

RADIO  
AT  
ULTRA-HIGH FREQUENCIES

Volume II

---

(1940-1947)

---

**RADIO  
AT  
ULTRA-HIGH FREQUENCIES**

**Volume II**

---

**(1940-1947)**

---

*Edited by*

**ALFRED N. GOLDSMITH  
ARTHUR F. VAN DYCK  
ROBERT S. BURNAP  
EDWARD T. DICKEY  
GEORGE M. K. BAKER**

**JULY, 1948**

**Published by**

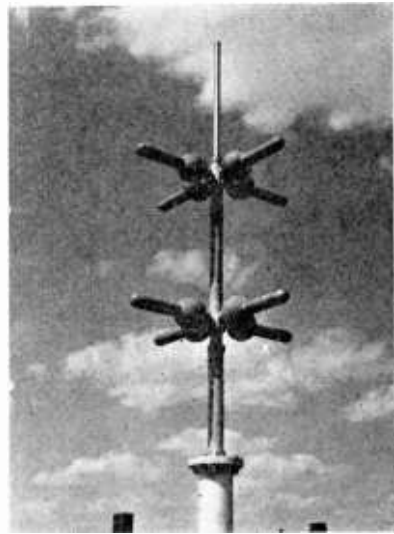
**RCA REVIEW  
RADIO CORPORATION OF AMERICA  
RCA LABORATORIES DIVISION  
Princeton, New Jersey**

Copyright, 1948, by  
Radio Corporation of America,  
RCA Laboratories Division

Printed in U.S.A.



*U-H-F electron tube*



*288-megacycle antenna*

---

**RADIO AT ULTRA-HIGH FREQUENCIES**

---



*Microwave radio relay*



*Microwave radar*

# RADIO AT ULTRA-HIGH FREQUENCIES

## Volume II

---

(1940-1947)

---

### PREFACE

RADIO AT ULTRA-HIGH FREQUENCIES, Volume II, is the eighth volume in the RCA Technical Book Series and the second on the general subject of radio at the higher frequencies. RADIO AT ULTRA-HIGH FREQUENCIES, Volume I, covered the period 1930-1939. The present volume includes the years 1940-1947.

Papers are presented in seven sections: antennas and transmission lines; propagation; reception; radio relays; microwaves; measurements and components; and navigational aids. As additional sources of reference, the appendices include a bibliography in the field of ultra-high-frequency radio, and summaries of all papers appearing in RADIO AT ULTRA-HIGH FREQUENCIES, Volume I, which is now out of print.

While it is realized that the ultra-high-frequency band is often limited to the frequencies 300-3,000 megacycles, the editors have taken some liberties with this concept. In certain cases, techniques applicable to U-H-F are discussed in papers covering V-H-F or microwave frequencies; such papers are included in this volume. Consequently, the title of this book indicates a limitation not strictly observed by the subject matter; it has been retained, however, in the interests of continuity and simplicity.

The bibliography has been included to insure that applicable material on U-H-F is available in this volume—at least in reference form. Papers concerning tubes and circuits which relate to specific applications such as television, frequency modulation, or facsimile, are listed in the bibliography; they are covered, however, in other volumes of the Technical Book Series.

\* \* \*

RCA REVIEW gratefully acknowledges the courtesy of the Institute of Radio Engineers (*Proc. I.R.E.*), the McGraw-Hill Publishing Com-

pany, Inc. (*Electronics*), the American Institute of Electrical Engineers (*Elec. Eng.*), The American Institute of Physics (*Jour. Appl. Phys.*), the Bryan-Davis Publishing Company (*Communications*), and the FM Company (*FM and Tele.*) in granting to RCA REVIEW permission to republish material by RCA authors which has appeared in their publications. The appreciation of RCA REVIEW is also extended to all authors whose papers appear herein.

\* \* \*

The importance of the U-H-F portion of the radio-frequency spectrum may be clearly understood when it is realized that research and development work in the higher radio frequencies underlies many of the recent advances in a score of widely different fields. Furthermore, overcrowding in the frequencies below 300 megacycles points to the need for utilization of the higher frequencies. While, in many cases, the characteristics of these higher bands raise problems of some magnitude, they frequently make possible the existence of services which could operate only with reduced effectiveness, if at all, in the lower bands.

RADIO AT ULTRA-HIGH FREQUENCIES, Volume II, is, therefore, being published for scientists, engineers, and others interested in the field of ultra-high-frequency radio, with the sincere hope that the material here assembled may help to speed developments in the higher radio-frequency bands.

*The Manager, RCA REVIEW*

RCA Laboratories,  
Princeton, N. J.  
May 18, 1948

# RADIO AT ULTRA-HIGH FREQUENCIES

## Volume II

(1940-1947)

### CONTENTS

	PAGE
FRONTISPIECE . . . . .	—v—
PREFACE . . . . . <i>The Manager, RCA REVIEW</i>	—vii—
ANTENNAS AND TRANSMISSION LINES	
Experimentally Determined Impedance Characteristics of Cylindrical Antennas . . . . . G. H. BROWN AND O. M. WOODWARD, JR.	1
Radio-Frequency Resistors as Uniform Transmission Lines . . . . . D. R. CROSBY AND C. H. PENNYPACKER	15
Comparator for Coaxial Line Adjustments . . . . . O. M. WOODWARD, JR.	27
Phase-Front Plotter for Centimeter Waves . . . . . H. IAMS	40
Circularly-Polarized Omnidirectional Antenna . . . . . G. H. BROWN AND O. M. WOODWARD, JR.	46
Slot Antennas . . . . . N. E. LINDENBLAD	57
<i>Summaries:</i>	
An Ultra-High-Frequency Antenna of Simple Construction . . . . . G. H. BROWN AND J. EPSTEIN	73
Water-Cooled Resistors for Ultra-High Frequencies . . . . . G. H. BROWN AND J. W. CONKLIN	73
The RCA Antennalyzer—An Instrument Useful in the Design of Directional Antenna Systems . . . . . G. H. BROWN AND W. C. MORRISON	74
Input Impedance of a Folded Dipole . . . . . W. VAN B. ROBERTS	75
PROPAGATION	
Propagation of Ultra-High-Frequency Waves . . . . . D. E. FOSTER	76
Ultra-High-Frequency Propagation Through Woods and Underbrush . . . . . B. TREVOR	90
Propagation Studies on 45.1, 474 and 2800 Megacycles Within and Beyond the Horizon . . . . . G. S. WICKIZER AND A. M. BRAATEN	93
RECEPTION	
Field Strength of Motorcar Ignition Between 40 and 450 Megacycles . . . . . R. W. GEORGE	117
The Distribution of Amplitude with Time in Fluctuation Noise . . . . . V. D. LANDON	125
The Absolute Sensitivity of Radio Receivers . . . . . D. O. NORTH	147
An Analysis of the Signal-to-Noise Ratio of Ultra-High-Frequency Receivers . . . . . E. W. HEROLD	159
Some Aspects of Radio Reception at Ultra-High Frequency . . . . . E. W. HEROLD AND L. MALTER	189
Part I—The Antenna and the Receiver Input Circuits . . . . .	189
Part II—Admittances and Fluctuation Noise of Tubes and Circuits . . . . .	224
Part III—The Signal-to-Noise Ratio of Radio Receivers . . . . .	245
Part IV—General Superheterodyne Considerations at Ultra-High Frequencies . . . . .	267
Part V—Frequency Mixing in Diodes . . . . .	286
<i>Summaries:</i>	
U-H-F Oscillator Frequency-Stability Considerations . . . . . S. W. SEELEY AND E. I. ANDERSON	305
Ultrashort Electromagnetic Waves VI—Reception . . . . . B. TREVOR	305

*CONTENTS (Continued)*

<b>RADIO RELAYS</b>		<b>PAGE</b>
Radio-Relay-Systems Development by the Radio Corporation of America	C. W. HANSELL	306
A Microwave Relay System . . . . .	L. E. THOMPSON	336
<i>Summaries:</i>		
Micro-Wave Television Relay . . . . .	W. J. POCH AND J. P. TAYLOR	353
Development of Radio Relay Systems . . . . .	C. W. HANSELL	353
A Microwave Relay Communication System . . . . .	G. G. GERLACH	354
Pulse Time Division Radio Relay . . . . .	B. TREVOR, O. E. DOW AND W. D. HOUGHTON	354
<b>MICROWAVES</b>		
Attenuation of Electromagnetic Fields in Pipes Smaller Than the Critical Size	E. G. LINDER	355
Resonant-Cavity Measurements	R. L. SPROULI AND E. G. LINDER	362
Absorption of Microwaves by Gases II . . . . .	J. E. WALTER AND W. D. HERSHBERGER	379
<i>Summaries:</i>		
Wave Guides and the Special Theory of Relativity . . . . .	W. D. HERSHBERGER	396
The Absorption of Microwaves by Gases . . . . .	W. D. HERSHBERGER	396
Thermal and Acoustic Effects Attending Absorption of Microwaves by Gases . . . . .	W. D. HERSHBERGER, E. T. BUSH, AND G. W. LECK	397
Mica Windows as Elements in Microwave Systems . . . . .	L. MALTER, R. L. JEPSEN, AND L. R. BLOOM	397
<b>MEASUREMENTS AND COMPONENTS</b>		
Receiver Input Connections for U-H-F Measurements	J. S. RANKIN	398
A Coaxial-Line Diode Noise Source for U-H-F . . . . .	H. JOHNSON	407
An Ultra-High-Frequency Low-Pass Filter of Coaxial Construction . . . . .	C. L. CUCCIA AND H. R. HEGBAR	424
<i>Summaries:</i>		
Measurement of Iron Cores at Radio Frequencies . . . . .	D. E. FOSTER AND A. E. NEWLON	432
Direct-Reading Wattmeters for Use at Radio Frequencies . . . . .	G. H. BROWN, J. EPSTEIN, AND D. W. PETERSON	432
Special Applications of Ultra-High-Frequency Wide-Band Sweep Generators . . . . .	J. A. BAUER	433
<b>AIDS TO NAVIGATION</b>		
<i>Summaries:</i>		
An Omnidirectional Radio-Range System . . . . .	D. G. C. LUCK	434
Part I—Principles of Operation . . . . .		434
Part II—Experimental Apparatus . . . . .		435
Part III—Experimental Results and Methods of Use . . . . .		435
Radiating System for 75-Megacycle Cone-of-Silence Marker . . . . .	E. A. LAPORT AND J. B. KNOX	436
Shoran Precision Radar . . . . .	S. W. SEELEY	436
Teleran, Part I—Air Navigation and Traffic Control by Means of Television and Radar . . . . .	D. H. EWING AND R. W. K. SMITH	437
Teleran, Part II—First Experimental Installation . . . . .	D. H. EWING, H. J. SCHRADER AND R. W. K. SMITH	438
— x —		
APPENDIX I—U-H-F Bibliography . . . . .		439
APPENDIX II—Summaries of Papers Published in RADIO AT ULTRA-HIGH FREQUENCIES, Volume I . . . . .		454



# EXPERIMENTALLY DETERMINED IMPEDANCE CHARACTERISTICS OF CYLINDRICAL ANTENNAS\*†

BY

GEORGE H. BROWN AND O. M. WOODWARD, JR.

Research Department, RCA Laboratories Division,  
Princeton, N. J.

*Summary*— Measurements of resistance and reactance of cylindrical antennas operated against ground have been made, with a wide variation of both antenna length and diameter. These data are displayed by means of a series of graphs.

The maximum values of resistance encountered are displayed. The shortening effect near the quarter-wave resonance point is also shown.

Terminal conditions, such as capacitance of the base of the antenna to ground, are briefly considered, and a series of measurements shows the wide variation in impedance for varying terminal conditions.

Measurements made in the course of the investigation show that the impedance of the antenna is independent of whether the top of the radiator is open or closed. The measured impedance data are also directly applicable to the case of a center-fed dipole.

## I. INTRODUCTION

**A** KNOWLEDGE of the base impedance of vertical antennas as a function of antenna length and diameter is very helpful in devising terminating networks for antenna systems. Much has been written concerning the mathematical difficulties of rigorously solving the antenna problem, and several methods of approximation have been proposed. Very little information of an experimental nature has been published. A number of years ago, the writers decided to undertake a systematic investigation of the problem. Other projects of a more pressing nature have seriously impaired our plans. However, the work of measuring the resistance and reactance of simple cylinders has been completed and the data compiled. The purpose of this paper is to present these data in a form that may prove useful.

## II. METHOD OF MEASUREMENT

The physical arrangement for making the measurements is shown in Figure 1. A large circular metallic screen 12 feet in diameter and 15 wires to the inch was placed on the surface of the earth. A concen-

\* Decimal classification: R241.1×R320.

† Reprinted from *Proc. I.R.E.*, April, 1945.

tric transmission line ran below this screen back to a slotted section of measuring line. Here a sensitive probe indicated the ratio of minimum-to-maximum voltage on the line as well as the position of a voltage minimum on the line. These two quantities together with the characteristic impedance of the feed line establish the impedance that exists at the end of the line. The inner diameter of the outer conductor of the feed line was 0.785 inch, while the diameter of the inner conductor was 0.25 inch. The cylinder which formed the antenna was closed at the bottom with a circular metal plate.

The writers rather like the method of notation which expresses dimensions in electrical degrees. For instance, in Figure 1, the dimension  $a$  which is the physical length from the ground plane to the top of the antenna may be used to compute the length  $A$  in electrical degrees.

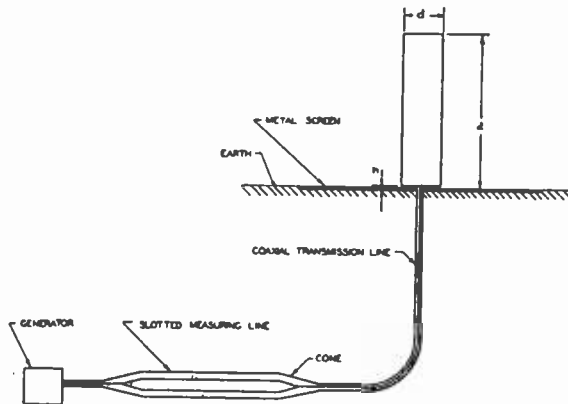


Fig. 1—Physical arrangement used in making impedance measurements.

$$A \text{ (degrees)} = 360a / \lambda \quad (1)$$

where  $\lambda$  is the free-space wavelength measured in the same units in which  $a$  is measured. The actual diameter  $d$  may be used in the same way to express the diameter  $D$  in electrical degrees.

Two simple and useful formulas for computing  $A$  are

$$A \text{ (degrees)} = a_{ft} f_{kc} / 2725 \quad (2)$$

and

$$A \text{ (degrees)} = a_{\text{inches}} f_{mc} / 32.7. \quad (3)$$

Measurements were made on wires and cylinders of various diameters, with  $D$  ranging from 0.1 degree to 20 degrees. This range was chosen with an eye to practical considerations, for a 3-inch diameter

mast at 1 megacycle represents a value of  $D$  close to 0.1 degree, while a diameter of 1.3 inches at 500 megacycles is approximately 20 degrees.

The spacing  $h$  between the ground plane and the metal plate closing the bottom of the cylinder was chosen so that this electrical spacing  $H$  was one degree.

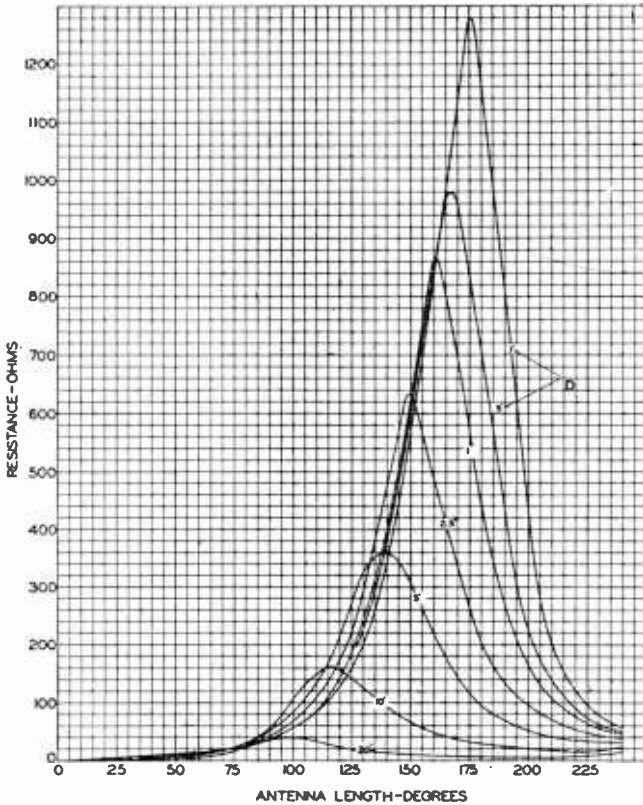


Fig. 2—Measured resistance curves versus antenna length in degrees, for a number of fixed diameters. Here the frequency is held constant and the physical length of the antenna is changed.

### III. RESISTANCE AND REACTANCE VARIATION, WITH DIAMETER AND FREQUENCY CONSTANT, AND THE ANTENNA LENGTH VARIABLE

A complete series of measurements was made by choosing a cylinder of a certain diameter, maintaining a fixed frequency of 60 megacycles, while the physical length of the antenna was changed. The resulting resistance curves are shown in Figure 2, while the corresponding reactance values are presented in Figure 3.

From Figure 2, we see that the maximum value of resistance for

each diameter becomes greater and occurs closer to  $A = 180$  degrees as the diameter becomes smaller. This point is illustrated strikingly

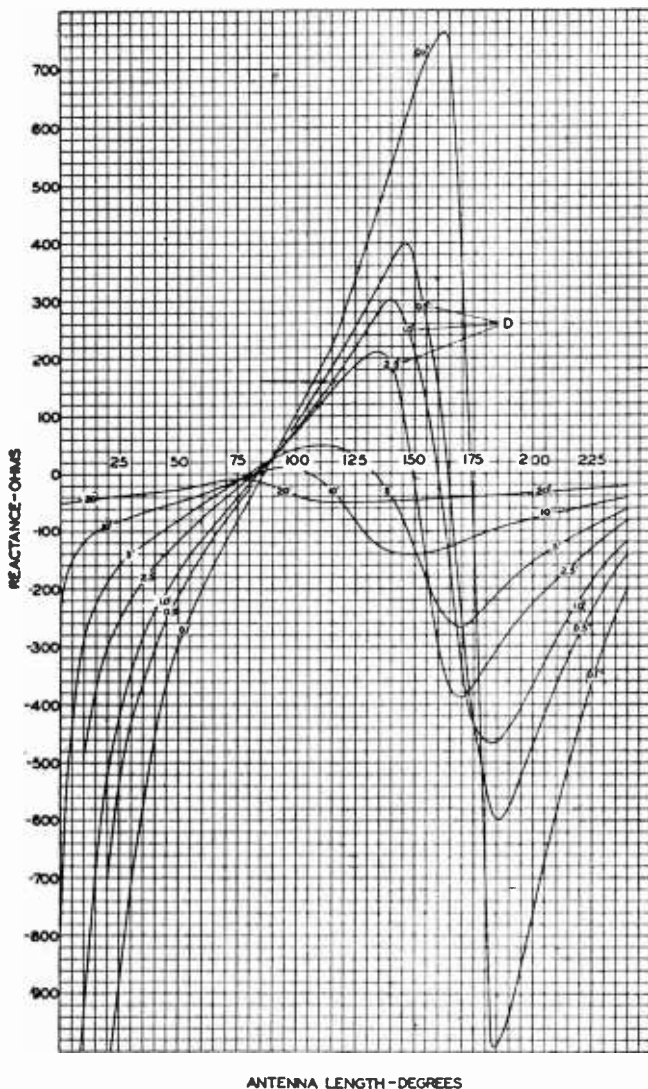


Fig. 3—Measured reactance curves versus antenna length in degrees. Again the frequency is held constant and the physical length of the antenna is changed.

by Figure 4. This diagram was constructed from Figure 2. The top curve in Figure 4 shows the antenna length  $A$  at which maximum resistance occurs for each value of  $D$ . The corresponding value of the

maximum resistance is shown by the lower curve. The upper curve extrapolates very nicely and shows that as  $D$  approaches zero, for maximum resistance,  $A$  approaches 180 degrees. The lower curve shows that there is a good chance of the resistance approaching infinity as the diameter approaches zero.

Figure 3 shows that as the antenna becomes very short, the reactance approaches a definite limiting value. The effect is particularly striking in the case where  $D$  is 20 degrees. Actually, in our measurements, the antenna length did not go down to zero degrees, for when the antenna has been trimmed entirely away, the plate which formed the bottom of the cylinder still remained, so that we measured the reactance of this disk hung on the end of the measuring line. It should be realized that all of our measurements shown in Figures 2 and 3 are

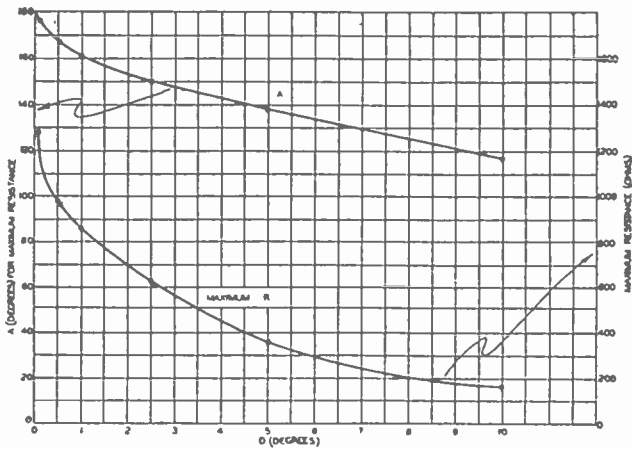


Fig. 4—Maximum resistance versus antenna diameter  $D$  and the antenna length  $A$  at which the maximum resistance occurs versus antenna diameter.

the combined impedances of the antenna proper in parallel with the base reactance. Theoreticians may well object that this prevents comparison between theoretical and experimental results. It is entirely possible to imagine a cylinder with the base removed and excited by a number of tiny generators connected between the periphery and the ground plane. Then a knowledge of the relationship between the generator voltage and the current delivered by the generators would give an answer closer to the ideal, since the base charging current would not be present. However, a realistic consideration of the problem soon indicates that these measurements taken under true existing conditions are likely to be of more value from a design standpoint.

It might be added that the effect of this base capacitance only makes itself felt where  $D$  is larger than one degree.

It may be observed from Figures 2 and 3, that the reactance curve crosses through zero close to the point where the resistance is maximum. There is, however, some slight departure from true correspondence. The solid curve in Figure 5 shows the antenna length for zero reactance as a function of the diameter,  $D$ . By calculation from Figures 2 and 3, the writers determined the zero reactance point when the base reactance was removed. The resulting values of antenna length are shown by the broken curve of Figure 5.

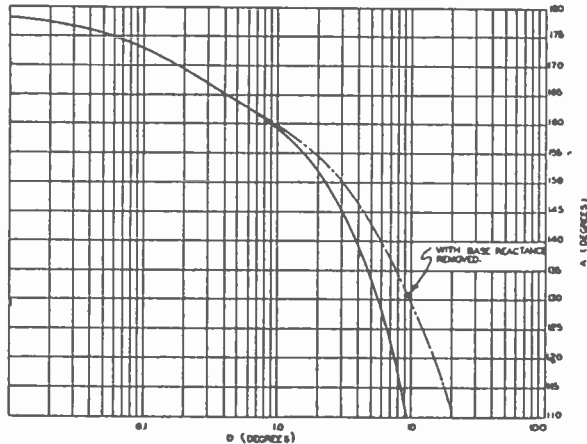


Fig. 5—The solid curve shows the antenna length  $A$  for zero reactance (near the maximum resistance point) as a function of the diameter  $D$ . This information is taken from measured data. The broken curve shows the same quantities when the base reactance is removed by calculation.

#### IV. RESISTANCE AND REACTANCE VARIATION, WITH DIAMETER AND LENGTH CONSTANT, AND WITH VARIABLE FREQUENCY

The curves of Figures 2 and 3 show the impedance variation when the antenna length is varied. Often, it is of interest to know the action for a fixed antenna as the frequency is varied. By working through the curves of Figures 2 and 3, and by cross-plotting much of the experimental data, the writers were able to build up Figures 6 and 7. Here the resistance and reactance variation is shown for a fixed ratio of antenna length to diameter, and the variation of the electrical length of the antenna is secured by varying the frequency.

It may be noted that the reactance curves approach infinite values as the antenna length approaches zero, since the approach to zero antenna length is secured by approaching zero frequency.

Figures 6 and 7 may prove to be useful in designing antennas to cover a wide frequency range.

Figure 8 presents the data of Figure 6 in a somewhat different

fashion. Here each curve shows the antenna resistance as a function of the ratio of antenna length to diameter ( $A/D$ ) for a fixed antenna length. Since the antenna length is fixed for each curve, large values of  $A/D$  represent very thin wires, while small values of  $A/D$  correspond to fat antennas. It is interesting to note that the resistance of a wire whose length  $A$  equals 90 degrees and whose  $A/D$  value is greater than 100 is very close to the theoretical value of 36.6 ohms obtained from the assumption of a simple sine-wave distribution of current.

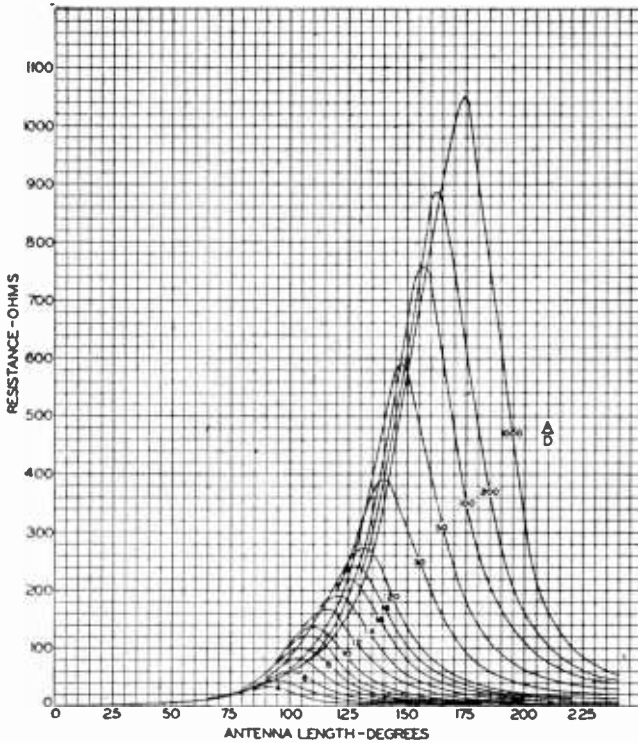


Fig. 6—Antenna resistance versus antenna length  $A$ , when a constant ratio of length to diameter  $A/D$  is maintained. Here the length and diameter are held constant while the frequency is changed.

Reactance curves as a function of  $A/D$  are given by Figure 9. Many of these curves would be altered remarkably by removing the shunting reactance at the base, or by altering the terminal conditions.

Reference to Figure 6 helped in the preparation of Figure 10, where the maximum resistance as a function of  $A/D$  is shown.

Another interesting bit of information may be extracted from the data shown in Figure 7 and Figure 9. It is generally known that the first resonance in a vertical antenna occurs close to a length of  $A$  equal

to 90 degrees, and it is also general knowledge that the antenna should be shortened slightly from the 90-degree length to obtain this resonance or zero-reactance condition. By cross-plotting the data of Figures 7 and 9, the writers obtained Figure 11, which shows the shortening (expressed in per cent of 90 degrees or one-quarter wavelength) necessary to secure zero reactance for each value of  $A/D$ .

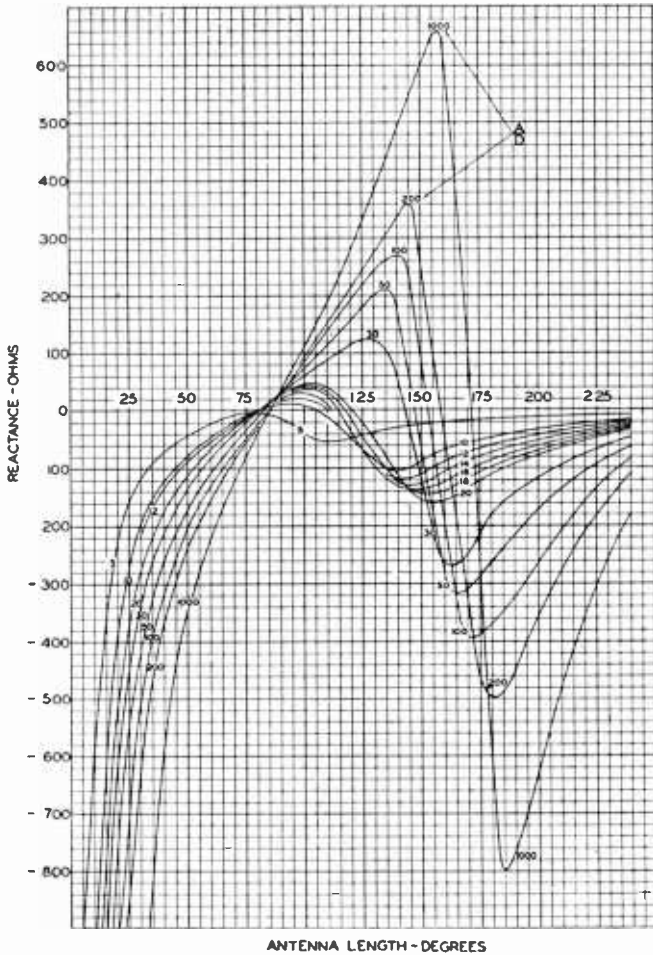


Fig. 7—Reactance curves corresponding to the resistance curves of Fig. 6.

#### V. REACTANCE OF THE BASE-PLATE

As has been stated, the disk which closes off the bottom of the radiator forms a shunt capacity across the terminals of the radiator. We may estimate the amount of the base shunting reactance by calcu-



lating the capacitance of the disk, neglecting fringing at the edges, and assuming that all displacement currents flow from the bottom of the disk to the ground plane. Then the shunt reactance is

$$X_s = \frac{\mu c^2 h}{\omega (\pi d^2 / 4)} \tag{4}$$

- where  $\mu$  = permeability of free space =  $4\pi \times 10^{-9}$
- $c$  = velocity of radio waves in free space =  $3 \times 10^{10}$  centimeters per second
- $h$  = spacing of disk from plane (centimeters)
- $d$  = diameter of disk (centimeters)
- $\omega = 2\pi f$
- $f$  = frequency in cycles per second

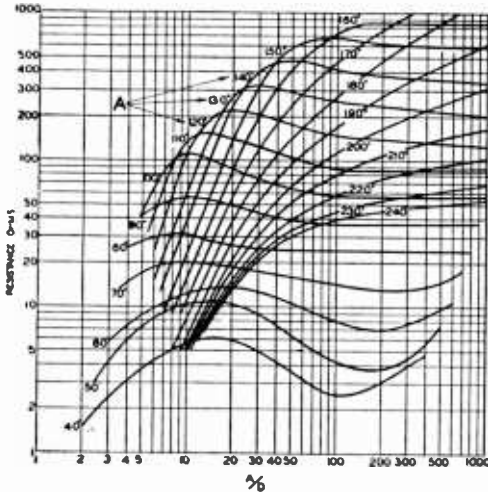


Fig. 8—Resistance versus the ratio  $A/D$  with antenna length  $A$  as a parameter.

Then we may rewrite (4) as

$$X_s = \frac{480 (\omega h / c)}{(\omega d / c)^2} \tag{5}$$

However, if we express the spacing in electrical degrees  $H$  and the diameter in the same way  $D$ , (5) becomes

$$X_s = 27,500 H / D^2 \tag{6}$$

In making the measurements shown in Figures 2 and 3, we kept  $H$  equal to 1 degree. Thus, for  $D$  equal to 20 degrees, we see that the shunt capacitive reactance is 68.3 ohms, a quantity which is not at all negligible. However, when  $D$  is 1 degree, the shunt reactance is 27,500 ohms, a rather high value compared to any value of impedance encountered during the course of measurement.

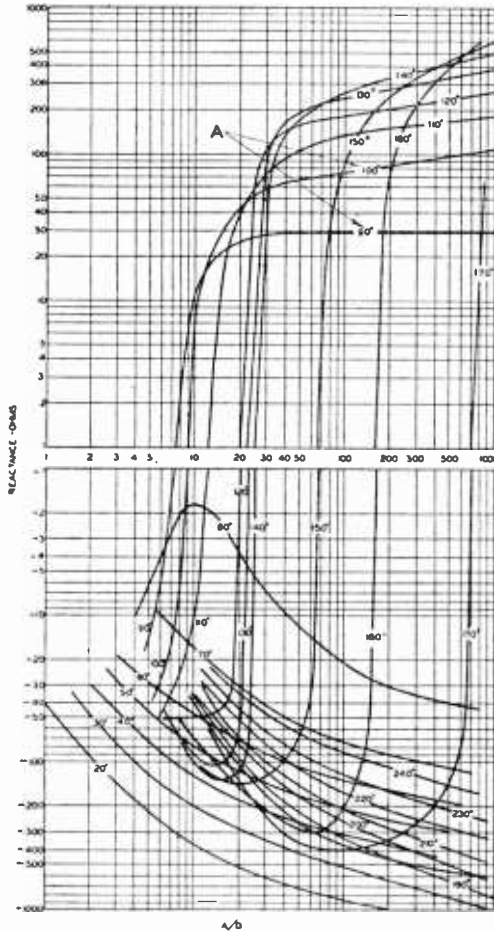


Fig. 9—Antenna reactance versus the ratio  $A/D$  for a number of values of antenna length  $A$ .

### VI. COMPARISON OF IMPEDANCE MEASUREMENTS WITH VARYING TERMINAL CONDITIONS

For the previously disclosed measurements with large diameters, the experimental arrangement looked something like that shown in

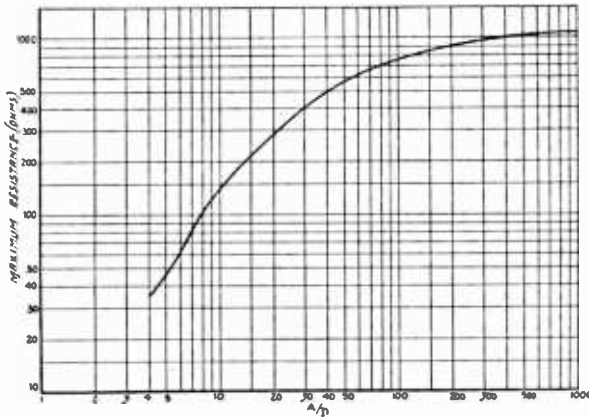


Fig. 10—Maximum resistance as a function of the ratio  $A/D$ .

Figure 12(a). Another experimental arrangement used for comparison purposes was that shown in Figure 12(b). Here the inner conductor of the measuring line was the same diameter as the antenna. In fact, the antenna was simply the extension of the inner conductor. The system was so arranged that no insulators were in the measuring line between the point of measurement and the antenna. In these comparative measurements, the antenna diameter was maintained at 20.6 degrees. Three sizes of tubing were chosen for the outer conductor of the transmission line. The diameters of the transmission line as well as the characteristic impedance are given in the captions for Figures 13 and 14.

Figure 13 shows the measured resistance values for the arrangements, while Figure 14 shows the corresponding reactance curves. Curve A in both figures shows the measured values for the arrangement of Figure 12(a), with a diameter of 20.6 degrees. For this diameter,

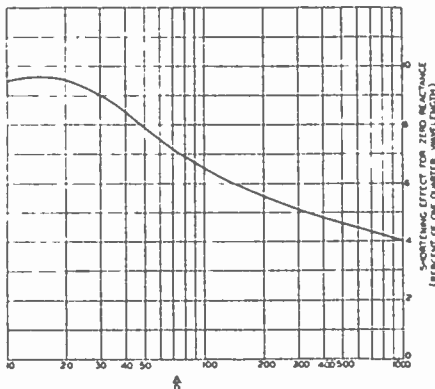


Fig. 11—Shortening effect near the quarter-wave point.

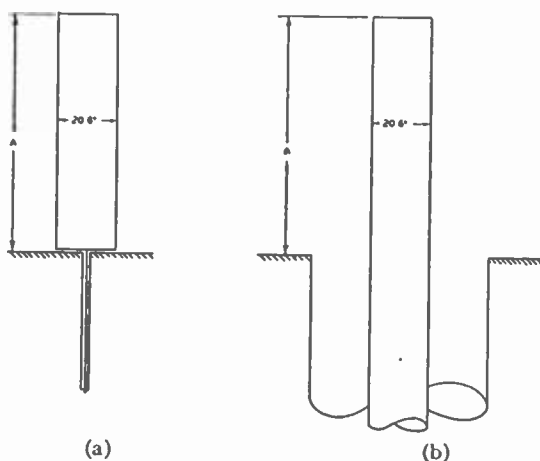


Fig. 12—Experimental arrangement for obtaining curves in Figs. 13 and 14. (a) For curve A. (b) For curves B, C, and D.

(6) shows that the shunt capacitive reactance is 65.0 ohms. To knock out the effect of this shunting reactance, we may imagine an inductive reactance in shunt with the antenna, where this auxiliary reactance has a value of 65.0 ohms. Curve *E* on Figures 13 and 14 was computed in exactly this fashion.

For instance, with an antenna length of 100 degrees, curve A shows that  $R_A$  is 42.0 ohms and  $X_A$  is  $-39.5$  ohms. Then to find the impedance

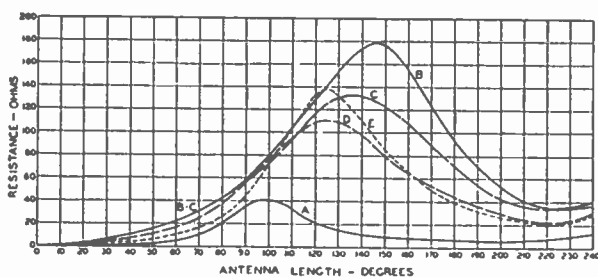


Fig. 13—Resistance as a function of antenna length *A*. The diameter *D* is 20.6 degrees.

Curve A—The arrangement shown in Fig. 12(a).

Curve B—The arrangement of Fig. 12(b), with the diameter of the outer conductor equal to 74 degrees. The characteristic impedance of the transmission line is 77.0 ohms.

Curve C—The outer conductor diameter is 49.5 degrees, and the transmission line has a characteristic impedance of 52.5 ohms.

Curve D—The diameter of the outer conductor is 33 degrees. The characteristic impedance is 28.3 ohms.

Curve E—This curve was obtained by tuning out the base reactance with an inductive reactance of 65.0 ohms.

without the shunt capacitance, we calculate the parallel circuit conditions.

$$R_E + jX_E = \frac{j65.0(42.0 - j39.5)}{42.0 + j25.5} = 74.0 + j20.5 \text{ ohms.}$$

Examination of Figures 13 and 14 shows that curve *E* fits in with the group formed by curves *B*, *C*, and *D*, particularly with regard to reactance values. This illustrates the point that the excessive base shunting reactance materially effects the measured impedance values. The difference between curves *B*, *C*, and *D* may be attributed again to changing terminal conditions.

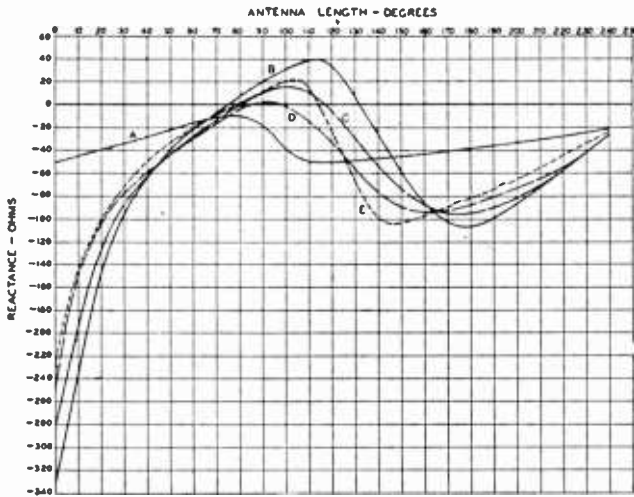


Fig. 14—Reactance curves corresponding to the resistance curves of Fig. 13.

The fact that curve *E* does not conform better to the curves *B*, *C*, and *D* is probably due to the fact that the simple conditions postulated in setting up (6) do not take full account of conditions near the terminals, and in addition to the fact that curve *A* was measured at 60 megacycles, while curves *B*, *C*, and *D* were obtained at a frequency of 540 megacycles.

#### VII. COMPARISON OF IMPEDANCE WITH TOP OF RADIATOR CLOSED AND OPEN

Some workers in the field have suggested that results obtained with the radiator closed at the top would be different than when the radiator

is open.<sup>1</sup> The writers continually checked this point throughout the course of the experiments. A great number of measurements were made with an open radiator, and then repeated with a disk soldered into place at the top of the radiator. Particularly careful observations were made with a radiator 20 degrees in diameter.

It was originally planned to display these experimental data. This plan was abandoned when it was discovered that opening or closing the top of the radiator made not the slightest difference in the measured impedance.

#### VIII. APPLICATION OF THE MEASURED CURVES TO CENTER-FED DIPOLES

All the data presented in this paper have applied to an antenna fed against ground. In case a center-fed dipole is to be considered, the antenna length  $A$  throughout this paper becomes the half length of the dipole, while all values of resistance and reactance shown in this paper must be doubled to give the proper values for a dipole. Due consideration must also be given the terminal conditions.

#### IX. CONCLUSION

Measured values of resistance and reactance of cylindrical antennas operated against ground have been displayed in a number of ways. It has been demonstrated that the exact conditions at the terminals are extremely important in determining the impedance conditions.

---

<sup>1</sup> L. Brillouin, "The Antenna Problem," *Quart. Appl. Math.*, Vol. I, p. 214; October, 1943.

# RADIO-FREQUENCY RESISTORS AS UNIFORM TRANSMISSION LINES\*†

BY

D. ROGERS CROSBY AND CAROL H. PENNYPACKER

Engineering Products Department, RCA Victor Division,  
Camden, N. J.

*Summary*—A theoretical study is made of the behavior of resistors, particularly the type where the resistance element is in the form of a film so there is negligible skin effect. When the electrical length of the resistor is a small fraction of a wavelength, it is shown that certain optimum proportions of the resistor exist in order best to terminate a radio-frequency transmission line.

## INTRODUCTION

THE theoretical and experimental behavior of resistors employed as transmission lines has been discussed frequently.<sup>1,2</sup> The material presented here is largely in the form of curves intended to give an easily grasped perspective of the subject. These curves are also suitable for design purposes. The dimensionless parameters used in plotting these curves are thought to be particularly convenient for engineering use. The existence of certain optimum values of the parameters is shown.

This paper is an analysis of the classical transmission-line equations. We thus assume that the resistors employed as transmission lines are long compared to the diameter of the shields surrounding them, so that the current flowing in the short circuit at the far end has an electromagnetic field which is small compared to the total electromagnetic field surrounding the resistor. It is further assumed that the resistance per unit length is independent of frequency. This is substantially true in the film-type resistors used at radio frequencies, since the current penetration through the film is substantially complete for the usual resistance values. Particular attention has been given to the case where the resistor is intended to terminate or "match" a coaxial transmission line. A family of curves showing standing-wave

\* Decimal classification: R383 × R144.

† Reprinted from *Proc. I.R.E.*, February, 1946.

<sup>1</sup> G. H. Brown and J. W. Conklin, "Water-Cooled Resistors for Ultra-High Frequencies," *Electronics*, Vol. 14, pp. 24-28; April, 1941.

<sup>2</sup> J. A. Fleming, *THE PROPAGATION OF ELECTRIC CURRENTS IN TELEPHONE AND TELEGRAPH CONDUCTORS*, D. Van Nostrand Co., Inc., New York, N. Y., 1911, Chap. III, Eq. (51).

ratio for various values of line resistance, as a function of frequency, has been plotted.

Consider the most common radio-frequency transmission line, made of copper. As the frequency of such a short-circuited line is raised from zero, the input resistance rises, reaching a maximum when the line is about a quarter wave long. For higher frequencies, the resistance oscillates with maxima slowly decreasing in amplitude. When the transmission-line conductor consists of a resistance that is not negligible compared to the characteristic impedance of the transmission line, the above impedance function is not obtained, since, as the frequency increases from zero, the input resistance may increase or decrease from the direct-current value. For frequencies a few times greater than the first resonant frequency, the input resistance may have a negligible amount of oscillation.

Consider a resistance employed as a transmission line and short-circuited at the far end (Figure 1).

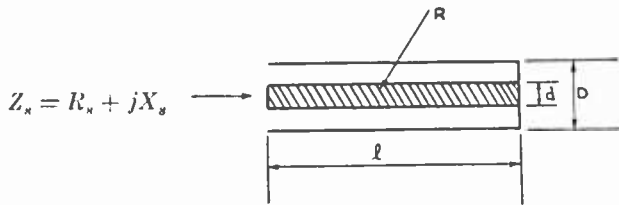


Fig. 1—Resistance employed as a transmission line. Far end is short-circuited.

$l$  = length of line in inches

$D$  = diameter of inside of outer conductor in inches

$d$  = diameter of resistor in inches

$Z_s$  = input impedance to line in ohms

$Z_0$  = characteristic impedance of line in ohms when  $R$  is zero

$R$  = total value of series resistance of line in ohms

$L$  = inductance of line in henries

$C$  = capacitance of line in farads

$f_{mc}$  = operating frequency in megacycles

$\lambda$  = free-space wavelength in inches

$\omega = 2\pi f = 2\pi f_{mc} \times 10^6$

From the classical theory



$$Z_0 = 138 \log_{10} \frac{D}{d} \quad (1)$$

$$Z_0 = \sqrt{\frac{L}{C}} \quad (2)$$

$$C = \frac{l}{\lambda} \times \frac{1}{Z_0 \times f} \quad (3) \quad L = \frac{l}{\lambda} \times \frac{Z_0}{f} \quad (4) \quad \frac{l}{\lambda} = \frac{l \times f_{mc}}{11,800} \quad (5)$$

$$Z_s = \sqrt{\frac{R + j\omega L}{G + j\omega C}} \tanh \sqrt{(R + j\omega L)(G + j\omega C)}. \quad (6)$$

We consider only the case where  $G$  is negligibly small. From the above equations, we obtain

$$\frac{Z_s}{Z_0} = \sqrt{1 - j \frac{R}{Z_0} \frac{1}{2\pi(l/\lambda)}} \cdot \tanh \sqrt{-4\pi^2 \left(\frac{l}{\lambda}\right)^2 + j2\pi \frac{l}{\lambda} \frac{R}{Z_0}}. \quad (7)$$

Two independent parameters are now involved,  $R/Z_0$  and  $l/\lambda$ . The term  $R/Z_0$  is independent of frequency, and is fixed by the proportion of the resistor to the jacket diameter. The term  $l/\lambda$  is proportional to frequency, so the plot of the impedance versus this term gives the frequency characteristic of the resistor.

The plot of (7) is given in Figures 2, 3, 4, 5, 6, 7, 8, 9, and 10, and shows:

1. For values of  $R/Z_0$  appreciably less than unity, both the resistance and reactance oscillate over a wide range of values.
2. For values of  $R/Z_0$  much greater than unity, the oscillations are of minor amplitude.
3. For larger values of  $R/Z_0$ , the reactance is always negative. For some short resistors, the reactance is positive, and for others it is negative.

Three special values of  $l/\lambda$  are of interest:

$$l/\lambda \text{ very small; } l/\lambda \text{ very large; } l/\lambda = 1/4.$$

#### SMALL VALUES OF $l/\lambda$

Expanding (7) in powers of  $2\pi l/\lambda$  we obtain

$$\frac{R_s}{Z_0} = \frac{\bar{R}}{Z_0} + (2\pi l/\lambda)^2 \left( \left(\frac{R}{Z_0}\right) \frac{2}{2} - \frac{2}{15} \left(\frac{R}{Z_0}\right)^3 \right) + (2\pi l/\lambda)^4 ( ) + \dots$$

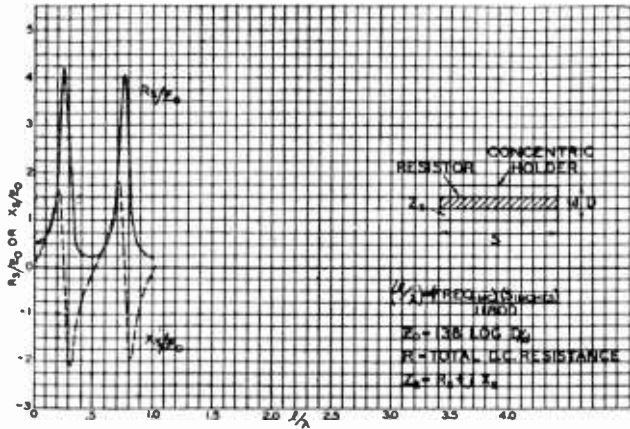


Fig. 2—Impedance of short-circuited transmission line.  $R/Z_0 = 0.5$ .

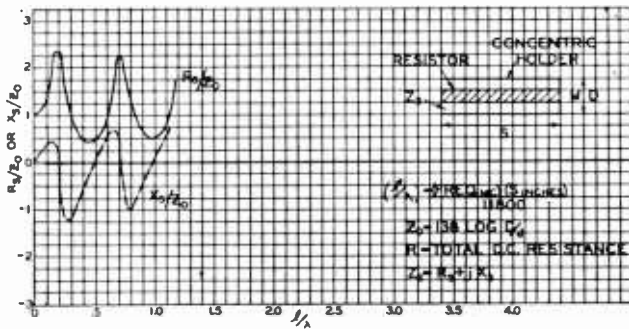


Fig. 3—Impedance of short-circuited transmission line.  $R/Z_0 = 1.0$ .

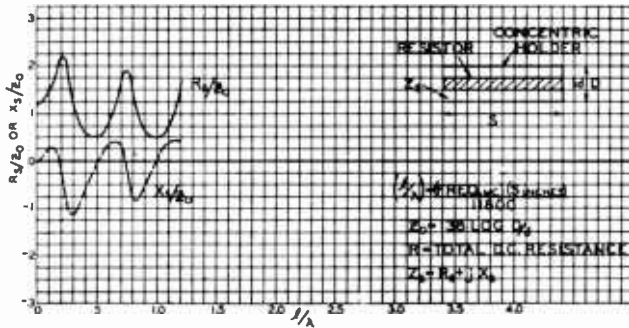


Fig. 4—Impedance of short-circuited transmission line.  $R/Z_0 = 1.2$ .

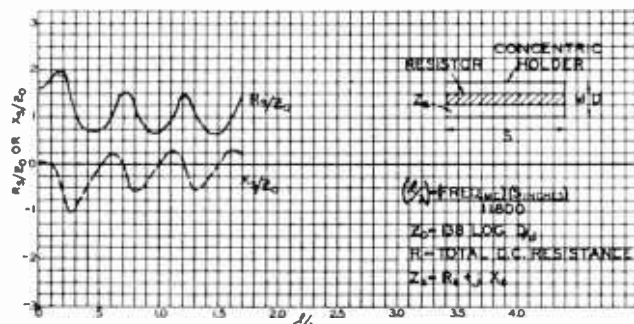


Fig. 5—Impedance of short-circuited transmission line.  $R/Z_0 = 1.6$ .

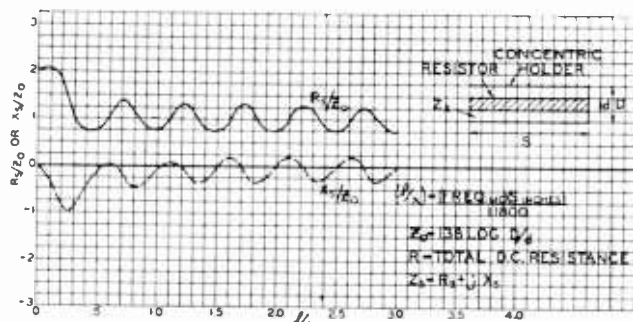


Fig. 6—Impedance of short-circuited transmission line.  $R/Z_0 = 2.0$ .

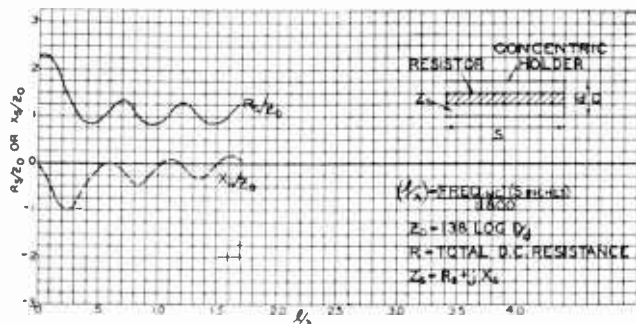
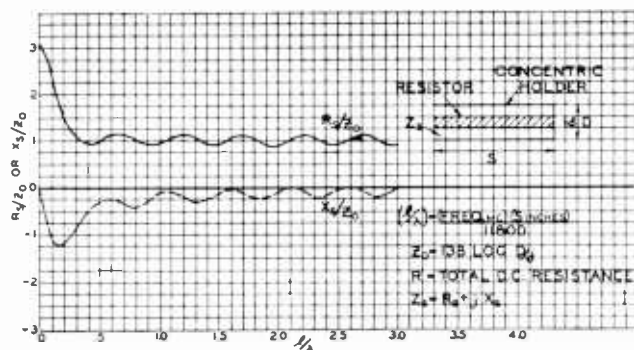
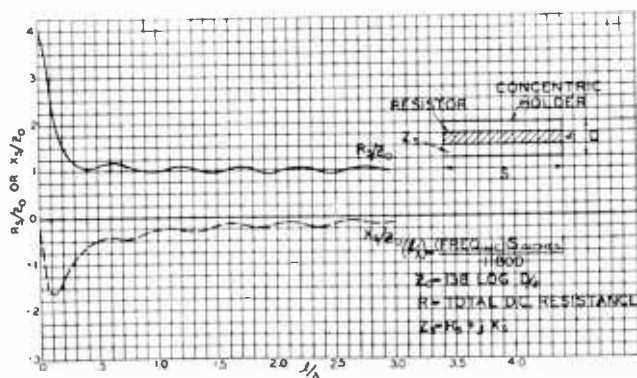
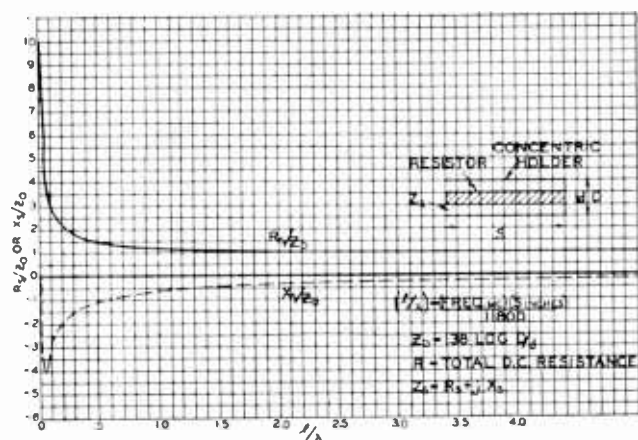


Fig. 7—Impedance of short-circuited transmission line.  $R/Z_0 = 2.25$ .

Fig. 8—Impedance of short-circuited transmission line.  $R/Z_0 = 3.0$ .Fig. 9—Impedance of short-circuited transmission line.  $R/Z_0 = 4.0$ .Fig. 10—Impedance of short-circuited transmission line.  $R/Z_0 = 10.0$ .

$$l/\lambda) \left( 1 - \left( \frac{R}{Z_0} \right)^2 \frac{1}{3} \right) + (2\pi l/\lambda)^3 (\dots) + \dots \quad (8)$$

*n*th derivative of a function expressed in a power series in the variable is zero, the coefficient of the *n*th term in the series must be zero.

Since the expression for  $R_n/Z_0$ , the term involving  $(l/\lambda)$  to the first power is missing, we conclude that the slope of all the resistance curves will be zero at  $l/\lambda = 0$ . Figures 2, 3, 4, 5, 6, 7, 8, 9, 10, and 11, illustrate this. For  $R/Z_0 = \sqrt{3}$ , the coefficient of the second term in the expression for  $R_n/Z_0$  vanishes. Thus for this value the curvature of the resistance characteristic will be zero at  $l/\lambda = 0$ .

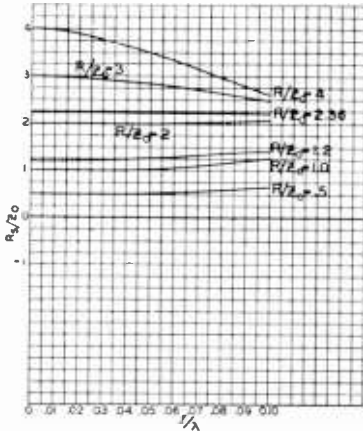


Fig. 11—Resistance of short-circuited transmission line. All slopes are zero at  $l/\lambda = 0$ . For  $R/Z_0 = \sqrt{3}$ , curvature is zero at  $l/\lambda = 0$ .

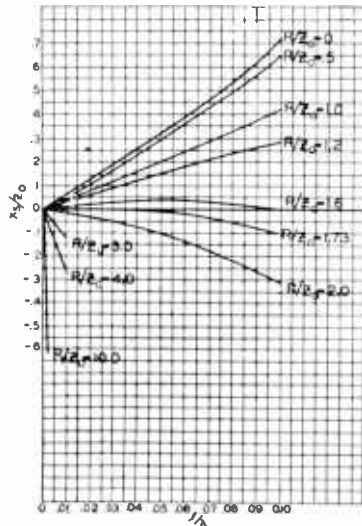


Fig. 12—Reactance of short-circuited transmission line. For  $R/Z_0 = \sqrt{3}$ , slope is zero at  $l/\lambda = 0$ .

Since in the expression for  $X_n/Z_0$ , the term involving  $l/\lambda$  to the second power is missing, we conclude that the curvature of all the reactance curves (Figure 12) will be zero at  $l/\lambda = 0$ . For  $R/Z_0 = \sqrt{3}$ , the coefficient of the first term in the expression for  $R_n/Z_0$  vanishes. Thus, for this value, the slope of the reactance curve will be zero at  $l/\lambda = 0$ .

When resistors are used for terminating transmission lines, the principal cause of standing waves is the presence of reactance. Thus

the derived relation  $R/Z_0 = \sqrt{3}$  gives the widest frequency range for a fixed minimum standing-wave ratio. The RCA patent called to our attention U. S. patent No. 2,273,547 filed in 1939 by Radinger of Berlin, Germany, which also gives the  $\sqrt{3}$  ratio as being optimum. Radinger refers to German patent No. 618,678 filed in 1932 by Roosenstein. Roosenstein discloses the method of finding the optimum value. Due to an error in an expansion, he arrived at  $\sqrt{2}$  instead of  $\sqrt{3}$ .

A plot has been made in Figure 13 to show how the standing-wave ratio varies with frequency when a coaxial line is terminated with a resistor. The value of  $R$  is taken equal to the characteristic imped-

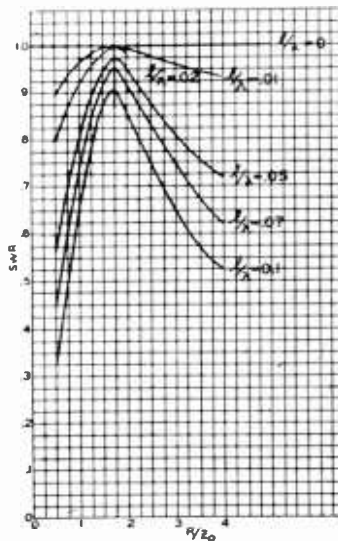


Fig. 13—Standing-wave ratio versus  $R/Z_0$  for constant  $l/\lambda$ . Note as  $l/\lambda$  increases, the standing-wave ratio is minimum for  $R/Z_0 = \sqrt{3}$ .

ance of the line to be terminated. This insures that the line will be matched at low frequencies.

The value of  $R/Z_0$  is determined by the ratio of the resistor diameter to the diameter of the transmission-line jacket in which the resistor is mounted. Thus the value  $Z_0$  is independent of the characteristic impedance of the line to be terminated. From Figure 13 it can be seen that the standing-wave ratio nearest unity occurs for  $R/Z_0 = \sqrt{3}$ .

Suppose we have a resistor 12 inches long and plan to use it up to 100 megacycles. Using (5) we obtain

$$l/\lambda = 0.1.$$

From the curves of Figure 13, we see that if the jacket is chosen so  $R/Z_0 = \sqrt{3}$ , the standing-wave ratio at 100 megacycles will be 0.9.

From this plot, we see that with the proper jacket, the standing-wave ratio will be 0.97 for  $l/\lambda = 0.05$ . Putting this value in (5)

$$0.05 = \frac{l \times f_{mc}}{11,800} \quad (9)$$

or approximately

$$f_{mc} = \frac{600}{l}.$$

This rounded constant 600 is convenient for quick design. Thus a resistor 1 inch long can have good characteristics up to 600 megacycles, and a resistor 12 inches long up to 50 megacycles.

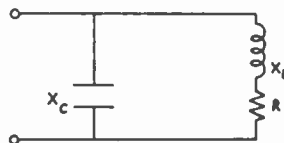


Fig. 14—Equivalent lumped circuit of resistor.

The curves of Figure 13 were computed using the formulas

$$\text{standing-wave ratio} = \frac{1 - |K|}{1 + |K|} \quad K = \frac{1 - \frac{Z_s}{R_0}}{1 + \frac{Z_s}{R_0}} \quad (10)$$

where  $K$  is the reflection coefficient.

That the resistance may either increase or decrease as the frequency is raised from zero can also be shown from an equivalent lumped circuit of the resistor.<sup>3,4</sup> The equivalent circuit of the resistor is shown in Figure 14, where  $Z_0 = \sqrt{L/C}$  and  $Q = Z_0/R$ .

It can be shown that the reactance slope for the above circuit is zero at zero frequency for

<sup>3</sup> D. B. Sinclair, "The Type 663 Resistor—a Standard for Use at High Frequencies," *Gen. Rad. Exper.*, Vol. 13, pp. 6-11; January, 1939.

<sup>4</sup> R. G. Anthes, "Behavior of Resistors at Radio Frequencies," *Electronic Industries*, Vol. 3, pp. 86-88; September, 1944.

$$\frac{R}{Z_0} = 1.$$

The condition at which the resistance begins to decrease as the frequency is raised is

$$\frac{R}{Z_0} = \sqrt{2}.$$

The corresponding two values from the transmission-line analysis are  $\sqrt{3}$  and  $\sqrt{5}$ . Thus the lumped-circuit analysis gives only an approximate answer.

When resistors of the order of 10,000 ohms or higher are employed, it is not practical to mount them so that the  $Z_0$  of the circuit is near the optimum value of

$$\frac{R}{Z_0} = \sqrt{3}.$$

When such resistors are mounted near a ground plane,  $R/Z_0$  is usually several hundred. When such resistors are mounted well above a ground plane, the connecting leads to the resistor violate the assumption of this analysis.

#### LARGE VALUES OF $l/\lambda$

To study the impedance characteristic for large values of  $l/\lambda$ , it is convenient to consider separately the two terms in our exact equation (7). The first term approaches a limit as  $l/\lambda$  becomes large.

$$\sqrt{1 - j \frac{R}{Z_0} \frac{1}{2\pi(l/\lambda)}} = \left[ 1 - j \left( \frac{R}{Z_0} \right) \frac{1}{4\pi(l/\lambda)} + \dots \right]. \quad (11)$$

This term gives the normalized characteristic impedance of the line, and approaches unity in the limit as  $l/\lambda$  increases. Since the total resistance of the line is held constant, we should expect from physical reasoning that the impedance angle of the characteristic impedance would approach zero as the line length increases.

The second term of (7) does not approach a limit as  $l/\lambda$  increases, but oscillates between values dependent on  $R/Z_0$ . For  $l/\lambda$  large,



$$\tanh \sqrt{-4\pi^2(l/\lambda)^2 + j2\pi \frac{l}{\lambda} \frac{R}{Z_0}} = \frac{\tanh \frac{R}{2Z_0} + j \tan 2\pi \frac{l}{\lambda}}{1 + j \tanh \frac{R}{2Z_0} \tan 2\pi \frac{l}{\lambda}}. \quad (12)$$

As  $l/\lambda$  increases, the real part of this expression oscillates between  $\tanh R/2Z_0$  and the reciprocal,

$$\frac{1}{\tanh \frac{R}{2Z_0}}.$$

The amplitude of the oscillation of the  $j$  part is much smaller, being

$$\frac{1}{2} \left[ \tanh \frac{R}{2Z_0} - \frac{1}{\tanh \frac{R}{2Z_0}} \right].$$

This behavior is in contrast to the common case in which the frequency is held constant and the line length is increased. The total line resistance then increases indefinitely, and the input impedance of the line approaches a limit, which is the characteristic impedance of the line.

Consider the example plotted in Figure 6.

$$\frac{R}{Z_0} = 2 \quad \tanh \frac{R}{2Z_0} = 0.762.$$

The normalized resistance oscillates for large  $l/\lambda$  between 0.76 and 1.31 while the reactance oscillates between  $\pm 0.28$ . These values are obtained by substituting in the above expressions. The plot in Figure 6 shows how the oscillation approaches a finite limit for its amplitude.

The oscillations of the plot of Figure 10 are negligible since  $R/Z_0 = 10$  and  $\tanh R/2Z_0 = 0.9999$ .

#### DISCUSSION OF $l/\lambda = 1/4$

For small value of  $R/Z_0$ , the resistance maximizes nearly  $l/\lambda = 1/4$ . The value of this maximum resistance is approximately

$$\left( \frac{R}{Z_0} \right)_{\max} = \frac{2Z_0}{R}.$$

In Figure 2,  $R/Z_0 = 0.5$  and the first maximum is approximately 4, as the plot shows. This situation has been discussed by Terman.<sup>5</sup>

---

<sup>5</sup> F. E. Terman, "Resonant Lines in Radio Circuits," *Elec. Eng.*, Vol. 53, pp. 1046-1053; July, 1934.

# COMPARATOR FOR COAXIAL LINE ADJUSTMENTS\*†

BY

O. M. WOODWARD, JR.

Research Department, RCA Laboratories Division,  
Princeton, N. J.

*Summary*—High-frequency line impedance measurements in laboratory or field can be simplified by this compact comparison instrument that essentially replaces the slotted coaxial line and sliding-probe voltmeter technique for checking match or determining standing-wave ratio and reactive component. The paper discusses the use of the device in the measurement of standing-wave ratios, use of fixed loop for matching, and the absolute magnitude of load impedance and the resistive component of load impedance. An example of one application is included.

IN MATCHING a load with several adjustable elements, such as an antenna array, to coaxial transmission lines the process may prove to be tedious using the conventional slotted line and probe indicator. At low frequencies such lines become long and inconvenient to construct.

The simple instrument illustrated in Figure 1 is a comparator consisting of a coaxial T-junction with a current pickup loop symmetrically placed to couple magnetically to the center of the junction. The T-junction joins the generator, the load whose characteristics are to be obtained, and a line terminated with a resistance or reactance equal to its characteristic impedance.

Electrostatic shielding between the coaxial lines and the loop is provided by a number of slots cut in each of the three lines near the center of the junction. The loop may be rotated in the plane of the junction to assume the various positions shown in Figure 2. The output of the loop is fed to an indicator such as a linear receiver. Assembled and exploded views of the completed comparator are shown in Figures 3 and 4.

## STANDING-WAVE RATIO

Referring to Figure 5 the three lines have a common voltage  $\bar{E}$  at the center of the T-junction. Hence the impedance of the load line at the junction  $L$  is

---

\* Decimal Classification: R244.3.

† Reprinted from *Electronics*, April, 1947.

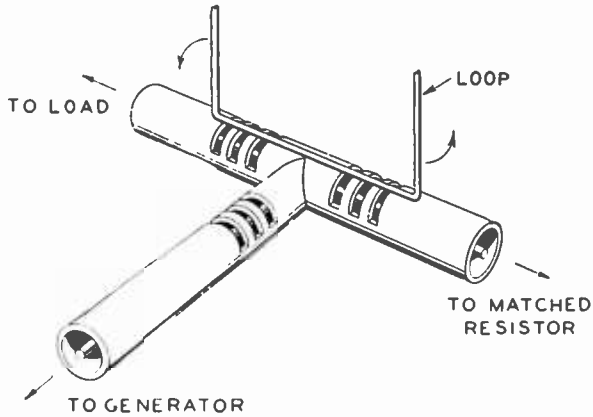


Fig. 1—Simplified drawing of T-junction, showing connections and the pickup loop that can be rotated to couple to them.

$$\bar{Z}_L = \bar{E}/I_L \tag{1}$$

Since the opposite line is matched,

$$Z_c = \bar{E}/I_c \tag{2}$$

and

$$I_L = I_c (Z_c/\bar{Z}_L) \tag{3}$$

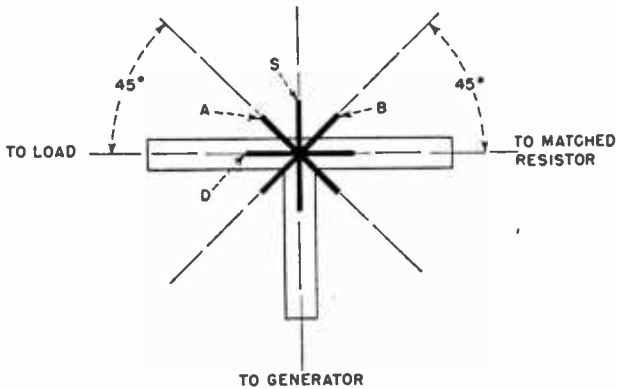


Fig. 2—Detail of the pickup loop positions with relation to the junctions, and the notation used in designating position.

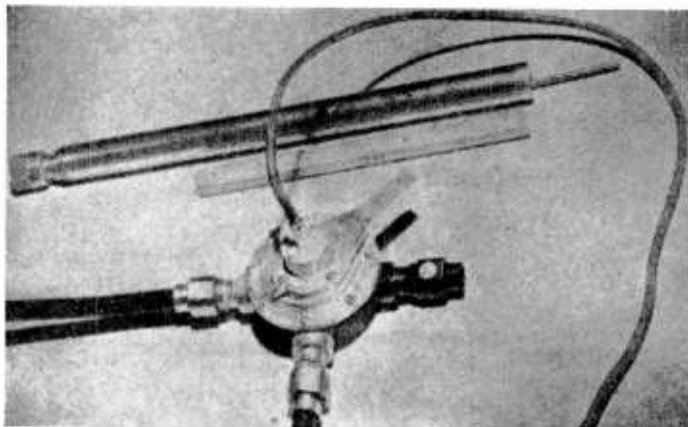


Fig. 3—The shorted one-eighth wave coaxial line at the top replaces the matched resistor when determining the algebraic value of the load reactance.

The impedance at a voltage minimum is a pure resistance equal to the product of the standing-wave ratio  $P$  and the characteristic impedance  $Z_c$  of the line, where  $P$  is taken to be the ratio of the minimum voltage to the maximum voltage.

By means of the usual impedance transfer equation the impedance may be determined in terms of the resistance at a voltage minimum  $X$  located a distance of  $\rho$  electrical degrees on the load line.

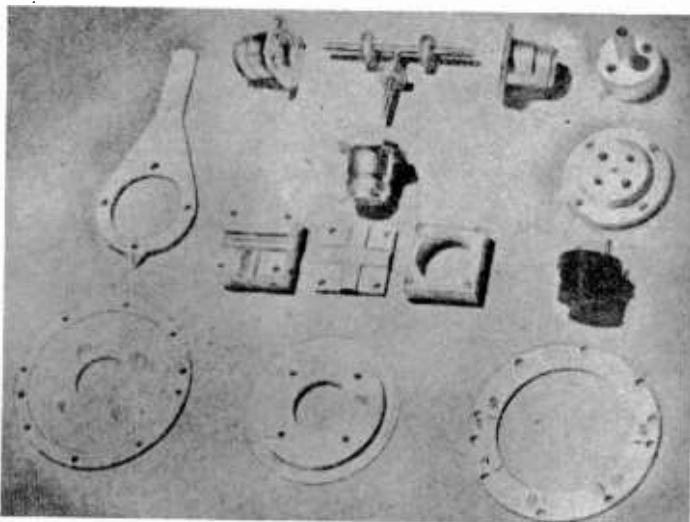


Fig. 4—Exploded view. Slotted openings in the T-junction cover provide electro-static shielding between the junction (upper center) and the rotating loop at right.

$$\bar{Z}_L = \frac{P Z_c + j Z_c \tan \rho}{Z_c + j P Z_c \tan \rho} Z_c \quad (4)$$

Combining Equations 3 and 4

$$I_L = I_C \left( \frac{1 + j P \tan \rho}{P + j \tan \rho} \right) \quad (5)$$

With the loop in position D (Figure 2) parallel to the load and matched lines, a voltage will be induced in the loop producing a current  $I_D$ , proportional to the vector difference of the load and matched line currents.

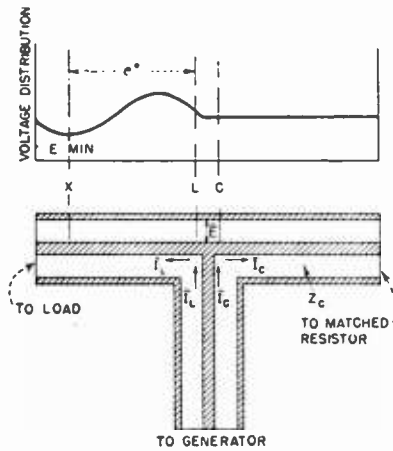


Fig. 5—Graphical representation of the standing wave formed on one arm of the T-junction when the load is not matched.

$$\begin{aligned} I_D &= T (I_L - I_C) = (T I_C) \left( \frac{1 + j P \tan \rho}{P + j \tan \rho} - 1 \right) \\ &= (T I_C) \frac{(1 - P) (1 - j \tan \rho)}{(P + j \tan \rho)} \quad (6) \end{aligned}$$

where  $T$  is a proportionality constant depending upon the frequency, physical dimensions of the comparator components, and the input impedance of the receiver.

After rectification in the receiver the output current  $I_D$  will be proportional to the absolute magnitude of Equation 6, or

$$I'_D = T'|I_c| \left( \frac{1 + \tan^2 \rho}{P^2 + \tan^2 \rho} \right)^{\frac{1}{2}} (1 - P) \tag{7}$$

where the proportionality constant  $T'$  also includes the receiver gain factor. Similarly, with the loop in position S parallel to the generator line a voltage will be induced in the loop producing a current  $I'_S$  proportional to the vector sum of the load and matched line currents.

$$I'_S = T(I_L + I_c) = (TI_c) \frac{(1 + P)(1 + j \tan \rho)}{(P + j \tan \rho)} \tag{8}$$

The receiver output current will then be

$$I'_S = T'|I_c| \left( \frac{1 + \tan^2 \rho}{P^2 + \tan^2 \rho} \right)^{\frac{1}{2}} (1 + P) \tag{9}$$

$$\frac{I'_D}{I'_S} = \frac{1 - P}{1 + P} = K \tag{10}$$

The ratio of the receiver output currents for the two coil positions is equal to the magnitude of the reflection coefficient  $K$  on the load line.

In practice, the loop is placed in position S and the receiver gain or generator power adjusted to produce full-scale reading on the receiver output meter. The loop is then rotated to position D and the reflection coefficient is directly indicated on the meter as the percentage of full-scale reading. Equation 10 shows that the reflection coefficient reading obtained is independent of the relative position of the standing wave with respect to the comparator. If the receiver is not linear, suitable correction of the meter calibration must be made.

This relationship also may be shown in another manner. The loop currents for the two positions D and S are

$$I_D = T(I_L - I_c) = \frac{T\bar{E}}{Z_L} \left( 1 - \frac{\bar{Z}_L}{Z_c} \right) \tag{11}$$

and

$$I_S = T(I_L + I_c) = \frac{T\bar{E}}{Z_L} \left( 1 + \frac{\bar{Z}_L}{Z_c} \right) \tag{12}$$

The well-known transmission line equation expressing the current at

a point down the line in terms of the load characteristics and line constants is

$$I_p = \underbrace{\frac{I_L}{2} \left[ 1 - \frac{\bar{Z}_L}{Z_c} \right]}_{\text{Reflected wave}} \epsilon^{\gamma P} + \underbrace{\frac{I_L}{2} \left[ 1 + \frac{\bar{Z}_L}{Z_c} \right]}_{\text{Main wave}} \epsilon^{-P\gamma} \quad (13)$$

Hence the ratio of the receiver output currents for the two loop positions D and S is seen to be the ratio of the reflected wave to the main wave, or the coefficient of reflection.

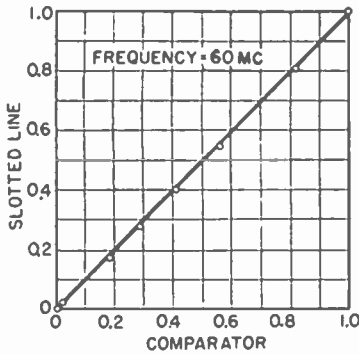


Fig. 6—Standing-wave ratios obtained with a slotted line inserted between adjustable load and comparator at 60 megacycles.

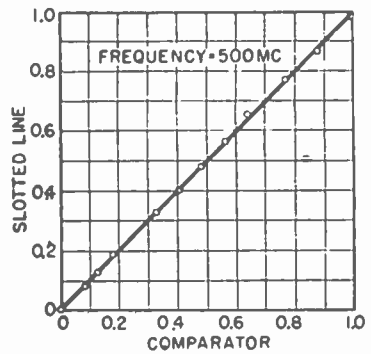


Fig. 7—Good agreement is found at 500 megacycles between slotted-line and comparator measurements of standing-wave ratios.

$$\frac{I_D}{I_S} = \left| \frac{\left( 1 - \frac{\bar{Z}_L}{Z_c} \right)}{\left( 1 + \frac{\bar{Z}_L}{Z_c} \right)} \right| \quad (14)$$

Assuming that a matched line may be provided, correct operation is independent of frequency up to the range where the loop couples to an appreciable fraction of a wavelength on the lines. In this region the loop current will not be a function of the currents flowing in the lines at the immediate T-junction only.

To obtain an experimental check on the accuracy of operation, a slotted measuring line was inserted between an adjustable load and the comparator. Standing-wave ratio readings obtained from the two instruments for various loads and frequencies are comparable as shown in Figures 6 and 7.



## FIXED LOOP FOR MATCHING

For certain applications, such as final matching adjustments of antennas in the field, the comparator may be simplified by fixing the loop in position D. In use, the load matching elements are adjusted in rotation for a null on the receiver output meter. Referring to Equation 7 it is seen that a null is obtained only when P is unity.

A comparator of this type covering the frequency range of 400 megacycles to 1,700 megacycles, in which the receiver is replaced by a fixed crystal and microammeter for simplicity, is shown in Figure 8. The loop consists of an adjustable quarter-wave tuning stub to which is coupled the fixed crystal. The matched load is a selected resistor equal to the characteristic impedance of the lines used. The exploded view (Figure 9) shows the construction of the electrostatic screen and

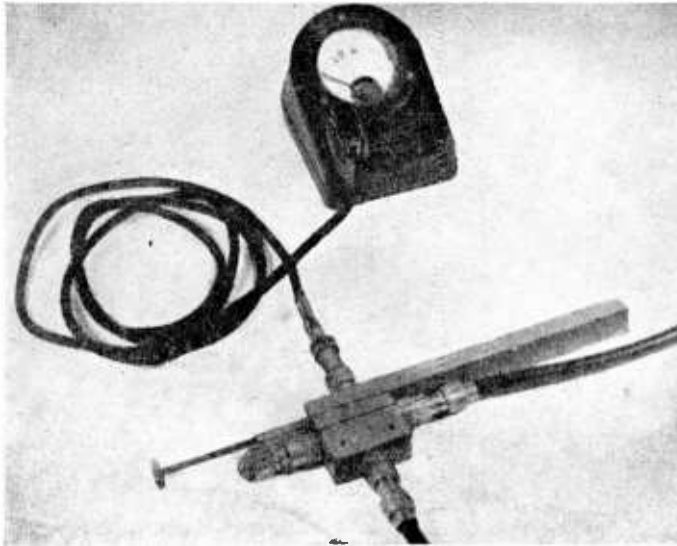


Fig. 8—A comparator designed for use in the frequency range 400 to 1,700 megacycles, using a self-contained fixed crystal detector and microammeter.

other component parts. Although simpler in construction, this modification of the comparator does not indicate the degree of mismatch.

For a given standing wave on the load line the load current and hence the loop current will be a function of the relative position of the standing wave with respect to the T-junction. If the line between the load and the comparator is of such a length as to give a voltage minimum at the T-junction ( $\rho = 0$ ) the loop current from Equation 7 is seen to be proportional to  $(1-P)/P$ . For the same load a change in line length of one-quarter wavelength will result in a voltage maximum

appearing at the T-junction ( $\rho = 90$ ), and the loop current will be proportional to  $(1-P)$ .

The ratio of the minimum loop current to the maximum loop current for a given load and a variable shift of the standing-wave along the load line is seen to be equal to the standing-wave ratio.

$$\frac{I_p \text{ min.}}{I_p \text{ max.}} = \frac{(1-P)}{(1-P)/P} = P \quad (15)$$

Thus, as a match is approached on the load line by adjustment of the matching elements, the possible meter deflection diminishes rapidly.

Using a square-law crystal detector the relative meter deflection as a function of the standing-wave ratio and its position on the load line

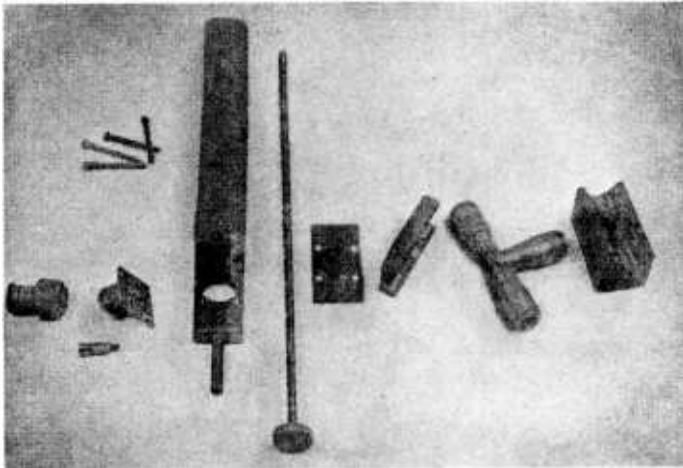


Fig. 9—Exploded view of the uhf comparator.

is plotted in Figure 10. The shaded area indicates the possible deflection change for any shift of the standing wave along the line. A constant T-junction voltage  $E$  is assumed for these calculations.

#### ABSOLUTE MAGNITUDE OF LOAD IMPEDANCE

Other load characteristics may be obtained from the comparator with the rotating loop. The absolute magnitude of the load impedance  $|Z_L|$  at the T-junction is found by taking the ratio of the linear receiver output readings for two additional loop positions. From Figure 2 it is seen that with the loop in position B the loop current is

$$I_B = T \left( \frac{I_c}{\sqrt{2}} + \frac{I_c}{\sqrt{2}} \right) = \sqrt{2} T I_c \tag{16}$$

since the loop is at an angle of 45 degrees and couples equally with both of the T lines. Components of the load current in the loop are equal and opposite in this case. Similarly, with the loop rotated 90 degrees to position A, the current is

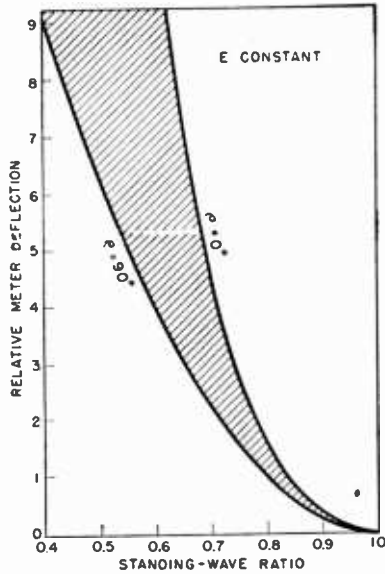


Fig. 10—Relative meter deflection shown as a function of standing-wave ratio and its position on the load arm and of the T-junction.

$$I_A = T \left( \frac{I_L}{\sqrt{2}} + \frac{I_L}{\sqrt{2}} \right) = \sqrt{2} T I_L \tag{17}$$

Forming the ratio and combining with Equation 3,

$$\frac{I_B}{I_A} = \frac{|Z_L|}{Z_c} \tag{18}$$

where  $|Z_L|$  is expressed in terms of the characteristic impedance of the lines. In practice the receiver output meter is set to full scale at the loop position giving the larger reading. The loop is then rotated 90 degrees to the other position and the ratio of  $|Z_L|/Z_c$ , or  $Z_c/|Z_L|$  as the

case may be, is read directly on the meter as the percentage of full scale deflection.

#### RESISTIVE COMPONENT OF LOAD IMPEDANCE

Having obtained the reflection coefficient  $K$  and the absolute magnitude of the load impedance  $|Z_L|$  from the four loop positions, the resistive component  $R_L$  of the load impedance may be found. From Equation 4

$$\frac{Z_L}{Z_c} = \frac{P + j \tan \rho}{1 + j P \tan \rho} = \frac{R_L + j X_L}{Z_c} \quad (19)$$

Equating the real terms and imaginary terms respectively

$$R_L - X_L P \tan \rho = Z_c P \quad (20)$$

and

$$R_L P \tan \rho + X_L = Z_c \tan \rho \quad (21)$$

Eliminating  $\tan \rho$  and solving for  $R_L/Z_c$

$$\frac{R_L}{Z_c} = \left( \frac{P}{P^2 + 1} \right) \left[ \left( \frac{|Z_L|}{Z_c} \right)^2 + 1 \right] \quad (22)$$

since  $P = (1 - K)/(1 + K)$

$$\frac{R_L}{Z_c} = \frac{(1 - K^2)}{2(1 + K^2)} \left[ \left( \frac{|Z_L|}{Z_c} \right)^2 + 1 \right] \quad (23)$$

Although the arithmetic value of the reactive component  $X_L$  may be derived knowing  $R_L$  and  $|Z_L|$ , the algebraic sign of  $X_L$  is not found since the same loop reading of  $\rho$  and  $|Z_L|$  will be obtained whether the reactive component is positive or negative. Also for some values of the load impedance having a small phase angle, low accuracy is obtained in determining the arithmetic value of  $X_L$ .

To obtain the algebraic value of the reactance, the matched resistor (Figure 5) is replaced with a shorted coaxial line one-eighth wavelength long having the same characteristic impedance  $Z_c$  as the T-junction lines. Since the reactance of the eighth-wave shorted stub is  $+jZ_c$ ,

$$I_c = \bar{E}/ + jZ_c \quad (24)$$

Hence  $I_c = I_L \left( \frac{X_L}{Z_c} - j \frac{R_L}{Z_c} \right)$  (25)

With the loop in position D,

$$I_D = T(I_L - I_c) = TI_L \left( 1 - \frac{X_L}{Z_c} + j \frac{R_L}{Z_c} \right)$$
 (26)

Likewise, with the loop in position S,

$$I_S = T(I_L + I_c) = TI_L \left( 1 + \frac{X_L}{Z_c} - j \frac{R_L}{Z_c} \right)$$
 (27)

Designating the ratio of the receiver output currents in this case by  $K'$

$$K' = \frac{I'_D}{I'_S} = \left[ \left( 1 - \frac{2X_L}{Z_c} + \frac{|Z_L|^2}{Z_c^2} \right) / \left( 1 + \frac{2X_L}{Z_c} + \frac{|Z_L|^2}{Z_c^2} \right) \right]^{1/2}$$
 (28)

Solving for  $X_L/Z_c$ ,

$$\frac{X_L}{Z_c} = \frac{(1 - K'^2)}{2(1 + K'^2)} \left[ \left( \frac{|Z_L|}{Z_c} \right)^2 + 1 \right]$$
 (29)

The ratio of the receiver currents for the loop positions B and A will be the same whether the stub or the matched resistor is used. It is seen that the equations for the resistive component and the reactive components are identical in form. The adjustable stub may be calibrated in terms of frequency for convenience in use.

Since the reactance of a shorted line  $\theta$  electrical degrees in length is given by

$$X = j Z_c \tan \theta$$
 (30)

it is seen that the stub may be somewhat shorter than an eighth-wave in length if its characteristic impedance is raised, the only requirement being that its reactance be equal to the characteristic impedance of the load line.

For a particular frequency of operation the stub length to give the required reactance may be found quite easily without the use of the slotted measuring line equipment. The load line is replaced by the stub, and the matched resistor connected to the opposite side of the comparator. Since it was shown in Equation 18 that the absolute

magnitude of the load impedance in terms of the characteristic impedance was equal to the ratio of the loop currents for loop positions B and A, the stub is simply adjusted until this ratio is unity.

A chart is given in Figure 11 from which the resistive and reactive components of the load impedance may be obtained from the various loop positions of the comparator.

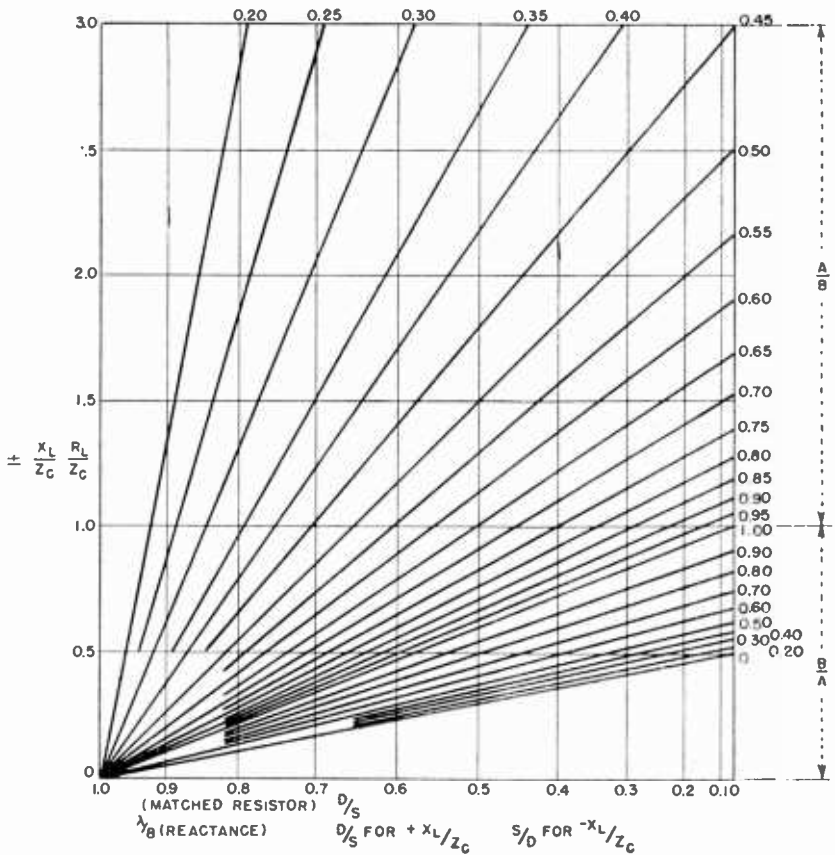


Fig. 11—Chart showing resistive and reactive components of the load impedance as obtained from various loop positions and detector voltage readings.

EXAMPLE

As an example of its use, an unknown load and the matched resistor are connected as shown in Figure 2. The loop is rotated in the four positions to give the current ratios of  $D/S$  and  $A/B$  (or  $B/A$ ). For a  $D/S$  ratio of 0.46 and a  $A/B$  ratio of 0.65 the resistive component of the load impedance in terms of the characteristic impedance is found

to be 1.10. The matched resistor is then replaced by the eighth-wave stub and the current ratio D/S (or S/D) determined. Using the same A/B value of 0.65 previously found, it is seen that the reactive component of the load impedance in terms of the characteristic impedance is equal to  $-0.75$  for a S/D ratio of 0.62. For a characteristic impedance equal to 52 ohms the load impedance is then equal to

$$(1.10 - j 0.75) (52) = 57.2 \text{ ohms} - j 39 \text{ ohms} \quad (31)$$

An adjustable impedance was measured with the comparator and the slotted line apparatus at a frequency of 200 megacycles to provide an experimental check of the accuracy of the comparator. The results are tabulated below.

Comparator	Slotted line
18.3 + j 6.5	18.2 + j 6.5
44.7 — j 70.4	44.8 — j 67.2
36.2 — j 20.3	38.4 — j 19.3
58.3 — j 100.0	56.8 — j 101.0

ACKNOWLEDGMENT

The author wishes to acknowledge the useful suggestions and valuable contribution by G. H. Brown in the development of the comparator.

# PHASE-FRONT PLOTTER FOR CENTIMETER WAVES\*†

By

HARLEY IAMS

Research Department, RCA Laboratories Division,  
Princeton, N. J.

*Summary*—In the centimeter-wave range it is not unusual to have an antenna, dish, or horn across which the phase of the radiation should be constant, or should vary in some predetermined manner. To test such behavior a machine was evolved which is capable of recording on a sheet of paper lines showing the regions in space which have the same phase.

This plotter can be used to test centimeter-wave antennas, to demonstrate principles of physical optics, or to measure the refractive index of dielectrics. The recordings are equivalent to pictures of radio waves.

**D**IRECTIONAL patterns of antennas are determined by both the amplitude and phase of the radiated energy. The need for improved methods of measuring relative phase across apertures many wavelengths wide arose in connection with the testing of rapid-scanning antennas for centimeter waves. A machine was developed to record on a sheet of paper lines showing the regions in space having the same phase. This device has proved useful for many purposes in addition to the one for which it was originally built.

One of the uses of the phase-front plotter is the making of pictures of radio waves as they pass through space. These pictures can be used by an antenna designer to determine the electrical center of a horn, to observe the relative phase at different parts of a structure, and to study the operation of a new antenna. Workers in the field of propagation can observe refraction, diffraction and reflection of radio-frequency energy. Another use is the measurement of the refractive index of dielectrics at radio frequencies; this does not require the preparation of special specimens nor involved computation.

## OPERATION

The principle of operation of the plotter may be explained with the aid of Figure 1, which is a photograph of one form of the device. A centimeter-wave transmitter (not shown) keyed at audio frequency

---

\* Decimal Classification: R246.

† Reprinted from *RCA REVIEW*, June, 1947.



supplies power to the horn *H*, which is being tested. The small movable probe *A* picks up some of the radiated energy, which is transferred by means of wave guides and rotary joints to the crystal detector *D*. Some of the transmitter power is also conveyed directly to the detector through a wave guide and an attenuator *R* (which is used to control the amplitude of this reference signal). The signals which reach the detector over the two routes may or may not be in the same phase, depending upon the position in which the probe is placed. The detector output is a maximum when the phase is the same, and a minimum when it differs by 180 degrees. This output is carried by cable *E* to an amplifier, the output of which is connected to stylus *S* placed directly below the probe. A sheet of current-sensitive paper on which the stylus rests is darkened in proportion to the detector output.

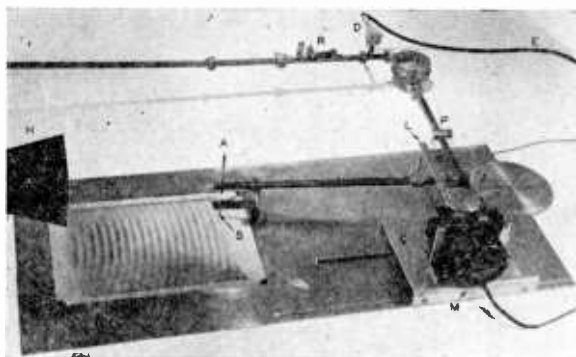


Fig. 1—Automatic plotter.

A motor *M* causes the probe to scan the area in front of the horn; through link *L* the waveguide is rocked back and forth, and it is moved in a second direction by the motion of carriage *C*.

In a few minutes a complete record is made, showing which parts of the scanned area have the same phase. The degree of darkening is an indication of the amplitude. Such a record may be said to be a picture of the radio waves; a photograph of ripples on a pond is also a record of the regions which vibrate in the same phase. By means of "line stretcher" *P* (in Figure 1) a line of maximum darkening of the paper can be made to pass through any desired point; this corresponds to the selection of the time at which water waves are photographed.

Wavelengths in the neighborhood of one centimeter are particularly suitable for phase-front plotting, since they are short enough to include a number of wavelengths in even a small scanned area and

long enough that the construction of models of typical antennas is not difficult. The use of  $1\frac{1}{4}$ -centimeter wavelength in the plotter of Figure 1 led to the selection of a combination of rigid wave guides and rotary joints to transfer the radio-frequency energy to the detector. At this wavelength there is, as far as it is known, no suitable transmission line or flexible wave guide which does not change its electrical length when flexed. Fortunately, the rotary joints which were tested proved very satisfactory in this respect.

When numerical data are to be taken, as is sometimes necessary in testing an antenna, the position of the phase fronts can be determined most accurately by moving the probe by hand, following lines along which the detector output is a minimum. To record the posi-

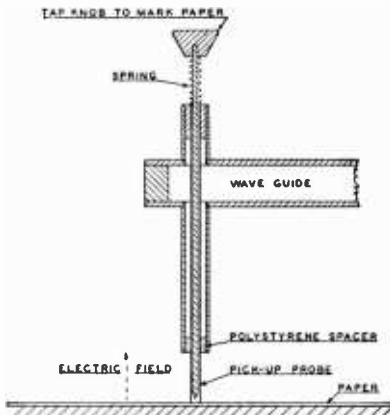


Fig. 2—Self-plotting probe.

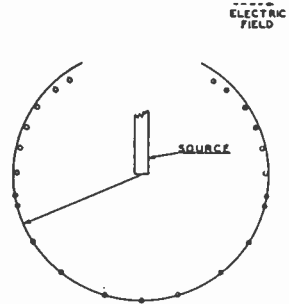


Fig. 3—Phase front near the open end of a waveguide.

tions, a self-plotting probe such as the one shown in Figure 2 is very convenient. When care is taken, it is possible to repeat readings to within  $\pm 0.010$  inch, which is  $\pm 1/50$  of a wavelength at the frequency used. A sample of such a plot is given in Figure 3.

When records are to be made at longer wavelengths than those mentioned it may be desirable to reduce the scale at which the plotting is done. This can be done by moving the stylus or plotting device by means of a pantograph attached to the probe, or by using a facsimile recorder synchronized with the motion of the probe.

#### APPLICATIONS

An example of the testing of a "pillbox" antenna is given in

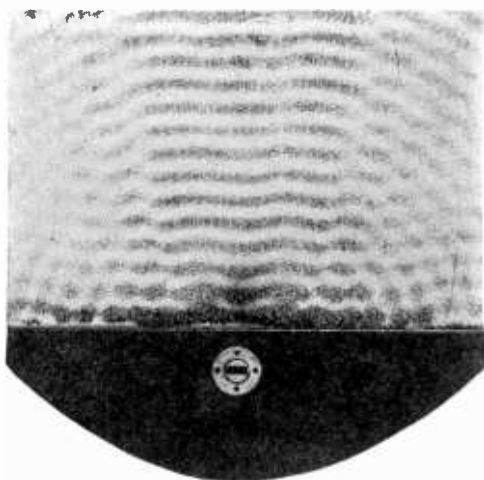


Fig. 4—Phase fronts from a “pillbox.”

Figures 4 and 5. Such an antenna focuses the radiation from a wave guide by reflecting it from a parabolic surface; the emerging waves should be straight. As Figure 4 shows, one such “pillbox” did produce nearly straight phase fronts—and some curved ones, as well. An examination of the curved waves shows that they are centered in the area masked by the wave guide. They are the result of the masking; one explanation is that the interrupted part of the wave could also have been produced by energy from another transmitter, equal in

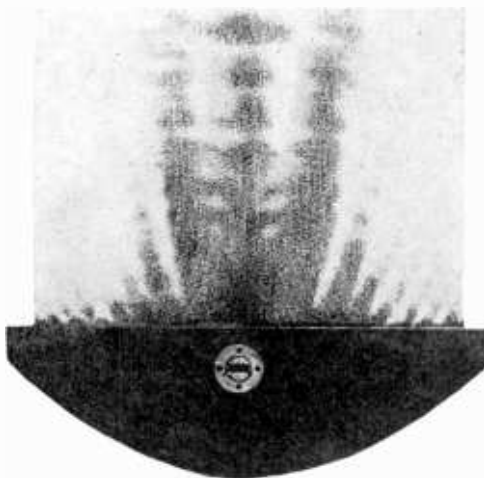


Fig. 5—Intensity pattern near a “pillbox.”

amplitude and opposite in phase to the energy supplied in this region by the reflector. Figure 5 is an intensity pattern from the same "pill-box" recorded by cutting off the reference signal. It shows how the interference between the straight and curved phase fronts acts to produce side lobes. Because the recording was made near the antenna the lobes have not assumed their final angular positions.

The phase fronts can be recorded in a series of layers when it is desired to obtain information in three dimensions. Also, the plane

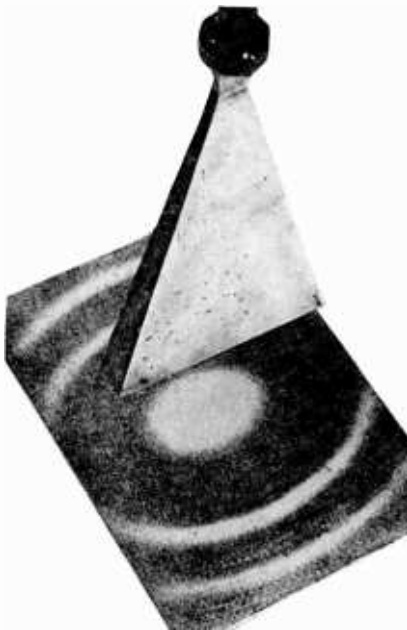


Fig. 6—Phase fronts at right angles to horn axis.

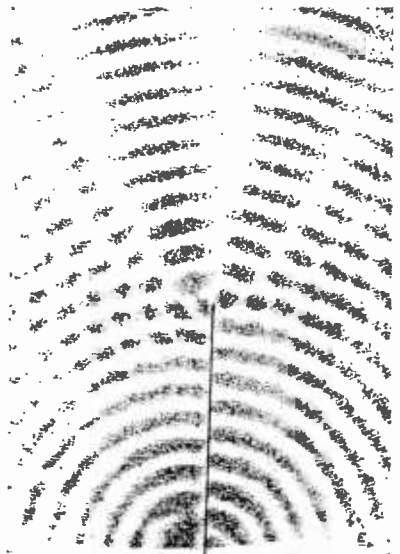


Fig. 7—Waves from a long-wire antenna.

which is scanned may be at right angles to the direction of propagation, as it was in Figure 6. A plot of this kind is, to a first approximation, a contour map of the lens which would be required to focus the radiation into a parallel beam.

Models of antennas usually used at longer wavelengths can also be tested. Figure 7 shows the recording which was made by scanning in a plane just grazing a single wire antenna about ten wavelengths long.

Problems in physical optics can be investigated in similar fashion. Figure 8 shows how radiation was focused by a pair of polystyrene lenses. While these lenses were not designed to give perfect focus,

the recording is illustrative of the limit to attainable spot size which is set up by the wavelength and angle of convergence of the radiation.

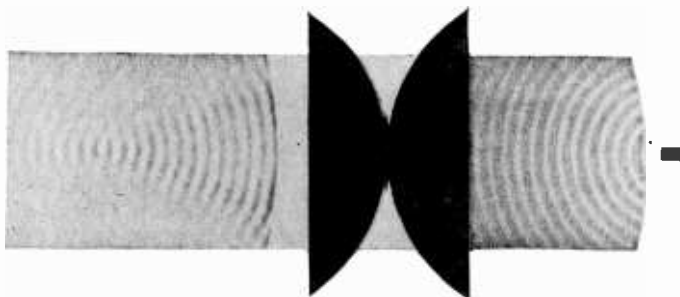


Fig. 8—Waves focused with lenses.

The refractive index of a dielectric (which is the square root of its dielectric constant) can be measured very easily. A sheet of the material is placed between the source and the probe, and the resulting displacement of a phase front is measured. The refractive index is  $1 + S/T$ , where  $S$  is the added phase delay and  $T$  is the thickness of the sample. When care is used in making the adjustments, it is possible to observe even the small phase shift resulting from interposing a sheet of paper, or blowing one's humid breath into one of the wave-guides.

#### ACKNOWLEDGMENTS

In conclusion, the writer wishes to express his appreciation for information and stimulation received from members of the staff of Radiation Laboratory; their pioneer work on the measurement of relative phase of radio waves at different points in space has not yet been published. Reference should also be made to work done at Ohio State University,<sup>1</sup> which takes a somewhat different approach to the problem. In connection with the wave-guide structure, plotting methods, two-dimensional scanning and automatic recording, valuable suggestions have been received from a number of RCA Laboratories staff members.

<sup>1</sup> *Engineering Experiment Station News*, Ohio State University, Vol. XVIII, No. 5, December, 1946.

# CIRCULARLY-POLARIZED OMNIDIRECTIONAL ANTENNA\*†

By

GEORGE H. BROWN AND O. M. WOODWARD, JR.

Research Department, RCA Laboratories Division,  
Princeton, N. J.

*Summary*—This paper describes a circularly-polarized antenna which has been developed specifically for ground station use in airport-to-airplane communication. After briefly considering the necessary field conditions in space to bring about circular polarization, a combination of a vertical dipole and a horizontal loop antenna is treated theoretically. An equivalent arrangement using four dipoles is also studied and a number of factors influencing the performance are displayed.

The theoretical treatment is followed by a description of an antenna which was constructed according to the principles outlined. Test results show that the antenna produced a substantially circularly-polarized wave over a rather wide frequency range without readjustment.

## INTRODUCTION

EXPERIENCE in airport-to-airplane communication has indicated a need for more reliable communication, free from random polarization changes caused by banking of the aircraft and from amplitude variations due to ground reflections. It has been suggested that a circularly-polarized antenna at the ground station would help to stabilize signal transmission, and permit maximum freedom of choice of antenna location on the aircraft.

The antenna described in this paper is the result of an extensive investigation which included experiments with slotted cylinder radiators, dipole and loop combinations, and spiral radiators.

## THEORETICAL CONSIDERATIONS

### (a) A Circularly-Polarized Wave

A circularly-polarized wave may quite properly be considered as made up of a vertically-polarized wave imposed on a horizontally-polarized wave with both waves traveling in the same direction. At any chosen point, the fields of the two waves are in time quadrature with one another.

The electric field intensity of the vertically-polarized wave is represented by the expression  $e_v = A \cdot \sin \omega t$  (1)

This field intensity component is vertical.

\* Decimal Classification: R320.

† Reprinted from *RCA REVIEW*, June, 1947.

The electric field intensity of the horizontally-polarized wave has the same peak value, but differs in phase by 90 degrees. This component, which is horizontal, is given by  $e_H = A \cdot \cos \omega t$  (2)

At any given instant of time, the resultant field intensity vector has a magnitude equal to  $\sqrt{e_V^2 + e_H^2} = A$ , and this vector makes an angle

$$\alpha \text{ with the horizontal where } \tan \alpha = \frac{e_V}{e_H} = \tan \omega t \quad (3)$$

The field intensity vector is seen to be constant in magnitude and rotates in the plane of the wave at synchronous speed.

When the observer looks in the direction of travel of the wave and sees the vector rotating clockwise, the wave is said to be right-hand circularly polarized. When the vector rotates counterclockwise, the wave is left-hand circularly polarized.<sup>1</sup>

#### (b) *The Combination of a Vertical Dipole and a Horizontal Loop*

A horizontal loop antenna, with a vertical half-wave dipole piercing the center of the loop, may be used to produce a circularly-polarized wave.

At a remote point in the horizontal plane, the vertical half-wave dipole produces a vertical electric field given by

$$E_V = \frac{j60I_V}{r} \epsilon^{-jkr} \quad (4)$$

The horizontal loop produces a horizontal electric field at the same point.

$$E_H = \frac{-60\pi kR \cdot J_1(kR)}{r} I_H \epsilon^{-jkr} \quad (5)$$

where  $I_V$  = the current at the center of the dipole,

$I_H$  = the current in the loop,

$\lambda$  = the wavelength,  $k = 2\pi/\lambda$ ,

$r$  = the distance from the antenna to the remote point,

<sup>1</sup> Standards on Radio Wave Propagation, (Definition of Terms—p. 2), Institute of Radio Engineers, New York, N. Y., 1942.

$R$  = the radius of the loop,

$J_1(kR)$  = the Bessel function of the first kind and first order.

It may be seen from equations (4) and (5) that the vertical and horizontal fields are in phase quadrature, when the currents in the loop and the dipole are in phase.

To make the two field components be equal to achieve circular polarization, the following relation must be satisfied:

$$I_V/I_H = \pi kR \cdot J_1(kR) \tag{6}$$

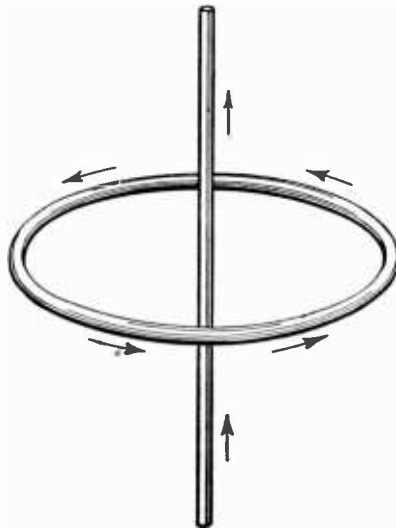


Fig. 1—Current flow relationships in a horizontal loop and a vertical dipole which radiate a right-hand circularly-polarized wave.

Typical values of this ratio, as a function of the radius of the loop, are given below:

$R/\lambda$	$I_V/I_H$
0.05	0.152
0.10	0.587
0.15	1.25
0.20	2.02
0.25	2.8

When the currents in the loop and dipole flow as shown in Figure 1, the resultant wave is right-hand circularly polarized.



While this combination of a loop and a dipole appears to be a simple arrangement, one soon finds that the necessary plumbing to achieve the proper current division while maintaining the currents in phase is quite elaborate and the adjustments are critical. This is particularly true when a wide band of frequencies is used.

(c) *An Equivalent Arrangement*

An arrangement which produces the same result but which is not difficult to attain has been proposed by Lindenblad.<sup>2, 3</sup> His plan may be described best in two steps. First, several vertical dipoles are disposed uniformly about the periphery of a circle which lies in the

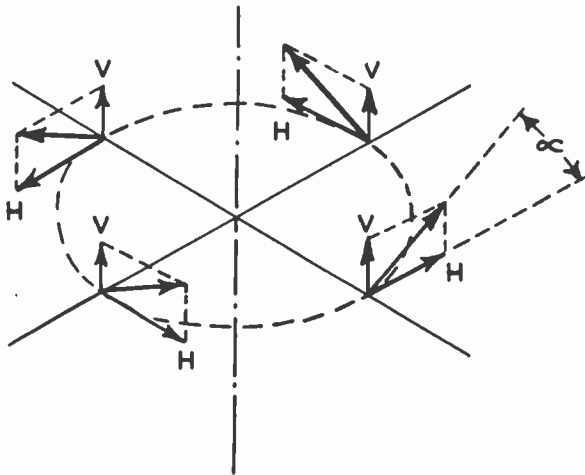


Fig. 2—The effective-current components in the slanted-dipole antenna arrangement.

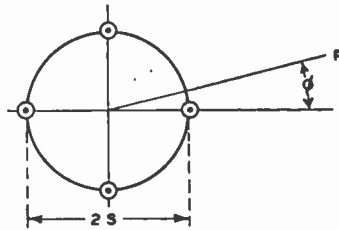
horizontal plane. Then each dipole is rotated about its center point, with the rotation taking place in a vertical plane which is tangent to the imaginary circle. Each dipole is rotated in the same angular direction. Figure 2 may help to clarify the description. Here four dipoles are used and the heavy arrows represent the direction of current flow in the dipoles. The vertical components of these currents are shown, all pointing upward and acting somewhat as a single vertical radiator. The horizontal components may be seen to flow just as the currents in a continuous loop antenna flow.

<sup>2</sup> N. E. Lindenblad, "Antennas and Transmission Lines at the Empire State Television Station", *Communications*, Vol. 21, No. 4, pp. 13-14, April, 1941.

<sup>3</sup> N. E. Lindenblad, U. S. Patent 2,217,911.

Figure 3 shows the plan view with the vertical current components all in phase, and the lower part of the same diagram shows the plan view for the horizontal current components.

PLAN VIEW-VERTICAL POLARIZATION



PLAN VIEW-HORIZONTAL POLARIZATION

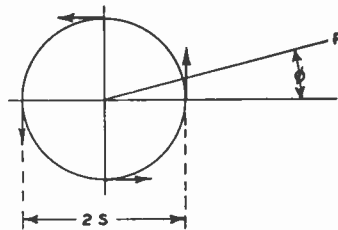


Fig. 3—Plan views showing the relative disposition of the vertical and horizontal components of antenna current.

Using the four radiators shown in Figures 2 and 3, we may write the expressions for the vertical and horizontal components of electric field at a remote point  $P$  thus:

$$E_V = j \frac{120 I \epsilon^{-jkr}}{r} \cdot \sin \alpha \cos \theta \left[ \cos (kS \cos \phi \cos \theta) + \cos (kS \sin \phi \cos \theta) \right] \quad (7)$$

$$\text{and } E_H = \frac{-120 I \epsilon^{-jkr}}{r} \cdot \cos \alpha \left[ \cos \phi \sin (kS \cos \phi \cos \theta) + \sin \phi \sin (kS \sin \phi \cos \theta) \right] \quad (8)$$

where  $S$  = the radius of the circle on which the antennas are located  
 $\alpha$  = the angle between each radiator and the horizontal plane

$\phi$  = the angle that locates the point  $P$  in the horizontal plane

$\theta$  = the angle which locates the point  $P$  in the vertical plane.  
(When this angle is zero, the point lies in the horizontal plane.)

$I$  = the current in each radiator.

The symbols  $k$  and  $r$  have been defined earlier in this paper.

Digressing for a moment, the case is considered where the dimension  $S$  is very small compared to a wavelength. Then the following approximations may be used:

$$\cos (kS \cdot \cos \phi \cos \theta) \doteq 1$$

$$\cos (kS \cdot \sin \phi \cos \theta) \doteq 1$$

$$\sin (kS \cdot \cos \phi \cos \theta) \doteq kS \cdot \cos \phi \cos \theta$$

$$\sin (kS \cdot \sin \phi \cos \theta) \doteq kS \cdot \sin \phi \cos \theta$$

and (7) becomes 
$$E_V = j \frac{120 I \epsilon^{-jkr}}{r} \cdot 2 \sin \alpha \cos \theta \quad (9)$$

while (8) takes the form

$$\begin{aligned} E_H &= \frac{-120 I \epsilon^{-jkr}}{r} \cdot \cos \alpha [kS \cos^2 \phi \cos \theta + kS \sin^2 \phi \cos \theta] \\ &= \frac{-120 I \epsilon^{-jkr}}{r} \cdot kS \cos \alpha \cos \theta \end{aligned} \quad (10)$$

Equations (9) and (10) show that, for small values of  $S$ , both the vertical and horizontal components of electric field are independent of the angle  $\phi$ . In other words, the radiation pattern is uniformly circular. Both vertical patterns vary simply as  $\cos \theta$ . Hence, if we satisfy the condition

$$2 \cdot \sin \alpha = kS \cos \alpha$$

or 
$$\tan \alpha = kS/2 \quad (11)$$

the radiated field will be circularly polarized at all points in space.

When the dimension  $S$  is not sufficiently small, perfect circular polarization will not be achieved at all points. However, elliptical polarization which closely approaches circular polarization may be

readily obtained. For example, if it is desired to insure true circular polarization in the horizontal plane at positions corresponding to values of  $\phi$  equal to 0, 90, 180, and 270 degrees, it is merely necessary to satisfy the relation

$$\sin \alpha [1 + \cos (kS)] = \cos \alpha \sin (kS)$$

or

$$\tan \alpha = \tan (kS/2) \quad (12)$$

To obtain circular polarization at points corresponding to  $\phi$  equal to 45, 135, 225, and 315 degrees, it is necessary to satisfy the relation

$$\tan \alpha = \frac{1}{\sqrt{2}} \tan \left( \frac{kS}{\sqrt{2}} \right) \quad (13)$$

The relation between the tilt angle of the dipoles and the dimension  $S$  may be seen in the following tabulation.

$S$ (wavelengths)	$kS$ (degrees)	$\alpha$ (degrees)	
		From equation (12)	From equation (13)
0	0	0	0
0.0833	30	15°	15° 22'
0.166	60	30°	32° 55'
0.25	90	45°	55°

#### DESCRIPTION OF A CIRCULARLY-POLARIZED ANTENNA

An antenna has been constructed, following the basic design principles established by Lindenblad, and is shown in Figure 4. The antenna consists of four in-phase dipoles arranged on the circumference of a circle having a diameter of approximately one-third wavelength. Hence  $kS$  is 60 degrees, so from Equation (12) it is found necessary to incline each dipole at an angle of 30 degrees from the horizontal plane.

Each of the four dipoles is fed with a RG-11U solid-dielectric coaxial cable placed inside one of the two tubular support legs, with the cables each one-quarter wave in length at the mid-band frequency of operation. The inner conductor of the cable extends through a protecting end seal to the end of the other support leg, providing a balanced feed to the dipole. This method of securing balanced feed is illustrated in Figure 5.

The impedance offered to the transmission line at this point consists of the antenna impedance shunted by the inductive reactance of

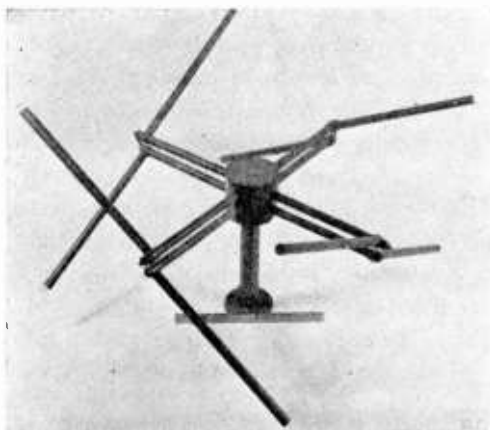


Fig. 4—The development model designed to operate over the frequency range from 110 to 132 megacycles. (This model radiates a left-hand circularly-polarized wave.)

the parallel-bar support legs. The dipoles are made somewhat less than a half wave, so the antenna impedance consists of a resistive component and a capacitive reactance. The dimensions were so chosen that the inductive reactance of the support legs just parallel-resonated the dipole. In addition, at resonance the resistance of the combination is 100 ohms. The RG-11U cable has a characteristic impedance of 72 ohms. Hence, the impedance looking into the quarter-wave section which feeds the dipole is approximately 52 ohms. It is of interest to

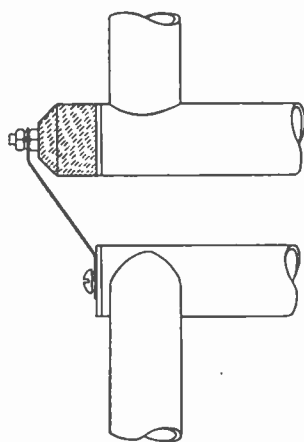


Fig. 5—The method used to secure balanced feed of the dipole from a concentric transmission line.

note that the velocity in this solid-dielectric cable is two-thirds of the velocity of radio waves in free space so the quarter wavelength of cable has an actual physical length of one-sixth of a free-space wavelength and thus just reaches from the end-seal of the dipole to the center of the large cylinder shown in Figure 4. The four cables join in this cylinder. Since they are all in parallel, they offer a resistance of 13 ohms. A quarter-wave transformer with a characteristic impedance of 26 ohms is contained in the central vertical support post. This transformer steps the 13-ohm resistance up to 52 ohms. Thus an impedance match is offered to the 52-ohm feed line which leads from the transmitter to the antenna. The result is a well-matched

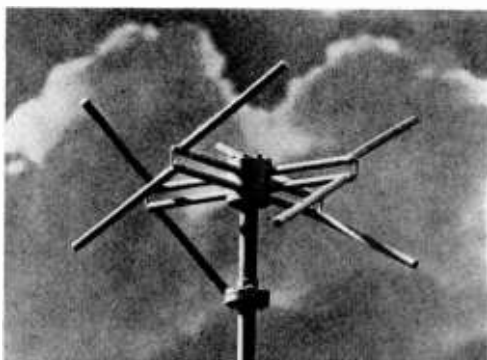


Fig. 6—A very small model of the circularly-polarized antenna. (This model radiates a right-hand circularly-polarized wave.)

antenna radiating a substantially circularly-polarized wave. Equal currents in the dipoles, all in phase, are obtained simply from the symmetrical construction and depend in no way upon the method of securing an impedance match.

While it is true that the central support pole lies in the field of the antenna, tests proved that it was not necessary to use a quarter-wave sleeve around the support pole to secure the desired radiation characteristics.

The weight of the completed antenna is less than 30 pounds, exclusive of the mounting pole and feed line.

An inspection of Figures 1 and 4 reveals that the antenna shown in Figure 4 will radiate a left-hand circularly-polarized wave. A small model of this type of antenna is shown in Figure 6. This model is constructed to yield a right-hand circularly-polarized wave.

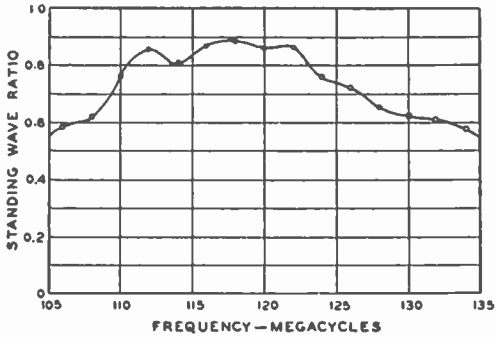


Fig. 7—The measured standing-wave ratio as a function of frequency.

### TEST RESULTS

The antenna was designed to cover a band of frequencies lying between 110 and 132 megacycles. The standing-wave ratio on the main feed line, as a function of frequency, is shown in Figure 7. It may be seen that the standing-wave ratio is better than 0.5 over the entire band.

To learn how well circular polarization had been achieved, a transmitter was connected to the antenna and a dipole at the receiver was rotated on a horizontal axis. This test was made at many points around the antenna and at several frequencies. Figure 8 shows typical results. A possible explanation of the departure of the measured curve from a perfect circle is the slight shading or shielding effect experienced by

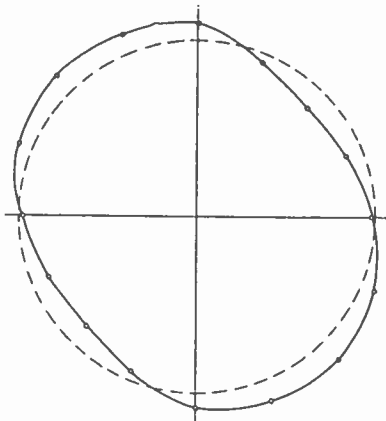


Fig. 8—Experimental data showed the close approach to a true circularly-polarized wave.

the radiators or portions of radiators farthest from the receiver, behind the central pipe support and cable connector box.

Vertical radiation patterns were found to obey the  $\cos \theta$  law rather well throughout the band of frequencies.

Radiation patterns in the horizontal plane were measured at a number of frequencies. The patterns were found to be essentially circular for all frequencies in the band. Typical measurements taken at 122 megacycles are shown in the tabulation below. The theoretical values were calculated from Equations (7) and (8).

Angle $\phi$ (degrees)	Horizontally-polarized field		Vertically-polarized field	
	Theoretical	Measured	Theoretical	Measured
0	1.0	1.0	1.0	1.02
22.5	1.05		0.992	
45	1.095	1.015	0.976	1.042
67.5	1.05		0.992	
90	1.0	0.98	1.0	1.042
135	1.095	1.015	0.976	1.065
180	1.0	1.0	1.0	1.075
225	1.095	1.015	0.976	1.052
270	1.0	0.98	1.0	1.032
315	1.095	1.015	0.976	1.032

### CONCLUSION

The antenna described in this paper produces a substantially circularly-polarized wave over a rather wide frequency range without readjustment. In fact, the initial adjustments are far from critical.

The signal radiated by this antenna may be received on a dipole or loop antenna. The receiving antenna may be oriented in any position, with the reservation that the receiving antenna does not have a null in its pattern at this position. For example, a dipole could be rotated about a horizontal axis and receive a substantially constant signal if this axis coincides with the line from the transmitter to the receiver. However, if the rotation were such that the receiving antenna assumed a position which coincided with the axis mentioned above, no signal would be received.

If a circularly-polarized antenna is used to receive the circularly-polarized wave, it is necessary that both antennas be capable of producing a right-hand circularly-polarized wave or that they both be capable of producing a left-hand circularly-polarized wave. For example, if the transmitting antenna were the one shown in Figure 4 and the receiving antenna similar to the antenna of Figure 6, the receiving antenna would be blind to the transmitter.



# SLOT ANTENNAS\*†

BY

N. E. LINDENBLAD

Research Department, RCA Laboratories Division,  
Rocky Point, L. I., N. Y.

*Summary*—The development of flush-type radiators of the slot and pocket type is described. Special emphasis is given to types applicable to aircraft. Specific solutions to altimeter and marker beacon pickup antennas are described. Reference to application in other fields is also made.

The general aspects of the phenomena which are involved are examined, and it becomes evident that workable solutions, in the majority of cases, can be obtained only by means of actual experiment, since variations in the surroundings have first-order influence upon such vital characteristics as radiation patterns, slot impedance, and bandwidth.

Progress before and during the war is described in somewhat chronological manner. It is pointed out that, while this progress has been considerable, an appreciable amount of skillful investigation remains to be done before slot antennas can be brought to maximum usefulness.

## INTRODUCTION

FOR a number of years, extending throughout the war, the engineers of the RCA Laboratories Division at Rocky Point, L. I., N. Y., have been engaged in the study of such fundamental antenna problems as bandwidth, and the effect of surroundings and location of antennas upon their radiation characteristics.

During this development period the speed of aircraft has been greatly increased. Consequently, streamlining became a necessary consideration. An all-out effort to provide for efficient radiation from flush surfaces was made in order to meet this increasing need. The result of this work is the slot antenna. It comprises slots in the metal surface of an aircraft. These slots are backed by metal cavities inside the surface. Impedance regions exhibiting stability over widest possible frequency bands are chosen or arranged within the cavity for connection to the feed lines.

It is the purpose to briefly review the general aspects of the problems involved in such designs and to describe somewhat chronologically the steps of development. It is hoped this description will serve as a stimulant to further developments.

---

\* Decimal Classification: R326.81 × R525.

† Reprinted from *Proc. I.R.E.*, December, 1947.

## GENERAL CONSIDERATIONS

An early idea that may be considered associated with so-called slot antennas was a scheme devised in 1939 by G. L. Usselman, of the RCA Laboratories Division at Rocky Point, L. I., N. Y., to feed an array of dipoles by a slotted wave guide. The dipoles were distributed along the slot and attached to its edges. By choice of phase-velocity characteristics of the wave guide thus loaded, either broadside or end-fire excitation could be achieved. Usselman also suggested that arrays of closely spaced dipoles may be replaced by continuous sheets of widths corresponding to the length of the dipoles.

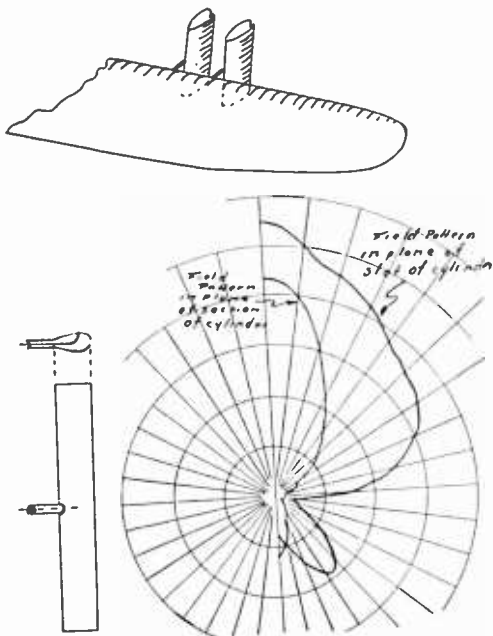


Fig. 1 — Open-ended and streamlined, slotted cylinder antennas mounted in front of leading edge of airplane wing. Polarization perpendicular to cylinders. Polar radiation diagrams for one antenna element are included.

This latter method had special merits worthy of further development, which was undertaken in a joint effort by the U. S. Navy, Radio Test, under Lieutenant Commander A. S. Born (now Captain, U.S.N.), and the Rocky Point Section of RCA Laboratories, beginning in 1941.

The primary purpose was to apply the slot-feed principle to airborne antennas. Slotted wave guides having teardrop or streamlined cross section were used in some of the early experiments (Figures 1 and 2). No special antenna elements were attached to this streamlined body, but by arranging for co-operative coincidence of internal and external characteristics, its own exterior served as a radiator. While having great usefulness in other fields of application, the limited use-

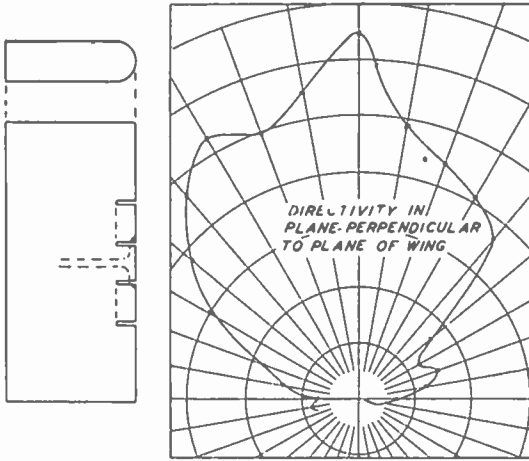


Fig. 2(a)—Combination of four slots across the leading edge of a wing, each pair having a common quarter-wave deep-backing cavity. Polarization in plane of the wing.

fulness of slotted cylinders for airborne purposes became quickly evident in view of the advancing speeds of aircraft.

Antennas for a high-speed aircraft must not add external structure. The designer must consider the possibilities of providing for the emergence of radiation from the surface of the plane. The least radical procedure is, perhaps, to mount a conventional radiation element in an indentation in the plane surface which is then covered with a dielectric window. The primary radiation fields thus originate with a con-

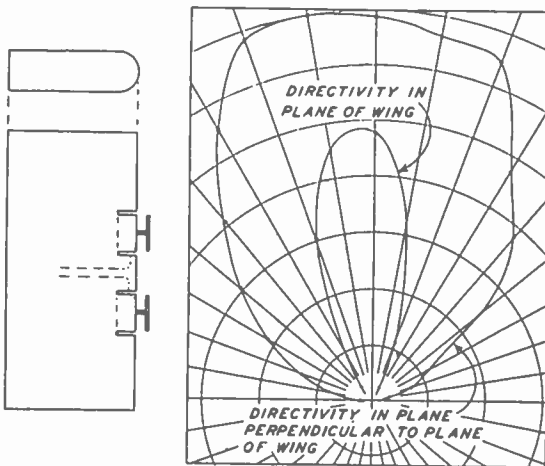


Fig. 2(b)—Same combination as in Fig. 2(a) with parasitic radiators added proximity one-quarter wave in front of each slot pair.

ventional radiation element. The cavity is open and nonresonant. The aperture, however, may be made smaller and the cavity itself be made resonant, eliminating the need of a distinct radiation element. The aperture may be in the form of a slot of sufficient dimensions for emergence of radiation from the interior of the cavity. A surface section may be electrically uncoupled from the rest of the skin by means of cavity-backed slots. In this case the currents, in the separated area, isolated by the high-impedance slots, may be considered the origin of radiation. Actually, it is difficult to draw any definite lines of distinction between these various methods, since surface currents are always part of the diffraction phenomenon around apertures. Only when the apertures are very large relative to the wavelength, or when the aperture is isolated, by surrounding high-impedance slots, may the adjacent surfaces be considered as possessing a high degree of nonparticipation in the radiation phenomenon. The dimensions of the total metal area thus very often has considerable influence upon the radiation pattern, and may sometimes become the antenna itself.

It is now evident that the most controllable method is the one where an aperture or an area is isolated by high-impedance cavity-backed slots. Of these, the least cumbersome appears to be that of isolating an area. In cases when complete flush mounting is not required, it is possible to mount the isolating cavities like external pockets. They can also be made in the form of a sheet, rolled up like a jelly roll, forming a spiral cavity.

#### DEVELOPMENT

One of the earliest attempts to utilize this idea was to cut pairs of half-wave-spaced vertical slots across the leading edge of an airplane wing. The resulting half-wave ribbon, which then was part of the leading edge, was backed by an approximately quarter-wave-deep cavity. Each side of the ribbon was connected at its maximum voltage point to a transmission line. These lines were then connected together in series or in parallel. This arrangement provided a rather wide, forward-spreading radiation pattern. When spaced coupled parasitic radiators or "directors" were placed a quarter-wave outside and in front of the strip between the paired slots, higher gain was obtained, as shown in Figure 2(b). This method, however, introduced difficult wing design and aerodynamic conditions, and was not continued.

The practical possibilities of isolating an area had been indicated, and experiments were directed toward flat surfaces. Figure 3 shows the cross section of one of these early forms of double-slot antennas, affectionately dubbed "bathtubs" by the Navy. In Figure 4 is shown

a photograph of an antenna consisting of a pair of double-slot antennas. As can be seen, the spacing between adjacent slots of different pairs is less than a half-wave. This spacing was determined experimentally with the aim in view of obtaining the cleanest radiation pattern. Figures 5, 6, and 7 show typical radiation patterns and the standing-wave-ratio curve as measured by the Navy Radio Test group. Figure 8 shows a form by means of which it was possible to obtain wider frequency response. As may be noted, the center conductor of the transmission line here expands gradually as a flat wedge before connecting to the slot edge.

It should be of interest to notice that the double-slot antennas possess a natural characteristic which is of advantage to lobe switching.

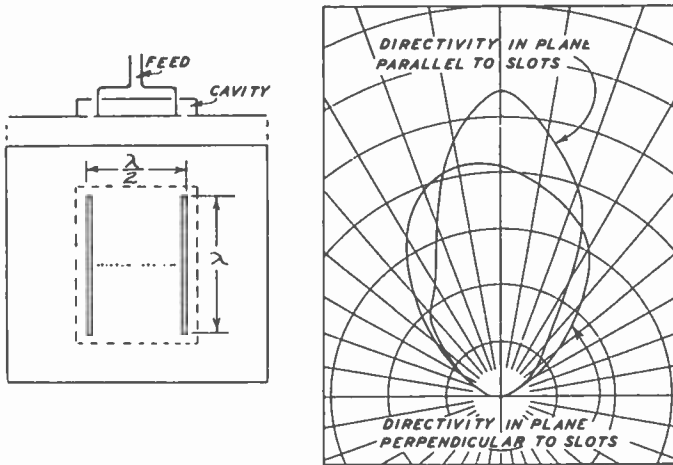


Fig. 3—Simple double-slot antenna.

If only one of the two slots is fed, the radiation pattern will lean toward the fed slot. In this way the same antenna can be used for both lobes by simply shifting the feed. This makes it equivalent to one slot per lobe (Figure 9).

A particular use was made of this phenomenon in a double-slot antenna used as the focal primary in a parabolic-reflector-type antenna at 1250 megacycles. It was found, however, that this design could be further simplified to permit the omission of a spark or contact switch. It was only necessary to provide a rotating patch of very small dimensions relative to the wavelength, which would alternately cover a portion of one or the other of the slots (Figure 10). In order to provide up and down switching, the vertical slot was divided in two sections, parallel fed, but having high coupling impedance. In this way, the patch, which was a piece of foil cemented in an eccentric position to an insulating

rotatable disk, would cover the upper and the lower half of one slot, and then in sequence the lower and the upper half of the other slot. In this way the same effect as that obtained with the mechanically more difficult type of nutating dipole was obtained. A simplified form of nutating antenna energized by either a single- or by a double-slot primary was, however, also developed. It consisted of a diametrically resonant disk rotated eccentrically at a distance of about one-quarter

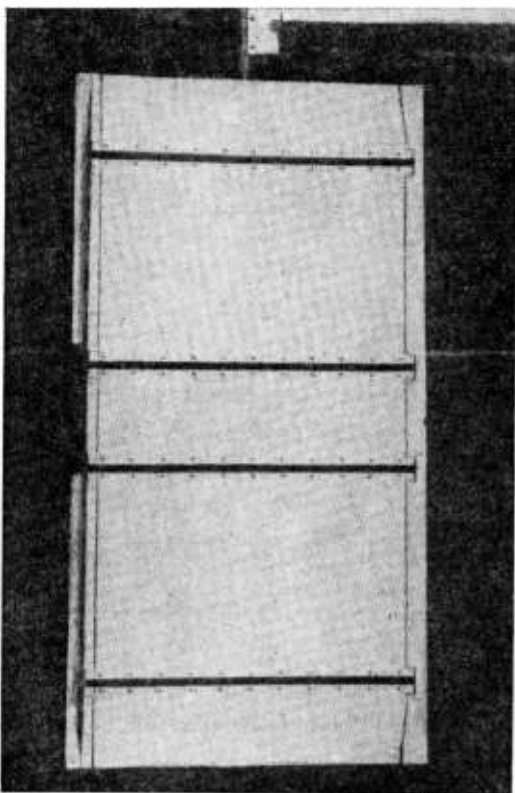


Fig. 4—Pair of double-slot three-quarter by half-wave antennas. This is the Navy "bathtub." Note close spacing between pairs for elimination of secondary lobes. Design by U. S. Navy.

of a wave or less in front of the double-slot antenna to which it was thus space-coupled (Figure 11).

The work so far described served the useful purpose of proving the practical possibilities of nonprotruding radiators. It had been shown that the slot principle was sound and workable and that it furnished tools for a new approach to radiator problems. The development was, however, insufficient to meet some of the applications for which it was most needed.

Thanks to the interest shown by other researchers who would from

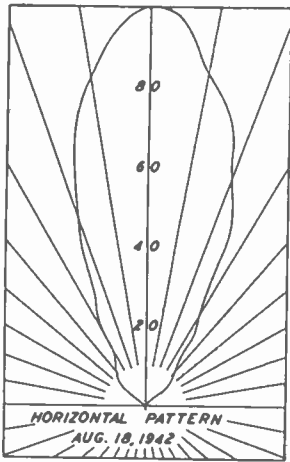


Fig. 5—Slot-crosswise pattern of antenna of Fig. 4. This data taken by U. S. Navy.

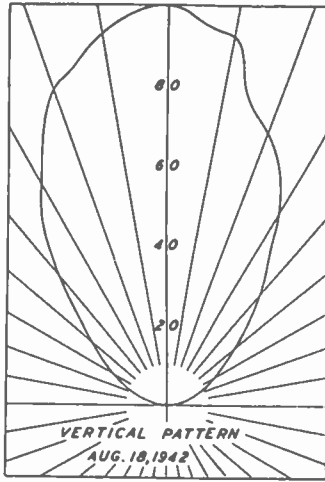


Fig. 6—Slot-lengthwise pattern of antenna of Fig. 4. Data by U. S. Navy.

now on contribute toward both the general and the special development of the slot principle, it was felt that the work could be directed toward specific applications. Slot antennas for altimeter and marker purposes were chosen as subjects of these efforts. These antennas would have to be applicable to all plane types, including the smallest and fastest. The operating frequencies are relatively low, especially

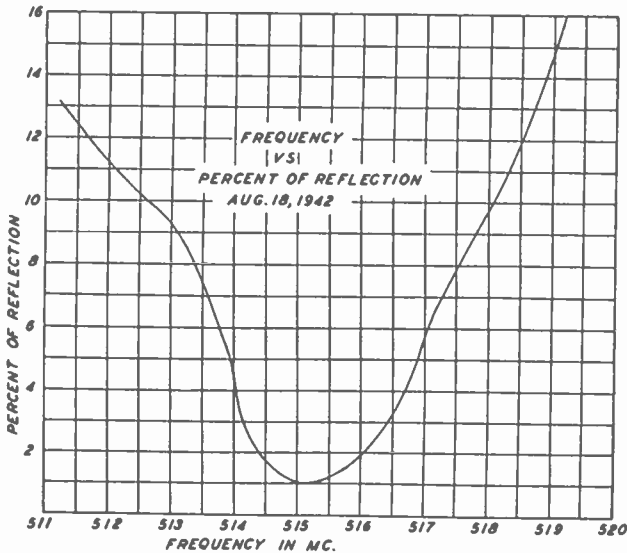


Fig. 7—Standing-wave-ratio curve taken from antenna of Fig. 4. Data by U. S. Navy.

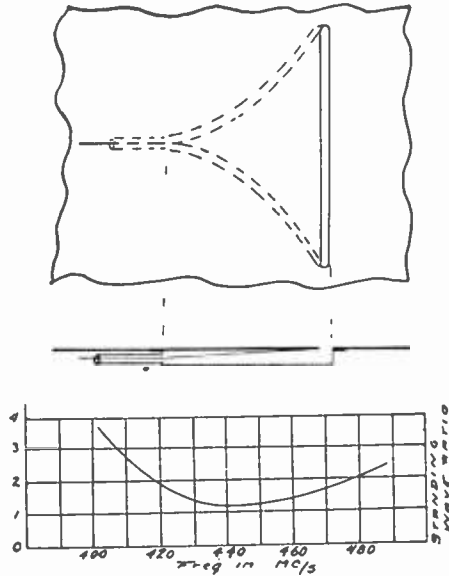


Fig. 8—Expanding wedge feed for single-slot antenna and the standing-wave-ratio curve for wedge antenna as shown.

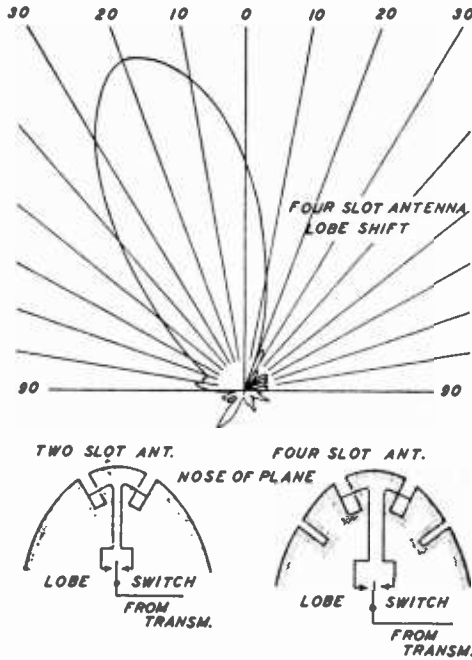
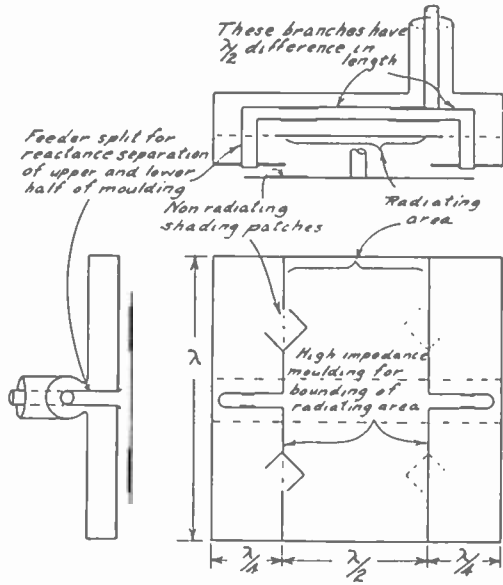


Fig. 9—Shiftable, single-slot feed for lobe switching. Note the application of this slot antenna to the curved contour of the model of the nose of an airplane.



Fig. 10—External pocket-border type, one by one-half-wave surface radiator. As the primary in a parabolic reflector, the lobe switching is performed by 90-degree-displaced rotatable shading patches. Note electrical sectionalizing of pockets and feeders to facilitate "pull" by shading patches, a very practical arrangement. A single patch provides diagonal and a double patch vertical-horizontal lobe pulling.



in the case of the marker antenna. Altimeter antennas must be so arranged that transmitter and receiver may be operated simultaneously. The frequency-response band required by the altimeter equipment is also relatively considerable. All such considerations which have a direct bearing upon the antenna dimensions must, in the practical application of slot antennas to aircraft, be accommodated without sacrifice of structural strength. Careful search for minimum dimensions must, therefore, be made.

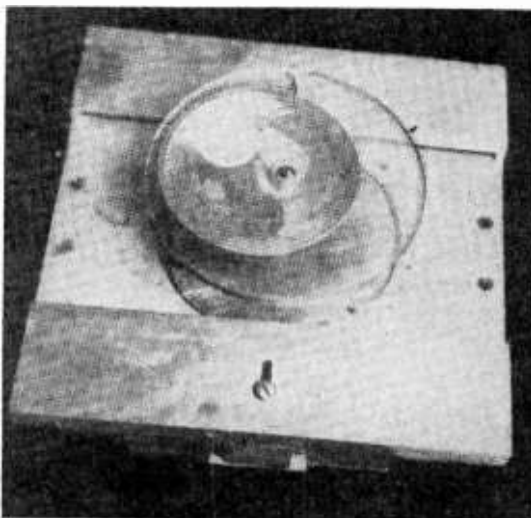


Fig. 11—External pocket-border type, one by one-half-wave surface radiator. The major radiating "area" is located between slots. The diametrically resonant disk in front, eccentrically rotatable, acts as a nutating facility for lobe switching when the combination serves as a focal reflector in a parabolic reflector system.

As a general rule, a cavity with generous cross-section dimensions make it easier to meet wide-frequency-band requirements. The slot and corresponding cavity length does not contribute in the same way and can, therefore, be reduced to the order of magnitude of a half-wave before it becomes a serious band limiting factor.

The view taken here is that it is always well, in antenna developments, to aim at as much "self"-bandwidth as possible, since it eliminates or reduces either the need or the complexity of impedance-correcting networks. The power of the network method in practical application is, reversely, greatly facilitated by good primary frequency response, especially in cases of exacting requirements of low reflection.

In view of the substantial reduction in bulk that could be obtained by the use of single slots, it was decided that these be given careful consideration. Although future equipment developments may not permit the use of the less exactly shaped radiation patterns obtained by single slots, their other virtues made them appear as the most practical expedients at the present stage of development.

At first, bandwidths greater than needed were aimed at. The opening of a longitudinally elliptic cavity was partitioned by means of a longitudinal strip to form two closely located, parallel slots (Figures 12 and 13). The cavity was likewise partitioned by a longitudinal wall. Point connections were made between this partition and the narrow strip between the slots. Thus a certain amount of internal coupling was maintained between the two half-sections. Each cavity half-section was again partitioned. The transmission line entering the cavity at bottom center connected to the top edge of one of the side partitions by means of an elliptic tongue. This multiple partitioning was an expedient by means of which a region of frequency-flat impedance balance could be obtained which was suitable for direct connection to the transmission line. A bandwidth of 30 per cent at 2:1 reflection tolerance was obtained (Figure 14). These experiments were done with a slot length of 0.75 wavelength and a maximum cavity depth of 0.2 wavelength. The cavity width was 0.135 wavelength.

Further reduction of size, however, continued to be very desirable. It appeared that this would then have to be done at the expense of bandwidth. In the case of the altimeter antenna, a search was made for the minimum dimensions required for the maintenance of the necessary 10 per cent bandwidth. A series of tests were carried out in which the influence of varying size and parameters was carefully noted. The partitions were eliminated. The tongue feed was maintained, but the tongue was now bent over itself and shape and position determined empirically for best conformity with region of flat

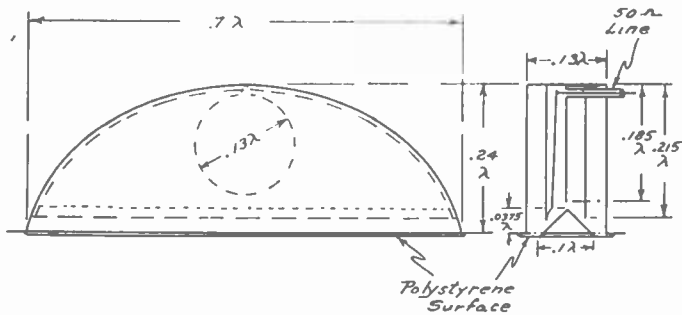
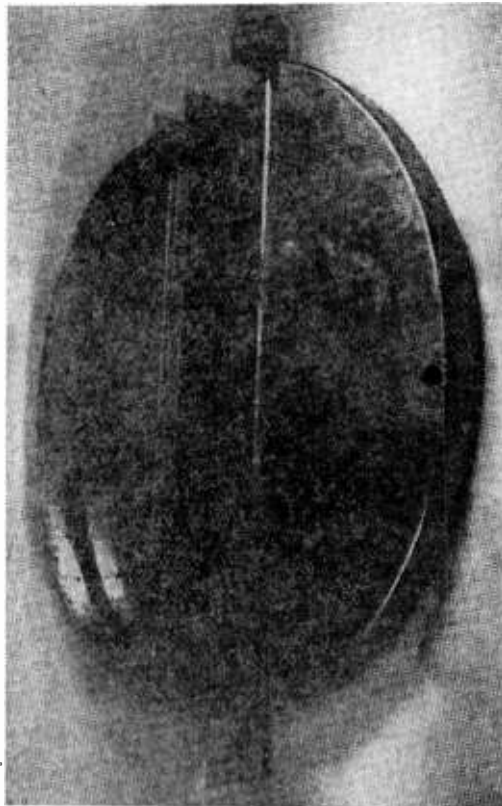


Fig. 12—Elliptic-cavity, wide-band, twin-slot antenna. The slots are spaced one-tenth of a wave-length.

impedance balance (Figure 15 and 16). In the illustrated example the slot and cavity length was 0.575 wavelength, the cross section was 0.1 by 0.135 wavelength. The bandwidth at 2:1 reflection standard was above 14 per cent.

As may be anticipated, further reduction of size calls for capaci-

Fig. 13 — Showing cavity sections of the antenna of Fig. 12. Note the hole in the feed tongue which divides it into two curved, parallel-connected expanded wedges.



tance loading of the cavities at their open end. This was first done by using narrowed slots and eventually by adding capacitances across the slots. In these continual attempts to reduce the cavity dimensions it became necessary to revise the feed methods from time to time, since their operation is subject to certain parametric conditions.

In the model which was considered sufficiently small to be practical, the attempts to establish a suitably broad impedance zone within the antenna proper into which the feed system may be introduced had not been entirely satisfactory. It was found that a simpler expedient could be had by resorting to external compensation by means of a line stub. This, however, was convenient only because such relatively high standing-wave ratios as 2:1 or 1.5:1 were considered permissible so

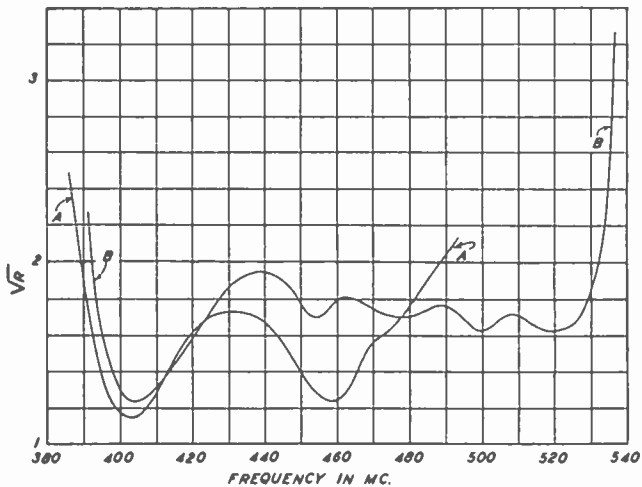
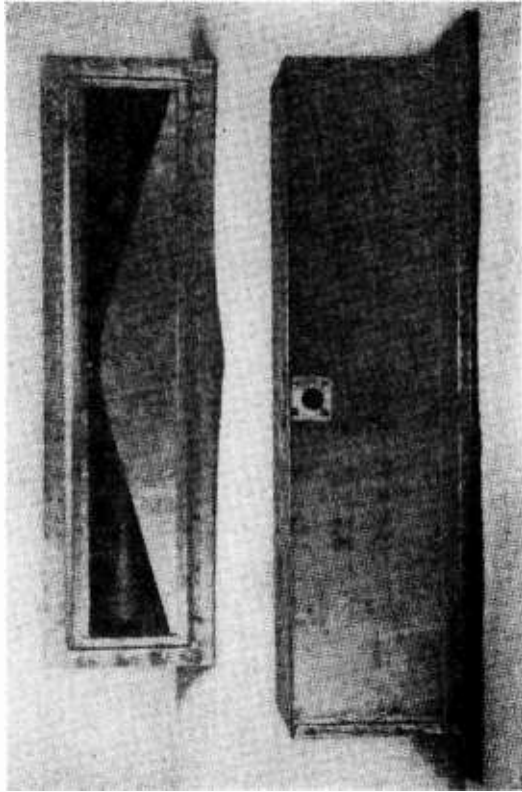


Fig. 14—Standing-wave-ratio curve of the antenna of Fig 12 as compared with the standing-wave-ratio of the antenna without subdivided cavity.

that the resulting hump in the s.w.r. curve, often unavoidable with such circuits, would not be objectionable. More complicated networks can, of course, be provided which will subdivide or level off such bumps.

The antenna of Figure 17 has a slot length of 0.4 wavelength. The cross section is 0.1 by 0.1 wavelength. Figure 18 shows a typical s.w.r. curve for this model. The tail stub which forms a continuation of the feed conductor across the cavity has an approximate length of three-quarters of a wavelength. Its characteristic impedance is 50 ohms. Line stubs of other impedance values can be used if the feed coupling is correspondingly adjusted. This coupling is varied by changing the distance from the coupling rod to the bottom of the cavity. It should be noted, however, that the rod must be located empirically to find the

Fig. 15 — Rolled-feed tongue, keyhole-slot antenna. Slot length, 0.575 wavelength. The rolled tongue can be seen inside the cavity.



position where the electric and magnetic field parameters co-operate in optimum fashion at a given characteristic line impedance and standing-wave ratio. Otherwise, considerable bandwidth is easily lost. Using a stub having a characteristic impedance of 50 ohms appeared satisfactory and aided in simplifying the system by being of the same

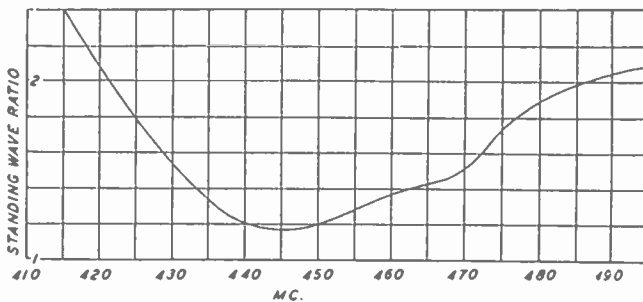


Fig. 16—Standing-wave-ratio curve of the antenna of Fig. 15.

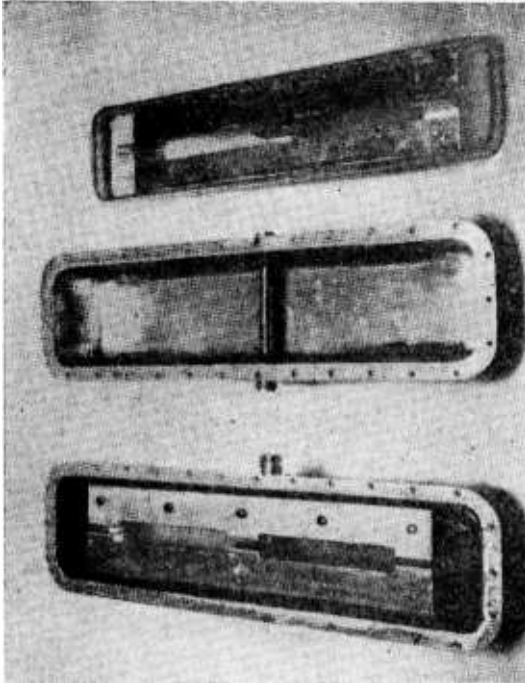
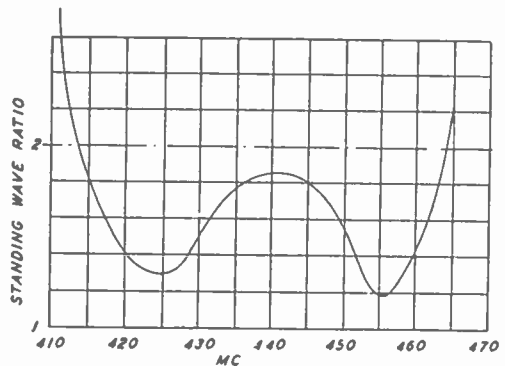


Fig. 17— Three - point capacitance - loaded *H*-slot altimeter antenna. Slot length, 0.4 wavelength.

value as that of the feed line. The cavities are pressed from a single aluminum sheet. The cover consists of Formica. The total weight of a complete antenna and stub combination to operate at a midfrequency of 440 megacycles is one pound.

In applying such antennas to altimeter equipment, where transmitter and receiver must operate simultaneously, it has been found that the coupling between transmitter and receiver antennas is generally about twice as high as that encountered with dipoles. It appears, however, that this does not exceed the coupling tolerance of the equipment.

Fig. 18— Standing-wave-ratio curve for the antenna of Fig. 17.



In such cases where smaller tolerance must be provided, these antennas can be arranged in series or parallel to form double-slot antennas, which then, due to the nature of such a combination, provides lesser coupling.

The marker beacons of the airways operate at present on a frequency of 75 megacycles. The conventional external antennas for receiving these signals are cumbersome and inefficient due to this rather low frequency. A slot antenna of such small dimensions as  $20 \times 4 \times 5$  inches has been developed. The slot length of this antenna is only 0.125 wavelength. The slot is heavily capacitance loaded. As can be understood, an antenna of such dimensions relative the wavelength must of necessity have a very high  $Q$ . The s.w.r. curve obtained by the aid of a series stub line is shown in Figure 19. The signals obtained are better than equal to those obtained with external wire antennas located

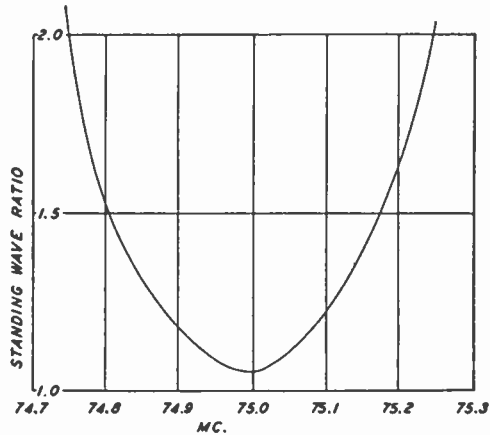


Fig. 19 — Standing-wave-ratio curve for marker-beacon antenna.

close to the ship. Greater bandwidth would be desirable, but it is gratifying at this stage of slot-antenna development to be able to report that antennas of such small dimensions relative to the frequency will work at all.

The marker-beacon signals do not call for any large bandwidth. The chief reason for not wishing to apply antennas of too narrow bandwidths is their sensitivity to moisture and ice. A sharply tuned antenna is easily detuned by small reactance variations. Trimming capacitors or inductances can, of course, be used, but they are not very satisfactory. It appears better to rely on means for preventing internal condensation of moisture, as well as both internal and external ice formation. Danger of external icing can be greatly reduced by proper location. The problem of eliminating internal condensation is more formidable. The antenna has either to be kept perfectly sealed to all

the pressure variations to which it is subjected as an airplane changes altitude or it must be thoroughly ventilated. The latter is the easiest but does not at times appear entirely adequate, unless heating elements or moisture-absorbing substances be added. This again is, of course, not very attractive.

It has been suggested that the dimensions of a cavity antenna may be decreased by filling it with a dielectric. When analyzing this proposal relative to radiation resistance and bandwidth, there appears to be nothing to gain by such procedure. A magnetic material operable at very-high frequencies would, on the other hand, provide a filler by which the circulating currents in the cavity could be reduced and bandwidth gains could be made. No such material is known at the present.

Dielectric fillers have, however, been considered for the purpose of keeping out the moisture of cavities. Desirable characteristics for such material are: low dielectric constant, low loss, homogeneity, and low weight. Foam is unsuitable, due to surface losses throughout the material. Boundary losses appear to be difficult to avoid even with the use of very solid materials.

#### CONCLUSION

An attempt has been made to describe the general aspects of slot antennas. Such antennas are a "must" in high-speed aeronautics and in radio-controlled missiles.

It has been shown that many of the tasks performed by external antennas can be performed by this flush-type radiator. Subjected to careful scientific investigation, as is possible in peacetime, their usefulness should eventually be greatly extended.

#### ACKNOWLEDGMENT

The author is indebted to the Navy Radio Test personnel and especially to Captain A. S. Born, R. M. Silliman, and Lieutenant J. B. Stout for encouragement during the early stages of development. Similar acknowledgment is due to various members of the radio technical groups of the Army.

To RCA, special acknowledgment is due to H. H. Beverage, C. W. Hansell, P. S. Carter, R. E. Franklin, and W. A. Miller for help and guidance freely given.



## AN ULTRA-HIGH-FREQUENCY ANTENNA OF SIMPLE CONSTRUCTION\*†

BY

GEORGE H. BROWN# AND J. EPSTEIN#

RCA Manufacturing Company, Inc.,  
Camden, N. J.

### Summary

*Two difficulties present in most of simple and popular types of U-H-F antennas are discussed with reference to the design of a new type of U-H-F antenna, the first model of which was tested and built in 1938. The paper covers the electrical and mechanical details of the new antenna, a vertical quarter-wave radiator supported above four horizontal ground rods. Subsequent structural modifications growing out of experience in the use of the new antenna resulted in a simplification of the construction which gave much greater matching flexibility. The frequency characteristics of the antenna are presented. Laboratory and field tests show that the antenna is efficient and of practical design. The chief advantages may be summed up as follows: equipment is mechanically simple and rugged; field adjustments are not required; transmission line is properly terminated; the concentric feed line is not exposed to high frequency fields; and the antenna is grounded.*

(3 pages; 8 figures)

---

\* Decimal Classification: R326.7.

† *Communications*, July, 1940.

# Now with the Research Department, RCA Laboratories Division, Princeton, N. J.

## WATER-COOLED RESISTORS FOR ULTRA-HIGH FREQUENCIES\*†

BY

G. H. BROWN# AND J. W. CONKLIN

RCA Manufacturing Company, Inc.,  
Camden, N. J.

### Summary

*Television transmitter development and other u-h-f services require the use of resistors capable of dissipating large amounts of power over a*

---

\* Decimal Classification: R383.22.

† *Electronics*, April, 1941.

# Now with the Research Department, RCA Laboratories Division, Princeton, N. J.

wide band of frequencies, without displaying inductive or capacitive effects. A water-cooled coaxial design which serves the purpose adequately is here described. Some of the applications in television transmission where high-power, water-cooled resistors are used are: circuit-loading resistors for damping or broadening tuned circuits; "dummy" antennas for testing and power measuring; terminating resistors in antenna filter networks; and coupling resistors for video-frequency circuits.

(6 pages; 14 figures)

## THE RCA ANTENNALYZER—AN INSTRUMENT USEFUL IN THE DESIGN OF DIRECTIONAL ANTENNA SYSTEMS\*†

BY

GEORGE H. BROWN AND WENDELL C. MORRISON

Research Department, RCA Laboratories Division,  
Princeton, N. J.

### Summary

The equations for the radiation patterns of directional antenna systems are well known, but the arithmetical work necessary to secure a plot of the radiation pattern is tedious and time-consuming. Several mechanical plotting devices to assist with the problem have been described in the literature. A brief review of a few of these instruments is presented. These mechanical devices yield the radiation pattern for a given choice of configuration and antenna constants. In general, however, the designer of a directional antenna for broadcast-station use knows the pattern required and is faced with the problem of determining the antenna configuration which will yield this pattern. The RCA Antennalyzer was developed to synthesize or to analyze. The instrument is entirely electrical, with no moving parts except the potentiometers which change the various parameters. Developed specifically for the design of directional antennas for broadcast use, the Antennalyzer, as constructed, will yield the radiation pattern of directional antennas which have as many as five towers or sources of radiation. Each source is characterized by four parameters: (1) the distance from a reference point; (2) the azimuth angle with respect to a base line; (3) the amount of current in the antenna; and (4) the phase angle of this antenna current. Thus the Antennalyzer has four potentiometers associated with each antenna, with one exception. One antenna is located at the reference point and carries unit current at zero phase. Hence, no controls are required for this antenna. The radiation pattern is displayed directly on the face of a cathode-ray tube either in polar or rectangular co-ordinates. The Antennalyzer may be used in two ways. The dials may be set to correspond to a given antenna configuration. Then the resulting pattern is observed on the cathode-ray tube. However, when a given pattern is the goal, the dials may be twiddled until the proper

\* Decimal Classification: R221.

† Proc. I.R.E., December, 1946.

pattern is obtained. Then the dial settings are recorded. These dial settings tell where to locate the towers, as well as the current ratios and phase angles to use. With a little practice, this operation of analysis may be performed in a few minutes. Metering devices are included in the Antennalyzer so that the ratio of maximum field intensity to root-mean-square field intensity is obtained. Some of the unusual circuit details are discussed. (8 pages; 15 figures)

## INPUT IMPEDANCE OF A FOLDED DIPOLE\*†

BY

W. VAN B. ROBERTS

Research Department, RCA Laboratories Division,  
Princeton, N. J.

### Summary

*The folded dipole has become a familiar expedient to provide increased input impedance over that of a dipole antenna and permit more efficient transmission line matching. The input impedances of standard configurations are well known; however, there has been no convenient way of determining the actual input impedance in the general case of elements of arbitrary size, shape, number and arrangement. This paper presents an analysis which attempts to provide necessary formulas and a physical picture of the operation of the folded dipole. The presentation is in two parts—folded dipole with equal elements, and folded dipole with unequal conductors.*

(12 pages; 10 figures)

---

\* Decimal Classification: R321.3.

† RCA REVIEW, June, 1947.

# PROPAGATION OF ULTRA-HIGH-FREQUENCY WAVES\*†

BY

DUDLEY E. FOSTER

RCA License Laboratory, New York, N. Y.

*Summary*—The increased use of frequencies above 25 megacycles, particularly for television and frequency-modulated wave broadcasting, has led to more general interest in the propagation characteristics of such waves. It has been recognized for a number of years that the U-H-F waves have certain peculiarities in propagation which differ from those for lower frequencies. The characteristic most commonly emphasized is that the useful U-H-F wave transmission is essentially limited to line-of-sight distances. In this respect, as in many others, such waves are quasi-optical in character and many of the principles applying to light waves, such as reflection, refraction and diffraction, are applicable to the ultra short radio waves.

## PRINCIPLES OF U-H-F PROPAGATION

A complete and exact treatment of the theory of U-H-F propagation is an involved process and has been the subject of many technical papers. For the use of those engineers interested in an extended treatment a bibliography is given at the end of this bulletin. A brief mathematical treatment of the theory is given in the appendix to this bulletin, but in this section the emphasis will be placed on physical principles and the simplified quantitative treatment.

## TRANSMISSION OVER A PLANE EARTH

Before considering the influence of the earth's curvature on the received signal, let us investigate the conditions of transmission over a plane surface.

The radiation field from a dipole in free space is given by the expression

$$E_o = \frac{60 \pi H I}{\lambda d} \quad (1)$$

where  $E_o$  is field intensity at distance  $d$

$H$  is the effective height of the antenna

---

\* Decimal Classification: R111 X R113.706.

† Material prepared February 9, 1940.

$I$  is the antenna current

$\lambda$  is wave length

Now a half wave doublet has an effective height of  $2\lambda/\pi$  and a resistance of 73 ohms. Substituting in expression (1) gives us the field from a half wave doublet as

$$E_o = \frac{7 \sqrt{W}}{d} \quad (2)$$

where  $W$  is power delivered to the antenna.

Thus, in free space, the field intensity from a half wave doublet

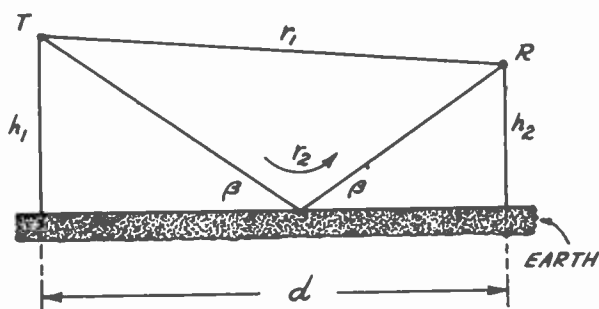


Fig. 1.

varies directly as the square root of the radiated power and inversely as the first power of the distance.

The presence of the surface of the earth considerably changes the conditions. The earth acts as a reflector so that we must consider both the direct and the reflected rays. The wave undergoes a change in both magnitude and phase on reflection, the phase angle change and the magnitude of change on reflection depending upon the nature of the reflecting surface, and also on whether the wave is horizontally or vertically polarized. As may be seen from Figure 1, the signal arriving at the receiving antenna  $R$  from the transmitting antenna  $T$ , is due to the vector sum of the direct and reflected rays. The direct ray travels a distance  $r_1$  and the reflected wave a distance  $r_2$ . The difference between horizontal and vertical polarization reflection characteristics depends not only upon the nature of the reflecting surface (the earth) but also upon the angle of incidence  $\beta$  (as in optical reflection, the angle of incidence is equal to the angle of reflection.) Therefore the

relative phase and magnitude of the direct and reflected rays at the receiver depend upon the heights of the two antennas  $h_1$  and  $h_2$  and the distance between them, as well as upon the polarization sense and earth coefficients. In the generalized case the reflection coefficient is a complex quantity, having both real and imaginary components.

Under the conditions usually encountered in practice the conditions are simplified. At ultra-high-frequencies, dry ground acts essentially as a perfect dielectric. When the angle of incidence is small, that is when the distance is large compared with the antenna heights, both horizontally and vertically polarized waves undergo no loss at reflection, but do undergo a 180-degree phase reversal. This means that the direct and reflected waves arrive at the receiver with equal amplitudes and, except for difference in path lengths, would be out of phase 180 degrees, so that the resultant field intensity would be zero. However, distance  $r_2$  of Figure 1 is greater than  $r_1$  so that the direct and reflected waves do not arrive 180 degrees out of phase. The path difference  $r_2 - r_1$  is approximately

$$\cdot \quad 2 \frac{h_1 h_2}{d} \quad (3)$$

so that the phase lag is  $2\pi/\lambda$  times as great or

$$\delta = \frac{4\pi h_1 h_2}{\lambda d} \quad (4)$$

The resultant of two equal voltages nearly 180 degrees out of phase is given by

$$E = E_0 2 \sin \frac{\delta}{2} \quad (5)$$

where  $\delta$  is 180 degrees plus the angle between them or  $\frac{4\pi h_1 h_2}{\lambda d}$ . The field then is given by

$$E = 2 E_0 \sin \frac{2\pi h_1 h_2}{\lambda d} \quad (6)$$

When the angle is small, the sine is equal to the angle, so with that limitation (6) becomes

$$E = E_o \frac{4\pi h_1 h_2}{\lambda d} \quad (7)$$

Substituting the value of  $E_o$  from (1) gives

$$E = 240\pi^2 HI \frac{h_1 h_2}{\lambda d^2} \quad (8)$$

For a half-wave doublet this becomes

$$E = 88 \sqrt{W} \frac{h_1 h_2}{\lambda d^2} \quad (9)$$

Where the units are volts per meter, watts in the transmitting antenna, heights in meters, distance in meters and wavelength in meters.

Converting  $h_1$  and  $h_2$  into feet and  $d$  into miles gives

$$E = 0.0105 \sqrt{W} \frac{h_1 h_2 f}{d^2} \text{ microvolts per meter} \quad (10)$$

when  $f$  is in megacycles.

This expression is in a very useful form but in using it the conditions under which it is valid must be borne in mind. These conditions are:

1. The transmitter dipole is a half-wave doublet.
2. The angle of incidence is small. For horizontal polarization at U-H-F, angles up to about 10 degrees are permissible. For vertical polarization, over earth or fresh water the angle should be less than 1 degree and for sea water less than 0.15 degree.
3. The antennas are at least one and one half wave lengths above the earth plane.

With these restrictions, the expression applies for either vertical or horizontal polarization.

It may be seen that under these conditions the signal intensity varies directly with the elevation of both transmitting and receiving antennas, directly as the frequency, and inversely as the square of the distance.

## EFFECT OF CURVATURE OF THE EARTH

The foregoing expressions have been derived on the basis of a plane earth. In actual cases the effects of the curvature of the earth must be taken into account. The expressions derived may be used within the distance where the direct ray does not intersect the earth, that is where the receiving antenna is not below the line of sight from the transmitting antenna.

At distances less than the electrical horizon, the curvature of the earth necessitates a correction to the heights  $h_1$  and  $h_2$  for use in expression (10). This may be visualized by considering the situation when the distance is exactly the optical horizon. Then the line-of-sight is tangent to the earth and the effective height of the transmitting and receiving antennas above this tangent plane is nil.

Under such conditions the angle of incidence is zero and direct and reflected rays coincide and, under the assumptions made for a plane earth, the received field would be zero at that distance and for any greater distance.

There are two effects, however, which permit reception beyond the optical horizon, namely, refraction and diffraction.

Refraction causes a bending of the rays, and is due to the effect of the earth's atmosphere. Diffraction causes some signal intensity beyond the distance where the rays intersect the earth's surface. The diffraction phenomenon for radio waves is analogous to the same phenomenon in optics.

In the case of light rays, if an object is interposed between the light source and a plane, the shadow region is not perfectly dark but receives some light from the rays passing the edge of the shadowing object. Similarly the field intensity of a radio wave does not drop suddenly to zero beyond the horizon but decreases gradually with distance although much more rapidly than for distances within the horizon.

In optics the sharpness of shadow is greater for short wavelength light than for long wavelength light. Likewise in radio transmission, the signal drops off beyond the horizon more rapidly for the higher frequencies.

The effect of diffraction for a given frequency is constant whereas the effect of refraction varies with atmospheric conditions. The signal beyond the horizon is therefore not constant but, because of varying refractive effect, varies with atmospheric conditions. An effect is present then in U-H-F propagation at distance greater than the horizon, similar to the effect of fading on the longer waves.



The distance to the horizon is given by the expression

$$D_h = 1.225 \sqrt{h} \quad (11)$$

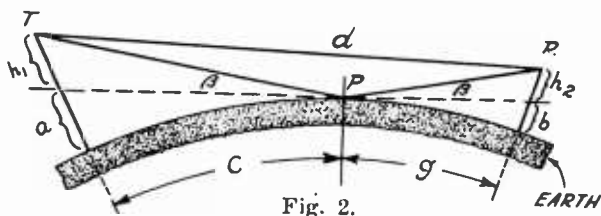
where  $D_h$  is in miles  
 $h$  is in feet

This expression is calculated for the mean diameter of the earth at approximately 40 degrees latitude.

It has been stated that refraction causes a bending of the rays and this bending is equivalent to an increase in the earth's diameter in its effect on the electrical horizon. The average refraction has been found to be equivalent to an increase in the diameter of the earth of 33 per cent. With refraction taken into account the distance to the electrical horizon becomes

$$D'_h = 1.41 \sqrt{h} \quad (12)$$

where the units are the same as for expression (11).



Because of the variation of refraction with the condition of the earth's atmosphere, signal intensity at distances beyond the optical horizon varies considerably with time. The signal intensity may vary under these conditions plus or minus 15 or 20 decibels.

Let us consider how to apply the relations expressed in formula (10) taking into account the earth's curvature and the average refraction.

The conditions are then as shown in Figure 2. As in Figure 1 the transmitter and receiver are designated  $T$  and  $R$  respectively and the distance between them by  $d$ . The reflected ray has an angle of incidence, and an equal angle of reflection  $\beta$ , which determines the ratio of distance  $c$  to distance  $g$ . The tangent plane through the point of reflection  $P$  intersects the transmitting and receiving antenna supports so that the effective elevation becomes only the portion  $h_1$  and  $h_2$  above the tangent plane intersection.

The height of the tower at the transmitter is  $h_1 + a$  and at the receiver  $h_2 + b$ . Knowing the tower heights the effective elevations  $h_1$  and  $h_2$  may be determined from the expression for the optical hori-

zon. If we take into account the average effect of refraction,  $a$  and  $b$  may be expressed by

$$a = \frac{c^2}{2} \qquad b = \frac{g^2}{2} \qquad (13)$$

where, as before,  $c$  and  $g$  are in miles and  $a$  and  $b$  in feet.

Subtracting these heights from the tower heights gives the effective elevations  $h_1$  and  $h_2$  which may then be substituted in (10) to find the received field intensity.

Expression (10) indicates that the field intensity varies directly with frequency so that as the frequency is increased less radiated power is required for a given field intensity for a given height and distance. Beyond the horizon conditions are materially different however, because it has been found that the signal then varies inversely as some power of the distance increasing rapidly with frequency.

Beverage has found empirically that the attenuation of signal beyond the horizon follows the law shown by Figure 3. It may be seen from this figure that at 40 megacycles the signal field intensity decreases inversely as the 3.6th power of the distance, whereas at 90 megacycles it decreases as the 5th power of distance. Since this is an experimentally determined curve it takes into account diffraction and average refraction. In applying this empirical law of variation of received field with distance the optical horizon rather than the electrical horizon should be used, as the electrical horizon, which is on the average 15 per cent greater than the optical horizon, is based on refraction effects. Likewise in using these experimental data the heights of the antennas used are those for plane earth. If the modifications for the earth's curvature were used the received signal would drop to zero at the electrical horizon since no account is taken in that case of diffraction, refraction only being considered. Therefore for reception near or beyond the optical horizon the expression for received field intensity becomes

$$E = \frac{0.0105 \sqrt{W} h_1 h_2 f D_k N^2}{D^N} \qquad (14)$$

where

$E$  is received field in microvolts per meter

$W$  is radiated power in watts

$h_1$  is transmitting antenna height in feet

$h_2$  is receiving antenna height in feet  
 $D_h$  is distance to the horizon in miles  
 $D$  is distance in miles  
 $f$  is frequency in megacycles

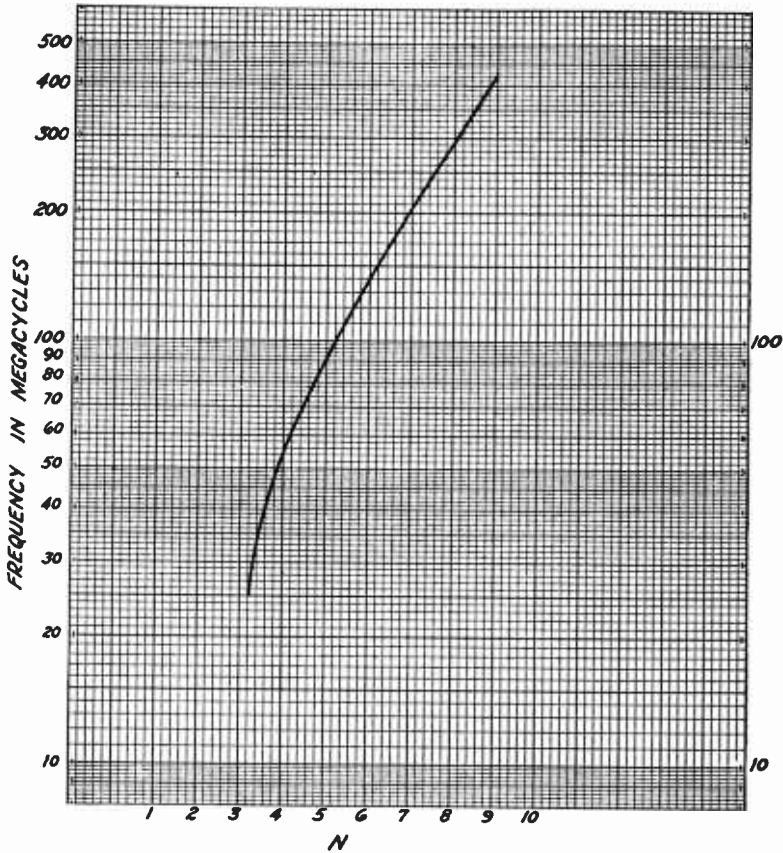


Fig. 3—Law of attenuation beyond the horizon for U-H-F transmission.

$$E \propto \frac{1}{D^N} \text{ where } D = \text{distance}$$

$N$  is the exponent given in Figure 3 as a function of frequency. Within the horizon exponent  $N$  is equal to two regardless of frequency so that  $D_h^{N-2}$  equals unity

$$D_h = 1.225 \sqrt{h_1} + 1.225 \sqrt{h_2} \tag{15}$$

In Figure 4 the calculated variation of received field intensity with distance has been plotted for the case of 1 kilowatt radiated, a transmitter antenna height of 500 feet, a receiving antenna height of 30 feet and a frequency of 40 megacycles. This curve illustrates the more rapid attenuation of signal beyond the horizon as well as the inverse square law variation within the horizon.

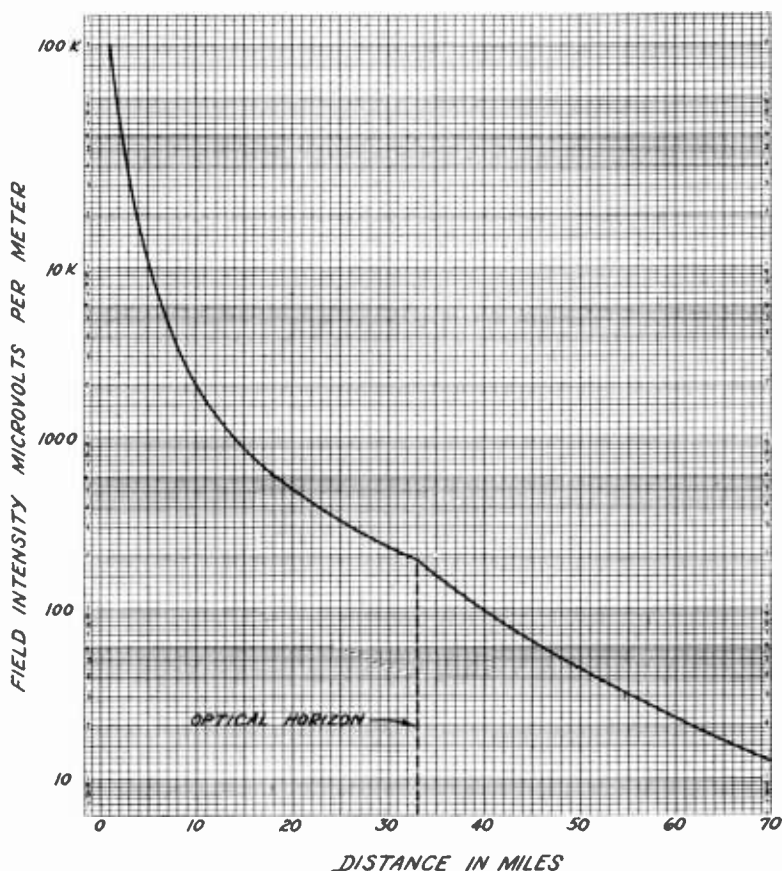


Fig. 4—Calculated field intensity variation

$W = 1$  kw.     $h$  Trans. = 500 ft.     $h$  Recvr. = 30 ft.     $f = 40$  mcs.

Measured field intensities frequently equal but seldom exceed the calculated values because of surface irregularities. The transmitter is usually located in an urban territory so that the effects of buildings are present at short distances and at longer distances hills frequently enter the picture to cause variations from the idealized smooth attenuation curve. The field intensity rises, often above the

calculated value, on the front slope of hills and drops below the calculated value behind the hill.

APPENDIX

It has been mentioned above that the simplified expressions are valid only for small angles of incidence and for earth with poor conductivity. For larger incidence angles, and in general over sea water for vertical polarization, more rigorous expressions are required because of the complex nature of the reflection coefficient.

The general expression for received field intensity is:

$$E = E_o \sqrt{(1 - K)^2 + 4K \sin^2 \frac{\phi}{2}} \tag{16}$$

where

- $E_o$  is the free space field given by (1) or (2)
- $K$  is the magnitude of the reflection coefficient
- $\phi$  is the phase difference in direct and reflected rays

The angle  $\phi$  includes phase change due to path difference,  $\delta$ , given by (4) and the phase rotation on reflection  $\alpha$ .

That is

$$\phi = \delta - \alpha \pm \pi \tag{17}$$

The complex reflection coefficient  $B$  being  $-Ke^{j\alpha}$

The complex reflection coefficient may be calculated from the following for vertical polarization:

$$B_v = \frac{\epsilon_o \sin \beta - \sqrt{\epsilon_o - 1 + \sin^2 \beta}}{\epsilon_o \sin \beta + \sqrt{\epsilon_o - 1 + \sin^2 \beta}} \tag{18}$$

$$= a_v + j b v$$

For horizontal polarization

$$B_H = \frac{\sin \beta - \sqrt{\epsilon_o - 1 + \sin^2 \beta}}{\sin \beta + \sqrt{\epsilon_o - 1 + \sin^2 \beta}} \tag{19}$$

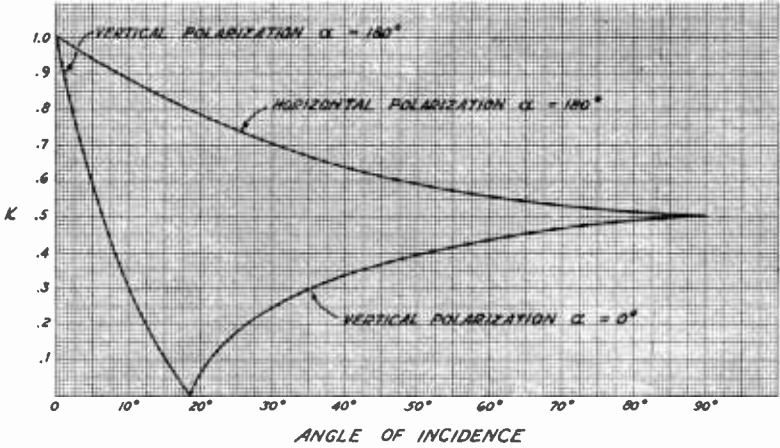


Fig. 5—Reflection Coefficient for Sandy Soil

$E = 9 \quad \sigma = 1 \times 10^6 \quad f = 50 \text{ mcs.}$

$$= a_H + j b H$$

$$\text{Then, } K = \sqrt{a^2 + b^2} \tag{20}$$

$$\alpha = \tan^{-1} \frac{a}{b} \tag{21}$$

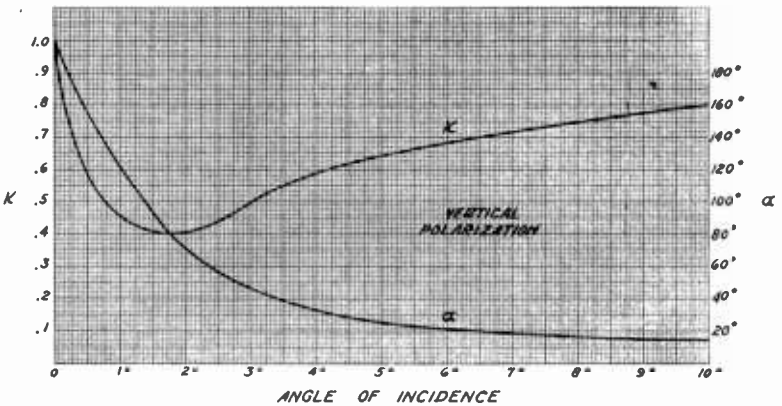


Fig. 6—Reflection coefficient for sea water.

$E = 80 \quad \sigma = 40 \times 10^9 \text{ e.s.u.} \quad f = 50 \text{ mcs.}$

For horizontal polarization  $K = 1.0 \quad \alpha = 180^\circ$

$$\epsilon_o = \epsilon - j \frac{2\sigma}{f} \quad (22)$$

$\beta$  = angle of incidence

Where

$\epsilon$  = dielectric constant of reflecting surface

$\sigma$  = conductivity of reflecting surface in e.s.u.

$f$  = frequency in cycles per second

Some typical values for  $\epsilon$  and  $\sigma$  are:

Type of Ground	$\epsilon$	$\sigma$
Sea Water	80	$40 \times 10^9$ e.s.u.
Fresh Water	80	$45 \times 10^6$
Sandy Soil	9	$1 \times 10^6$
Dry Soil	4	$0.1 \times 10^6$
Fertile Farm Land	15-25	$50-150 \times 10^6$

The complex reflection coefficient for the two cases of special interest, dry sandy soil and sea water, are plotted in Figure 5 and 6 respectively.

It may be seen that for vertical polarization under the dry ground condition changes from 180 degrees to 0 degrees at an angle of incidence of 18.5 degrees. This is the polarization or Brewster's angle in optics and is the angle at which  $\cot \beta = \sqrt{\epsilon}$ .

#### BIBLIOGRAPHY

1. G. N. Watson                      The diffraction of electric waves by the earth. *Proc. Royal Society, A*, 95, 1918.
2. R. Jouaust                         Some details relating to the propagation of very short waves. *Proc. I.R.E.*, March, 1931.
3. T. L. Eckersley                    Radio transmission problems treated by phase integral methods. *Proc. Royal Society, A*, 136 1932.
4. L. F. Jones                         A study of the propagation of wavelengths between three and eight meters. *Proc. I.R.E.*, March, 1933.

5. B. Trevor and P. S. Carter      Notes on propagation of waves below ten meters in length. *Proc. I.R.E.*, March, 1933.
6. J. C. Schelleng, C. R. Burrows, and E. B. Ferrell      Ultra-short-wave propagation. *Proc. I.R.E.*, March, 1933.
7. C. R. Englund, A. B. Crawford and W. W. Mumford      Some results of a study of ultra-short-wave transmission phenomena. *Proc. I.R.E.*, March, 1933.
8. C. B. Feldman      Optical behavior of the ground for short radio waves. *Proc. I.R.E.*, June, 1933.
9. W. H. Wise      Note on dipole radiation theory. *Physics*, October, 1933.
10. P. S. Epstein      On the bending of electro-magnetic micro-waves below the horizon. *Proc. Nat. Acad. Sci.*, January, 1935.
11. C. R. Burrows, L. E. Hunt and A. Decino      Mobile urban ultra-short-wave transmission characteristics. *Elec. Eng.*, January, 1935.
12. B. Trevor and R. W. George      Notes on propagation at wavelengths of seventy-three centimeters. *Proc. I.R.E.*, May, 1935.
13. C. R. Burrows      Radio propagation over spherical earth. *Proc. I.R.E.*, May, 1935.
14. Ross Hull      Air-mass conditions and the bending of ultra-high-frequency waves. *QST*, June 1935.
15. C. R. Englund, A. B. Crawford and W. W. Mumford      Further results of a study of ultra-short-wave transmission phenomena. *Bell Sys. Tech. Jour.*, July, 1935.
16. C. R. Burrows, A. Decino and L. E. Hunt      Ultra-short-wave propagation over land. *Proc. I.R.E.*, December, 1935.
17. P. von Handel and W. Pfister      Ultra-short-wave propagation along the curved earth's surface. *Proc. I.R.E.*, March, 1937.
18. P. S. Carter and G. S. Wickizer      Ultra-high-frequency transmission between the RCA building and the Empire State Building in N. Y. C. *Proc. I.R.E.*, August, 1936.
19. K. A. Norton      The propagation of radio waves over the surface of the earth and in the upper atmosphere. *Proc. I.R.E.*, October, 1936.
20. H. H. Beverage      Some notes on ultra-high-frequency propagation. *RCA Review*, January, 1937.
21. C. R. Burrows      Radio propagation over plane earth . . . field strength curves. *Bell Sys. Tech. Jour.*, January, 1937.



22. W. H. Wise                               The physical reality of Zenneck's surface wave. *Bell Sys. Tech. Jour.*, January, 1937.
23. C. R. Burrows                           The surface wave in radio propagation over plane earth. *Proc. I.R.E.*, February, 1937.
24. Ross Hull                               Air wave bending of ultra-high-frequency waves. *QST*, May, 1937.
25. T. L. Eckersley                       Ultra-short-wave refraction and diffraction. *Jour. I.E.E.*, 80, 1937.
26. K. A. Norton                           Physical reality of space and surface waves in the radiation field of radio antennas. *Proc. I.R.E.*, September, 1937.
27. K. A. Norton                           The propagation of radio waves over the surface of the earth and in the upper atmosphere. Part II. *Proc. I.R.E.*, September, 1937.
28. C. R. Burrows, A. Decino and L. E. Hunt                   Stability of two-meter waves. *Proc. I.R.E.*, May, 1938.
29. T. L. Eckersley and G. Millington                   Application of the phase integral method to the analysis of the diffraction and refraction of wireless waves around the earth. *Phil. Trans. Ray Soc.*, June 10, 1938.
30. B van der Pol and H. Bremmer                       The propagation of radio waves over a finitely conducting spherical earth. *Phil. Mag. Supp.*, June, 1938.
31. C. R. Englund, A. B. Crawford and W. W. Mumford           Ultra-short-wave transmission and atmospheric irregularities. *Bell Sys. Tech. Jour.*, October, 1938.
32. R. W. George                           A study of ultra-high-frequency wide band propagation characteristics. *Proc. I.R.E.*, January, 1939.
33. R. I. Smith-Rose and A. C. Stickland                   Ultra-short-wave propagation. *Wireless Engineer*, March, 1939.
34. H. O. Peterson                       Ultra-high-frequency propagation formulas. *RCA Review.*, October, 1939.
35. M. G. Crosby                           The Service Range of Frequency Modulation Waves. *RCA Review*, January, 1940.

# ULTRA-HIGH-FREQUENCY PROPAGATION THROUGH WOODS AND UNDERBRUSH\*†

BY

B. TREVOR#

Engineering Department, RCA Communications, Inc.,  
Riverhead, L. I., N. Y.

*Summary*—Measurements of the attenuation of field strength through 500 feet of woods and underbrush on a frequency of 500 Mc showed a loss of approximately 17 to 19 db in summer and 12 to 15 db in winter as compared with the propagation over level ground. No great difference was found between horizontal and vertical polarization.

At 250 Mc the attenuation through the same section of woods in winter showed a 10 db loss with horizontal and a 14 db loss with vertical polarization.

Transmission of 500-Mc signals over low scrub pines compared with that over sand ground showed a reduction of signal due to vegetation which can be interpreted as showing reflection rather than absorption of the indirect ray from a level considerably above ground or near the top of the vegetation.

## INTRODUCTION

SINCE the use of frequencies above three or four hundred megacycles is finding increased usefulness the question naturally arose concerning the effect of foliage on the propagation of these frequencies. We might ask two questions:

1. What is the attenuation introduced by woods and underbrush by transmission through such a mass?
2. What effect does the foliage have on the indirect ray reflected from ground when the direct ray is in the clear above the underbrush?

## MEASUREMENTS

A few experiments have been made in an attempt to partially answer these questions. A square patch of woods 500 feet per side on level ground was found which allowed a small 500-megacycle oscillator to be set up at one corner of the woods. The radiating antenna was nearly six feet above ground. The receiver in a car was driven from the remote corner of the woods along its edge, passing the corner of the woods 500 feet from the transmitter, and emerging in the clear in order to observe the difference in signal intensity as propagated over flat ground as compared with propagation through the trees and undergrowth. The receiving antenna was about 7 feet above ground.

\* Decimal Classification: R113.5.

† Reprinted from *RCA REVIEW*, July, 1940.

# Now with the Research Department, RCA Laboratories Division, Riverhead, L. I., N. Y.

Measurements were made in July with full foliage out and again in November with no foliage present. Figure 1 shows a photograph of this patch of woods under winter conditions.

The results of these tests showed no appreciable difference between vertically and horizontally polarized transmissions in summer and an attenuation of 17 to 19 db due to the trees as compared with transmission over plain ground.

In November somewhat lower attenuations were obtained since the foliage had dropped off. Using vertical antennas the attenuation was approximately 15 db and with horizontal antennas 12 db.

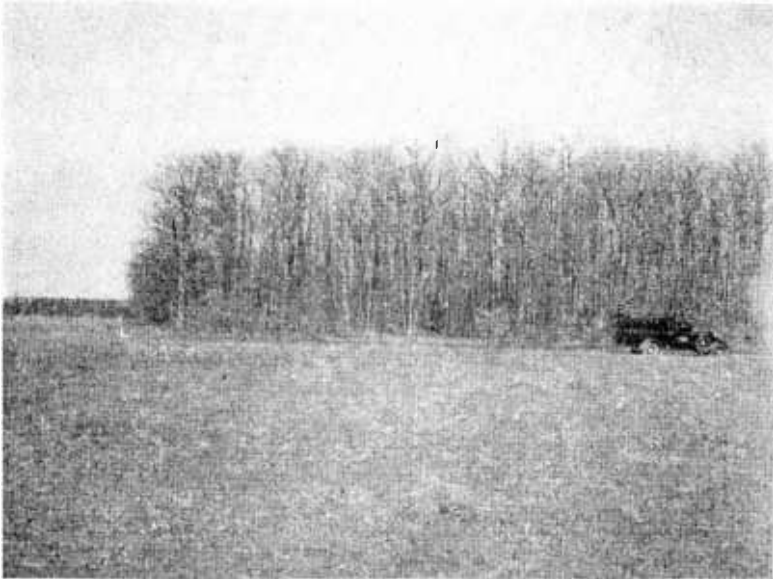


Fig. 1

The growth of vegetation was sufficiently dense to obstruct the view of the transmitter even with no foliage present.

Also in November a similar test was made on a frequency of 250 Mc. In this case the attenuation was measured to be 14 db with vertical and 10 db with horizontal antennas. Summer measurements on this frequency have not been made.

It should be pointed out that the accuracy of these measurements is not very great due to the bad standing wave patterns in space which were observed on the far side of the woods. The values shown above represent the best average that could be obtained.

In July 500-Mc transmissions were observed over a 500-foot span

of level ground and compared with transmissions of 500 feet over low scrub pines. The antennas were above  $8\frac{1}{2}$  feet above ground and the height of the undergrowth was approximately 5 or 6 feet. The ground at this location was nearly pure sand. With vertical antennas transmission over the vegetation showed a loss of 8 db compared with transmission in the clear. With horizontal antennas the attenuation was 6 db. Figure 2 is a photograph showing a portion of the scrub pine area.

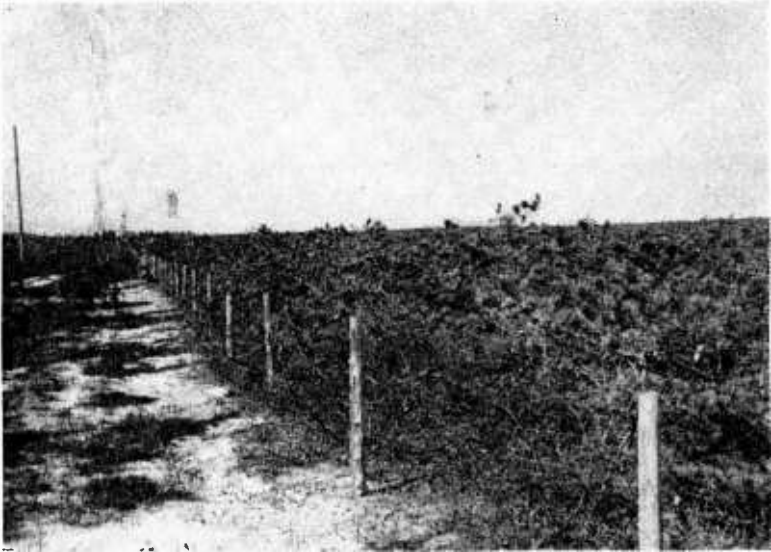


Fig. 2

#### CONCLUSION

From these measurements we conclude that there is considerable attenuation of ultra-high-frequency waves in passing through woods and underbrush and that there is little difference between vertically and horizontally polarized waves. And there is a noticeable difference in the attenuation between summer and winter conditions due to the absence of green foliage in winter. There is an indication that the horizontally polarized waves are attenuated somewhat less, particularly under winter conditions.

Since the signal was attenuated with transmission over low scrub pines we are led to conclude that the indirect ground ray was reflected from a level above that of the sand ground rather than absorbed by the vegetation. Under the conditions of measurement an absorption of the ground ray by the vegetation would have given an increase in signal.

# PROPAGATION STUDIES ON 45.1, 474, AND 2800 MEGACYCLES WITHIN AND BEYOND THE HORIZON\*†

BY

GILBERT S. WICKIZER AND ARTHUR M. BRAATEN

Research Department, RCA Laboratories Division,  
Riverhead, L. I., N. Y.

*Summary*—Continuous recordings of field strength on 474 and 2800 megacycles, over a period of 13 months, revealed maximum values three to four times the free-space field at distances of 42.5 and 70.1 miles from the transmitting site atop the Empire State Building, New York City. Recordings on 45.1 megacycles during the same period, on a reduced schedule, did not exhibit the large variation found on the higher frequencies. Refraction was found to be greater in the summertime, the strongest periods occurring at night or in the early morning. Refraction greater than normal was not evident when the average wind velocity was above 13 miles per hour. A study of weather conditions during the periods of strongest refraction indicated that roughly 60 per cent of the gradients were of the frontal type, involving different air masses, and approximately 60 per cent of the gradients were higher than 100 feet above the earth's surface.

## INTRODUCTION

PROPAGATION studies in the very-high-frequency region (30 to 300 megacycles) have been reported by a number of investigators. The effects of reflection, diffraction, and refraction were outlined in an early paper by Schelleng, Burrows, and Ferrell.<sup>1</sup> As the laws governing propagation within the horizon became better known, more interest was focussed on the subject of variations observed at greater distances. Burrows, Decino, and Hunt have reported on the stability and fading characteristics of 150 megacycles over a nonoptical path.<sup>2</sup> Analysis on a statistical basis and correlation with atmospheric conditions require continuous observations for extended periods to attain worth-while results. The relatively early work of Hull on this subject was a valuable contribution in explaining the nature of refraction and revealing the magnitude of its effects.<sup>3-5</sup> Englund, Crawford,

\* Decimal classification: R113.501.

† Reprinted from *Proc. I.R.E.*, July, 1947.

<sup>1</sup> J. C. Schelleng, C. R. Burrows, and E. B. Ferrell, "Ultra-short-wave propagation," *Proc. I.R.E.*, vol. 21, pp. 427-463; March, 1933.

<sup>2</sup> C. R. Burrows, A. Decino, and L. E. Hunt, "Stability of two-meter waves," *Proc. I.R.E.*, vol. 26, pp. 516-528; May, 1938.

<sup>3</sup> R. A. Hull, "Air-mass conditions and the bending of ultra-high-frequency waves," *QST*, vol. 19, pp. 13-18; June, 1935.

and Mumford suggested that seasonal variation in refraction was due to corresponding changes in water-vapor content of the air, and they were able to verify the existence of dielectric-constant gradients through frequency-sweep methods.<sup>6,7</sup> MacLean and Wickizer demonstrated that fading was random and increased with distance.<sup>8</sup>

The rapid extension of the frequency spectrum in the centimeter region as a result of wartime research opened up a new field for propagation studies. The application of new techniques permitted construction and operation of equipment at frequencies far above the range of previous propagation studies. Thus a need was suddenly created for information on the propagation of signals in the ultra- and super-high-frequency bands (300 to 30,000 megacycles). The present paper describes the results of simultaneous field-strength measurements on 45.1, 474, and 2800 megacycles at two distant points, one of which was beyond the horizon. The more important meteorological factors influencing refraction in the lower atmosphere were studied.

### PROPAGATION PATHS AND EQUIPMENT

#### *Transmission Paths*

The transmitters were located in the tower of the Empire State Building, New York City, and the receiving locations were at Hauppauge and Riverhead, Long Island, New York, 42.5 and 70.1 miles distant, respectively. The transmission paths are shown on the map in Figure 1. The difference in azimuth between the two paths is 3 degrees. Although transmission was over land, the presence of large bodies of water on both sides no doubt influenced propagation conditions to some extent.

The profiles along the two transmission paths are depicted in Figures 2 and 3. Elevations above sea level are plotted vertically, while distances along the earth's surface are plotted horizontally. The datum line corresponding to sea level is in the form of a parabola, elevation

---

<sup>4</sup> R. A. Hull, "Air-wave bending of ultra-high-frequency waves," *QST*, vol. 21, pp. 16-18, 76-82; May, 1937.

<sup>5</sup> A. W. Friend, "A summary and interpretation of ultra-high-frequency wave-propagation data collected by the late Ross A. Hull," *Proc. I.R.E.*, vol. 33, pp. 358-373; June, 1945.

<sup>6</sup> C. R. Englund, A. B. Crawford, and W. W. Mumford, "Further studies of ultra-short-wave transmission phenomena," *Bell Sys. Tech. Jour.*, vol. 14, pp. 369-387; July, 1935.

<sup>7</sup> C. R. Englund, A. B. Crawford, and W. W. Mumford, "Ultra-short-wave transmission and atmospheric irregularities," *Bell Sys. Tech. Jour.*, vol. 17, pp. 489-519; October, 1938.

<sup>8</sup> K. G. MacLean and G. S. Wickizer, "Notes on the random fading of 50-megacycle signals over nonoptical paths," *Proc. I.R.E.*, vol. 27, pp. 501-505; August, 1939.

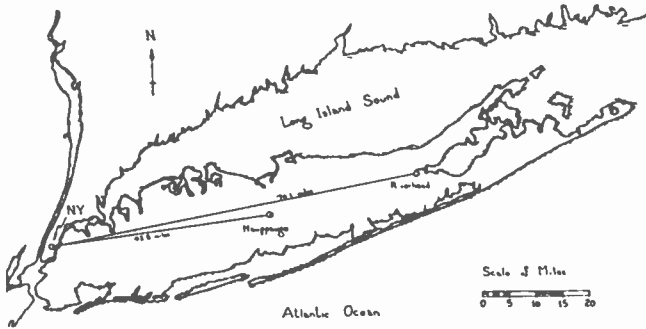


Fig. 1—Map of Long Island, showing locale of measurements. Transmission paths from Empire State Building to receiving sites at Hauppauge and Riverhead are indicated.

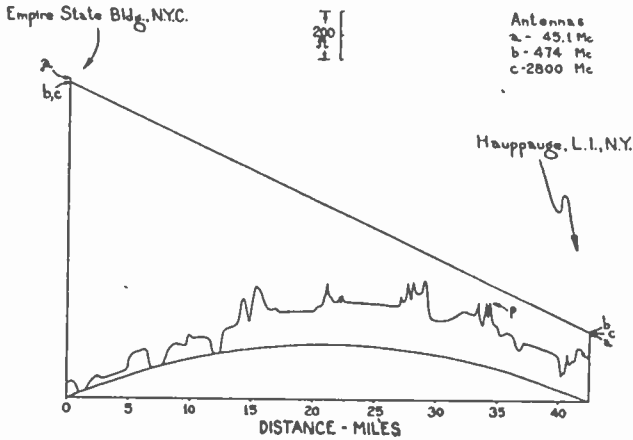


Fig. 2—Profile along optical path between New York and Hauppauge. Earth radius of  $4/3$  assumed, for condition of standard refraction. Observe elevated location of transmitters as compared with that of the receivers, and absence of unobstructed reflecting regions.

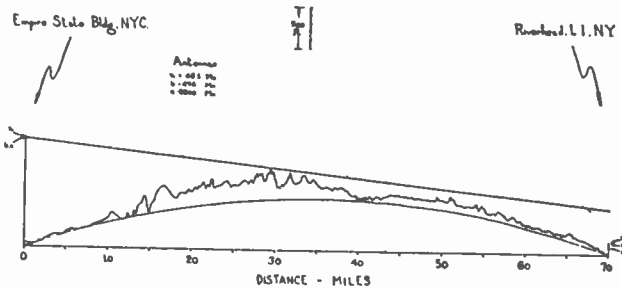


Fig. 3—Profile along nonoptical path between New York and Riverhead, based on  $4/3$  earth radius. Note presence of relatively high ground near center of path.

falling with distance from the mid-point of the path according to the relation

$$h = \frac{d^2}{2} \quad (1)$$

where  $h$  is in feet and  $d$  in statute miles. This relation is based on an earth's radius of  $4/3$  to correct for standard atmospheric refraction.

The foregoing method of representing transmission-path profiles is simple and convenient. Because of the radically different scale factors for height and distance which must be employed to show a useful amount of detail, curved lines and angles will become distorted; but all straight lines, such as the paths taken by direct and reflected rays, remain straight. The accuracy with which elevations and distances can be read from such a profile is limited only by the respective scales chosen for plotting.

The transmission path from the Empire State Building to the receiving site at Hauppauge was "optical" on a  $4/3$ -earth's-radius profile. The clearance between the direct ray and ground level at a distance of 34.3 miles from the transmitter was 70 feet. This point is indicated by  $p$  in Figure 2.

The transmission path to Riverhead was beyond the horizon; the receiving antennas were roughly 450 feet below line-of-sight on a  $4/3$ -earth's-radius profile. The earth's-radius factor had to be greater than 2.3 to provide an "optical" path to the two lower-frequency antennas, and the path to the 2800-megacycle antenna became "optical" when the radius factor was greater than 3.

### *Transmitting Equipment*

The regular transmissions of W2XWG, the frequency-modulated transmitter of the National Broadcasting Company, were used for the propagation study on 45.1 megacycles. The radiated power from this transmitter was equivalent to 750 watts in a horizontal half-wave doublet. The transmission schedule was from 2 to 10 P.M., Eastern Standard Time, daily, except Thursdays and Fridays. The power output was maintained within 0.5 decibel.

The transmitter on 474 megacycles was of the master-oscillator power-amplifier type, with a high degree of frequency stability. The transmitter output was 17.6 watts at the beginning of the test and 4.1 watts at the end of the test, a decrease of 6.3 decibels. The antenna was a special horn having a total aperture of 7 square feet. The width



of the radiated pattern at half-power points was 44 degrees in the horizontal plane and 27 degrees in the vertical plane. The equivalent radiated power was not measured directly, but was expressed as the resulting free-space field  $E_0$ . This was obtained from local measurements using the same receiving antenna as was used in the final installation. The voltage delivered by the receiving antenna and transmission line was measured under conditions of free-space propagation, at distances of 30 to 100 feet. The measured values were then extrapolated to distances of 42.5 and 70.1 miles to serve as the values of free-space received voltage at the distant receiving points. The output of a thermocouple monitor pickup in the transmitter horn was recorded continuously to provide a record of transmitter output. Vertical polarization was used on this frequency.

The 2800-megacycle transmitter contained a Westinghouse WL-410 klystron. The transmitter output decreased from 4.2 watts at the beginning of the test to 0.7 watt at the end of the test, a change of 7.8 decibels. The transmitter output was fed through a wave guide to a small horn having an aperture of 1.66 square feet. The width of the radiated pattern at half-power points was 14 degrees in the horizontal plane and 17 degrees in the vertical plane. The antenna was equipped with a thermocouple monitor similar to that in the 474-megacycle horn. Transmissions were vertically polarized on this frequency.

### *Receiving Equipment*

The receiving equipment at Hauppauge was installed in a temperature-controlled room and all supply voltages were regulated. Only the 474-megacycle receiver was equipped with automatic frequency control. The diode outputs of the three receivers were recorded individually on an Englehard four-color recorder, which operated at a chart speed of  $\frac{3}{4}$  inch per hour. Calibrations of receiver gains were checked with standard-signal generators three times weekly. A summary of the antenna systems used at Hauppauge is given in Table I.

The antenna facilities and receiving equipment at Riverhead were essentially duplicates of the Hauppauge installation. The receiving equipment was installed in two separate buildings which were temperature controlled. A small building housed the 45.1- and 474-megacycle receivers, while the 2800-megacycle receiver was located in one of the laboratory spaces where it could be watched more conveniently. An Englehard two-color recorder was used on 45.1 and 474 megacycles, and a Bristol moving-pen recorder was used on 2800 megacycles. The chart speed on the latter was 1 inch per hour. The antenna heights at Riverhead are listed in Table II.

Table I—Hauppauge Antennas

Frequency, (mega- cycles)	Antenna Type	Height, feet		Transmission Line	
		Above ground	Above sea level	Type	Loss (decibels)
		45.1	$\lambda/2$ doublet	82	280
474	Parabolic reflector, area 12.5 square feet	100	298	Coaxial	4.6
2800	Horn, area 5.6 square feet	90	288	Wave guide	1.3

Table II—Riverhead Antenna Heights

Antenna frequency (megacycles)	Height, feet	
	Above ground	Above sea level
45.1	132	154
474	124	145
2800	68	87

## DISCUSSION OF RESULTS

*General Observations*

The signal recordings from the three charts were analyzed, and plotted to show hourly ranges of signal strength on all frequencies at both receiving locations. The received fields were compared to their free-space values  $E_0$ , and the comparison expressed in decibels. This method of expressing field strength provides comparative measurements on the transmission path only, since equipment factors such as transmitter power, antenna gain, and transmission-line loss are measured and removed from the result. Thus, the quality of the transmission path may be quickly recognized. Sample plots illustrating the general performance of the three frequencies at Hauppauge and Riverhead, in summer and winter, are found in Figures 4 and 5.

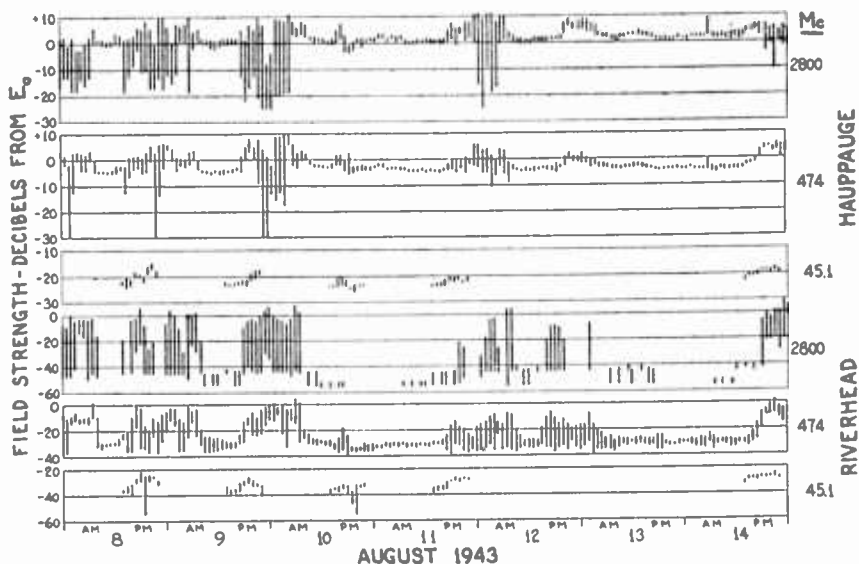


Fig. 4—Hourly ranges of field intensity, on three frequencies, at Hauppauge and Riverhead for period of August 8 to 14, 1943.

Continuous recordings of signal strength near the horizon usually exhibit a diurnal pattern in which the record is disturbed during the night and is relatively smooth during the daylight hours. The least disturbed period occurs in the early afternoon, usually about 2 P.M.,

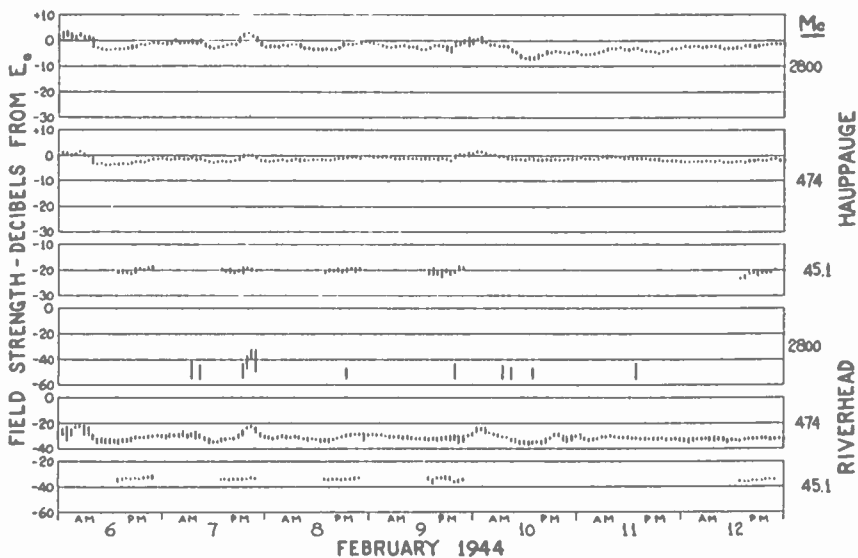


Fig.5—Same as Fig. 4, but for period of February 6 to 12, 1944.

local standard time. At this time of day, any atmospheric stratification which may have formed during the previous night has been broken up by convection, and transmission is through a turbulent medium. The amount of refraction at such times will be referred to here as "normal refraction," and the corresponding signal strength will be called the "undisturbed level." Usually, this level is easily recognized on the two higher frequencies, and is a convenient reference level to use as a basis for fading analyses.

*Transmission Within the Horizon*

As would be expected, reception within the horizon was marked by strong signals, with some fading present. Signal-strength variations were larger on the two higher frequencies, especially in the case of fading minimums. A summary of the measurements at Hauppauge is complicated somewhat by slight seasonal variations in the undisturbed levels. Values for the undisturbed levels contained in Table III are average values obtained over the period of the recording.

*Table III—Hauppauge Signal-Strength Summary*  
(All compared to  $E_0$ , in decibels)

Frequency (megacycles)	Undisturbed Level	Highest Maximum	Lowest Minimum
45.1	-21	-13	-29
474	- 4	+10.5	Below -30
2800	- 2	+12	Below -25

Attempts at determining the field strengths to be expected at Hauppauge on a theoretical basis, on the three widely separated frequencies, brought to light several interesting points. It will be evident, by referring to Figure 2, that regular reflections of the Empire State transmissions reaching the receiving antennas would be expected to originate in a region some eight miles short of Hauppauge. As can be seen, the profile in the vicinity of this point is quite irregular and is not an ideal reflecting surface. The terrain consists of several areas of reasonably flat ground a few miles in extent, separated from each other by small ranges of hills rising to about 100 feet above the surrounding ground. At 45.1 megacycles these hills represent roughness in the reflecting surface of 4 to 5 wavelengths in height. Theoretically, such roughness should not impair reflection at angles near grazing,

provided the roughness is fairly well distributed. Such does not appear to be the case here, as an examination of the profile will reveal. Nevertheless, reflection apparently is not seriously affected. The undisturbed level of 21 decibels below free space received on 45.1 megacycles at Hauppauge would be realized with a reflection coefficient of 0.9, with the reflection taking place on a plane coinciding with the top of the ridge designated by  $p$  in Figure 2. Any diffraction effect occurring on this frequency would appear to be masked by the relatively greater reflection effect.

At 474 and 2800 megacycles, the hills at  $p$  represent roughness of approximately 50 and 300 wavelengths, respectively, and these orders of roughness are theoretically too large to allow regular reflections. Calculated fields on the basis of reflection theory on these frequencies were not in as good agreement with measured values as they were on 45.1 megacycles. Evidently, on the higher frequencies, with obstruc-

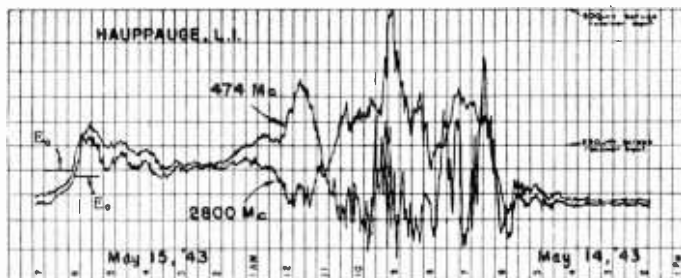


Fig. 6—Example of synchronous fading of opposite phase over an optical path, transcribed from record taken at Hauppauge.

tions of this size, the effects of diffraction predominate, and it was found that calculations on the basis of diffraction theory produced values which agreed well with measured values of undisturbed levels.

Signal traces on the two higher frequencies were observed to move in opposite directions during many of the disturbed periods. This opposite fading usually took the form of an increase in strength on 474 megacycles, and a slight increase, followed by a decrease, on 2800 megacycles. In many cases the 474-megacycle signal passed through a maximum at the same time that the 2800-megacycle signal was near its minimum level. This condition is not easily explained on the basis of the same transmission path for both frequencies, since the path difference to produce the first maximum on 474 megacycles would be 31.6 centimeters, while the path difference to produce the first minimum on 2800 megacycles would be 10.6 centimeters. An interesting section of chart, illustrating opposite fading within the horizon, is found in Figure 6. Two distinct types of signal-strength variation are present,

one in which the two frequencies vary in opposite directions, and the other in which both frequencies move together. This suggests that, in this case, a distinct change in propagation conditions took place between midnight and 1 A.M. The weather instruments at Hauppauge indicated a steep surface gradient in dielectric constant from midnight to 6 A.M., and the weather map taken at 1:30 A.M. showed the presence of relatively dry air at the surface, with overlying maritime tropical air, so it is quite possible that the opposite fading in the early evening was due to refraction at higher altitudes, and the smooth fading after midnight was due to the surface gradient.

The Hauppauge records were inspected to determine what proportion of the time that opposite fading occurred. Each month was

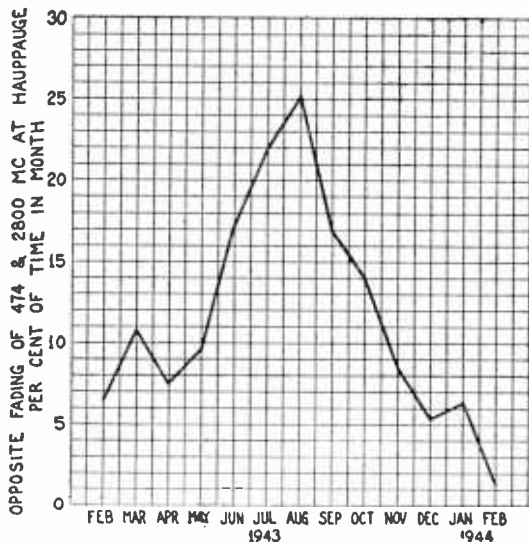


Fig. 7—Per cent of time in months in which opposite fading occurred on 474 and 2800 megacycles at Hauppauge.

analyzed separately, on an hourly basis, and the result plotted in Figure 7. Since opposite fading on this particular path was found to be an indication of strong refraction, it appears from this graph that conditions were most disturbed during August, and least disturbed during February, 1944.

A statistical analysis of the field-strength variation at Hauppauge is found in Figures 8, 9, and 10. Due to lack of time, it was not possible to analyze the 474- and 2800-megacycle signals with respect to  $E_0$ . Referring to Figure 8, the performance of 45.1 megacycles within the horizon exhibits a resemblance to a normal probability distribution, especially the data for the month of August. The relatively sharp drop

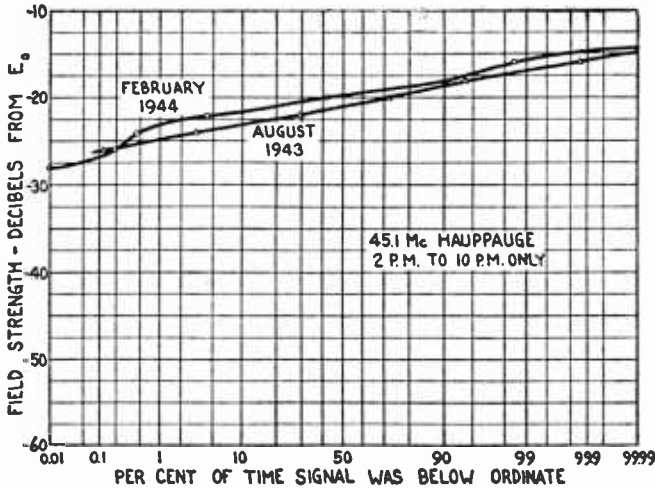


Fig. 8—Per cent of time per month that received field at Hauppauge on 45.1 megacycles was less than indicated level, referred to free space. Summer and winter conditions.

at the low end of the February curve was due to a single deep fade which may not have been representative, since there were three fades below  $-26$  decibels during August, which were not as long nor as deep. It is of interest to note that the field strength was generally greater in the winter, by a measurable amount. The average normal-refraction level in February was found to be 2.5 decibels higher than in August. It is possible that the reduction in field strength during the summer

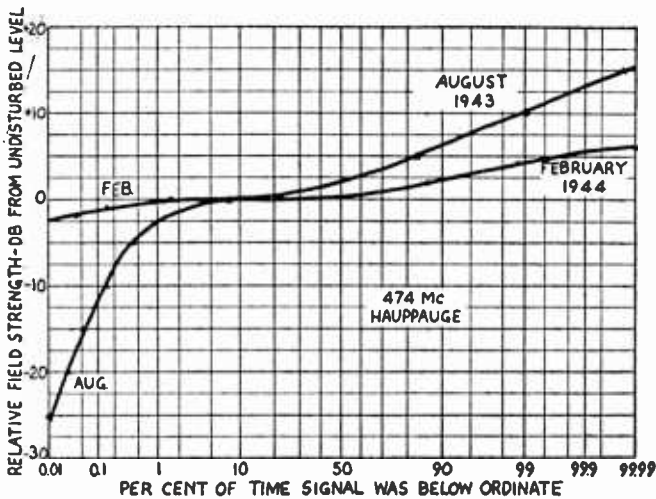


Fig. 9—Same as Fig. 8, but for frequency of 474 megacycles. Note that field here is compared to undisturbed level, rather than free space.

was due to improved reflection from vegetation, thus reducing the resultant of the direct and reflected rays. The normal-refraction level during August was 22.7 decibels below  $E_0$ , and during February, 20.2 decibels below  $E_0$ . Note that these curves are for the daily period of 2 P.M. to 10 P.M. Eastern Standard Time, only.

The greater signal-strength variation on 474 megacycles is evident in Figure 9, as is the difference in performance during summer and winter. In February, 474 megacycles showed less over-all variation than 45.1 megacycles, but more variation was present in the summer, especially below the undisturbed or normal-refraction level. On this frequency, the undisturbed level was also higher in February, by 3.3 decibels. The normal-refraction level in August was 5.8 decibels below  $E_0$ , and in February, 2.5 decibels below  $E_0$ .

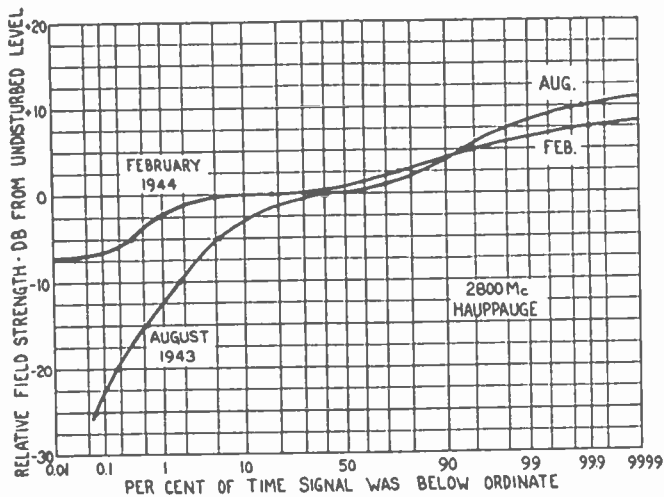


Fig. 10—Same as Fig. 9, but for 2800 megacycles.

Signal-strength variation on 2800 megacycles was greater than that on 474 megacycles, as indicated by Figure 10. Points of interest are the large proportion of the time that the higher frequency was below the undisturbed level in August, and the low minimum values of field strength recorded. During the summer, 2800 megacycles, within the horizon, was below the normal-refraction level for roughly ten times the length of time that 474 megacycles was. Comparison of the normal-refraction level in winter and summer on 2800 megacycles reversed the condition observed on the lower frequencies. The normal-refraction level in August was 0.8 decibel above  $E_0$ , and in February, 3.3 decibels below  $E_0$ , a difference of 4.1 decibels.



*Transmission Beyond the Horizon*

Performance beyond the horizon was marked by lower signal levels and greater variations than within the horizon. Comparing normal-refraction fields within and beyond the horizon, the highest frequency was attenuated most in passing over the horizon, and the lowest frequency was attenuated the least. Variations generally took the form of an increase in field strength, with the highest frequency showing the largest increase.

Curves showing the performance of 45.1 megacycles at Riverhead are found in Figure 11. The field strength was more variable in the summer, so at times there was no undisturbed level, or it was not clearly defined. From the available data, the undisturbed level appeared to be about 35 decibels below  $E_0$ , both summer and winter.

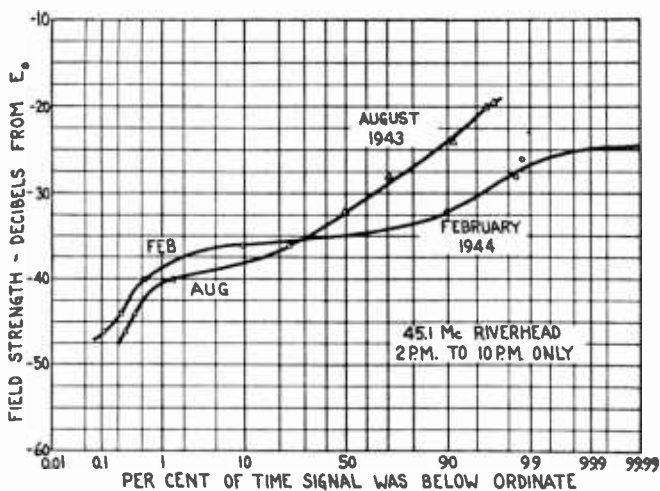


Fig. 11—Per cent of time per month that received field at Riverhead on 45.1 megacycles was less than indicated level, referred to free space. Summer and winter conditions.

The signal on 474 megacycles was more variable than that on 45.1 megacycles, as shown in Figure 12. The curves are approximate below  $-5$  decibels (from the undisturbed level) in August, and below  $0$  decibels in February, due to the low signal levels received on this frequency beyond the horizon. The undisturbed level on this frequency was about  $3$  microvolts delivered to the receiver input terminals. It is interesting to note that  $474$  megacycles beyond the horizon attained signal levels more than  $35$  decibels above the normal-refraction level. The maximum recorded on this frequency was  $10.5$  decibels above  $E_0$ . The normal-refraction level was slightly higher in the summer, being  $31.5$  decibels below  $E_0$  in August and  $33$  decibels below  $E_0$  in February, a difference of  $1.5$  decibels.

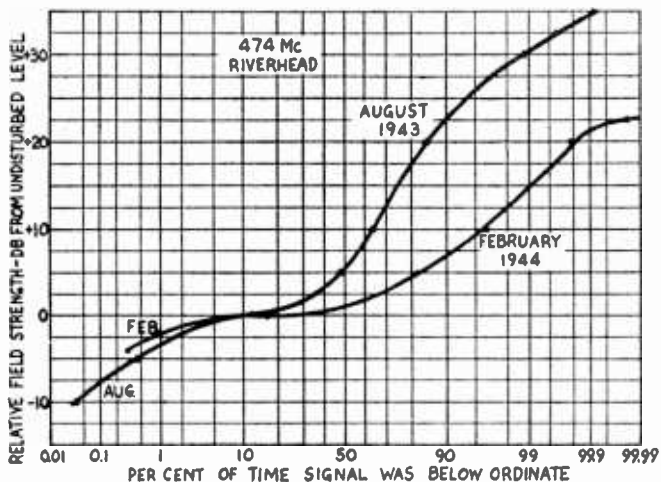


Fig. 12—Same as Fig. 11, but for frequency of 474 megacycles. Note that field here is compared to undisturbed level.

The normal-refraction level on 2800 megacycles at Riverhead was 50 to 60 decibels below the free-space value, and was too weak to measure quantitatively. For this reason, the field-strength recordings were compared to  $E_0$ , as shown in Figure 13. The seasonal variation is quite striking, as are the slopes of the curves. The maximum signal received was 13 decibels above  $E_0$ , and the minimum could not be discerned, so it is quite likely that the signal level was zero at times. In general, field-strength levels were appreciably higher on this frequency in the summer. In August, the signal could be heard through the day-

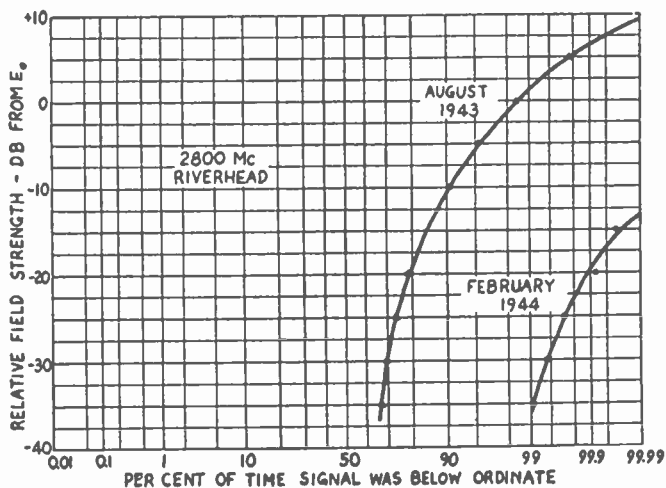


Fig. 13—Same as Fig. 11, but for 2800 megacycles.

light hours, with an average strength about 50 decibels below  $E_0$ . In February, however, the signal could be heard at 2 P.M. only about one day out of ten, at a level from 50 to 55 decibels below the free-space value. In general, the signal levels on 474 and 2800 megacycles followed the same broad pattern beyond the horizon, although the 474-megacycle signal showed less over-all variation.

Since the 2800-megacycle signal was most responsive to changes in propagation conditions, its performance was chosen for further study. The recordings were analyzed to determine the proportion of time that the signal was above  $-35$  decibels from the free-space value. A graph showing this characteristic by months is shown in Figure 14.

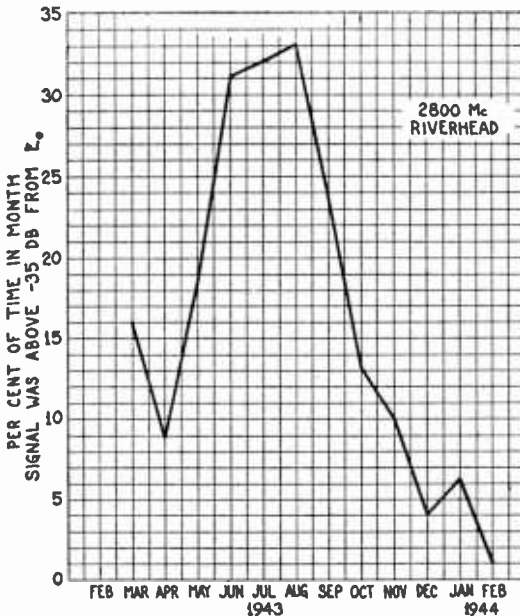


Fig. 14—Per cent of time, by months, that the 2800-megacycle field was sufficiently strong to produce a recordable signal beyond the horizon at Riverhead.

This graph is very similar to Figure 7, showing opposite fading at Hauppauge, especially during the winter months. While there appears to be, over a long period of time, a general correlation between opposite fading at Hauppauge and reception of 2800 megacycles at Riverhead, comparisons over shorter periods than a month do not show as good correlation. Under conditions of opposite fading at Hauppauge, the 2800-megacycle signal was usually received at Riverhead, but the converse did not hold. The seasonal nature of abnormal refraction is clearly demonstrated by this graph, with the most consistent strong

refraction occurring in the three summer months of June, July, and August.

The days and hours during which the 2800-megacycle signal exceeded 6 decibels above the free-space value at Riverhead were tabulated, and the corresponding weather conditions were analyzed. It was found that the signal exceeded the above level in 65 hourly periods, distributed over 37 days. Figure 15 shows the distribution of these conditions by months. The days with unusually strong refraction were rather uniformly distributed through the summer months, including the month of September. Although this graph indicates a definite maximum in August, 1943, the vagaries of the weather could conceivably shift the maximum to one of the other three months in which

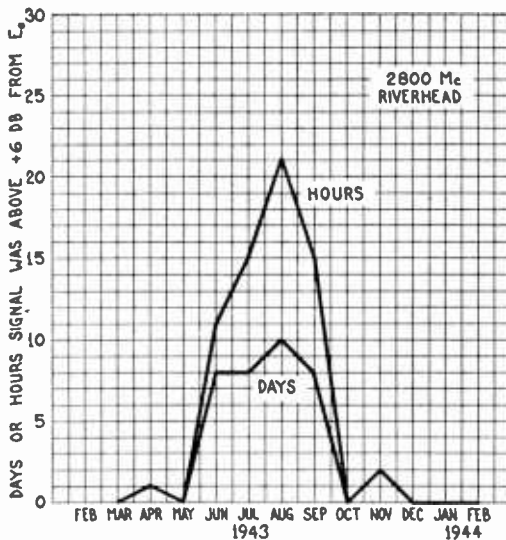


Fig. 15—Number of days and hours, by months, during which 2800 megacycles at Riverhead exceeded twice the free-space value.

unusually strong refraction periods occurred. Diurnally, the most prevalent time of unusually strong refraction was between 5:30 and 6:30 A.M.

## WEATHER STUDIES

### *Atmospheric Gradients*

The exceptionally high signal levels reached by the 2800-megacycle signal at Riverhead could not fail to arouse an interest in knowing more about the weather conditions which produced such strong refraction. Although very little time could be devoted to such a broad field,

it was hoped that some information could be obtained with the limited facilities available.

Two hair-type hygrothermographs loaned by the Radiation Laboratory of the Massachusetts Institute of Technology were installed at Hauppauge to record temperature and relative humidity of the air at two heights above the ground. From the measurements of temperature, pressure, and relative humidity, the dielectric constant of the air may be calculated from the following formula:

$$(\epsilon - 1) 10^6 = \frac{157.5}{T} \left[ p + \frac{4800e_m}{T} (R.H.) \right] \tag{2}$$

- where  $\epsilon$  = dielectric constant of the atmosphere
- $T$  = absolute temperature in degrees Kelvin
- $p$  = total atmospheric pressure in millibars
- $e_m$  = maximum water vapor pressure in millibars
- $R.H.$  = relative humidity ( $e/e_m$ ), in terms of pressure.

Knowing the value of the dielectric constant at two heights above ground establishes the dielectric-constant gradient,  $d\epsilon/dh$ . The labor of calculating the dielectric constant for continuous recording was shortened appreciably by neglecting the variations in atmospheric pressure, leaving only the constant pressure difference due to height, and by the construction of special nomograms which were much more accurate than the recording instruments. From the dielectric-constant gradient, the earth's-radius factor  $k$  was obtained from the relation

$$k = \frac{1}{1 + 10.4 \frac{d\epsilon}{dh} \times 10^6} \tag{3}$$

where  $d\epsilon/dh$  = dielectric-constant gradient.

Two plots comparing reception of signals at Riverhead with the equivalent earth's-radius factor measured at Hauppauge are found in Figures 16 and 17. There appears to be some correlation between the surface refraction at Hauppauge and reception of signals at Riverhead in the month of April, but refraction, in terms of  $k$ , in July is negative (i.e., bending greater than earth's curvature) most of the time. It might be pointed out that, under the circumstances, good agreement should not be expected. The concept of the factor  $k$  as a

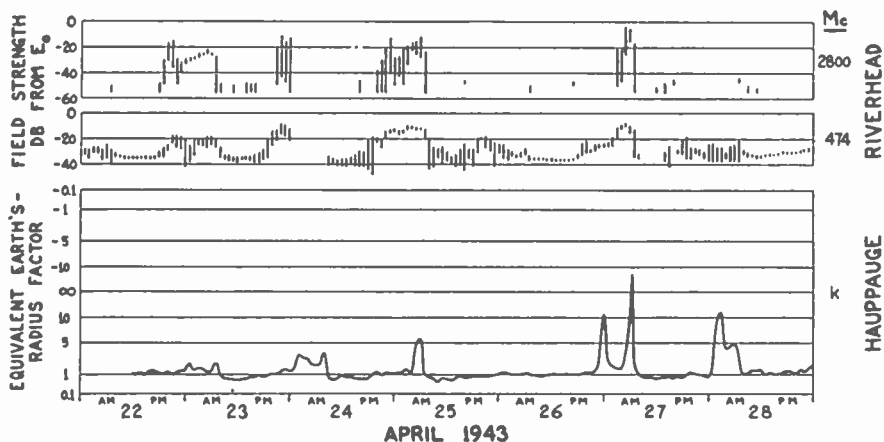


Fig. 16—Comparison of received fields on 474 and 2800 megacycles at Riverhead to surface refraction near center of path at Hauppauge, in April in terms of equivalent earth's radius.

measure of refraction presupposes a homogeneous atmosphere in which uniform bending of the ray takes place throughout the path. For the Riverhead path, such a condition, over an extended period of time, would be rarely encountered; atmospheric conditions, in general, would not be uniform either horizontally or vertically. A sample of the atmosphere taken at a single point along the path, and near the surface, would obviously not be representative of conditions along the path as a whole. Furthermore, it is quite likely that instrument errors were responsible for some of the extreme values of  $k$  in Figure 17.

The degree of accuracy required in weather instruments used for

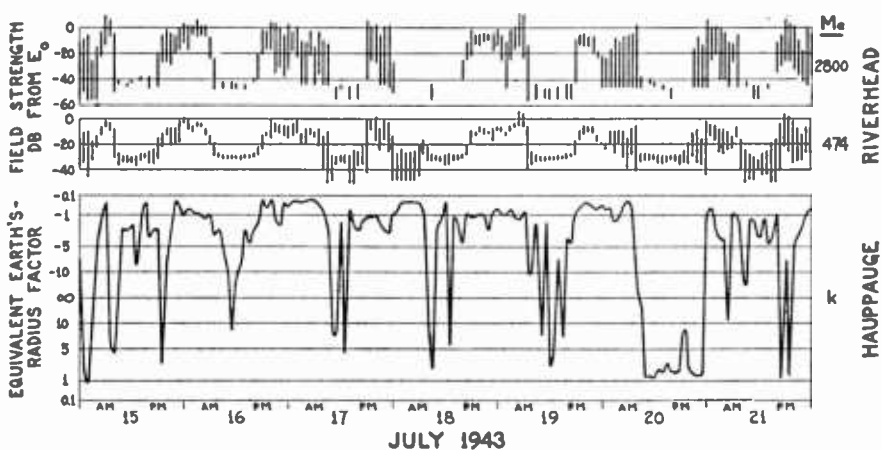
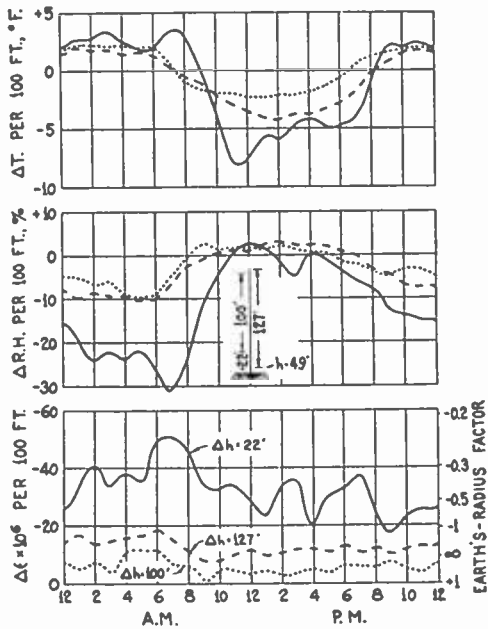


Fig. 17—Same as Fig. 16, but for month of July. Note sustained periods of strong refraction.

measurement of dielectric-constant gradients (and consequently  $k$ ) was found to be very great. This is due, for the most part, to the fact that the dielectric-constant gradient is determined from the difference between two values of dielectric-constant measured in a relatively small height interval. Working with height intervals in the vicinity of 100 feet, it was found desirable to be able to read temperature to 0.1 degree Fahrenheit, and relative humidity to 0.5 per cent.

In spite of the limitations of the weather instruments, it was hoped that some information of value could be derived from a study of records obtained with various height intervals, near the earth's

Fig. 18—Atmospheric gradient conditions at Hauppauge. Changes in temperature, relative humidity, and dielectric constant (for a constant height interval of 100 feet) for three layers near the earth's surface.



surface. If hourly values of difference in temperature and relative humidity are averaged over a sufficient period of time, any existing diurnal trend in the related dielectric-constant gradient should become apparent. The effects of random instrument errors would be minimized, although, of course, constant errors would be unaffected.

In Figure 18 will be found a comparison of gradients measured near the ground, at three different spacings in height. These three conditions permit inspection of a "thin" and a "thick" layer of air near the ground, and a fairly thick layer somewhat removed from the direct influence of the ground. In plotting the curves, all gradients were converted to a common height interval of 100 feet, in order to compare

their slopes. Unfortunately, it was not possible to conduct simultaneous measures at the various heights, but it was felt that the average of two weeks' data for each condition should be significant, especially if interpreted with the help of other weather information. Inspection of available weather records indicated that the general weather conditions were practically the same for the three measurement periods, which covered the interval from July 14 to August 28, 1943.

The curves of temperature and relative-humidity gradients (Figure 18) show, as might be expected, a temperature inversion and higher relative humidity at the surface during the night. However, the curves of the derived dielectric-constant gradients do not exhibit the definite trends of the corresponding temperature and relative-humidity gradients. In the diurnal heating and cooling of the same air mass, the relationship of the temperature and relative humidity is such as to result in a compensating effect on the value of the dielectric constant as calculated from (2). Thus it is possible to have definite changes in temperature and relative humidity, with little change in corresponding dielectric constant. Close inspection reveals a fairly definite increase of gradient about two hours after sunrise; this agrees with the early-morning increase in signal strength observed many times on the records at Riverhead.

From Figure 18, it is apparent that the steepest dielectric-constant gradients were in the 22-foot layer nearest the ground, followed by the 127-foot layer, with the smallest gradients in the 100-foot layer which was above the ground. This apparent irregularity is explicable as follows. The 100-foot layer was well above ground, and thus did not embrace gradients near the surface; the 127-foot layer included this surface region. Thus, the three curves are in agreement, and indicate that the largest dielectric-constant gradients are found nearest the earth's surface.

The general weather conditions prevailing during the periods of unusually strong refraction (Figure 15) were studied in an attempt to divide the types of gradient into three classes: (1) the frontal type, involving different air masses; (2) the radiation type, in which the lower layers of the same air mass are modified by the influence of the earth's temperature; and (3) a combination of the two types. Weather information was obtained from the daily weather maps, temperature and humidity recordings at two heights above ground at Hauppauge, and local observations at Riverhead. The Weather bureau co-operated by furnishing radiosonde data on days of especial interest. As a rule, the weather conditions to produce unusually strong refraction were definite enough to permit the type of gradient to be classified. The



analysis indicated that frontal gradients accounted for 62 per cent of the total number of hourly periods of unusually strong refraction; radiation gradients, 23 per cent; and a combination of the two, 15 per cent. Analysis of the temperature and relative-humidity recordings at Hauppauge revealed that a steep surface gradient of dielectric constant was present in 39 per cent of the hourly periods of unusually strong refraction, and no appreciable gradient was indicated in the remaining 61 per cent. Although these figures appear to duplicate those already given, there were cases of local movements of different air masses which were measured in a height difference of 100 feet, and there were other typical examples of radiation-type gradient in which both instruments indicated a high value of dielectric constant. Under the latter condition, the gradient producing the refraction was

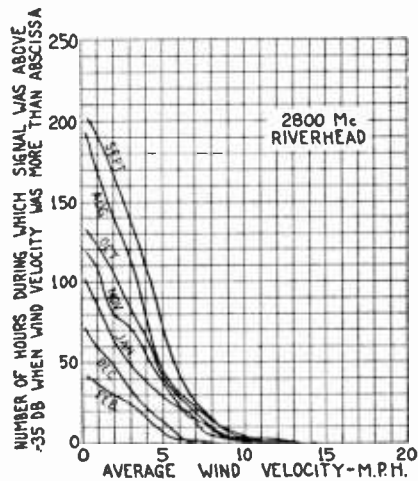


Fig. 19—Comparison, by months, of 2800-megacycle reception and surface wind velocity at Riverhead.

evidently above the weather instruments. From the above discussion, it may be concluded that the controlling gradient is more than 100 feet above the ground in about 60 per cent of the cases when unusually strong signals are received beyond the horizon on this particular transmission path.

*Wind Effects*

Since strong refraction is dependent on more or less stratified layers of air, the effect of wind would be to break up this stratification, especially near the surface of the earth. An anemometer was installed above 70 feet above the ground at Riverhead, to record the average wind velocity. Results of a study of the effect of surface wind velocity on the reception of 2800 megacycles at Riverhead are found in Figure 19. The curves represent the number of hours during

which the signal was above the receiver threshold when the average wind velocity was greater than indicated. The "number of hours" was obtained from the analyzed data for convenience, and does not represent true integrated time; the figure for wind velocity was an hourly average. The curves indicate a fairly definite upper limit to the surface wind velocity which would permit strong refraction on this radio circuit. This value was slightly over 13 miles per hour. The slopes of the separate curves are relatively constant at low velocities, suggesting that strong refraction was independent of surface wind velocity below 6 to 8 miles per hour. The gradual change in the slope of the curves for the individual months as the weather became colder is also of interest. The curve for August represents only 19 days; September was the first full month of wind-velocity recording.

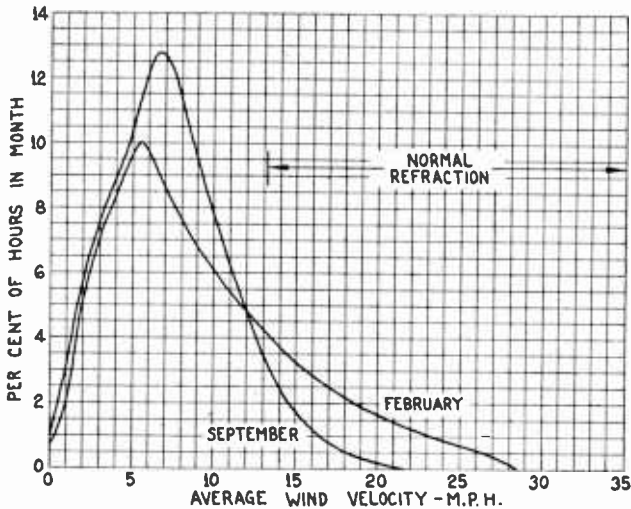


Fig. 20—Comparison of surface wind velocities for months of September and February. Normal refraction usually obtained for wind velocities above 13 miles per hour.

Figure 20 contains direct plots of the average wind velocity at Riverhead during the months of September, 1943, and February, 1944. The comparison indicates the more active circulation of air in the winter, which prevented the formation of gradients. Another point of interest is that, although the wind performance below 5 miles per hour was practically the same for September and February, the slopes of the curves for these months in Figure 19 are quite different, a direct indication that factors other than wind velocity were controlling refraction.

The weather records during the periods of unusually strong refraction shown in Figure 15 were chosen for further study. The

average wind velocity, during period of wind-velocity recording at Riverhead, was found to be 3.3 miles per hour, a value well down on the curves of Figure 19. The average water-vapor content of the air, as measured by the specific humidity, was 11.6 grams per kilogram of air. This corresponds to air at 70 degrees Fahrenheit, 74 per cent relative humidity, and 1000 millibars pressure, typical of summer conditions on Long Island. Since refraction is dependent on both temperature and water-vapor content, these cannot be discussed separately. In general, strong refraction was more frequent when the water-vapor content was high, as indicated above. Although refraction greater than normal was evident on rare occasions with specific humidities one-tenth the above value, such quantities of water vapor require severe temperature inversions to produce strong refraction, a condition seldom experienced on Long Island due to the stabilizing influence of the Atlantic Ocean and Long Island Sound.

### CONCLUSIONS

Within the horizon, the normal-refraction signal level tended to approach the free-space value as the frequency increased. Variations in field strength also increased with frequency, usually taking the form of a reduction in field strength at the highest frequency. Maximum levels observed on the higher frequencies were three to four times the free-space value. Opposite fading between 474 and 2800 megacycles within the horizon was most prevalent during the summer months, and, in general, was accompanied by strong refraction for the signals beyond the horizon.

Beyond the horizon, under conditions of normal refraction, the highest frequency became the weakest of the three. Variations in field strength were generally in the nature of an increase in field strength, especially at the highest frequency. Maximum values on 474 and 2800 megacycles were three and four times the free-space value, respectively. Refraction, as indicated by the reception of 2800 megacycles beyond the horizon, was at a maximum in August, and at a minimum in February.

In the field of weather studies, strong refraction did not take place when the surface wind velocity was greater than about 13 miles per hour. In studying gradients of dielectric constant near the earth's surface, the steepest gradients were found nearest the earth. Periods of unusually strong refraction beyond the horizon occurred most frequently in the summer, with the boundaries between different air masses predominating in the formation of gradients, usually at heights more than 100 feet above the surface of the earth.

## ACKNOWLEDGMENT

The project yielding the data upon which the material in this article is based was carried on under the sponsorship of the National Defense Research Committee of the Office of Scientific Research and Development. Many groups and individuals were instrumental in contributing to the success of the investigations. In particular, valuable assistance was given by the Propagation Group of the Radiation Laboratory of the Massachusetts Institute of Technology. The Empire State Building staff of the National Broadcasting Company rendered aid in operating the transmitting equipment. The Rocky Point group of RCA Laboratories designed and built the 474-megacycle transmitter used in the tests. Of those of the Riverhead group of RCA Laboratories who assisted in the work, particular credit is due E. N. Brown, who prepared the original nomograms used in the weather studies, and who did most of the analyzing of the recorded signal intensities.

# FIELD STRENGTH OF MOTORCAR IGNITION BETWEEN 40 AND 450 MEGACYCLES\*†

BY

R. W. GEORGE‡

RCA Communications, Inc., Riverhead, L. I., N. Y.

*Summary*—Measurements of motorcar-ignition peak field strength were made on frequencies of 40, 60, 100, 140, 180, 240, and 450 megacycles. Propagation was over Long Island ground and the receiving antennas were 35 feet high and 100 feet from the road. Under these conditions, the average field strength varied about 2 to 1 over the frequency range. Curves show the maximum field strength versus frequency for 90, 50, and 10 per cent of all the measurements. Vertical and horizontal polarization are compared showing slightly greater field strength, in general, for vertical polarization. New cars, old cars, and trucks are compared showing no large differences of ignition field strength.

Some of the factors involved in motorcar-ignition radiation are mentioned. Theoretical propagation curves are included and the measuring system is briefly discussed.

IT IS generally appreciated that motorcar ignition produces radio waves which are rather difficult to measure and evaluate. The annoyance factor of ignition interference cannot be established without reference to the type of communication service, the nature of the intelligence to be received, the over-all discrimination against, or tolerance for such interference, propagation factors, and the sources.

Ignition interference can, for a large number of services, be estimated when the probable peak value of ignition field strength is known. It is not practical to consider in this paper all the factors involved, but a given application will indicate the factors, some of which may be evaluated from the experimentally derived peak ignition field-strength curves. These curves were made from data taken with the receiving antenna 35 feet high and 100 feet from a standard two-lane highway near Riverhead, L. I., N. Y. The peak ignition field strength of each car was measured as it passed the point nearest the antenna.

The geometry of the propagation paths is shown in Figure 1. This receiving antenna height and distance were chosen as being what might be considered a fairly common receiving condition. If the height  $h$  above ground of the ignition source is assumed to be 2 feet, the angle

---

\* Decimal classification: R270.

† Reprinted from *Proc. I.R.E.*, September, 1940.

‡ Now with the Research Department, RCA Laboratories Division, Riverhead, L. I., N. Y.

of reflection  $\theta$  is about 20 degrees which is near the Brewster angle for Long Island ground. For this condition it was thought that vertically polarized waves would be received with a minimum of indirect-wave interference and therefore indicate the relative power radiated at the different frequencies. Apparently too many unknown transmission factors are involved to assume this to be true.

#### MEASURING EQUIPMENT AND METHODS

The receiver was of the superheterodyne type covering from 60 to 500 megacycles. The input to the first intermediate-frequency amplifier of 40 megacycles was brought to terminals to permit reception of 40-megacycle signals. The second intermediate-frequency amplifier at 4.1 megacycles was equipped with a relatively strong local oscillator to beat with incoming signals. The audio-frequency output was passed through a 5-kilocycle low-pass filter in order to determine the band width corresponding with the peak measurements. The filter output

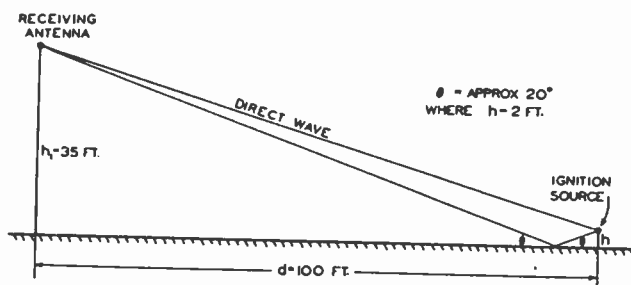
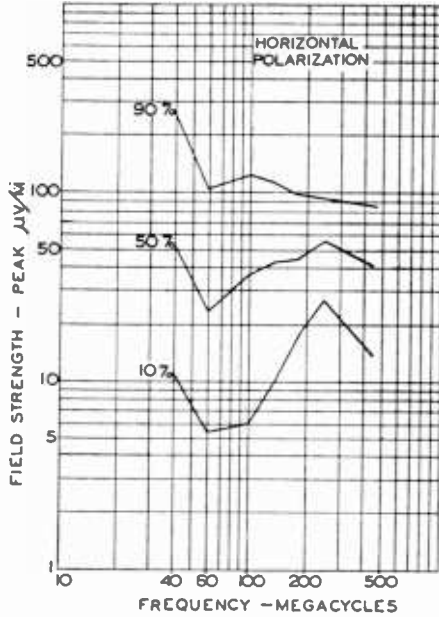


Fig. 1—Geometry of propagation paths.

was subsequently amplified and measured by means of a peak-voltage-indicating instrument. The peak-indicator circuits were such that only one or two short impulses, the minimum lengths of which were determined by the band width of the audio-frequency filter, were required to charge the condenser in a resistance-capacitance time circuit to over 90 per cent of the peak voltage of the impulse. The charging time was on the order of 15 microseconds. A decay-time constant of 1 second was used. This gave sufficient time to read the peak deflection on a properly damped milliammeter which was indirectly operated by the voltage across the time circuit.

Calibration of the peak indicator was obtained by reference to signal frequencies supplied by standard-signal generators connected to the transmission line in place of the antenna. Over-all equipment calibrations of this kind were made at each frequency. Half-wave dipoles were used to provide known antenna constants. At 450 megacycles, the dipole was backed by a parabolic reflector giving 11 decibels

Fig. 2—Motorcar-ignition radiation, horizontal polarization. Peak field strength versus frequency for a 10-kilocycle band. 90, 50, and 10 per cent of all cars and trucks produce less than the field strength indicated by the curves. Receiving antenna 35 feet high and 100 feet from road.



gain over a dipole in free space. This gain at 450 megacycles was desirable in order to provide signals strong enough to override the receiver noise. It is estimated that the errors of measurement were within plus or minus 2 decibels.

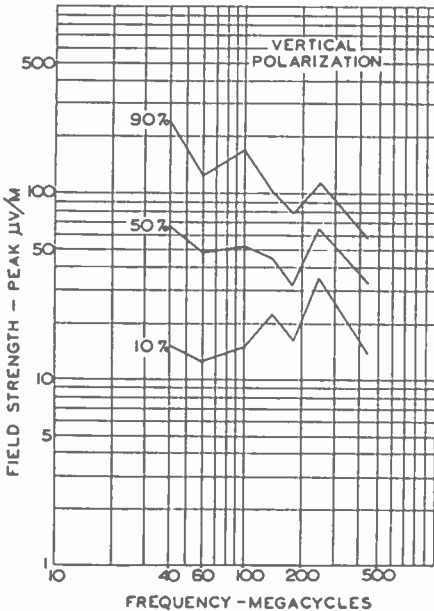


Fig. 3—Motorcar-ignition radiation, vertical polarization. Peak field strength versus frequency for a 10-kilocycle band. 90, 50, and 10 per cent of all cars and trucks produce less than the field strength indicated by the curves. Receiving antenna 35 feet high and 100 feet from road.

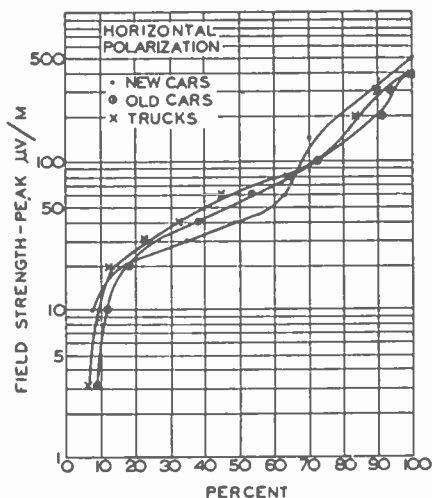


Fig. 4—Motorcar-ignition radiation at 40 megacycles for horizontal polarization. Curves show per cent of cars or trucks giving less than the indicated peak field strength for a 10-kilocycle band. Receiving antenna 35 feet high and 100 feet from the road.

The equipment was set up on a level plot of ground having a front-age clear of obstructions for over 100 feet on both sides. A few power and telephone wires on the opposite side of the road were not considered to be objectionable. Between 22 and 50 cars of each classification were measured at each frequency and polarization.

#### DATA

The peak ignition field-strength data are summarized in a general way in Figures 2 and 3. It will be noted that all data in this paper are for a band width of 10 kilocycles.

Figures 4 and 5 are for horizontal and vertical polarization, re-

Fig. 5—Motorcar-ignition radiation at 40 megacycles for vertical polarization. Curves show per cent of cars or trucks giving less than the indicated peak field strength for a 10-kilocycle band. Receiving antenna 35 feet high and 100 feet from the road.

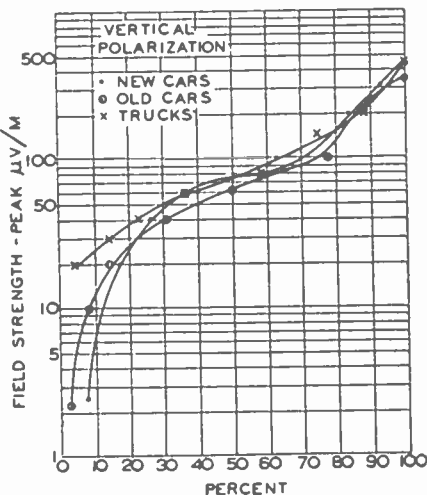
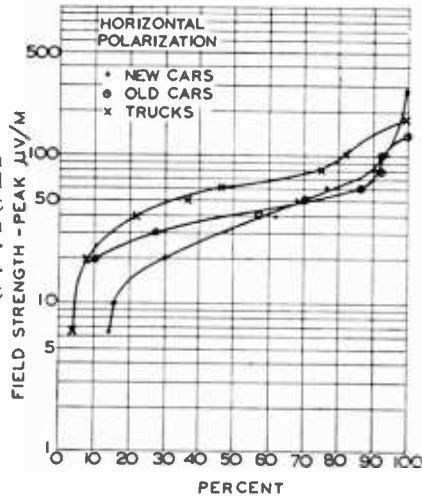




Fig. 6—Motorcar-ignition radiation at 180 megacycles for horizontal polarization. Curves show per cent of cars or trucks giving less than the indicated peak field strength for a 10-kilocycle band. Receiving antenna 35 feet high and 100 feet from the road.



spectively, showing the maximum field strength for 0 to 100 per cent of new cars (approximately 1936 to 1940 models), old cars, and trucks, at 40 megacycles. Figures 6, 7, 8, and 9 are data of the same type for the frequencies of 180 megacycles and 450 megacycles.

Figures 10 and 11 are theoretical propagation curves based on the use of a transmitting antenna 2 feet high and a receiving antenna 35 feet high. Calculations for both horizontal and vertical polarization are for reflection from earth having a dielectric constant of 10 and negligible conductivity in order to conform reasonably with the conditions under which the previous data were measured. From these curves the field strength at distances from 50 to 200 feet can be esti-

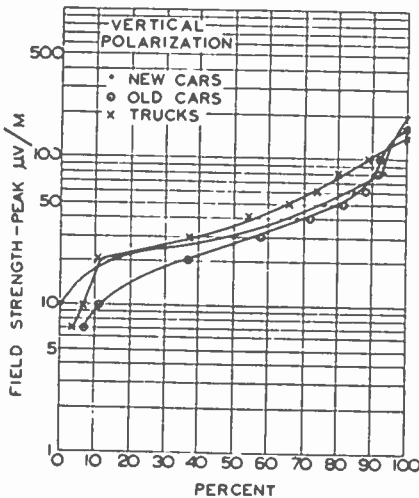


Fig. 7—Motorcar-ignition radiation at 180 megacycles for vertical polarization. Curves show per cent of cars or trucks giving less than the indicated peak field strength for a 10-kilocycle band. Receiving antenna 35 feet high and 100 feet from the road.

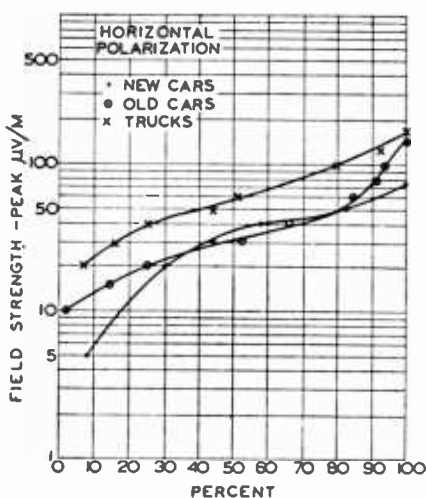


Fig. 8—Motorcar-ignition radiation at 450 megacycles for horizontal polarization. Curves show per cent of cars or trucks giving less than the indicated peak field strength for a 10-kilocycle band. Receiving antenna 35 feet high and 100 feet from the road.

ated by multiplying the actual field strength measured at a distance of 100 feet, by the indicated factor. The height of the transmitting source is assumed to be 2 feet which may be reasonable, however, this factor is probably variable and is difficult to determine.

#### CONCLUSIONS

Although these data are not comprehensive of the subject, they do show that appreciable motorcar-ignition interference can be expected at frequencies up to 450 megacycles. The height of the source above ground is indefinite. The radiation from the ignition system undoubtedly is modified by the body of the car which surrounds it.

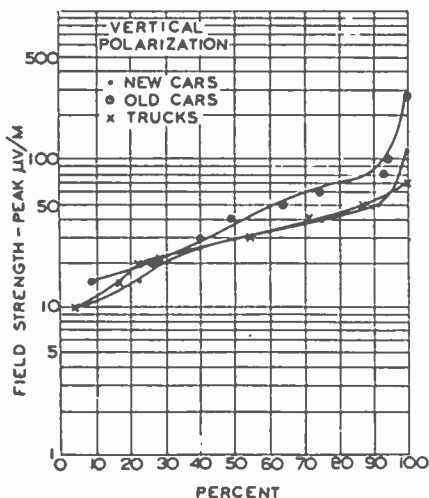


Fig. 9—Motorcar-ignition radiation at 450 megacycles for vertical polarization. Curves show per cent of cars or trucks giving less than the indicated peak field strength for a 10-kilocycle band. Receiving antenna 35 feet high and 100 feet from the road.

The polarization of the radiation can be of all kinds. Furthermore, these and other particulars are subject to variation even between cars of identical design. There are several factors which are favorable to the production of ignition interference at the higher frequencies. More or less obvious, these are improved propagation conditions due to increased phase difference between direct and reflected waves at

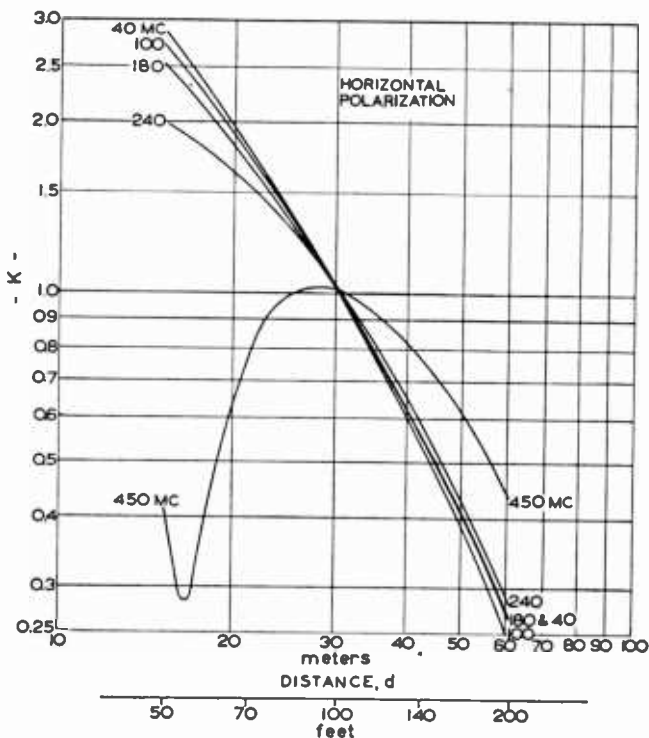


Fig. 10—Theoretical propagation curves for horizontal polarization. Field strength at distance  $d$  equals the field strength measured at a distance of 100 feet, times the indicated factor  $K$ . Transmitting and receiving antennas 2 feet and 35 feet high. Propagation over ground having a dielectric constant of 10 and negligible conductivity.

a given point except for short distances; and the metal sections of the car and the ignition leads are more comparable in size with short wavelengths, thus acting as less effective shields and more effective radiators. It will be apparent that the radio-frequency power in ignition systems could fall off considerably with increasing frequency and still produce substantial field strengths.

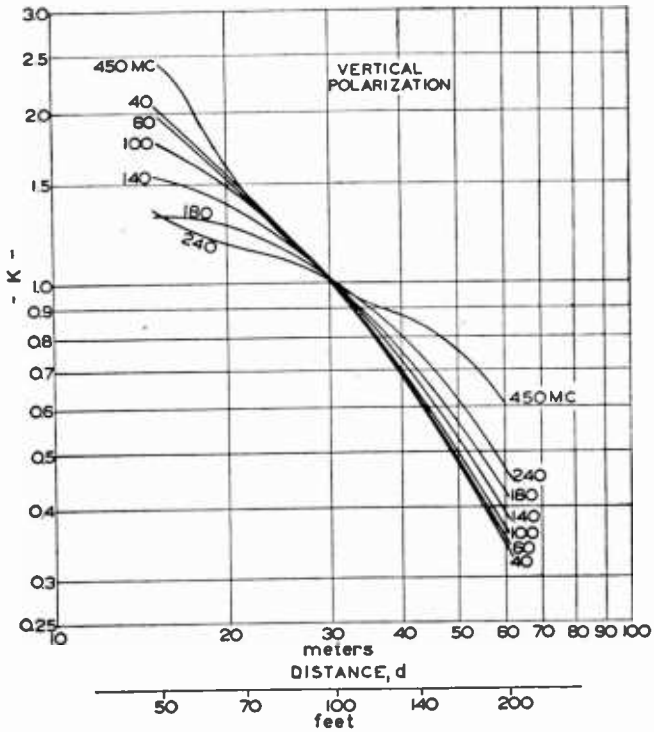


Fig. 11—Theoretical propagation curves for vertical polarization. Field strength at distance  $d$  equals the field strength measured at a distance of 100 feet, times the indicated factor  $K$ . Transmitting and receiving antennas 2 feet and 35 feet high. Propagation over ground having a dielectric constant of 10 and negligible conductivity.

# THE DISTRIBUTION OF AMPLITUDE WITH TIME IN FLUCTUATION NOISE\*†

BY

VERNON D. LANDON‡

RCA Manufacturing Company, Inc., Camden, N. J.

*Summary*—The purpose of this paper is to show that fluctuation noise has a statistical distribution of amplitude versus time which follows the normal-error law. This fact is also correlated with the measurements of crest factor made on the noise output of band-pass amplifiers by various investigators.

It is shown that the distribution of noise amplitude continues to follow the normal-error law, even after the noise has been passed through frequency-selective circuits. It is shown why the measurements of crest factor, made by various experimenters, group around the value 4, but it is pointed out that this is not a true crest factor because the voltage occasionally goes considerably higher. The ratio of the average to the effective voltage is shown to be 0.798. A discussion is given of the kinds of noise which do not follow this normal-error law.

FLUCTUATION noise is a name applied to thermal-agitation noise or to shot-effect noise. Thermal-agitation noise is the noise caused by the thermal motion of electrons in conductors. Shot-effect noise is the noise caused by the granular structure of the plate current of a vacuum tube. The term is sometimes reserved for the condition of no space charge. In the presence of space charge the noise amplitude is reduced. For this condition the noise may be called shot-effect noise as before or simply tube noise. These various types of noise source produce noises which cannot be distinguished one from the other by any known test.

Several investigators,<sup>1,4</sup> have made experimental investigations of the "crest factor" of fluctuation noise. The crest factor is defined as the ratio of the amplitude of the highest peaks to the root-mean-square

\* Decimal classification: R270.

† Reprinted from *Proc. I.R.E.*, February, 1941.

‡ Now with the Research Department, RCA Laboratories Division, Princeton, N. J.

<sup>1</sup> V. D. Landon, "A Study of the Characteristics of Noise," *Proc. I.R.E.* Vol. 24, pp. 1514-1521; November, 1936.

<sup>2</sup> M. G. Crosby, "Frequency Modulation Noise Characteristics," *Proc. I.R.E.*, Vol. 25, pp. 472-514; April, 1937.

<sup>3</sup> Karl G. Jansky, "An Experimental Investigation of the Characteristics of Certain Types of Noise," *Proc. I.R.E.*, Vol. 27, pp. 763-768; December, 1939.

<sup>4</sup> E. H. Plump, "Storverminderung durch Frequenzmodulation," *Hochfrequenz. und Electroakustik*, Vol. 52, pp. 73-80; September, 1938.

voltage. Various values have been obtained ranging from 3.4 to 4.5. It now appears that the required data can best be obtained from purely theoretical considerations.

From the standpoint of theory the term "crest factor" would seem to be a misconception. It will be shown that the noise is made up of an infinite number of components differing in frequency by infinitesimal amounts. If all these components should get in phase, the voltage would rise to an indefinitely large value, but the probability of this happening is infinitesimal. Nevertheless, if any finite crest factor is chosen, the probability that it will be exceeded at a given instant is a finite fraction. This probability is another name for the fraction of the time that the voltage will exceed the chosen value in a given long period of time.

To make the conception clearer let it be supposed that the noise output of a high-gain band-pass amplifier is fed to a diode. An adjustable direct-current bias is applied to the diode simultaneously and a tape recorder is arranged to record the time during which the diode is drawing current. With a given direct-current bias on the diode it would be possible to determine, by examining the tape, the percentage of the time during which the diode was drawing current. A point-by-point curve could then be plotted of direct-current bias, against the probability that the bias would be exceeded at a given instant.

By letting  $r$  stand for the ratio between any given direct voltage  $V$  and the root-mean-square value of the noise  $E$  and letting  $p$  stand for the probability that the noise will exceed the given direct voltage, it should be possible to find an analytical relationship  $p = F(r)$  which would determine the above curve from purely theoretical considerations.

#### THE CONDITIONS OF THE PROBLEM

Following is a review of the facts which are known about the problem. The energy of the noise is distributed uniformly over the frequency spectrum. If the noise is passed through a frequency-selective network the root-mean-square value of the noises in the output is proportional to the square root of the effective band width of the network. The noise is made up of a continuous spectrum of frequency components. The relative phase of the various components is random.

The last statement requires some further explanation. Considering shot effect as a typical example of fluctuation noise, the noise unit is due to the arrival of one electron on the plate. This may be considered to be an infinitesimal unit impulse. Unit impulse (the first derivative of the unit step) is known to have a uniform distribution of energy over the frequency spectrum. However, the phase of these

components is not random. The components are all in phase at the instant the unit impulse occurs. If two unit impulses occur at different times, the frequency components add with various phases. The resultant components have phases differing from the phases of components of the same frequency in either pulse alone. Exceptions are the few individual frequencies where the phases are the same for the two impulses. When the impulses occur at random times and the number of impulses is increased to an indefinitely large value, the relative phases of the various components have no discernible relationship and are said to be random. The term, random phase, is difficult to define accurately. As applied to only two incommensurable frequency components, the term is meaningless because the relative phase inevitably assumes all possible values as the two frequencies beat together. When speaking of a continuous spectrum of frequency components the phase may be said to be random if the following statement may be made about each frequency component. Let the phase of the component be observed every time the noise voltage passes through a certain value. The phase is as likely to have one value as another, regardless of what voltage is chosen for the measurements. Thus randomness of phase is seen to be a necessary condition to insure the accuracy of the relation that the root-mean-square value is proportional to the square root of the band width.

#### DERIVING THE ANALYTICAL RELATIONSHIP

The desired relation may be represented by

$$p = F(r) = F\left(\frac{V}{E}\right) = F\left(\frac{V}{\sqrt{n}}\right)$$

where  $n = E^2$ .

Let

$$p_v' = \frac{dp}{dV}$$

where  $dp$  is the probability of the voltage lying between  $V$  and  $V + dV$ .

Let the mean-square value of the noise be increased by adding an infinitesimal frequency component  $\Delta$ .

This added component is assumed to be very small compared to  $E$  as are all the other components of the noise. The magnitude is not necessarily equal to that of the other components, however. The probability  $p_v'$  will also be changed by the addition of this component. An equation relating this change in  $p_v'$  to the change in the mean-square voltage is derived below:

$\Delta$  is the root-mean-square value of an oscillatory voltage. The instantaneous value is  $\sqrt{2}\Delta \sin 2\pi ft$ . At any value of the time  $t_0$

the probability that the total resultant voltage will have the value  $V_0$  is the value of  $p_v'$  corresponding to  $V = (V_0 - \sqrt{2}\Delta \sin 2\pi ft)$ . Since the added component is negative just as much as it is positive,  $p_v'$  will change only if the curve has curvature at the point under consideration.

The relationship can be seen more clearly by expanding the value of  $p_v'$  as a Taylor's series.

Let  $p_0'$  be the value of  $p_v'$  corresponding to  $V_0$  in the absence of  $\Delta$ . Then with  $\Delta$  added

$$p_v' = p_0' + \frac{dp_v'}{dV} \sqrt{2} \Delta \sin 2\pi ft + \frac{d^2p_v'}{dV^2} \frac{1}{2} (\sqrt{2} \Delta \sin 2\pi ft)^2 + \dots \quad (1)$$

The second term does not affect the long-time value of  $p_v'$  because the average value is zero. The third term does change the value of  $p_v'$  because  $\sin^2 2\pi ft$  is always positive. The higher-order terms are negligible if  $\Delta$  is small. Hence,

$$\begin{aligned} dp_v' &= \frac{d^2p_v'}{dV^2} \frac{1}{2} 2\Delta^2 \sin^2 2\pi ft \\ &= \frac{d^2p_v'}{dV^2} \Delta^2 \frac{1 - \cos 2(2\pi ft)}{2} \end{aligned} \quad (2)$$

Averaged over a long time

$$dp_v' = \frac{\Delta^2}{2} \frac{d^2p_v'}{dV^2} \quad (3)$$

Now  $n = E^2$

$$n + dn = E^2 + \Delta^2.$$

Hence

$$\frac{dp_v'}{dn} = \frac{1}{2} \frac{d^2p_v'}{dV^2} \quad (4)$$

This is a well-known differential equation. The solution is

$$p_v' = \frac{A}{\sqrt{n}} e^{-V^2/2n} = \frac{A}{E} e^{-V^2/2E^2} = \frac{A}{E} \exp\left(-\frac{V^2}{2E^2}\right) \quad (5)$$

Now

$$\int_{-\infty}^{+\infty} p_v' dV = 1. \quad (6)$$

But

$$\frac{A}{E} \int_{-\infty}^{+\infty} \exp\left(-\frac{V^2}{2E^2}\right) dV = \frac{A}{E} \frac{2\sqrt{\pi} E}{\sqrt{2}} = 1 \quad (7)$$



Therefore

$$A = \frac{1}{\sqrt{2\pi}} \tag{8}$$

Therefore

$$p_v' = \frac{1}{\sqrt{2\pi} E} \exp\left(-\frac{V^2}{2E^2}\right) = \frac{1}{\sqrt{2\pi n}} \exp\left(-\frac{V^2}{2n}\right) \tag{9}$$

This solution may be checked by differentiating

$$\frac{dp_v'}{dn} = \frac{1}{\sqrt{2\pi n}} \exp\left(-\frac{V^2}{2n}\right) \left(\frac{V^2}{2n^2} - \frac{1}{2n}\right) = \frac{1}{2} \frac{d^2 p_v'}{dV^2} \tag{10}$$

As might have been expected, the desired function turns out to be the probability integral. The probability that the noise amplitude will lie between zero and any given voltage at a given instant is

$$p_a = \frac{1}{\sqrt{2\pi}} \int_0^r \exp\left(-\frac{r^2}{2}\right) dr = \frac{1}{2} \operatorname{erf}(r/\sqrt{2}) \tag{11}$$

where *erf* means the error function.

The probability that the given voltage will be exceeded is

$$p_b = \frac{1}{\sqrt{2\pi}} \int_r^\infty \exp\left(-\frac{r^2}{2}\right) dr = \frac{1}{2} \operatorname{erfc}(r/\sqrt{2}) \tag{12}$$

where *erfc* means the complement of the error function.

Since the probability that the given voltage will or will not be exceeded in a negative direction is the same as in a positive direction

$$2(p_a + p_b) = \sqrt{\frac{2}{\pi}} \int_0^\infty \exp\left(-\frac{r^2}{2}\right) dr = 1. \tag{13}$$

Functions described by the probability integral are said to follow the normal-error law. Other synonymous terms are the Maxwell-Boltzmann distribution or Maxwell distribution.

It has previously been demonstrated that a similar function applies to the velocity distribution of electrons emitted from a hot cathode.<sup>5-7</sup> However, the behavior of the resultant current in an associated external selective circuit was not considered in any of this previous work.

<sup>5</sup> Irving Langmuir, "The Effect of Space Charge and Initial Velocity on the Potential Distribution and Thermionic Current Between Parallel Plane Electrodes," *Phys. Rev.*, Vol. 21, pp. 419-435; April, 1923.

<sup>6</sup> Thornton C. Fry, "The Thermionic Current Between Parallel Plane Electrodes; Velocities of Emission Distributed According to Maxwell's Law," *Phys. Rev.*, Vol. 17, pp. 441-452; April, 1921.

<sup>7</sup> D. O. North, "Fluctuations in Space Charge Limited Currents at Moderately High Frequencies, Part II—Diodes and Negative-Grid Triodes," *RCA Review*, Vol. 4, pp. 441-472; April, 1940.

Dunn and White<sup>8</sup> relate the function to noise amplitude but give no theory or details.

#### ADDITIVE PROPERTY OF NORMAL-ERROR LAW

An important property of the normal-error law is expressed by the following theorem:

When the normal-error law applies to each of two voltages it also applies to their sum.

When the normal-error law does apply, then in any electrical network, the probability that a given voltage will be exceeded at a certain instant is

$$\begin{aligned} p_1 &= \frac{1}{\sqrt{2\pi}} \int_r^{\infty} \exp\left(-\frac{r^2}{2}\right) dr \\ &= \frac{1}{E_1\sqrt{2\pi}} \int_V^{\infty} \exp\left(-\frac{V^2}{2E_1^2}\right) dV \end{aligned} \quad (14)$$

where  $V$  is any direct voltage and  $E_1$  is the root-mean-square value of the noise.

In a second network

$$p_2 = \frac{1}{E_2\sqrt{2\pi}} \int_V^{\infty} \exp\left(-\frac{V^2}{2E_2^2}\right) dV. \quad (15)$$

When the noise outputs of the two networks are added algebraically the expression must retain the same form.

That is to say

$$p_3 = \frac{1}{E_3\sqrt{2\pi}} \int_V^{\infty} \exp\left(-\frac{V^2}{2E_3^2}\right) dV \quad (16)$$

where the subscript 3 refers to the two networks with outputs added.

Then  $E_3$  should equal  $\sqrt{E_1^2 + E_2^2}$ .

This theorem is proved in the following paragraphs.

#### PROOF OF THE ADDITIVE THEOREM

Now the probability that a noise voltage will lie between any two finite values of voltage is a finite number. However, as one value approaches the other the value of the probability approaches zero. That is, the probability of the voltage having a certain definite value is zero, unless a certain tolerance or range is allowed. However, the relative probability of the voltage having one value or another has a real meaning. This is best expressed as the probability per voltage

<sup>8</sup>H. K. Dunn and S. D. White, "Statistical Measurements on Conversational Speech," *Jour. Acous. Soc. Amer.*, Vol. 11, pp. 278-288; January, 1940.

interval. That is, of course, equivalent to the slope of the curve or  $dp/dV$ .

Thus the relative probability that the voltage of network 1 will have a certain fixed value  $V$  within any small fixed tolerance is

$$\frac{dp_1}{dV} = \frac{-1}{E_1\sqrt{2\pi}} \exp\left(-\frac{V^2}{2E_1^2}\right). \quad (17)$$

The relative probability that the voltage of network 2 will have a value  $V_0 - V$  is

$$\frac{-1}{E_2\sqrt{2\pi}} \exp\left(-\frac{(V_0 - V)^2}{2E_2^2}\right).$$

The relative probability that both voltages occur simultaneously and add to the value  $V_0$  is

$$\frac{1}{E_1E_22\pi} \exp\left(-\frac{V^2}{2E_1^2}\right) \exp\left(-\frac{(V_0 - V)^2}{2E_2^2}\right).$$

The summation of this probability for all possible values of  $V$  is

$$\frac{dp_3}{dV} = \frac{1}{E_1E_22\pi} \int_{-\infty}^{+\infty} \exp\left(-\frac{V^2}{2E_1^2} - \frac{(V_0 - V)^2}{2E_2^2}\right) dV. \quad (18)$$

Now

$$\begin{aligned} & \frac{V^2}{2E_1^2} + \frac{(V_0 - V)^2}{2E_2^2} \\ &= \frac{1}{2} \left[ \frac{E_1^2 + E_2^2}{E_1^2E_2^2} \left( V - V_0 \frac{E_1^2}{E_1^2 + E_2^2} \right)^2 + \frac{V_0^2}{E_1^2 + E_2^2} \right]. \end{aligned} \quad (19)$$

Hence

$$\begin{aligned} \frac{dp_3}{dV} &= \frac{1}{E_1E_22\pi} \exp\left(-\frac{V_0^2}{2(E_1^2 + E_2^2)}\right) \\ & \int_{-\infty}^{+\infty} \exp\left[\left(-\frac{E_1^2 + E_2^2}{2E_1^2E_2^2}\right) \left( V - V_0 \frac{E_1^2}{E_1^2 + E_2^2} \right)^2\right] dV \\ &= \frac{1}{E_1E_22\pi} \exp\left(-\frac{V_0^2}{2(E_1^2 + E_2^2)}\right) \\ & \cdot \int_{-\infty}^{+\infty} \exp\left(-\frac{E_1^2 + E_2^2}{2E_1^2E_2^2} S^2\right) dS \end{aligned} \quad (20)$$

where

$$S = V - V_0 \frac{E_1^2}{E_1^2 + E_2^2}$$

$$\frac{dp_3}{dV} = \frac{-1}{\sqrt{2\pi}\sqrt{E_1^2 + E_2^2}} \exp\left(-\frac{V_0^2}{2(E_1^2 + E_2^2)}\right) \quad (21)$$

$$p_3 = \frac{1}{\sqrt{2\pi}\sqrt{E_1^2 + E_2^2}} \int_{V_0}^{\infty} \exp\left(-\frac{V_0^2}{2(E_1^2 + E_2^2)}\right) dV_0. \quad (22)$$

This is the desired form of expression and  $E_3$  in (16) is found to equal  $\sqrt{E_1^2 + E_2^2}$  as required.

It has now been proved that when the normal-error law holds for each of two networks it will also hold for the sum of their outputs. (A similar theorem is proved by Scarborough.)<sup>9</sup>

The foregoing paragraphs prove that the summation of a large number of small sinusoidal components follows the normal-error law, regardless of the relative magnitudes of the various components, providing the phases are random. It is true, therefore, that the fluctuation-noise output of any frequency-selective network follows the normal-error law regardless of the shape of the selectivity curve.

This should not be taken to mean that the noise output of a vacuum tube follows this law at all times. Deviations from the law may be caused by a large hum component, microphonic noises, faulty insulation, flicker effect, etc. Nevertheless, if the noise is primarily of the type called fluctuation noise or hiss then the normal-error law does apply.

Hence in the output of any network passing fluctuation noise the expression

$$p = \frac{1}{E\sqrt{2\pi}} \int_V^{\infty} \exp\left(-\frac{V^2}{2E^2}\right) dV \quad (23)$$

is the probability that the noise voltage at any given instant will exceed the voltage  $V$  chosen at random. This may also be written in the form

$$p = \frac{1}{2} [1 - \text{erf}(r/\sqrt{2})] \quad (24)$$

where  $r = V/E$ , and  $\text{erf}$  denotes the error function.

In Figure 1 a curve is plotted of  $p$  versus  $r$ . The data for the curve were obtained from tables of the probability integral. The point on the curve at  $r = 0$ ,  $p = 0.5$  indicates that the voltage is above the zero axis half the time. The point at  $r = 1$ ,  $p = 0.16$  indicates that the voltage exceeds the root-mean-square value (in a positive direction)

<sup>9</sup>J. B. Scarborough, "Numerical Mathematical Analysis." Johns Hopkins, Baltimore, Md., 1930.

16 per cent of the time. The point at  $r = 4$ ,  $p = 0.000032$  indicates that the voltage exceeds 4 times the root-mean-square value for a total of 3.2 seconds out of 100,000 seconds. The curve is for one side of the wave only. For the probability that the absolute magnitude of the voltage will exceed a certain value, the probabilities given on the curve should be doubled.

#### AUDIO-FREQUENCY NOISE IN THE OUTPUT OF A DETECTOR

The foregoing applies only to the output of amplifiers or filters containing linear circuit elements. When radio-frequency noise from a band-pass network is applied to a detector the distribution of noise amplitude in the detector output circuit does not follow the normal-

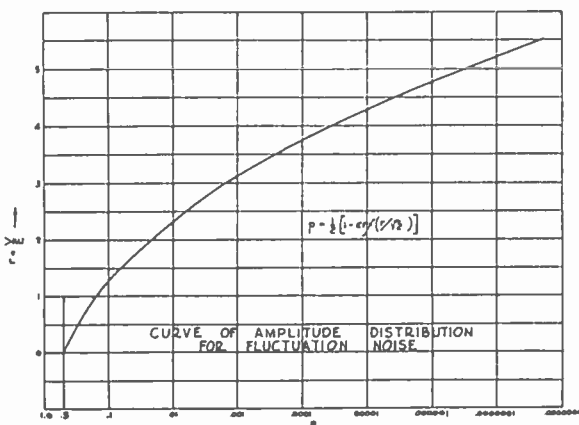


Fig. 1

error law. If no signal is present the deviation from the normal-error curve is quite marked. This is due to the fact that the audio-frequency output is the envelope of the peaks on one side only. The zero audio-frequency level corresponds approximately to the average of the radio-frequency voltage. The audio-frequency peaks in one direction correspond to zero radio-frequency voltage and thus are limited in amplitude to the value of the average radio-frequency voltage. Thus there is a distinct lack of symmetry. The voltage crests in one direction are definitely limited and in the other direction the voltage exceeds the values predicted by the normal-error law.

If a continuous-wave signal is applied to the detector at the same time as the radio-frequency noise, the audio-frequency noise in the output deviates less from the normal-error curve. If the carrier is considerably stronger than the highest peaks of the noise, the deviation becomes negligible. This statement is established by the following argument.

Consider a single-frequency component, differing from the signal carrier wave by a frequency interval  $f$ . This component will beat with the carrier, producing the frequency  $f$  in the detector output.

Now consider a group of components extending from the carrier frequency to the band limit. The audio-frequency output will consist of a group of audio-frequency components distributed from zero to the frequency corresponding to the difference between the carrier frequency and the band-limit frequency. The radio-frequency noise consists of a continuous spectrum of components having a random distribution of phase. The audio-frequency output of the detector will also consist of a continuous spectrum of components having a random distribution of phase. Therefore, it too will have an amplitude distribution following the normal-error law. Deviation from the law will occur only when the signal carrier does not exceed the noise sufficiently.

#### THE NUMBER OF CRESTS EXCEEDING $4E$ IN ONE SECOND

For convenience, in the following discussion, the response of an amplifier to unit impulse will be called a typical pulsation. In the low-pass case, the pulsation will have a shape of the general form of half a cycle of a sine wave or perhaps, roughly, the shape of the function  $\sin 2\pi f_c t/t$ . The exact shape depends on the attenuation characteristics. In the band-pass case the pulsation consists of a wave train. The intercepts of the zero line occur at the mean frequency of the pass band. The envelope of the wave train is the same as the pulsation wave shape of the low-pass case. In each case the time duration of the pulsation is about  $1/f_c$ , where  $f_c$  is the cutoff frequency in the low-pass case, and one half the band width in the band-pass case.

If the output of an amplifier consists of fluctuation noise, the wave form of the higher crests of the noise will be closely the same as the wave form of a pulsation due to unit impulse excitation. This statement is justified by the following reasoning. No peak can be narrower than a typical pulsation because this would require a wider pass band. The probability that a given peak will be much wider than a typical pulsation is small, particularly at the higher amplitudes. This is supported by the following data taken from the curve. The probability that the voltage at a given instant will exceed  $2E$  is 0.023. The probability that it will exceed  $3E$  is 0.001.

Of those peaks which exceed  $4E$  in amplitude the average height appears from the curve to be about  $4.15E$ . Using graphical methods, this leads to the following conclusion. The average peak which exceeds  $4E$ , exceeds it for about  $1/6$  of the duration of a typical pulsation, or for  $1/6f_c$  second. Thus the number of crests per second in excess of  $4E$  is approximately  $6f_c$  times 0.00003. When the band width is 10,000

cycles there will be an average of about 18 such peaks in 10 seconds.

The foregoing brings out the following curious fact. When a noise which follows the normal-error law has an equal distribution of components at all frequencies, then the value of the voltage at a given instant is quite independent of its values at preceding instants. On the other hand, when the frequency range of the noise is limited and the preceding wave form is given, the wave form may be extrapolated into the future for a short distance. This is particularly true if the instant chosen coincides with the time of occurrence of an unusually high peak, since the peak will probably have the form of a typical pulsation of the circuit which was used to limit the frequency band. Nevertheless, the normal-error law still applies over a long period of time.

It should also be pointed out that when random impulses are the source of noise and the frequency range is practically unlimited, the number of impulses must be very large if the normal-error law is to apply. When the frequency range is limited, then a smaller number of impulses will suffice. The restricted frequency band is necessary to cause the individual pulsations in the output to overlap adjacent pulsations. Even ignition interference may cause a noise which approximately follows the law if the noise is coming from many cars simultaneously and if the received frequency band is sufficiently restricted.

#### VARIATIONS IN MEASURED CREST FACTOR

It follows from the above that the number of peaks exceeding  $4E$  in a given time is proportional to the band width of the amplifier. Some observers might tend to set the limit at a certain number of peaks per second regardless of band width. If this were done, the "crest factor" derived on this basis would tend to be slightly greater for wide-band amplifiers than for narrow. This may account for the apparent variation in crest factor shown by Plump<sup>1</sup> (Figure 2 in his paper).

#### THE VALUE OF THE AVERAGE VOLTAGE

It may be of some interest to give the value of the average voltage using the error function. Sokolnikoff<sup>10</sup> shows how the average value of the error function is derived.

The mean absolute value of the voltage is twice the summation of all positive values of the voltage multiplied by the probability of occurrence of each. That is,

<sup>10</sup> I. S. and E. S. Sokolnikoff, "Higher Mathematics for Engineers and Physicists," McGraw-Hill Book Company, New York, N. Y., 1934, p. 393.

$$|\bar{V}| = 2 \frac{1}{\sqrt{2E\sqrt{\pi}}} \int_0^{\infty} V \exp\left(-\frac{V^2}{2E^2}\right) dV \quad (25)$$

$$= \sqrt{\frac{2}{\pi}} \frac{1}{E} \left[ E^2 \exp\left(-\frac{V^2}{2E^2}\right) \right]_0^{\infty} = \sqrt{\frac{2}{\pi}} \frac{1}{E} E^2 \quad (26)$$

$$= E\sqrt{2/\pi} \quad (27)$$

$$\frac{|\bar{V}|}{E} = \sqrt{2/\pi} = 0.798. \quad (28)$$

The measured value obtained by Jansky<sup>3</sup> is 0.85.

### CONDITIONS FOR VALIDITY

As previously pointed out, the curve of Figure 1 is valid regardless of the shape of the selectivity curve of the band-pass amplifier under consideration. The only requirement is that the noise-frequency spectrum be continuous and that the components have random phase angles.

It is well known that certain types of noise have a voltage distribution differing widely from that of the curve of Figure 1. In any given case the reason for the departure can usually be found. Ignition noise is a prominent example and, of course, the reason for the deviation is at once apparent in this case. The cause of the noise is a series of discrete impulses. Each impulse causes its own independent wave train in the output. In general the wave trains do not overlap. The frequency components of a given wave train are not of random phase but start out all having the same phase. Thus the normal-error law does not apply.

With other exceptions also, the reason for the failure to follow the law can usually be found after a moderate amount of study. For example, in Crosby's paper,<sup>2</sup> the "crest factor" of fluctuation noise is shown to rise under certain conditions in a frequency-modulated receiver. The required condition is that the root-mean-square value of the noise be in the neighborhood of one quarter of the peak voltage of the carrier. Certain noise peaks then exceed the "improvement threshold" of the receiver and come through unduly amplified.

### CONCLUSION

It has been shown that the fluctuation-noise output of band-pass amplifier has a distribution of voltage versus time following the normal-error law. Thus a theoretical basis is established for appraising the measurements of crest factor made on the noise output of band-pass amplifiers by various investigators.<sup>1-4</sup> It is shown that there is some



slight justification for assigning the fixed value 4 to the crest factor, for convenience in making rough calculations. However, it must be remembered that it is not a true crest factor since occasional peaks go considerably higher. The ratio of the average to the effective voltage is shown to be 0.798. A discussion is given of the kinds of noise which do not follow the normal-error law.

#### ACKNOWLEDGMENT

The author wishes to acknowledge the invaluable suggestions and helpful criticism made by Dr. J. L. Barnes, Mr. B. J. Thompson, Dr. D. O. North and Dr. D. S. Bond.

---

#### DISCUSSION ON

#### "The Distribution of Amplitude with Time in Fluctuation Noise"†

K. A. NORTON<sup>1</sup>: In this paper the author finds that the distribution with time of the instantaneous amplitude of fluctuation noise is represented by the normal distribution. His derivation of this analytical result is not entirely clear and is apparently incorrect. If fluctuation noise may be represented analytically by a large number of unit impulses, each occurring at randomly different times, then, at any given frequency, the fluctuation noise may be considered to consist of a large number of oscillations (at that frequency) with random relative phases. Many years ago Lord Rayleigh<sup>2</sup> determined the probable distribution with time of the instantaneous amplitude of a large number  $n$  of oscillations with equal unit amplitudes and with random relative phases. The probability  $dp$  of a resultant amplitude between  $V$  and  $V + dV$  was found to be

$$dp = \frac{2}{n} e^{-(\exp - V^2/n)} V dV \quad (1a)$$

so that, after a simple integration, we find that the instantaneous

---

† Reprinted from *Proc. I.R.E.*, September, 1942.

<sup>1</sup> Office of the Chief Signal Officer, War Department, Washington, D. C.

<sup>2</sup> Lord Rayleigh, "On the resultant of a large number of vibrations of the same pitch and of arbitrary phase," *Phil. Mag.*, vol. 10, pp. 73-78; 1880; see also the book "Theory of Sound," 1894, second edition, paragraph 42a.

amplitude  $V$  will be exceeded for the percentage of time  $P$  given by

$$P = 100p = 100e(\exp - V^2/n), \tag{2a}$$

The above result may be generalized to apply to the case of a large number  $n$  of waves with random relative phases and with *unequal* amplitudes  $E_1, E_2, \dots, E_n$  such that  $E_i^2 \ll E_1^2 + E_2^2 + \dots + E_n^2$  for  $i = 1$  to  $n$ . In this case (1a) and (2a) become

$$dp = \frac{2}{E_1^2 + E_2^2 + \dots + E_n^2} e(\exp - V^2/(E_1^2 + E_2^2 + \dots + E_n^2)) V dV \tag{1b}$$

$$P = 100e(\exp - V^2/(E_1^2 + E_2^2 + \dots + E_n^2)). \tag{2b}$$

If we write  $E$  for the root-mean-square value of the resulting disturbance, then

$$E^2 = \int_0^\infty V^2 dp = E_1^2 + E_2^2 + \dots + E_n^2 \tag{3}$$

and we obtain the interesting result that the root-mean-square value of the resulting disturbance is equal to the root-sum-square value of the amplitudes of the individual oscillations. Thus we see that (1b) and (2b) may be expressed in terms of the root-mean-square value  $E$  of the resulting disturbance as follows:

$$dp = \frac{2}{E^2} e(\exp - (V/E^2)) V dV \tag{1c}$$

$$P = 100e(\exp - (V/E^2)). \tag{2c}$$

Equation (2c) is given graphically in Figure 1. We see by (2c) that  $V > 4E$ , for a percentage of time  $P = 0.0000113$  per cent;  $V > 3E$ , for a percentage of time  $P = 0.0123$  per cent; and  $V > 2E$ , for a percentage of time  $P = 1.83$  per cent.

The average value of the disturbance may also be easily determined. Thus

$$\bar{V} = \int_0^\infty V dp = \frac{\sqrt{\pi}}{2} E = 0.886E. \tag{4}$$

This value lies somewhat nearer the value  $0.85E$  as determined experimentally by Jansky<sup>3</sup> than the theoretical value of  $0.798E$  determined by Landon from the normal distribution.

It is obvious from (1b) and (2b) that the instantaneous amplitude of two disturbances, each with amplitudes distributed according to the Rayleigh law and with root-mean-square values  $E_a$  and  $E_b$ , would also be distributed according to the Rayleigh distribution and would have a root-mean-square value equal to  $\sqrt{E_a^2 + E_b^2}$ .

Having established the above theoretical relations, it is desirable to examine further the postulates on which these relations are based. In deriving the above equations, it was tacitly assumed that the amplitudes of the individual oscillations  $E_i$  remain constant over the period of time required for a measurement of  $E$ ,  $\bar{V}$ , or of  $P$ ; actually, a necessary and sufficient condition for the applicability of (1c), (2c), and

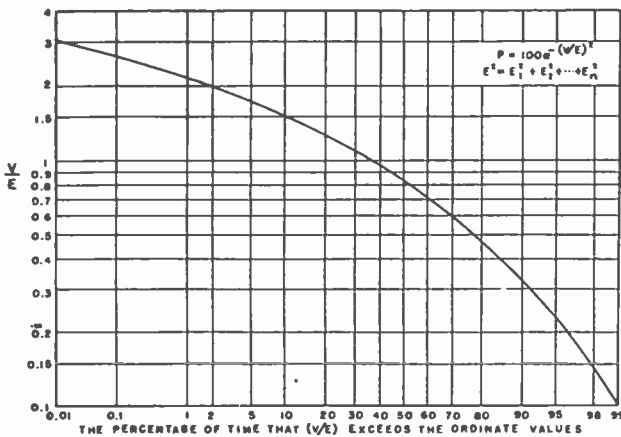


Fig. 1—The Rayleigh distribution.

(4) to fluctuation noise is the constancy of  $E$  over the period of time in question. If  $E$  also varies with time, then its distribution will be superimposed upon that given by the Rayleigh distribution.

It may be mentioned in passing that this same distribution applies to the instantaneous intensity of ionospheric waves (sky waves), irrespective of the radio frequency, but does not apply to tropospheric waves. In the study of the variation of ionospheric-wave intensities with time, since the root-mean-square value  $E$  of the disturbance varies with changes in the ionosphere absorption, the Rayleigh distribution will only apply for periods of time which are short enough not to include any large variations of ionospheric absorption; for frequencies in the

<sup>3</sup> Karl G. Jansky, "An experimental investigation of the characteristics of certain types of noise," *Proc. I.R.E.*, vol. 27, pp. 763-768; December, 1939.

standard broadcast band this period of time is of the order of one hour on the average.

VERNON D. LANDON<sup>4</sup>: The mathematics in Mr. Norton's discussion appears to be substantially correct (with minor exceptions). Paradoxically, the mathematics in my paper also is believed to be correct. The apparent discrepancy is due to the fact that we are not talking about exactly the same thing. The point can be cleared up by reference to Figure 2. In this figure the value of a noise voltage at a certain instant is represented by the point *V*. The instantaneous value of the envelope corresponding to *V* is represented by the point *A*. The *V* of my mathematics is the *V* of the figure. However, the *V* of Mr. Norton's mathematics is apparently the *A* of the figure.

Perhaps the choice of words in the title to my paper could have been improved upon. Had the title been "The Distribution of Voltage with

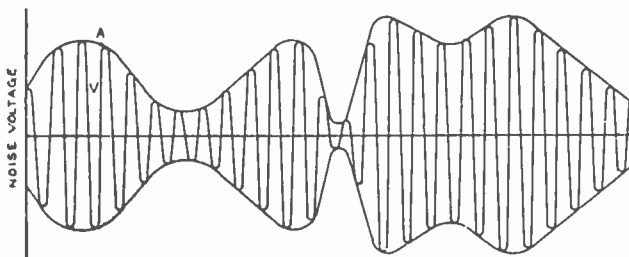


Fig. 2—Noise voltage wave showing envelope.

Time in Fluctuation Noise" there would have been less opportunity for misinterpretation. Instantaneous amplitude can perhaps be interpreted as meaning the value of the envelope. Actually, what was meant was the instantaneous voltage.

As I proved in my paper, the probability that the instantaneous voltage lies between *V* and *V* + *dV* is

$$dp_V = \frac{-1}{E \sqrt{2\pi}} \exp\left(-\frac{V^2}{2E^2}\right) dV. \tag{5}$$

Experimental proof is provided by Dunn and White<sup>5</sup> (Figure 14 of their paper). On the other hand, it can be shown that the probability that the instantaneous value of the envelope lies between *A* and *A* + *dA* is<sup>6</sup>

<sup>4</sup> RCA Manufacturing Company, Inc., Camden, New Jersey.

<sup>5</sup> H. K. Dunn and S. D. White, "Statistical measurements on conversational speech," *Jour. Acous. Soc. Amer.*, vol. 11, pp. 278-288; January, 1940.

<sup>6</sup> This relationship was first pointed out to me by Dr. D. O. North of the Research Laboratories of the RCA Manufacturing Company, Harrison, N. J.

5-

$$dp_A = \frac{A}{E^2} \exp\left(-\frac{A^2}{2E^2}\right) dA. \tag{6}$$

If the symbol  $V$  is substituted for  $A$  and the symbol  $n/2$  for  $E^2$ , the result is Mr. Norton's equation (1a). Mr. Norton bases his equations on Lord Rayleigh's work. Lord Rayleigh was concerned with the resultant amplitude when a large number of sine waves of the same frequency are added with random phase. By "amplitude" he meant the peak value of the resultant sine wave. When this peak value varies from moment to moment, it evidently traces out the envelope of the wave.

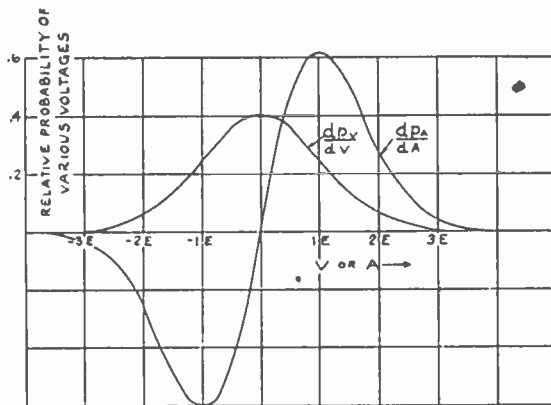


Fig. 3—Relative probability curves for instantaneous voltage and envelope.

I have defined  $E$  as the root-mean-square value of the noise voltage. In Mr. Norton's work,  $E$  is the root-mean-square summation of the *peak* values of a number of waves. Hence, his value of  $E$  is larger than mine by a factor  $\sqrt{2}$ .

The relationship between (5) and (6) can be made clear by reference to Figure 3 where  $dp_V/dV$  and  $dp_A/dA$  are plotted as functions of  $V$  and  $A$ . It should be noted that the probability of the envelope  $A$  going to zero is infinitesimal, while zero is the most probable value of the instantaneous voltage  $V$ . The reasonableness of this can be seen by reference to Figure 2.

It should be pointed out that the concept of an envelope to the noise voltage has a definite meaning only for noise which is confined to a relatively narrow frequency spectrum. If the noise has a bandwidth comparable to the mean frequency, or if the band includes zero frequency, then the fluctuations of the envelope occur about as rapidly

as the fluctuations of the voltage wave itself. For this case the concept of an envelope has little meaning.

It is of interest to note the similarity between the equations for molecular motion in a perfect gas and (5) and (6) of the present discussion. The distribution of molecular velocities in one, two, and three dimensions is as follows:

$$dp_u = - \sqrt{\frac{a}{\pi}} \exp(-au^2) du = \frac{-1}{\sqrt{2\pi E}} \exp\left(-\frac{u^2}{2E^2}\right) du \quad (7)$$

$$dp_r = 2ar \exp(-ar^2) dr = \frac{r}{E^2} \exp\left(-\frac{r^2}{2E^2}\right) dr \quad (8)$$

$$dp_s = 4 \sqrt{\frac{a^3}{\pi}} s^2 \exp(-as^2) ds = \sqrt{\frac{2}{\pi}} \frac{s^2}{E^3} \exp\left(-\frac{s^2}{2E^2}\right) ds \quad (9)$$

where  $u$ ,  $r$ , and  $s$  are, respectively, the magnitudes of the velocities on the  $x$  axis, in the  $xy$  plane, and in space.  $E$  is the root-mean-square velocity along the  $x$  axis in each case and  $a = 1/2E^2$ .

It can be seen that the expressions for  $dp_u$  and  $dp_r$  are identical to the expressions for  $dp_v$  and  $dp_A$  of (5) and (6).

The following additional facts about the envelope may be of some interest.

#### *The Probability that the Envelope Will Exceed the Value A*

The probability that the envelope will be greater than a certain voltage  $A$  at a given instant is

$$p_A = \int_A^\infty \frac{A}{E^2} \exp\left(-\frac{A^2}{2E^2}\right) dA = \exp\left(-\frac{A^2}{2E^2}\right). \quad (10)$$

Mr. Norton omits the 2 in the denominator of the exponent and, hence, his values are in error. Actually, if  $A = 4E$ , then  $p_A = e^{-8} = 0.00034$ . If  $A = 3E$ , then  $p_A = e^{-9/2} = 0.011$ . If  $A = 2E$ , then  $p_A = 2^{-2} = 0.135$ . As would be expected, these values are from ten times to three times the corresponding values for  $p_v$ . The increased values would be expected because the envelope encloses more area than the wave itself.

#### *The Most Probable Value of A*

The most probable value of the envelope is where  $d^2p_A/dA^2$  goes to zero.

$$\frac{d^2 p_A}{dA^2} = \frac{A}{E^2} \left( \frac{-A}{E^2} \right) \exp \left( -\frac{A^2}{2E^2} \right) + \frac{1}{E^2} \exp \left( -\frac{A^2}{2E^2} \right) = 0 \quad (11)$$

$$\frac{A_p^2}{E^4} = \frac{1}{E^2} \quad A_p = \pm E. \quad (12)$$

Thus, the most probable value of the envelope of a radio-frequency noise wave is equal to the root-mean-square value of the wave.

*The Mean Value of A*

The mean value of  $A$  is the integral from 0 to  $\infty$  of  $A$ , times the probability of occurrence of  $A$ .

$$\bar{A} = \int_0^\infty A \frac{A}{E^2} \exp \left( -\frac{A^2}{2E^2} \right) dA = E \sqrt{\frac{\pi}{2}} = 1.252E. \quad (13)$$

(Mr. Norton's value of  $0.886E$  is in error by the factor  $\sqrt{2}$  because in (1b),  $E_1, E_2$ , etc., are peak values not root-mean-square values. The mean absolute value of  $V$  is  $|\bar{V}| = 0.798E$  as proved in my paper.)

The value of  $\bar{A}$  is of some importance because it is the value of the direct-current output voltage from an ideal diode detector (when the ideal diode detector is defined as one in which the output voltage follows the envelope of the wave exactly).

*The Root-Mean-Square Deviation of A from its Mean Value*

The root-mean-square deviation of  $A$  from its mean value is the root-mean-square audio output of an ideal diode detector with noise but no signal applied. It is obtained by a simple integration as follows:

$$\begin{aligned} A_r &= \sqrt{\int_0^\infty \left( A - E \sqrt{\frac{\pi}{2}} \right)^2 \frac{A}{E^2} \exp \left( -\frac{A^2}{2E^2} \right) dA} \\ &= E \sqrt{2 - \frac{\pi}{2}} = 0.655E. \end{aligned} \quad (14)$$

*The Root-Mean-Square Value of A*

The root-mean-square value of  $A$  may be obtained directly by integration or from the following:

$$A_{rms} = \sqrt{A^2 + A_r^2} = \sqrt{2}E. \quad (15)$$

K. A. NORTON<sup>1</sup>: As Mr. Landon admits, his equations are for the distribution of voltage rather than amplitude with time. The equations given in my discussion give the correct distribution for the amplitude with time in fluctuation noise. There is no error of  $\sqrt{2}$  as Landon states; this may be seen by reference to (3) which proves that the root-mean-square value of the instantaneous amplitudes  $V$  of the disturbance averaged over a long period of time is equal to  $E$ . Landon was apparently confused by my statement that "the root-mean-square value of the resulting disturbance is equal to the root-sum-square value of the amplitudes of the individual oscillations"; as far as the experimenter is concerned, only the resulting disturbance can be observed and its root-mean-square value is just  $E$ .

Mr. Landon states that my equations are for the distribution of the envelope; that is correct to the extent that any useful meaning may be attached to the envelope of a noise disturbance in which the fluctuations are varying just as rapidly as the fluctuations of the voltage wave itself. My equations, however, are always applicable to the distribution of the amplitude of the fluctuation noise; this amplitude, which I have denoted by  $V$  (but which Landon denotes by  $A$ ), may be defined by the following equation for the instantaneous voltage of a disturbance of angular frequency  $\omega$  and phase  $\phi$ .

$$v = V \sin (\omega t + \phi) \quad (16)$$

where  $v$  denotes the instantaneous voltage and  $\phi$  is the phase of the instantaneous value of the disturbance. Note that  $V$  has positive values only while  $v$  will be negative for half of the time.

It is important to note that in Jansky's experimental work the average value of the envelope  $V$ , rather than the average value of the voltage  $v$ , was measured; this probably explains the close agreement between his experimental value and my theoretical value.

It is instructive to determine the distribution of the voltage  $v$  of fluctuation noise directly from (16). Since  $V$  is distributed between 0 and  $\infty$  in accordance with the probability law

$$dp/dV = \frac{2V}{E^2} e^{-(V/E)^2} \quad (17)$$

and since  $U \equiv \sin (\omega t + \phi)$  is independently distributed between  $-1$  and  $+1$  in accordance with the probability law



$$dp/dU = \frac{1}{\pi\sqrt{1-U^2}} \tag{18}$$

Then, using a theorem due to Huntington,<sup>7</sup> we may write for the distribution of the product  $UV = v$

$$dp/dv = \frac{2}{\pi E^2} \int_{-\infty}^{+\infty} \frac{V}{\sqrt{V^2 - v^2}} e(\exp - (V/E))^2 dV \tag{19}$$

If we set  $V^2 - v^2 = X^2$ , the integration may be performed and we obtain

$$dp/dv = \frac{1}{E\sqrt{\pi}} e(\exp - (V/E))^2 \tag{20}$$

This equation is not directly comparable to (5) for the probability of a voltage between  $v$  and  $v + dv$  since the  $E$  in (20) is the root-mean-square value of  $V$ . If we write  $E_v$  for the root-mean-square value of  $v$  we obtain

$$E_v^2 = \int_{-\infty}^{+\infty} v^2 dp = \frac{1}{E\sqrt{\pi}} \int_{-\infty}^{+\infty} v^2 e(\exp - (V/E))^2 dv = \frac{E^2}{2} \tag{21}$$

and we see that the root-mean-square value of  $V$  is  $\sqrt{2}$  times the root-mean-square value of  $v$ .

When  $E_v$ , as determined by (21), is substituted for  $E$  in (20) and (17) we obtain Landon's equations (5) and (6). Thus there is no discrepancy in the mathematics. However, since it is the distribution of the envelope  $V$ , which was measured experimentally by Jansky rather than the distribution of the voltage  $v$ , my relation  $\bar{V} = 0.886E$  is the one applicable to the experimental results instead of Landon's relation  $\bar{v} = 0.798E_v$ .

VERNON D. LANDON<sup>4</sup>: It now appears that Mr. Norton and I are in almost perfect agreement providing we both charitably agree to use the other fellow's latest definitions in reading his earlier work.

Thus in the title of my original paper, "The Distribution of Amplitude with Time in Fluctuation Noise," the word amplitude must be interpreted as the instantaneous voltage, as I intended. Fortunately,

<sup>7</sup> E. V. Huntington, "Frequency distribution of product and quotient," *Annals Math. Statistics*, vol. 10, pp. 195-198; June, 1939.

a more accurate wording is used in many places in the body of the paper.

In Mr. Norton's discussion when he speaks of "the root-mean-square value of a wave," he means not the root-mean-square voltage but something larger by the factor  $\sqrt{2}$ . (See equation (21).) Similarly, when he speaks of the average value of the wave he means not the average voltage but the average magnitude of the envelope.

Of the three of us, Jansky alone was quite lucid on these definitions. His use of the words, "effective, or root-mean-square voltage," and his defining equations (1) and (2) leave no room for doubt. He was trying to measure the ratio of the average voltage to the effective voltage, not the ratio of the average value of the envelope to the root-mean-square value of the envelope. What he actually measured is something else again. From his circuit diagrams, it appears that his measure of the average voltage might be nearer to the average value of the envelope, while his measure of the effective voltage might be accurate. If this were true the expected value of the ratio would be 1.252, which is still further from a check. Perhaps the point is not worth belaboring further. There seems to be no question now as to the theoretical values of the various ratios.

I, too, have derived the voltage distribution from the envelope distribution by a method similar to that of Mr. Norton. It should be pointed out that the proof depends on the assumption that the phase angle is random when the value of the envelope is given. This assumption appears to be quite justified.

It is a curious fact that the reverse derivation cannot be carried out by this method. Given the value of the instantaneous voltage, the phase angle is not random! This derivation has been carried out by another method but it is somewhat involved and need not be repeated here.

In spite of the initial misunderstanding I believe that the discussion has brought out important material not previously published. It is to be hoped that the controversy will not becloud the issue. I believe that (accepting the above definitions) either Mr. Norton's work or my own is an accurate treatment. Certain of the details brought out in the discussion should find important practical applications.

# THE ABSOLUTE SENSITIVITY OF RADIO RECEIVERS\*†

BY

D. O. NORTH ‡

Research Laboratories, RCA Manufacturing Company, Inc., Harrison, N. J.

*Summary*—The total random noise originating in a receiver has customarily been described in terms of the equivalent noise voltage at the receiver input terminals. A comparison of the signal-to-noise ratios of two receivers working out of identical antennas is thereby facilitated, but only so long as the coupling between antenna and receiver input is extremely loose.

This paper describes a method for rating and measuring the noise in complete receiving systems, antenna included. The proposed rating appears particularly applicable to ultra-high-frequency services and, more generally, to any service in which signal-to-noise ratio is made a prime consideration in receiver design and operation.

A portion of the study deals with the properties of receiving antennas, yielding as a by-product an alternative derivation of Nyquist's theorem concerning thermal fluctuations in passive networks.

A formula for absolute sensitivity is developed, which shows how the minimum usable signal-field strength is related to the operating wavelength, the antenna directivity, the local noise-field strength, the receiver bandwidth, and a number called the "noise factor", which is a basic measure of the internal noise sources of the receiver.

THE "Standards on Radio Receivers" adopted and published by the Institute of Radio Engineers in 1938, define the sensitivity of a radio receiver as "that characteristic which determines the minimum strength of signal input capable of causing a desired value of signal output".<sup>1</sup> So defined, the sensitivity is a measure of gain. The same report<sup>2</sup> takes cognizance of the fact that random fluctuations (noise) originating in the receiver set a limit to the useful sensitivity. Leaving a precise definition to those who write standards, we shall refer to this useful limit as the "absolute sensitivity", indicate in an elementary way its dependence upon certain properties of the receiver<sup>3</sup> and antenna, suggest methods for measuring it in the laboratory, and consider its modification by noise induced in the antenna.

\* Decimal Classification: R161.2.

† Reprinted from *RCA REVIEW*, January, 1942.

‡ Now with the Research Department, RCA Laboratories Division, Princeton, N. J.

<sup>1</sup> "Standards on Radio Receivers", 1938, definition 1R36.

<sup>2</sup> Page 42, section 13.

<sup>3</sup> A more thorough consideration of this aspect is the purpose of a companion paper by E. W. Herold, "An Analysis of the Signal-to-Noise Ratio of Ultra-High-Frequency Receivers", *RCA Review*, Jan. 1942.

The conventional method of describing receiver noise in terms of an equivalent-noise-side-band input, while possessing a limited utility, does not ever permit an immediate positive judgment of signal-to-noise ratio, nor even a comparison of two receivers, unless additional information is given concerning the antennas and the means for coupling. It will be seen, on the other hand, that a description of the absolute sensitivity of a receiver, antenna included, provides a direct basis for the judgment of a complete receiving system, and facilitates the inter-comparison of receiving equipments, no matter how diverse their characteristics.<sup>4</sup> A rating of this kind is particularly valuable in the ultra-high-frequency field, where antennas are designed as an integral part of the receiver, or, for that matter, in any service wherein maximum signal-to-noise ratio is an important factor in design and operation. It was during an attempt, two years ago, to find a sound basis for the comparison of television receivers, that the considerations reported below were crystallized.

#### MEASUREMENTS IN THE LABORATORY

Consider an ultra-high-frequency receiver constructed to work out of a specific antenna. This implies a specific radiation resistance, antenna reactance, and ohmic loss (such as might be present in a long down-lead). The important essentials of a laboratory simulation of the real antenna, therefore, appear to be

1—a signal generator providing a known radio-frequency voltage source,  $e$ , in series with

2—a resistor,  $R_a$ , whose resistance equals the radiation resistance of the prescribed real antenna;

3—tunable reactance to simulate the  $Q$  of the real antenna; perhaps

4—additional losses to simulate unavoidable losses in the real antenna, and possibly

5—a low-loss transformer to correct *minor* defects in the attempted similitude.

In many cases, the real antenna is prescribed to have a low  $Q$ , to permit reception over a wide range of frequencies. In this event, and provided the antenna  $Q$  is small in comparison with the  $Q$  of the receiver input circuit, item (3) is of minor importance. By the same token, emphasis upon “low-loss” in item (5) becomes less severe. Furthermore, item (5) will often be found incorporated in the receiver proper, in which case the responsibility for making it loss-free lies with the receiver designer.

---

<sup>4</sup> This same subject has recently received the capable attention of R. E. Burgess, “Noise in Receiving Aerial Systems”, *Proc. Phys. Soc.*, Vol. 53, p. 293, May, (1941).

Consider next methods for measuring the noise output. Present I.R.E. standards prescribe measurement of noise after detection.<sup>2</sup> This method not only requires a known modulation for the signal generator, but also makes the noise measurement a function of the frequency response of the circuits which follow the detector. On the premise that post-detection filters are, or should be made sufficiently flat and broad to pass uniformly all frequencies offered by the pre-detection part of the receiver, it is here proposed to measure noise prior to detection. The natural point at which to insert a meter is just ahead of the detector. But occasionally latitude is permissible, and the demands made upon the meter and its position may thus be summarized.

1—It must be preceded by all the filters which materially determine the r-f and i-f selectivity, and must not, in itself, modify the selectivity.

2—It must be preceded by all of the significant sources of random fluctuations.

3—Its response to both noise and signal (preferably, to any admixture of these) must be known.

Item (1) is often too stringent, and may be relaxed in circumstances where it is known that the frequency spectrum of the noise power presented to the meter input terminals conforms essentially to the shape of the power-selectivity curve at that point. This point will be elaborated later.

A schematic of such a laboratory arrangement is shown in Figure 1, which, in addition displays *one* of the sources of noise, namely, thermal agitation in the resistor  $R_a$  which, at room temperature  $T_o$ , is simulating radiation resistance. The quantity  $k$  appearing in the formula,

$$\overline{e_i^2} = 4k T_o R_a \Delta f \quad (1)$$

is Boltzmann's constant. The quantity  $\Delta f$  we will consider related to the overall selectivity curve in the usual way. That is, if  $f_o$  be the nominal operating frequency of the receiver, and if  $G(f)$  be the response of a linear output meter to input signal  $e(f)$ , then

$$\Delta f = \int \frac{G^2(f)}{G^2(f_o)} df \quad (2)$$

By any of various methods which avoid overloading any portion of the system, it is possible to find a signal  $e(f_o)$  which produces (as indicated by the meter) an output signal power equal in magnitude to the output noise power. Were the receiver ideal in the sense that it possessed no sources of noise save that originating in the dummy

<sup>2</sup> loc. cit.

antenna, it would be found that

$$\overline{e^2}(f_o) = 4k T_o R_a \Delta f \tag{3}$$

A fundamental description of the noise generated in the laboratory by a receiver equipped with a dummy antenna is, therefore, provided by the dimensionless measure

$$N = \frac{\overline{e^2}(f_o)}{4k T_o R_a \Delta f} \tag{4}$$

The number  $N$  we shall refer to as the "noise-factor". Expressed as a number, it states the ratio of actual noise power to that developed by an ideal receiver. Or, it may, of course, be given in decibels referred to the ideal receiver as a zero level. That is, the lower limit of  $N$  is unity, or zero decibels.

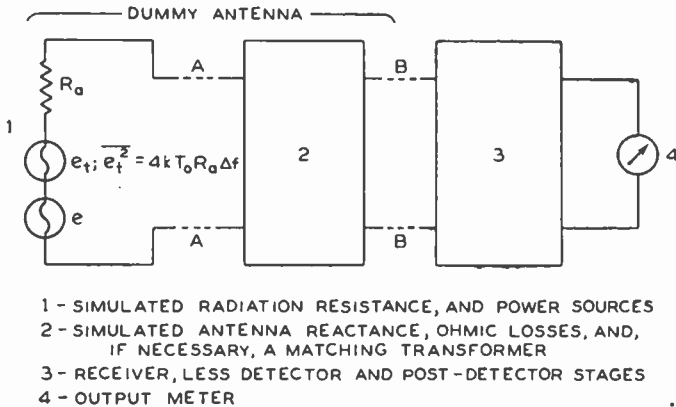


Fig. 1—Schematic of a receiving system with dummy antenna and output meter for laboratory measurements.

This proposed method for quoting laboratory measurement of receiver noise is particularly valuable for two reasons.

First, it is generally fairly insensitive to modifications in the selectivity, as was hinted above. For, unless the frequency spectrum of the noise power output differs materially from the power-selectivity curve,  $\overline{e^2}(f_o)$  is proportional to  $\Delta f$ . The noise factor  $N$  thus provides a reasonably just basis for the comparison of equipments possessing selectivity curves widely different as to both shape and width.

Second, the quantity  $e^2/R_a$  is invariant in a transformation through a loss-free transformer. Consequently, whenever there are no prescribed ohmic losses in the antenna, and when the object of the measurement is not simply to measure  $N$ , but rather, to adjust the antenna coupling to an optimum which then produces the *lowest pos-*

sible  $N$ , one need not be limited to a value of  $R_a$  precisely equal to the radiation resistance of the prescribed antenna. One need only make sure that the prescribed antenna  $Q$  is provided, and even this requirement loses importance when the  $Q$  is too low to affect materially the overall selectivity. For all special, but highly significant measurements of this kind, it becomes unnecessary to know either the voltage calibration of the signal generator, or the precise value of  $R_a$ . Since only the quantity  $\overline{e^2/R_a}$  appears in the expression for the noise factor, it is sufficient to know simply the power the combination will deliver to a matched load. In view of this property, it is seen that the minimum noise factor provides, also, a reasonably just basis for the comparison of equipments working out of antennas possessing widely different radiation resistances.

#### SOME PROPERTIES OF RECEIVING ANTENNAS

Although we have obtained a method for determining and rating the noise of a receiver with dummy antenna, we are not yet in a position to describe its absolute sensitivity in operation. We must first learn two things: one, the connection between signal-field strength and voltage  $e$  produced thereby at the open terminals of an antenna of radiation resistance  $R_a$ ; two, the rôle played by noise picked up by the antenna.

The rôle played by antenna reactance is altogether silent and will be ignored.

Consider two antennas as pictured in Figure 2. The reciprocity law (which is only a dignified way of saying that transfer impedances for passive networks are the same in both directions) assures us that if  $i$  is the current fed to one antenna, and  $e$  the resulting open-circuit voltage at the other, then

$$e = k i$$

and  $k$  is symmetrical in the two antennas. But if antenna (b) is transmitting, its power output is

$$P = i^2 R_b$$

And if antenna (a) is receiving some of that power, its open-circuit voltage will be proportional to the square-root of  $P$ . Therefore,

$$e \propto \sqrt{P} = \sqrt{R_b} i$$

It follows that  $k$  is proportional to  $\sqrt{R_b}$ , and, being symmetrical in the two antennas, must be proportional to  $\sqrt{R_a}$  also. It is, in addition, proportional to a space-attenuation factor and to the product of the directivities of the two antennas.

We are thus enabled to write the relation between signal field strength and open-circuit antenna voltage. Let  $\Omega$  represent the two angular coordinates which define a direction in space. Let  $\phi$  represent the azimuth in a normal plane, to define the direction of polarization of a Poynting vector  $S(\Omega, \phi)$  which describes the signal field. Let  $D^2(\Omega, \phi)$  be the function which describes the power-directivity receiving pattern (identical with the radiation pattern in unencumbered

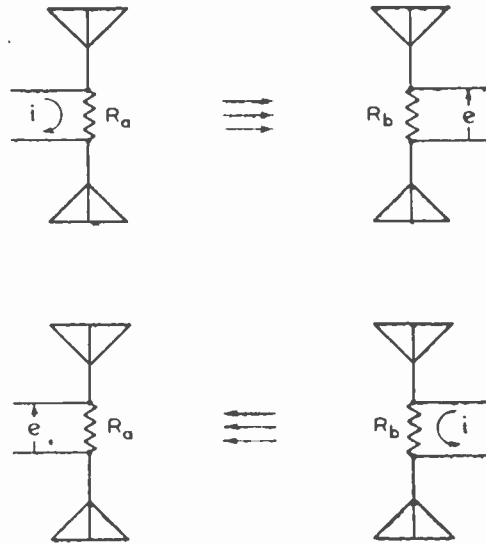


Fig. 2—The reciprocity law for two antennas with individual radiation resistances  $R_a$  and  $R_b$ .

space), and let it be normalized so that, averaged over all values of  $\Omega$  and  $\phi$ ,  $\overline{D^2(\Omega, \phi)} = 1$ . It follows that

$$e^2 = A R_a D^2(\Omega, \phi) S(\Omega, \phi) \quad (5)$$

The coefficient  $A$  is evaluated in the Appendix by an appeal to Nyquist's theorem, for which an additional derivation is produced, proving (if, indeed, proof be needed) its valid application to radiation resistance as well as ohmic resistance. The result, Equation (15), is

$$A = \lambda^2/2\pi$$

where  $\lambda$  is the wavelength.

$$\text{Hence,} \quad e^2 = \frac{\lambda^2}{2\pi} R_a D^2(\Omega, \phi) S(\Omega, \phi) \quad (6)$$

When practical units are used, and  $\lambda$  is given in meters, the relation between  $S$  (watts per square meter) and its associated field strength  $E$  (volts per meter) is

$$S = E^2/120\pi \quad (7)$$



The open-circuit voltage produced at the antenna terminals by a signal field is then

$$e^2 = \frac{\lambda^2}{2\pi} \frac{R_a}{120\pi} D^2(\Omega, \phi) E^2 \quad (8)$$

The voltage produced by a noise field may be likewise expressed. It is certain that if the antenna were exposed solely to the isotropic equilibrium-radiation of an enclosure maintained at room temperature  $T_o$ , the noise voltage would be

$$\overline{e_i^2} = 4k T_o R_a \Delta f$$

It is equally certain that this is not the case. The strength of local noise fields has been, and will always continue to be, the subject of much serious speculation and measurement.<sup>5</sup> While it is known already that both man-made noise and atmospherics decrease rapidly with  $\lambda$ , the "resolving power" of receivers is not yet sufficient to determine what limit, if any, is approached. Furthermore, the development of new communications equipment for shorter wavelengths will always, of itself, implement the production of what must necessarily be regarded, from certain points of view, as new noise fields.

Local noise fields may be crudely divided into three groups:

1—Strictly random fluctuations similar to those generated within the receiver proper, and characterized by a proportionality between noise power and bandwidth.

2—Noise consisting of impulses, random enough, but occurring at a mean rate too low in comparison with the bandwidth to be included with (1), and, therefore, characterized by a lack of proportionality between noise power and bandwidth.

3—All other unwanted fields.

It is beyond our present purposes to discuss the relative amounts of service disturbance engendered by equal amounts of noise power in each of these categories. This vastly complex problem is receiving attention elsewhere.<sup>6</sup> Concerning ourselves with a measure of the

<sup>5</sup> For example, K. G. Jansky, "Minimum Noise Levels Obtained on Short-Wave Radio Receiving Systems", *Proc. I.R.E.*, Vol. 25, p. 1517, December, (1937).

R. K. Potter, "An Estimate of the Frequency Distribution of Atmospheric Noise", *Proc. I.R.E.*, Vol. 20, p. 1512, September, (1932).

G. Reber, "Cosmic Static", *Proc. I.R.E.*, Vol. 28, p. 68, February, (1940).

<sup>6</sup> C. M. Burrill, "Progress in the Development of Instruments for Measuring Radio Noise", *Proc. I.R.E.*, Vol. 29, p. 433, August, (1941).

power alone, we note that the difference between two determinations of the noise factor, conducted as described, one with a dummy antenna, the other with the real antenna in the absence of a signal field, provides just such a measure. We may go even further and, simply for convenience, express this measure in terms of an essentially fictitious temperature  $T_a$  of local space, writing

$$\overline{e^2} = 4k T_a R_a \Delta f$$

for the net open-circuit voltage produced by the local noise field at the antenna terminals, so that<sup>7</sup>

$$N(\text{operating}) = N + \frac{T_a}{T_o} - 1 \quad (9)$$

The total equivalent noise voltage at the antenna terminals of a system in operation may consequently be written

$$\overline{e^2} = 4k T_o R_a \Delta f \left[ N + \frac{T_a}{T_o} - 1 \right] \quad (10)$$

Should it be ascertained that the local noise field consists entirely of the first kind,  $T_a$  will then be independent of bandwidth, but not necessarily independent of operating frequency; and if the noise field is not isotropic,  $T_a$  will naturally be a function of antenna orientation and directivity. To the extent that noise fields of the second and third kinds are present,  $T_a$  cannot even be presupposed independent of bandwidth.

#### ABSOLUTE SENSITIVITY

If, by the term "absolute sensitivity", we refer to the r-m-s signal field strength which produces at the open antenna terminals a mean-square voltage equal to the equivalent mean-square noise voltage, then, from (8) and (10), that field strength is

$$\overline{E^2} = \frac{240\pi^2}{\lambda^2} \cdot \frac{4k T_a \Delta f}{D^2(\Omega, \phi)} \left[ N + \frac{T_a}{T_o} - 1 \right] \quad (11)$$

<sup>7</sup> E. W. Herold, Reference 3, exhibits the general functional relationship of  $N$  to the important sources of noise *within the receiver*, and to the circuit arrangements dictated by the service for which it is designed.

If  $E$  is conventionally expressed in *microvolts per meter*,  $\lambda$  in meters,  $\Delta f$  in megacycles, and  $T_o$  set equal to 300 degrees Kelvin (room temperature),

$$\overline{E^2} = \frac{39\Delta f}{\lambda^2 D^2(\Omega, \phi)} \left[ N + \frac{T_a}{300} - 1 \right] \quad (12)$$

The expression shows clearly the distinct, prominent contributions of receiver proper, antenna directivity, and local noise fields.

The economy of efforts to improve the laboratory noise factor is seen to be bounded, in some cases sharply, by the existence of local noise. The use of tuned antennas for broadcast reception is, in many locations, a costly luxury. In some recent experiments, W. R. Ferris<sup>8</sup> and the author produced a noise factor  $N = 3.2$  in an attempt to determine the lower limit for television service at 100 megacycles. Such a receiver would probably be unappreciated in metropolitan districts. On the other hand, at higher frequencies,  $T_a$  appears to decline, as stated before, while minimum  $N$  rises rapidly for a number of tube and circuit reasons.<sup>3</sup> There is surely much to be gained from improved  $N$ 's at very short wavelengths.

The economy of antenna structures needs similar consideration. For half-wave dipoles in free space,  $D^2$  is not a function of wavelength. For dipoles beamed by parabolas large in comparison with  $\lambda$ ,  $D^2$  (maximum) is proportional to  $A/\lambda^2$ , where  $A$  is the area of the parabola's aperture. Even were the noise factor to remain fixed as one moved towards shorter wavelengths, the absolute sensitivity would certainly suffer if one continued to use dipoles and would, indeed, still suffer, despite the switch to a parabola, unless the aperture of the parabola were given an area comparable to the square of the initial wavelength.

#### CONCLUSION

Because of the ease of interpretation, and the simplicity of measurement method, it is hoped that the material presented above may be considered as a basis for the adoption of a standard of "absolute sensitivity" for radio receivers.

#### APPENDIX

Thermodynamic reasoning alone is sufficient to justify the application of Nyquist's theorem<sup>9</sup> concerning thermal agitation to any

<sup>3</sup> loc. cit.

<sup>8</sup> Research Laboratories, RCA Manufacturing Company, Inc., Harrison, New Jersey.

<sup>9</sup> H. Nyquist, "Thermal Agitation of Electric Charge in Conductors", *Phys. Rev.*, Vol. 32, p. 110, July, (1928).

passive network. But it is, at least, interesting to develop the theorem in detail for a microscopic dipole exposed to equilibrium radiation.<sup>10</sup>

Using electrostatic units, we know that the radiation resistance of a dipole of length  $l$  ( $l \ll \lambda$ ) in vacuum is<sup>11</sup>

$$R_a = \frac{8}{3} \frac{(\pi f l)^2}{C^3} \tag{13}$$

where  $f$  is the operating frequency,  $C$  the velocity of light.

The energy density of equilibrium radiation at temperature  $T$  is<sup>12</sup>

$$\rho = \frac{8\pi h f^3 df}{C^3} \left[ e^{\frac{hf}{kT}} - 1 \right]^{-1}$$

wherein  $h$  is Planck's constant,  $k$  is Boltzmann's constant. But since  $hf/kT \sim 10^{-4}$  for  $f = 1,000$  megacycles and  $T = 300$  degrees Kelvin, the Rayleigh-Jeans approximation is sufficiently accurate. Thus,

$$\rho = \frac{8\pi kT f^2}{C^3} df$$

But, being isotropic,

$$\rho = \frac{\overline{E^2}}{4\pi} = \frac{\overline{E_x^2} + \overline{E_y^2} + \overline{E_z^2}}{4\pi} = \frac{3\overline{E_z^2}}{4\pi}$$

Hence, the mean-square field strength at the antenna in its susceptible direction ( $z$ ) is

$$\overline{E_z^2} = \frac{32(\pi f)^2}{3 C^3} kT df$$

Therefore, the mean-square open-circuit voltage at the antenna terminals is, with the help of (13),

$$\overline{e^2} = \overline{E_z^2} l^2 = 4 \left[ \frac{8(\pi f l)^2}{3 C^3} \right] kT df = 4kT R_a df \tag{14}$$

\* \* \* \* \*

To evaluate the coefficient  $A$  in (5), we submerge any antenna in equilibrium radiation and demand that the open-circuit voltage appear-

<sup>10</sup> A more general derivation was given by Burgess, Reference 4.  
<sup>11</sup> For example, Hund, "High-Frequency Measurements", p. 399, (McGraw-Hill, 1933).  
<sup>12</sup> For example, Ruark and Urey, "Atoms, Molecules, and Quanta", p. 58, Eq. 10, (McGraw-Hill, 1930).

ing at its terminals obey Nyquist's theorem. Since  $D^2(\Omega, \phi)$  has been defined to have an average value of unity, and since (in *e.s.u.*)

$$\bar{S} = \frac{C \overline{E^2}}{4\pi}$$

it follows that

$$4kT R_a df = \overline{e^2} = A R_a \bar{S} = A R_a \frac{C \overline{E^2}}{4\pi} \Rightarrow \frac{2\pi A}{\lambda^2} \cdot 4kT R_a df$$

whence

$$A = \frac{\lambda^2}{2\pi} \tag{15}$$

This result enables one to state a perfectly general relationship between the "effective height" of an antenna, its radiation resistance, and its directivity. The effective height  $h(\Omega, \phi)$  is defined

$$h = \frac{e}{E}$$

Hence, from (8), we have, in practical units,<sup>13</sup>

$$h^2(\Omega, \phi) = \frac{\lambda^2 R_a}{2\pi 120\pi} D^2(\Omega, \phi) \tag{16}$$

We further find, in agreement with Burgess,<sup>4</sup> that the mean-square effective height averaged over all orientations with respect to a fixed signal vector is then

$$\overline{h^2} = \frac{\lambda^2 R_a}{2\pi 120\pi} \tag{17}$$

<sup>13</sup> The quantity,  $120\pi$ , carries the dimension, ohms. It is, in fact, the characteristic impedance of a strip  $x$  units broad of a transmission line consisting of two parallel infinite planes  $x$  units apart, supporting plane-wave transmission.

<sup>4</sup> loc. cit.

Finally, with reference to (6), it is to be noticed that the power an antenna can extract from a signal Poynting vector is proportional to

$$\frac{e^2}{R_a} = \frac{\lambda^2}{2\pi} D^2(\Omega, \phi) S(\Omega, \phi)$$

The radiation pattern of dipoles shorter than a half-wavelength is sensibly independent of the length; this leads to the curious observation that such dipoles extract sensibly equal amounts of power, no matter how short they are. In the language of physical optics this would be known as a diffraction phenomenon. In the language of atomic physics, we can only conclude that the capture-cross-section of short dipoles for passing Poynting vectors is of the order of  $\lambda^2$ .

# AN ANALYSIS OF THE SIGNAL-TO-NOISE RATIO OF ULTRA-HIGH-FREQUENCY RECEIVERS\*†

By

E. W. HEROLD

Research Laboratories, RCA Manufacturing Company, Inc., Harrison, N. J.

*Summary*—This paper presents an elementary analysis of the effect of the various sources of fluctuation noise on the signal-to-noise ratio of radio receivers. Because the noise induced in negative grids at high frequencies is included, the work is particularly applicable at ultra-high frequencies. It is found that the signal-to-noise ratio depends on the antenna noise; in addition, when bandwidth is not a consideration, it depends on the ratio of equivalent noise resistance to input resistance of the first tube, and, when bandwidth is a major consideration, on the product of input capacitance and equivalent noise resistance. The coupling from antenna to first tube is an important variable in receiver design and an optimum coupling is found which results in an improvement in signal-to-noise ratio. This optimum condition is often considerably different from the adjustment for maximum gain and, by its use, the noise induced in the grid becomes relatively unimportant. The noise from the second stage of the receiver is also evaluated. It is shown that the thermal noise from a wide-band interstage circuit may be made negligible by concentrating all the damping on the secondary side. Calculations of typical receiver arrangements using triode type 955 and pentode type 954 mixers are given for 300, 500 and 1,000 megacycles.

## I—INTRODUCTION

THE useful reception of radio and other types of signals is limited, in the main, to those signals which exceed the unavoidable random fluctuation noise of the communicating system. Because there are other sources of noise in addition to normal random noise, such as static and man-made interferences, the signal must usually exceed the random noise by a considerable factor, under most conditions of reception. However, since random noise imposes a readily calculated absolute limit to sensitivity, it is usually used to designate receiver performance. This criterion is particularly appropriate when the noise which is inherent in the receiving antenna is included. At low frequencies, up to say 20 megacycles, the chief sources of noise in the usual receivers are due to atmospherics and allied causes, to thermal agitation in the antenna<sup>1,2</sup> and in the input circuits of the first tube,

\* Decimal Classification: R361.211.

† Reprinted from *RCA REVIEW*, January, 1942.

‡ Now with the Research Department, RCA Laboratories Division, Princeton, N. J.

<sup>1</sup> F. B. Llewellyn, "A Rapid Method of Estimating the Signal-to-Noise Ratio of a High Gain Receiver", *Proc. I.R.E.*, Vol. 19, pp. 416-420, March, 1931.

<sup>2</sup> R. E. Burgess, "Noise in Receiving Aerial Systems", *Proc. Phys. Soc.*, Vol. 53, Part 3, pp. 293-304, May 1, 1941.

and to shot-effect in the plate circuit of the first tube. At higher frequencies, however, the noise induced in the input grid by the passage of electrons<sup>3,4,5</sup> must also be considered as a contributing factor. When the gain of the first tube is low, it is also important to consider noise contributed by the coupling circuit to the following tube and also the noise contributed by the following tube itself.

In all cases, the most convenient evaluation of the total noise energy is made by referring all sources of noise to a given point in a receiver. For example, if the grid of the first tube is used as reference point, the noise voltage resulting from shot noise in the plate may be divided by the gain of the tube to give an entirely fictitious, but equivalent noise voltage at the grid reference point. This noise voltage may be added in the usual mean-squared manner to other independent noise voltages referred to this same point to give a total noise value. In estimating receiver performance, however, it is necessary to refer the received signal to this same point, if the signal-to-noise capability of the receiver is desired. In a companion paper,<sup>6</sup> D. O. North has shown that the absolute sensitivity of a receiving system depends upon a noise factor,  $N$ , of the receiver itself. The relations found in the present paper will show how  $N$  varies with tube and circuit constants and how receivers may be designed to minimize it.

Studies of signal-to-noise ratio in the input circuit of receivers have previously been made qualitatively by Llewellyn<sup>1</sup> and quantitatively by Williams<sup>7</sup> and by Fränz.<sup>8</sup> The present paper is an extension of the work of these men to include wide-band and ultra-high-frequency applications. In addition, a study of interstage coupling has been included for those cases when the gain of the first stage is low. This information is particularly necessary in ultra-high-frequency superheterodynes when a wide band is used with a low-gain converter stage.

## II—BASIC RELATIONS

A tuned antenna of radiation resistance  $R_a$  will be assumed to be coupled to the receiver through a perfect transmission line of characteristic impedance  $Z_o = R_a$ . Coupling to the input of the first tube will

<sup>1</sup> loc. cit.

<sup>3</sup> Stuart Ballantine, "Schrot Effect in High-Frequency Circuits", *Journ. of Frank. Inst.*, Vol. 206, pp. 159-167, August, 1928.

<sup>4</sup> D. O. North and W. R. Ferris, "Fluctuations Induced in Vacuum-Tube Grids at High Frequencies", *Proc. I.R.E.*, Vol. 29, pp. 49-50, February, 1941.

<sup>5</sup> C. J. Bakker, "Fluctuations and Electron Inertia", *Physica*, Vol. 8, pp. 23-43, January, 1941.

<sup>6</sup> D. O. North, "The Absolute Sensitivity of Radio Receivers", *RCA REVIEW*, January, 1942.

<sup>7</sup> F. C. Williams, "Thermal Fluctuations in Complex Networks", *J. I.E.E.*, Vol. 81, pp. 751-760, December, 1937.

<sup>8</sup> K. Fränz, "The Limiting Sensitivity in the Reception of Electric Waves and Its Attainability", *Elektrische Nachrichten-Technik*, Vol. 16, p. 92, 1939.



be assumed to be through a network which is the equivalent of a transformer whose leakage reactances are eliminated by tuning, and whose step-up, or effective turns ratio, is  $m^*$ . An equivalent circuit then is as shown in Figure 1. The total input impedance of the tube with the antenna disconnected, as determined by circuit and lead losses as well as transit-time loading, is lumped as  $R_1$  in the figure. The open-circuit antenna signal voltage is shown as  $e_a$ . Feedback effects which may change the signal-to-noise ratio in the tube will be neglected in this analysis. The noise sources which must be considered are:

1. Thermal and other noise in the antenna.
2. Thermal noise of circuit and leads.
3. Induced input electrode noise in first tube.
4. Plate noise of the first tube referred to the input circuit.
5. Noise of parts of receiver subsequent to the first tube, and also referred to the input circuit.

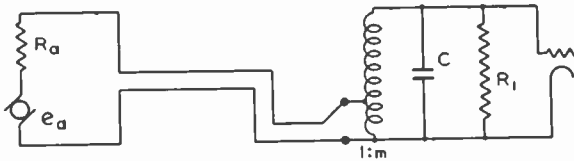


Fig. 1—Basic equivalent circuit of receiver input.

The noise of the antenna is conveniently introduced by considering this noise as if it were noise due to thermal agitation in the radiation resistance of the antenna and assigning to this resistance an effective temperature,  $T_a$ . Under ordinary circumstances, at frequencies below 20 megacycles, this effective temperature may be considerably higher than the ambient temperature.<sup>9</sup> At ultra-high frequencies, where directive antennas are employed and atmospherics are negligible, the value of  $T_a$  will more nearly approach the ambient temperature and may even go below it. When a conventional method of measuring receiver sensitivity is employed, a resistor at ambient temperature is substituted for the antenna resistance and the results obtained will correspond to  $T_a$  equal to the ambient temperature. These cases will be given special attention in this paper.

To distinguish between items 2 and 3 of the above list it will be convenient to divide  $R_1$  into two parallel components, one having thermal noise and representing circuit and leads, and the other having induced grid noise and representing electronic loading. If the con-

\*  $m$  is the ratio of output voltage to input voltage of the network.

<sup>9</sup> K. G. Jansky, "Minimum Noise Levels Obtained on Short-Wave Radio Receiving Systems", *Proc. I.R.E.*, Vol. 25, pp. 1517-1530, December, 1937.

ductances of these two components are  $g_{\Omega}$  and  $g_e$ , respectively, then

$$g_{\Omega} + g_e = \frac{1}{R_1}$$

The noise induced in the input circuit by the passage of electrons has been found by North and Ferris<sup>4</sup> for tubes with an input control grid adjacent to the cathode. Their results for oxide-coated cathode tubes showed the noise to be equivalent to the thermal noise of a resistor of a value equal to the electronic loading and whose temperature is about 5 times room temperature. Furthermore, their work has shown that, theoretically, to a first approximation, induced grid noise may be added to the plate noise (referred to the grid) of the same tube as if they were independent sources of noise. Their results have made the application of this analysis to ultra-high frequencies possible.

With respect to induced grid noise in tubes whose control grid is not adjacent to the cathode, the problem is not yet completely solved, although a start has been made by Bakker.<sup>5</sup> The emphasis in the present paper will be on the more common tubes with oxide-coated cathodes and an adjacent control grid which is also the input grid. However, for the sake of completeness, the results which apply to the other forms of tube are given in an appendix.

One of the more common feedback effects in ordinary tubes at high frequencies is due to cathode lead inductance which introduces an input loading very similar in nature to the electronic loading. However, it has been shown<sup>10</sup> that this feedback leaves the signal-to-noise ratio unaffected, at least in the first approximation. In using the results of the present paper, therefore, input conductance due to cathode lead inductance should not be included in the evaluation of the electronic conductance,  $g_e$ . If the conductance due to the cathode lead is included in  $g_{\Omega}$  as if it were an ohmic loss the error will be small in most practical cases.

The plate noise of the first tube will be referred to the grid in the usual manner by making use of an equivalent-noise-resistance concept.<sup>11</sup> In many practical cases, the gain of the first tube will be sufficiently high so that noise of succeeding stages will be negligible. However, to preserve complete generality, the other sources of noise will be assumed to be included by adding a second equivalent noise resistance which is

<sup>4</sup> loc. cit.

<sup>5</sup> loc. cit.

<sup>10</sup> M. J. O. Strutt and A. Van der Ziel, "Methods for the Compensation of the Effects of Shot Noise in Tubes and Associated Circuits", *Physica*, Vol. 8, pp. 1-22, January 1941.

<sup>11</sup> See Part V of B. J. Thompson, D. O. North and W. A. Harris, "Fluctuations in Space-Charge-Limited Currents at Moderately High Frequencies", *RCA REVIEW*, Vol. V, pp. 505-524, April 1941 and Vol. VI, pp. 115-124, July 1941.

calculated at the grid of the first tube by using the squares of the gains between this point and the actual sources of noise, in the usual manner. A later section will include the evaluation of this second equivalent-noise-resistance factor as applied to the second stage. The total equivalent noise resistance at the grid will be designated by  $R_{eq}$  and will be the sum of the noise resistance of the first tube and that calculated from all succeeding stages.

Using the above concepts, by assuming an overall receiver passband which is not wider than that of the circuits considered in the analysis, it now becomes possible to redraw the circuit to include all the noise sources. This is done in Figure 2 in which all noise sources are shown as constant-current generators except the equivalent-noise-resistance source,  $R_{eq}$  which is shown as a voltage. Throughout this analysis,  $T_a$  represents the effective antenna temperature,  $T_R$  represents ambient or room temperature in degrees Kelvin,  $k$  is Boltzmann's constant

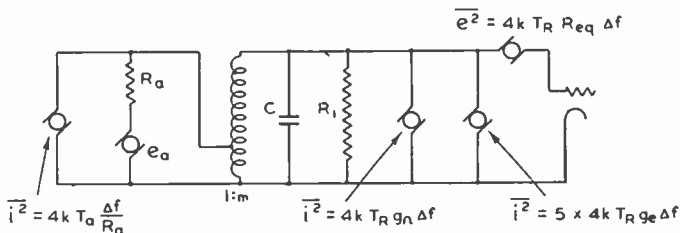


Fig. 2—Equivalent circuit of receiver input with noise sources included.

(equal to  $1.37 \times 10^{-23}$  joules per  $^{\circ}K$ ) and  $\Delta f$  is the overall effective passband of the receiver for noise purposes.<sup>11</sup> The induced noise in the input grid is shown in the form suitable for oxide-coated cathode tubes with control grid adjacent to the cathode.

Since the antenna resistance referred to the input circuit secondary is equal to  $m^2 R_a$  (where  $m$  is the effective turns ratio, or step-up, of the input circuit), the antenna noise referred to the grid is just the thermal noise of a resistor  $m^2 R_a$  at a temperature  $T_a$  in parallel with

the resistance  $R_1 = \frac{1}{g_{\Omega} + g_e}$  already there. Thus, another equivalent circuit can be shown in Figure 3a.

In order to simplify the analysis still further, let us replace the reflected antenna conductance,  $1/m^2 R_a$ , by the symbol  $g_a$ . The two resistances of Figure 3a in parallel will then be equivalent to the single resistance of Figure 3b. Furthermore, by remembering that

<sup>11</sup> Thompson, North and Harris, loc. cit.

$$g_{\Omega} + g_e = \frac{1}{R_1}$$

we can rewrite the expression for the constant-current noise generator as shown in the latter figure. It will be well to keep in mind that the condition for maximum gain (impedances matched) corresponds to  $g_a R_1 = 1$ .

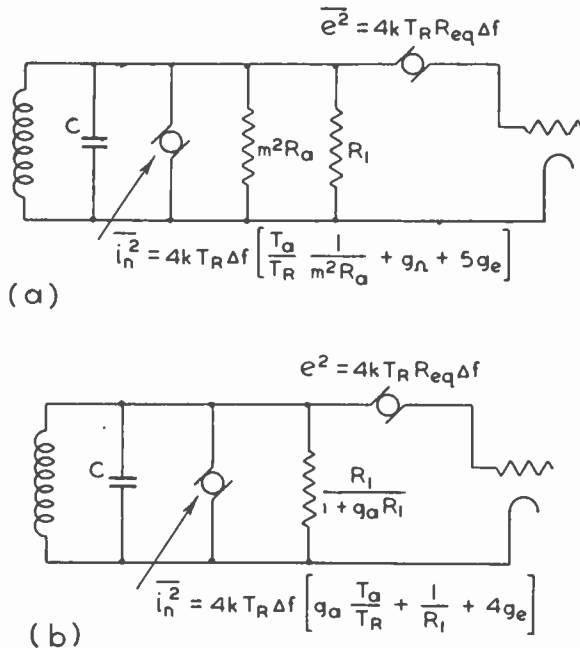


Fig. 3—(a) Equivalent circuit with antenna loading and noise shown as reflected values in secondary of antenna transformer; (b) Simplified equivalent obtained by introducing  $g_a$  for the reflected antenna conductance.

When the circuit is reduced to the simple one of 3b, the relations for the signal voltage and noise voltage are readily written down. As to the signal, in Figure 3b it could have been represented as a constant-current generator of value  $e_a/mR_a$ . In terms of the reflected antenna conductance,  $g_a$ , the signal voltage on the tube grid is then

$$e_{\text{grid}} = e_a \frac{\sqrt{g_a R_1}}{1 + g_a R_1} \sqrt{\frac{R_1}{R_a}} \quad (1)$$

This expression reduces to the expected value for matched impedances if  $g_a R_1$  is given the value unity.

The mean-squared noise voltage on the grid, from Figure 3b, is then

$$\overline{e_n^2} = 4k T_R \Delta f \left[ R_{eq} + \left( g_a \frac{T_a}{T_R} + \frac{1}{R_1} + 4 g_e \right) \frac{R_1^2}{(1 + g_a R_1)^2} \right] \quad (2)$$

The signal-to-noise ratio is given by dividing (1) by the square-root of (2) and is

$$\frac{e_{\text{signal}}}{\sqrt{\overline{e_n^2}}} = \frac{e_a}{\sqrt{4k T_R R_a \Delta f}} \times \left[ \frac{1}{\frac{T_a}{T_R} + 2 \frac{R_{eq}}{R_1} + (g_a R_1) \frac{R_{eq}}{R_1} + \frac{1}{(g_a R_1)} \left( 1 + \frac{R_{eq}}{R_1} + 4g_e R_1 \right)} \right]^{\frac{1}{2}} \quad (3)$$

The denominator inside the radical of Equation (3) is the noise factor,  $N$ , whose importance in limiting the absolute sensitivity is discussed in a companion paper.<sup>6</sup>

For the sake of completeness, another relation, which is of some interest, is the bandwidth of the input circuit (which has been assumed equal to, or greater than,  $\Delta f$ ). The total bandwidth, from points 3 db down on each side of the resonance curve, may be compared with that of a simple tuned circuit of capacitance  $C$  shunted by a resistance

$$\frac{R_1}{1 + g_a R_1} \text{ and is}$$

$$\text{Input band width} = \frac{1 + g_a R_1}{2\pi C R_1} F \text{ (for 3 db down)}$$

where  $F$  is equal to unity for an input circuit which is equivalent to a single-tuned circuit. For coupled circuits, or other band-pass arrangement,  $F$  may be somewhat greater.

Equations (1) to (4) are the fundamental relations which are applicable to the input circuit. Their interpretation will be made more clear by the subsequent discussion.

### III—CONDITIONS WHEN GAIN IS MAXIMUM (IMPEDANCES MATCHED)

From Equation (1), maximizing with respect to  $g_a R_1$ , it is found that the maximum grid signal is given when  $g_a R_1 = 1$  as, of course, is expected. This condition means simply that

$$m^2 R_a = R_1$$

<sup>6</sup> D. O. North, loc. cit.

and the antenna impedance is exactly matched to the tube impedance by the input circuit. It is the usual condition of adjustment and warrants further consideration.

The signal-to-noise ratio (from Equation (3)), when  $g_a R_1 = 1$ , is

$$\left. \frac{e_{\text{signal}}}{\sqrt{e_n^2}} \right] g_a R_1 = 1 = \frac{e_a}{\sqrt{e_t^2}} \sqrt{\frac{1}{\left( \frac{T_a}{T_R} + 1 \right) + 4 \frac{R_{eq}}{R_1} + 4 g_e R_1}} \quad (5)$$

where  $\overline{e_t^2}$  is the open-circuit, mean-squared thermal noise voltage of the antenna at room temperature. This expression shows that the signal-to-noise ratio for a given signal, antenna noise and bandwidth depends only on the ratio of the tube equivalent noise resistance\* to the total input resistance and on the fraction of this input resistance which is electronic in nature. The latter fraction, shown as  $g_e R_1$  in the equation, must lie, of course, between 0 and 1. Thus, the signal-to-noise ratio must always lie between the two limits imposed by the above equation for  $g_e = 0$  and for  $g_e R_1 = 1$ .

The minimum open-circuit antenna signal which will just equal the noise under the matched-impedance condition, is given by

$$\left. e_a \right]_{\text{min}} = \sqrt{\overline{e_t^2}} \sqrt{2 + 4 \frac{R_{eq}}{R_1} + 4 g_e R_1} \quad (6)$$

an expression which is obtained by setting  $T_a = T_R$  as in receiver measurements with a dummy antenna. This minimum value may be used as a criterion for receiver performance.† Values of  $\overline{e_t^2}$  computed for  $T_a = 293^\circ K$ ,  $R_a = 75$  ohms, and various bandwidths are as follows:

$\Delta f,$ kc	$\sqrt{\overline{e_t^2}},$ $\mu V$
10	0.11
200	0.49
2000	1.55
4000	2.2

\* i.e., when noise of other tubes is small and  $R_{eq}$  is substantially due to first tube, only. Otherwise,  $R_{eq}$  includes noise of following stages also.

† As North has shown in Reference 6,  $e_a/\sqrt{\overline{e_t^2}}$  cannot be changed by antenna design except by changing the directivity.

With the condition of matched impedances, which applies to Equation (6), the signal, when measured at the receiver input terminals, will be just half of the open-circuit signal,  $e_a$ .

A curve of the factor  $(2 + 4 R_{eq}/R_1 + 4 g_e R_1)^{1/2}$  plotted against  $R_1/R_{eq}$  is shown in Figure 4. The lower curve is for the case when  $g_e R_1 = 0$  while the upper curve is for the case when  $g_e R_1 = 1$ . Results for all practical receivers, when adjusted for maximum gain, must lie between these two curves. Further discussion of these data will be given later in the paper.

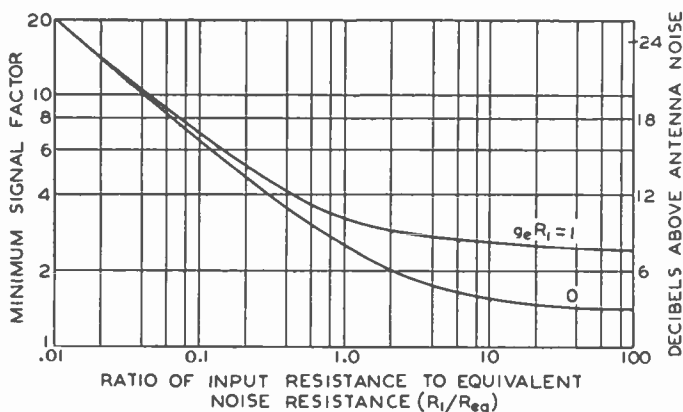


Fig. 4—The relative fluctuation noise of a receiver whose input circuit is adjusted for maximum gain.

#### IV—CONDITIONS WHEN SIGNAL-TO-NOISE RATIO IS MAXIMUM

Referring to Equation (3) of the basic relations, if this expression is maximized with respect to  $g_a$ , it will be found that best signal-to-noise ratio is given when

$$(g_a R_1)^2 = 1 + \frac{R_1}{R_{eq}} (1 + 4 g_e R_1) \tag{7}$$

In terms of the step-up,  $m$ , of the input circuit the maximum signal-to-noise ratio is given when

$$m = \sqrt{\frac{R_1}{R_a}} \quad 4 \sqrt{\frac{1}{1 + \frac{R_1}{R_{eq}} (1 + 4 g_e R_1)}}$$

Substituting (7) in (3) gives the maximum signal-to-noise ratio as

$$\left[ \frac{e_{\text{signal}}}{\sqrt{e_n^2}} \right]_{\text{min.}} = \frac{e_n}{\sqrt{e_i^2}} \sqrt{\frac{1}{\frac{T_u}{T_R} + 2 \frac{R_{eq}}{R_1} + 2 \sqrt{\frac{R_{eq}}{R_1} \left( 1 + \frac{R_{eq}}{R_1} + 4 g_a R_1 \right)}}}} \quad (8)$$

It is again seen that the signal-to-noise ratio for a given signal, antenna noise, and bandwidth, depends only on the ratio  $R_{eq}/R_1$  and on  $g_a R_1$ .

The minimum open-circuit antenna signal which will just equal the noise is then

$$e_n \Big]_{\text{min}} = \sqrt{\frac{e_i^2}{1 + 2 \frac{R_{eq}}{R_1} + 2 \sqrt{\frac{R_{eq}}{R_1} \left( 1 + \frac{R_{eq}}{R_1} + 4 g_a R_1 \right)}}}} \quad (9)$$

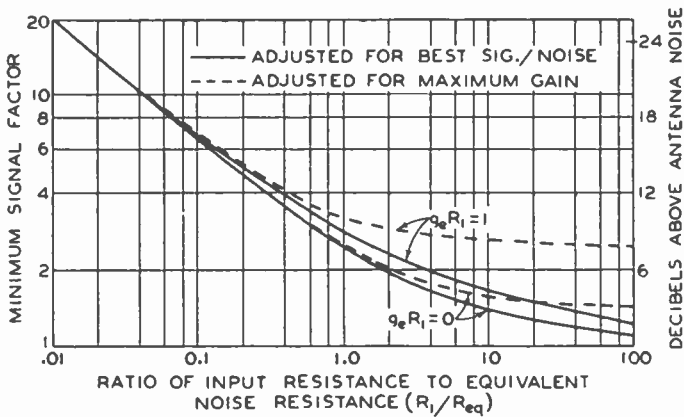


Fig. 5—The relative fluctuation noise of a receiver whose input circuit is adjusted for best signal-to-noise ratio as compared with one adjusted for maximum gain.

where  $T_u$  has been set equal to  $T_R$  for the lowest possible antenna noise (as with a dummy antenna). A curve of the factor included under the right hand radical plotted against  $R_1/R_{eq}$  is shown in Figure 5 for each of the two limiting cases  $g_a R_1 = 0$  and  $g_a R_1 = 1$ . In order to facilitate comparison, the curves of Figure 4 are drawn with dotted lines.

It is, of course, necessary to sacrifice signal-voltage gain in order to achieve the improved signal-to-noise ratio. The ratio of the signal-voltage, antenna-to-grid gain (Equation (1)) with best signal-to-noise ratio to that with optimum-gain coupling is

$$\frac{\text{Actual Gain}}{\text{Max. Gain}} = \frac{2 \sqrt{g_a R_1}}{1 + g_a R_1} \quad (10)$$



where  $g_a R_1$  is the value given by Equation (7) for best signal-to-noise. Equation (10) represents, therefore, the gain-reduction factor.

Curves showing the reduction in gain as well as the improvement in signal-to-noise ratio\* which are made possible with this coupling in comparison with optimum-gain coupling are shown in Figure 6. It is seen that over the range of values usually encountered ( $R_1/R_{eq} < 10$ ), the signal-to-noise ratio improvement is appreciable though not startling even for  $g_a R_1 = 1$ . The reduction in gain is very nearly equal to the improvement in signal-to-noise ratio in this range. It should be noted that the bandwidth of the overall input circuit is *increased* by a change in coupling from that for best gain in the direction of that for best signal-to-noise ratio. The amount of the increase is readily found from Equation (4) using the value of  $g_a R_1$  found from Equation (7).

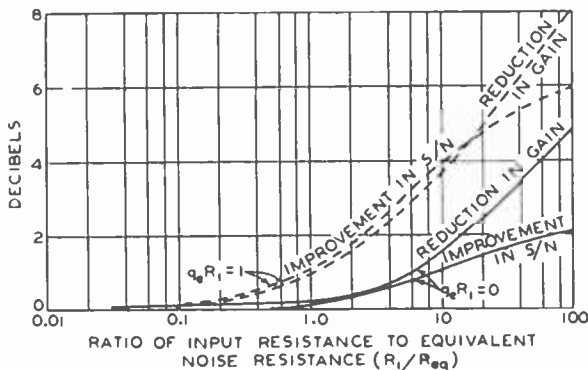


Fig. 6—Comparison of coupling for best signal-to-noise ratio,  $S/N$ , with coupling for best gain.

#### V—DISCUSSION OF RESULTS OF SECTIONS III AND IV

Perhaps the most interesting feature of the analysis has been that, no matter whether impedances are matched or whether best signal-to-noise ratio is desired, the signal-to-noise ratio depends mainly on the ratio of equivalent noise resistance,  $R_{eq}$ , to the total effective shunt resistance,  $R_1$ , of the input to the tube. When  $R_{eq}$  is chiefly due to the first tube (as it is when the gain of the first tube is reasonably high) and  $R_1$  is also chiefly a result of the first tube (i.e., when circuit losses are negligible), a figure of merit for the first tube is  $R_1/R_{eq}$ . Unfortunately, this ratio varies with frequency. Its use, however, together with the curves of Figure 5, lead to a clear picture of receiver performance. It is seen, for example, that in an ultra-high-frequency

\* i.e., the reduction in minimum signal which it is possible to receive.

amplifier or converter tube, an improvement in input resistance is just as valuable as a reduction in equivalent-noise resistance.

Referring to Figure 4, for the impedance-matched condition, the data show that little improvement is to be obtained in signal-to-noise by an increase in  $R_1/R_{eq}$  much greater than unity. Thus, if impedance matching is maintained, and a tube is found to have a minimum signal factor corresponding to  $R_1/R_{eq} = 1$  it will not be possible to improve the performance much more, unless perhaps  $g_e R_1$  can be reduced by a reduction in electronic loading so as to change from the upper curve towards the lower. However, if a mis-match is permitted, as shown in Figure 5, a definite improvement in signal-to-noise can be expected as  $R_1/R_{eq}$  is increased even up to 100.

At all times, the minimum thermal noise voltage of the antenna ( $T_a = T_R$ ) sets a definite lower limit to receiver sensitivity. As an example, consider the minimum usable signal of a television receiver. A receiver with a 4-megacycle bandwidth designed for the reception of amplitude-modulated signals must have a signal-to-noise ratio of around 30 db for a satisfactory picture. Since the antenna thermal noise is 2.2 microvolts (for a 75-ohm antenna), a satisfactory picture requires a signal of 70 microvolts as a minimum and no amount of improvement in the receiver can possibly decrease this value.

One of the conclusions to be drawn from Figures 4 and 5 is that the presence of induced grid noise does not affect the signal-to-noise performance by a large amount. Under most practical high-frequency conditions,  $R_1/R_{eq}$  is well under 10 and if a tube and circuit whose major loading is electronic is compared with one whose loading is entirely resistive a maximum difference of only 1.4 db will be found when the coupling is adjusted for best signal-to-noise ratio.

The curves of Figure 6 indicate that adjustment for maximum gain (impedance-matching) is reasonable only as long as  $R_1/R_{eq} < 1$ . If the latter ratio can be improved markedly, by an improved circuit, tube, or both, so as to exceed unity by a significant amount it becomes profitable to mis-match somewhat to take advantage of the improved signal-to-noise ratio which is then attained.

There is still one other aspect of the signal-to-noise problem which is of importance in the normal broadcast band, for example. In a receiver design which is suitable for a wide variety of antennas, it is customary to couple the antenna very loosely to the input circuit. In this way variations of antenna impedance will have a minimum of effect on receiver line-up and performance. The condition of loose coupling corresponds to a very small reflected conductance, i.e.,  $g_e R_1 \ll 1$ . This condition, when included in Equation (3), shows the signal-to-noise ratio to be

$$\frac{e_{\text{signal}}}{\sqrt{e_n^2}} = \frac{e_a}{\sqrt{e_i^2}} \sqrt{\frac{g_a R_1}{\left(1 + \frac{R_{eq}}{R_1} + 4 g_e R_1\right)}} \tag{11}$$

If  $g_a R_1$  is held fixed, the ratio  $R_{eq}/R_1$  is again seen to be of primary importance. Greatest improvement in signal-to-noise, however, will be accomplished by increasing the antenna coupling so as to increase  $g_a$ .

VI—SIGNAL-TO-NOISE RATIO WHEN BANDWIDTH IS OF PARAMOUNT IMPORTANCE

This section is concerned with those instances where the unavoidable tube or circuit capacitance is so great that the input circuit bandwidth is too narrow when the coupling is adjusted for best signal-to-noise (the bandwidth, in this case, will be even narrower for the impedance-matched condition). It will now be necessary either to adjust the reflected antenna conductance for the correct bandwidth, or to decrease the shunt resistance  $R_1$  by adding a loading resistor. From Equation (4), it is seen that the relation between  $R_1$ , the bandwidth, the reflected conductance, and the capacitance is fixed as

$$g_a R_1 = \frac{2\pi \Delta f' C R_1}{F} - 1$$

$$= \frac{\Delta \omega C R_1}{F} - 1$$

where  $\Delta \omega$  is introduced for  $2\pi \Delta f'$ . The bandwidth  $\Delta f'$  is the *r-f circuit* bandwidth and is to be distinguished from  $\Delta f$  which is the total effective bandwidth for noise purposes. When this expression for  $g_a R_1$  is substituted in Equation (3) it is found that the *signal-to-noise* ratio is

$$\frac{e_{\text{signal}}}{\sqrt{e_n^2}} = \frac{e_a}{\sqrt{e_i^2}} \sqrt{\frac{1}{\frac{T_a}{T_R} + \frac{\Delta \omega C R_{eq}}{F} + \frac{1 + (\Delta \omega C R_{eq})/F + 4 g_e R_1}{(\Delta \omega C R_1)/F - 1}}} \tag{12}$$

It is now evident that, in this special case and once the r-f bandwidth is assigned, a low value of  $R_{eq} C$  is the desideratum for best signal-to-noise. When  $R_{eq}$  and  $C$  are mainly contributed by the first tube, a possible figure of merit for the first tube is then  $\frac{1}{2\pi C R_{eq}}$  which is expressible in cycles per second. It is also evident that, when  $R_1$

approaches infinity, the best possible upper limit to the signal-to-noise ratio is obtained since the right hand term in the denominator then vanishes. The input circuit bandwidth is then obtained by the antenna loading only. Thus, the addition of a loading resistor to obtain bandwidth always results in a needless reduction of signal-to-noise ratio.

A point of some interest is that a pair of coupled circuits, with coupling adjusted for flat-top response and with  $R_1$  approaching infinity gives a value of  $F = \sqrt{2}$ . With this coupled-circuit input arrangement, the minimum signal which is just equal to the noise is then

$$e_{\min} = \sqrt{e_i^2} \sqrt{1 + 0.7(2\pi\Delta f') C R_{eq}}$$

where  $\Delta f'$  is still defined by points 3 db down at each side of the resonance curve.

#### VII.—EFFECT OF OUTPUT CIRCUIT AND SECOND TUBE ON TOTAL EQUIVALENT NOISE RESISTANCE, $R_{eq}$

A. Maximum gain: bandwidth not important—In some receivers, particularly those used at ultra-high frequencies with a low-gain amplifier or converter, it becomes necessary to consider the thermal noise and tube noise subsequent to the input stage. The calculation is most convenient if carried out in terms of an equivalent noise resistance due to the second circuit and tube, but referred to the grid of the *first* tube. The value so calculated must be added to the equivalent noise resistance of this first tube itself to obtain the total  $R_{eq}$  which has been assumed in the preceding analyses. The results are applicable whether the first tube be an amplifier or a converter. Induced grid noise will be neglected in this section.

In receiver arrangements where the bandwidth of the circuit coupling the first and second tubes is, a priori, wider than the overall bandwidth of the receiver, the coupling circuit is designed for maximum gain. With a single tuned circuit of resonant impedance  $R_2$  and with a second tube of equivalent noise resistance  $R_{eq2}$  the mean-squared noise at the grid of the second tube is proportional to  $(R_2 + R_{eq2})$ . This may be referred to the grid of the first tube by dividing by the square of the grid-to-grid gain. The total effective equivalent noise resistance at the grid of the first tube is then

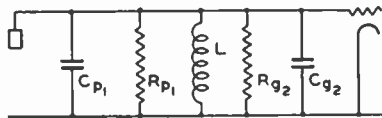
$$R_{eq} = R_{eq1} + \frac{R_2 + R_{eq2}}{(\text{GAIN})^2} \quad (13)$$

where  $R_{eq1}$  is the equivalent noise resistance of the first tube. When a pair of coupled circuits is used, with coupling adjusted for maximum gain, it is necessary to consider both primary and secondary im-

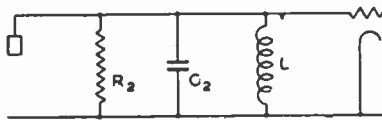
pedances. If we call the first of these  $R_{p1}$  and the second  $R_{g2}$ , the gain of the first tube will be proportional to  $\frac{1}{2}\sqrt{R_{p1}R_{g2}}$ . The mean-squared noise voltage at the grid of the second tube will be proportional to  $R_{g2}/2 + R_{eq2}$  since the primary load with optimum coupling halves the value of  $R_{g2}$  for noise-calculating purposes. Thus, the total effective equivalent noise resistance referred to the grid of the first tube is, in this case,

$$R_{eq} = R_{eq1} + \frac{\frac{R_{g2}}{2} + R_{eq2}}{(\text{GAIN})^2} \tag{14}$$

In both Equations (13) and (14) the gain has been assumed to be the grid-to-grid gain. It will be found that for given first and second



(a) SINGLE-TUNED CIRCUIT



(b) EQUIVALENT CIRCUIT

$$C_2 = C_{p1} + C_{g2}$$

$$R_2 = \frac{R_{p1} R_{g2}}{R_{p1} + R_{g2}}$$

Fig. 7—Circuit and its equivalent for coupling first tube to second tube.

tubes, there is little to choose between the single-circuit and the coupled-circuit cases represented by Equations (13) and (14) as regards ultimate signal-to-noise ratio. This is in marked distinction to the wideband analysis to follow.

B. Wideband operation: bandwidth a major consideration—It now becomes necessary to consider the receiver in which the bandwidth of the coupling circuit between first and second tubes is an important, if not paramount, consideration. When the first tube is a converter or mixer, for instance, the bandwidth of the coupling circuit is almost always of primary concern since it is the first i-f circuit. When the coupling circuit is a single-tuned circuit, as in Figure 7, the effective bandwidth between points 1 db down on the curve is

$$\text{Bandwidth } \Delta f' = \frac{1}{4\pi C_2 R_2} \quad (\text{for 1 db down}) \quad (15)$$

When the value of  $R_2$  from (15) is substituted in (13) and the bandwidth is  $\Delta f'$ , the total effective noise resistance becomes\*

$$R_{eq} = R_{eq1} + \frac{1 + 4\pi C_2 \Delta f' R_{eq2}}{4\pi C_2 \Delta f' (\text{GAIN})^2} \quad (16a)$$

However, the gain is also expressible as  $g_{m1} R_2$  where  $g_{m1}$  is the transconductance (or conversion transconductance) of the first tube. Thus (16a) can also be written (using again the value of  $R_2$  from (15))

$$R_{eq} = R_{eq1} + \frac{4\pi C_2 \Delta f'}{(g_{m1})^2} (1 + 4\pi C_2 \Delta f' R_{eq2}) \quad (16b)$$

It is seen clearly that, for the second tube as well as for the first, and when the bandwidth is a major consideration, the performance is

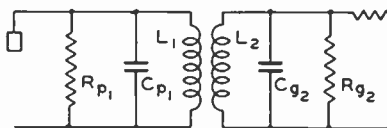


Fig. 8—Double-tuned circuit for coupling first tube to second tube.

specified by the product of a capacitance and the equivalent noise resistance, or  $C_2 R_{eq2}$ .

For wideband applications it is highly advantageous to separate the two capacitances in an interstage coupler as is done by use of the pair of coupled circuits of Figure 8 or its equivalent  $T$  or  $\pi$  network. The fluctuation noise analysis in this instance is complicated for the first time by the possibility of a triangular instead of a rectangular noise spectrum. In a pair of coupled circuits (see Figure 8) adjusted for flat-top transfer impedance (i.e., second derivative of gain vs. frequency deviation set equal to zero), the impedance looking in at one pair of terminals may be decidedly double-humped if the circuits are of unequal  $Q$ . Thus the mean-squared thermal noise across such a pair of terminals must be obtained by integrating the resistive component of impedance over the pass band. Because the complete discussion is unimportant at this point, the derivation will be given in Appendix A and only the results discussed here. It is found that, by having a low- $Q$  secondary circuit and a high- $Q$  primary circuit, a

\* It is assumed that the total thermal noise is  $4kTR_2 \Delta f$ . Actually if  $\Delta f = \Delta f'$ , due to dropping off of the tuned impedance near the edge of the pass band, this would be about 8 per cent too high, a negligible correction.

substantial reduction in thermal noise is made possible with no sacrifice in gain or circuit bandwidth.

The effective bandwidth of a pair of coupled circuits (Figure 8) taken between points 1 db down on each side and adjusted for flat response is

$$\begin{aligned} \text{Bandwidth } \Delta f' &= \frac{1}{4\pi} \left( \frac{1}{C_{p_1} R_{p_1}} + \frac{1}{C_{g_2} R_{g_2}} \right) \\ &= \frac{\omega_o}{4\pi} \left( \frac{1}{Q_1} + \frac{1}{Q_2} \right) \end{aligned} \tag{17}$$

where  $\omega_o$  is the angular frequency at the center of the band and  $Q_1$  and  $Q_2$  are primary and secondary  $Q$ 's, respectively. As shown in the appendix, the equivalent noise resistance at the grid of the first tube is then

$$\begin{aligned} R_{eq} &= R_{eq_1} + \frac{4\pi\Delta f' C_{p_1}}{g_{m_1}^2} \times \\ &\left\{ \frac{0.96 \left( 1 + \frac{Q_1}{Q_2} \right) \left( 1 + 0.158 \frac{Q_1}{Q_2} \right) + \left( 1 + \frac{Q_1}{Q_2} \right)^2 2\pi\Delta f' C_{g_2} R_{eq_2}}{1 + \left( \frac{Q_1}{Q_2} \right)^2} \right\} \end{aligned} \tag{18}$$

where  $g_{m_1}$  is the transconductance or conversion transconductance of the first tube. It is easily shown that (18) is lowest when  $Q_1 \gg Q_2$  (see appendix) and this choice should always be made whenever possible. The part of the noise due to thermal agitation in the coupling network is reduced considerably by the choice. With this condition (i.e.,  $Q_1 \gg Q_2$ )

$$R_{eq} = R_{eq_1} + \frac{4\pi\Delta f' C_{p_1}}{g_{m_1}^2} (0.15 + 2\pi\Delta f' C_{g_2} R_{eq_2}) \tag{19}$$

Again, as in the previous cases, it is evident that the noise of the second tube is determined by the product  $C_{g_2} R_{eq_2}$  which should be as small as possible. It is of considerable importance that the primary capacitance,  $C_{p_1}$ , (which is determined largely by the output capacitance of the first tube) should be as small as possible. If the condition  $Q_1 \gg Q_2$  is fulfilled, it will seldom be found that the thermal noise of the inter-stage circuit is appreciable compared with the noise produced by the

second tube. Thus, for most practical purposes, (19) may be replaced by

$$R_{eq} = R_{eq1} + \frac{R_{eq2}}{(\text{GAIN})^2} \quad (19a)$$

provided coupled circuits are used as indicated. Equation (19a) is obtained from (19) by neglecting the factor, 0.15, substituting  $|Z_t|$  for its equivalent, and finally letting  $g_{m1} |Z_t| = \text{GAIN}$ .

#### VIII—PRACTICAL APPLICATION TO U-H-F RECEIVERS

Examples of the application of the foregoing analysis are readily made to ultra-high-frequency receivers for operation above 300 megacycles. In the following applications, it must be emphasized that feedback effects have been neglected and that, to some extent, this neglect may lead to discrepancies between measured results and those calculated herein. Furthermore, since the purpose of this discussion is primarily illustrative, the tube data to be used will be only approximate. Exact tube data at frequencies above 300 megacycles or so are not available in any event.

The triode mixer, used in the converter stage of the receiver, will form an important part of the discussion and it may be well to offer a word of explanation. A triode in the converter stage, followed by a low-noise i-f system, seems to offer the greatest promise for a good overall signal-to-noise ratio with tubes now commercially available. In the ordinary triode mixer, signal-frequency feedback from the i-f circuit (which looks like a capacitance at the signal frequency) through the grid-plate capacitance may be very important in reducing the input resistance. However, in receivers designed to cover a very limited tuning range, a simple expedient may be used to greatly reduce feedback. If the i-f output circuit is designed so as to present a very low impedance to signal frequency, the signal-frequency voltage on the plate may be reduced so that feedback becomes negligible. As a simple example, consider the primary winding of the i-f transformer. At signal frequency, this winding is above its natural resonance, and behaves as a capacitance. If we add, in series with it, a small inductance (a loop of wire or a length of lead) and adjust the latter to series resonance with the effective distributed capacitance of the i-f coil, we obtain a series resonant output circuit at signal frequency without affecting, in any way, the i-f circuit. As a minor point in connection with the triode mixer, the input capacitance and output capacitance are each increased by the amount of the grid-plate capacitance.



The equivalent noise resistances which will be used are taken from formulas given in another paper.<sup>12</sup> The conversion transconductance is assumed to be adjusted to optimum value. The electronic input conductance figures are based on available data with fixed voltages applied and, in the case of the converter stage, are averaged over the oscillator cycle. The capacitance figures which will be used represent reasonable approximations.

The data will be presented in the form of a table. In the table, the electronic input conductance is expressed in micromhos per (megacycle)<sup>2</sup>. Thus, to obtain the input conductance at any one frequency, the constant given must be multiplied by the square of the frequency in megacycles. In somewhat similar fashion, the non-electronic input loss is expressed in micromhos per megacycle. The figure given represents only a rough guess, but since this part of the loss is small in comparison with the electronic loss, its exact value is unimportant. Circuit losses, if any, will be assumed to be included in the non-electronic conductance figure. The Type 955 is assumed to be operated at a plate voltage of 180, the 954 at a screen voltage of 100. The column giving the peak oscillator voltage required is of importance in estimating the power required from the local oscillator. The grid bias of the mixer tube is assumed equal to the peak oscillator voltage in all cases.

TABLE I

First Tube and Method of Operation	Equiv. Noise Resist. $R_{eq}$ , Ohms	Trans-conduct. $g_m$ or $g_c$ , $\mu\text{mhos}$	Electronic $g_e$ Per (Mc) <sup>2</sup> , $\mu\text{mhos}$	Non-Electronic $g_n$ Per Mc., $\mu\text{mhos}$	Approx. Peak Oscillator Volts
955 Mixer—At Oscillator Fundamental	5,200	700	0.0030	0.2	5
955 Mixer—At Oscillator 2nd Harmonic	12,000	350	0.0015	0.2	12
955 Mixer—At Oscillator 3rd Harmonic	15,000	230	0.0010	0.2	34
954 Mixer—At Oscillator Fundamental	30,000	700	0.0030	0.2	5
954 Amplifier	6,000	1,400	0.0050	0.2	—

Each example to be computed will be considered at three signal frequencies, 300, 500, and 1,000 megacycles. The intermediate fre-

<sup>12</sup> E. W. Herold, "The Operation of Frequency Converters and Mixers for Superheterodyne Reception", submitted for publication to *Proc. I.R.E.*

quency (i-f) is chosen as 30 megacycles and the overall bandwidth of the radio portion of the receiver is 7 megacycles, in order to minimize tuning difficulties and to permit wideband operation, as for television. However, when the relative sensitivities (signal equal to noise) are computed, they will be referred to an arbitrary bandwidth of 10 kilocycles. The actual sensitivity for other bandwidths following the second detector, is readily computed by multiplying by the square-root of the bandwidth ratio, in the usual way, with a negligible error.

A. The i-f tube and circuit—It is observed from Equation (19) that the best tube to select for the i-f amplifier is one with the lowest product of  $C_{g_2}$  and  $R_{eq_2}$ . It is easily determined that the type 6AC7/1852 is the best of the commercially available tubes in this respect, since it has a value for  $R_{eq_2} = 780$  ohms and an effective  $C_{g_2}$  (including circuit and leads) which can be made as low as 20 micromicrofarads. This tube will, therefore, be chosen. In each example, the tube working into the i-f system will be an "Acorn" type and a total effective output capacitance of 5 micromicrofarads ( $C_{p_1}$ ) will be assumed. This value is high enough to include circuit and leads. There is no significant difference between the 954 and 955 types in output capacitance because, with the latter, it is necessary to add the grid-to-plate capacitance as well. Because the i-f system is common to each example, we may compute its contribution to the noise immediately. The output plate impedance of a 955 mixer or converter is easily shown to be in excess of 20,000 ohms, while the 6AC7/1852 has an input impedance of around 5,000 ohms. Thus, if we use a pair of coupled circuits as the first i-f transformer,  $Q_1 > 19$  and the secondary loaded by the 6AC7 only will have  $Q_2' = 19$ .† These  $Q$ 's are so much higher than required to give our desired 7-megacycle circuit bandwidth that a damping resistance must be added.

Following the low-noise design exemplified by the discussion following Equation (18) we will add all the damping to the secondary. For simplicity, let us assume  $Q_1 = 19$  in every case.‡ Then Equation (17) gives

$$\frac{1}{Q_1} + \frac{1}{Q_2} = 2 \frac{\Delta\omega}{\omega} = 2 \frac{7}{30} = 0.47$$

If  $Q_1 = 19$  we see that  $Q_2$  must be 2.4 and that we must add a shunt resistance of 730 ohms across the input to the 6AC7. Under these

† Obviously the i-f transformer losses can be neglected.

‡ This implies adding a 20,000-ohm shunt resistance across the primary of the i-f transformer when a pentode mixer is used.

circumstances,  $Q_1/Q_2 = 7.9$  and the transfer impedance is 1,600 ohms, approximately. From Equation (18) we find the effective equivalent noise resistance at the grid of the converter stage is

$$R_{eq} = R_{eq_1} + \frac{523 \times 10^{-6}}{g_c^2}$$

Using the values from Table I for  $R_{eq_1}$  and  $g_c$ , we find  $R_{eq}$  for each of the converter stage possibilities.

B. Converter as first stage—It is first necessary to determine whether the input circuit bandwidth is sufficiently wide. The narrowest bandwidth of any example considered, will be obtained with the lowest frequency, 300 megacycles, and the highest value of input resistance, obtained with the 955 mixer operating at the third harmonic of the applied oscillator frequency. Using Equation (4) and letting  $g_a R_1 = 1$  (the lowest value which should be considered in a low-noise design), the circuit bandwidth is at least

$$\Delta f' = \frac{1}{\pi C R_1} = \frac{1}{\pi \times 5 \times 10^{-12} \times \left( \frac{10^6}{0.001 \times (300)^2 + 0.2 \times 300} \right)} = 9.6 \text{ megacycles}$$

Thus, it is found that the r-f bandwidth need not be increased in any of the examples and the receiver may be designed for best signal-to-noise ratio. Section IV of this paper is then applicable.

The calculations for each example are straightforward and only one will be carried out in detail. The others will be tabulated later in this section of the paper. We see from Equation (9) that we need only  $R_{eq}$ ,  $R_1$ , and  $g_e$ . Let us choose for the detailed example the 500-megacycle receiver with a 955 mixer operating at oscillator fundamental. Then

$$R_{eq} = R_{eq_1} + \frac{523 \times 10^{-6}}{g_c^2} = 5200 + 1070 = 6270 \text{ ohms}$$

Also

$$R_1 = \frac{1}{g_e + g_\Omega} = \frac{10^6}{0.003 \times (500)^2 + 0.2 \times 500} = 1180 \text{ ohms}$$

Finally

$$g_e R_1 = 0.003 \times (500)^2 \times 10^{-6} \times 1180 = 0.88$$

Using Equation (9), we find  $e_{a_{min}} = \sqrt{e_i^2} \times 5.1$

For  $R_a = 75$  and  $\Delta f = 10 \text{ kc}$ ,  $\sqrt{e_i^2} = 0.11$  microvolts so that the minimum open-circuit antenna signal to equal the noise is  $e_{a_{min}} = 0.56$  microvolts. If a signal generator is used which has been calibrated

for the matched impedance condition, its calibration should indicate just half of the above value.

It is interesting to compare the sensitivity just computed with that which would obtain if the impedance-matched condition had been used. Using Equation (6), we find

$$\text{impedance-matched } e_a = 0.57 \text{ microvolts}_{min}$$

This represents a negligible reduction in signal-to-noise ratio. The result should have been expected from inspection of the curves of Figure 6 which are nearly coincident at the value of  $R_1/R_{eq}$  appropriate to this example.

C. Amplifier as first stage—Let us assume a 954 amplifier followed by a converter stage with the lowest noise equivalent (the 955 operated at oscillator fundamental). The calculations will be made neglecting the induced grid noise in the converter and assuming an idealized condition with no feedback in the r-f stage. In this example, the interstage circuit impedance will be given by half of the geometric mean of the 954 output impedance and the converter input impedance. Recent data on the 954 indicate an output conductance due to lead losses etc. roughly equal to

$$954 \text{ output } g = 0.0006 \times (\text{megacycle})^2 \text{ (in micromhos)}$$

For this relation, the 300-, 500-, and 1,000-megacycle interstage transfer impedances are then 3,700, 1,400, and 360 ohms, respectively. With  $g_m = 1,400$  micromhos, the grid-to-grid gains are then 5.2, 2.0, and 0.5, respectively. The value of  $R_{eq_2}$  will be taken as 6,270 ohms (to include i-f noise) while  $R_{eq_1}$  (Table I) is 6,000 ohms. We find from Equation (14)

$$R_{eq} = R_{eq_1} + \frac{\frac{R_{v_2}}{2} + R_{eq_2}}{(\text{GAIN})^2} = \begin{cases} 6,300 \text{ ohms for 300 megacycles} \\ 6,700 \text{ ohms for 500 megacycles} \\ 32,000 \text{ ohms for 1,000 megacycles} \end{cases}$$

Using the conductance data from Table I, we find

$$R_1 = \begin{cases} 2,000 \text{ ohms for 300 megacycles} \\ 740 \text{ ohms for 500 megacycles} \\ 190 \text{ ohms for 1,000 megacycles} \end{cases}$$

The minimum open-circuit antenna signal is then readily computed. For Equation (9) (the condition for best signal-to-noise ratio), the relative open-circuit antenna signals ( $R_a = 75$ ,  $\Delta f = 10$  kilocycles) are

$$e_a = \begin{cases} 0.46 \text{ microvolts at 300 megacycles} \\ 0.70 \text{ microvolts at 500 megacycles} \\ 2.9 \text{ microvolts at 1,000 megacycles} \end{cases}_{min}$$

It is evident from these figures that a 954 r-f amplifier stage is inferior to the 955 converter stage, from a signal-to-noise point of view, even at 300 megacycles. This was already in evidence in Table I since both  $R_{eq_1}$  and  $g_e$  were lower for the 955 mixer than for the 954 amplifier.

TABLE II

First Tube	Minimum Open-Circuit Antenna Signals		
	300 Mc	500 Mc	1,000 Mc
955 Mixer—At oscillator fundamental	0.39 $\mu$ V	0.56 $\mu$ V	1.02 $\mu$ V
955 Mixer—At oscillator 2nd harmonic	0.45	0.66	1.20
955 Mixer—At oscillator 3rd harmonic	0.47	0.69	1.23
954 Mixer—At oscillator fundamental	0.75	1.15	2.22
954 Amplifier—Followed by 955	0.46	0.70	2.9

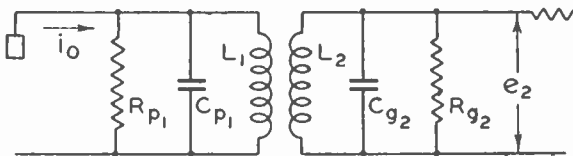


Fig. 9—Double-tuned circuit with constant-current drive.

D. Tabulated results for all examples—It is assumed that  $R_a = 75$  ohms,  $\Delta f = 10$  kilocycles and the design for best signal-to-noise is used (Equation (9)).

One of the more interesting aspects of the table is the fact that the 955 used as a mixer at 2nd or 3rd harmonic of the applied oscillator is less than 2 db poorer in signal-to-noise ratio than it is with the oscillator fundamental. It is, of course, necessary to apply a considerably larger oscillator voltage when harmonic conversion is desired.

APPENDIX A

Calculation of Noise in Wide Band Coupled Circuit Fed by Constant-Current Source

Because the behavior of coupled circuits is reasonably well known, no attempt to derive the basic relations for transfer impedance, bandwidth, etc. will be made here. The relations which will be used represent the usual approximations which hold exactly only for high Q's (i.e., bandwidth small compared to center frequency), but which are

qualitatively correct even for a low- $Q$  circuit. Referring to the figure, if  $Q_1 = \omega C_{p1} R_{p1}$ , the primary circuit  $Q$ , and  $Q_2 = \omega C_{p2} R_{p2}$ , the secondary circuit  $Q$ , then the transfer impedance is

$$\left| \frac{e_2}{i_o} \right| = |Z_t| = \frac{\sqrt{2}}{\omega_o \sqrt{C_{p1} C_{p2}}} \frac{\sqrt{\frac{1}{Q_1^2} + \frac{1}{Q_2^2}}}{\left( \frac{1}{Q_1} + \frac{1}{Q_2} \right)^2} \sqrt{\frac{1}{1 + \frac{2^6}{\left( \frac{1}{Q_1} + \frac{1}{Q_2} \right)^4} \left( \frac{\delta\omega}{\omega_o} \right)^4}} \quad (20)$$

where  $\delta\omega$  is the deviation from the center angular frequency,  $\omega_o$ . This equation assumes flat-top response, i.e., zero second derivative of  $|Z_t|$  at center frequency. The total bandwidth,  $\Delta f'$ , for one  $db$  down on each side is then twice the deviation frequency for a one  $db$  decrease in  $|Z_t|$  and is

$$2\pi\Delta f' = \Delta\omega = \frac{\omega_o}{2} \left( \frac{1}{Q_1} + \frac{1}{Q_2} \right) \quad (21)$$

Using (21) in (20) we get

$$|Z_t| = \frac{0.707}{\Delta\omega \sqrt{C_{p1} C_{p2}}} \frac{\sqrt{1 + \left( \frac{Q_1}{Q_2} \right)^2}}{1 + \frac{Q_1}{Q_2}} \sqrt{\frac{1}{1 + 4 \left( \frac{\delta\omega}{\Delta\omega} \right)^4}} \quad (22)$$

The real part of the impedance looking into the  $C_{p2}$ ,  $R_{p2}$  terminals is

$$Rl \text{ part of } Z_{\text{secondary}} = \frac{1}{\Delta\omega C_{p2} \left( 1 + \frac{Q_1}{Q_2} \right)} \frac{1 + 2 \frac{Q_1}{Q_2} \left( \frac{\delta\omega}{\Delta\omega} \right)^2}{1 + 4 \left( \frac{\delta\omega}{\Delta\omega} \right)^4} \quad (23)$$

It is interesting to note that, if  $Q_1 \gg Q_2$ , a curve of Equation (23)

is decidedly double-humped as shown qualitatively in Figure 10. Since the thermal noise is proportional to this variable, the noise spectrum is non-uniform and, in fact, the noise at center band is very small. This behavior results in a very low average thermal noise over the pass band when  $\Delta f = \Delta f'$ . It should be remembered that  $\Delta f$ , the effective pass band for noise purposes, is largely determined by the system following the final demodulation of an incoming signal whereas  $\Delta f' = \frac{\Delta \omega}{2\pi}$  is the circuit bandwidth. Since the maximum noise will occur when  $\Delta f = \Delta f'$ , the calculations will be made on this basis. Since, as will be

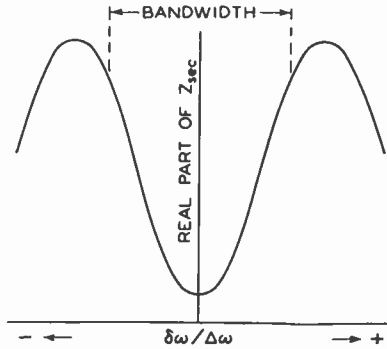


Fig. 10—The real part of the secondary impedance of a flat-top, double-tuned circuit for frequency deviations around mid-band and with primary Q much higher than secondary Q.

found, the thermal noise of the coupled circuits may be made very low, the correction which might have been applied when  $\Delta f \ll \Delta f'$  would not have been of significance in any event.

We are now in a position to compute the thermal-noise voltage at the grid of the second tube, add to it the equivalent second-tube noise voltage, and, if we choose, refer the total back to the grid of the preceding tube by dividing by the square of the gain,  $(g_{m1}Z_t)^2$ . The mean-squared noise of thermal agitation at the grid of the second tube is

$$\left( \overline{e_{t_2}^2} \right)_{\text{circuit}} = 4kT_R \frac{1}{2\pi} \int_{\omega_0 - \frac{\Delta \omega}{2}}^{\omega_0 + \frac{\Delta \omega}{2}} \text{Rl part of } Z_{\text{sec}} d\omega$$

where  $\omega_0$  is the mid-band angular frequency. This is equivalent to the thermal noise of a resistance at the second-tube grid of value

$$\begin{aligned}
 R_{t_2} &= \frac{1}{\Delta\omega} \int_{\omega_0 - \frac{\Delta\omega}{2}}^{\omega_0 + \frac{\Delta\omega}{2}} \text{Rl part of } Z_{\text{sec}} d\omega \\
 &= 2 \int_0^{\frac{1}{2}} \text{Rl part of } Z_{\text{sec}} d\left(\frac{\delta\omega}{\Delta\omega}\right)
 \end{aligned}$$

where  $\delta\omega$  is the angular frequency deviation from the center-band point and  $\Delta\omega$  is the angular bandwidth to points 1 db down. Using Equation (23), we obtain

$$\begin{aligned}
 R_{t_2} &= \frac{2}{\Delta\omega C_{\rho_2} \left(1 + \frac{Q_1}{Q_2}\right)} \int_0^{\frac{1}{2}} \frac{1 + 2 \frac{Q_1}{Q_2} x^2}{1 + 4x^4} dx \left(\text{where } x = \frac{\delta\omega}{\Delta\omega}\right) \\
 &= \frac{0.96}{\Delta\omega C_{\rho_2}} \frac{1 + 0.158 \frac{Q_1}{Q_2}}{1 + \frac{Q_1}{Q_2}} \quad (24)
 \end{aligned}$$

Equation (24) shows that  $R_{t_2}$  varies over a 6:1 range as  $Q_1/Q_2$  is varied from one extreme ( $Q_1 \gg Q_2$ ) to the other ( $Q_2 \gg Q_1$ ). When  $Q_1 \gg Q_2$ , the noise spectrum is non-uniform and, at mid-band frequency, the thermal noise is very much reduced over that at the edge of the band.\* The transfer impedance (i.e., the gain) is, of course, constant over the band by the a priori relations.

The total effective noise resistance at the second-tube grid is ( $R_{eq_2} + R_{t_2}$ ) where  $R_{eq_2}$  is the equivalent noise resistance of the second tube. The noise may be referred back to the first-tube grid by using (21), (22), and (24) to get

$$R_{eq} = R_{eq_1} + \frac{R_{eq_2} + R_{t_2}}{(g_m |Z_t|)^2}$$

\* It should be emphasized that the thermal noise-reduction possibilities of coupled circuits cannot be utilized in the antenna-to-grid circuit in the same way.



$$= R_{eq1} + \frac{2\Delta\omega C_{p1}}{g_{m1}^2} \times \left\{ \frac{0.96 \left(1 + \frac{Q_1}{Q_2}\right) \left(1 + 0.158 \frac{Q_1}{Q_2}\right) + \left(1 + \frac{Q_1}{Q_2}\right)^2 \Delta\omega C_{p2} R_{eq2}}{1 + \left(\frac{Q_1}{Q_2}\right)^2} \right\} \quad (25)$$

The factor in the bracket of Equation (25) is determined by the choice of  $Q_1/Q_2$  which is usually up to the designer. Curves of this factor are plotted in Figure 11. They show that  $Q_1/Q_2$  should be high,

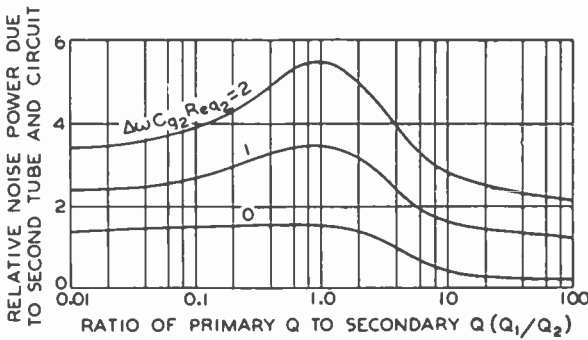


Fig. 11—The total fluctuation noise of a flat-top, double-tuned circuit of bandwidth  $\Delta\omega$  whose secondary is connected to a tube of equivalent-noise-resistance,  $R_{eq}$ , and whose total secondary capacitance is  $C_{p2}$ .

i.e., the wide-band circuit damping should be concentrated in the secondary. The overall noise improvement to be obtained by such a choice is ordinarily considerably less than the theoretical maximum of 8 db because of the major role played by the first-tube equivalent noise resistance,  $R_{eq1}$  not to mention the noise of the second tube as expressed in  $R_{eq2}$ . However, since there appear to be no major disadvantages to the choice, it can be concluded that best design of the interstage coupling circuit will occur with the damping on the secondary only.

APPENDIX B

*Signal-to-Noise Ratio for Mixer and Converter Tubes with Control Grid Not Adjacent to Cathode*

In some mixer and converter tubes the input or signal grid is not adjacent to the cathode and the preceding formulas must be modified

before they are applicable. Furthermore, the electronic conductance of a tube of this kind is usually negative<sup>12</sup> so that some consideration must be given to this aspect. The analysis and measurements of induced grid noise in such tubes gives the noise in terms of an equivalent saturated diode current,  $I_d$ .<sup>5</sup> Thus the mean-squared grid noise current is

$$\overline{i_n^2} = 2 e I_d \Delta f$$

and this noise current cannot be expressed in a simple manner in terms of  $g_e$ , the electronic input conductance, as when the control grid is adjacent to the cathode. However, at frequencies for which the transit angles are not too great,  $I_d$  increases with the square of the frequency just as does the magnitude of  $g_e$ .

The formulas developed in the body of the paper assumed the induced noise current to be  $\overline{i_n^2} = (5 \times 4k T_R g_e \Delta f)$  so that, for the present case, we find that the quantity  $4g_e R_1$  of the formulas becomes

$$4 g_e R_1 = \left( \frac{\overline{i_n^2}}{4k T_R \Delta f} - g_e \right) R_1 = (20 I_d - g_e) R_1 \quad (26)$$

For the tubes we are now considering,  $R_1$  may be negative and it must be appreciated that stability requirements demand that the reflected antenna resistance be lower than  $R_1$ . An even more stringent requirement is that imposed by bandwidth. This requirement is given by Equation (4) and may be written

$$g_a \geq \Delta \omega C - \frac{1}{R_1} \quad (27)$$

where  $\Delta \omega$  is  $2\pi\Delta f'$  and a single-tuned circuit is assumed.

The value of  $g_a$  for optimum signal-to-noise ratio, irrespective of bandwidth, is given by Equation (7). This optimum coupling condition is rewritten (using Equation (26))

$$\begin{aligned} g_a^2 &= \frac{1}{R_1^2} + \frac{1 - g_e R_1 + 20 I_d R_1}{R_1 R_{eq}} \\ &= \frac{1}{R_1^2} + \frac{g_\Omega + 20 I_d}{R_{eq}} \end{aligned} \quad (28)$$

If the value of  $g_a$  from Equation (28) is larger than that from (27) it is possible to obtain a signal-to-noise advantage by using (28). Otherwise, condition (27) must be used to assure proper bandwidth.

<sup>5</sup> C. J. Bakker, loc. cit.

<sup>12</sup> E. W. Herold, loc. cit.

Using (26) and the bandwidth condition (27), the minimum signal which is equal to the noise is found from Equation (3) to be

$$e_a \Big]_{\min} = \sqrt{4k T_R R_a \Delta f} \sqrt{\frac{T_a}{T_R} + \frac{g_\Omega + 20 I_d + (\Delta\omega C)^2 R_{eq}}{\Delta\omega C - \frac{1}{R_1}}} \quad (29)$$

If, on the other hand, the bandwidth is not a limiting consideration, we may use (26) and (28) in (3) to get the lowest possible noise and find

$$e_a \Big]_{\min} = \sqrt{4k T_R R_a \Delta f} \sqrt{\frac{T_a}{T_R} + 2 \frac{R_{eq}}{R_1} + 2 \sqrt{\frac{R_{eq}}{R_1} \left( \frac{R_{eq}}{R_1} + g_\Omega R_1 + 20 I_d R_1 \right)}} \quad (30)$$

When  $R_1$  is negative, as here contemplated, the sign of the inner square root must nevertheless be taken as positive if the result is to be valid.

LIST OF SYMBOLS

- $C$  = Total capacitance of input circuit to first tube.
- $C_{p1}$  = Total capacitance of primary circuit of interstage transformer.
- $C_{g2}$  = Total capacitance of secondary circuit of interstage transformer.
- $C_2$  = Sum of  $C_{p1}$  and  $C_{g2}$ . Total shunt capacitance effective across a single-tuned circuit between first and second tubes.
- $e_a$  = Open-circuit signal voltage from antenna.
- $e_i^2$  = Open-circuit mean-squared noise voltage from an antenna which can be considered at room temperature.
- $F$  = Factor by which double-tuned antenna transformer is better than single-tuned as regards bandwidth.
- $\Delta f$  = Overall receiver bandwidth for noise purposes (usually determined after final demodulation of signal).
- $\Delta f'$  = Circuit bandwidth. This has a minimum value equal to  $\Delta f$ .
- $\Delta\omega$  = Overall angular circuit bandwidth; equal to  $2\pi\Delta f'$ .

$\delta\omega$  = Angular-frequency deviation from center of a band-pass circuit.

$\omega_0$  = Center frequency of band-pass circuit.

$g_a$  = Reflected antenna conductance in secondary of input circuit.

$g_e$  = Electronic input conductance of first tube.

$g_\Omega$  = Circuit and "cold" tube loading conductance of input to first tube.

$g_{m1}$  = Transconductance or conversion transconductance of first tube.

$k$  = Boltzmann's constant ( $1.37 \times 10^{-23}$  joules per °K).

$m$  = Effective turns ratio or step-up of antenna-to-grid circuit.

$Q_1$  = Ratio of shunt resistance to reactance of primary circuit of interstage transformer.

$Q_2$  = Ratio of shunt resistance to reactance of secondary circuit of interstage transformer.

$R_a$  = Radiation resistance of antenna.

$R_1$  = Impedance of secondary side of antenna-to-grid circuit with tube connected but with antenna disconnected.

$R_{p1}$  = Shunt resistance across primary of interstage transformer.

$R_{p2}$  = Shunt resistance across secondary of interstage transformer.

$R_2$  = Shunt resistance across single-tuned circuit as interstage network.

$R_{e,q}$  = Total equivalent noise resistance at grid of first tube including noise due to first tube, interstage circuit, and second tube.

$R_{eq1}$  = Equivalent noise resistance of first tube at its grid.

$R_{eq2}$  = Equivalent noise resistance of second tube at its grid.

$T_a$  = Temperature of a resistance equal to antenna radiation resistance and having same mean-squared noise as antenna.

$T_R$  = Room, or ambient, temperature.

$|Z_t|$  = Magnitude of transfer impedance of interstage transformer.

# SOME ASPECTS OF RADIO RECEPTION AT ULTRA-HIGH FREQUENCY\*†

BY

E. W. HEROLD‡ AND L. MALTER#

## Part I. The Antenna and the Receiver Input Circuits

BY

E. W. HEROLD

*Summary*—This paper is in five parts, of which this is the first, and includes material prepared by the authors for a lecture course given during 1941-1942.

At ultra-high frequencies the fluctuation noise of tubes and circuits in the receiver is sufficiently greater than antenna noise and other forms of interference so as to limit the reception of weak signals. Signal-to-noise ratio is often one of the chief problems in reception at ultra-high frequencies. The bandwidth of the receiver is also of great importance, both for the determination of the maximum speed at which intelligence can be received and for the determination of the total noise which will be encountered. Circuit and noise bandwidth are not always the same and are distinctly separated in the analyses. Finally, selectivity is a third important aspect of ultra-high-frequency reception.

It is shown that the receiving antenna "captures" an amount of the transmitted power which, at a given wavelength, depends only on the directivity. Thus, receiving-antenna design is chiefly concerned with directivity, which determines the maximum signal-to-noise ratio, and with bandwidth, or  $Q$ , which determines the useful frequency range. The  $Q$  of the half-wave dipole is determined by its surge impedance which in turn depends on the ratio of diameter to length of the conductors. The antenna  $Q$  is low even for small diameters and is lowered even further by the receiver load. Coupling the antenna to the receiver requires low-loss transmission lines and proper impedance matching. The amount of reflection at line-coupling elements or at insulating beads can easily be calculated and formulas are given for cases in which the nonuniform sections are short compared with the wavelength. The losses due to such reflections rise with frequency and may be appreciable even for rather small beads, if isolated.

The selectivity of superheterodyne receivers is largely obtained in the intermediate-frequency stages. However, the receiver input circuits, prior to the mixer stage, determine the image response. It is found that the image-to-signal ratio depends on the ratio of the input-circuit bandwidth to intermediate frequency. Thus, high intermediate frequencies are desirable. The design of resonant-line input circuits between the antenna and

\* Decimal classification: R320 × R361.2.

† Reprinted from *Proc. I.R.E.*, August 1943.

‡ Research Department, RCA Laboratories Division, Princeton, N. J.

# Tube Department, RCA Victor Division, Lancaster, Pa.; now with the Research Department, RCA Laboratories Division, Princeton, N. J.

*the tube to obtain any desired bandwidths can be carried out by use of lumped-circuit equivalents. This procedure is simplified since distributed losses in the line circuits can often be neglected in comparison with the lumped loss introduced by connection of a tube. If a bandwidth is too narrow, the Q can be lowered by coupling the antenna tighter. If the bandwidth is too wide, the Q can be raised by coupling the tube more loosely to the circuit.*

*An Appendix gives useful data for transmission-line circuits including their equivalents in the form of lumped L and C circuits.*

## I. INTRODUCTION

**D**URING the winter of 1941-1942, a lecture course entitled "Ultra-High-Frequency Practice" was conducted in the northern New Jersey area by the Newark College of Engineering and Rutgers University under the auspices of the Engineering, Science and Management War Training Program. Most of the following material was prepared for the portion of the course dealing with reception and was presented to seven sections of the course by the authors. The material was also used by E. W. Herold in a portion of an ESMWT course given at the Polytechnic Institute of Brooklyn during the summer of 1942.

The work is intended to be useful to those who, although familiar with radio technique at lower frequencies, have only recently encountered the problems peculiar to the very high frequencies. It is also intended that this series survey the field in a broad way so as to acquaint the specialist in other ultra-high-frequency fields with the basic problems of reception. Many of the aspects covered have been previously published in scattered papers and frequent reference is made to the more important of these. They must be consulted for detailed information since this presentation is necessarily condensed.

The subject has been divided into five parts, chiefly corresponding to individual lectures of the aforementioned course, and each part is essentially complete in itself. These five parts are:

Part I. The Antenna and the Receiver Input Circuits — E. W. Herold

Part II. Admittances and Fluctuation Noise of Tubes and Circuits — L. Malter

Part III. The Signal-to-Noise Ratio of Radio Receivers — E. W. Herold

Part IV. General Superheterodyne Considerations — L. Malter

Part V. Frequency Mixing Diodes — E. W. Herold

## II. THE CHIEF PROBLEMS IN ULTRA-HIGH-FREQUENCY RECEPTION

1. *Signal-to-Noise Ratio*

One of the chief differences between the ultra-high-frequency problem and reception at lower frequencies lies in the fact that there is frequently only one receiver for each transmitter. At lower frequencies, one of the major fields is broadcasting whereas at ultra-high frequencies (above 100 megacycles) it is not usual to use a single transmitter covering a very large number of receivers. Instead, we often have what is called point-to-point communication. This is a factor which greatly influences receiver and receiving-antenna design. At the antenna, it leads to directive arrays; these are all the more useful at ultra-high frequency because of the high directivity which may be obtained in a small space. In the receiver it means better design and more justification for good performance irrespective of cost. For example, suppose a distance  $d$  must be covered by a transmitter of power  $P_t$ . The received power will vary as some rapidly diminishing function of the distance  $f(d)$ , and is

$$P_r = kf(d)P_t$$

However, in any receiving system, we have a certain amount of unavoidable interference which we may broadly class as "noise":

1. The noise received by the antenna along with the signal.
2. The noise generated in a receiver during the process of reception. We may call the total noise power at the receiver  $P_N$  and, for the signal to be heard readily,  $P_r > P_N$ . Thus the transmitter power

$$P_t > \frac{P_N}{kf(d)}$$

and it is important that the total noise power be small if  $d$  is large since then  $f(d)$  is small. Now at frequencies below 20 megacycles, the receiver noise may be made small compared with that received by an efficient antenna. Jansky<sup>1</sup> found that the antenna noise was always at least four times that of his receiver at 20 megacycles. Antenna noise at lower frequencies is chiefly a result of local atmospheric but at 20 megacycles much of it appears to come from interstellar radiation. From 20 megacycles up to about 70 megacycles the noise received by the antenna diminishes although ignition noise and man-made inter-

<sup>1</sup> K. G. Jansky, "Minimum noise levels obtained on short-wave radio receiving systems," *Proc. I.R.E.*, vol. 25, pp. 1517-1530; December, 1937.

ferences are present. Above 70 megacycles the antenna noise level becomes so small compared with receiver noise that there is no clear evidence as to its magnitude. At ultra-high frequencies, therefore, receiver noise is the chief component of  $P_N$  and one is faced with quite a different problem from that encountered at lower frequencies.

In a good all-wave radio receiver, with a tuned radio-frequency stage properly coupled to an antenna, we would not, as a rule, find any contribution to  $P_N$  by receiver noise. The same radio-frequency stage, which might use an ordinary broadcast receiving tube such as the type 6SK7, could be made operative at 100 megacycles. At this frequency, however, laboratory measurements would show that the receiver contributed something like 31 times as much noise as the dummy antenna and  $P_N$  would be about 32 times the antenna noise, a high value. By choice of the proper ultra-high-frequency tube, a receiver could be designed to reduce  $P_N$  to around four times the dummy antenna noise. We could then reduce our transmitter power to  $\frac{1}{8}$ , a saving of  $\frac{7}{8}$  of its original power. This simple example shows that a reduction in receiver noise, which is the same as an improved signal-to-noise ratio, is worth many dollars in terms of transmitter power.

As the frequency gets higher, the antenna noise level remains small and the receiving tubes are less efficient so that the contribution of the receiver to  $P_N$  is larger and larger in comparison with our ultimate noise level. Every improvement in the receiver, therefore, cuts the transmitter power.

These points are emphasized because the most important fundamental problem of receiver design at ultra-high frequency is the signal-to-noise ratio.

## 2. Bandwidth

The next aspect of ultra-high-frequency receiver design which must be emphasized is bandwidth. As we know, a steady, unvarying direct current can transmit no intelligence. If this current varies slowly, it transmits information slowly, i.e., at a low rate. The more rapid the variations, the more intelligence can be transmitted in a given time. However, radio transmissions operate by modulating the carrier by the intelligence, so the carrier must be transmitted. That is, the carrier frequency must be at least as high as the highest modulating frequency. If many channels are required, a very high carrier frequency must be used. In very many ultra-high-frequency applications, a wide band is necessary; bands of 1 or 2 megacycles are common and for television purposes bands of 10 megacycles or more are desirable. It may be pointed out that, even if one wishes to send only voice transmission on



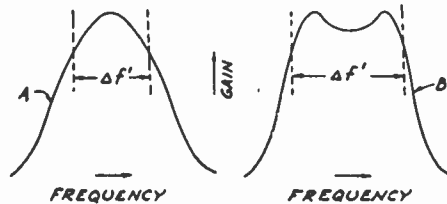
an ultra-high-frequency carrier one must consider the frequency stability of the oscillator. Thus the receiver band must be considerably wider than 10 kilocycles to take care of possible frequency drift.

Now, to return to bandwidth, as the frequency becomes higher, circuit  $Q$ 's become higher but often tubes load down the circuits to some extent and the net  $Q$  is not far from that at low frequencies. Thus, since the bandwidth of a circuit tuned to a frequency  $f$  is

$$\Delta f' \text{ (3 decibels down)} = \frac{f}{Q}$$

it is found that a loaded circuit of over-all  $Q = 100$  still has considerable bandwidth. In general, the circuit  $Q$ 's in the ultra-high-frequency field are very high and the low over-all  $Q$  is the result of connecting a tube with its associated lead and electronic losses. However, by tapping down on the circuit, it is possible to drive a tube and yet keep the over-all  $Q$  high, with a slight sacrifice in signal.

Fig. 1—Frequency responses of typical amplifiers or receivers. The circuit bandwidth  $\Delta f'$  is defined roughly by points 3 decibels down from the maxima.



While on the subject of bandwidth, there are two quantities, between which we must distinguish, both of which are called bandwidth. If we have a circuit, or an amplifier, or a receiver, it will have an output-versus-frequency curve such as *A* or *B* of Figure 1. If all the frequencies in a transmitted signal are to be received with a specified fidelity we design our receiver response to be reasonably smooth and then define the bandwidth arbitrarily in terms of this fidelity. In Figure 1, for example, a bandwidth  $\Delta f'$  is indicated on both curves and is defined by the 3-decibel down points. For noise purposes, however, this bandwidth has no direct significance. Suppose we consider a noise which is distributed uniformly over all frequencies so that the noise output spectrum has the same amplitude shape as the selectivity curves of Figure 1. The measurement of the noise must be made in terms of the over-all effect. Since the noise may be considered as similar to a large number of different frequencies (closely spaced) we must add them in root-mean-square fashion or better yet, add their power. The noise power is proportional to the *square* of the curves of Figure 1;

such squared curves are shown in Figure 2. The total area under the curves in Figure 2 gives the total noise power output

$$\text{noise power} = k_n \int_0^\infty G^2(f) df$$

where  $k_n$  is a measure of the noise input power per unit bandwidth and  $G(f)$  is the gain at a frequency  $f$ . Now if the signal was also *uniformly* distributed over the band we could compare the noise power to the signal power by using  $k_n$  only, without regard to the integral, which would be the same for both signal and noise. This would be true, for example, if we used a calibrated noise source as the source of signal. Actually, in most measurements and tests, a single-frequency signal is used. Suppose this signal is tuned in at a frequency  $f_0$ . Then our signal output power is

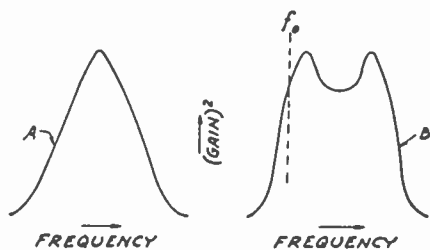


Fig. 2—Square of the frequency response of the typical amplifiers or receivers of Figure 1. Frequency  $f_0$  denotes position of a possible signal for signal-to-noise comparison.

$$\text{signal power} = k_s G^2(f_0)$$

where  $k_s$  is a measure of the signal input power. Then

$$\frac{\text{noise power}}{\text{signal power}} = \frac{k_n \int_0^\infty G^2(f) df}{k_s G^2(f_0)} = \frac{k_n}{k_s} \Delta f$$

and we define  $\Delta f$  as the noise bandwidth. What it represents is simply the bandwidth of a rectangle of height  $G^2(f_0)$  having the same noise as  $\int G^2(f) df$ . It is clear that  $\Delta f$  is altered if the frequency  $f_0$  of the test signal is altered. It differs markedly, therefore, from the circuit bandwidth  $\Delta f'$ , which was shown in Figure 1.

In this discussion,  $\Delta f$  will stand for the noise bandwidth and  $\Delta f'$  for the circuit or receiver bandwidth for signal purposes, as exemplified in Figure 1.

### 3. Selectivity

The final item which is needed in a receiver is *selectivity*. We must be able to distinguish between two signals of different frequency so as to select one of them. The superheterodyne principle is universally employed to improve selectivity since, with it, the same selectivity is obtained for all stations and the intermediate-frequency amplifier is easily designed to meet any requirements. With the superheterodyne there is, however, one factor which gives trouble and that is the response to the so-called image frequency. A signal whose frequency is *higher* than that of the local oscillator will give the same intermediate frequency as one which is *lower* by the same amount and both can be heard. If we use a high intermediate frequency the two responses are far apart and our radio-frequency signal circuit will separate them. This is the cure usually adopted at ultra-high frequency. In a broadcast receiver, the intermediate frequency is of the order of 450 kilocycles. In the ultra-high-frequency receiver, it is commonly above 10 megacycles and is sometimes as high as 100 megacycles when really excellent image reduction is desired.

## III. THE RECEIVING ANTENNA

### 1. Induced Signal Voltage, Directivity, and the Equivalent Circuit

The purpose of the receiving antenna is to "capture" some of the transmitted radiation so as to enable one to utilize the transmitted intelligence. It should be made clear at the outset that the effectiveness of the receiving antenna in picking up the transmission imposes a fundamental limitation on the signal-to-noise ratio. We cannot think about, or compute, the absolute sensitivity of a receiving system without first knowing the absolute sensitivity of the antenna. Actually a receiving antenna may be considered as having an induced electromotive force (induced by the transmitted signal) and an internal resistance, the radiation resistance. Thus the available received signal power is a definite quantity which we must know before the signal-to-noise ratio can be discussed in Part III of this series. We shall now demonstrate that this received signal power at a given wavelength is a function of only one quantity which can be controlled at the receiver, namely, the receiving-antenna directivity. As a result, the design of the receiving antenna is concerned only with directivity, which determines the maximum signal-to-noise ratio and with bandwidth or  $Q$  which determines the useful frequency range.

For most ultra-high-frequency applications, the so-called reciprocity law holds and it may be used to demonstrate the fundamental property

of the receiving antenna. Following the analysis of D. O. North,<sup>2</sup> if antenna *B* transmits to an antenna *A*, as in Figure 3, we know that the open-circuit voltage at antenna *A* is proportional to the current into *B*; i.e.,

$$e_a = k i_b.$$

The reciprocity law in one of its forms<sup>3</sup> tells us that, if antenna *A* is used at the transmitter end, *k* is the same in both directions; i.e.,

$$e_b = k i_a.$$

We also know that antenna *B* will have a radiation resistance  $R_b$ , and radiates a power  $i_b^2 R_b$ , so that the receiving antenna *A* will have a voltage proportional to the square root of this power,

$$e_a \propto \sqrt{R_b} i_b.$$

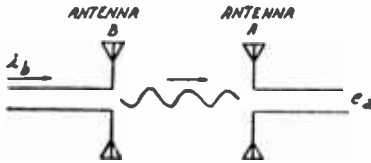


Fig. 3—Transmission of signal from antenna *B* to antenna *A*. A current  $i_b$  in the transmitting antenna induces an open-circuit electromotive force  $e_a$  in the receiving antenna.

But if *A* were the transmitter

$$e_b \propto \sqrt{R_a} i_a.$$

So we see that *k* must be proportional to the square root of the radiation resistances of both transmitting and receiving antennas. Thus

$$e_a = k' \sqrt{R_a R_b} i_b.$$

Now we know more about  $k'$ ; we know that it becomes smaller as our distance increases, and we also know that it depends on the product of directivities of receiving and transmitting antennas. Thus we may write

$$e_a = \sqrt{A} f(d) D_a D_b \sqrt{R_a R_b} i_b$$

or, squaring

<sup>2</sup> D. O. North, "The absolute sensitivity of radio receivers," *RCA REVIEW*, vol. 6, pp. 332-343; January, 1942.

<sup>3</sup> S. A. Schelkunoff, "Electromagnetic Waves," D. Van Nostrand Co., New York, N. Y., 1943.

$$e_a^2 = Af^2(d) D_a^2 D_b^2 R_a R_b i_b^2$$

where  $A$  is some constant and  $D_a^2$  and  $D_b^2$  are directivities. North<sup>2</sup> defines the directivities to represent the ratio of effectiveness of transmission or reception at a particular direction and polarization angle to the average over all directions and angles. That is,  $D_a^2$  represents the power gain of the receiving antenna over a hypothetical completely nondirectional unpolarized antenna.<sup>4</sup> We may associate  $S = f^2(d) D_b^2 i_b^2 R_b$  with the transmitter, and write

$$e_a^2 = AR_a D_a^2 S$$

where  $S$  is not controllable at the receiver. Actually  $S$  represents simply the fraction of the total transmitter power which is effective at the receiver. It may be expressed as the density of radiation in watts per square meter and is called the Poynting vector. The relation between  $S$  and the field strength  $E$  is simple and is

$$S = \text{watts/meter}^2 = E^2/120\pi$$

where  $E$  is in volts per meter and  $120\pi$  has the dimension of ohms. For any received radiation,  $S$  has a definite direction and  $D_a$  is also a function of direction. Finally, it was shown by North<sup>2</sup> that  $A = \lambda^2/2\pi$ . Hence

$$e_a^2 = \frac{\lambda^2}{2\pi} R_a D_a^2 S.$$

All this is perfectly reasonable. First, consider the dependence on  $\lambda^2$ . We know a half-wave dipole has a radiation resistance of some 73 ohms and a certain directivity pattern, no matter what the wavelength is. But surely at  $\lambda = 1$  meter where the dipole is  $1/2$  meter long we would expect less pickup than at 10 meters where the dipole is 5 meters long. Ordinarily we say

$$e_a = Eh$$

where  $E$  is the field strength and  $h$  the "effective height." For a half-wave dipole, approximately,  $h = (2/\pi)l$  where  $l$  is the length  $\lambda/2$  so that we see in this example that the square of  $e_a$  is proportional to  $\lambda^2$ . The same should be true of any antenna.

Next it is seen in the equation that  $e_a^2$  depends on  $R_a$ , the radiation

<sup>4</sup> By this definition the half-wave dipole has a value of  $D_a^2$  of about 3.3 and a non-directional but polarized antenna has a  $D_a^2 = 2$ .

resistance. This is again reasonable. The quantity  $e_a^2/R_a$  is a power and is just four times the maximum power we might extract from the receiving antenna. Surely this depends on the radiation density  $S$  from the transmitter and  $\lambda^2 D_a^2/2\pi$  is four times the "capture" area. That is,  $S$  is watts per square meter and the effective area of the receiving antenna is  $\lambda^2 D_a^2/8\pi$ .

The importance of these considerations is that we now know that, no matter what the antenna is like, its open-circuit voltage depends only on the wavelength, the directivity, the radiation resistance, and, of course, on the intensity of received radiation. We may substitute for the real antenna, then, an equivalent circuit consisting of a generator  $e_a$ , a resistor  $R_a$ , and the antenna reactance  $X_a$ , as in Figure 4. For a given transmitter and a given wavelength, we see that  $e_a^2/R_a$  is only affected by a change in the directivity. In other words, the maximum power we can abstract from the receiving antenna can only be increased by increasing the directivity; we cannot, for example, redesign an antenna to give a different radiation resistance and expect improved reception unless, at the same time, the directivity has been increased.

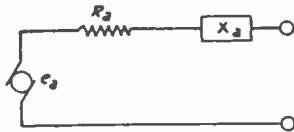


Fig. 4—Equivalent circuit of receiving antenna. At a given wavelength the quantity  $e_a^2/R_a$  is a function only of the directivity and field strength of the transmitter. The antenna reactance is represented by  $X_a$ .

Let us look into this property of directivity and "capture" area a little further by again considering the half-wave dipole as an example. The directivity factor  $D_a^2$  is approximately 3 so that the effective "capture" area is

$$\text{area} = \frac{\lambda^2}{8\pi} D_a^2 \approx \frac{\lambda^2}{8} \approx \frac{l^2}{2}$$

or the area of a square each of whose sides is  $l/\sqrt{2}$ . Thus the half-wave dipole captures the radiation from a square whose diagonal is a half wavelength. For a large reflector or some other type of array large compared with the wavelength, we should expect that the maximum "capture" area is fairly close to the actual area; i.e., that  $e_a^2/4R_a$  is approximately equal to the product of  $S$  and the actual area. We can, therefore, get some idea of the directivity of a large reflector or array by its area. The power gain of a large array over a half-wave dipole will be given very approximately by the ratio of the area to  $\lambda^2/8$  and is

power gain of reflector or array =  $8 \frac{\text{area of array}}{\lambda^2}$  (very approximate).

This assumes that the area of the reflector is large compared with the wavelength.

## 2. Antenna Frequency Range (Bandwidth)

Although we have now found a first equivalent circuit for the antenna it is still necessary to discuss the nature of the antenna reactance. For practically all ultra-high-frequency applications, the antenna is tuned by itself; that is, our antenna reactance is practically zero somewhere in the frequency range. This means we need not tune out the reactance at that frequency but, on the other hand, we must examine the frequency limits over which our antenna may be used. Excellent papers<sup>5-7</sup> on antennas and their bandwidths are available and should be consulted. We will look into the simple half-wave dipole as an illustrative example, since this antenna is the basis of practically all ultra-high-frequency designs.



Fig. 5—A half-wave dipole formed by two conical conductors of apex angle  $2\psi$ . Such a biconical dipole presents a uniform surge impedance to waves traveling along the length of the conductors.

To begin with, the ordinary half-wave dipole is nothing but an opened-out transmission line. However, if the dipole is uniform in cross section, it is a line of variable surge impedance. A very simple change which makes very little difference physically but which makes all the difference theoretically, is to assume that the conductors are conical.<sup>7</sup> Then the surge impedance is uniform and a wave starts at the center and travels out to the ends as on a uniform line. The surge impedance of such an antenna with the conical conductors having an angle  $2\psi$  at the apex (Figure 5) is

$$Z_0 = 120 \log_e \cot \psi/2 \approx 120 \log_e \frac{2r}{\rho} \quad (\text{for small } \psi\text{'s})$$

<sup>5</sup> P. S. Carter, "Simple television antennas," *RCA REVIEW*, vol. 4, pp. 168-185; October, 1939.

<sup>6</sup> N. E. Lindenblad, "Television transmitting antenna for Empire State Building," *RCA REVIEW*, vol. 3, pp. 387-408; April, 1939.

<sup>7</sup> S. A. Schelkunoff, "Theory of antennas of arbitrary size and shape," *Proc. I.R.E.*, vol. 29, pp. 493-521; September, 1941.

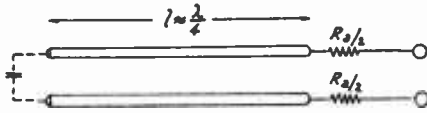


Fig. 6—Parallel-wire line circuit which is equivalent to the biconical dipole of Fig. 5. The radiation resistance is shown in lumped form. A small capacitance at the open end is also due to radiation.

where  $\rho$  is the radius of the cone at a distance  $r$  from the apex. This approximate expression is identical with that for the surge impedance of a parallel-wire line of spacing  $2r$  and radius of wire  $\rho$ . Thus we may replace the dipole by a uniform open-ended  $\lambda/4$  line, Figure 6, but there is one difference between this equivalent line and the lines usually used. Usually the line spacings are small compared with the wavelength and radiation may be neglected. In the dipole equivalent, however, radiation is the major source of loss. For all the practical cases of reasonably small  $\psi$ , the radiation effects may be lumped as a 73-ohm (approximately) resistance at the input terminals and a reactance term which acts as a small capacitance at the end<sup>7</sup> as shown in Figure 6. By shortening the dipole slightly, we may forget about the reactance since this restores tuning to the originally contemplated wavelength. We may remember that an open-ended  $\lambda/4$  line behaves like a series resonant circuit.<sup>8</sup> The lumped-circuit equivalent of the dipole is therefore as shown in Figure 7.  $L$  and  $C$  are the equivalent inductance and capacitance and are determined in terms of  $Z_0$ .

Now we may easily find the bandwidth of the antenna, near its  $\lambda/2$  resonance. The  $Q$  is

$$Q = \frac{\omega L}{R} = \frac{\pi}{4} \frac{Z_0}{R_a + R_L}$$

where  $R_L$  is the load imposed by the transmission line or receiver. Thus, if  $Z_0$  is high, the  $Q$  is high and the bandwidth is narrow. The actual antenna bandwidth for 3 decibels down is just  $1/Q$  times the resonance frequency. However, as very clearly shown by Carter,<sup>5</sup> it is not advisable to use an antenna as far out in frequency as its 3-decibel down band edge if one also wishes to use a long low-loss transmission line between antenna and receiver. Near such a band edge the antenna reactance approximately equals the antenna resistance and the im-

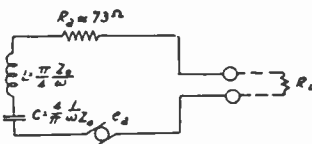


Fig. 7—Equivalent lumped circuit of typical dipole receiving antenna near its half-wave resonance.

<sup>8</sup> See the Appendix to this part for an outline of lumped-circuit equivalents to transmission-line circuits.



pedance at the far end of the transmission line (as seen by the receiver) goes through very extreme variations for a rather small change in frequency. For example, consider a transmission line of length  $l$ . Its electric length is

$$\theta = \frac{2\pi l}{\lambda} = \frac{2\pi fl}{v}$$

where  $v$  is the velocity of propagation on the line. Thus, the rate of change of the electrical length with the frequency is

$$\frac{d\theta}{df} = \frac{2\pi l}{v}$$

which increases linearly with the length. Thus for a long line a very small change in frequency will result in a  $\lambda/4$  change in line length. This causes an extreme impedance nonuniformity at the receiver when a reactive term is present in the antenna impedance, as occurs near the band edge. The curves given by Carter<sup>5</sup> show the results in striking fashion. The antenna should be designed, therefore, to give a much lower  $Q$  than that required by the frequency range, at least whenever a transmission line is used.

In most practical cases, dipoles are cylindrical in cross section rather than conical. However, the above results are only slightly affected by this difference in shape. As Schelkunoff<sup>7</sup> has shown, the cylindrical dipole may be considered roughly in terms of an *average* surge impedance along its length which is

$$Z_0 = 120 \log_e \frac{2l}{a} - 120$$

where  $2l$  is the total length and  $a$  is the radius. Thus the surge impedance is just 120 ohms less than that of the narrow-angle biconical dipole of over-all length  $2l$  and end radius  $a$ . In other words the  $Q$  of the cylindrical dipole is slightly less than that of the small-angle biconical dipole. The wide-angle cone behaves quite differently and will not be treated.

At 300 megacycles a cylindrical dipole of 1-inch diameter at the end will have a  $Z_0$  of approximately 325 ohms and a  $Q$  of 4 when short-circuited. The  $Q$  is halved when working into a matched load. This means a maximum frequency range (3 decibels down) of from 263 to 337 megacycles when short-circuited or something approaching from

225 to 375 megacycles when matched. However, if our dipole had been a number 36 wire  $Z_0$  would be 980 ohms and  $Q$  would be 11. This would still give a 27-megacycle frequency range. If a long low-loss transmission line is used with the antennas of the above examples, it would be wise to consider the useful frequency range to be only a fraction of the figures given so as to avoid extreme variations in the impedance seen at the receiver end when tuning from one end of the range to the other.

To summarize, a *cylindrical* dipole of total length  $2l$  and radius  $a$  will have a short-circuited  $Q$  of approximately

$$Q \approx 1.4 \left( \log_e \frac{2l}{a} - 1 \right)$$

and, of course, a lower  $Q$  when operated into a load. The frequency range of the antenna is given roughly by  $f/Q$  (where  $f$  is the resonant frequency of the antenna) when short transmission lines are used, but is much less with long, low-loss lines.

### 3. Random Noise of the Antenna

An antenna picks up radiation from all points within its directivity pattern. Since, due to temperature, there is a thermal-energy exchange which is random as regards frequency, we might expect one type of noise which is equivalent to thermal-agitation noise. It has been shown<sup>2</sup> that, if an antenna is placed in an enclosure at a uniform temperature  $T_a$ , the noise it will pick up is the same as thermal agitation in its radiation resistance

$$\overline{e_n^2} = 4kT_a R_a \Delta f$$

where  $\overline{e_n^2}$  is the open-circuit noise voltage,  $k = 1.37 \times 10^{-23}$  joule per degree Kelvin, and  $\Delta f$  is the effective noise bandwidth as previously defined.

Actually, an antenna is not in such an enclosure, but, if it receives its entire radiation from *within* the Heaviside layer, it would amount to the same thing. At ultra-high frequency, however, we would expect the waves to pass right through the Heaviside layer so that if we have an antenna directed toward interstellar space, it might be receiving little or no thermal noise; i.e., its effective temperature, as far as noise is concerned, would be zero. It is interesting to realize that, with such a condition, a resistor connected to the antenna would be cooled at a very slow rate by the radiation at antenna frequency. In practice, a

directive antenna might be turned in almost any direction and the noise will presumably vary considerably. Because receiver noise is so high, it has not been possible to measure the effective antenna temperature at ultra-high frequency.

Of course, there are other sources of noise received by the antenna, and, at *low* frequencies, these far outweigh the thermal noise we have been talking about. At ultra-high frequency it is no longer certain that other noise sources than actual man-made interference are present and we may usually assume that, under favorable conditions, the antenna noise will be as low or lower than thermal noise corresponding to room temperature.

#### 4. *Dummy Antenna for Laboratory Measurement*

For measurement of a receiver in the laboratory, we may replace an actual antenna by an equivalent circuit. As we already saw (Figure 4) a known voltage source, a resistance equal to radiation resistance, and a reactance, represent our antenna. If the dummy antenna is to be complete,  $R_a$  should be at the temperature  $T_a$  corresponding to antenna thermal noise. If other sources of noise are present, they should be added. Until measurements to the contrary are made, it is convenient to assume that a lower noise than  $T_a =$  room temperature is not to be expected. It is, therefore, a simple matter to replace the radiation resistance  $R_a$  by a lumped resistance at room temperature.

As to the reactance, in almost every ultra-high-frequency application, the antenna is tuned; i.e., its reactance is zero or very small in the frequency band in which we are interested. We may go further and assume that, if the antenna is correctly designed, its bandwidth is so wide (i.e., its  $Q$  is so low) so that the reactance is negligible at any point near its resonance. Thus the dummy antenna circuit may omit  $X_a$ , the reactance.

It is now possible to outline the chief requirements of a signal generator for receiver measurements since such a generator must supply the known voltage source. It should have a known internal impedance, which is a pure resistance, if possible. If it contains internal reactance, the latter must either be tuned out or be very small in magnitude compared with the radiation resistance (i.e., the equivalent dummy-antenna resistance). If the signal generator has a low internal impedance, the dummy antenna may be added externally. Otherwise the internal impedance must be considered as part or all of the dummy antenna.

At the very high frequencies, it is extremely difficult to get a lumped, reactance-free resistance to replace the antenna-radiation resistance for use in the dummy antenna. Ordinary carbon resistors (e.g., of 75 ohms direct-current resistance) are entirely satisfactory

over much of the ultra-high-frequency region, however. They have an effective inductance of the order of  $10^{-8}$  henry, which is not too bad; they should be regarded with suspicion at those frequencies at which their reactance exceeds 20 to 30 ohms. One expedient which may be used at the very high frequencies is to connect a long length of transmission line with appreciable loss between the signal source and the receiver. Such a line will look like its surge impedance and, if the loss per wavelength is not too great, it will be almost resistive and independent of frequency. The line loss becomes the equivalent of the radiation resistance in the dummy antenna. However, the signal output voltage must be continuously calibrated by some independent means since the loss of many transmission lines varies markedly with temperature and humidity.

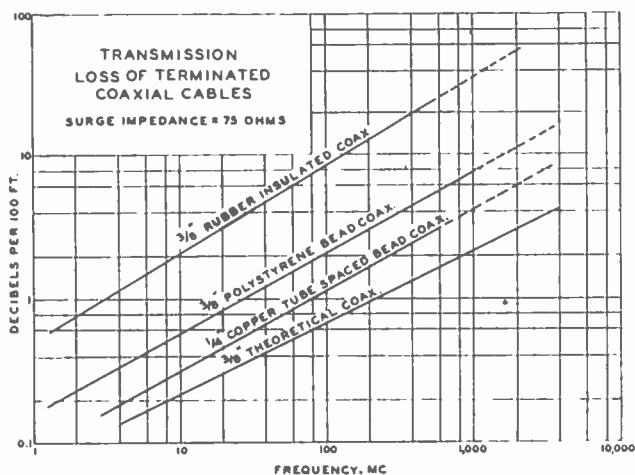


Fig. 8—Attenuation of properly terminated coaxial cable as a function of frequency.

#### IV. COUPLING THE ANTENNA TO THE RECEIVER

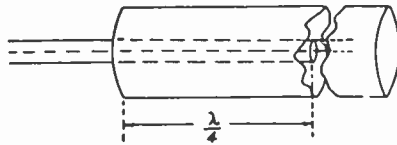
##### 1. Magnitude of Transmission-Line Losses versus Frequency

Let us now consider how to run a lead from the antenna to the receiver. As a first approximation the antenna may be considered as a resistance  $R_a$  with a voltage generator  $e_a$  and the simplest connection is made by using a transmission line of impedance  $R_a$ . If this is possible, at the receiver end, we shall see an impedance  $R_a$  and a voltage generator of reduced magnitude, depending on the line losses. The line losses are most easily expressed in decibels per 100 feet and typical values are given in the curves of Figure 8. Obviously, every decibel of line loss must be supplied by the transmitter and a 3-decibel loss means doubled transmitter power at the noise-level limit. It is, therefore,

highly desirable to place early tubes of a receiver near the antenna.

A word in regard to choice of surge impedance. An air-insulated, solid-outer-conductor, coaxial cable has only copper loss which is a minimum at slightly over 75 ohms impedance.<sup>9</sup> For this reason 75 ohms has been a widely used value. The impedance which will give highest voltage-handling capacity without breakdown is about 60 ohms, and highest power-handling capacity without breakdown about 30 ohms. In cables not air-insulated, the losses are increased by the dielectric and the impedance for minimum attenuation is usually less than 75 ohms but is not the same for all cables. Balanced open-wire lines are much higher in impedance but twisted-pair or balanced shielded lines are usually between 75 and 150 ohms. At the lower frequencies, where radiation loss is not too serious, the high-impedance, balanced, open-wire line is probably the lowest cost line for a given attenuation and has had frequent application. At the higher frequencies, however, it is desirable to use coaxial lines because of their low loss and freedom from radiation; there is a growing tendency to choose an impedance of either 50 or 75 ohms for such coaxial lines.

Fig. 9—The quarter-wave skirt for connecting the unbalanced (coaxial) line to a balanced line (or antenna). The coaxial is extended a quarter-wave inside the outer skirt.



For further information attention is directed to the early and excellent paper of Sterba and Feldman,<sup>9</sup> much of which is applicable to ultra-high-frequency practice.

## 2. Matching Circuits for Antenna to Line

When a balanced antenna such as a dipole or dipole array is used, even though the line impedance may match it, in order to preserve the balance, it is desirable to make use of *balanced* lines or two parallel coaxial lines. Because of its shielding and lower loss, a *single* coaxial line is most widely used and we may well review the special coupling methods which permit its use without detriment to a balanced antenna. The most obvious method is the quarter-wave skirt. To change a coaxial to a balanced line, we simply make a double coaxial for a length equal to a quarter wavelength as in Figure 9. This causes both inner and outer conductors to have a high impedance to ground. The quarter-wave section, being tuned, acts as an open circuit at its resonance. However, although the arrangement is ideal only at resonance, its band-

<sup>9</sup> E. J. Sterba and C. B. Feldman, "Transmission lines for short-wave measuring systems," *Proc. I.R.E.*, vol. 20, pp. 1163-1202; July, 1932.

width is fairly wide. The impedance of the outer coaxial section at an angular frequency  $\omega$  is

$$Z = Z_0' \tan \frac{2\pi l}{\lambda} = Z_0' \tan \frac{\pi}{2} \frac{\lambda_0}{\lambda} = Z_0' \tan \frac{\pi}{2} \frac{\omega}{\omega_0}$$

where  $Z_0'$  is the surge impedance of the outer coaxial section and  $\omega_0$  is its resonant angular frequency. If the inner coaxial has an impedance  $Z_0$ , and  $Z_0'$  is made much higher than  $Z_0$ , the band extends from  $1/2 \omega_0$  to  $3/2 \omega_0$  with safety. If  $Z_0'$  is comparable with  $Z_0$ , safer limits are  $0.8 \omega_0$  to  $1.2 \omega_0$ , i.e., a bandwidth of 40 per cent. For example, such a matching skirt at 300 megacycles would cover a band from 240 to 360 megacycles.

A second means of coupling a coaxial line to a balanced antenna is shown in Figure 10. This is suitable only for vertical antennas. It operates by folding back the outer conductor of the coaxial line to form

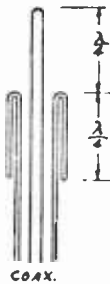


Fig. 10—A method of connecting a coaxial transmission line to a vertical half-wave dipole.

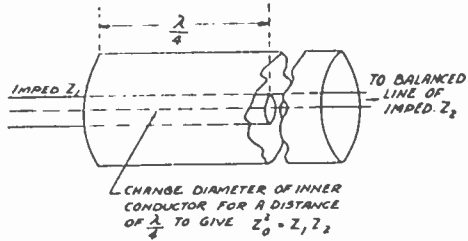
the lower half of the radiating dipole. There are also other means whereby the coupling from an unbalanced transmission line may be made to a balanced antenna, many of which have been described in the patent literature.

Now suppose a balanced antenna, or balanced line is to be connected to a coaxial line of a different surge impedance. Here one may use the basic impedance transformer, the  $\lambda/4$  section of line.<sup>9</sup> In a  $\lambda/4$  line terminated in a resistor  $R$  the input looks like

$$Z = \frac{Z_0^2}{R}$$

so that we may use this section to step up  $R$  to a higher value. Thus, to match two lines of different impedance  $Z_1$  and  $Z_2$ , we may join them by a  $\lambda/4$  section whose impedance is

Fig. 11—The use of a combination of quarter-wave skirt with a quarter-wave transformer for matching an unbalanced line of one surge impedance to a balanced line of another surge impedance.



$$Z_0^2 = Z_1 Z_2.$$

This is true for any type of line, balanced or coaxial. We may, then, modify the skirted coaxial line, as in Figure 11, by a reduced inner-conductor diameter. However, the total bandwidth free from reflection is now greatly reduced. An impedance transformation of more than 2:1 is good only for frequency deviations of a few per cent.<sup>5</sup> By using two  $\lambda/4$  sections and a progressive impedance rise, greater bandwidths are obtainable. This leads to the impedance matching by a tapered line. If two lines of different surge impedance are joined by a tapered section several waves long, a good wide-band match is obtained with very little reflection loss.

The best-known impedance-raising transformer for the dipole is the folded-dipole arrangement wherein the antenna itself forms the transformer as in Figure 12. The paper by Carter<sup>5</sup> gives all details.

### 3. The Connection of Transmission Line to Receiver

In connecting the antenna to the receiver through transmission line, an impedance mismatch at the receiver end leads to standing waves on the line and thus increases the line losses somewhat. Thus, when the receiver is strictly a power-operated device, it is desirable to maintain an impedance match at the receiver end as well as at the antenna. On the other hand, a receiver is not necessarily power-operated<sup>10</sup> and there

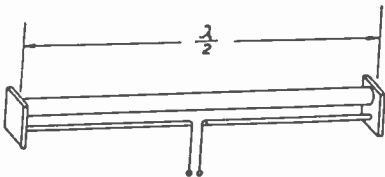


Fig. 12—An impedance-raising transformer for a half-wave dipole antenna. The impedance ratio is determined by the relative diameters of the two parallel dipole conductors.

<sup>10</sup> For example, the receiver might conceivably have an infinite, or even a *negative* input resistance. The latter condition need not be an unstable one since the antenna loading may be made sufficient for completely stable operation.

is sometimes an improvement in signal-to-noise ratio or in frequency response by a mismatch at the receiver terminals. This aspect of receiver design will be taken up in more detail in Part III of this series. When, in such a case, there is a mismatch at the receiver, the resulting reflection will lead to an increased apparent power loss but, since optimum power transfer is not the criterion of receiver performance, this is not pertinent. However, when the receiver is mismatched to the line it is important to maintain a good match at the antenna end or else there will be a decrease in signal-to-noise ratio due to increased line losses.

Thus, we may lay down the general rule that, when the best receiver performance is obtained with maximum power to it, the transmission line should be matched at both ends. When a mismatch improves the receiver performance, the transmission line should be matched to the antenna and the mismatch should occur between the transmission line and the receiver.

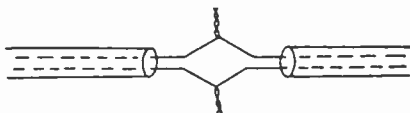


Fig. 13—Two pieces of balanced low-impedance transmission line connected by a joint which may give rise to serious reflection.

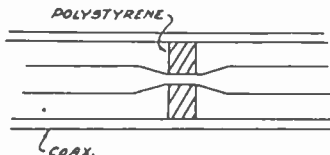
If an antenna is operated at a frequency slightly off from its natural resonance, its impedance presents a small reactance which does not greatly affect the magnitude of the impedance but which nevertheless creates a mismatched condition to a transmission line. The result at the other end of a long, low-loss line is an impedance which may change appreciably with a small change in frequency, as clearly shown in the curves by Carter.<sup>5</sup> With a wide-band receiver, the impedance change may appreciably affect the frequency response. The effects are minimized by using the lowest possible antenna  $Q$  and the shortest possible transmission-line length. The effects are also less severe when the line losses are appreciable.

#### 4. Reflection Loss by Line Couplings

While on the subject of impedance match the effect of connectors must not be forgotten. When two pieces of line are joined by a connector, care must be taken to see that the reflection at the connection is minimized. For example, two pieces of 75-ohm balanced line might be joined by an open connection as in Figure 13. When the frequency is high, this connection can easily cause an appreciable loss. By pushing the two pieces of wire at the joint close together and adding some rubber tape to lower the surge impedance, the loss can be greatly reduced. In designing connectors, therefore, one should try to match



Fig. 14—Method of introducing a polystyrene support in a coaxial line so as to minimize reflection.



impedance. If a polystyrene support is used, in a coaxial cable, as in Figure 14, its dielectric constant is 2.5. The inner conductor should then be restricted as shown so as to maintain  $Z_0 = (1/v_0 \sqrt{\epsilon} C_0)$  a constant where  $\epsilon$  is the dielectric constant. In the case of a 75-ohm coaxial line, the ratio of diameters, when air insulation is used, is approximately 3.5 to 1. With polystyrene insulation, this ratio being 7.2 to 1, at a point of support, the inner conductor diameter should be cut roughly in half.

It is of interest to calculate the reflection coefficient when no such precautions are taken at a connection or point of support. An idea of the magnitude is readily obtained by assuming that the discontinuity represents added shunt capacitance or added series inductance depending on whether the surge impedance is decreased or increased at the point on the line under consideration. The added capacitance, or added inductance may be computed and the reflection ratio estimated from the usual formula

$$\text{reflection ratio} = \frac{Z - Z_0}{Z + Z_0}$$

where  $Z_0$  is the normal surge impedance and  $Z$  is the combination of added capacitance in parallel with  $Z_0$  or added inductance in series with  $Z_0$ . Figure 15 shows the equivalent circuit for the two cases, i.e., a

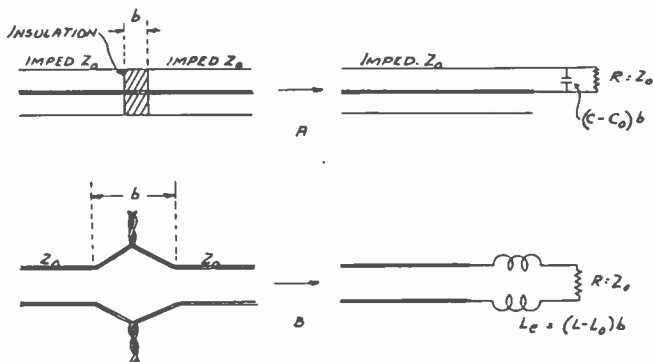


Fig. 15—Equivalent circuits which may be used to calculate the reflection at an insulating bead or a transmission-line connection; A, coaxial line with bead, B, balanced line with joint of higher surge impedance.

decrease in surge impedance at a point, and an increase in surge impedance at a point. Although the method is easily extended to include discontinuities of any length, the equivalent circuits shown in the figure are exact only for discontinuities short compared with the wavelength. With this approximation, the reflection ratio for the illustration of Figure 15A can be shown to be

$$\text{reflection ratio} \approx j\pi (\epsilon - 1) \frac{b}{\lambda} \quad (b \ll \lambda)$$

where  $j = \sqrt{-1}$ ,  $\epsilon$  is the dielectric constant of the bead,  $b$  is its length, and  $\lambda$  is the free-space wavelength of the transmitted radiation. For the case of Figure 15B, where the reflection is due to a short length of increased surge impedance, as in the twisted joint of a parallel-wire line, the reflection ratio is

$$\text{reflection ratio} \approx j\pi \left( \frac{L}{L_0} - 1 \right) \frac{b}{\lambda} \quad (b \ll \lambda)$$

where  $L$  is the average inductance per unit length at the joint and  $L_0$  is the normal inductance per unit length of the line. It should be noted that the maximum possible power-loss ratio due to reflection alone is given by the square of the reflection ratio in the above case. The total power loss can be less than this maximum under special conditions but it can also be higher if there is any loss in the discontinuity (which was assumed purely reactive in the above analysis).

We may notice that the reflection ratio becomes worse as the wavelength is decreased; i.e., as we approach higher frequencies. For example, an isolated polystyrene disk only  $\frac{1}{8}$  inch long may cause an appreciable loss when the frequency is sufficiently high. In cases where there are many regular reflections, such as in a beaded cable, the losses can be reduced by proper spacing of the beads.

## V. THE RECEIVER INPUT CIRCUIT

### 1. *Selectivity and Image Response*

The purpose of the receiver input circuit is first to match properly the antenna and its associated transmission line to the first tube of the receiver, and second to provide some selectivity, particularly against the image response. Let us consider the second purpose first.

If we are tuned to a frequency  $f_s$  and the intermediate frequency is  $f_i$  then we know that our local oscillator frequency  $f_0$  will be given by

$$f_s \pm nf_0 = f_i$$

where  $n$  is an integer. Usually  $n = 1$  and we operate at the fundamental of the local oscillator. The receiver will respond at frequencies

$$f = f_0 - f_i, f_0 + f_i, 2f_0 - f_i, 2f_0 + f_i, 3f_0 - f_i, 3f_0 + f_i$$

and the intermediate-frequency circuit will not distinguish between them. The input circuit must select the desired one and discriminate against the others. Now if one of these is chosen as the signal, the next nearest one differs by the frequency  $2f_i$ , so the input must discriminate between a frequency  $f_s$  and a frequency  $f_s \pm 2f_i$ . For most cases,  $f_i$  is not more than  $1/5$  of  $f_s$  so that, if we have an input circuit tuned to  $f_s$ , and it has a reasonably symmetrical response, the rejection of  $f_s + 2f_i$  and  $f_s - 2f_i$  will be the same, and it makes little difference upon which side of the signal the local oscillator frequency is placed.

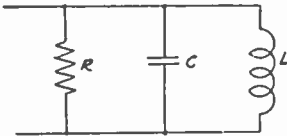


Fig. 16—Equivalent lumped-circuit analog to many resonant-line input circuits.

Many input circuits, though they may be tuned sections of transmission line, have a lumped circuit equivalent which is a simple parallel-tuned circuit such as shown in Figure 16. Such a circuit has a bandwidth

$$\Delta f' \text{ (3 decibels down)} = \frac{f_s}{Q} = \frac{1}{2\pi CR}$$

and in using such a circuit for selectivity it is necessary to tap the unavoidable load resistances (e.g., the tube input) down on the circuit so as to obtain the desired bandwidth (or, if one likes, the desired  $Q$ ). At the image frequency ( $f_s + 2f_i$ ) such a circuit behaves as a reactance

$$x_c = \frac{1}{2\pi C} \frac{f_s + 2f_i}{4f_i(f_s + f_i)}$$

Thus the ratio of its response at image frequency to its response at frequency is

$$\frac{\text{image response}}{\text{signal response}} = \frac{1}{R} \frac{1}{2\pi C} \frac{f_s + 2f_i}{4f_i(f_s + f_i)} = \frac{\Delta f'}{4f_i} \frac{f_s + 2f_i}{f_s + f_i}$$

$$\approx \frac{\Delta f'}{4f_i} \text{ when } f_i \ll f_s.$$

The value of a high intermediate frequency is readily apparent.

A pair of coupled circuits has much greater discrimination against image response, for the same bandwidth. In fact, if the intermediate frequency is small compared with the signal frequency, the ratio is approximately

$$\frac{\text{image response}}{\text{signal response}} \approx \left( \frac{\Delta f'}{4f_i} \right)^2$$

which is just the square of the single-tuned circuit ratio, or the equivalent of two single-tuned circuits in cascade.

## 2. *Signal-to-Noise Ratio*

Although major consideration of the signal-to-noise ratio will be reserved for Part III of this series, it may be well at this point to emphasize the effect which the input circuit may have on this important factor. Although there are some instances where important noise sources are present in a receiver ahead of, or in the input of the first tube, in very many cases the major noise source occurs in the output of the first tube. In the latter event, best signal-to-noise ratio will be obtained by designing an input circuit to deliver the maximum possible signal voltage on the input electrode. This implies, first of all, a reduction of all losses to a minimum which is usually imposed by the electronically active portion of the tube input and second, it implies impedance matching from the antenna or transmission line to the tube input. The first implication is a valid one in all cases.

It is, however, a mistake to worship the matched-impedance condition to the extent to which it is sometimes done. In an ideal receiver with no losses in the input tube or circuit, for example, impedance matching is also equivalent to zero bandwidth and is not a practicable operating condition. By a mismatch to the antenna, the bandwidth may be increased with a minimum loss in signal and hence a minimum reduction in signal-to-noise ratio. In many receivers, there are sources of noise present in the input (such as thermal agitation in the input circuit and induced noise in the tube input electrodes) which cannot be neglected. Again a mismatch to the antenna is advantageous and leads to an improved signal-to-noise ratio.

The input circuit is, therefore, an important part of receiver de-

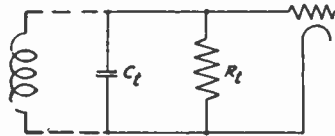
sign for best signal-to-noise ratio, since it permits an adjustment of the coupling between the antenna and the tube input.

### 3. Wide-Band Considerations

We have already introduced the bandwidth  $\Delta f'$  into selectivity considerations. This is a bandwidth which must usually be considered in the initial design. If the image rejection is sufficient, one may, however, let the radio-frequency circuit bandwidth be as wide as desired since the intermediate-frequency circuits will give adequate selectivity. But the radio-frequency bandwidth cannot be permitted to be too narrow. Since the bandwidth of a circuit depends inversely on its  $Q$  and for the same resonant impedance depends on the total effective circuit capacitance, we usually desire low capacitances.

In wide-band ultra-high-frequency receivers, it is invariably found that the circuits may be made very low loss and most of the losses are in the tubes, leads to the tubes, etc. In fact we may neglect the circuit losses, as a rule, and assume the circuits to be perfect, but we must

Fig. 17—The connection of a loss-free inductance to a tube of input resistance  $R_t$  and capacitance  $C_t$  to form an input circuit.



be careful to introduce the tube and lead losses properly. Suppose we have a tube and we find that it behaves like a resistance  $R_t$  in parallel with a capacitance  $C_t$ . If we connect a loss-free inductance (with no distributed capacitance) we get a circuit (Figure 17) of

$$Q = \omega C_t R_t$$

$$\Delta f' = \frac{f}{Q} = \frac{1}{2\pi C_t R_t}$$

and the smaller the value of  $C_t$ , the wider is the band. If, as always happens, the added inductance has a distributed capacitance, the bandwidth is always less than that expected with an ideal inductance. When the inductance consists of a transmission line its effective capacitance is sometimes as high as half of its total capacitance.<sup>11</sup> Thus wide-band circuits require low- $C$  line circuits, or high surge-impedance line circuits.

It is seen that when  $R_t$  is increased,  $C_t$  must be decreased to keep

<sup>11</sup> See Appendix for appropriate formulas.

the same bandwidth. We shall see later that the bandwidth may be varied by the effect of antenna loading on the input circuit.

4. Equivalent Circuits of Input Transformers

We have talked a great deal about line circuits but have not shown anything but lumped-circuit diagrams. This is because the easiest way for one versed in low-frequency technique to understand line circuits is in terms of lumped circuit equivalents. A table of useful data including such equivalent circuits has been prepared and is attached in an Appendix to this part. Only one arrangement will be discussed in detail here.

A typical input transformer to a tube will be a concentric cylinder,<sup>12</sup> quarter-wave line with a tap for the antenna such as shown in Figure 18. Let us assume a connection to a tube whose parallel resistance is  $R_t$  and whose capacitance is  $C_t$ . The condition for resonance is then  $Z_0 \tan \theta = 1/\omega C_t$ , where  $\theta$  is the electrical length of line  $2\pi l/\lambda$ . To

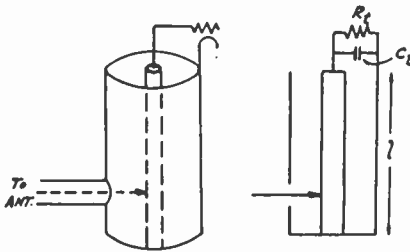


Fig. 18—A typical concentric-line, resonant circuit used as an input transformer with a tube input resistance  $R_t$  and capacitance  $C_t$ . The length  $l$  determines the resonant frequency.

obtain a transformer action, the antenna may be tapped down on the line. From the table in the Appendix, it is found that, with the antenna line disconnected,

$$Q = \frac{1}{2} \left[ \omega C_t R_t + \frac{\theta}{\sin^2 \theta} \frac{R_t}{Z_0} \right].$$

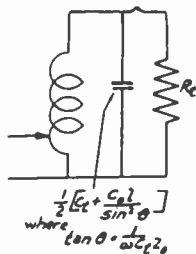
If the antenna tap is moved up until the impedances are matched, the  $Q$  will be just half of this. By moving the tap up further, the  $Q$  can be lowered as much as desired (until the  $Q$  of the antenna itself is approached). The equivalent lumped circuit is as shown in Figure 19. It is also possible to couple in the antenna by a loop inserted in the line. If this is done it is usually best to couple near the short-circuited end so as to link the strongest magnetic field. The coupling loop will have some reactance but, as a rule, this may be tuned out by a readjustment of tuning.

<sup>12</sup> C. W. Hansell and P. S. Carter, "Frequency control by low power factor line circuits," *Proc. I.R.E.*, vol. 24, pp. 597-619; April, 1936.

The tuning-up of the circuit and the adjustment of antenna coupling is often a cut-and-try process, with each adjustment made to get either highest signal into the receiver or highest over-all signal-to-noise ratio. Since the antenna equivalent is a voltage in series with a resistance, optimum signal voltage on the first tube will occur with impedances matched. In the material which follows in Part III of this series, much more will be learned about antenna-coupling adjustment from the signal-to-noise point of view, and it will be found that coupling for the highest signal-to-noise ratio is not always the same as that which gives optimum signal on the tube.

Suppose in the above example that the antenna circuit has too narrow a bandwidth when it is adjusted for best gain (antenna coupled in). This means that  $Q$  is too high. Although there are many ways in which  $Q$  can be lowered, and they will all serve equally well to increase the bandwidth, they are not all alike in their effect on the signal-to-noise ratio. For example, if we add a shunt resistor for additional

Fig. 19—Input circuit which is equivalent to the resonant-line circuit of Fig. 18. The line length  $l$  is included in the angle  $\theta = 2\pi l/\lambda$  and  $C_0$  is the capacitance per unit length of the resonant line while  $Z_0$  is its surge impedance.



damping, the  $Q$  will be lowered but will be accompanied by marked reduction of signal gain and hence a reduction in signal-to-noise ratio. A second remedy is to couple the antenna more tightly than optimum. This will lower the  $Q$  with little change in the signal-to-noise ratio (it may even improve in some cases). A third possibility is the use of degenerative feedback in the first tube. If this is correctly done, by feeding back both signal and noise in like amounts, the effective tube input resistance may be reduced with little or no change in signal-to-noise ratio.<sup>13</sup> Finally, the best of all, the  $Q$  may be reduced by choice of a lower capacitance, higher input-resistance tube and the use of a lower capacitance circuit.

For wide-band input circuits, a considerable advantage in flatness of response and in image rejection is obtained by the use of a double-tuned input circuit. A possible design is shown in Figure 20. In the figure, two end-to-end resonant coaxial-line circuits are shown, one as a primary which has the antenna coupled to it and the other used as

<sup>13</sup> Further discussions will be reserved for Part III of this series entitled, "The Signal-to-Noise Ratio of Radio Receivers."

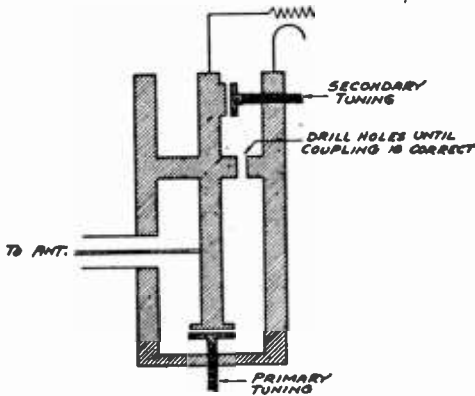


Fig. 20—A double-tuned transformer of resonant coaxial-line sections, as used for coupling antenna to the first tube of a receiver.

a secondary circuit driving the first tube. The coupling between primary and secondary may be adjusted by drilling the central short-circuiting bar until the response curve has the proper flat-top shape. The use of capacitive tuning, as shown in Figure 20, is simple and convenient but is disadvantageous in that the total circuit capacitances are increased.

Suppose, on the other hand, we have a single-tuned transformer and the bandwidth is so *wide* that we could well afford to narrow it so as to improve image response. Here we wish to raise the  $Q$ . Even with a double-tuned transformer we may find the secondary  $Q$  is too low. One method of raising the  $Q$  is to add low-loss capacitance preferably by use of a lower surge-impedance line circuit and this is probably a satisfactory remedy. Another expedient makes use of the fact that the  $Q$  of an unloaded, resonant-line transformer is usually very high. If we couple the tube more loosely to the line, as by tapping it down on the line, the over-all effective  $Q$  can be raised until it approaches the  $Q$  of the unloaded line alone. Part 2a of the Appendix gives a formula which is applicable when the tube, of capacitance  $C_t$ , resistance  $R_t$ , is tapped down on the resonant line. We may obtain a physical understanding of the behavior by considering the lumped-circuit analogy shown in Figure 21. In A of the figure the tube is

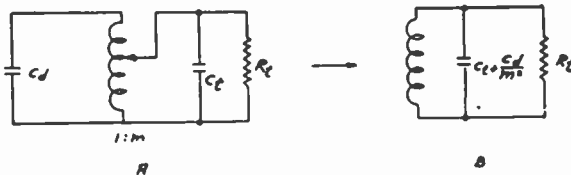


Fig. 21—Equivalent lumped circuits showing the effect of tapping a tube of capacitance  $C_t$ , resistance  $R_t$  down on a very high  $Q$  circuit. The over-all  $Q$  is thereby increased over a straight parallel connection.



shown tapped down on a resonant circuit whose inherent capacitance is  $C_d$  and whose  $Q$  may be considered very high. The equivalent circuit shown in Figure 21B, discloses that the over-all  $Q$  is

$$Q = \omega R_t \left( C_t + \frac{C_d}{m^2} \right)$$

where  $m$  is the effective turns ratio of the tapped-down section of the transformer to the total. Thus, if the tap is brought down on the circuit,  $m$  is made smaller and  $Q$  is made higher. Of course the upper limit to  $Q$  is imposed by the circuit losses which, in the case of resonant lines, are often small enough to permit attainment of a  $Q$  of 1000 or more. The antenna can be coupled into the circuit in the usual way and no appreciable loss of signal need result if the  $Q$  is raised a moderate amount by the tapping-down process.

As an example of a particular design of input transformer, suppose we have the following problem:

$$\Delta f' = 3.5 \text{ megacycles}$$

$$\lambda_0 = 86 \text{ centimeters}$$

$$f = 350 \text{ megacycles}$$

$$Q = \frac{f}{\Delta f'} = 100,$$

The input tube is to be a type 955 mixer used at oscillator fundamental. We will find that the input conductance of this tube as a mixer<sup>14</sup> is about 435 micromhos corresponding to  $R_t = 2300$  ohms and the input capacitance  $C_t$  (considering the plate as radio-frequency ground) is about 4 micromicrofarads or so.

Let us use a concentric-cylinder line circuit, in the quarter-wave mode. Such a line, designed for maximum  $Q$ , may have an inner conductor of  $\frac{1}{4}$ -inch diameter copper, and a surge impedance of 77 ohms, corresponding to an inside diameter of 0.975 inch for the outer conductor. The line alone, if made a quarter wave long, would be 21.4 centimeters long and would have a  $Q$  as follows: (see Appendix for formula)

$$Q = 5.2 \times 10^4 \frac{1/8 \times 2.54}{\sqrt{86}} \approx 1780.$$

This  $Q$  is obviously high enough to be neglected in comparison with the desired  $Q$  of 100, so we may use the data in the Appendix of equivalent

<sup>14</sup> E. W. Herold, "An analysis of the signal-to-noise ratio of ultra-high-frequency receivers," *RCA REVIEW*, vol. 6. pp. 302-331; January, 1942.

circuits (which neglects line losses). We find, if the tube is connected to the open end of the line as in Figure 18, that the 4-micromicrofarad capacitance will require the line length to be reduced to

$$l = \frac{\lambda_0}{2\pi} \theta = \frac{\lambda_0}{2\pi} \sin^{-1} \sqrt{\frac{1}{1 + (\omega Z_0 C_t)^2}}$$

Using some of the relations given in the Appendix we find that

$$C_0 = \frac{33}{Z_0} = 0.43 \text{ micromicrofarad per centimeter.}$$

Thus

$$\omega Z_0 C_t = \frac{6.2 C_t}{\lambda_0 C_0} = 0.67$$

$$l = \frac{\lambda_0}{2\pi} \times 0.98 = 13.4 \text{ centimeters}$$

and

$$\sin^2 \theta = 0.69.$$

The equivalent lumped circuit gives, therefore, an equivalent-lumped-circuit capacitance

$$C = \frac{1}{2} \left[ C_t + \frac{1C_0}{\sin^2 \theta} \right] = 6.2 \text{ micromicrofarads}$$

and

$$Q = \omega C R_t = 31.$$

This gives a bandwidth of 11 megacycles even before connecting the antenna and is much too broad.

We must consider tapping down the tube on the line and we refer to the last of the cases treated in Part 2a of the Appendix. It must be remembered that we wish a final  $Q$  of about 100 but that when the antenna is coupled in, and approximately matched to the circuit, the  $Q$  will roughly be halved. The circuit by itself must therefore be designed for a  $Q$  of around 200, if the antenna impedance is to be somewhere near matched. This means the effective lumped equivalent capacitance must be about 40 micromicrofarads. Trying out  $l_1 = 4.0$  centimeters,  $\theta_1 = 0.29$  radian, we find

$$\cos^2 \theta_2 = 0.12, \quad l_2 = 16.6 \text{ centimeters}$$

so that

$$C = 42 \text{ micromicrofarads}$$

which gives a value of  $Q$  of 212. As shall be shown later, it is preferable to couple the antenna just a little more tightly than optimum and this will lower the  $Q$  to less than half. Thus, we may consider the choice as satisfactory and the antenna coupling can then be adjusted to give an over-all  $Q$  of 100. It should be noted that by this simple expedient of tapping the tube down on the line we have narrowed the bandwidth to the desired value without appreciable sacrifice in signal strength or reduction in signal-to-noise ratio.

Let us note that the image response ratio for an intermediate frequency of 25 megacycles is

$$\frac{\text{image response}}{\text{signal response}} = \frac{\Delta f'}{4f_i} = \frac{1}{29} \text{ or about 29 decibels.}$$

This is usually considered adequate. A local oscillator may be coupled in inductively or capacitively and the coupling should be very loose so as not to affect the impedance.

It is hoped that this example will suffice to show the utility of the lumped-circuit-equivalent formulas given in the Appendix. They can, of course, be used equally well for other input-circuit problems.

## APPENDIX

### *Useful Data for Resonant Transmission-Line Circuits*

In most applications to ultra-high-frequency receivers, the radio-frequency ohmic losses in the parts external to the tube are so small in comparison with the loading introduced by the tube, that they may safely be neglected. Thus, when the external circuits are resonant sections of line, we may safely neglect their distributed ohmic losses and make computations on the assumption that they are negligibly small. Under these conditions, a resonant section of transmission line, near one of its resonant modes, behaves in a fashion similar to lumped reactance elements. The loss and capacitance which are introduced by the connection of a tube, for example, are then readily affixed in lumped form to form an equivalent circuit. These equivalent lumped circuits are illuminating to the engineer familiar with low-frequency technique, and, in addition, greatly simplify circuit analysis.

1—Uniform Low-Loss Lines.

a. SYMBOLS

- $\epsilon$  = dielectric constant of insulating material.
- $C_0$  = capacitance per unit length of air-insulated line, farad/meter
- $C = \epsilon C_0$  = capacitance per unit length of dielectric-insulated line, farad/meter
- $L_0$  = inductance per unit length, henries/meter.
- $v_0$  = velocity of propagation on air-insulated line =  $3 \times 10^8$  meter/sec
- $v$  = velocity of propagation on dielectric-insulated line =  $v_0/\sqrt{\epsilon}$
- $\lambda_0$  = wavelength, meters on air-insulated line =  $v_0/f$ .
- $\lambda$  = wavelength, meters on dielectric-insulated line =  $v/f$
- $Z_0$  = surge impedance, ohms.
- $l$  = length of line, meters.
- $f$  = frequency, cycles per second.
- $\omega = 2\pi f$ , angular frequency, radians per sec.
- $n$  = any integer.

b. GENERAL RELATIONS

$$v_0 = \frac{1}{\sqrt{L_0 C_0}} \qquad v = \frac{1}{\sqrt{\epsilon L_0 C_0}}$$

$$Z_0 = \sqrt{\frac{L_0}{C}} = \frac{1}{\sqrt{\epsilon}} \sqrt{\frac{L_0}{C_0}} = v L_0 = \frac{v_0}{\sqrt{\epsilon}} L_0 = \frac{1}{vC} = \frac{1}{veC_0} = \frac{1}{v_0 \sqrt{\epsilon} C_0}$$

c. OPEN AND SHORTED LINES

Impedance of shorted line =  $j Z_0 \tan\left(\frac{2\pi l}{\lambda}\right)$


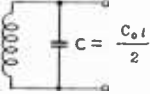
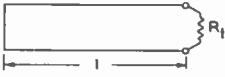
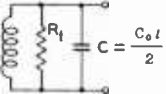

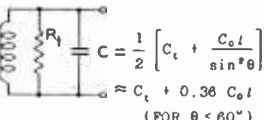
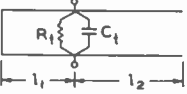
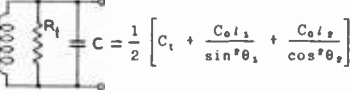
Impedance of open line =  $-j Z_0 \cot\left(\frac{2\pi l}{\lambda}\right)$

d. CHARACTERISTIC OF PARTICULAR LENGTHS OF LINE (Losses Neglected)

Line Length	Far-End Termination	Input Impedance	Equivalent Lumped Circuit
$l \ll \lambda$	0	$j\omega l L_0$	
$l \ll \lambda$	$R = Z_0$	$Z_0$	
$l \ll \lambda$	$\infty$	$1/(j\omega l C_0)$	
$l = (2n-1)\lambda/8$	0	$jZ_0$	
$l = (2n-1)\lambda/8$	$R = Z_0$	$Z_0$	
$l = (2n-1)\lambda/8$	$\infty$	$-jZ_0$	
$l = (2n-1)\lambda/4$	0	$\infty$	
$l = (2n-1)\lambda/4$	$Z_1$	$Z_0^2/Z_1$	
$l = (2n-1)\lambda/4$	$\infty$	0	
$l = n\lambda/2$	0	0	
$l = n\lambda/2$	$Z_1$	$Z_2$	
$l = n\lambda/2$	$\infty$	$\infty$	

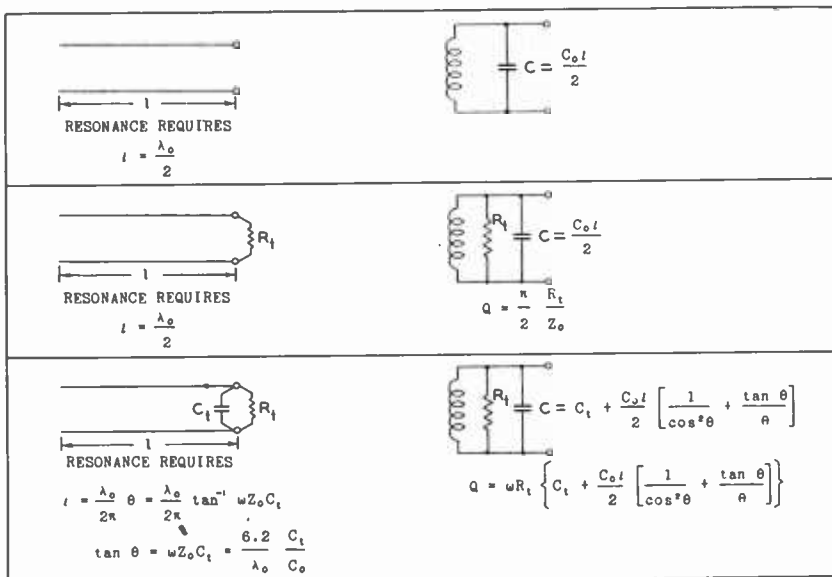
The following compilation of transmission-line information is, therefore, based on the assumption that the losses may be lumped at one point. In the figures, although parallel-wire lines are schematically indicated, the results are, of course, applicable to coaxial or to any other uniform line configuration.

2a—Equivalent Circuits of Quarter-Wave Short-Circuited Lines with Negligible Line Loss.

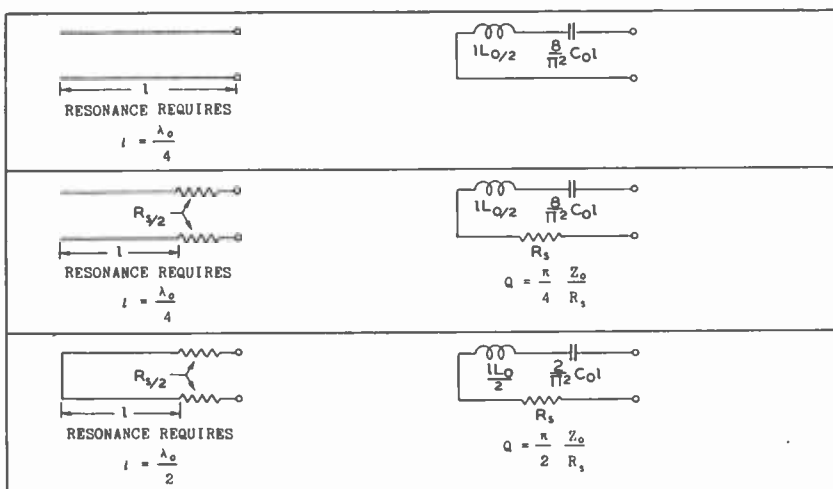
 <p>RESONANCE REQUIRES</p> $l = \frac{\lambda_0}{4}$	 <p><math>Q = \text{THAT OF LINE ALONE}^*</math> (ASSUMED VERY HIGH)</p>
 <p>RESONANCE REQUIRES</p> $l = \frac{\lambda_0}{4}$	 <p><math>Q = \omega \frac{C_0 l}{2} R_t = \frac{\pi}{4} \frac{R_t}{Z_0}</math></p>
 <p>RESONANCE REQUIRES</p> $l = \frac{\lambda_0}{2\pi} \theta = \frac{\lambda_0}{2\pi} \sin^{-1} \sqrt{\frac{1}{1 + (\omega Z_0 C_t)^2}}$ $\sin^2 \theta = \frac{1}{1 + (\omega Z_0 C_t)^2}$	 <p><math>C = \frac{1}{2} \left[ C_t + \frac{C_0 l}{\sin^2 \theta} \right]</math> <math>\approx C_t + 0.38 C_0 l</math> (FOR <math>\theta &lt; 60^\circ</math>)</p> <p><math>Q = \frac{\omega R_t}{2} \left[ C_t + \frac{C_0 l}{\sin^2 \theta} \right]</math> <math>= \frac{1}{2} \left[ \omega C_t R_t + \frac{\theta}{\sin^2 \theta} \frac{R_t}{Z_0} \right]</math></p>
 <p>RESONANCE REQUIRES</p> $l_1 = \frac{\lambda_0}{2\pi} \theta_1, \quad l_2 = \frac{\lambda_0}{2\pi} \theta_2$ <p>CHOOSING <math>l_1</math>, OR <math>\theta_1</math>, THEN</p> $\cos^2 \theta_2 = \frac{1}{1 + (\cot \theta_1 - \omega C_1 Z_0)^2}$	 <p><math>C = \frac{1}{2} \left[ C_t + \frac{C_0 l_1}{\sin^2 \theta_1} + \frac{C_0 l_2}{\cos^2 \theta_2} \right]</math></p> <p><math>Q = \frac{\omega R_t}{2} \left[ C_t + \frac{C_0 l_1}{\sin^2 \theta_1} + \frac{C_0 l_2}{\cos^2 \theta_2} \right]</math></p>
<p>USEFUL RELATIONS: IF <math>C_0</math> IS IN <math>\mu\text{mf PER CM}</math>, <math>C_t</math> IN <math>\mu\text{mf}</math>, <math>\lambda</math> IN CM.</p> $C_0 = \frac{33}{Z_0} \quad Z_0 = \frac{33}{C_0} \quad \omega Z_0 C_t = \frac{6.2}{\lambda_0} \frac{C_t}{C_0}$	

\* The maximum  $Q$  of concentric-cylinder, copper,  $\lambda/4$  line is given when  $Z_0 = 77$  ohms and is  $Q_{line} = 5.2 \times 10^4 (a/\sqrt{\lambda_0})$ , where  $a$  is radius of inner conductor in centimeters and  $\lambda_0$  is also in centimeters.

2b—Equivalent Circuits of Open Lines in Half-Wave Resonance.



2c—Lines in Series Resonance.



The general method which was used to derive the equivalent, *parallel*, lumped circuits of Parts 2a and 2b of the Appendix made use of the voltage distribution  $V(x)$  as a function of the distance  $x$  along the

resonant line. This distribution, which is composed of appropriate portions of a sinusoid, was then used to calculate the total stored energy by integrating the product  $\frac{1}{2}C_0V^2$  over the total length, where  $C_0$  is the capacitance per unit length. The stored energy was equated to the stored energy of an equivalent lumped circuit having the same voltage as the terminals of the line circuit. Thus the effective, equivalent, lumped capacitance (excluding the externally added capacitance) was just

$$C = \frac{C_0}{V_t^2} \int_0^l V^2(x) dx$$

where  $V_t$  is the voltage at the terminals and  $l$  is the length. For example, in the first illustration of Part 2a below,  $l = \lambda/4$  and  $V(x) = V_t \sin 2\pi x/\lambda$  so that

$$\begin{aligned} C &= C_0 \int_0^{\lambda/4} \sin^2 \frac{2\pi x}{\lambda} dx \\ &= C_0 \frac{\lambda}{8} \\ &= C_0 \frac{l}{2} . \end{aligned}$$

In some of the more complicated cases the result can be expressed in many different forms by trigonometric manipulation.

Equivalent, lumped, *series* circuits, such as those in part 2c of the Appendix, were most easily found by using the *current* distribution on the resonant line and integrating the total stored magnetic energy, again equating the total to the energy of a lumped circuit having the same current as the terminals of the resonant line.

## Part II. Admittances and Fluctuation Noise of Tubes and Circuits†

BY

L. MALTER

*Summary*—The signal-to-noise ratio of radio receivers depends in part upon tube and circuit admittances and upon noise sources present in tube and circuit elements. Tubes operating in a linear fashion can be represented by a 4-terminal network consisting of admittances, of which the most important are the input, output, and feedback admittance, and by two constant-current generators of which the more important is the one which determines the transadmittance.

The input admittance of conventional type tubes is determined largely by: 1. ohmic losses; 2. interelectrode capacitances; 3. electrode self and mutual inductances; 4. lead self and mutual inductances; 5. the space-charge conditions within the tube; and 6. the magnitude of the cathode—control-grid transit angle. The cathode lead inductance, which may be the most important, results in an input admittance term which varies as the first power of the transconductance, and as the square of the frequency. The cathode—control-grid transit angle introduces a similarly varying admittance term which is also proportional to the transit angle, (provided the latter is not too large). These added admittance terms are positive for the case of space-charge-limited emission and negative for temperature-limited emission. Similarly, the input capacitance is increased over the “cold-cathode” value in the space-charge-limited emission case and decreased in the temperature-limited emission case.

The transadmittance does not vary greatly in magnitude as a function of frequency, although its phase angle may vary considerably. The feedback admittance (primarily a capacitance) may reverse in sign at a particular frequency. The output admittance is generally altered less than the input admittance by an increase in frequency.

Various noise sources, which are factors in determining the signal-to-noise ratio of receivers, are treated. These include thermal fluctuations, shot noise, current division, induced noise, and secondary emission. The concept of equivalent noise resistance of a tube is introduced, it being a fictitious resistance of such value that if placed across the input terminals of a tube, it will result in an increase in the plate-circuit noise equal to the shot noise of the plate current. Its utility will be brought out in Part III of this series.

### I. INTRODUCTION

AS WAS pointed out in Part I of this series, the function of the receiving antenna is to “capture” a portion of the transmitted power. In general, a portion of the captured power is consumed in the first tube of the receiver through the mechanism of the input circuit. In some cases, however, when the tube has an infinite or *negative* input resistance, the tube will not be power-consuming.<sup>1</sup> The

† Reprinted from *Proc. I.R.E.*, September, 1943.

<sup>1</sup> See Part I, Section II, 3 of this series for added discussion of this point.



ultimate goal in many receiver designs is maximum possible signal-to-noise ratio, that being aimed after, regardless of the nature of the input resistance of the first tube, subject to the condition that the bandwidths of the various circuits be adequate for the utilization of all the information contained in the received signal. If the receiver input is strictly power-operated, the condition for maximum signal-to-noise ratio coincides with that for maximum signal on the control electrode of the same tube, it merely being necessary to maintain an impedance match at the tube input terminals. Whether the receiver input is strictly power-operated or not, the signal-to-noise ratio of the receiver will be determined in part by the tube and circuit admittances. As a consequence, a study of tube admittances is of prime importance as a prelude to the investigation of receiver response. The signal-to-noise ratio of a receiver is determined not only by the tube and circuit admittances, but by the unavoidable noise voltages due to thermal agitation, electron emission, the division of current, and other "noise sources" which will be discussed in detail below. This part of the series on ultra-high-frequency reception will concern itself with a discussion and evaluation of tube admittances and with the noise present in the components of radio receivers. In Part III it will be shown how the influence of these factors may be combined to give a measure of the so-called noise factor of a radio receiver.

## II. THE TUBE AS A 4-TERMINAL NETWORK

A tube, as e.g., a triode or pentode, operating over a linear portion of its characteristics can be represented by the 4-terminal network shown in Figure 1 where

$I_g$  is the effective alternating component of grid current.

$I_p$  is the effective alternating component of plate current.

$E_p$  is the effective alternating component of plate voltage.

$y_m E_g$  is the effective alternating component of plate current due to the effect of grid voltage  $E_g$  upon electron current to the plate.

$y_n E_p$  is the effective alternating component of grid current due to the effect of plate voltage  $E_p$  upon electron current to the grid.

$y_m E_g$  and  $y_n E_p$  are thus currents over and above those which would flow in the plate and grid circuits in the absence of electron emission, the circuit in that case being purely passive in nature with currents determined by impressed voltages and impedances of circuit elements only.

It should be clearly realized that the representation of a tube by the 4-terminal network is, strictly speaking, permissible only if the

tube is linear in operation. This effectively limits the representation to amplifiers only, excluding such devices as mixers or detectors. However, even in the case of nonlinear devices, a 4-terminal representation can be made for successive small portions of the characteristic as are effectively linear, and the results for these successive portions then combined for the whole region of operation so as to give useful information.

From Figure 1 it can be seen that the following relations hold:

$$I_p = y_m E_g + y_p E_p + (E_p - E_g) y_{pg}$$

$$I_g = y_n E_p + y_g E_g + (E_g - E_p) y_{pg}$$

If the output terminals are short-circuited  $E_p = 0$ ; then,

$$I_p = y_m E_g - y_{pg} E_g$$

$$I_g = y_g E_g + y_{pg} E_g$$

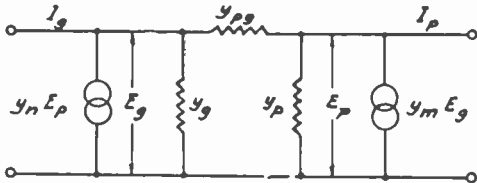


Fig. 1—Representation of a vacuum tube by a 4-terminal network which contains as elements, admittances and constant-current generators.

If there were no emission,  $y_m E_g = y_n E_p = 0$ . It is then seen that  $y_{pg}$  is the feedback admittance between plate and grid.  $y_m$  is defined as the grid-plate transadmittance, and  $y_g$  as the input admittance. If the input terminals are short-circuited,  $E_g = 0$ ; then,

$$I_p = y_p E_p + y_{pg} E_p$$

$y_p$  is defined as the output admittance;  $y_n$ , which is defined as the plate-grid transadmittance, in general plays a minor role and may usually be neglected. The above treatment is applicable to practically all types of receiving tubes if by the term "grid" in the preceding discussion, it is understood that one refers to the "control electrode." The various tube admittances will now be considered in turn, as a preliminary to the consideration of their influence upon the signal-to-noise ratio of a receiver.

### III. INPUT ADMITTANCE

#### Case 1. Cold Cathode

To enable the influence of electron emission upon the input admittance to be determined, it will be of value first to consider the case of

a tube with a cold cathode, where, since no emission is present, the 4-terminal network becomes passive in nature, and the problem is purely a circuit one.

The input circuit of a multielectrode tube with the cathode cold may be represented as shown in Figure 2. The combination of inductances and capacitances, when examined at the input terminals, exhibit series and parallel resonances at various frequencies. As a rule the lowest frequency resonance is of the series type, wherein the input lead inductances resonate with the remainder of the circuit, which behaves like a capacitance at that frequency. As one attempts to tune to this frequency, the external circuit diminishes in size until it finally consists of a short circuit across the input terminals. To operate at higher frequencies it then becomes necessary to use a transmission-line circuit operating at a three-quarter or higher mode. However, with tube types employing wire leads through the envelope, the ohmic losses are usually increasing rapidly with frequency in this region, so that satisfactory performance cannot always be obtained.

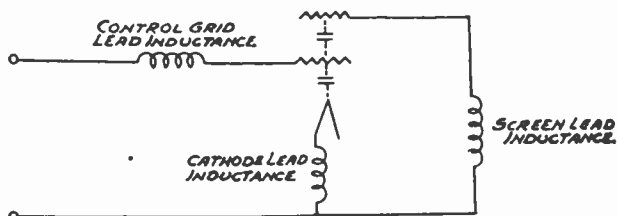


Fig. 2—Tube-input circuit indicating presence of inductance in electrode leads.

### Case 2. Hot Cathode

When emission is present, the picture is altered in that the input conductance becomes increasingly large at ultra-high frequencies. This conductance serves to load down the input circuit, thus limiting the gain obtainable from the antenna to the signal grid. The input conductance, frequently referred to as loading, arises primarily from two distinct sources, 1) the inductance and resistance of the tube leads, and 2) the finite transit time of the electrons in traversing the tube. These will be considered in turn.

#### (a) Lead Effects

A complete study of the input admittance involves the consideration of the effects of lead self and mutual inductances as well as of capacitances between leads and of distributed capacitances. This problem

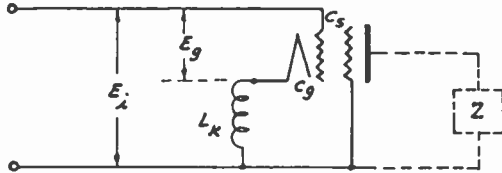


Fig. 3—Tube circuit indicating presence of cathode-lead inductance.

has been handled in a thorough fashion by Strutt.<sup>2</sup> It will suffice for the purpose of illustration to consider the simple case wherein self-inductance is present in the cathode lead only, as shown in Figure 3. This is due to the fact that in certain cases it is the cathode lead inductance which plays the preponderant role in determining the input conductance at ultra-high frequency.

For the circuit of Figure 3, there can be substituted its equivalent as shown in Figure 4.

$C_g$  is the cathode—control-grid capacitance.

$C_s$  is the control-grid—screen-grid capacitance.

$L_k$  is the cathode lead inductance.

$E_g$  is the effective alternating voltage between grid and cathode.

$E_i$  is the effective alternating voltage across the input terminals.

$g_m$  is the sum of the transconductances as measured between the control grid and all other electrodes to which electron current flows.

The  $g_m E_g$  generator across  $L_k$  is a current generator which supplies the plate current, screen current, etc., which flow through  $L_k$ , the cathode lead inductance.

$$\text{Then, } E_i = E_g + j\omega L_k g_m E_g$$

$$= E_g (1 + j\omega L_k g_m)$$

$$I_y = E_g j\omega C_g + E_i j\omega C_s$$

$$= (E_i j\omega C_g) / (1 + j\omega L_k g_m) + E_i j\omega C_s$$

$$= E_i (j\omega C_g + \omega^2 L_k C_g g_m) / (1 + \omega^2 L_k^2 g_m^2) + E_i j\omega C_s$$

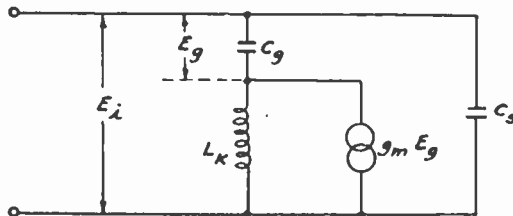


Fig. 4—Equivalent input circuit of tube represented in Fig. 3.

<sup>2</sup> M. J. O. Strutt, "The causes for the increase of the admittances of modern high-frequency amplifier tubes on short waves," *Proc. I.R.E.*, vol. 26, pp. 1011-1033; August, 1938.

If the discussion is limited to the case for which  $\omega^2 L_k^2 g_m^2 \ll 1$ , then

$$I_g = E_i [j\omega(C_g + C_s) + \omega^2 L_k C_g g_m]$$

and finally  $y_g = I_g/E_i = j\omega(C_g + C_s) + \omega^2 L_k C_g g_m$ .

If the screen lead inductance is appreciable and of value  $L_s$ , the expression for input admittance becomes

$$A = j\omega(C_g + C_s) + \omega^2(g_m L_k C_g - g_s L_s C_s)$$

where  $g_s$  is the grid-screen transconductance.

Thus the cathode and screen lead inductances result in the introduction into the input admittance of real components, which vary as the first power of transconductance and as the square of the impressed frequency. The effect of the screen lead inductance is to tend to "neutralize" the effect of the cathode lead inductance. However, due

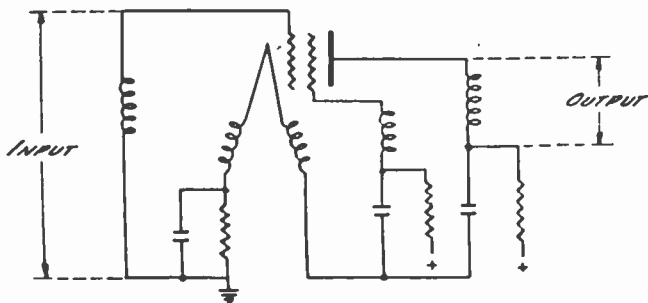


Fig. 5—Circuit of tube with two cathode-leads.

to the fact that  $g_s$  is usually a fraction of  $g_m$  the neutralization could be complete only by making  $L_s$  several times  $L_k$ , a method which is unsatisfactory in that it results in screen "swinging."

One method of decreasing the loading effects of cathode lead inductance is to use two separate cathode leads to separate the input and output circuits, so that the plate current does not affect the input loading. This method, which has been made use of in tubes produced for ultra-high-frequency operation, is illustrated in Figure 5.

### (b) Capacitance Changes and Transit-Time Loading

The influence of the flow of electrons within the tube upon the input capacitance and conductance will now be examined. It is customary to think of current flow occurring to an electrode only when electrons strike it, a concept which is strictly valid only for static conditions. A more appropriate concept is best arrived at by examining the behavior

of a diode, in which it can be seen that plate current begins to flow as soon as electrons leave the cathode. Every electron in the space between cathode and plate induces an "image" charge on the plate; the magnitude of the charge depending upon the proximity of the electron to the plate. Because the proximity changes with electron motion, there is a current flow through the external circuit due to the motion of electrons in the space between cathode and plate.

This concept of current flow can be used to envisage the way in which the grid current flows in a triode as illustrated in Figure 6.  $e_g$  is the instantaneous value of the alternating component of grid voltage. In this triode, the plate is positive with respect to the cathode and the grid is negatively biased. Due to the motion of electrons between cathode and grid there is a current  $i_a$  flowing into the grid and in addition there is a current  $i_b$  flowing out of the grid due to the

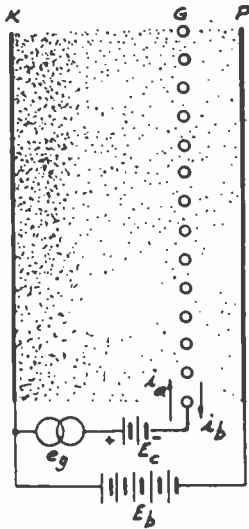


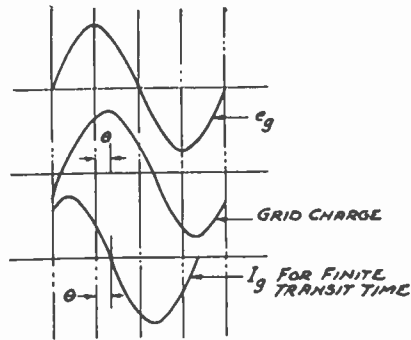
Fig. 6—Triode showing presence of electron space charge.

motion of electrons away from the grid toward the plate. When no alternating voltages are present  $i_a = i_b$  and the net grid current  $i_g = 0$ . While under static conditions no current flows in the grid circuit, the presence of electrons in the space causes a positive image charge to appear on the grid. Now if the grid potential is varied in the positive direction, the positive charge on the grid will be increased, the increase being due in part to the effect of the capacitance between the grid and other electrodes, and in part to the increase of electron space charge in the region surrounding the grid. The increase in space charge results from the increased electron current caused by the grid going more positive. From the fact that the positive charge on the grid is increased

over and above the charge due to the capacitance with the cathode cold, it may be seen that the space charge effectively results in an increase in the effective capacitance between the grid and the other electrodes. This added capacitance depends upon the electron space charge and increases with decreasing grid bias.

If a small alternating voltage  $e_g$  is applied to the grid, the electron current will vary correspondingly and consequently the grid charge too. If the time taken for the electrons to traverse the region between the cathode and grid is small compared with the period  $T$  of the alternating voltage  $e_g$ , the charge on the grid due to the electron space charge will vary in phase with  $e_g$  and thus the added input admittance resulting from current flow will be purely susceptive. The time taken for the electrons to traverse the region between cathode and grid is referred to as the cathode-grid transit time and is denoted by  $T_g$ . The transit time between grid and plate  $T_p$  is generally small compared with  $T_g$ ,

Fig. 7—Variations of grid potential, grid charge, and grid current in tube with appreciable cathode—control-grid transit angle.



due to the high average electron speed in this region. As a consequence consideration of the effects of transit times upon input admittance may be restricted to the cathode—control-grid transit time  $T_g$ .

It is frequently convenient to make use of the quantity "transit angle" which is defined as  $\omega T = 2\pi fT = 2\pi(T/T)$ . For the above case where  $T_g \ll T$ ,  $\omega T_g \ll 2\pi$ . Now if the cathode-grid transit angle is appreciable, which is just another way of saying that the time taken for an electron to traverse the cathode-grid region is not negligible compared with the period of the impressed signal, the grid charge will go through its maximum value somewhat later than the instant when the grid voltage passes through its maximum. This "lag" in the grid charge denoted by  $\theta$  in Figure 7, results in a corresponding lag in the grid current. The courses of the grid voltage, charge, and current for this case are depicted in Figure 7. Since the grid voltage and current are not in quadrature, the input admittance is complex and contains a real or conductance term. From Figure 7 it may be seen that the

conductance term is positive indicating that the effect of finite transit angle is the introduction of a real conductance across the grid-cathode terminals. This problem has been investigated by Ferris<sup>3</sup> and North<sup>4</sup> who found that if the transit angle is not too great the input conductance is given by  $A = kg_m\omega^2T_g^2$  where  $k$  is a constant and  $T_g$  is the cathode-grid transit time. If the transit angle is greater than about  $\pi/2$ , the behavior may be quite different, in that the input conductance and susceptance may oscillate through positive and negative values as the transit angle increases.<sup>4</sup> It will be noted that this expression is similar to that for the input conductance due to lead inductances in that it varies as the first power of  $g_m$  and the square of the applied frequency. The similarity of the two expressions makes their experimental unraveling difficult.<sup>5</sup>

For the purposes of illustration, the input loading and capacitance change of a 6AC7 are shown in Figure 8 as a function of plate current. While the measurements were made at 40 megacycles, they can be extended to other frequencies by making use of the facts that the input conductance varies as the square of the frequency and that, to a first approximation, the change in input capacitance is independent of the frequency.

The preceding discussion applies to the case of space-charge-limited emission. For temperature-limited emission the behavior is the converse, the capacitance change being negative and the input conductance due to finite transit time also being negative. That this is so can be seen by considering the behavior of a space-charge grid tube (see Figure 9) wherein a grid  $G_1$  interposed between cathode and control grid  $G_2$  is operated at a positive potential. The current passing through the control grid  $G_2$  and then through the screen grid  $G_3$  to the plate is practically unaffected by variations in control-grid-voltage. There is, of course, some variation in plate current as the grid voltage is varied. However, for small changes in the grid voltage, the variations in current transmitted through the grid are small compared with the average or quiescent value of this current. As a consequence, to a first approximation the space current may be considered as constant for small variations in control grid voltage.

The current passing through the grid  $G_2$  in Figure 9 (considered constant) is given by  $\rho v$  where  $\rho$  is the space-charge density and  $v$  is

<sup>3</sup> W. R. Ferris, "Input resistance of vacuum tubes as ultra-high-frequency amplifiers," *Proc. I.R.E.*, vol. 24, pp. 82-105; January, 1936.

<sup>4</sup> D. O. North, "Analysis of the effect of space charge on grid impedance," *Proc. I.R.E.*, vol. 24, pp. 108-136; January, 1936.

<sup>5</sup> M. J. O. Strutt, "Moderne Kurzwellen-Empfangstechnik," pp. 113-118, Julius Springer, Berlin, Germany, 1940.



Fig. 8—Variation of input conductance and of input capacitance as function of plate current in 6AC7 pentode measured at 40 megacycles.  
 $E_f = 6.3$  volts  
 Plate volts = 250  
 Suppressor volts = 0  
 Screen volts = 150  
 Gridvolts = varied  
 Frequency = 40 mcs.

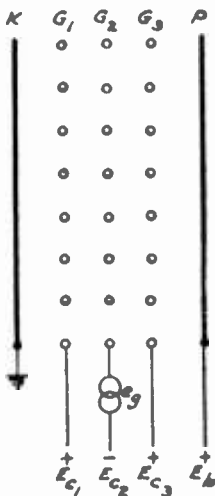
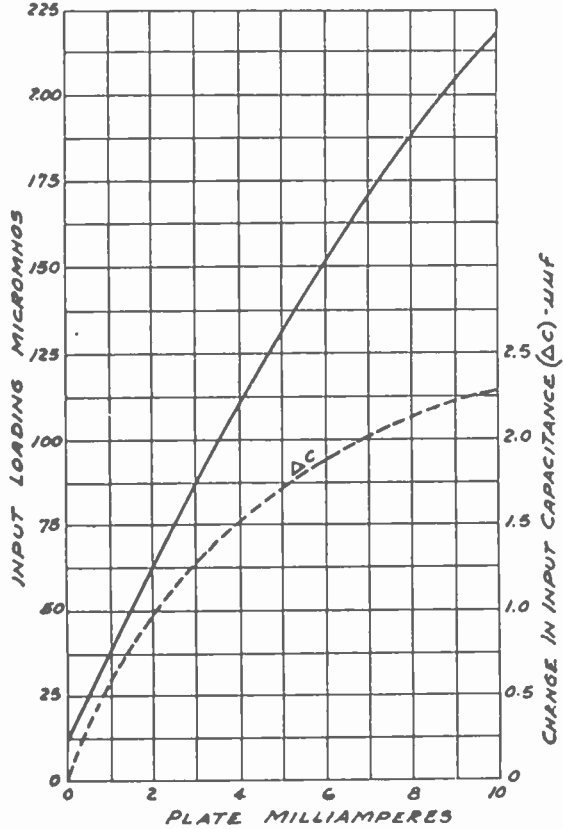


Fig. 9—Space-charge-grid tube in which effect of space charge is to lower effective input conductance and capacitance.

the average velocity of the electrons in the  $G_2$  plane. Suppose now that a small alternating voltage  $e_g$  is connected to grid  $G_2$  as indicated. During the part of the cycle when  $e_g$  is increasing the electrons in the space between  $G_2$  and  $G_3$  are accelerated and their velocities increased. Since  $\rho v$  (the current) is a constant,  $\rho$  must decrease, and (if the transit angle is negligibly small) the charge on the grid due to the electrons must vary 180 degrees out of phase with the grid voltage. By comparison with the space-charge-limited case wherein the grid charge was in phase with the grid voltage it is seen that electrons serve to produce a negative capacitance change.<sup>6</sup> A finite transit angle will produce a lag in the grid current with respect to the grid voltage. Just as a finite transit angle for the positive capacitance case results in a positive input conductance, the lag in this case, wherein the capacitance change is negative, results in a negative input conductance.

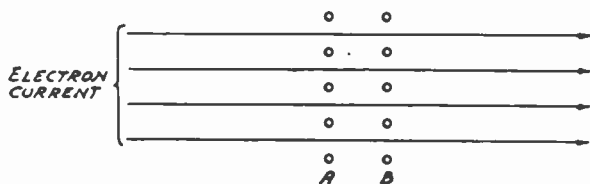


Fig. 10—Velocity-modulating grids traversed by electron current.

(c) *Input Admittance of Velocity-Modulation Devices*

In recent years, a new method for the control of electron beams or current has been described,<sup>7-9</sup> wherein the velocity rather than the magnitude of a current is affected by voltages applied to control electrodes. In Figure 10 let  $A$  and  $B$  represent grids which are connected to the opposite terminals of a radio-frequency circuit and which are traversed by an electron current or beam. If the transit angle in the space between  $A$  and  $B$  is not too great, the beam will experience a "velocity modulation." Thus, when the radio-frequency electric field is such that  $B$  is positive with respect to  $A$ , the electrons will be accelerated as they traverse the region between  $A$  and  $B$  and will be slowed down during the opposite phase. If the region beyond  $B$  is free of radio-frequency fields, the velocity modulation will be retained in that region. By methods described,<sup>7</sup> e.g., deflection conversion, drift tube

<sup>6</sup> L. C. Peterson, "Impedance properties of electron streams," *Bell Sys. Tech. Jour.*, vol. 18, pp. 465-482; July, 1939.

<sup>7</sup> W. C. Hahn and G. F. Metcalf, "Velocity-modulated tubes," *Proc. I.R.E.*, vol. 27, pp. 106-117; February, 1939.

<sup>8</sup> A. A. Heil and O. Heil, "A new method for the production of short electromagnetic waves," *Zeit. für Phys.*, vol. 95, pp. 752-762; July 12, 1935.

<sup>9</sup> R. H. Varian and S. F. Varian, "A high frequency oscillator and amplifier," *Jour. Appl. Phys.*, vol. 10, pp. 321-327; May, 1939.

conversion (bunching), or retarding-field conversion, the velocity modulation can be transformed into a current modulation which can be used to develop signal voltage in an output circuit.

If the transit time between *A* and *B* is infinitesimal, no net interchange of energy between the electrons and circuit takes place since the energy transfer from the circuit to the beam during the portion of the cycle when the beam is accelerated is balanced exactly by the transfer of energy in the reverse direction during the opposite phase of the oscillation. For finite transit angles less than  $\pi$  radians, however, there is a net transfer of energy from the circuit to the electron stream, this being evidenced externally by an apparent loading of the circuit between grids *A* and *B* of Figure 10. The shunt conductance is given by<sup>10</sup>  $g = (i_0/V_0) (\omega^2 T^2/6)$  where  $i_0$  is the beam current and  $V_0$  is the average volt velocity of the beam. This expression, which holds very closely up to transit angles of about  $\pi/2$ , is similar to those for the other forms of input loading in that the conductance increases as the square of the transit angle.

#### (d) *Transadmittance*

In the case of grid control tubes, transadmittance is more uniform in magnitude as a function of frequency than the other admittance terms of the 4-terminal equivalent network described above.<sup>11</sup> Whereas, the input conductance is already radically altered at frequencies for which the transit angle is  $\pi$  radians, the transadmittance is practically unaltered in magnitude for the same frequencies. Its phase, as measured by the relative phase of plate current with respect to signal-grid voltage, may, however, be radically altered. Lead effects, too, may considerably affect its phase. These phase changes are of no importance in amplifier operation, except through the effect of plate-grid feedback, but for the case of self-excited oscillators, the phase of the feedback must obviously be altered to compensate for phase changes in the transadmittance.

#### (e) *Output Admittance*

The output circuit of a multielectrode tube may be represented as shown in Figure 11. The behavior of this circuit is similar to that at the input end of a tube as discussed in Section III, 2, above, and the same general conclusions are valid. The influence of the electron space charge upon the output capacitance is negligible due to the high speed

<sup>10</sup> D. L. Webster, "Cathode ray bunching," *Jour. Appl. Phys.*, vol. 10, pp. 501-508; July, 1939.

<sup>11</sup> M. J. O. Strutt, "Messungen der Komplexen Steilheit Moderner Mehrgitterrohren im Kurzwellen Gebeit," *Elek. Nach. Tech.*, vol. 15, pp. 103-111; April, 1938.

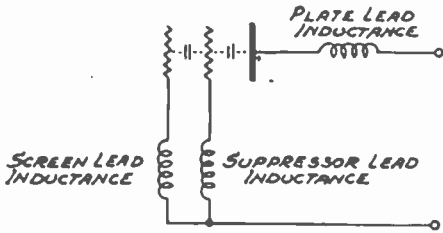


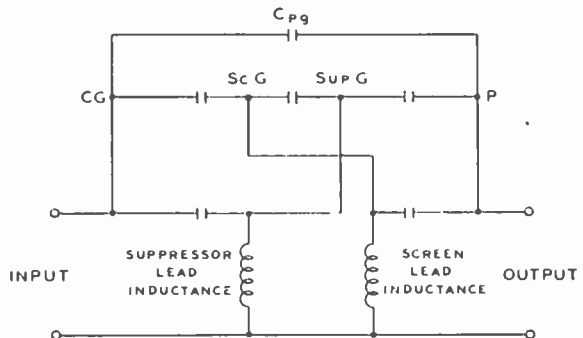
Fig. 11—Output circuit of multielectrode tube.

of the electrons in the output region. Its influence upon the output conductance, while not negligible, is many times less than upon the input conductance. Consequently, in an amplifier employing a number of tubes (except in the case wherein a matching transformer is employed between stages), the output conductance due to electron flow may play a minor role in loading down the circuits, when account is taken of the influence of the input conductance of the following tube. However, unless particular attention is paid to the matter of minimizing ohmic losses in the leads, these losses may exercise a preponderant role in both input and output at extremely high frequencies.

(f) *Feedback Admittance*

There still remains for consideration the remaining term in the 4-terminal network equations, i.e., the feedback admittance. At low frequencies, this is obviously capacitive in character, the capacitance being the static capacitance of plate to grid. Consider the equivalent circuit of a typical pentode as shown in Figure 12. At low frequencies, the lead inductances to screen and suppressor exert a negligible influence and so the effective feedback capacitance is given by  $C_{(pg)0}$  (the static capacitance). At high frequencies, the lead inductances become of importance, and the effective capacitance is given by a very complex expression derived in the paper by Strutt.<sup>2</sup> This complex expression can be represented at moderately high frequencies by  $C'_{pg} = C_{(pg)0} - A\omega^2$ .

Fig. 12—Equivalent circuit of pentode.



$A$  is of the order of  $10^{-19}$  when  $C_{pg}$  is expressed in micromicrofarads and  $\omega = 2\pi f$  where  $f$  is measured in cycles per second. Thus with increasing frequency, the effective feedback capacitance decreases and finally passes through zero at the so-called self-neutralization point, and becomes negative at still higher frequencies. This expression shows that for wide tuning-range receivers, neutralization at ultra-high-frequencies may be a serious problem in view of the rapid frequency variation of the effective feedback capacitance.

#### IV. NOISE DUE TO STATISTICAL FLUCTUATIONS

In the preceding sections, the high-frequency behavior of tube admittances, which directly affects the over-all gain of any amplifier system, was studied. However, it is not gain alone that sets a limit to the sensitivity of a receiver, since, after all, any desired gain can be achieved by increasing the number of stages (provided, of course, the gain of the individual stages is greater than unity).

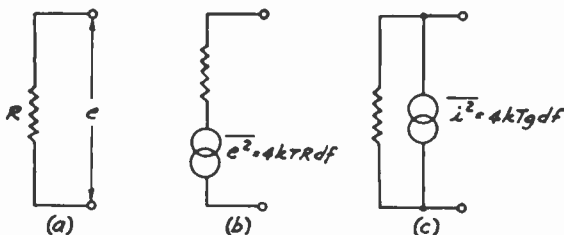


Fig. 13—(a), (b), and (c) are equivalent if the resistor  $R$  in (a) is a normal noisy resistor, while those in (b) and (c) are noise-free but connected to the voltage or current noise generators as shown.

The actual sensitivity limit is also determined in part by the statistical fluctuations of the electric charge within a conductor, or fluctuations of electron emission. These give rise to "noise," which sets a lower limit to the signal which can be detected. In this section some general theoretical results concerning noise will be presented and in Part III of this series these results will be used to compute the limiting sensitivity of radio receivers.

##### 1. Thermal Agitation Noise

Consider a resistor  $R$  as shown in Figure 13(a). Due to the internal random motion of the electrons within  $R$ , a mean-square open-circuit voltage will be present across its terminals given by<sup>12</sup>  $\bar{e}^2 = 4kTRdf$  where  $k$  is Boltzmann's constant  $= 1.37 \times 10^{-23}$  joule per degree centigrade and  $T$  is the temperature in degrees Kelvin.

<sup>12</sup> J. B. Johnson, "Thermal agitation of electricity in conductors," *Phys. Rev.*, vol. 32, pp. 97-110; July, 1928.

$df$  is the element of bandwidth in cycles per second. In the general case one limits oneself to an element  $df$  for the reason that the value of  $R$  may be a function of frequency in which case it becomes necessary to perform an integration, if the noise voltage squared over a finite bandwidth is desired. If  $R$  is independent of frequency, the noise voltage produced over any bandwidth is the same regardless of its position in the frequency spectrum.

The "noisy" resistor can be represented by means of an ideal noise-free resistor in series with a constant-voltage generator of mean-square voltage  $\overline{e^2} = 4kTRdf$  as shown in Figure 13(b) or by means of a noise-free resistor in parallel with a constant-current generator of mean-square current  $\overline{i^2} = 4kTgdf$  where  $g = 1/R$ . That the constant-voltage series generator and the constant-current shunt generator modes of representation are completely equivalent as far as external effects are concerned may be seen readily by connecting an impedance  $Z$  across the output terminals of Figures 13(b) and 13(c). Then for the constant-voltage-generator representation the mean-square current through  $Z$  is given by

$$\overline{i_z^2} = e^2 / (R + Z)^2 = 4kTRdf / (R + Z)^2.$$

For the constant-current generator representation the mean-square current through  $Z$  is given by

$$\overline{i_z^2} = \overline{i^2} \frac{R^2}{(R + Z)^2} = \frac{4kTdf}{R} \frac{R^2}{(R + Z)^2} = \frac{4kTRdf}{(R + Z)^2}$$

which is identical with that derived above, thus demonstrating the interchangeability of the constant-current and constant-voltage representations.

The choice of which concept to use depends in general upon the nature of the application. For parallel combinations the constant-current concept is more useful since the separate mean-square noise currents are simply added to produce the resultant mean-square noise current. Similarly for series connections the voltage generator concept is the more useful one since, for this case, the separate mean-square noise voltages add to produce the resultant.

In the preceding discussion reference was made only to resistors. The results given are actually applicable to any passive two-terminal networks subject to the condition that for  $R$  one uses the real part of the complex impedance. Thus, consider the parallel resonant circuit of Figure 14, with real part  $R$  of its impedance as function of frequency

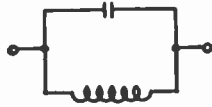


Fig. 14—Parallel resonant circuit.

as shown in Figure 15. For this case the mean-square noise voltage between frequency limits  $f_1$  and  $f_2$  is given by

$$\overline{e^2} = 4kT \int_{f_1}^{f_2} Rdf.$$

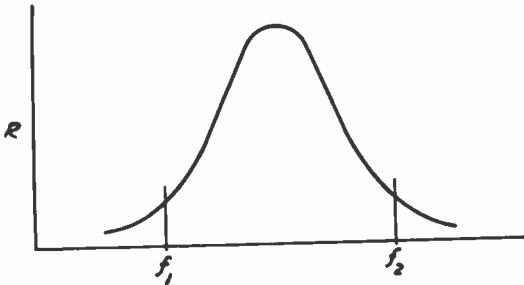
## 2. Tube Noise

Schottky<sup>13</sup> predicted that the emission in a temperature-limited diode would contain a fluctuation component given by  $\overline{i^2} = 2eIdf$  where  $e$  is the electronic charge and  $I$  is the average total emission. It is assumed in this that the transit time through the diode is small compared with the frequencies whose noise components are under study.

If the diode anode is operated at a uniform negative potential with respect to the cathode so that the arrival or nonarrival of an electron at the anode is determined by its emission velocity solely, then the mean-square noise current is given by  $\overline{i^2} = 2eI_b df$  where  $I_b$  is the actual plate current.

For the intermediate conditions wherein the emission is space-charge-limited, the so-called shot noise is less than that due to the same current under temperature-limited conditions and is given by<sup>14</sup>  $\overline{i^2} = 2eI_b \Gamma^2 df$  where  $\Gamma$  is a factor depending upon the ratio of available emission to actual plate current and upon the value of the anode potential.

If the available emission is large compared with the plate current, and the anode potential is not too close to that of the cathode,  $\Gamma$  is less than 0.2 for conventional structures, indicating how considerable a

Fig. 15—Real part  $R$  of impedance of circuit of Fig. 14, as a function of frequency.

<sup>13</sup> W. Schottky, "Spontaneous current fluctuation in various conductors," *Ann. der Phys.*, vol. 57, pp. 541-567; December 20, 1918.

<sup>14</sup> D. O. North, "Fluctuations in space charge limited currents at moderately high frequencies," *RCA REVIEW*, vol. 4, pp. 441-473; April, 1940.

reduction in the noise current is produced by the presence of the space charge. North<sup>14</sup> has shown that if the available emission is large compared with the actual current drawn from the cathode, then  $I^2 = 1.29 (kT_K/e) g/I_b$  where  $e$  is the electronic charge,  $k$  is Boltzmann's constant and  $T_K$  is the absolute temperature of the cathode and  $g$  is the conductance of the diode, given by  $g = \partial I_b / \partial E_b$  where  $I_b$  is the plate current and  $E_b$  the plate voltage. If this is substituted in the expression for  $\overline{i^2}$ , one obtains

$$\overline{i^2} = 2.58eI_b(kT_K/e)(g/I_b)df = 0.64(4kT_K)gdf.$$

This indicates that for a space-charge-limited diode, wherein large excess emission is available, the noise current is a linear function of the conductance and does not involve the plate current directly. For an oxide-coated cathode ( $T_K = 1000$  degrees Kelvin),  $I^2 = 0.11(g/I_b)$  and  $\overline{i^2} = 3.54 \times 10^{-20}gdf$ .

It is interesting to look into the physical picture of the process in order to see exactly how noise reduction is brought about by the presence of space charge. Under space-charge-limited conditions, a potential minimum exists in the region between the cathode and anode and is very close to the cathode. In the region between the cathode and the potential minimum electrons are traveling in both directions. The electrons returning toward the cathode are those emitted with a volt velocity less than that of the potential minimum so that they are unable to get over the "crest." Now if in the normal course, as determined by probability considerations, there is a sudden excess emission of charge, a depression of the potential minimum will occur which will in turn cause some electrons to be turned back that might otherwise have reached the plate. The variations in the potential minimum in correspondence with the fluctuations in emission current thus tend to smooth out the fluctuations in current passing through the potential minimum to the plate.

The above expressions, which are based on the theoretical work of North,<sup>14</sup> are not in agreement with the measured values for space-charge-limited diodes. Actually, for this case the noise is considerably greater than predicted by theory. North<sup>14</sup> indicates that the explanation for this is most likely that elastic reflections of electrons at the anode (which is operating at a comparatively low potential) contribute to an increase in the noise in the plate circuit. For the temperature-limited case, wherein the anode can operate at much higher potential, the agreement between theory and experiment is excellent.

From the noise standpoint, a negative-grid triode can be looked upon as a diode whose anode potential is equal to the effective potential



in the grid plane. Since all electrons which pass the grid plane are collected by the plate, the theoretical results for the space-charge-limited diode should (and do) describe the actually observed values for the negative-grid-triode, if for  $g$ , the conductance, one substitutes  $g_m$ , the grid-plate transductance.

### 3. Equivalent Noise Resistance

For many purposes it is convenient to suppose that the current flow in a tube is noise-free but that the noise in the plate current arises from the presence of a noise-voltage generator in series with the grid. We can set for the mean-square voltage of this fictitious generator  $\bar{e}^2 = 4kT_R R_{eq} df$ , where  $R_{eq}$  is a fictitious resistance at room temperature ( $T_R = 300$  degrees Kelvin) and of such value that, if shunted across the input of a noise-free tube, the noise current in the plate circuit is the same as that for the noisy tube with shorted input. An expression for  $R_{eq}$  may be derived as follows:

$$\bar{i}^2 = 2eI_b I^2 df$$

$$= g_m^2 \bar{e}^2$$

$$\bar{e}^2 = 4kT_R R_{eq} df$$

where

$$\begin{aligned} R_{eq} &= \bar{e}^2 / 4kT_R df = \bar{i}^2 / g_m^2 4kT_R df \\ &= 2eI_b I^2 df / g_m^2 4kT_R df = 20I_b I^2 / g_m^2. \end{aligned}$$

If for  $I^2$  one inserts the approximate value for negative-grid triodes with oxide-coated cathode  $I^2 = 0.11g_m/I_b$ , there results

$$R_{eq} = 20I_b / g_m^2 \times 0.11 (g_m / I_b) = 2.2 / g_m.$$

A list of values of  $R_{eq}$  for various types of tubes has been prepared by Harris.<sup>15</sup>

$R_{eq}$  is a totally fictitious resistance and must, under no circumstances, be considered as actually being present in the circuit. The noise-voltage generator is represented as being directly in series with the grid, the tube internal capacitance or loading being effectively external to the generator so that the full generator voltage is effective across the input circuit. This is illustrated for a simple case in Figure 16, where  $R_{inp}$  is due to input loading and  $C_{inp}$  is the input capacitance of the tube.

$R_{eq}$  is an excellent measure of the "noisiness" of a tube and varies

<sup>15</sup> W. A. Harris, "Fluctuations in vacuum tube amplifiers and input systems," *RCA REVIEW*, vol. 5, pp. 505-525; April; and vol. 6, 115-124; July, 1941.

from values as low as 220 ohms for a 6AC7 operating as a triode amplifier to values of hundreds of thousands of ohms for multigrid converters such as the 6SA7. In the case of converters, the value of the conversion transconductance rather than the amplifier transconductance enters into the expression for the equivalent noise resistance. Since optimum conversion transconductance is always less than maximum amplifier transconductance for a given tube, the equivalent noise resistance of a tube when operating as a converter is usually greater than when operating as an amplifier. This conclusion should be borne in mind as reference will be made to it in Part IV of this series when consideration is given to the question of whether to use an amplifier or mixer for specific applications.

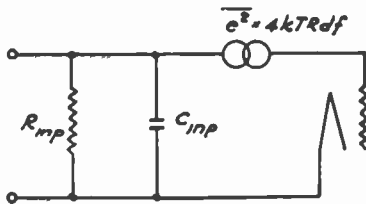


Fig. 16—Tube circuit wherein plate noise is represented as being due to noise-voltage generator in series with grid lead.

#### 4. Noise Due to Current Division

In multielectrode tubes the electron current usually divides between several electrodes at a positive potential which gives rise to additional fluctuations. For example, in the case of a pentode, the fluctuations arise from the fact that the chance of any electron hitting a screen wire or of landing on the anode is purely random. If there is no secondary emission from any of the electrodes drawing current, as in the case of pentodes, theory indicates<sup>16,17</sup> that the noise in the plate circuit will in general exceed that for a similar triode with the same plate current but will never exceed that due to the same value of temperature-limited plate current.

#### 5. Effects of Secondary Emission

Secondary electron emission enters into the noise picture in one of two ways: 1) by the noise introduced by secondaries emitted at any electrode which then go to a more positive electrode, or 2) in the use of a secondary-emission multiplier to multiply an electron current. The first of these is of no importance in triodes or pentodes but is a factor in tetrodes and some multigrid tubes.<sup>18</sup>

<sup>16</sup> D. O. North, "Multi-collectors," *RCA REVIEW*, vol. 5, pp. 245-260; October, 1940.

<sup>17</sup> C. J. Bakker, "Current distribution fluctuations," *Physica*, vol. 5, pp. 581-592; July, 1938.

<sup>18</sup> C. J. Bakker and B. van der Pol, "Spontaneous fluctuations," *Compt. Rend. de l'Union Radio-Scientifique Internationale*, Venise 5, pp. 217-227; 1938.

At times an electron multiplier is used to multiply a modulated electron current. If there were no fluctuations in the secondary electron emission, i.e., if each primary produced the same number of secondary electrons, no more, no less, then the signal and the noise would be multiplied alike so that the signal-to-noise ratio would be unchanged. This method of amplification would be superior to the normal use of a following tube with coupling impedance, since the noise introduced by the coupling impedance and following tube would be eliminated. However, secondary electron emission is also a "statistical" phenomenon in that the secondary-emission ratio  $n$  is actually the average of a distribution of ratios for all the primary electrons. As a consequence the ratio of signal-to-noise in the output of an electron multiplier is always less than in the input. If the secondary-emission ratio of the initial stage is not too small, say 5 or greater, the decrease in signal-to-noise ratio by an electron multiplier is almost negligible. It is thus extremely desirable to use electron multipliers in cases where the tube geometry permits.<sup>19</sup>

As a final item it must be emphasized that in the preceding discussion it was tacitly (and incorrectly) assumed that the multiplication of a varying signal is the same as that of a direct current. The amplification of a multiplier decreases with frequency due to the spread in transit angle resulting from nonuniform initial velocities and differing paths. At ordinary intermediate frequencies this is of no importance, so that the use of multipliers for amplifying the intermediate-frequency signal of a converter or mixer is feasible. However, since the gain of ordinary multipliers begins to drop off at frequencies of only a few hundred megacycles, care must be used in applying electron multiplication to the amplification of ultra-high-frequency signals.<sup>20</sup>

## 6. Induced Noise

### (a) Induced Noise in Grid-Controlled Tubes

This is the one source of noise which may be considered as an ultra-high-frequency noise in that it is present only when transit angles are appreciable and increases with frequency. It arises from the fact that for finite transit angles through the tube the noise-current fluctuations in the emission current induce noise current on the grid which in turn react upon the electron current traversing the tube. North and

<sup>19</sup> V. K. Zworykin, G. A. Morton, and L. Malter, "The secondary emission multiplier—a new electronic device," *Proc. I.R.E.*, vol. 24, pp. 351-376; March, 1936.

<sup>20</sup> L. Malter, "Behavior of electrostatic multipliers as a function of frequency," *Proc. I.R.E.*, vol. 29, pp. 587-598; November, 1941.

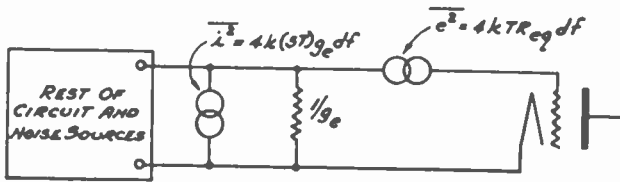


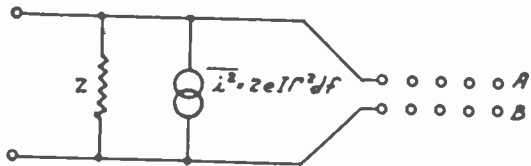
Fig. 17 — Circuit indicating how induced noise in a triode may be represented as being due to a constant-current generator in shunt with a conductance.

Ferris<sup>21</sup> have shown that induced noise current in grid-controlled tubes is equivalent to the thermal-noise produced by a resistor whose reciprocal is equal in value to the input conductance due to finite transit angle and whose temperature is about 5 times room temperature. They have also shown that, to a first approximation, induced grid noise may be added to the plate noise (referred to the grid) of the same tube as if they were independent sources of noise. The representation is shown in Figure 17, where  $g_c$  is the input conductance due to finite transit angle.

(b) Induced Noise in Velocity-Modulation Devices

If the electron stream traversing the region between the velocity-modulation grids *A* and *B* of Figure 9 is current-modulated as, e.g., by noise-current components, a serious type of induced noise comes into existence. A current-modulated beam passing between *A* and *B* induces a current in the circuit of which *A* and *B* are part, this current approaching in value the modulated component of the stream for small transit angles between *A* and *B*. If this induced current be denoted by  $i$ , then a potential difference will be established between *A* and *B* given by  $e = iZ$  where  $Z$  is the circuit impedance. This varying voltage  $e$  will make itself felt upon the beam in the form of a velocity modulation. If  $i$  is due to noise, the resultant noise source can be represented by the circuit of Figure 18.  $I$  is the beam current and  $I^2$  the space-charge reduction factor. Since in tubes of this type beams are generally employed, noise due to current division generally is introduced at focusing electrodes preceding the velocity-modulation grids. As a consequence there exists a "wiping out" of space-charge reduction effects, resulting in a final  $I^2$  approaching unity. As a consequence, the contribution of the induced noise to the total noise may be considerable or even preponderant.

Fig. 18 — Representation of induced noise in velocity modulation device as being due to a constant-current generator in shunt with conductance as measured between velocity-modulating grids.



<sup>21</sup> D. O. North and W. R. Ferris, "Fluctuations induced in vacuum-tube grids at high frequencies," *Proc. I.R.E.*, vol. 29, pp. 49-50; February, 1941.

## Part III. The Signal-to-Noise Ratio of Radio Receivers†

By

E. W. HEROLD

*Summary*—The signal-to-noise ratio of a radio receiver can best be analyzed by finding all the various noise sources and then referring them to a single point. When the equivalent-noise-resistance concept is used at the input to express the output noise of the first tube of a series, noise sources beyond this point are also conveniently referred back to this same input. Thus, a single equivalent noise resistance  $R_n$  can be used to express all the noise sources at or beyond the first tube. In the simplest case, where noise sources at the input of the first tube can be neglected, the maximum signal at the input also gives best signal-to-noise ratio. The signal-to-noise ratio then depends on the ratio of tube input resistance (which determines the maximum signal) to equivalent noise resistance.

When there is induced noise in the input of the first tube, the optimum signal-to-noise ratio is obtained by coupling the antenna somewhat more tightly to the tube input than for maximum power transfer. Although this reduces the signal at the grid from its maximum value, the reduction of impedance is more marked and causes an even greater reduction in induced noise. The optimum signal-to-noise ratio depends on the product of induced noise and equivalent noise resistance. Even when the input resistance is infinite or negative, the optimum signal-to-noise ratio is limited either by this induced noise or by the bandwidth of the input circuit. Exact analysis, including all noise sources, is more complex but the behavior is qualitatively the same as for the simpler cases.

The effect of feedback, either degenerative or regenerative, on signal-to-noise ratio is often minor, since in many instances both signal and noise are fed back alike. Thus, when this is so, the signal-to-noise ratio may be estimated as if the feedback did not exist and the tube input resistance to be used for such an estimate should not include the part due to feedback.

The signal-to-noise ratio is always inherently limited by the receiving antenna and associated transmission line which have noise of their own. In the laboratory the antenna noise is simply thermal agitation in the dummy-antenna resistance. The ratio of total receiver noise to that produced by the dummy antenna may be used to evaluate the performance of receivers. This ratio, which was introduced by North and is called noise factor, is readily measured, and for a completely noise-free receiver, is unity. All signal-to-noise ratio estimates are conveniently put in this form, since the noise factor is often independent of bandwidth and of antenna-radiation resistance.

## I. INTRODUCTION

## 1. Prefatory Remarks

THIS third paper of the series is concerned almost entirely with one phase of receiver performance, the signal-to-noise ratio. It has already been shown that this is of extreme importance at ultra-high frequencies and, very fortunately, it is a subject which is no longer difficult to understand. Some years ago, the subject of fluctua-

---

† Reprinted from *Proc. I.R.E.*, September, 1943.

tion noise was considerable of a mystery even to the best scientists and engineers. In 1928, Johnson<sup>1</sup> and Nyquist<sup>2</sup> cleared up the subject of thermal agitation noise in circuits. Since about 1935 or so, fluctuation noise in the plate circuit of amplifier tubes has been fairly completely worked out<sup>3</sup> and, with some additional work on mixer and converter noise,<sup>4,5</sup> it is now possible to use accurate quantitative data on tube noise for receiver calculations. Finally, at high frequencies, induced input noise must also be considered and this has also been evaluated.<sup>6,7</sup> In Part II of this series some of the fundamental noise relations were discussed.

The signal-to-noise ratio of a radio receiver at ultra-high-frequencies is primarily dependent on the above-mentioned noise relations for tubes and circuits but, in addition, consideration must be given to the input signal and its transfer to and through the receiver. However, the earlier published work<sup>8-10</sup> on signal-to-noise ratio did not include induced input noise and hence was not strictly applicable at ultra-high frequencies. Furthermore, until North's exposition<sup>11</sup> of the quantity known as noise factor, there appeared to be no widely accepted basis on which experimental or analytical results could be quantitatively compared. The extension of the analysis to include induced noise has now been made<sup>12</sup> and the interpretation of results in terms of noise factor is now common. As a result, it is possible to discuss signal-to-noise ratio at ultra-high-frequencies with considerably greater clarity.

<sup>1</sup> J. B. Johnson, "Thermal agitation of electricity in conductors," *Phys. Rev.*, vol. 32, pp. 97-109; July, 1928.

<sup>2</sup> H. Nyquist, "Thermal agitation of electric charge in conductors," *Phys. Rev.*, vol. 32, pp. 110-113; July, 1928.

<sup>3</sup> B. J. Thompson, D. O. North, and W. A. Harris, "Fluctuations in space-charge limited currents at moderately high frequencies," *RCA REVIEW*, pp. 269-285; January; pp. 441-472; April; pp. 115-124; July; pp. 244-260; October, 1940; pp. 371-388; January; April; pp. 505-524; July, 1941.

<sup>4</sup> E. W. Herold, "Superheterodyne converter system considerations in television receivers," *RCA REVIEW*, vol. 4, pp. 324-337; January, 1940.

<sup>5</sup> E. W. Herold, "The operation of frequency converters and mixers," *Proc. I.R.E.*, vol. 30, pp. 84-103; February, 1942.

<sup>6</sup> D. O. North and W. R. Ferris, "Fluctuations induced in vacuum-tube grids at high frequencies," *Proc. I.R.E.*, vol. 29, pp. 49-50; February, 1941.

<sup>7</sup> C. J. Bakker, "Fluctuations and electron inertia," *Physica*, vol. 8, pp. 23-43; January, 1941.

<sup>8</sup> F. B. Llewellyn, "A rapid method of estimating the signal-to-noise ratio of a high gain receiver," *Proc. I.R.E.*, vol. 19, pp. 446-420; March, 1931.

<sup>9</sup> F. C. Williams, "Thermal fluctuations in complex networks," *Jour. I.E.E.* (London), vol. 81, pp. 751-760; December, 1937.

<sup>10</sup> K. Fränz, "The limiting sensitivity in the reception of electric waves and its attainability," *Elek. Nach. Tech.*, vol. 16, pp. 92-96; April, 1939.

<sup>11</sup> D. O. North, "The absolute sensitivity of radio receivers," *RCA REVIEW*, vol. 6, pp. 332-343; January, 1942.

<sup>12</sup> E. W. Herold, "An analysis of the signal-to-noise ratio of U-H-F receivers," *RCA REVIEW*, pp. 302-331; January, 1942.

## 2. The Simple Amplifier and Its Equivalent Noise Resistance

It is instructive to examine the simplest possible amplifier case and see what is meant by a calculation of signal-to-noise ratio. In Figure 1(a) there is shown a signal source connected to a tube, delivering a voltage  $e_s$ . In the plate of the tube is connected an amplifier and finally some sort of indicating device which may be a loudspeaker, a cathode-ray tube, or any other utilization means. It is known that the tube plate current, although it has an average value  $I_b$  will actually have very minute fluctuations around this average value. These fluctuations are called shot noise and to evaluate them some sort of average value must be found. Since they go as much above as below the average direct current of the tube, an ordinary averaging process will give no information. If the instantaneous fluctuating component of current is squared, however, all the fluctuations, both positive and negative, will give a positive contribution which may then be averaged. Such an average is called the "mean-squared value" of the fluctuation. At the same time, it should be appreciated that such an averaging will give a quantity proportional to noise power. Furthermore, since noise is random, if there are two independent noise sources at one point, their total effect is obtained by simple addition of their noise power, or by just adding their mean-squared values. If the noise fluctuations are in plate current, they may be called  $\overline{i_{pn}^2}$ , where the bar indicates the averaging of the squares of the fluctuations. Now, in general, random noise is distributed over all frequencies. The total noise effect is, therefore, dependent on what frequencies are able to pass through the amplifier and affect the measuring circuit. Thus, the tube noise which reaches the output of an amplifier will depend on the power-gain-versus-frequency characteristic. If the noise is compared with a signal, or if the noise response is compared with the response at some reference frequency, it becomes possible to use the quantity  $\Delta f$ , an effective noise bandwidth which was discussed in Part I. In the discussion to follow, such a comparison is implicitly intended.

We may say, therefore, that the tube noise is  $\overline{i_{pn}^2} = k_n \Delta f$  remembering always that the value of  $\Delta f$  depends on the response at some reference frequency.<sup>13</sup> It is of interest to note that, for most tubes which do not include secondary emitters,  $k_n$  has a *maximum* value of  $2eI_b$  where  $e$  is the electron charge and  $I_b$  is the average plate current. It is usually less than this value, however, as pointed out in Part II.

To go back to the original simplified problem, the tube noise may be shown on Figure 1(a) by the constant-current noise generator of value  $\overline{i_{pn}^2}$ . Since the signal output current is  $g_m e_s$ , it is seen that the

<sup>13</sup> See the discussion of bandwidth at the beginning of Part I of this series.

signal-to-noise ratio at the input to the final amplifier is

$$\frac{\text{signal}}{\text{noise}} = \frac{S}{N} = \sqrt{\frac{g_m^2 e_s^2}{i_{pn}^2}} = e_s \sqrt{\frac{g_m^2}{i_{pn}^2}}$$

If no other sources of noise are present, this will be the over-all signal-to-noise ratio. To eliminate the square root, it is advantageous to consider the square of the signal-to-noise ratio and, this will be done from now on. The use of  $(S/N)^2$  instead of  $(S/N)$  merely means that the results are expressed as a power ratio instead of as a voltage or current ratio. This is always a convenience when several noise sources must be considered, since it is their powers which add.

In this simple problem the signal-to-noise ratio was very easily calculated as follows. First, the origin of the noise was located and

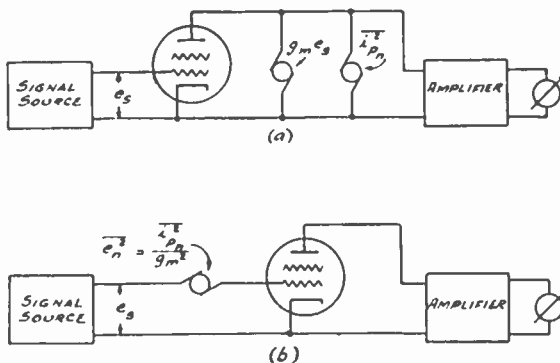


Fig. 1—Simple amplifier case to illustrate the concept of signal - to - noise ratio; (a) noise generator introduced at point of origin, (b) fictitious but equivalent noise generator introduced in grid by use of transconductance  $g_m$ .

then a generator was put in which represented the noise magnitude. Finally, the signal was calculated at that point. This is not the only way in which the same answer could have been obtained and, obviously, if the noise sources are distributed at a number of different points, some other procedure must be adopted. If the *real* noise generator is removed from the plate circuit, and an *entirely fictitious* one put in the grid circuit, it is possible to find a magnitude for the latter generator which would give the same answer for the signal-to-noise ratio. If a fictitious grid noise generator,  $\overline{e_{n1}^2}$ , is substituted for the actual plate noise as in Figure 1 (b), then the plate noise current due to the fictitious generator is  $\overline{i_{pn}} = \overline{e_{n1}^2} g_m^2$ . Thus it is found that for the same plate noise as in Figure 1 (a), the fictitious noise generator must have a value  $\overline{e_{n1}^2} = \overline{i_{pn}^2} / g_m^2$ . The signal at the grid is still  $e_s$  so that

$$(S/N)^2 = e_s^2 / e_{n1}^2 = e_s^2 (g_m^2 / i_{pn}^2)$$



the same as before. It is thus seen that it is not always necessary to evaluate noises at their point of origin; they may, instead, be referred to some other point. Although, in the simple case analyzed, one method has no advantage over another, if there were many noise sources, it would be advantageous to refer them all to the one point.

It is common practice to refer tube noise back to the input as we have done, but it usually is done in terms of an equivalent grid noise resistance. The advantages of this are apparent to those who have been greatly concerned with noise although it may seem like an additional complication at this point. An actual resistor of value  $R$  will have a mean-squared noise voltage due to thermal agitation of<sup>14</sup>  $\overline{e_{n1}^2} = 4kT_R R \Delta f$  where  $k = 1.37 \times 10^{-23}$  joule per degree Kelvin and  $T_R$  is the temperature in degrees Kelvin (i.e., ambient temperature). Thus,  $R = \overline{e_{n1}^2} / 4kT_R \Delta f$ . In the case of the tube,  $\overline{e_{n1}^2}$  is not really due to thermal agitation noise. In fact it is not a *true* noise source at all but simply an *equivalent* to the true noise. Thus, as long as this is fictionalized anyway, we may go further and call  $R_{eq}$  the value of a resistance whose open-circuit noise voltage is the same as  $\overline{e_{n1}^2}$ .

Hence 
$$R_{eq} = \overline{e_{n1}^2} / 4kT_R \Delta f = \overline{i_{pn}^2} / 4kT_R \Delta f g_m^2.$$

If this is used, 
$$(S/N)^2 = e_s^2 (1/4kT_R R_{eq} \Delta f).$$

In this simple example, the signal-to-noise ratio depends simply on the reciprocal of the equivalent noise resistance. The same considerations apply to frequency-changing tubes, except that the conversion transconductance  $g_c$  is used instead of the transconductance  $g_m$ .

In any actual receiver there are many sources of noise. In particular, those sources of noise which follow the first tubes are of small importance in most cases, because the previous sources of noise are much more amplified and exceed these later fluctuations. Thus, as a rule, one may forget the later noise sources and concentrate on those sources in, and ahead of, the first tube, since these receive greatest amplification. For the sake of complete generality, however, let us show that the later sources of noise may be easily accounted for by a slight change in the concept of  $R_{eq}$ . Suppose there is a second noise source, at a point  $k$  in the amplifier as in Figure 2(a). If this *real* noise source is removed and an *equivalent* substituted at the input grid, the same total output noise must still be present. A noise generator  $\overline{e_n^2}$  at the input will produce at point  $k$  a noise  $\overline{e_{nk}^2} = \overline{e_n^2} A_k^2$  where  $A_k$  is the gain of the system from the input to point  $k$ . Thus it is found that  $\overline{e_n^2} = \overline{e_{nk}^2} / A_k^2$ . If there are many noise sources the total mean-squared noise

<sup>14</sup> See Part II of this series.

at the input is

$$\overline{e_n^2} \text{ total} = \sum_k \frac{e_{nk}^2}{A_k^2}$$

Using an equivalent noise resistance concept,

$$R_{eq} = \overline{e_n^2} \text{ total} / 4kT\Delta f = R_{eq1} + R_{eq2} + \dots$$

where the values of  $R_{eq2}$ , etc., are computed using squares of gains. In the remainder of this paper, the concept of  $R_{eq1}$  may, therefore, be considered to include all noise at or beyond the anode of the first tube.

A numerical example may be of interest. A type 955 triode mixer for an ultra-high-frequency receiver has a plate noise, for a 7-megacycle noise bandwidth of<sup>15</sup>  $\overline{i_{pn}^2} = 2.8 \times 10^{-16}$  (ampere)<sup>2</sup>. Since the con-

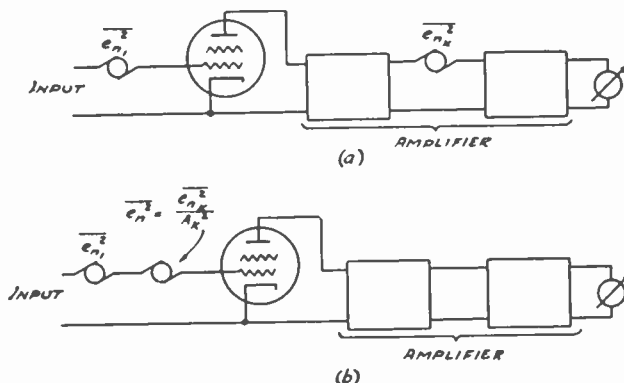


Fig. 2—Noise sources at any point in an amplifier system may be considered in terms of fictitious but equivalent sources at the input; (a) noise introduced at point of origin, (b) equivalent noise generator in input by use of the voltage gain  $A_k$  between input and point of origin.

version transconductance  $g_c$  is  $700 \times 10^{-6}$  mho, the equivalent grid noise voltage is  $\overline{e_n^2} = \overline{i_{pn}^2} / g_c^2$  and  $R_{eq1} = 5200$  ohms. This tube is followed by a single-tuned intermediate-frequency circuit of impedance 520 ohms (so as to give a 7-megacycle bandwidth) and a type 6AC7 tube whose equivalent noise resistance is 700 ohms. At the grid of the second tube there are two noise sources; one is the thermal agitation noise in the intermediate-frequency circuit and the second is the 6AC7 tube noise referred to its own grid. In terms of equivalent resistance, at the first grid (i.e., the grid of the 955 mixer)

<sup>15</sup> This value was obtained by utilizing the triode mixer formulas in footnote reference 4.

$$R_{eq2} = \frac{520}{(\text{gain})^2} = \text{contribution of the thermal noise of the intermediate-frequency circuit}$$

$$R_{eq3} = \frac{700}{(\text{gain})^2} = \text{contribution of the first intermediate-frequency tube noise}$$

If other noise sources are negligible, the total equivalent noise resistance is then  $R_{eq} = R_{eq1} + R_{eq2} + R_{eq3}$ . Since the gain from mixer grid to intermediate-frequency grid is just  $g_c \times 520 = 0.36$  it is seen that  $R_{eq} = 5200 + 520/(0.36)^2 + 700/(0.36)^2 = 5200 + 9400 = 14,600$  ohms. With a properly designed double-tuned intermediate-frequency transformer, it should be noted, this could have been reduced to 6270 ohms.<sup>12</sup> Since the design of interstage coupling networks for best signal-to-noise ratio is beyond the scope of this paper, the reader is referred to Section VII of footnote reference 12 for details.

## II. THE ANALYSIS OF THE SIGNAL-TO-NOISE RATIO OF AN ULTRA-HIGH-FREQUENCY RECEIVER—NOISE FACTOR

### 1. Simple Relations Using Only One Noise Source—Matched Impedance

In many well-designed ultra-high-frequency receivers using conventional triodes or pentodes above about 300 megacycles, it will be found that the chief sources of noise are at the plate of the first tube and at points which follow it. For this reason, the simplified case of a receiver with only these noise sources will be taken up. A very simple relation for the signal-to-noise ratio can then be derived. Furthermore, it will be fairly accurate for triodes and pentodes whose control grid is adjacent to the cathode since, with these tubes, induced input noise is often negligible. Finally, the result is simple and will lead to a better picture of the more complex cases to follow.

We start with a typical input circuit similar to the one which was discussed in Part I. As we saw then, the actual antenna may be replaced by a resistor  $R_a$  and a signal voltage source  $e_a$ . The circuit and its approximate equivalent is shown in Figure 3 and the tube indicated may be an amplifier or a mixer of any kind other than the diode. Let us first assume that the input-transformer tap is adjusted for maximum gain and that the input-circuit bandwidth with such an adjustment is adequate. Maximum gain will result when the impedances are matched, and this means that, looking at the input terminals of the receiver, their impedance will look like the value  $R_a$ . Thus,  $e_a$  is equally divided between  $R_a$  and the transformer. The primary voltage is  $e_a/2$ . The secondary voltage applied to the grid is

$$e_g = m(e_a/2) = (e_a/2) \sqrt{R_t/R_a}$$

since the effective turns ratio  $m$  is fixed by the impedance match. The signal-to-noise ratio is then

$$\begin{aligned} (S/N)^2 &= e_g^2/e_n^2 \approx (e_a^2/4) (R_t/R_a) (1/4kT_R R_{eq} \Delta f) \\ &\approx (e_a^2/4kT_R R_a \Delta f) (1/4) (R_t/R_{eq}). \end{aligned}$$

Remembering from Part I that  $e_a^2/R_a$  depends only on the antenna directivity, it is seen that the only other method to increase the signal-to-noise ratio lies in an improvement of  $R_t/R_{eq}$ , that is, by an increased ratio of input resistance to equivalent noise resistance. Because only

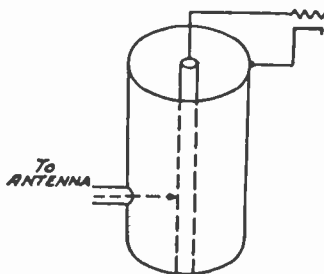
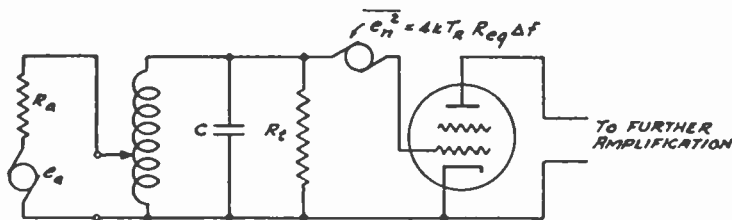


Fig. 3—Receiver input circuit and its equivalent for noise analysis. Noise sources at plate of first tube and at subsequent points of amplifier are included in an equivalent generator at the input.



noise sources at or beyond the anode of the first tube were included, the signal-to-noise ratio computed by this formula will always be better than can actually be obtained in practice and for this reason the relation has been written as an approximation rather than an equality. It is shown in this simple example that the input resistance of the tube is just as important as the equivalent noise resistance in determining signal-to-noise performance since it is only their ratio which matters.

Before leaving this simplified illustration, it should be noted that the antenna itself may have noise associated with its radiation resistance (see Part I of this series). If this may be considered at room temperature  $T_R$ , as with a dummy antenna, the limiting maximum signal-to-noise ratio will be that of the antenna itself, namely the ratio of its signal voltage to its thermal agitation noise voltage,

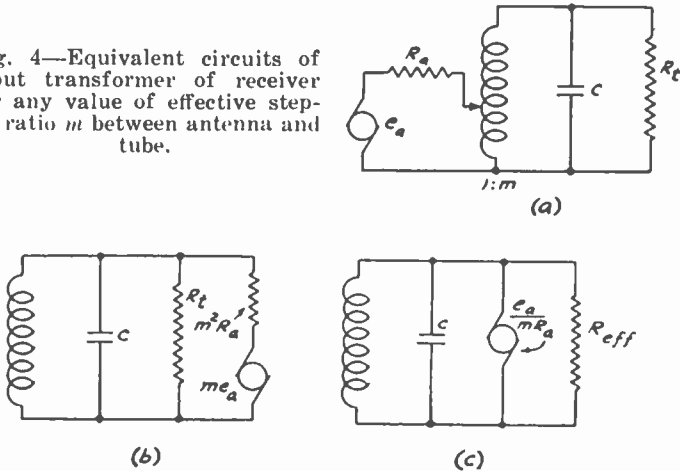
$$\text{antenna } (S/N)^2 = e_a^2 / 4kT_r R_a \Delta f.$$

The ratio of this antenna signal-to-noise ratio to the actual signal-to-noise ratio computed above is then

$$F = \frac{\text{antenna } (S/N)^2}{\text{over-all receiver } (S/N)^2} \approx 4 \frac{R_{eq}}{R_t} \text{ (when } R_{eq}/R_t \gg 1).$$

Actually, of course,  $F$  cannot be less than unity since this would imply that the over-all  $(S/N)^2$  was greater than that of the antenna itself. Hence, it is seen that the approximation which was implicit by neglecting input-circuit noise sources breaks down for values of  $R_{eq}/R_t$  which approach unity or less. The quantity  $F$  is the same as North's noise factor<sup>11</sup> and it will be discussed at greater length in a later part of this

Fig. 4—Equivalent circuits of input transformer of receiver for any value of effective step-up ratio  $m$  between antenna and tube.



paper. Suffice it to say at this point that the lower the quantity  $F$ , the more nearly noise-free is the receiver and the better the signal-to-noise ratio.

## 2. Effect of Transformer Step-up Adjustment

It has been seen how easily the signal-to-noise ratio is obtained from the matched-impedance condition. Let us next examine what happens when the antenna tap on the transformer is varied. The transformer, only, may be considered first. The effect of the primary may be determined by using its reflected value as seen in the secondary. Thus, approximately equivalent circuits, as shown in Figure 4(a), (b), and (c), may be derived, where in Figure 4(c) the signal is expressed as a constant-current generator and  $R_{eff} = 1 / (1/R_t + 1/m^2 R_a)$ . The signal

voltage  $e_g$  is then just the current  $e_a/mR_a$  multiplied by the total shunt resistance  $R_{eff}$ ,

$$e_g = e_a [m^{-1} + m(R_a/R_t)]^{-1}.$$

An expression of this kind is one which is frequently encountered in signal-to-noise computations; the denominator is of the form  $f(x) = (ax^{-1} + bx)$ . It has a minimum value which may be found to occur at  $x^2 = a/b$  and the minimum is

$$f(x) ]_{min} = f(\sqrt{a/b}) = 2\sqrt{ab}.$$

So that, in the above case where  $x$  corresponds to  $m$ ,

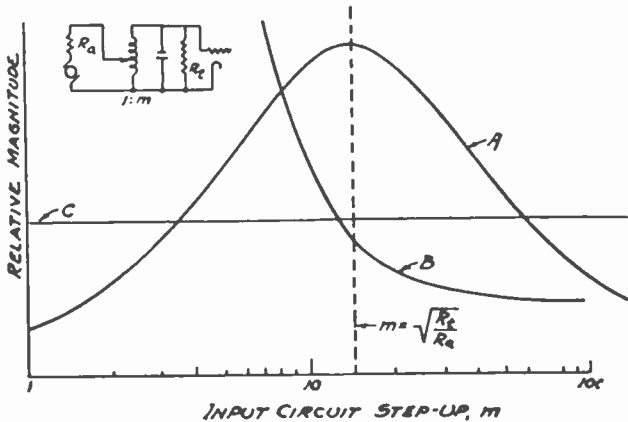


Fig. 5—Curves showing effect of variations of input circuit step-up ratio  $m$ . Curve A shows the signal voltage at the grid of the first tube. Curve B shows the bandwidth of the input circuit. Curve C shows the contribution of noise sources at or beyond the plate of the first tube.

$$e_g ]_{max} = e_a (1/2) \sqrt{R_t/R_a} \quad (\text{for } m^2 = R_t/R_a)$$

which, of course, is the matched-impedance condition which was already used in Section II, 1. If the signal voltage is plotted against  $m$  a curve is obtained similar to that shown in A of Figure 5.

Let us now find the bandwidth of the input circuit. Calling the equivalent-lumped-circuit capacitance  $C$  (see Appendix to Part I), the circuit bandwidth<sup>16</sup>  $\Delta f'$  between points 3 decibels down from resonance, is

$$\Delta f' = \frac{f}{Q} = \frac{f}{\omega CR_{eff}} = \frac{1}{2\pi C} \left( \frac{1}{R_t} + \frac{1}{m^2 R_a} \right).$$

<sup>16</sup> As distinguished from the noise bandwidth  $\Delta f$ .

The bandwidth varies with  $m$  because of the antenna loading, and a typical curve is shown in  $B$  of Figure 5; this curve can be understood physically. If  $m$  is very large the antenna is practically not coupled at all and the tap on the transformer of Figure 4(a) is near the bottom. The bandwidth is then the same as that of the circuit alone. As the tap is moved up on the transformer of Figure 4(a),  $m$  is decreased and the bandwidth gets wider. At  $m = \sqrt{R_t/R_a}$  the bandwidth is just double that of the circuit alone.

In Part I it was shown that the bandwidth can always be reduced by tapping the tube down on the circuit, which has the same effect as increasing the capacitance  $C$ . Furthermore, if circuit losses are negligible, this entails no loss in signal voltage. It is now seen that the bandwidth may be *increased* by overcoupling the antenna, but it is also seen from Figure 5 that some sacrifice in signal voltage will then result. However, this method of increasing bandwidth is less harmful in this respect than that of lowering  $R_t$ .

Finally, we may consider the noise. In this simple example, the only sources of noise were at or beyond the plate of the first tube. These noise sources, of course, do not vary with changes in  $m$ . The noise can, therefore, be drawn as a horizontal line  $C$  in Figure 5. Obviously, therefore, the signal-to-noise ratio is a maximum when the impedances are matched since this is when the signal is a maximum. As will be shown later, this is not usually the optimum condition when noise sources in the input are appreciable.

### 3. Wide-Band Adjustment

If the input-circuit bandwidth is too narrow for the receiver requirements, it can be seen from the curve  $B$  of Figure 5 that a lower value of  $m$  is then in order, although this means a reduction in signal-to-noise ratio. As a special case, let us consider what happens when  $R_t$  becomes very large. It might be expected that the signal-to-noise ratio would also rise to its maximum value. However, this is not the actual case because the design must always be based on some particular bandwidth. If  $R_t$  is very large, then the bandwidth equation of the preceding discussion may be solved to give

$$m^2 R_a \approx 1/2\pi\Delta f' C \approx 1/\Delta\omega C \quad (\text{assuming } \Delta\omega CR_t \gg 1)$$

where  $\Delta\omega$  is introduced for  $2\pi\Delta f'$ . The grid signal is then

$$e_g = \frac{e_a}{(1/m) + m(R_a/R_t)} \approx m e_a \approx \frac{e_a}{\sqrt{\Delta\omega CR_a}}$$

In this case, since the noise is again  $4kTR_{eq}\Delta f$ ,

$$\left(\frac{S}{N}\right)^2 \approx \frac{e_a^2}{4kT_R R_a \Delta f} \frac{1}{\Delta\omega CR_{eq}} \quad (\text{assuming } \Delta\omega CR_l \gg 1).$$

Far from having its maximum value, the  $S/N$  ratio is definitely limited by the product of  $CR_{eq}$ . The noise factor in this example is then  $F' \approx \Delta\omega CR_{eq}$ .

All that has been given so far is qualitatively applicable to every exact analysis which might be made and is very useful in understanding the behavior of the more complicated expressions which occur in exact analyses. It is now opportune to consider another interesting example in which an important additional and independent noise source is present in the input.

#### 4. *The Signal-to-Noise Ratio with Induced Input Electrode Noise*

In all tubes used for high frequencies, the input electrode also has noise current flowing in it<sup>6,7</sup> whereas, up to this point, only the plate noise of a tube has been considered. For example, in an ordinary grid-controlled tube, the electron current has fluctuations, and induces a fluctuating charge on the control grid. The rate of change of charge represents a grid current, which therefore fluctuates also. However, at low frequencies, the transit time is but a small fraction of the period and the charge induced as an electron approaches the grid is very nearly canceled by the reverse charge induced as the electron leaves so that the noise currents are small. The induced-noise current in grid-controlled tubes rises with the frequency and cannot be entirely neglected at high frequencies. However, when the control grid is adjacent to the cathode, the induced noise is subject to space-charge damping and does not play an important role, as has been seen.<sup>6,12</sup> With other control methods, the noise may be large at low frequencies as well.

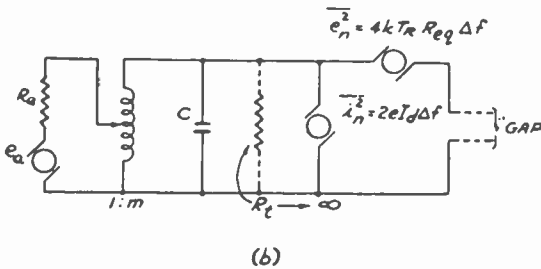
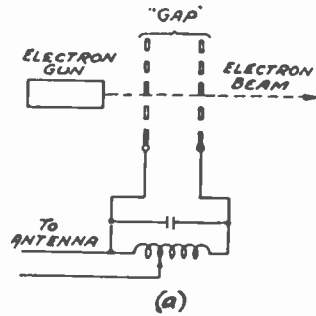
To illustrate the behavior of a tube when induced input noise is present, we shall use as an example a velocity-modulation mixer<sup>17</sup> because, as was shown in Part II of this series, this type of tube has a very large induced noise in the input which is roughly independent of frequency. The mixer, rather than the amplifier, is used because then the input noise and the output noise occupy different frequency bands and may be considered independently. The tube is indicated in Figure 6(a) and has an equivalent circuit as shown in Figure 6(b) where the voltage input to the tube corresponds to the "gap" voltage

<sup>17</sup> W. C. Hahn and G. F. Metcalf, "Velocity-modulated tubes," *Proc. I.R.E.*, vol. 27, pp. 106-116; February, 1939.



of the velocity-modulated control. Any of the described methods<sup>17</sup> of operating the tube as a mixer may be used and the one selected is immaterial to the discussion. For small transit angles, the full beam current through the "gap" of the tube induces noise in the input circuit, so that across the "gap" there exists a noise generator containing the full mean-squared noise current of the beam. If it be assumed that this is full shot noise it will be  $\overline{i_n^2} = 2eI_d\Delta f$  where  $I_d$  is the beam current. Such a tube will also have output noise and there may be subsequent noise sources as well but these may be referred back to the "gap" as an  $R_{eq}$  in the same way as before. Thus the equivalent circuit of Figure 6(b) is justified. The total impedance across the gap is usually

Fig. 6—A velocity-modulation type of mixer tube and its equivalent circuit. Two noise generators are shown, one as a voltage generator  $\overline{e_n^2}$  equivalent to noise at the anode and at points beyond, and the other as a current generator  $\overline{i_n^2}$  corresponding to induced noise across the input electrodes.



very high; in fact the electron loading may be made negligible if the transit time is made very small<sup>18</sup> and the circuit may be very low loss. So, for illustrative purposes, we may assume an infinite circuit impedance, i.e.,  $R_t \rightarrow \infty$ . Let us examine the signal-to-noise ratio as the antenna coupling  $m$  is varied. The signal voltage at the gap, assuming an infinite impedance, is  $e_v \approx me_a$ . The noise voltage is

$$\begin{aligned} \overline{e_n^2} &= 4kT_R R_{eq} \Delta f + 2eI_d \Delta f (m^2 R_a)^2 \\ &= 4kT_R \Delta f [R_{eq} + 20I_d (m^2 R_a)^2] \end{aligned}$$

(since  $2e/4kT_R = 20 \text{ volts}^{-1}$ ).

<sup>18</sup> See Part II of this series for transit-time loading in such a tube.

The signal-to-noise ratio is then

$$\begin{aligned} (S/N)^2 &\approx (e_a^2/4kT_R\Delta f)m^2[R_{eq} + 20I_d(m^2R_a)^2]^{-1} \\ &\approx (e_a^2/4kT_RR_a\Delta f)1/[R_{eq}/m^2R_a + 20I_dm^2R_a]^{-1} \end{aligned} \quad (\text{assuming } R_t \rightarrow \infty).$$

The denominator is again of the form  $(ax^{-1} + bx)$  which was studied in Section II, 2, above and has a maximum value at  $m^4R_a^2 = R_{eq}/20I_d$ . This gives

$$(S/N)^2]_{\max} \approx (e_a^2/4kT_RR_a\Delta f)1/(2\sqrt{20I_dR_{eq}}) \quad (\text{assuming } R_t \rightarrow \infty).$$

This may be understood better by a consideration of curves of the various factors plotted against the coupling  $m$ . Referring to Figure 7, the signal voltage at the gap increases directly with  $m$  and its square  $S^2$ , which is plotted, is therefore parabolic. The plate noise, as given by  $R_{eq}$ , is constant and does not vary with coupling. The input-circuit impedance varies as  $m^2$ , so that the mean square of the induced input noise varies as  $m^4$  and so rises more steeply than the signal. The total noise  $N^2$ , which in this example is the sum of the plate noise and the induced noise, is also plotted. Finally the squared signal-to-noise ratio,  $(S/N)^2$  is shown and has a definite optimum. This optimum is the result of the rapid increase in total noise when the input impedance (as seen by the tube) is increased by lowering the damping effect of the antenna (i.e., increasing the effective step-up  $m$ ).

As the analysis shows, it is desirable in such a tube to have the lowest possible product of  $R_{eq}$  and beam current. Once again, the results may be interpreted in terms of a noise factor  $F \approx 2\sqrt{20I_dR_{eq}}$ .

The bandwidth of the input circuit must sometimes be considered and is shown as a curve on Figure 17. If this is too narrow when the coupling is adjusted for best signal-to-noise ratio, it may be widened by decreasing  $m$ . In this event,  $m$  may be chosen from  $\Delta\omega$  (3 decibels down)  $\approx 1/m^2R_aC$  so that  $m^2R_a \approx 1/\Delta\omega C$  and

$$(S/N)^2 \approx (e_a^2/4kT_RR_a\Delta f)1/[\Delta\omega CR_{eq} + 20I_d/\Delta\omega C].$$

The signal-to-noise ratio of this type of tube is handicapped by the high noise in the input. If such a tube is used, it is clear that the antenna coupling should not be adjusted for maximum gain if it is desired to obtain best signal-to-noise ratio.

### 5. The Exact Signal-to-Noise Ratio

Up to this point the noise of the antenna has been neglected and

also the thermal agitation noise of the part of the input resistance which is due to ohmic losses. Even in the treatment just preceding, the induced input noise was treated only for the simplified case wherein the input resistance  $R_i$  was very high, approaching infinity. If the exact case is to be treated, it is necessary to split  $R_i$  into its two pos-

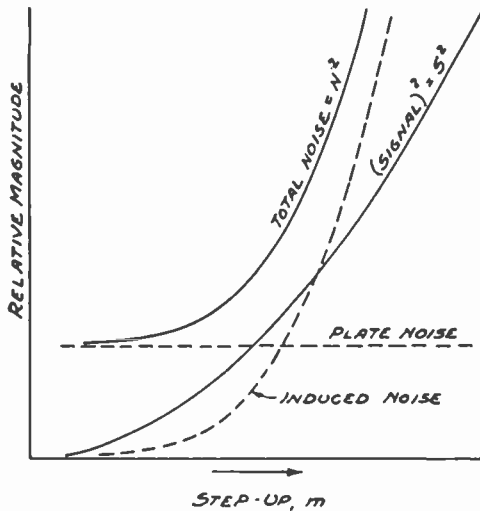
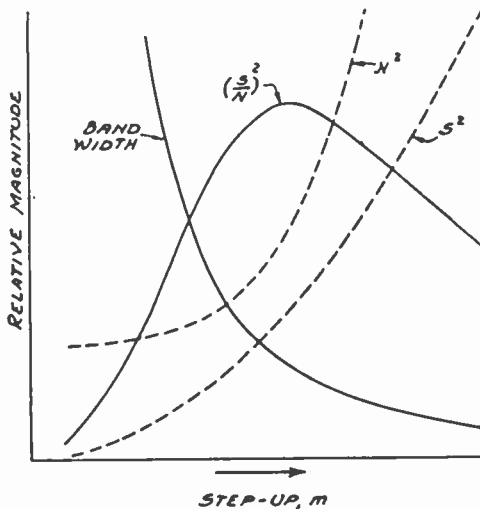


Fig. 7 — Relative magnitudes of signal, noise, bandwidth, and signal-to-noise ratio for a case where input resistance is infinite. The curves are divided into two groups only to void confusion; the  $S^2$  and  $N^2$  curves are common to both groups.



sible components, the ohmic and the electronic. The former is accompanied by thermal agitation noise, whereas the latter component may be said to be noise-free, since its noise is already included in what has been called induced input noise. With grid-controlled tubes,

whose control grid is adjacent to the cathode, the induced noise bears a direct relationship to the electronic loading.<sup>6</sup> In other types of tubes there may be no simple relationship at all. In the following, the induced noise will be considered in terms of an equivalent saturated-diode noise  $2eI_d\Delta f$ . For the control-grid-adjacent-to-cathode tubes with oxide-coated cathodes it was found<sup>6</sup> that  $I_d \sim (1/4)g_e$ , where  $g_e$  is the electronic input conductance of the tube in mhos and  $I_d$  is in amperes. In the treatment, induced input noise will be regarded as a noise source independent of (i.e., not coherent with) the anode noise, since this is approximately correct in most ordinary tubes at small transit angles or under mixer conditions.

The equivalent circuit for a transformer with effective step-up  $m$  is shown in Figure 8 where the noise generators have been omitted. In the figure, the reflected antenna conductance is shown as  $g_a$ , and the resistance  $R_t$  is considered as composed of the electronic conductance  $g_e$  and the ohmic conductance  $g_\Omega$ . In terms of current generators, the mean-squared noise currents are: antenna noise =  $4kT_{eff}g_a\Delta f$ ; thermal noise =  $4kT_Rg_\Omega\Delta f$ ; induced noise =  $2eI_d\Delta f$ ; and plate noise and be-

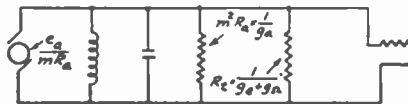


Fig. 8—Equivalent circuit of receiver input with the antenna signal  $e_a$  and antenna resistance  $R_a$  introduced in terms of their reflected value in the secondary. The effective step-up of the transformer is  $m$ . The tube input resistance  $R_t$  is split into electronic and ohmic components whose conductances are  $g_e$  and  $g_\Omega$ , respectively.

yond =  $4kT_R R_{vq} \Delta f (g_a + g_\Omega + g_e)^2$  where  $T_{eff}$  is the effective noise temperature of the antenna and its associated transmission line which will be discussed in a later section. The signal in Figure 8 is also shown as a current generator  $e_a/mR_a$  so that the signal-to-noise ratio may be written directly

$$\left(\frac{S}{N}\right)^2 = \frac{e_a^2}{4kT_R R_a \Delta f} \frac{1}{\frac{T_{eff}/T_R + g_\Omega/g_a + (2e/4kT_R)(I_d/g_a) + R_{vq}(g_a + g_\Omega + g_e)^2/g_a}{e_a^2}} = \frac{e_a^2}{4kT_R R_a \Delta f} \frac{1}{\frac{T_{eff}/T_R + 2(R_{vq}/R_t) + (g_\Omega + 20I_d + R_{vq}/R^2t)/g_a + g_a R_{vq}}{(e_a^2/4kT_R R_a \Delta f)(1/F)}}$$

As in the previous cases, this general result is best interpreted in terms of the noise factor  $F$ . The one variable in  $F$  is the quantity  $g_a$  which depends on the antenna coupling  $m$ . We may see immediately that  $F$  has a minimum since the denominator again contains a function of the type  $ax^{-1} + bx$  which was analyzed in Section II, 2. Using the relation for the minimum therein found

$$\begin{aligned} F_{\text{minimum}} &= T_{\text{eff}}/T_R + 2(R_{\text{eq}}/R_t) \\ &\quad + 2\sqrt{(R_{\text{eq}}/R_t)^2 + g_\Omega R_{\text{eq}} + 20I_d R_{\text{eq}}} \\ &= T_{\text{eff}}/T_R + 2(R_{\text{eq}}/R_t) \\ &\quad + 2\sqrt{(R_{\text{eq}}/R_t)^2 + R_{\text{eq}}/R_t + (20I_d - g_c) R_{\text{eq}}}. \end{aligned}$$

The matched-impedance noise factor is obtained by letting  $g_a = 1/R_t$  in the original expression, since this equates the antenna reflected resistance to the input resistance. This is

$$F_{\text{matched}} = 1 + T_{\text{eff}}/T_R + 4(R_{\text{eq}}/R_t) + (20I_d - g_c)R_t.$$

The bandwidth of the input circuit is given by the expression

$$\begin{aligned} \Delta f' \text{ (3 decibels down)} &= \Delta\omega/2\pi = (1/2\pi)(g_a + g_\Omega + g_c)/C \\ &= (1/2\pi)(g_a + 1/R_t)/C. \end{aligned}$$

When  $R_t$  is high, or negative, the bandwidth may be too narrow and it will be necessary to increase  $g_a$  so as to realize the required bandwidth. We may solve for the necessary value, which is  $g_a = \Delta\omega C - 1/R_t$ . This value may be substituted in the basic  $(S/N)^2$  expression to find the noise factor

$$F_{\text{wide band}} = \frac{T_{\text{eff}}}{T_R} + \frac{1/R_t + (20I_d - g_c) + (\Delta\omega C)^2 R_{\text{eq}}}{\Delta\omega C - 1/R_t}.$$

These exact expressions all show the same basic phenomena that we observed in the approximate relations previously derived, namely that the lowest possible value of  $R_{\text{eq}}/R_t$  is desired for best signal-to-noise ratio and, in the wide-band case, that  $R_t$  should be high while  $\Delta\omega C R_{\text{eq}}$  should be small. Furthermore, it may be seen that induced noise can seriously affect the noise factor, especially when  $R_{\text{eq}}/R_t$  is high. In each of the above cases, the substitution  $I_d \approx (1/4)g_c$  makes the results applicable to oxide-coated-cathode tubes whose control grid

is adjacent to the cathode provided the transit angles are not too great.<sup>6</sup> It should be noted that, for laboratory measurements with a dummy antenna,  $T_{eff} = T_R$ . Further discussion of the magnitude of  $T_{eff}$  will be found below in Section II, 7. More details of the exact signal-to-noise ratio analyses are to be found in footnote reference 12.

#### 6. Effect of Feedback on Signal-to-Noise Ratio

The analyses made thus far have neglected feedback. If the first tube or tubes of a receiver are radio-frequency amplifiers, however, feedback in one form or another (i.e., degenerative, regenerative, or both) must often be considered in the operation of the amplifier. However, the effect of feedback on signal-to-noise ratio is often relatively minor.<sup>19</sup> We may see this by thinking of a vacuum tube in the terms of an equivalent circuit containing a noise generator of mean-squared value  $\overline{i_{pn}^2}$  and a signal-current generator  $g_m e_g$  in the plate circuit. If any of the plate output is fed back to the input, the apparent input impedance and gain of the tube may be radically raised or lowered but the ratio of the noise generated to the signal generated as given by  $\overline{i_{pn}^2}/g_m^2 e_g^2$  remains approximately unchanged. Thus, noise will always be fed back along with the signal and in about the same ratio. If the feedback is regenerative, the input impedance is raised, the gain is increased, the grid signal is augmented by the energy fed back, but the noise is also increased and in approximately the same proportion as the increase in signal. For the degenerative case, the signal and noise are *decreased* by just about the same ratio. Thus, the effect of feedback on signal-to-noise ratio is chiefly due to the noise sources which are not fed back, and these are, in some instances, of minor importance.

To obtain a rough estimate of the signal-to-noise ratio of an amplifier in which a known and definite feedback exists, one may, therefore, make the computation as in the previous cases, making sure that the feedback effects are not included in the values of equivalent-noise resistance and tube-input resistance which are used in the formulas.

There is one common form of feedback which is worth a little more discussion, namely, that due to cathode-lead inductance. It was shown in Part II of this series that this is a degenerative form of feedback which leads to a lowering of the input resistance. In the case of a triode, we should follow the above rule: neglect the lowered resistance due to lead effects and compute the signal-to-noise ratio as if the tube had the higher input impedance of one with an ideal cathode connection. In the case of a pentode, the noise current flowing in the cathode

<sup>19</sup> W. A. Harris, "Fluctuations in space-charge-limited currents at moderately high frequencies—Part V," *RCA REVIEW*, vol. 6, pp. 122-124; July, 1941.

lead is only a fraction of the noise in the plate lead. The screen-grid-distribution-noise current<sup>20</sup> flows between screen and plate and is not in the cathode lead; it is not fed back through the cathode-lead inductance at all. Thus the noise is not reduced by the feedback as much as the signal, and the signal-to-noise ratio is worse than the one computed by neglecting the cathode-lead feedback. However, it is possible to feed back some of the screen-lead noise (e.g., through an impedance in the lead and capacitance to the control grid) so as to obtain an improved signal-to-noise ratio, even approaching that of the triode.<sup>21</sup>

A practical effect of the feedback which exists in most ultra-high-frequency receivers is to invalidate some of the cruder methods of checking the signal-to-noise ratio which are based on detuning the input.<sup>8,9</sup> For example, it has been proposed that if the noise output is observed both with the input circuit normally connected and with it short-circuited, the relative contributions of tube and thermal input noise can be found. This is only true if there is no induced-input noise and if the feedback remains constant; neither condition is generally so at ultra-high frequencies.

#### 7. Attenuation and Thermal Noise of Transmission Line

A transmission line which connects the antenna to the receiver will obviously decrease the possible signal-to-noise ratio if it attenuates the received signal. At the same time, its losses may contribute to thermal noise in the input. In the exact analysis that was discussed above, the antenna and its associated transmission line (if any) were considered as having a signal voltage  $e_a$  and a noise voltage whose mean-squared value was  $4kT_{eff}R_a\Delta f$ . It is a simple matter to determine how these two quantities depend on an associated transmission line or other passive network between the actual antenna and the connection to the receiver.

Let the actual antenna have an open-circuit signal voltage  $e_a'$ , and a radiation resistance  $R_a'$ . The available signal power is then  $(e_a')^2/R_a'$  of which one quarter can be delivered to a matched transmission line or other transducer. At the other end of the line or transducer, there will be an open-circuit voltage  $e_a$  and a resistance  $R_a$  (which may or may not equal  $R_a'$ ). Thus the ratio of output power available to available input power is

<sup>20</sup> D. O. North, "Fluctuations in space-charge-limited currents at moderately high frequencies—Part III," *RCA REVIEW*, vol. 5, pp. 244-260; October, 1940.

<sup>21</sup> M. J. O. Strutt and A. van der Ziel, "Methods for the compensation of the effects of shot noise in tubes and associated circuits," *Physica*, vol. 8, pp. 1-22; January, 1941.

$$M = \text{output power/input power} \\ = (e_a^2/R_a) / [(e_a')^2/R_a']$$

which, of course, is a maximum when the antenna is matched to the line or transducer. This power ratio is often expressed in decibels, and is called the attenuation.

If the antenna is at an effective noise temperature of  $T_a$  it will have a noise voltage  $\bar{e}^2 = 4kT_a R_a' \Delta f$ . The available noise power at the antenna is then

$$\text{noise power at antenna} = \bar{e}^2/R_a' = 4kT_a \Delta f.$$

At the other end of the line or transducer, i.e., at the receiver, this is  $M$  times as great,

$$\text{noise power from antenna getting to receiver} = M4kT_a \Delta f.$$

The transducer or transmission line will have thermal agitation associated with its losses at a temperature which we shall call  $T_L$ . Thus, if in a hypothetical case, the antenna and transducer were both at this temperature  $T_L$ , the available noise power at the receiver would be  $4kT_L \Delta f$ . This is too high by the quantity  $M4kT_L \Delta f$  which would be the antenna contribution in this hypothetical case. Thus, in the actual case,

$$\text{noise power from transducer getting to receiver} = (1 - M)4kT_L \Delta f.$$

The total available noise power at the receiver is, therefore,

$$\text{total noise power at receiver} = 4k \Delta f [T_L(1 - M) + MT_a]$$

and the effective noise temperature of the antenna and associated transducer is  $T_{\text{eff}} = T_L(1 - M) + MT_a$ . Ordinarily, the transmission line or transducer is at room temperature so that  $T_L = T_R$ .

It is seen by reference to the expression in Section II, §5, above, that the signal-to-noise ratio of an over-all system containing a transmission line whose power-loss ratio is  $M$  is reduced from that of one with a loss-free line, first by the factor  $M$  (which is the loss in  $e_a^2/R_a$ ), and second by the change of apparent antenna noise temperature from  $T_a$  to  $T_{\text{eff}}$ . This may be written

$$\left( \frac{S}{N} \right)^2 \Bigg]_{\text{with line}} = \left( \frac{S}{N} \right)^2 \Bigg]_{\text{with no line loss}} M \frac{T_a/T_R + F - 1}{T_{\text{eff}}/T_R + F - 1}$$



where  $F$  is the noise factor of the receiver alone as it would be with a dummy antenna (whose temperature is  $T_R$ ).

### III. THE RATING OF RECEIVERS

#### 1. The Noise Factor

It was found by the analyses above that all the signal-to-noise ratios could be written in the form

$$(S/N)^2 = (e_a^2/4kT_R R_a \Delta f) (1/F)$$

and the quantity  $F$  was identified with what North has called the noise factor.<sup>11</sup> In the laboratory, with a dummy antenna at room temperature it can be seen that  $F$  represents simply the number of times that the total receiver noise exceeds that of the dummy antenna and, as North showed, this may be made a general concept for any receiver whatever. The concept implies that, in a completely noise-free receiver, the total noise will be dummy antenna noise only and  $F_{\min} = 1$ . Thus the higher the number  $F$  which is measured in the laboratory, the poorer is the receiver compared with the ideal. It may be noted that it is not usually possible to obtain a noise factor approaching unity with a matched-impedance input connection except when the input impedance is a result of feedback. In other cases, the thermal noise of the receiver input impedance (or the matching impedance which may have been added), leads to a value of 2 for  $F$  even though no other noise sources are present.

In the field, with an actual antenna, we have seen that  $F$  contains a term which depends on the effective noise temperature of the antenna and its transmission line  $T_{\text{eff}}$ . Thus, with an antenna whose noise temperature is less than room temperature, and a low-loss line, an operating noise factor is obtained which is less than that measured in the laboratory and, with an ideal noise-free receiver, is less than unity. On the other hand, a noisy actual antenna and transmission-line system results in an increase in the operating noise factor over that measured in the laboratory. When the receiver noise greatly exceeds that of the antenna it becomes difficult to measure the actual operating noise factor directly so that this quantity is often not known at ultra-high frequencies.

Ordinarily, receivers are most easily compared in the laboratory and, as we shall see, a noise-factor measurement is a simple and straight-forward process. Thus the laboratory noise factor<sup>22</sup> was originally proposed<sup>11</sup> to define a method of rating receivers for signal-

<sup>22</sup> I.e., the noise factor when  $T_{\text{eff}} = T_R$ .

to-noise ratio, since noise factor is often independent of bandwidth and of the magnitude of the antenna radiation resistance from which the receiver was intended to operate. An important accompaniment of North's proposal was the analysis of the receiving antenna (also discussed in Part I of this series) which showed that the available received power from a given transmitter and at a given wavelength depends only on the receiving antenna directivity, and is independent of the radiation resistance.

Since the noise factor is a power ratio, it is conveniently expressed in decibels, so that an ideal, noise-free receiver, with  $F = 1$ , may also be said to have a noise factor of zero decibels. Similarly, a matched-impedance receiver which has a resistive input impedance which is at room temperature for noise purposes but wherein the receiver is otherwise noise-free, has a noise factor  $F = 2$  which corresponds to three decibels.

## 2. The Measurement of Receiver Noise Factor

In order to measure the receiver noise factor  $F$  we must measure the actual signal-to-noise ratio of a receiver and compare it with that of the dummy antenna  $e_a^2/4kT_R R_a \Delta f$ . To do this in the laboratory, a known voltage source  $e_a$  (e.g., a signal generator), and a dummy antenna of value  $R_a$  may be used. One possible procedure may be outlined.

We first apply a small signal of frequency  $f_0$  anywhere in the band to which the receiver is responsive and of a magnitude  $e_a$  somewhat in excess of the noise. In the output of the receiver, prior to any audio or video amplification, we connect a power-measuring device<sup>23</sup> (such as a thermocouple meter) suitable for reading the total output power over the entire frequency spectrum to be utilized. With the signal turned on, the output power will then be the sum of signal and noise powers. Let us call its value  $P_1$ . If the signal is now turned off, the output power will be that due to noise only, which may be called  $P_2$ . Then the signal-to-noise ratio is

$$(S/N)^2 = (P_1 - P_2)/P_2.$$

By the definition of noise factor  $F$ , however,

$$(S/N)^2 = (e_a^2/4kT_R R_a \Delta f) (1/F)$$

so that  $F = (e_a^2/4kT_R R_a \Delta f) P_2 / (P_1 - P_2)$

$$= 0.62 \times 10^{20} (e_a^2/R_a) (1/\Delta f) P_2 / (P_1 - P_2).$$

<sup>23</sup> Any other device responsive to signal and noise, such as a linear detector, may be used if a power calibration for the combination of signal and noise has been calculated or has been experimentally determined.

To compute  $F$  we need, in addition to the power measurement, therefore, only the quantity  $e_a^2/R_a$  and the noise bandwidth  $\Delta f$ . The former may be obtained if  $e_a$  and  $R_a$  are known and the latter (see Part I of this series) is defined as the ratio of the area under the power-selectivity curve to the height of this curve at the signal frequency  $f_0$ . Mathematically

$$\Delta f = \frac{1}{P(f_0)} \int_0^{\infty} P(f) df$$

where  $P(f)$  is the output power as a function of receiver signal input frequency,  $f$ .

Since the calculation of noise factor requires a knowledge of  $e_a^2/R_a$ , it is clear that  $F$  may be found without knowing  $e_a$  and  $R_a$  separately. In fact, all that is required is a shielded oscillator and attenuator with an ultra-high-frequency power-measuring device. If the oscillator is matched to the power-measuring device, it will measure the quantity  $e_a^2/4R_a$  and this will enable  $F$  to be computed. In practice, one usually must design the equipment for a specified value of  $R_a$  so that actually  $e_a$  and  $R_a$  will both be known.

---

#### Part IV. General Superheterodyne Considerations at Ultra-High Frequencies†

BY

L. MALTER

*Summary*—This paper presents a general survey of the problems encountered in the mixer or converter stage of superheterodyne receivers, particularly at ultra-high frequencies. The application of a strong local-oscillator voltage causes a periodic variation of the signal-electrode transconductance as a consequence of which intermediate-frequency-current components appear in the output circuit when a signal is also impressed upon the signal electrode. It is demonstrated that intermediate-frequency-current components are present in the output, which differ from the signal frequency by integral multiples of the local-oscillator frequency, if the Fourier analysis of the signal-electrode transconductance contains components which are integral multiples of the local-oscillator frequency. Methods of determining the conversion transconductance for so-called fundamental and harmonic conversion are given.

It is shown that the noise output and input loading of a mixer stage are given by averaging these quantities over a local-oscillator cycle. A discussion of mixer gain is included, with a demonstration that the gain

† Reprinted from *Proc. I.R.E.*, October, 1943.

of a mixer stage is given approximately by the product of the conversion transconductance and the impedance of the output circuit (for high-output-impedance tubes).

Considerations regarding image rejection and the undesirability of radiation of oscillator power lead to the conclusion that high intermediate frequencies are desirable.

An extended discussion of whether to use an amplifier or mixer stage in the first stage of a superheterodyne receiver is included. If the received signal is strong, one should convert immediately, unless image rejection or the prevention of oscillator radiation necessitate the use of radio-frequency stages. If the received signal is weak, an amplifier stage should be used below a certain frequency and a mixer above, the transition frequency depending upon the characteristics of the tubes available and the bandwidth required. In general the transition frequency occurs at the point where available tubes will no longer give appreciable radio-frequency gain for the bandwidth required.

## I. INTRODUCTION

IN PART II of this series we concerned ourselves primarily with the case wherein the signal voltages applied to the circuits and tubes of a receiver are so low in amplitude that the tubes can be considered as linear devices, wherein the output voltage or current is proportional to the signal-electrode voltage. This case will be recognized as being precisely that of the linear amplifier.

It is frequently convenient, however, to make use of the superheterodyne principle in receivers. In receivers of this type, the incoming signal is combined with a locally produced oscillation of different frequency to produce a third signal at a frequency referred to as the intermediate frequency, which is related to both the frequencies of the incoming signal and the locally produced oscillation. It is an essential characteristic of any electrical device, wherein the simultaneous application of oscillating voltages results in the production of one or more oscillating quantities whose frequencies differ from those of any of the impressed quantities, either that the device be *nonlinear*, i.e., that the relation between the output and input (i.e., impressed) variables be of such a nature that it cannot be reduced to a form wherein the variables appear as first-power terms, or that the nature of the device be such that, even though it be linear as regards the application of a single voltage, the simultaneous application of two voltages results in the appearance in the output of a quantity (e.g., a current change) which is dependent upon the product of the two impressed voltages. An example of such a device is a multigrid tube wherein two voltages may be impressed simultaneously on different grids. In this case the change in output current will be related to the changes in the two grid voltages by means of a relation of the form

$$i_p = b_0 + b_1e_1 + b_2e_2 + b_{12}e_1e_2 \quad (1)$$

where the  $b$ 's are constants,  $i_p$  is the change in plate current, and  $e_1$  and  $e_2$  are the changes in potential of the two grids. Since, in a superheterodyne receiver, the simultaneous application of two voltages of different frequencies results in the production of the intermediate-frequency signal whose frequency differs from those of the two original signals, the superheterodyne receiver must contain a device which has one of the two types of characteristics described above. This device is often a tube which may (among others) be a diode, triode, or multigrid tube. In some cases crystal diodes are employed.

In Figure 1 of Part V (which follows Part IV in this issue) there is shown an incoming signal and locally produced oscillation fed into a diode (tube or crystal) with the resultant production of intermediate-frequency output. The diode as a device for producing intermediate frequencies is sufficiently important and different from other tubes designed for the same purpose, so as to merit special treatment. It will form the subject matter of Part V of this series.

In the case of triodes or pentodes various modes of introducing the incoming signal and locally produced oscillation are possible. Thus, they may both be impressed between control-grid and cathode, as is illustrated in Figure 1, or the incoming signal may be impressed between the control grid and ground, while the locally produced oscillation is impressed between cathode and ground. In general the incoming signal and the locally produced oscillations need not be impressed upon the same electrodes. Throughout the remainder of this paper the term signal electrode will refer to the control electrode upon which the incoming signal is impressed.

For many superheterodyne applications at frequencies below 30 megacycles or so, it has been found convenient to make use of multigrid tubes. In this case, in addition to the possibility of impressing both voltages on the same electrode, one can also have the local-oscillator voltage applied to an electrode which precedes the signal electrode (inner-grid injection) or the converse (outer-grid injection). Since tubes of this type do not find much application at ultra-high frequencies, their consideration is here terminated, except to indicate that the interested reader may find a more extended treatment in the literature.<sup>1</sup>

Before launching into a discussion of the mechanism of mixer action, it may be to the point to outline briefly the outstanding reasons for the use of superheterodyne receivers at ultra-high frequencies:

<sup>1</sup> E. W. Herold, "The operation of frequency converters and mixers for superheterodyne reception," *Proc. I.R.E.*, vol. 30, pp. 84-103; February, 1942.

1. The tuned circuits in intermediate-frequency amplifiers are fixed in frequency, whereas in radio-frequency amplifiers they require tuning to the individual signal. If the receiver is to cover an extended frequency range, the tuning problem for the radio-frequency amplifier may be a serious one.

2. It is often possible to secure a higher gain per stage at intermediate frequencies than at radio frequencies.

3. Better control of frequency response can generally be achieved at intermediate frequencies, particularly if the receiver is to operate over an extended frequency range.

4. It may be possible to achieve a higher signal-to-noise ratio with a superheterodyne type receiver than with a radio-frequency amplifier type.

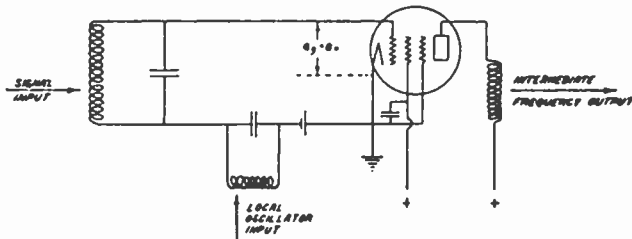


Fig. 1—Circuit of pentode mixer stage wherein incoming signal and local-oscillator voltage are both applied between control grid and cathode.

## II. THE MECHANISM OF MIXER ACTION

The mechanism whereby the combination of the incoming signal and the locally produced oscillation serves to produce an intermediate frequency is referred to as "mixing action." The locally produced oscillation may either be generated in the same tube as that in which the mixing action occurs in which case this tube that serves a double function, is referred to as a converter, or the locally produced oscillation may be produced in a separate tube in which case the tube in which the mixing action occurs is referred to as a mixer.

The fact that a nonlinear device can be used for the production of an intermediate-frequency signal, is readily demonstrated by means of a simple illustration. In Figure 1 there is shown a triode with input circuits upon which are impressed an incoming signal and a locally produced oscillation. These will result respectively in the impression upon the grid of the triode of two oscillating voltages  $e_s$  and  $e_0$ . The presence of these voltages will cause a change in plate current of an amount  $i_p$ . Since  $e_s$ ,  $e_0$ , and  $i_p$  are variations away from quiescent values, we can set (by the application of Taylor's theorem)

$$i_p = c_0 + c_1e + c_2e^2 + c_3e^3 + \dots \quad (2)$$

where  $e = e_s + e_0$  and the  $c$ 's are constants which depend upon the tube and circuit characteristics. For the amplifier case,  $e$  is so small that the terms of higher power than the first may be neglected. Equation (2) then becomes

$$i_p = c_0 + c_1e. \quad (2a)$$

From (2a) it may be seen that  $i_p$  will contain as components, terms whose frequency is the same as those present in  $e$ . For the generation of current components of frequencies different from those of  $e_s$  and  $e_0$  it is essential that  $e$  be sufficiently great so that some of the terms in (2) of the second or higher degree become of importance. Since  $e_s$  is, in general, comparatively small,  $e_0$  must be comparatively large in order that the relation between  $i_p$  and  $e$  be nonlinear. Actually, while  $e_s$  is generally of the order of microvolts or millivolts,  $e_0$  is usually measured in volts.

To see that a nonlinear relationship of the form of (1) results in the production of terms of frequencies different from those of  $e_s$  and  $e_0$ , let us consider the simple case wherein the terms of powers higher than the second may be neglected. Then

$$i_p = c_0 + c_1(e_s + e_0) + c_2(e_s + e_0)^2. \quad (3)$$

$$\text{Let } e_s = E_s \sin \omega_s t \quad (4)$$

$$e_0 = E_0 \sin \omega_0 t. \quad (5)$$

$$\begin{aligned} \text{Then } i_p &= c_0 + c_1 E_s \sin \omega_s t + c_1 E_0 \sin \omega_0 t \\ &\quad + c_2 E_s^2 \sin^2 \omega_s t + 2c_2 E_s E_0 \sin \omega_s t \sin \omega_0 t \\ &\quad + c_2 E_0^2 \sin^2 \omega_0 t \end{aligned} \quad (6)$$

$$\begin{aligned} &= c_0 + c_1 E_s \sin \omega_s t + c_1 E_0 \sin \omega_0 t + (c_2 E_s^2)/2 \\ &\quad + (c_2/2) E_s^2 \sin 2\omega_s t + c_2 E_s E_0 \cos (\omega_s - \omega_0) t \\ &\quad - c_2 E_s E_0 \cos (\omega_s + \omega_0) t + (c_2 E_0^2)/2 \\ &\quad + [(c_2 E_0^2)/2] \sin 2\omega_0 t. \end{aligned} \quad (7)$$

Thus, in addition to terms of angular frequency  $\omega_s$  and  $\omega_0$ , there appear in the plate current terms of angular frequency  $2\omega_0$ ,  $2\omega_s$ ,  $|\omega_s - \omega_0|$ , and  $|\omega_s + \omega_0|$ . If the output circuit in Figure 1 is resonant to angular

frequency  $|\omega_s - \omega_0|$ , voltage at this angular frequency will be developed across the circuit. This may then be applied to later intermediate-frequency amplifier stages. For the case just treated the intermediate frequency may be of angular frequency  $|\omega_s - \omega_0|$  or  $|\omega_s + \omega_0|$ . For the general case as represented by (2), the intermediate-frequency term will be of the form  $|n_1\omega_s \pm n_2\omega_0|$  where  $n_1$  and  $n_2$  are integers. The output circuit is made to resonate at the particular angular frequency which is chosen for intermediate-frequency amplification. The most common choice is the one wherein  $n_1 = n_2 = 1$  and  $\omega_i = |\omega_s - \omega_0|$ , where  $\omega_i$  is the angular frequency of the intermediate-frequency signal.

The preceding treatment, while of value in portraying the mechanism whereby the mixing action is brought about, is unsatisfactory for numerical computations, since, for normal tube characteristics, and for large oscillator voltages, it leads to exceedingly complex expressions and very laborious computations. A more elegant mode of attack upon the problem of computing mixer action has been described by Herold.<sup>1</sup> Before entering into this it is necessary to introduce the quantity known as conversion transconductance which is defined as the ratio of the intermediate-frequency output current to the signal-electrode input voltage.

As was pointed out above, one mode of operation is that in which the local-oscillator signal should be sufficiently large so as to result in nonlinear operation of the mixer or converter. While the nonlinearity was defined in terms of the relation of output-current-to-signal-electrode voltage, it is obvious that the nonlinearity must at the same time extend to the signal-electrode-to-plate transconductance. As a consequence, due to the presence of the "large" local-oscillator voltage, the instantaneous signal-electrode transconductance may be considered as varying periodically at local-oscillator frequency, and may thus be expressed in the form of a Fourier series

$$g_m = a_0 + a_1 \cos \omega_0 t + a_2 \cos 2\omega_0 t + \dots \quad (8)$$

where the  $a$ 's are constants which depend upon the tube characteristic, the quiescent or operating point, and upon the magnitude of the local-oscillator voltage. Since  $\omega_0 = 2\pi f_0$ , where  $f_0$  is the local-oscillator frequency, the signal-electrode transconductance may be considered as being made up of an infinite number of components, the first being an average value  $a_0$ , the second a term of oscillator frequency, the third a term of twice oscillator frequency, etc. Now, simultaneous with the application of the local-oscillator voltage, let a signal voltage  $E_s \sin \omega_s t$  be applied to the signal electrode. Then the plate current will be given by



$$i_p = g_m E_s \sin \omega_s t. \quad (9)$$

For  $g_m$  in (9) we substitute its value from (8) and obtain

$$i_p = a_0 E_s \sin \omega_s t + E_s \sum_{n=1}^{\infty} a_n \sin \omega_s t \cos n \omega_0 t \quad (10)$$

$$\begin{aligned} &= a_0 E_s \sin \omega_s t + E_s/2 \sum_{n=1}^{\infty} a_n \sin (\omega_s + n\omega_0) t \\ &\quad + E_s/2 \sum_{n=1}^{\infty} a_n \sin (\omega_s - n\omega_0) t. \end{aligned} \quad (11)$$

The plate current thus contains components of angular frequency  $\omega_s$ ,  $|\omega_s + n\omega_0|$ , and  $|\omega_s - n\omega_0|$ . The first of these is one at signal frequency and does not concern us. The other terms are those which characterize the device as a mixer since they represent new frequency terms related to the signal and local-oscillator frequencies. It is customary to insert a tuned circuit in the output lead of the converter or mixer which is tuned to angular frequency  $|\omega_s - \omega_0|$ . The voltage developed across this circuit is then fed into the intermediate-frequency amplifier. While this mode of operation (referred to as fundamental operation, since the intermediate frequency is equal in absolute value to the difference between the signal frequency and the fundamental local-oscillator frequency) is generally the preferred one, in certain cases it is convenient to operate at one of the other possible intermediate frequencies for which  $n \neq 1$ ; (referred to as harmonic operation). In these cases, the tuned output circuit is tuned to angular frequency  $|\omega_s - n\omega_0|$ . It should be noted that for harmonic operation it is not the oscillator voltage or tube current which must contain harmonic components, but the Fourier analysis of the signal-electrode transconductance, when the tube is operated as a mixer. Harmonic operation may be used when generation of a local-oscillator signal of sufficient power at fundamental frequency is difficult. However, in general, harmonic operation yields a lower signal-to-noise ratio than fundamental operation, and is thus avoided, if possible, where signal-to-noise ratio is of fundamental importance (as is the case in many ultra-high-frequency applications).

The conversion transconductance at the  $n$ th harmonic is given by

$$g_{c_n} = I_{i,f}/E_s = a_n/2. \quad (12)$$

If one substitutes the value of the Fourier coefficient, there results

$$g_{c_n} = \frac{1}{2\pi} \int_0^{2\pi} g_m \cos n\omega_0 t d\omega_0 t. \quad (13)$$

When  $n = 1$ , the fundamental conversion transconductance is obtained.

The method of determining conversion transconductance can be made clear by means of an illustrative example. Let Figure 2 represent the signal-electrode transconductance of a receiving tube as a function of oscillator-electrode voltage (it is assumed, as may be the case, that the oscillator voltage and signal voltage are not necessarily applied to the same electrode), and let  $A$  in the figure be the applied oscillator voltage (assumed to be sinusoidal). Then  $B$  is the resultant time variation of transconductance.

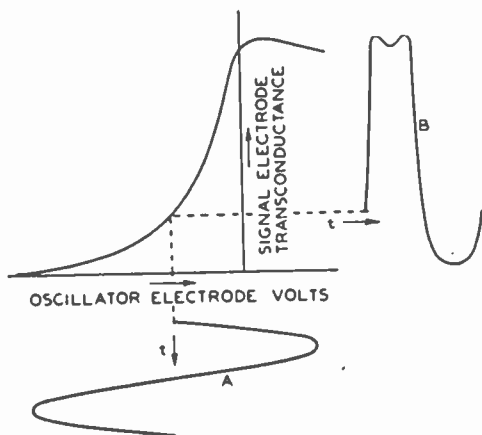


Fig. 2—Signal-electrode transconductance versus oscillator-electrode voltage for a typical mixer tube. The applied oscillator voltage is shown at  $A$  and the resultant time variation of the transconductance at  $B$ .

A Fourier analysis of  $B$  yields the desired conversion transconductance since for the  $n$ th harmonic mode of operation it is simply half the  $n$ th Fourier coefficient, as was shown above. If, as is usually the case, the oscillator voltage is sinusoidal in shape, it is possible to make use of some convenient formulas of sufficient accuracy for most purposes. Referring to Figure 3, a sinusoidal oscillator voltage is assumed and a seven-point analysis at 30-degree intervals is made. Then,<sup>1</sup> the conversion transconductances for the fundamental and the first two modes of harmonic operation are

$$g_{c_1} = \frac{1}{2} [(g_7 - g_1) + (g_5 - g_3) + 1.73(g_6 - g_2)] \quad (14)$$

$$g_{c_2} = \frac{1}{2} [2g_4 + \frac{3}{4}(g_3 + g_5 - g_6 - g_2) - (g_7 + g_1)] \quad (15)$$

$$g_{c_3} = \frac{1}{2} [(g_7 - g_1) - 2(g_5 - g_3)]. \quad (16)$$

The values  $g_1, g_2$ , etc., are obtained from the transconductance characteristic of Figure 3 by means of the 30-degree analysis there indicated. An examination of (14) for  $g_{e1}$  indicates that maximum possible fundamental conversion transconductance, (excluding negative transconductances) occurs when  $g_1, g_2$ , and  $g_3$  are zero and  $g_5, g_6$ , and  $g_7$  are large. This is achieved by operating so that the transconductance is cut off over slightly less than half the oscillator cycle and with oscillator-voltage amplitude of such magnitude that the tube operates to somewhat beyond the point of maximum transconductance.

In practical cases, wherein grid-controlled tubes are employed, the maximum possible fundamental conversion transconductance is given approximately<sup>1</sup> by 28 per cent of the maximum signal-grid-to-plate transconductance. The maximum attainable second-harmonic conver-

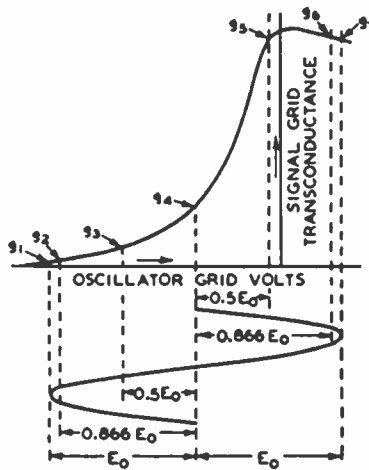


Fig. 3—Points used for 30-degree analysis of conversion transconductance.

sion transconductance is roughly half as great, and for third-harmonic conversion the maximum attainable transconductance is only about one third as great. Harmonic operation requires greater excitation, as a rule, than fundamental operation and the optimum operating point is differently located.

Thus an examination of the signal-electrode-to-plate transconductance curve quickly yields approximate values of the following quantities:

1. Optimum operating point for fundamental conversion.
2. Optimum local-oscillator excitation for fundamental conversion.
3. Conversion transconductances for fundamental, second harmonic, and third harmonic conversion.

## III. NOISE OF CONVERTER OR MIXER STAGE

As was shown in Parts II and III of this series, fluctuation noise is measured by its mean-square value. In most vacuum tubes, the important part of the fluctuation noise comes from the plate or anode current. Under static conditions or with very small signals the mean-square noise current may be written as  $\overline{i_{pn}^2}$ . In the converter stage of a receiver, a large local oscillator voltage is usually applied to the converter or mixer so that  $\overline{i_{pn}^2}$  fluctuates periodically at local-oscillator frequency. The mean-square noise current at the intermediate frequency, which is the one of concern here, is then the average value of the fluctuations, i.e., the time average over the oscillator cycle,

$$\overline{i_{i-f}^2} = \frac{1}{2\pi} \int_0^{2\pi} \overline{i_{pn}^2} d(\omega t).$$

Values for the plate noise  $\overline{i_{pn}^2}$  of different types of tubes have been computed theoretically<sup>2</sup> and checked closely experimentally (except in the case of diodes) so that the mixer noise can readily be estimated by use of the above averaging process.<sup>3</sup>

It is convenient to express mixer noise in terms of an equivalent noise resistance (except perhaps for the diode mixer). This resistance is defined as that which, if connected across the input of a noise-free mixer with conversion transconductance equal to that of the tube under study, will produce the same noise current in the plate circuit as is present in the actual tube. Thus

$$\overline{e_n^2} = \overline{i_{i-f}^2} / g_c^2 \quad (17)$$

where  $g_c$  is the conversion transconductance and  $\overline{e_n^2}$  is the mean-square noise voltage developed by the equivalent noise resistance.

$$R_{eq} = \overline{e_n^2} / (4kT\Delta f) \quad (18)$$

$$= \overline{i_{i-f}^2} / (4kTg_c^2\Delta f) \quad (19)$$

where  $k = 1.37 \times 10^{-23}$  joule per degree Kelvin,  $T$  is the absolute

<sup>2</sup> B. J. Thompson, D. O. North, and W. A. Harris, "Fluctuations in space-charge-limited currents at moderately high frequency," *RCA REVIEW*, vol. 4, pp. 269-285; January 1940; vol. 4, pp. 441-472; April, 1940; vol. 5, pp. 106-124; July 1940; vol. 5, pp. 244-260; October, 1940; vol. 5, pp. 371-388; January, 1941; vol. 5, pp. 505-524; April, 1941; vol. 6, pp. 114-124; July, 1941.

<sup>3</sup> E. W. Herold, "Superheterodyne converter considerations in television receivers," *RCA REVIEW*, vol. 4, pp. 324-337; January, 1940.

temperature, and  $\Delta f$  is the noise bandwidth as defined in Part I of this series. As was shown in Part III, it is desirable from a signal-to-noise point of view to have as small a value for  $R_{eq}$  as can be obtained.

A convenient table of equivalent noise resistance values for triode and pentode mixers was given by Herold<sup>1</sup> and is shown in Table I. In the table, it is assumed that optimum oscillator excitation (i.e., optimized for maximum  $g_c$ ) is used. The control-grid cutoff voltage is  $E_{c0}$ , the peak grid-to-cathode transconductance (usually taken at zero bias) is  $g_0$ , and the peak cathode current (also usually at zero bias) is  $I_0$ . (Grid-to-cathode transconductance is defined as the rate of change of cathode current with respect to signal-electrode voltage. It is thus the sum of the transconductances measured between the signal-grid and the screen and plate.) For triodes,  $\alpha = 0$ , where as for pentodes,  $\alpha$  is the ratio of screen current to plate current. It will be shown in a later section that the average transconductance is of value in estimating the electronic input loading.

In the ultra-high-frequency field, multigrid mixers are not widely used because they are greatly inferior to triodes and pentodes from a signal-to-noise point of view<sup>3</sup> and will not, as a consequence, be discussed here. The two-element mixer such as the diode. (tube or crystal), on the other hand, has been used to some extent<sup>4</sup> but is sufficiently different in behavior to justify a separate treatment.<sup>5</sup>

Table I—Mixer Noise of Triodes and Pentodes  
(Oscillator and Signal both Applied to Control Grid)

Operation	Approximate Oscillator Peak Volts	Average Transcon- ductance $\bar{g}_m$	Average Cathode Current $\bar{I}_c$	Conversion Transcon- ductance $g_c$	Equivalent Noise Resistance $R_{eq}$
At Oscil- lator Fun- damental	$0.7 E_{c0}$	$\frac{0.47}{1+\alpha} g_0$	$0.35 I_0$	$\frac{0.28}{1+\alpha} g_0$	$\frac{13}{g_0} + \frac{90}{g_0^2} \alpha$
At Oscil- lator 2nd Harmonic	$1.5 E_{c0}$	$\frac{0.25}{1+\alpha} g_0$	$0.20 I_0$	$\frac{0.13}{1+\alpha} g_0$	$\frac{31}{g_0} + \frac{220}{g_0^2} \alpha$
At Oscil- lator 3rd Harmonic	$4.3 E_{c0}$	$\frac{0.15}{1+\alpha} g_0$	$0.11 I_0$	$\frac{0.09}{1+\alpha} g_0$	$\frac{38}{g_0} + \frac{260}{g_0^2} \alpha$

<sup>4</sup> See "40-cm waves for aviation," *Electronics*, vol. 12, pp. 12-15; November, 1939.

<sup>5</sup> See Part V of this series.

## IV. CONVERTER OR MIXER GAIN

The gain in a converter or mixer stage may be treated in exactly the same manner as for the case of the more familiar amplifier stages. The gain is defined as the ratio of the intermediate-frequency voltage on the control grid of the first intermediate-frequency amplifier tube to the signal voltage on the signal electrode of the converter or mixer tube. While the "gain" is a definite quantity which is a measure of the voltage ratio on the grids of successive tubes, it is not a true measure of the "step-up" between stages except at low frequencies where the tube loading is negligible. What is generally of greater interest than gain, is the voltage "step-up" between an antenna and the grid of the first intermediate-frequency tube. At ultra-high frequencies, this is determined not only by the mixer gain, but by the input loading on the signal grid of the mixer. It is thus seen that care must be

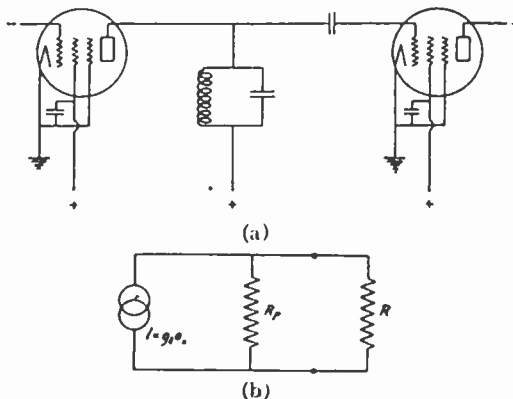


Fig. 4—(a) Circuit shows mixer stage coupled to intermediate-frequency stage by means of single-tuned circuit; (b) circuit which is equivalent of 4(a).

taken in attempting to arrive at a relative evaluation of different tubes from the standpoint of "gain."

In the general case gain depends upon the conversion transconductance, internal plate resistance of the mixer, and upon the input and transfer impedances of the circuit joining the two tubes. The simple case of a single-tuned circuit joining a pentode mixer to the intermediate-frequency amplifier is illustrated in Figure 4(a). The gain may be determined with the aid of the equivalent circuit shown in Figure 4(b), wherein  $R_p$  is the internal plate resistance of the mixer and  $R$  is the resonant impedance of the single-tuned network (assumed tuned to the intermediate frequency).  $g_c e_s$  represents a constant-current generator,  $g_c$  is the conversion transconductance, and  $e_s$  is the signal-grid voltage. The voltage developed across  $R$  (i.e., the intermediate-frequency voltage across the input to the intermediate-frequency amplifier) is  $g_c e_s (RR_p)/(R + R_p)$ . This divided by the

signal-grid voltage yields the conversion gain  $g_c(RR_p)/(R + R_p)$ . For pentodes, it is generally the case that  $R_p \gg R$ , and then conversion gain is equal to  $g_cR$ . This is similar to the corresponding expression for amplifier gain except that  $g_c$  replaces  $g_m$ . Under certain conditions the gain of a tube as an ultra-high-frequency amplifier bears a simple relation to its gain when employed as a mixer. In both cases it will be assumed that the operating conditions are adjusted for maximum transconductance. It will also be assumed that the tube in each case is operating into a single-tuned circuit of maximum possible resonant impedance. It can be shown that in each case the resonant impedance is given by the expression  $Z = 1/(2\pi C\Delta f')$  where  $C$  is the capacitance of the output circuit and  $\Delta f'$  is its effective circuit bandwidth as defined in Part I of this series. Since it is desired that  $Z$  be as large as possible,  $C$  must be reduced to the unavoidable minimum due to stray tube electrode, lead, and circuit distributed capacitances. The limiting capacitance is largely due to the tube and leads so that the minimum value of  $C$  is about the same for either the radio-frequency or intermediate-frequency cases, i.e., for amplifier or mixer operation. Furthermore, at ultra-high frequencies, as well as at intermediate frequencies, the value of  $\Delta f'$  is more often determined by the application at hand than by the unavoidable ohmic losses present in the circuit. Under these circumstances, the circuit must be "loaded down" with additional resistance so as to make its effective bandwidth sufficiently great to meet the needs of the application. Since this bandwidth requirement is the same regardless of the carrier frequency employed,  $\Delta f'$  is seen to be the same for the amplifier as for the mixer. As a consequence, the maximum output circuit impedance is the same regardless of whether the tube is used as an amplifier or as a mixer. The tube gain for this case has already been shown to be given by  $gR$  where  $g$  refers to  $g_m$  for the amplifier and to  $g_c$  for the mixer. Since  $R$ , the maximum output circuit impedance, is the same for both cases, the gains will be related in the same fashion as the transconductance. Since, as was indicated above, the maximum conversion transconductance is only about 28 per cent of the maximum amplifier transconductance, it follows that a given tube when used as an amplifier will produce about four times as much gain as when used as a mixer. While this conclusion was drawn for the case of a single-tuned coupling circuit it holds closely for more complicated network cases.

#### V. INPUT LOADING OF MIXER STAGE

In Part II of this series, the problem of input loading of vacuum tubes was discussed and expressions for loading due to lead inductances

and finite transit angle in the cathode-control-grid region of conventional-type tubes, and the loading in velocity-modulated devices were developed. In mixer operation, the input loading will vary periodically at local-oscillator frequency, so that to determine the actual loading it is necessary to average the instantaneous values over the oscillator cycle. The averaging process is identical with that outlined in Section III where the noise of mixer stages was discussed, and need not be outlined in detail. Since, in many instances, the input conductance varies directly with the transconductance, the average transconductance can be used as a measure of the relative loading.

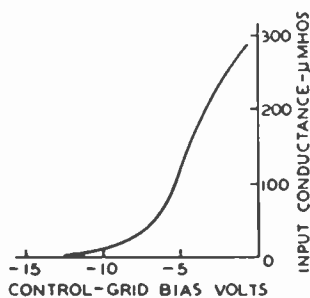


Fig. 5—Input conductance of a typical variable- $\mu$ , radio-frequency pentode at 60 megacycles.

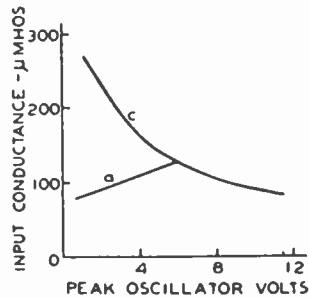


Fig. 6—Input conductance of a typical pentode when used as a mixer at 60 megacycles. *a* fixed-bias operation; *c* bias obtained by means of a high-resistance grid leak.

To see how the mixer loading is related to the instantaneous amplifier loading, let us examine an illustrative case treated by Herold.<sup>1</sup> Figure 5 depicts the input loading of a “typical pentode” at 60 megacycles as a function of control-grid bias. We consider two cases: 1. the tube is operated at a fixed bias, and 2. the bias is obtained by means of a high-resistance grid leak. The results obtained for mixer operation as a function of local-oscillator voltage (also applied to the control grid) are shown as curves *a* and *c* of Figure 6. It is interesting to note that the loading actually decreases with increasing excitation for the case of grid-leak bias. This is due to the fact that the grid is biased further back toward cutoff with increasing oscillator voltage, so that the cathode current (and consequently, the loading) is cut off over a greater portion of the cycle. Thus, as the oscillator voltage is increased, the loading across the input circuit is reduced, and as consequence  $R_t$  (the resonant impedance of over-all input circuit as defined in Part III) is increased. For *harmonic* operation the oscillator swing should be further increased for best results, so that  $R_t$  is greater than in the case of optimum fundamental conversion. At the same time, due to decreased  $g_m$ ,  $R_{eq}$  is also increased. It has been shown by



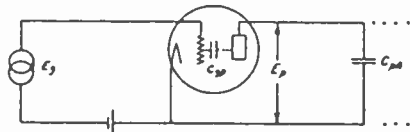
Herold<sup>6</sup> that the ratio  $R_i/R_{c1}$  in the cases of second- and third-harmonic conversion with triodes is only slightly reduced below the value for fundamental conversion. Since, as was shown in Part III, the signal-to-noise ratio depends largely on  $R_i/R_{c1}$ , it follows that for triode converters, the signal-to-noise ratio is not seriously affected by harmonic operation. The gain however, being determined by  $g_c$ , is reduced by harmonic operation. In addition, it may be difficult to obtain the larger oscillator excitation required.

From the fact that at ultra-high frequencies the input loading varies as the square of the frequency, the results for any one frequency may be immediately extended to others.

VI. FEEDBACK IN TRIODE MIXERS AT ULTRA-HIGH FREQUENCIES

In general, mixer feedback is due primarily to the capacitance between the plate and signal grid. Since this is appreciable only for triodes, the discussion will be limited to that tube type. A triode mixer feeds into a network designed to have the desired bandwidth

Fig. 7 — Effective radio-frequency circuit of a triode mixer.



at the intermediate frequency. For maximum possible intermediate-frequency circuit impedance (as a condition for maximum gain) the output capacitance should be a minimum. As was previously shown, this is generally accomplished by limiting the output-circuit capacitance to that unavoidably present within the tube and that due to leads and stray and distributed capacitances. Since such inductances as are in the plate circuit are designed so as to result in the desired circuit characteristics at the intermediate frequency, any radio frequency present in the plate circuit will “see” capacitance only. To understand how this output capacitance affects the tube behavior at radio frequency consider the effective triode circuit as shown in Figure 7. Let the triode be fed by a signal source of negligible internal impedance of voltage amplitude  $E_g$ . This will cause a current  $I_p$  to flow in the plate circuit of magnitude  $\overline{g_m}E_g$ , where  $\overline{g_m}$  is the average transconductance over the oscillator cycle. This in turn will result in voltage  $E_p$  across the effective output capacitance  $C_{pk}$  given by

$$E_p = (\overline{g_m}E_g) / (j\omega C_{pk}). \tag{20}$$

<sup>6</sup> E. W. Herold, “An analysis of the signal-to-noise ratio of ultra-high-frequency receivers,” *RCA REVIEW*, vol. 6, pp. 302-331; January, 1942.

A capacitive current will flow in the input circuit, given by

$$I_{gp} = j\omega C_{gp} E_p = \overline{g_m} (C_{gp}/C_{pk}) E_g. \quad (21)$$

Therefore the input admittance due to feedback will be

$$A_g = I_{gp}/E_g = \overline{g_m} (C_{gp}/C_{pk}). \quad (22)$$

This is in the form of a conductance which will load down the input circuit, over and above the loading due to ohmic losses, and the loading due to the effects of lead inductance and finite transit angles as was discussed in Part II of this series. Since  $C_{gp}/C_{pk}$  may be of the order of 0.3, it is seen that the input resistance due to feedback in a triode mixer may be of the order of several thousand ohms, and may thus have an appreciable effect upon the receiver performance.

#### VII. IMAGE FREQUENCIES AND INTERMEDIATE-FREQUENCY CONSIDERATIONS

Let us now consider a problem peculiar to mixers. It is best made clear by an example. If the signal frequency is 100 megacycles and the oscillator frequency is 101 megacycles, the frequencies in the output will include 100 megacycles, 101 megacycles, 201 megacycles (the sum frequency), and 1 megacycle (the difference frequency). Of these frequencies it can be assumed that the desired intermediate frequency is 1 megacycle. The undesired frequencies can be filtered out by the sharply tuned circuits in the intermediate-frequency amplifier. With the oscillator operating at 101 megacycles, it is obvious that an incoming signal of 102 megacycles will provide a difference frequency of 1 megacycle which is also capable of passing through the intermediate-frequency amplifier. Reception of this kind is known as image reception. This image should be avoided in good receiver design.

If a low value is chosen for the intermediate frequency it is difficult to attenuate the image without using tuned-radio-frequency stages ahead of the mixer. This may be undesirable because of practical tuning considerations or from the signal-to-noise standpoint. As a consequence it is generally desirable to use a high value for the intermediate frequency. For ultra-high-frequency applications this may range from 10 to 100 megacycles.

There is another factor which favors the use of high intermediate frequencies. Most ultra-high-frequency applications require the use of a wide-band amplifier following the second detector. Thus, e.g., the final amplification in a television amplifier occurs in the video ampli-

fier which may amplify frequencies up to 4 megacycles. If the intermediate frequency is too low, it becomes exceedingly difficult to keep some of it out of the video amplifier with resultant distortions and feed-backs of regenerative or degenerative nature.

#### VIII. RADIO-FREQUENCY AMPLIFICATION VERSUS CONVERSION IN FIRST STAGE OF A RECEIVER

On the basis of the preceding sections of this paper as well as of the earlier parts of this series we are now in a position to render judgment regarding a basic question which arises in the design of all superheterodyne-type receivers. Should one convert immediately in the first stage or should one first use one or more stages of radio-frequency amplification and then convert in a later stage? The answer to this question depends, in general upon the following considerations: 1. Magnitude of received signal; 2. Frequency of received signal; 3. Band-width required; 4. Image rejection; 5. Reradiation of local-oscillator power; and 6. Nature of tubes available, i.e., the "state of the art."

The first of these is tied up intimately with the importance of signal-to-noise ratio. If the received signal is large compared with the receiver noise, signal-to-noise ratio is of no importance. This simplifies the consideration of the strong signal case considerably. As was shown above, the gain of an amplifier stage is roughly four times that of a mixer stage. However, since a mixer stage must be used somewhere in a superheterodyne receiver, the lower gain of a mixer must be faced at some point, so that from gain considerations one can draw no positive conclusion concerning the location of the mixer stage. The important factors actually are those related to image rejection and reradiation. If the first stage were a mixer, the image rejection might be inadequate, in which case one or stages of radio-frequency amplification would be required. By use of a high value of intermediate frequency, immediate conversion may be possible.

In some applications, the radiation from the antenna of local-oscillator power may be a serious factor as regards local interference or in revealing the presence of the receiver. This can be minimized by the use of a radio-frequency stage to isolate the local oscillator from the antenna. If the first stage is a mixer, reradiation can be reduced by the use of a high value of intermediate frequency, so that the antenna and input circuit are far out of tune with the local-oscillator frequency or by the use of balanced (neutralizing) circuits. In general, however, if image rejection and reradiation are not serious, immediate conversion is preferred in order to avoid the difficulties

inherent in the tuning of radio-frequency amplifiers. This is particularly the case if the receiver is to be tunable. The bandwidth required and the nature of the tubes employed do not exercise an appreciable role for the case of strong-signal reception and will not be treated further at this point.

If the received signal is weak, the signal-to-noise ratio is of paramount importance. Let us first suppose that for a particular signal frequency and bandwidth application, a tube is available from which a radio-frequency gain considerably greater than unity can be obtained. We postulate further that the bandwidth requirements are such that the circuits must be "loaded down" with external shunt resistance, in order to achieve the desired bandwidth, i.e., in the relation  $Z = 1/2\pi C\Delta f'$ ,  $\Delta f'$  is determined by the application at hand and not by tube and circuit losses. As has already been pointed out, under these conditions, the mixer gain available from a tube is only about one quarter as great as the available amplifier gain, but since this reduced gain must be faced eventually, no conclusions can as yet be drawn as to whether to make use of radio-frequency amplification or conversion in the first stage. However, the equivalent noise resistance  $R_{eq}$  is much lower for the amplifier case than for the mixer, and since this often means a higher signal-to-noise ratio, the use of one or more amplifier stages before conversion is definitely indicated. Now, let us suppose, as a first variation, that the operating frequency is increased. In this case, the circuit impedance which includes the tube loading, decreases with increasing frequency so that the circuit requires less and less additional external loading to achieve the desired bandwidth. Above a certain frequency (which we may call the crossover frequency) the circuit bandwidth, with no external loading, exceeds that required by the application at hand, this being increasingly the case as the frequency goes higher and higher. As a consequence, amplifier gain drops off above the "crossover" frequency. A point will finally be reached for which the amplifier-stage gain drops to unity or lower, in which case it would obviously be foolish to use such a stage, and conversion should be employed in the first stage. In fact, better signal-to-noise response can usually be obtained by immediate conversion for cases in which the amplifier gain is still somewhat above unity. Since the intermediate-frequency-circuit resonant impedance is independent of the signal frequency, the mixer gain remains unaltered as the signal frequency increases, so that the mixer-stage gain may eventually exceed that of the amplifier stage. This constitutes a further argument for immediate conversion above a certain frequency, which we may refer to as the "transition frequency."

The decreased radio-frequency gain with increased frequency is determined largely by tube losses and these in turn depend upon the nature of the tubes available. Thus we may conclude that the transition frequency above which immediate conversion is preferred depends in part, upon the "state of the art." In recent years advances in ultra-high-frequency receiving-tube design have extended the frequency range over which radio-frequency amplification yields better signal-to-noise ratio than is available with converter operation, so that the "transition frequency" is now considerably higher than it was several years ago.

As a second variation, let us suppose that the bandwidth requirements are increased. In that case, the radio-frequency as well as the intermediate-frequency-circuit impedances must be lowered. As a consequence, since the tube loading plays a lesser role in this case, one can, in general, extend the range of amplifier operation to higher frequencies before the loss in gain becomes so serious as to justify immediate conversion.

#### IX. CONCLUSION

If the received signal is strong, one should convert immediately, unless image rejection or the prevention of oscillator radiation necessitate the use of radio-frequency stages. If the received signal is weak, an amplifier stage should be used below a certain frequency and a mixer above, the transition frequency depending upon the characteristics of the tubes available and the bandwidth required. In general the transition frequency occurs at the point where available tubes will no longer give appreciable radio frequency gain for the bandwidth required.

#### X. APPLICATION OF SECONDARY ELECTRON EMISSION TO SUPERHETERODYNE RECEIVERS

Secondary emission is ideally suited for application to converters and mixers. It was pointed out in Part II of this series that the gain of a secondary-emission multiplier falls off with increasing frequencies due to the transit-time spreads of secondary electrons. These spreads arise from the fact that different secondaries are emitted with different initial velocities and travel over different paths. This definitely limits the use of secondary-emission multipliers as ultra-high-frequency amplifiers. However, at the intermediate-frequencies used in ultra-high-frequency receivers, the loss in gain described above is negligible so that secondary-emission amplification after conversion is possible and is generally advantageous.

In Part III it was shown that the noise contribution of circuits and tubes following the first stage may be of importance. Anything that can be done to reduce the noise contributed by what follows the first tube will thus improve the signal-to-noise ratio of the complete receiver. The coupling impedance joining the first tube to the second in a conventional-type amplifier is a source of noise and by permitting the plate current of the first tube to go through a secondary-emission multiplier the coupling circuit with its resultant noise contribution is shifted to a later stage where its noise contribution is negligible in comparison with the now greatly amplified noise from earlier sources. One must be sure, however, that the secondary-emission multiplier does not contribute noise in excess of that due to a coupling circuit or resistor. It has been shown<sup>7</sup> that if the secondary-emission ratio  $n$  is high, the signal-to-noise ratio is inappreciably affected. If the primary current (plate current for our case) has only pure temperature-limited shot noise ( $\bar{i}^2 = 2eI\Delta f$ ) then the relative change in the signal-to-noise ratio due to a secondary-emission stage is given approximately by  $\sqrt{n/(n+1)}$ , which is obviously unimportant if  $n$  is large.

<sup>7</sup> V. K. Zworykin, G. A. Morton, and L. Malter, "The secondary emission multiplier—A new electronic device," *Proc. I.R.E.*, vol. 24, pp. 351-376; March, 1936.

## Part V. Frequency Mixing in Diodes†

BY

E. W. HEROLD

*Summary*—Although the diode (crystal or thermionic) is one of the simplest forms of device, the behavior of the diode mixer in superheterodyne reception has not been well understood. One reason for this is that the conversion process is more complex than in other mixers in that it is bilateral, a radio-frequency input voltage giving an intermediate-frequency output current and the resulting intermediate-frequency output voltage in turn giving a radio-frequency current in the input. Analysis of the behavior leads, however, to a very simple equivalent circuit consisting of a symmetrical  $\pi$  circuit of three conductances whose magnitudes are determined by the average diode conductance and by the conversion conductance of the diode. The present paper derives this circuit and uses it to find the conversion loss of the converter stage both with and without input circuit loss. The results, although arrived at independently, are in agreement with the recent publication of James and Houldin.

If the conversion loss is to be held small, the diode must be operated so as to obtain the highest ratio of conversion conductance to average con-

† Reprinted from *Proc. I.R.E.*, October, 1943.

ductance. The upper limit of this ratio is unity and this is attained only when the mixer-stage impedance is infinite. Thus, circuit losses prevent the attainment of the condition of no conversion loss in practice.

The signal-to-noise ratio of a receiver whose input stage is a diode converter is not determinable accurately because of uncertainties in the diode noise behavior. However, by using the conversion loss together with an effective noise temperature for the converter stage, an over-all noise factor can be given in terms of the noise factor of the intermediate-frequency amplifier,  $F_{i-f}$  which in the laboratory, is

$$F_{\text{over-all (in laboratory)}} = \frac{F_{i-f} + (1 - M)(T_i/T_R - 1)}{M}$$

where  $M$  is the ratio of intermediate-frequency output power to signal-input power of the converter stage, and  $T_i/T_R$  is the ratio of effective noise temperature to room temperature.

The analysis of the average and conversion conductances of particular diodes may be made by use of Fourier analysis in the same manner as with other mixer and converter tubes. The behavior of many diodes is qualitatively shown by an idealized diode whose volt-ampere characteristic is given by two intersecting straight lines. Curves are given showing the conversion loss as a function of the ratio of direct-bias-to-peak oscillator voltage and including input-circuit loss. It is found that conversion at the second or third harmonic of the local oscillator is more critical than at fundamental, but under optimum conditions, the conversion loss is only a few decibels higher.

## I. INTRODUCTION

THE general theory of superheterodyne frequency conversion is now well understood and it has given a reasonable complete understanding of the behavior as mixers of conventional triodes and multigrad tubes.<sup>1</sup> In the ultra-high-frequency region, however, the use of the two-element nonlinear device (e.g., the diode) as a frequency changer has been common. Although the diode is one of the simplest forms of device, its behavior as a mixer has been very poorly understood. M. J. O. Strutt<sup>2,3</sup> was early to publish on the subject but failed to make his analysis complete. During intervening years there has been unpublished work, notably that of W. A. Harris of the RCA Victor Division, but it was only a few months ago that a more adequate presentation has appeared in print.<sup>4</sup> The following analysis was developed independently by the present writer some years ago by

<sup>1</sup> E. W. Herold, "The operation of frequency converters and mixers," *Proc. I.R.E.*, vol. 30, pp. 84-103; February, 1942.

<sup>2</sup> M. J. O. Strutt, "On conversion detectors," *Proc. I.R.E.*, vol. 22, pp. 981-1008; August, 1934.

<sup>3</sup> M. J. O. Strutt, "Diode frequency changers," *Wireless Eng.*, vol. 13, pp. 73-80; February, 1936.

<sup>4</sup> E. C. James and J. E. Houldin, "Diode frequency changers," *Wireless Eng.*, vol. 20, pp. 15-27; January, 1943.

an extension of the method used for other types of converters or mixers.<sup>1</sup> However, it will be found that the end results are in agreement with those of James and Houldin.<sup>4</sup>

Most mixers and converters using separate signal-input and intermediate-frequency output electrodes are readily analyzed because there is no reverse conversion; i.e., the signal-electrode current is unaffected by the presence or absence of an intermediate-frequency voltage on the output electrode. The diode or two-terminal mixer, however, converts in both directions. The signal-frequency voltage is converted to an intermediate-frequency current and the resulting intermediate-frequency voltage is converted by the local oscillator to a signal-frequency current. Thus, the signal-frequency impedance of the mixer stage is affected by the intermediate-frequency load impedance and the output impedance is affected by the signal circuit. The problem of properly adjusting circuit bandwidths and of matching impedances becomes a complex one.

Finally, the problem of signal-to-noise relations in the two-terminal mixer is very involved. In the first place, the actual fluctuation noise of the two-terminal device must be known under actual operating conditions, i.e., with the local-oscillator voltage applied. Next, the proper connection between signal-frequency and intermediate-frequency noise components must be clearly established since the bidirectional conversion process ties these two components closely together. This aspect of the diode mixer is not yet completely understood.

## II. CONVERSION THEORY

### 1. Basic Analysis

The basic diode-converter stage consists of an input circuit tuned to the signal frequency, an output circuit tuned to the intermediate frequency, and a source of local-oscillator voltage. In operation, a signal-input voltage is impressed on the device and an output voltage of intermediate frequency is also present as a voltage drop across the intermediate-frequency circuit. Since, at the start, the phase relationship of these two voltages is unknown, it is best to proceed by assuming an arbitrary phase relationship, just as if the intermediate-frequency voltage were an *impressed* voltage rather than a voltage drop. After the currents flowing in the circuit have been found, the necessary conditions applicable to the actual case will be obvious and it will be possible to establish the correct phase relationship. The basic circuit is then shown in Figure 1 where signal- and intermediate-frequency voltages are indicated. The intermediate-frequency voltage is given an arbitrary phase angle  $\phi$ .



An analysis will be made which is valid for small signal- and intermediate-frequency voltages, although no restriction is imposed on the magnitude of the local-oscillator voltage. This is in accord with established mixer practice in which comparatively large oscillator voltages are used, but in which the received signals are small. The characteristic of the two-terminal device may be written  $i = f(e)$  so that, under mixer conditions,

$$i = f(e_0 + e_i + e_s) \tag{1}$$

where  $e_0$  is the sum of the local-oscillator voltage and the direct-current bias,  $e_i$  is the intermediate-frequency voltage, and  $e_s$  is the signal voltage. Since the latter components  $e_i$  and  $e_s$  are small, a Taylor's expansion may be made about the point of operation determined by  $e_0$ ,

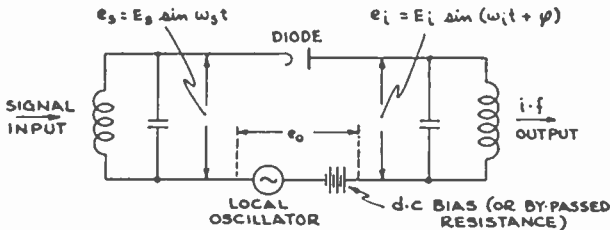


Fig. 1—Schematic circuit of diode converter stage.

$$i = f(e_0) + (e_i + e_s) f'(e_0) + \dots \tag{2}$$

Higher-order terms than those shown will be neglected, thus implying that  $(e_i + e_s)$  is sufficiently small. The first term of (2) contains only oscillator-frequency terms and is of no interest here. Since the conductance of the two-element device is  $g = di/de = f'(e)$  it is evident that the important part of (2) may be written

$$\begin{aligned} i &= g(e_s + e_i) \\ &= g[E_s \sin \omega_s t + E_i \sin (\omega_i t + \phi)] \end{aligned} \tag{3}$$

where  $g$  is the conductance of the two element device when oscillator voltage and bias only are applied, i.e., when  $e = e_0$ . Equation (3) might well have been written directly.

It is clear that  $g$ , the conductance, varies in time periodically at the frequency of the local-oscillator voltage. The conductance, therefore, may be written as a Fourier series whose fundamental component is at local-oscillator frequency

$$g = g_0 + \sum_{n=1}^{\infty} g_n \cos n\omega_0 t \quad (4)$$

where the cosine series implies that the conductance is single-valued and that the oscillator voltage varies as  $\cos \omega_0 t$ . The coefficients  $g_0$  and  $g_n$  are found by any of the usual methods of harmonic analysis based on the formulas<sup>5</sup>

$$g_0 = \frac{1}{2\pi} \int_0^{2\pi} g d(\omega_0 t)$$

$$g_n = \frac{1}{\pi} \int_0^{2\pi} g \cos n\omega_0 t d(\omega_0 t).$$

This is exactly the procedure followed in conventional converter theory. Substituting (4) in (3) we get

$$\begin{aligned} i &= g_0 E_s \sin \omega_s t + g_0 E_i \sin (\omega_i t + \phi) \\ &\quad + E_s \sum g_n \sin \omega_s t \cos n\omega_0 t + E_i \sum g_n \sin (\omega_i t + \phi) \cos n\omega_0 t \\ &= g_0 E_s \sin \omega_s t + g_0 E_i \sin (\omega_i t + \phi) \\ &\quad + E_s/2 \sum g_n \sin (\omega_s + n\omega_0) t + E_s/2 \sum g_n \sin (\omega_s - n\omega_0) t \quad (5) \\ &\quad + E_i/2 \sum g_n \sin [(\omega_i + n\omega_0) t + \phi] \\ &\quad + E_i/2 \sum g_n \sin [(\omega_i - n\omega_0) t + \phi]. \end{aligned}$$

If any one of the low-frequency components is chosen as the intermediate frequency  $\omega_i$ , then

$$\omega_i = \pm (\omega_s - n\omega_0) \quad (6)$$

where conversion is at the  $n$ th harmonic of the local oscillator. Rearranging (6) it is seen that

$$\pm \omega_i + n\omega_0 = \omega_s. \quad (7)$$

Using (6) and (7) in (5) and disregarding all the terms which contain frequencies other than  $\omega_s$  or  $\omega_i$ , the signal-frequency current  $i_s$  and the intermediate-frequency current  $i_{i-f}$ , are found to be<sup>6</sup>

<sup>5</sup> For derivation see any standard text, e.g., E. B. Wilson's, "Advanced Calculus," Ginn and Company, New York, N. Y., p. 458.

<sup>6</sup> It may be noted that the magnitude of the local-oscillator voltage  $E_0$  does not appear directly in the current relations. However, the Fourier coefficients  $g_0$  and  $g_n$  depend on the local-oscillator voltage and thus the currents are dependent on  $E_0$  to some extent.

$$i_s = g_0 E_s \sin \omega_s t + (g_n/2) E_i \sin (\omega_s t + \phi) \tag{8}$$

$$i_{1-f} = g_0 E_i \sin (\omega_i t + \phi) + (g_n/2) E_s \sin \omega_i t. \tag{9}$$

Finally, the original conception of  $E_i \sin (\omega_i t + \phi)$  as an *impressed* voltage may be dropped and this term now considered as a *voltage drop*. The new concept may be simplified by assuming the intermediate-frequency load resistance to be tuned to the intermediate-frequency so that it presents a pure resistance  $R_{1-f}$  and, at the same time, by assuming the other circuit impedances to be negligible at the intermediate frequency. Then the voltage drop is  $E_i \sin (\omega_i t + \phi) = -i_{1-f} R_{1-f}$ . Substituting the value of  $i_{1-f}$  from (9) and rearranging, it is found

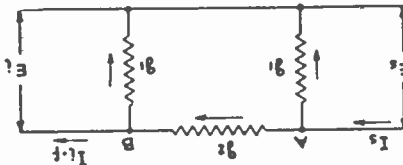


Fig. 2—Symmetrical  $\pi$  network whose equations resemble those for the diode mixer.

that  $(g_0 + 1/R_{1-f}) E_i \sin (\omega_i t + \phi) = -(g_n/2) E_s \sin \omega_i t.$  (10)

Since this relation must hold for all values of  $t$ , it is clear that  $\phi = \pi$ , and that  $E_i/E_s = g_{cn}/(g_0 + 1/R_{1-f})$  where  $g_{cn}$  has been written for  $g_n/2$ . It is seen, of course, that  $g_{cn}$  is simply the conversion conductance of the two-element mixer where conversion is at the  $n$ th harmonic of the local oscillator. It is analogous in every way to the conversion transconductance of other forms of mixer as given in a previous paper<sup>1</sup> and discussed in Part IV of this series.

Equations (8) and (9) can now be written (putting  $\phi = \pi$ )

$$i_s = g_0 E_s \sin \omega_s t - g_{cn} E_i \sin \omega_s t. \tag{12}$$

$$-i_{1-f} = -g_{cn} E_s \sin \omega_i t + g_0 E_i \sin \omega_i t. \tag{13}$$

It is now possible to solve (10), (12), and (13) and find all the desired quantities. However, it is not necessary to do this formally as will now be shown.

### 2. Equivalent Circuit for the Diode-Converter Stage

There is a similarity between (12) and (13) of the foregoing and the mesh equations for a symmetrical network of three conductances arranged in a  $\pi$ . Considering the symmetrical  $\pi$  network of Figure 2,

the Kirchhoff-law relation may be written for the sum of currents at points *A* and *B* respectively. It is seen that

$$I_s = E_s g_1 + (E_s - E_i) g_2$$

$$-I_{i-f} = E_i g_1 - (E_s - E_i) g_2$$

where currents entering the points are equated to those leaving the points. Rearranging it is found

$$I_s = E_s (g_1 + g_2) - g_2 E_i \tag{14}$$

$$-I_{i-f} = -E_s g_2 + (g_1 + g_2) E_i \tag{15}$$

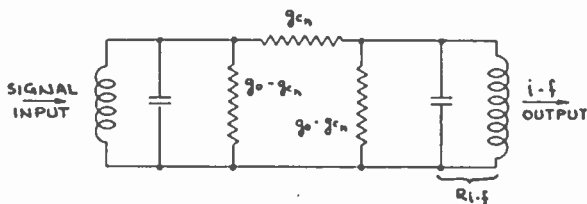


Fig. 3—The equivalent circuit for the diode mixer. This circuit gives the correct *magnitude* for input and output currents and voltages; however, the frequency of the input current and voltage is different from the output frequency.

A comparison of (14) and (15) with (12) and (13) shows that the mixer circuit may be considered as equivalent to Figure 2 as far as amplitudes of currents and voltages are concerned. As to frequencies, of course, the mixer circuit is always different from the passive network inasmuch as the frequency of the output voltage and current differs from the input frequency.<sup>7</sup> Furthermore, if  $g_0 = g_1 + g_2$  and  $g_2 = g_{cn}$  so that  $g_1 = g_0 - g_{cn}$  all the solutions to the mixer problem are found by simply solving the circuit of Figure 3. Almost every relation of importance can be written down by inspection of this simple equivalent circuit.<sup>8</sup>

### III. IMPEDANCES AND CONVERSION LOSS OF MIXER STAGE

#### 1. Maximum Power Transfer: Image or Iterative Impedance

It can be shown<sup>9</sup> that, barring negative resistance effects, the conversion conductance  $g_{cn}$  can never exceed the average conductance  $g_0$ .

<sup>7</sup> When the intermediate-frequency circuit has appreciable impedance at radio frequency or when the radio frequency circuit has impedance at intermediate frequency, these impedances should be included in the radio-frequency and intermediate-frequency branches of the circuit, respectively.

<sup>8</sup> To the writer's knowledge this equivalent circuit was first used by W. A. Harris of the RCA Victor Division.

<sup>9</sup> See Section IV, 1, of this paper.

Thus, in examining Figure 3, the shunt arms may be considered as positive conductances and it is clear that the intermediate-frequency output voltage can never exceed the radio-frequency signal voltage, no matter how high the intermediate-frequency circuit impedance is. The further discussion of the evaluation of  $g_0$  and  $g_{cn}$  will be left for a later section. For the present, let the characteristics of the diode mixer stage be examined as they are indicated by the equivalent passive network of Figure 3.

To begin with, it is clear that the mixer stage is basically a symmetrical  $\pi$ -type attenuator which, at the same time changes the frequency. If it is connected to the signal source and to the intermediate-frequency load through ideal transformers, maximum power transfer will occur when the transformers are adjusted to match the iterative or image impedance. This impedance is that which, when used as a termination, makes the input impedance of the mixer stage equal to this terminating value. In other words, by use of this impedance as a termination at each end, impedance matching is maintained throughout. The input conductance, when the intermediate-frequency conductance is  $g_x$ , can be written by inspection of Figure 3.

$$g_{in} = g_0 - g_{cn} + \frac{g_{cn}(g_0 - g_{cn} + g_x)}{g_0 + g_x}$$

$$= \frac{g_0^2 - g_{cn}^2 + g_0 g_x}{g_0 + g_x}. \quad (16)$$

If this input conductance is equated to  $g_x$  then  $g_x$  becomes what might be called the iterative conductance and is given by

$$g_x^2 = g_0^2 - g_{cn}^2. \quad (17)$$

This is one of the more important characteristics of the mixer stage.

## 2. Conversion Loss Under Matched Conditions: Circuit Losses Neglected

The minimum power loss in changing the signal frequency to the intermediate frequency occurs when the input and output are matched to  $g_x$  by ideal, loss-free circuits; the output-to-input power ratio is then given by the square of the voltage ratio (since the impedances are the same). Again examining Figure 3 it is seen that if a voltage  $E_s$  is impressed across the signal-input terminals, the voltage across the intermediate-frequency output  $E_i$  is by inspection.

$$\begin{aligned}
 E_t &= E_s \frac{(g_0 - g_{cn} + (1/R_{1-t}))g_{cn}}{g_0 + 1/R_{1-t}} \frac{1}{g_0 - g_{cn} + 1/R_{1-t}} \\
 &= E_s \frac{g_{cn}}{g_0 + 1/R_{1-t}}.
 \end{aligned}
 \tag{18}$$

If the intermediate-frequency load is matched to the diode mixer, then  $1/R_{1-t} = g_x$  and, using (17),

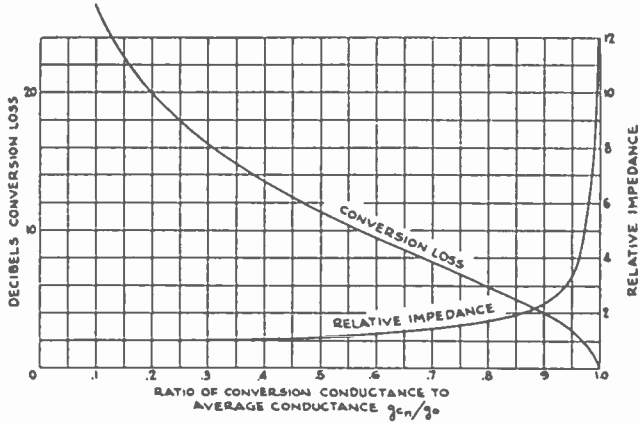


Fig. 4—The behavior of a diode mixer as a function of the two basic conductance components, assuming no loss in the input or output transformers and impedance matching throughout.

$$\begin{aligned}
 \frac{E_t}{E_s} &= \frac{g_{cn}}{g_0 + \sqrt{g_0^2 - g_{cn}^2}} \\
 &= \frac{g_{cn}/g_0}{1 + \sqrt{1 - (g_{cn}/g_0)^2}}
 \end{aligned}
 \tag{19}$$

Since the input and output impedances are the same, this relation may be expressed as a conversion loss in decibels; a curve of conversion loss is plotted against  $g_{cn}/g_0$  in Figure 4.

It is seen from Figure 4 that, unless  $g_{cn}/g_0$  is approximately unity the conversion loss is appreciable. However, an important factor to consider is the absolute magnitude of the matching conductance  $g_x$ . If this is very small (i.e., a very high impedance) it is not possible to match properly without the matching-circuit losses playing an important role. As  $g_{cn}/g_0$  approaches unity,  $g_x$  approaches zero and the impedances needed to match approach infinity. The relative matching impedance  $g_0/g_x$  is plotted on a second curve on Figure 4.

As will be seen later, the only way in which  $g_{cn}/g_0$  can approach unity in a diode-mixer stage is for  $g_{cn}$  and  $g_0$  separately to become very small. This in itself implies a very high matching impedance. If a particular diode is chosen, and by adjustment of operating conditions  $g_{cn}/g_0$  is made to approach unity, the curve of matching impedance would rise much more steeply than that shown in Figure 4.

It may be concluded first, that the diode mixer is not operable as a power-transfer device without appreciable conversion loss, and second, that circuit losses must be considered for any diode mixer whose conversion loss is small. Thus, it is logical to consider the next topic. ●

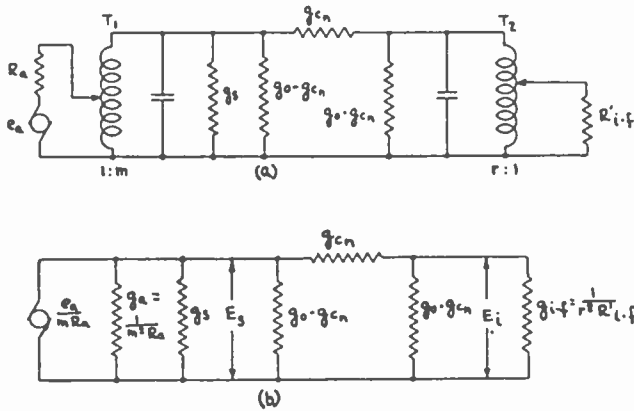


Fig. 5—(a) The schematic circuit of a diode mixer including input-circuit loss, shown as a conductance  $g_a$ . (b) An equivalent circuit wherein reflected current and conductances are substituted for the input and output transformers.

### 3. Conversion Loss Including Losses in Input Circuit

If the input circuit has a shunt loss which may be represented by a conductance  $g_s$ , the circuit becomes similar to the one shown in Figure 5(a). For the purposes of this analysis,  $T_1$  and  $T_2$  may be assumed to be ideal transformers whose step-up adjustments permit optimum power transfer to be obtained from the signal source  $e_a$  to the intermediate-frequency load  $R'_{1-f}$ . The transformers  $T_1$  and  $T_2$  may be removed to give the equivalent circuit of Figure 5(b) by inserting the impedances as seen from the diode-mixer input and output terminals. The conversion loss can now be computed from the ratio of power dissipated in the intermediate-frequency conductance,  $g_{1-f}$ , to that dissipated in the input, i.e.,  $g_s$  combined with the diode input conductance. The power dissipated in  $g_{1-f}$  is output power  $= E_i^2 g_{1-f}$  where  $E_i$  is the voltage across the output terminals (see Figure 5). The input power is input power  $= E_s^2 (g_s + g_{in})$  where  $E_s$  is the voltage

across the input terminals and  $g_{in}$  is the diode input conductance. From (16)

$$g_{in} = \frac{g_0^2 - g_{cn}^2 + g_0 g_{1-t}}{g_0 + g_{1-t}}$$

and from (18)

$$\frac{E_i}{E_s} = \frac{g_{cn}}{g_0 + g_{1-t}}$$

Using these relations

$$\begin{aligned} \frac{\text{output power}}{\text{input power}} &= \left( \frac{E_i}{E_s} \right)^2 \frac{g_{1-t}}{g_s + g_{in}} \\ &= \left( \frac{g_{cn}}{g_0 + g_{1-t}} \right)^2 \frac{g_{1-t}}{g_s + \frac{g_0^2 - g_{cn}^2 + g_0 g_{1-t}}{g_0 + g_{1-t}}} \end{aligned}$$

Multiplying out, it will be found that this becomes

$$\begin{aligned} \frac{\text{output power}}{\text{input power}} &= g_{cn}^2 \left[ (2g_0^2 + 2g_0 g_s - g_{cn}^2) \right. \\ &\quad \left. + (g_0/g_{1-t})(g_0^2 - g_{cn}^2 + g_s g_0) + g_{1-t}(g_0 + g_s) \right]^{-1} \end{aligned} \tag{20}$$

Considering  $g_{1-t}$  as a variable, the denominator contains the form  $(ax^{-1} + bx)$  which was treated in Section II, 2, of Part III of this series. The maximum power transfer (minimum denominator) occurs when

$$g_{1-t}^2 = \frac{g_0(g_0^2 - g_{cn}^2 + g_s g_0)}{g_0 + g_s} \tag{21}$$

and is

$$\begin{aligned} M &= \left. \frac{\text{output power}}{\text{input power}} \right]_{\max} \\ &= \frac{g_{cn}^2}{2g_0^2 + 2g_0 g_s - g_{cn}^2 + 2\sqrt{g_0(g_0 + g_s)(g_0^2 - g_{cn}^2 + g_s g_0)}} \end{aligned}$$



$$\begin{aligned}
 &= \frac{g_{cn}^2}{[\sqrt{g_0(g_0 + g_s)} + \sqrt{g_0^2 - g_{cn}^2 + g_s g_0}]^2} \\
 &= \left[ \frac{g_{cn}/g_0}{\sqrt{1 + g_s/g_0} + \sqrt{1 - (g_{cn}/g_0)^2 + g_s/g_0}} \right]^2. \quad (22)
 \end{aligned}$$

Since  $g_{cn}/g_0$  can approach unity only as  $g_{cn}$  and  $g_0$  each approach zero, the effect of the shunt-input loss  $g_s$  is to impose a practical optimum value for  $g_{cn}/g_0$  which is less than unity. Thus, the conclusion as to the impossibility of attaining conversion without appreciable loss seems to be further strengthened. In Figures 9, 10, and 11 of a later section, curves will be shown for an idealized diode-mixer stage which show how  $g_{cn}$  and  $g_0$  will vary with the operating parameters and which also illustrate the minimum conversion loss imposed by input-circuit loss.

#### 4. The Over-All Signal-to-Noise Ratio

The over-all signal-to-noise ratio of a receiver with a diode-converter stage is a quantity of considerable importance but is not accurately predictable on theoretical grounds. There are several reasons for this statement. In the first place, the measured fluctuation noise in diodes is usually larger than would be expected by theory. The discrepancy in space-charge-limited thermionic diodes was satisfactorily explained by North<sup>10</sup> as due to elastically reflected electrons which disturbed the virtual cathode so as to upset the space-charge reduction of shot noise. Thus, an accurate measure of the noise is not available in general, and presumably changes in anode structure or material of a diode may alter the noise without in other ways affecting the diode performance. Second, diode-noise fluctuations affect both the radio-frequency and the intermediate-frequency circuits and are not necessarily independent of each other. Finally, large-signal, transit-time effects cannot always be neglected at the ultra-high frequencies and may have a bearing on the noise behavior; such effects have not yet been fully investigated.

A rough qualitative notion of the effect of the diode-mixer stage on the signal-to-noise ratio of a receiver can be made, however. For one thing, the conversion loss cuts the signal available at the input of the intermediate-frequency amplifier so that the signal-to-noise ratio will be worse than that of the intermediate-frequency amplifier by a

<sup>10</sup> D. O. North, Part II of "Fluctuations in space-charge-limited currents at moderately high frequencies," *RCA REVIEW*, vol. 5, pp. 117-124; July, 1940.

predictable amount on this score alone. If the diode-mixer stage adds some noise, and it usually will, this decreases the over-all signal-to-noise ratio still more.

It can be seen that the converter stage acts as an attenuator of the signal and as an additional noise source itself. Thus, a radio receiver may consist of an antenna of radiation resistance  $R_a$ , whose effective noise temperature is  $T_a$ , and which is connected to the intermediate-frequency receiver through the mixer as in Figure 6. We may substitute for this combination of antenna and mixer, a resistance at the input to the intermediate-frequency amplifier by placing this resistor at an effective temperature  $T_{eff}$  for noise purposes and by assigning

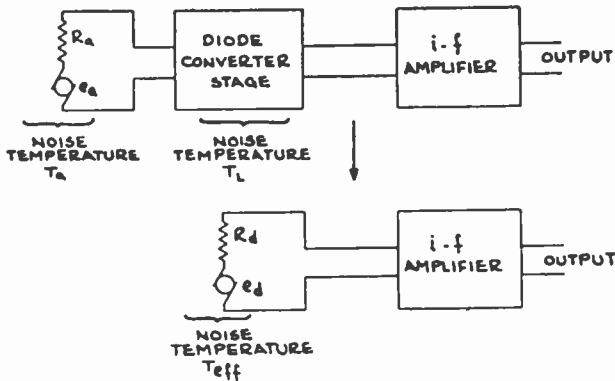


Fig. 6—A receiver consisting of an antenna, a diode mixer, and an intermediate-frequency amplifier may be analyzed for signal-to-noise ratio by replacing the antenna and diode mixer by an equivalent resistor at a noise temperature  $T_{eff}$ .

an available signal power ( $e_d^2/R_d$  of Figure 6) which is at a lower frequency and is less than that of the actual antenna by the conversion loss of the mixer. This is almost exactly the problem which was treated in Section II, 7, of Part III of this series where the effect on signal-to-noise ratio of a passive transducer between antenna and receiver was worked out. Thus, if the diode-mixer stage is considered as a noise source at an effective noise temperature  $T_L$ , reference to Part III gives

$$T_{eff} = T_L(1 - M) + MT_a \quad (23)$$

where  $M$  is the conversion loss expressed as the ratio of output power to input power of the diode mixer (equation (22) above).

The intermediate-frequency system may be measured as if it were a receiver by itself, using a dummy antenna of value  $R_d$  (the output impedance of the diode mixer) as shown in Figure 6. If this dummy antenna is at room temperature, as in the laboratory, the intermediate-

frequency system will have a noise factor<sup>11</sup>  $F_{1-t}$ . The over-all receiver including the diode-mixer stage will then have a noise factor

$$F_{\text{over-all}} = \frac{F_{1-t} - 1 + T_{\text{eff}}/T_a}{M}. \quad (24)$$

In the laboratory, an over-all measurement would be made with a dummy antenna so that  $T_a = T_R$  giving

$$T_{\text{eff}}/T_R = M + (1 - M) T_L/T_R$$

so that

$$F_{\text{over-all (in laboratory)}} = \frac{F_{1-t} + (1 - M) (T_L/T_R - 1)}{M}. \quad (25)$$

These relations are only of indirect value unless the effective noise temperature  $T_L$  of the converter stage is known. The measurement of  $F_{1-t}$ ,  $F_{\text{over-all}}$  and the conversion loss,  $M$ , will permit  $T_L/T_R$  to be calculated from (25).

The effective temperature will not be independent of operating conditions of the diode and may be substantially higher than would be expected on the basis of the highest temperature element in the converter stage. For a thermionic diode mixer with an oxide-coated cathode at 1000 degrees Kelvin, it would be improbable that  $T_L/T_R$  could be less than 2 and not out of reason to expect values of this ratio as high as 10 or more. A crystal diode will have lower values, perhaps between 1 and 3.

#### IV. THE EVALUATION OF AVERAGE AND CONVERSION CONDUCTANCES

##### 1. The General Case

It has already been brought out that best mixer performance will be obtained when the conversion conductance  $g_{cn}$  approaches the average conductance  $g_0$ , provided circuit losses can be neglected. The instantaneous conductance has been written as a Fourier series (equation (4)) so that the quantities  $g_0$  and  $g_{cn}$  are given directly in terms of the Fourier coefficients,

$$g_0 = \frac{1}{2\pi} \int_0^{2\pi} g d(\omega t) \quad (26)$$

<sup>11</sup> See discussion of noise factor in Part III of this series.

$$g_{cn} = \frac{g_n}{2} = \frac{1}{2\pi} \int_0^{2\pi} g \cos n\omega t \, d(\omega t). \quad (27)$$

If negative values of  $g$  are excluded, inspection indicates that, since the integrand of the second expression can never exceed that of the first (since  $\cos n\omega t$  can never exceed unity), the integral in the second case can never exceed the integral in the first case, i.e., the conversion conductance  $g_{cn}$  can never exceed the average conductance  $g_0$ . However, if the conductance  $g$  is an impulsive-type function of finite maximum value and if, during the entire time at which  $g$  is greater than zero,  $\cos n\omega t$  is substantially unity, then the two integrals will each become small and will approach equality. It is therefore seen that, only in the relatively ineffectual case where both  $g_0$  and  $g_{cn}$  are very small, can the two approach equality.

It should also be noted that, in general, the Fourier series for  $g$  (equation (4)) will be convergent, so that conversion at oscillator harmonics is progressively less efficient as the order of harmonic is raised. Again, with the ineffectual impulsive function, all the conversion conductances (at different oscillator harmonics) approach each other in magnitude, but only as they all approach zero.

For a diode, or any other two-element nonlinear device for that matter, the mixer behavior can be estimated from its conductance-versus-voltage characteristic. From this characteristic, the conductance-versus-time curve may be obtained for any particular local-oscillator injection voltage, and a Fourier analysis made. It is more usual to make an analysis directly from points on the curve of conductance versus bias, and some simple 7-point formulas for  $g_{c1}$ ,  $g_{c2}$ , and  $g_{c3}$  have been given.<sup>1</sup> It is also necessary to obtain  $g_0$ , in the present instance. Using Figure 2(a) of reference 1 it may be shown that, to a sufficient accuracy for most purposes,

$$g_0 = 1/12[g_1 + g_7 + 2(g_2 + g_3 + g_4 + g_5 + g_6)] \quad (28)$$

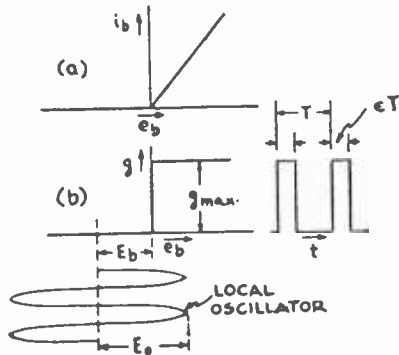
where the  $g_1$ ,  $g_2$ , etc., are points on the curve of the figure.<sup>12</sup> The formula for  $g_{c1}$  as given in the reference is

$$g_{c1} = 1/12[(g_7 - g_1) + (g_5 - g_3) + 1.73(g_6 - g_2)]. \quad (29)$$

It is clear by comparing these formulas for  $g_0$  and  $g_{c1}$  that highest  $g_{c1}$  and lowest  $g_0$  can be obtained by operating the device so that

<sup>12</sup> They are not to be confused with the  $g$ 's of the Fourier series used in the present paper in equation (4).

Fig. 7 — (a) Plate-current-versus-plate-voltage characteristic of an idealized diode. (b) Conductance characteristic of idealized diode showing an applied oscillator with a bias  $E_b$  and the resulting rectangular pulses of conductance versus time.



$g_1 = g_2 = g_3 = 0$ , if this is possible. It is interesting to note that no use is ordinarily found for the diode current-versus-voltage characteristic, except when the average direct current is required.

2. An Idealized Diode

Much can be learned from an examination of the behavior of the idealized diode whose current characteristic is shown in Figure 7(a) and whose conductance characteristic is shown in Figure 7(b). If a local-oscillator voltage, of peak value  $E_o$ , is applied, together with a direct-current bias of value  $E_b$  (from a battery or a by-passed resistor) then the conductance versus time will be the rectangular pulse function shown to the right of Figure 7(b). Such a function has Fourier components such that

$$g_0 = g_{max}\epsilon \tag{30}$$

$$g_{cn} = g_{max} \sin n\pi\epsilon/n\pi \tag{31}$$

where  $\epsilon$  is the fraction of the time during which current flows, i.e.,

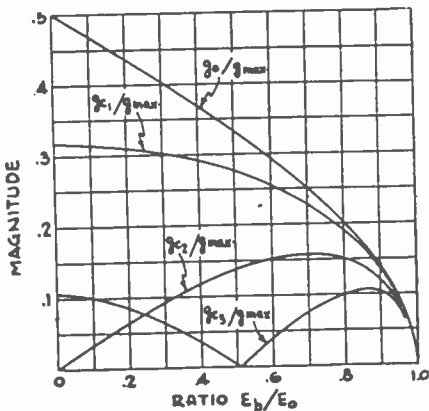


Fig. 8—Average conductance  $g_0$  and conversion conductances  $g_{c1}$ ,  $g_{c2}$  and  $g_{c3}$  for the idealized diode of Fig. 7 as a function of the ratio of direct-current bias to peak oscillator voltage. The curves are plotted as ratios of the conductance to the maximum diode conductance  $g_{max}$ .

$$\pi\epsilon = \cos^{-1} (E_b/E_0). \quad (32)$$

Thus, when  $\epsilon$  is small, it is seen that  $g_0$  and  $g_{cn}$  are approximately equal and the conversion conductances at the different harmonics are all nearly equal but are all very small. Figure 8 shows curves of the average diode conductance and of  $g_{c1}$ ,  $g_{c2}$ , and  $g_{c3}$  as the ratio of bias voltage to peak-oscillator voltage is varied. It is seen that harmonic operation requires a greater bias than fundamental operation.

Of more direct interest are the curves of Figure 9 which show the

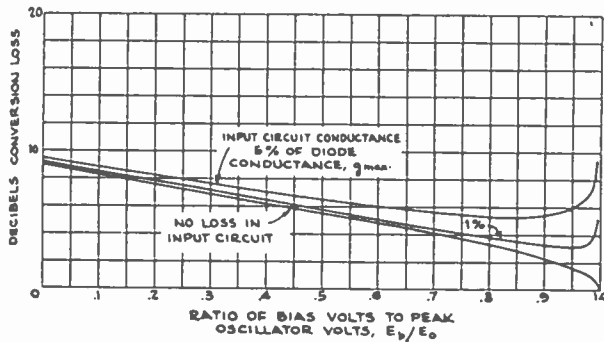


Fig. 9—The conversion-loss characteristic of an idealized diode whose maximum conductance is  $g_{max}$ . The curves are for conversion at oscillator fundamental and show the effect of loss conductance in the input circuit.

conversion loss, using oscillator fundamental, for the idealized diode, again as a function of the ratio of bias to peak oscillator voltage. These curves were computed from (22) and therefore represent optimum values. The curve for a perfect no-loss input circuit is an impracticable ideal which is shown only for comparison. The other curves give the results for an input circuit whose conductance  $g_s$  is 1 and 5 per cent, respectively, of the diode maximum conductance  $g_{max}$ .

A similar set of curves for conversion at second and third harmonics are shown in Figures 10 and 11. It is interesting to compare the optimum results for conversion at a harmonic with normal conversion at fundamental. Taking the minimum conversion losses from Figures 9, 10, and 11, Table I may be prepared. It is seen that harmonic operation is by no means out of the question if a decibel or two more conversion loss can be tolerated. However, Figures 9, 10, and 11 show that the adjustment for lowest conversion loss is much more critical when harmonic conversion is used.

Table I—Minimum Conversion Loss of Idealized Diode

Operation at	Decibel Loss $g_s = 0.01 g_{max}$	Decibel Loss $g_s = 0.05 g_{max}$
Fundamental	3.2	5.3
Second Harmonic	4.0	6.6
Third Harmonic	4.6	7.6

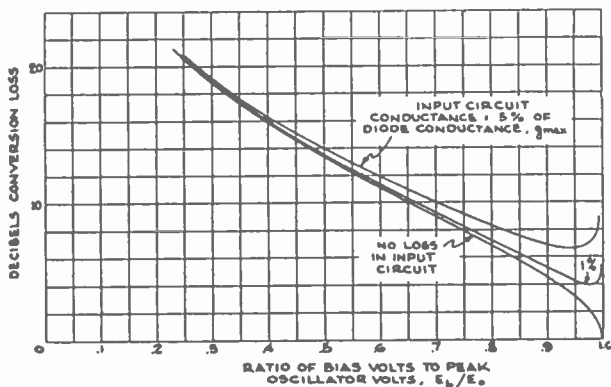


Fig. 10—Conversion loss of an idealized diode with second-harmonic conversion. The curves show the effect of loss conductance in the input circuit.

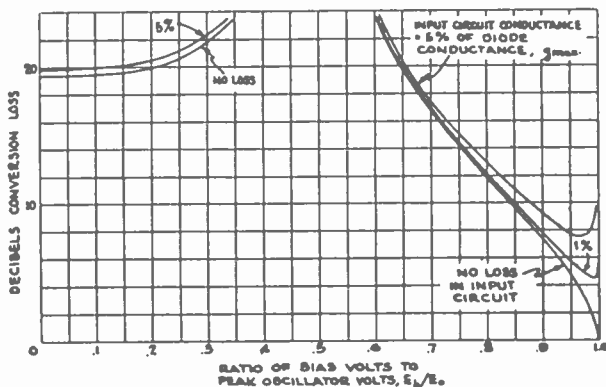


Fig. 11—Conversion loss of an idealized diode with third-harmonic conversion. The effect of loss in the input circuit is shown.

### 3. Discussion of Practical Diodes

Although the idealized diode which has been discussed in Section IV, 2, is not realizable in practice, the behavior shown is qualitatively applicable to practical diodes. Particular characteristic-curve shapes

may be more accurately analyzed by use of the general formulas in Section IV, 1, together with (22). The application of the integral formulas (26) and (27) to such a common characteristic as the 3/2-power law leads to results in terms of elliptic functions<sup>4</sup> and it is often more rapid to use the 7-point approximate formulas (28) and (29). This is certainly true for more complex characteristics for which the analytic expression is difficult to handle.

When, as in practical diodes, the conductance rises gradually with an increase in applied voltage up to the value  $g_{\max}$ , the results will, as a rule, be inferior to those shown in Figures 9, 10, and 11. However, a large oscillator swing together with appropriately large bias does permit an approach to the results shown. In some instances (e.g. crystal diodes), it may be necessary to take into account conduction in both directions. It is clear that this phenomenon increases the average conductance and decreases the conversion conductance under any conditions whatever, so that it becomes impossible to equal the performance of the idealized diode. Analysis shows that there is then an optimum operating condition even if the input circuit is loss-free, and this optimum, of course, has a finite conversion loss.



## U-H-F OSCILLATOR FREQUENCY-STABILITY CONSIDERATIONS\*†

BY

S. W. SEELEY# AND E. I. ANDERSON

RCA License Laboratory,  
New York, N. Y.

### Summary

*Each of the circuit components in an oscillator may change its characteristics with change in temperature. Some of them are subject to change with changes in humidity and operating parameters. These effects are discussed with particular emphasis on change in inductance with change in temperature, since less attention has generally been given this cause of oscillator instability. An oscillator designed to have very small drift is described.*

(12 pages; 3 figures)

---

\* Decimal Classification: R355.912.

† RCA REVIEW, July, 1940.

# Now Manager, Industry Service Laboratory, RCA Laboratories Division, New York, N. Y.

---

## ULTRASHORT ELECTROMAGNETIC WAVES VI — RECEPTION\*†

BY

B. TREVOR

Research Department, RCA Laboratories Division,  
Riverhead, N. Y.

### Summary

*This paper is the concluding article in a series of six on ultrashort electromagnetic waves, written by various engineers in the industrial and educational fields. Reception of ultrashort electromagnetic waves over line-of-sight paths under practical conditions is discussed. It is shown that, when directive antennas are employed, there is an optimum antenna height for which the direct and reflected rays are received in phase, producing maximum effect. The concept of excess-noise ratio is developed which evaluates the merit of a receiver in a manner independent of bandwidth, receiver-impedance, signal-generator impedance, or frequency. A useful reference list is appended to the paper.*

(5 pages; 3 figures)

---

\* Decimal Classification: R111.6.

† Elec. Eng., September, 1942.

# RADIO-RELAY-SYSTEMS DEVELOPMENT BY THE RADIO CORPORATION OF AMERICA\*†

BY

C. W. HANSELL

Research Department, RCA Laboratories Division,  
Rocky Point, L. I., N. Y.

*Summary*—Now that television is ready to provide a new American industry there is need for a nationwide network to distribute the programs. This network may handle many auxiliary services. Radio relays offer a promising means for establishing the network.

Twenty years of RCA radio-relay development made it possible, in 1940, to demonstrate a system for automatic relaying of the present standard television. It operated on frequencies near 500 megacycles, used frequency modulation with amplitude limiting in repeaters, and included a repeater retransmitting the waves on the same frequency as they were received.

The problems of relay-system design are reviewed and formulas, based on reasonable assumptions, are given for calculating the required repeater gain, the output power, and required antenna heights for various spacings between repeaters and for various frequencies. These indicate that the largest spacings for which adequate antenna height can be provided, and the highest frequencies up to some undetermined limit, result in least over-all repeater gain. Preliminary cost analysis indicates optimum repeater spacings will be 35 to 45 miles.

A striking characteristic of radio-relay systems is that they require much less repeater gain than existing coaxial-cable installations when both are adjusted to accommodate the present standard television modulation bands. This difference will be increased if the standards are raised.

Experimental data on cross couplings between antenna systems, an important factor in relay systems, and practical expedients for minimizing them are given.

It is proposed that minimum frequency bandwidths of 15 megacycles should be allowed for relay channels designed to carry the present standard television and it is pointed out that each band may be used over and over, not only in geographically separated areas but even for a number of channels in and out of the same city. This multiple use of frequency bands, and the great value to the public of television networks, justifies generous assignments of frequency space, and promises a great future for radio relaying.

## INTRODUCTION<sup>1</sup>

IF television and its auxiliary services are to expand rapidly, so as to provide a new American industry, and a source of large-scale employment after the war, we must have the means to carry pro-

\* Decimal Classification: R480 × R583.

† Reprinted from *Proc. I.R.E.*, March, 1945.

<sup>1</sup> M. E. Streiby, "Coaxial cable system for television transmission," *Bell Sys. Tech. Jour.*, vol. 17, pp. 438-457; July, 1938.

grams from city to city over nationwide distributing networks.

For years forward-looking research, invention, and development have been directed toward making it possible to provide these networks, and the need to provide them is almost upon us.

Two lines of approach, one through development of coaxial cables and repeaters, and one through development of radio relays, have been followed. The present paper is intended to outline work done by the Radio Corporation of America, on the development of radio-relay systems.

### HISTORICAL

RCA has now been engaged in radio-relay development for more than 20 years. In the course of that development the radio carrier frequencies used have increased from 182 kilocycles to 500 megacycles and the modulation bands have increased from 2000 cycles to 4 megacycles. The type of service has comprised relaying of telegraph signals, international broadcast programs, facsimile, and television. It has included five years' experience with an unattended radio-relay system in commercial service between New York and Philadelphia.

#### *1. 182-Kilocycle Relay for Transoceanic Telegraph Signals*

In 1923 RCA began the development of a radio-relay station at Belfast, Maine. Its purpose was to intercept long-wave transoceanic telegraph signals at a location where directional reception would reduce interference from summer lightning storms and to relay the intercepted signals on another frequency to the Riverhead receiving station for transfer to New York. The relay transmitter was designed to handle several telegraph signals simultaneously. It used single-side-band modulation with a carrier at 182 kilocycles and provided peak power of a few kilowatts. This station was operated experimentally for about a year, until it was replaced with a commercial receiving station connected with New York through wire lines.

#### *2. 3-Megacycle Relay for Transoceanic Broadcast Programs*

In 1924 a supplementary relay transmitter was completed at Belfast to operate on frequencies near 3 megacycles, with a maximum power output of about 250 watts. This transmitter is of incidental historical interest because it is believed to be the second transmitter in the world equipped for piezoelectric quartz-crystal frequency control, the first having been an assembly of units in the laboratory of Professor George H. Pierce at Harvard. It was the first crystal-controlled transmitter put to any practical use. It is also of interest because it relayed the first broadcast programs brought from London

to New York for rebroadcasting here. For RCA it marked the beginning of short-wave equipment development and propagation tests which, in combination with the work of others, resulted in the present world-wide networks for international radio communication.<sup>2</sup>

### 3. 80-Megacycle New York-to-Camden Television Relay<sup>3</sup>

In the meantime RCA and its associated companies carried forward a program of development designed to create a system of television. Eventually this program had made enough progress to justify the creation of an experimental television-broadcast station at the Empire State Building in New York City, and it had become apparent that television networks for carrying programs from city to city would be required.

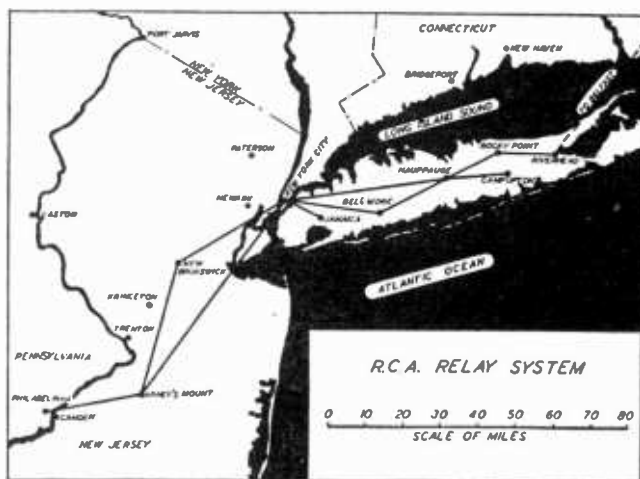


Fig. 1—Locations of radio-relay systems described in this paper.

In 1932 RCA and the National Broadcasting Company, in co-operation with General Electric and Westinghouse undertook the development of a relay station to carry experimental television from New York to Camden, New Jersey. It was demonstrated successfully in 1933. At that time television had reached the point where 120 lines per frame could be used, which required a modulation band of about 250,000 cycles.

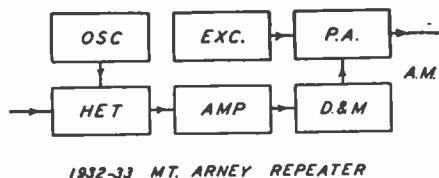
The relay station was located at Arney's Mount, near Mount Holly,

<sup>2</sup> H. H. Beverage, C. W. Hansell, and H. O. Peterson, "Radio plant of RCA Communications, Inc.," *Trans. A.I.E.E. (Elec. Eng., March, 1933)*, vol. 52, pp. 75-82; March, 1933.

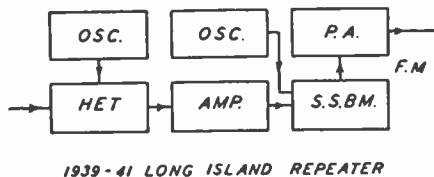
<sup>3</sup> E. W. Engstrom, R. D. Kell, A. V. Bedford, M. A. Trainer, R. S. Holmes, W. L. Carlson, W. A. Tolson and Charles J. Young, "An experimental television system," *Proc. I.R.E.*, vol. 22, pp. 1241-1294; November, 1934.

New Jersey. For reception of signals from the Empire State Building it used a broadside array of dipoles, with a reflector, mounted on a 165-foot steel tower, and for transmission used a resistance-terminated V antenna on 70-foot wooden poles. Most of the amplification in the repeater was done at an intermediate radio frequency so that modulation-frequency currents appeared at only one point in the transmitter.

The Arney's Mount repeater had only a short period of usefulness, for experimental purposes, because at about that time electronic methods of television were being field-tested, and the quality of the television images improved so rapidly with corresponding increases in bandwidth that the repeater very soon was entirely inadequate. It was foreseen that television relaying would have to be done at far



1932-33 MT. ARNEY REPEATER



1939-41 LONG ISLAND REPEATER



IDEAL REPEATER

Fig. 2—Experimental repeaters and ideal repeater.

higher frequencies than could be utilized at the time and that a long-range program of vacuum tube and equipment development would be necessary.

#### 4. 100-Megacycle Unattended Relay System between New York and Philadelphia<sup>4,5</sup>

A long-range program of television-relay development was begun but, in the meantime, an unattended automatic radio-relay system

<sup>4</sup> H. H. Beverage, "The New York-Philadelphia ultra-high-frequency facsimile relay system," *RCA REVIEW*, vol. 1, pp. 15-31; July, 1936.

<sup>5</sup> J. Ernest Smith, Fred H. Kroger, and R. W. George, "Practical application of an ultra-high-frequency radio-relay circuit," *Proc. I.R.E.*, vol. 26, pp. 1311-1326; November, 1938.

for two-way multiplexed telegraph printer and facsimile communication between New York and Philadelphia was undertaken in 1934. This relay system used two repeaters, in each direction, one at Arney's Mount and one at the RCA transoceanic station at New Brunswick, New Jersey. It operated in a range of frequencies near 100 megacycles and provided for a modulation range up to 20,000 or 30,000 cycles.

The system was placed in operation in 1936 and was a regular part of RCA facilities on the circuits from New York to Philadelphia, Baltimore, and Washington until the Federal Communications Commission ordered it shut down soon after the beginning of the war. Its approximately 5 years of continuous unattended operation gave us some valuable experience and provided a service of greater reliability than had been obtained with cable pairs over the same circuit. It proved that radio relaying with fully automatic, unattended repeaters is practical.

#### 5. 500-Megacycle Television-Relay Demonstrations<sup>6-9</sup>

By the end of 1939 enough progress had been made in the development of the new vacuum tubes for use at very high frequencies, and in the development of radio repeaters and relay stations that 450- to 500-megacycle experimental radio-relay stations had been established on Long Island, at Hauppauge, and at the Laboratory near the transoceanic transmitting station at Rocky Point. By means of these repeaters, television signals broadcast from the Empire State Building were picked up at Hauppauge and relayed automatically through Rocky Point to a terminal receiver in the Laboratory near the transoceanic receiving station at Riverhead. This relay system was designed to accommodate the full modulation bandwidth permitted by the present television standards.

It employed frequency modulation of the radio carrier current as a result of which the technical problems were simplified. It became possible to use simple amplitude limiting to control power levels in the system and the inherently nonlinear response characteristics of vacuum tubes were reduced to a smaller factor in the production of distortion.

---

<sup>6</sup> Andrew V. Haeff and Leon S. Nergaard, "A wide-band inductive-output amplifier," *Proc. I.R.E.*, vol. 28, pp. 126-130; March, 1940.

<sup>7</sup> H. M. Wagner and W. R. Ferris, "The orbital beam secondary-electron multiplier for ultra-high-frequency amplification," *Proc. I.R.E.*, vol. 29, pp. 598-602; November, 1941.

<sup>8</sup> F. H. Kroger, Bertram Trevor, and J. Ernest Smith, "A 500-megacycle radio-relay distribution system for television," *RCA REVIEW*, vol. 5, pp. 31-50; July, 1940.

<sup>9</sup> I. G. Maloff and W. A. Tolson, "A résumé of the technical aspects of RCA theatre television," *RCA REVIEW*, vol. 6, pp. 5-11; July, 1941.

Late in 1940 a third relay station was established at the former site of NBC broadcast station WCAF at Bellmore, Long Island, and a terminal receiving station was set up at the RCA Building in New York. This made it possible to relay from Hauppauge back into New York and many demonstrations of relaying were made, in 1940 and 1941, including demonstrations for the Federal Communications Commission and National Television System Committee.

These demonstrations should some day have much historic interest because they comprised all the elements of a complete television broadcast service including studio programs, programs brought from a distance by radio relay, and by coaxial cable, broadcasting of programs to home receivers, and showing of programs on a large screen in a theater.

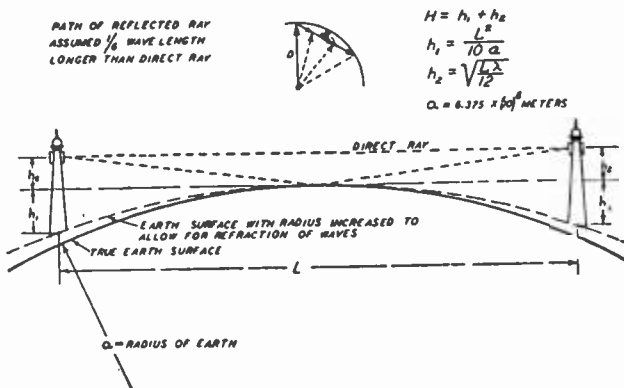


Fig. 3—Radio-relay space circuit, vector addition of direct and reflected waves for various efficiencies of reflection, and antenna heights for equivalent of free-space propagation.

An important part of these tests was the demonstration of radio relaying with a repeater so designed and adjusted that the input and output carrier frequencies were equal.

#### PRESENT STATUS OF RADIO-RELAY DEVELOPMENT

Before the development of radio-relay systems suitable for television had been interrupted by the war, the initial and most difficult pioneering work had been accomplished and the technical basis laid for a great nation-wide system of radio relays capable of providing not only television networks but many other important services. Many detail problems, such as must be solved in establishing any new service, still remained, but it could be stated with confidence that there were no insuperable technical obstacles remaining to prevent the establishment of a successful radio-relay service.

The range of frequencies which will be used for relaying is so high that it has become possible to utilize each frequency channel over and over again, not only over circuits which are spaced apart geographically but even, with some limitations, for a number of circuits in and out of the same city. It is this possibility of using the same frequency band over and over again which justifies the assignment of wide-channel bands to television relay systems and which promises a great future for radio relays.

A striking characteristic of properly designed radio-relay systems

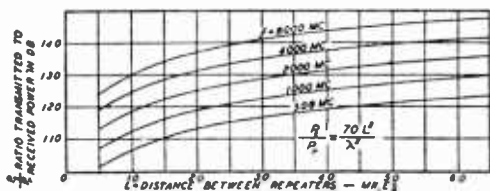


Fig. 4—Ratio of transmitted-to-received power for equivalent of short dipole antennas in free space.

Fig. 5—Power gain per hop due to antenna directivity as compared with short dipoles.

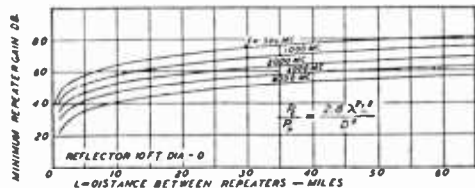
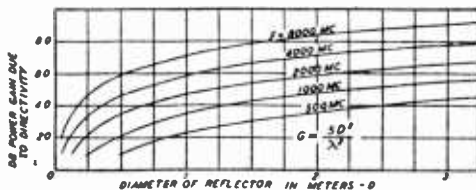


Fig. 6—Minimum power gain per repeater.

operated on frequencies above 500 megacycles is that they require much less amplification in a given distance than the concentric-cable systems, when both are required to meet the present and future television-modulation-bandwidth requirements.

As television broadcasting moves to the higher-frequency portions of the spectrum and as it becomes possible to include color, it is natural that the bandwidth required for transmission will be increased, and it then seems probable that radio relaying will receive greater recognition as the most promising means, technically and economically, for the distribution of television programs.

A fortunate circumstance is that, in establishing a radio-relay system, a major portion of the cost is represented by sites and towers



and that no developments which can be foreseen at present will destroy the value of these investments. Instead, it is anticipated, future developments will make it possible to utilize higher radio frequencies and to provide more perfect reproduction of modulations without requiring substantial alterations in sites and towers.

Before the war the development of vacuum tubes and repeaters had been carried far enough to make it practical to utilize frequencies for television relaying in the range of about 300 to 1000 megacycles. It is anticipated that, as soon as restraints due to the war are removed, the frequency range will be extended upward until, eventually, frequencies of 3000 megacycles or more may be used.

#### PHASE OR FREQUENCY MODULATION PREFERRED FOR RELAYING<sup>10-13</sup>

At the present time phase or frequency modulation of the radio carrier current by the video modulation frequencies is considered preferable to amplitude modulation. In practice a hybrid, or compromise, between phase and frequency modulation, obtainable by means of suitable pre-emphasis of the modulation currents in either a phase-modulated or a frequency-modulated terminal transmitter is preferred.

By using this hybrid type of modulation it is possible to strike some sort of optimum balance between the width of frequency band required for modulation side frequencies and the relative magnitude and frequency distribution of noise in the output of the relay system. This optimum balance may vary according to the character of the material transmitted so that the means to attain it should not be standardized but should be left to the agency operating the system.

When phase or frequency modulation is used in a radio-relay system it is possible to use simple amplitude limiting in each repeater as a means to overcome the effects of space-circuit variations. It is expected that this will make it unnecessary to employ pilot current channels with automatic level controls such as would be required in amplitude-modulated, or single-sideband-modulated systems.

Amplitude limiting makes it possible to operate the high-power portions of repeaters as class C amplifiers, or equivalent, which is a condition tending toward high-power-conversion efficiency.

In the phase- or frequency-modulated system the inherently non-

---

<sup>10</sup> Murray G. Crosby, "Communication by phase modulation," *Proc. I.R.E.*, vol. 27, pp. 126-136; February, 1939.

<sup>11</sup> Murray G. Crosby, "Frequency modulation noise characteristics," *Proc. I.R.E.*, vol. 25, pp. 472-514; April, 1937.

<sup>12</sup> Murray G. Crosby, "Frequency modulation propagation characteristics," *Proc. I.R.E.*, vol. 24, pp. 898-913; June, 1936.

<sup>13</sup> Edwin H. Armstrong, "A method of reducing disturbances in radio signaling by a system of frequency modulation," *Proc. I.R.E.*, vol. 24, pp. 689-740; May, 1936.

linear amplitude-response characteristics of amplifiers become a smaller factor in determining modulation wave-form distortions and the characteristics of frequency-selective intertube coupling circuits become relatively more important. For this reason it is desirable to keep the number of the coupling circuits to a minimum by providing high gain per tube, provided the high gain can be obtained in a stable manner.

Fortunately, a good start toward providing high gain per tube has been made through the use of secondary-emission amplification

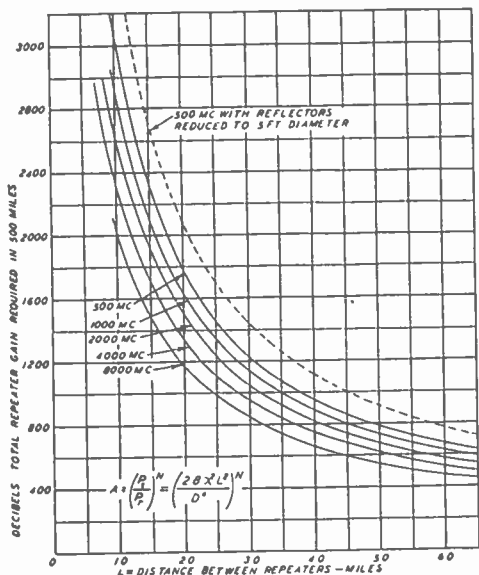


Fig. 7—Total repeater gain in 500 miles when using reflectors 10 feet in diameter.

to supplement the gain per tube obtainable by more conventional methods. In addition, the tube designers are making considerable progress in adapting tubes and circuits one to the other. Because of these and related developments the prospects for greatly improved repeaters, soon after the war, now seem to be good.

RELAY SYSTEM SIGNAL-TO-NOISE-RATIO REQUIREMENTS<sup>14-17</sup>

It is assumed that facsimile and television systems will be modulated by an electrical potential which differs from a reference value in proportion to the square root of brightness. Since brightness is a

<sup>14</sup> Donald G. Fink, "Television Standards and Practice," McGraw-Hill Book Co., Inc., New York, N. Y., 1943.

<sup>15</sup> Matthew Luckeish and Frank K. Moss, "The Science of Seeing," D. Van Nostrand Co., New York, N. Y., 1937.

<sup>16</sup> Heinrich Kluver, "Visual Mechanisms," The Jacques Cattell Press, Lancaster, Pa., 1942.

<sup>17</sup> E. E. Kenneth Mees, "The Theory of the Photographic Process," The Macmillan Company, New York, N. Y., 1944.

measure of radiated power, this assumption is that electrical power is made proportional to light power, when the reference value of potential is taken as zero. The resulting modulation characteristic is a fair approximation to the "approximately logarithmic" response characteristic suggested recently by the Television Panel of the Radio Technical Planning Board.

For message-type facsimile recording at a rate of one picture per frame, a reasonably satisfactory service can be provided if a brightness range of 20 to 1 is provided and brightness modulations due to relay system noise are held to an average value of about 1.5 per cent at the lowest brightness level. This corresponds, in an amplitude-modulated system, to a carrier-to-noise power ratio of 51.2 decibels.

In a frequency-modulated relay system, operated with a modulation index of 1, there is a 3-to-1 gain in ratio of signal power to noise power due to the noise-suppressing effect of frequency modulation. On the other hand there is a 2-to-1 power loss due to synchronizing pulses occupying a portion of the modulation characteristic. These two factors combined give a net gain of 1.5-to-1, or 1.8 decibels. We can, therefore, fulfill the operating specification stated in the previous paragraph with a carrier-to-noise power ratio of  $51.2 - 1.8 = 49.4$ , or say 50 decibels.

When it is desired to obtain an improved signal-to-noise ratio for the handling of higher-quality material it is possible to obtain the desired improvement by repeating the picture through any number of frames to form a single record in which the modulations due to noise are very largely averaged out into a nearly uniform minimum average power and brightness level. Much of the effect of this minimum average level upon the record can be eliminated by thresholding.

Fortunately, the noise requirements for television are less stringent than the assumed requirements for page-per-frame facsimile. In television the viewer cannot perceive individual successive images except perhaps for rare occasions when some object, not followed by the eyes, moves rapidly across the field. More generally the visual and mental mechanism causes the consciousness to combine the contributions of a considerable number of images.

If the contributions of all the successive images, attenuating with elapsed time, could be expressed in terms of an equivalent number of unattenuated images, then we might expect an averaging out of the effects of noise which would improve the image-to-noise power ratio in proportion to the equivalent number of unattenuated images. This averaging process is analogous to frequency selectivity in ordinary communications systems.

The equivalent number of images apparently can reach quite large values, depending upon the mental condition and attitude of the observer, the character of the pictures, and the degree to which interest and attention are centered on the program rather than on the technical perfection of reproduction.

In the absence of scientific-test results it seems fair to assume that, when still pictures are transmitted over a television system, the superposition of successive images results in a gain in image-to-noise ratio of 10 to 20 decibels.

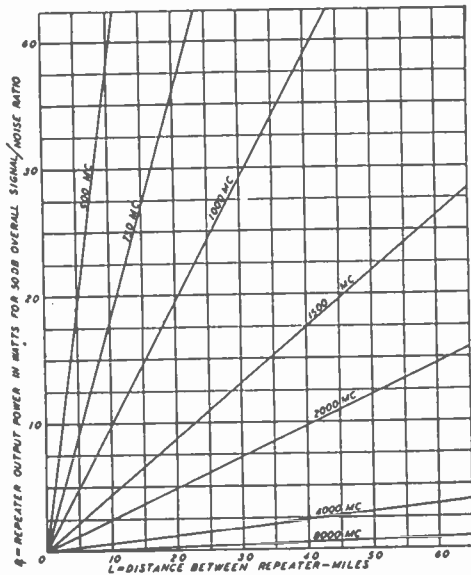


Fig. 8—Power output required from repeaters.  
 $P_r = (2.8 \times 10^{-12} L^2 NP_r) / D^4$ .

If the foregoing reasoning is correct it seems that if a relay system is designed to provide a 50-decibel carrier-to-noise power ratio it will be quite adequate for television and will not make any significant contribution to noise in television-broadcast systems. This figure of 50 decibels will be assumed in what follows.

#### THE OVER-ALL PROBLEM OF TELEVISION RADIO RELAYING

One of the first problems in planning a television radio-relay system is to make a proper choice of the average spacing between repeaters and the consequent height of repeater-station towers. In this problem the factors of cost are in conflict with the factors of over-all technical performance and reliability of service.

Assuming that no less than a 500-mile relay system will be required to provide an acceptable range of service, a calculation has been made of the over-all technical requirements for a system of this length.

In making the calculations the following assumptions were made:

1. The over-all length of the system would be 500 miles. This is roughly the length of a system linking Boston, New York, Philadelphia, Baltimore, Washington and some of the smaller cities along the route.
2. Smooth spherical earth was assumed, keeping in mind the fact that rolling country would cause variations in repeater spacings and heights of towers, probably in a manner to increase the system requirements beyond the calculated requirements. To allow for bending or refraction of the waves around the curvature of the earth,

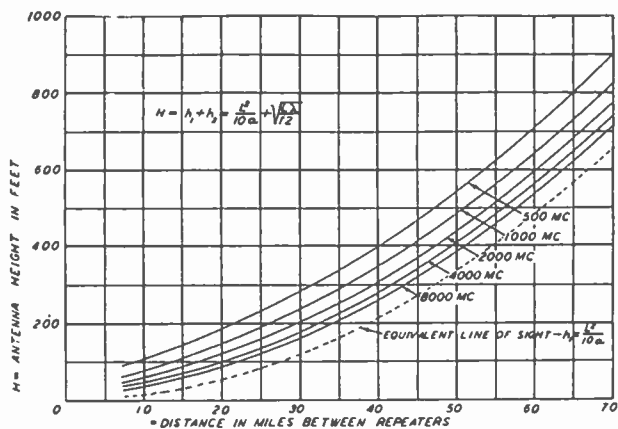


Fig. 9—Antenna heights to provide equivalent of free-space propagation.

it is customary to calculate the required heights of antennas using a formula which increases the earth's radius by 1.33. For the present calculation a more conservative factor of 1.25 was used, it being normal minima rather than average signal strengths which are considered important.

3. It was assumed that antennas with reflectors 10 feet in diameter would be used and that they would be mounted at such a height that the direct ray of radiation and the ray reflected from the ground would lack 60 degrees of phase opposition. Any lower height would cause a rapid decrease in average received signal strength and a rapid increase in variations of the received signal strength. A greater height would add to the cost of towers. This assumption makes it possible to ignore variations in the percentage of power absorbed or reflected by the ground without introducing serious error.

4. It was assumed that the final noise level at the output end of a relay system would be the summation of the noise levels introduced at all the repeaters and would therefore be proportional to the number of repeaters used in the 500-mile distance.

5. It was assumed that all noise in the system would be developed in the input ends of the repeaters themselves and that a 50-decibel over-all carrier-to-noise power ratio would be required in order that the relay system might not make a substantial contribution to the level of noise which can be observed in the viewer's receiver. It seems probable that repeater noise will be predominant except possibly for reception in cities where man-made noise reaches relatively high levels. Present experience seems to indicate that the noise generated in the head-end of receivers, or repeaters, is of the order of

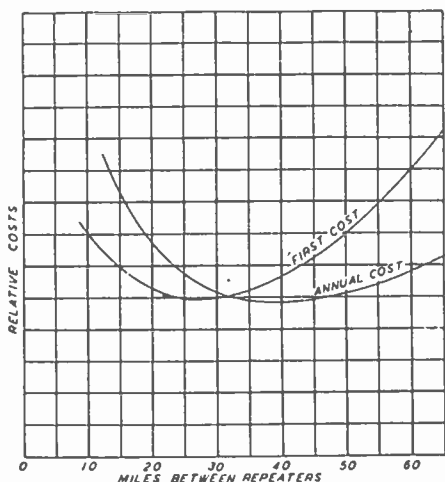


Fig. 10—Radio-relay relative costs.

30 times the power level produced by thermal agitation in the first input circuit. This ratio is not a constant for all frequencies nor for all periods of development, but will probably be representative of the state of the art as any new band of frequencies is opened up for radio-relay use. It is the ratio which is assumed here.

6. It was assumed that the effective frequency band-width of the system for determining carrier-to-noise ratio, to accommodate both modulation sidebands, would be 10 megacycles. This is believed to be a reasonable assumption, based upon the present television-broadcast standards. The actual total band occupied by a fully modulated carrier will be greater, perhaps 15 to 20 megacycles.

Based on the foregoing assumptions, calculations were made according to the following symbols and formulas:

#### LIST OF SYMBOLS

$a$  = radius of the earth in same units as  $\lambda$ .  
( $a = 6.375 \times (10)^6$  meters).

- $A$  = total amplification power ratio for a whole relay system.
- $B$  = effective frequency bandwidth of the relay system, in cycles per second. Normally this will be twice the band of modulation frequencies, all other noise at higher modulation frequencies being presumed invisible on the television receiver screens.
- $D$  = diameter of main parabolic reflector, in an antenna system of optimum design, in same units as  $\lambda$ .
- $E$  = radiation field strength in volts per meter.
- $G$  = power-gain ratio, due to directivity, as compared with a short capacitance-loaded dipole antenna.
- $h_1$  = antenna height required to give barely an equivalent line of sight between antennas at each end of a space circuit, taking into account refraction, assuming a smooth spherical earth.
- $h_2$  = additional antenna height required to give equivalent of free-space propagation between antennas at each end of a space circuit.
- $H = h_1 + h_2$  = total antenna height required to give equivalent of free-space propagation between antennas.
- $I$  = current in a short capacitance-loaded dipole in amperes.
- $\lambda$  = wavelength of the radio wave, in units consistent with other dimensions given in the formulas.
- $L$  = distance between repeaters in same units as  $\lambda$ .
- $N$  = number of space-circuit hops in a relay system.
- $P_m$  = minimum theoretical thermal-agitation noise power, in watts, in first circuit of each repeater.
- $P_n$  = practical equivalent noise level, in watts, in the input circuit of the terminal receiver required to match the accumulated noise of a relay system of  $N$  hops.
- $P_p$  = practical equivalent noise level, in watts, required in input circuit of each repeater to give the actual noise in the system which is expected in practice.
- $P_r$  = practical minimum required received power, in watts, after each hop, to provide a commercially acceptable relay system, assuming the noise to be substantially all repeater noise.
- $P_T$  = practical minimum required transmitted power, in watts, required for each hop to provide a commercially acceptable relay system, assuming the noise to be substantially all repeater noise, for any given set of assumed conditions.
- $R$  = radiation resistance of a short capacitance-loaded dipole antenna.
- $X$  = length of a short capacitance-loaded dipole in meters.

FORMULAS<sup>18 20</sup>

1.  $P_m = 0.8 \times (10)^{-20} B$  watt due to thermal agitation in each repeater-input circuit, at a temperature of 20 degrees centigrade. (Another  $0.8 \times (10)^{-20} B$  appears as radiated power in the matched-antenna system.)
2.  $P_n = 24 \times (10)^{-20} B$  watt due to all equipment causes, equivalent noise power in each repeater input circuit, at present stage of vacuum-tube development, in the frequency range from 500 to 4000 megacycles. At present the noise power level in good equipment is about 30 times the minimum thermal-agitation noise.
3.  $P_n = NP_n$  watts in final receiver-input circuit of a relay system, after  $N$  hops, due to accumulation of noise from all repeaters.
4.  $P_r = (10)^5 NP$  watts required to give a barely acceptable over-all signal-to-noise ratio in a radio-relay system of  $N$  hops. This assumes a 50-decibel signal-to-noise ratio in the relay system which is 10 to 20 decibels better than the minimum permissible at the final television-receiver screen.
5.  $G = 5D^2/\lambda^2$  maximum obtainable gain due to directivity from an antenna system with a main parabolic reflector of  $D/\lambda$  wavelengths in diameter. The value of  $G$  must be squared to give total gain per hop if the same type of antenna is used for both transmitting and receiving.
6.  $P_T/P_r = 70L^2/\lambda^2$  ratio of transmitted to received power for equivalent of free-space propagation between short dipole antennas.
7.  $P_T/P_r = 2.8\lambda^2 L^2/D^4$  ratio of transmitted to received power for equivalent of free-space propagation between directional antennas with main reflectors  $D/\lambda$  wavelengths diameter.
8.  $A = (P_T/P_r)^N = (2.8\lambda^2 L^2/D^4)^N$  the total amplification required in a relay system with a total length of  $LN/\lambda$  wavelengths.
9.  $P_T = 2.8 \times (10)^5 \lambda^2 L^2 NP_n/D^4$  watts minimum acceptable power output from each repeater in a system of  $N$  hops, each  $L/\lambda$  wavelengths long, using antennas with reflectors  $D/\lambda$  diameter, where  $P_n$  is the equivalent noise power in the first circuit of each repeater.
10.  $P_T = 6.72\lambda^2 L^2 BN/(10)^{14} D^4$  watts minimum acceptable power output from each repeater for giving 50 decibels over-all signal-to-equipment noise ratio in a system where the noise power in each repeater is 30 times that due to thermal agitation in the circuit of each repeater.
11.  $P_T = 6.72\lambda^2 L^2 N/(10)^7 D^4$  watts required to keep a 50-decibel signal-to-equipment noise ratio in a practical relay system with a bandwidth of 10 megacycles (modulation band of 5 megacycles).

<sup>18</sup> J. B. Johnson and F. B. Llewellyn, "Limits to amplification," *Trans. A.I.E.E. (Elec. Eng., November, 1941)*, vol. 53, pp. 1449-1454; November, 1934.

<sup>19</sup> "Valve and Circuit Noises," *Wireless World*, vol. 46, pp. 262-265; May, 1940.

<sup>20</sup> F. E. Terman, "Radio Engineers' Handbook," McGraw-Hill Book Co., Inc., New York, N. Y., 1943.



12.  $h_1 = L^2/10a$  the antenna heights required to give equivalent clear line of sight over smooth spherical earth of radius  $a/\lambda$  wavelengths, using a factor of 1/1.25 to account for normal refraction. The value of  $(a)$  in the above formula is 3960 miles, 6,370,000 meters or 20,900,000 feet. (All factors to be in same unit of measure.)
13.  $h_2 = \sqrt{L\lambda/12}$  additional height required to give equivalent of free-space propagation. This corresponds to 60 degrees from phase opposition for direct and reflected rays. Increasing  $h_2$  by  $\sqrt{3}$  will give phase addition of direct and reflected rays, a condition of maximum received signal strength where the received power can approach as a limit four times the received power for equivalent of free-space propagation.
14.  $H = h_1 + h_2 = L^2/10a + \sqrt{L\lambda/12}$  total antenna height over smooth spherical earth to give equivalent of free-space propagation.
15.  $E = 60XI/L\lambda$  field strength in volts per meter in the direction of maximum radiation from a short, capacitance-loaded, dipole antenna carrying a uniform current  $I$  over a length of conductor  $X$ .
16.  $R = 789X/\lambda^2$  ohms, the radiation resistance of a short capacitance-loaded doublet antenna.
17.  $P_r = I^2R = 789X^2I^2/\lambda^2$  the power radiated from a short capacitance-loaded doublet antenna.
18.  $P_r = E^2X^2/4R = E^2\lambda^2/3156$  watts, the received power from an impedance-matched short capacitance-loaded dipole antenna in a radiation field of  $E$  volts per meter (all other dimensions also in meters).

SAMPLE CALCULATION

Assume that we have a 500-mile radio-relay system comprising 10 hops of 50 miles each. Each repeater will use receiving and transmitting antennas with reflectors which are 3 meters (about 10 feet) in diameter, mounted at a height required to give the equivalent of free-space propagation. The frequency will be assumed to be 1000 megacycles, corresponding to a wavelength of 0.3 meter and the bandwidth will be taken as 10 megacycles.

Expressed in symbols, with dimensions in meters:

$$N = 10$$

$$\lambda = 0.3 \text{ meter}$$

$$D = 3 \text{ meters}$$

$$B = (10)^7 \text{ cycles}$$

$$L = 50 \times 1610 = 80,500 \text{ meters}$$

The minimum thermal-agitation noise power, at 20 degrees centigrade, effective in the first circuit of each repeater, assuming that the circuit is matched to the antenna system, and taking into account that half of the total thermal-agitation noise power is radiated, is  $P_m = 0.8 \times (10)^{-20} \times (10)^7 = 0.8 \times (10)^{-13}$  watt.

According to the present state of the art, the actual effective noise power in each repeater will be about 14.8 decibels, or 30 times greater than the minimum thermal-agitation noise power. This raises the effective noise level in each repeater, as referred to the input circuit, to the practical value of  $P_p = 30P_m = 24 \times (10)^{-13}$  watt.

Since there are 10 repeaters in cascade, and each adds its quota of noise power to the final signal-to-noise ratio, the final noise power accumulated and made effective in the terminal-receiver input circuit is  $P_n = 10P_p = 24 \times (10)^{-12}$  watt.

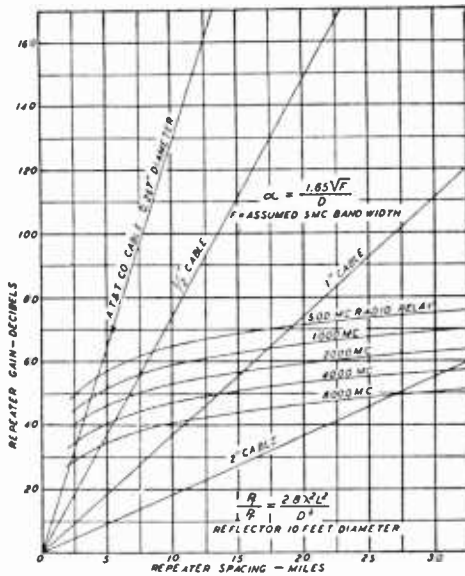


Fig. 11 — Cable and radio-relay systems, gain per repeater required for various repeater spacings.

The received power at each input circuit, required to give an overall 50-decibel signal-to-noise ratio for the relay system is  $P_r = (10)^5 P_n = 2.4 \times (10)^{-6}$  watt.

The ratio of transmitted to received power over each hop, if we assumed that short capacitance-loaded dipole antennas without reflectors were used, would be  $P_t/P_r = 70 \times (80,500)^2 / (0.3)^2 = 5.05 \times (10)^{12}$ , or 127 decibels.

If we use directional antennas for both transmission and reception, with maximum practical gain obtainable from parabolic reflectors, as compared with the short dipoles, the gain for each antenna will be about  $G = 5 \times (3)^2 / \lambda^2 = 500$  in power, or 27 decibels.

This gain is effective at both ends of the circuit and provides a total gain of  $G = 25 \times (10)^4$ , or 54 decibels.

The directional-antenna gain reduces the gain required for trans-

mission between short dipoles to  $P_T/P_r = (5.05 \times (10)^{12}) / (25 \times (10)^4) = 20 \times (10)^6$ , or 73 decibels.

This figure of  $20 \times (10)^6$ , or 73 decibels, is the required amplification gain per repeater in the system.

The total gain of the 10 repeaters in cascade is  $A = (P_T/P_r)^{10} = [20 \times (10)^6]^{10} = (10)^{73}$  approximately, or 730 decibels.

The output power required from each repeater is  $P_T = 20 \times (10)^6 \times 2.4 \times (10)^{-6} = 48$  watts.

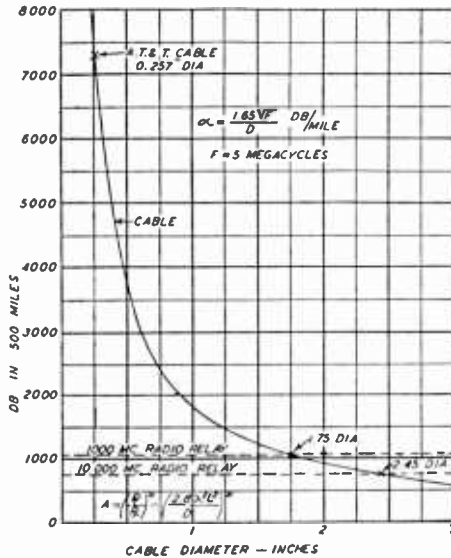


Fig. 12—Cable and radio-relay systems amplification required in 500 miles.

The antenna height required to give the equivalent of free-space propagation is

$$\begin{aligned}
 H &= (80,500)^2 / (10 \times 6.37 \times (10)^6) \\
 &\quad + \sqrt{(80,500 \times 0.3) / 12} \\
 &= 101.8 + 44.8 = 146.6 \text{ meters, or } 480.8 \text{ feet.}
 \end{aligned}$$

SUMMARY OF CALCULATIONS

Calculations made from the formulas led to the results outlined in Tables I, II, and III. The data in all of these tables are based on the assumption that antenna heights are adjusted to give the equivalent of free-space propagation and that reflector diameters are 3 meters (10 feet) in diameter.

The data contained in the tables indicate that the total decibels power gain, or total amplification of all the repeaters in cascade,

decreases rapidly as the spacing between repeaters is increased. Since the amount of repeater equipment in cascade, the probability of failures in operation, and the undesirable distortions of the useful modulation, all increase more or less in proportion to the total required power gain in the system, it will be evident that excellence of technical performance favors a large spacing between repeaters.

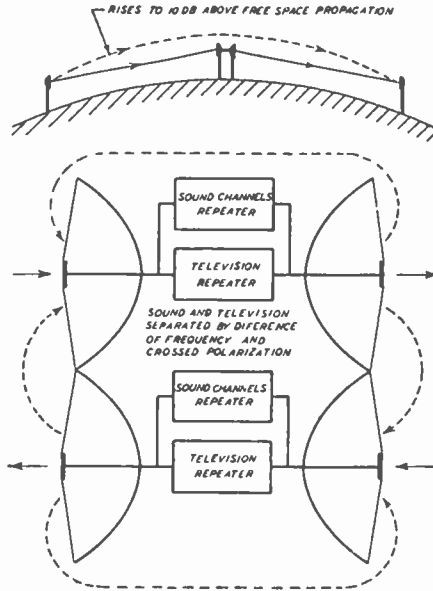


Fig. 13—Undesired coupling paths in radio-relay systems.

Table I—500-Megacycle Television Radio-Relay System

Repeater Spacing in Miles	Repeater Gain in Decibels	Repeater Power in Watts	Antenna Height in Feet
10	65	38.7	106.3
15	68.6	58	144.1
20	71	77.3	185.3
25	73	96.7	230.9
30	74.6	116	281.8
35	75	135.3	338
40	77.2	154.8	399.8
45	78.2	174	467.5
50	79	193.3	541.5
55	79.8	212.5	623
60	80.6	232	709.3
65	81.4	252	800.5
70	82	271	901.5
75	82.6	290	1005

Table II—1000-Megacycle Television Radio-Relay System

Repeater Spacing in Miles	Repeater Gain in Decibels	Repeater Power in Watts	Antenna Height in Feet
10	59	9.68	79.1
15	62.6	14.5	111.3
20	65.2	19.38	146.4
25	67	24.2	187.6
30	68.6	29.05	234
35	70	33.9	287.1
40	71	38.75	349
45	72.2	43.6	409.8
50	73	48.4	480.8
55	73.9	53.2	558.8
60	74.6	58.1	642.3
65	75.4	62.9	731
70	76	67.8	829.3
75	76.6	72.6	930.5

Table III—2000-Megacycle Television Radio-Relay System

Repeater Spacing in Miles	Repeater Gain in Decibels	Repeater Power in Watts	Antenna Height in Feet
10	53	2.41	59.8
15	56.6	3.62	87.1
20	59.2	4.825	119.4
25	61	6.03	157.1
30	62.6	7.25	200.9
35	64	8.45	250.9
40	65	9.65	306.6
45	66.2	10.9	368.8
50	67	12.1	437.5
55	67.9	13.3	513.8
60	68.6	14.5	595.2
65	69.4	15.7	681.8
70	70	16.9	778.3
75	70.6	18.1	877.5

Opposed to the use of large spacings between repeaters is the necessity to use higher output power and greater gain at each repeater, which increases the equipment and repeater-station-development difficulties. In addition, large spacing between repeaters requires the use of high and costly towers. A contributing factor of unknown future importance is the mutual hazard which high towers and airplanes provide for each other. This may result in a need for co-ordination and compromise in respect to regulations which at present appear to limit heights of radio structures without similarly limiting other structures, such as chimneys.

An attempt has been made to arrive at the relative cost per mile year for radio-relaying systems for several assumed radio frequencies

and for various spacings between repeaters. The costs have had to be based upon more or less arbitrary assumptions and cannot be accurate for determining actual costs, but are believed to be nearly correct for relative costs for various assumed conditions. They have led to the conclusion that, over ideal smooth spherical earth, if that were possible, repeater spacings in the range of 35 to 45 miles would provide minimum annual cost.

These cost studies indicate that the investment cost and annual cost per television channel can decrease quite rapidly as the number of channels provided over a given system is increased above the assumed minimum of one channel in each direction, operable simultaneously. This suggests that, whenever possible, each relay system should be designed to handle a number of channels in each direction.

As to choice of radio-carrier frequency, it is quite evident that the highest possible frequency should be used up to some unknown limit where it is no longer possible to make effective use of a certain size of antenna, and where the space-circuit propagation becomes too variable. Before the war the highest frequencies which could be used were in the neighborhood of 500 megacycles, but it is possible that frequencies up to 3000 megacycles or more might be chosen if there were no equipment limitations.

At the present time it is a reasonable assumption that, except for unusual cases where natural obstacles require very long distances between repeaters, television relaying can be started soon after the end of the war in the range of 300 to 1500 megacycles.

Assuming that sufficient incentive, in the form of business opportunities for qualified organizations, is held out it may be anticipated that repeater development soon will extend the range of available frequencies up to, and perhaps beyond, 3000 megacycles.

#### COUPLINGS BETWEEN DIRECTIONAL ANTENNAS

Several years ago a series of measurements were made to determine the order of magnitude of the coupling between directional-antenna systems of the type which comprise simple dipole radiators in parabolic reflectors. These measurements are considered reliable only for determining order of magnitude, because there are many variations in conditions which can have an effect upon practical results. The results obtained may be summarized very briefly as follows:

##### *1. Antennas Close Together Pointed in Same Direction*

- (a) Radiators Either in Same Straight Line or with One Turned by 90 Degrees

In this case the ratio of power transmitted from one antenna to power picked up by the other can be approximately  $P_T/P_r = 60,000 (D/\lambda)^4$ .

(b) Radiators Turned Parallel, at Right Angles to Line between Them

$$P_T/P_r = 600 (D/\lambda)^4.$$

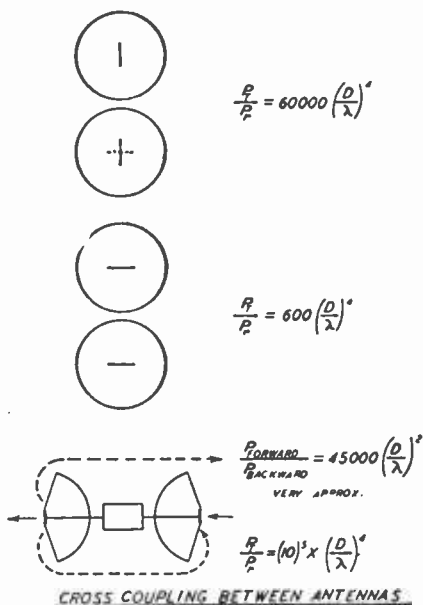


Fig. 14—Order of magnitude of ratio of transmitted power to power received over undesired coupling paths.

### 2. Effect of Spacing between Reflectors

If the spacing between reflectors is increased from substantially zero to a distance between the closest points equal to the diameter, the cross coupling is reduced by about 10-to-1 in power for antennas with reflectors about 5 wavelengths in diameter. However, for radiators end to end, the change was not smooth but showed oscillations over a range of about 20 decibels upward from the values which would be given by the foregoing formula for  $P_T/P_r$ . These oscillations are undoubtedly due to passing through conditions which balance portions of the coupling paths against other portions.

No oscillations of feedback coupling with increasing spacing were observed when the dipoles in the reflectors were set parallel to one another and at right angles to the line between them. In this case the energy fed across from one to the other falls off smoothly as the distance between reflectors is increased.

### *3. Ratio of Power Forward to Power Backward*

From general theoretical considerations it might be expected that the ratio of power forward to power backward from an antenna system with a parabolic reflector would vary about in proportion to  $(D/\lambda)^{2.5}$ . However, in practice, lack of symmetry of objects near the reflector, such as are caused by the supporting structure, and reflections backward from objects on the ground out in front are likely to cause a lower ratio.

For the present it seems safer and more realistic to say that our experience indicates, when reflectors 5 to 10 wavelengths in diameter are used, the ratio of power in the forward direction to power in the backward direction can be of the order of that obtained by using the following formula:  $P_{\text{forward}}/P_{\text{backward}} = 45,000 (D/\lambda)^2$ .

### *4. Coupling between Radiators with Crossed Polarization, in Same Reflector*

It is possible, theoretically, to place two radiators in the same reflector which are polarized at right angles, and which have couplings between them balanced out. Our experience would indicate that this expedient should not be relied upon to provide more than about 20 decibels of uncoupling between the radiators. Even this figure may prove to be too optimistic under conditions of snow and ice on the antenna system.

### *5. Artificial Balancing of Cross Couplings*

It is theoretically possible, in any particular case, to introduce a balancing or neutralizing coupling to obtain a reduction in net coupling between antennas. In one trial of this we were able to reduce the coupling between two antenna systems from an initial value of 70 decibels to a final value of 85 decibels, a gain of 15 decibels. However, in wide-band service such balancing methods may prove difficult and complicated because there probably will be a variety of component coupling paths of different length and time delay, each of which would require its own balancing path. In the experimental trial mentioned above it was found that there were a number of relatively short paths and other paths corresponding to distances down to the ground and back over the supporting structure, or out to near-by reflecting objects and back.

In any practical case it would seem that, if artificial balancing is used, it must be done with care to provide proper time delays and, at least until it is covered by more experience, should not be relied upon for improvements of more than 10 to 20 decibels.



### 6. Polarization Discrimination over Long Distances

Insufficient information is available to indicate to what degree differences in polarization may be relied upon to discriminate between channels working in the same direction over the same space circuit. Our experience indicates only that such discrimination may be of substantial aid, but only tests for long periods over actual operating circuits can give us information as to how much discrimination can be relied on. As a conservative and very preliminary guess we might place the figure at about 10 decibels.

### 7. Coupling Between Antennas with Reflectors Pointed in Opposite Directions

The coupling between antennas in reflectors pointed in nearly opposite directions is more subject to the conditions under which they are mounted than is the coupling in the other cases considered. In general it should be possible, by using all the available technical expedients, to count on a reduction of coupling to about  $P_T/P_r = (10)^5 \times (D/\lambda)^4$ .

This would indicate that, by using reflectors 10 wavelengths or more in diameter it will generally be possible to receive and retransmit without shift of carrier frequency in the repeater.

However, this matter of relaying without shift of carrier frequency, while it has been demonstrated in one of our relay experiments, is a matter which should receive more experimental development. All we can say with certainty at present is that we are confident that it can be done in most instances and that higher radio frequencies and large antennas will help to make it possible.

## BANDWIDTHS REQUIRED FOR TELEVISION RELAYING INTENDED TO SERVE PRESENT STANDARD TELEVISION-BROADCAST STATIONS

The present television-broadcast standards provide for modulation frequencies ranging from 0 to about 4.25 megacycles.

In a relay system it is considered essential to transmit the zero or very low-frequency components of the modulation so that the synchronizing pulses may occupy a fixed range of the modulation characteristic. Otherwise, variations in image background level may modulate the wave form and amplitude of the synchronizing pulses in a manner to detract from the quality of reproduced images. This means that the highest frequency modulations of the frequency-modulated carrier current will be superimposed upon a carrier frequency which can vary between the values set for the black-and-white levels. This requires that the radio-frequency bandwidth be equal to twice the

highest modulation frequency plus the range of frequency lying between the black-and-white levels.

According to the present standards, the difference between the black-and-white levels occupies about 75 per cent of the modulation characteristic. Therefore, if we so design the modulator that it can produce plus and minus 4.25 megacycles frequency deviation at any modulating frequency from 0 to 4.25 megacycles, then the minimum band required for a frequency-modulated radio-relay system, to match the present standards, will be  $B = (2 \times 4.25) \times 1.75 = 14.9$  megacycles.

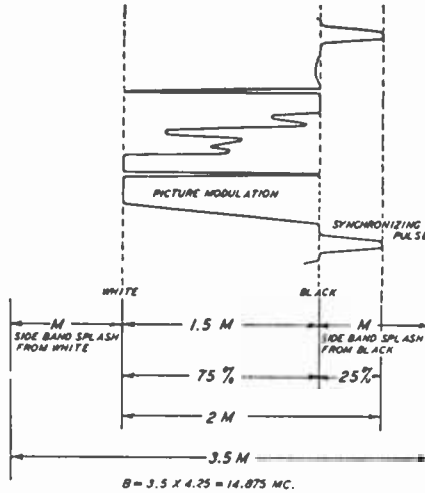


Fig. 15—Frequency range of frequency-modulation television modulated-carrier current.

From this we may conclude that the nominal bandwidth allowed for a television-relay channel should be at least 15 megacycles.

In practice, a larger frequency band is desirable to permit some increase in quality and reduction in noise, to help guarantee that the relay system will not be a substantial factor in detracting from the quality of service from the broadcast stations which it serves.

It is therefore suggested that relay channels to serve the present standard television-broadcast stations should be allowed a nominal channel band of 20 megacycles.

#### BANDWIDTHS REQUIRED FOR RELAY SYSTEMS TO SERVE TELEVISION IN THEATERS

It now appears that future needs of theater television will call for an increase in the picture resolution over that now considered standard for television broadcasting. This is particularly true where television

programs may be interspersed with motion pictures, affording almost direct comparisons.

For some classes of theater television, it is, therefore, assumed that more scanning lines would be used and, for the purpose of the present analysis, a minimum bandwidth in a radio-relay system for theater television programs of 60 megacycles and a nominal bandwidth of 80 megacycles is assumed.

It may be noted that, if this bandwidth is available for theater television, it may be used also for carrying future color television to the home with the same or better definition than is provided by the present standard for black-and-white images.

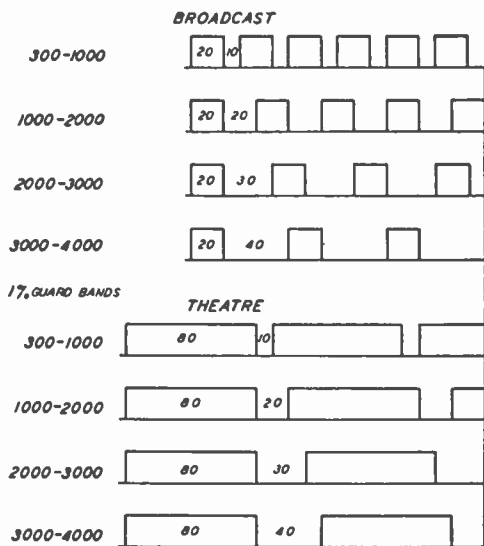


Fig. 16—Suggested minimum channel spacings for any one relay system—megacycles.

GUARD BANDS BETWEEN CHANNELS WORKING IN THE SAME DIRECTION OVER THE SAME SYSTEM

In existing television-broadcast systems, operating near 50 megacycles, a frequency interval of 0.5 megacycle is allowed within which to provide cutoff with a filter, for preventing interference between vision and sound transmitters. This suggests that guard bands between channels, for single-hop relays, might be nominally 1 per cent of the carrier frequency.

In multiple-hop relays there tends to be an accumulation of the effects of cross coupling between channels, but perhaps this can be

balanced off against the reduction in cross-coupling effects provided by use of frequency modulation and by the effects of expedients other than frequency selectivity, such as polarization discrimination. It therefore seems reasonable, until further data are available, to assume that guard bands between channels should be 1 per cent or more of the carrier frequency.

A suggested allowance for various ranges of frequency is shown in Table IV.

*Table IV*—Circuits in Same Direction over Same Relay Path

Range in Megacycles	Megacycles Guard Band	Total Band Per Channel	
		Broadcast	Theater
300 to 1000	10	30	90
1000 to 2000	20	20	100
2000 to 3000	30	50	110
3000 to 4000	40	60	120

#### GUARDS BETWEEN CHANNELS WORKING IN OPPOSITE DIRECTIONS OVER THE SAME SYSTEM

For channels working in opposite directions the interference introduced at each repeater between channels is provided by the cross coupling between antennas pointing in the same direction, one of which is transmitting and the other receiving. This cross coupling, which has been given in a previous section, is determined by the approximate formula  $P_T/P_r = 60,000 (D/\lambda)^4$ .

If this ratio is the same as the gain required in each repeater, our receiving conditions will be identical with those where two channels operate in the same direction.

Ordinarily, the gains per repeater may be on the order of 80 decibels or 100,000,000-to-1 in power. Therefore  $P_T/P_r = 100,000,000 = 60,000 (D/\lambda)^4$ , or  $D/\lambda = 6.4$ .

From this we conclude that the spacing between channels going in opposite directions may be the same as that between channels going in the same direction provided the reflectors for the antennas are 6.5 wavelengths or more in diameter, in a system engineered as outlined in the early part of this paper.

#### PROBABLE FUTURE USES FOR RADIO-RELAY SYSTEMS

Since the only justification for investing large sums of money in radio-relay systems, and for becoming involved in the toils of technical

development, business promotion, and government regulation, is the usefulness of the systems, it may be appropriate to consider what some of the uses may be.

Radio relays have such outstanding technical and economic advantages for the distribution of television that, eventually, they should be regarded as essential for this service. However, the costs for adequate radio-relay systems are substantial and, unless the costs of relay-station sites, towers, and facilities can be spread over a number of channels and services, they may be so burdensome as to delay the initial spread of television service.

In holding unit costs down it is essential that the relay stations be designed and utilized to provide several television channels, all utilizing the same towers. It is also essential that the investment and operating expenses be shared with as many secondary services as possible.

In general, relay stations will occupy the highest points and provide the highest towers in each community. They are, therefore, the natural choice for location of radio broadcast stations. By combining relaying and broadcasting, where this is possible, both can benefit.

High towers, occupying the highest points, are natural gathering places for pleasure seekers and the curious. In many cases, observation platforms at the top of the towers, television theaters, restaurants and other entertainment facilities may be provided to give a greater public service and to help in paying the costs.

One of the most natural secondary services, from a technical standpoint, will be that of facsimile communication, by which is meant the transmission of any sort of picture or message which is to be recorded at the receiving end as a copy of the original. An adequate television-radio-relay circuit has a potential speed of transmission of 108,000 pages per hour.

There are as many uses for facsimile service as there are for the existing telegraph and mail services. It is a means for giving the service with far greater speed and less effort. Soon, for example, it could provide a nationwide newspaper delivery faster than papers can now be printed. Newspaper publishers then will no longer be dependent upon the slow and inefficient type of delivery service which was already in use when printing was invented.

There is another probably important use for future radio-relay systems which is closely related to the struggle just beginning to obtain the use of frequencies above 30 megacycles. It is that of providing radio services to airplanes.

As the number of airplanes in flight increases, the demands for

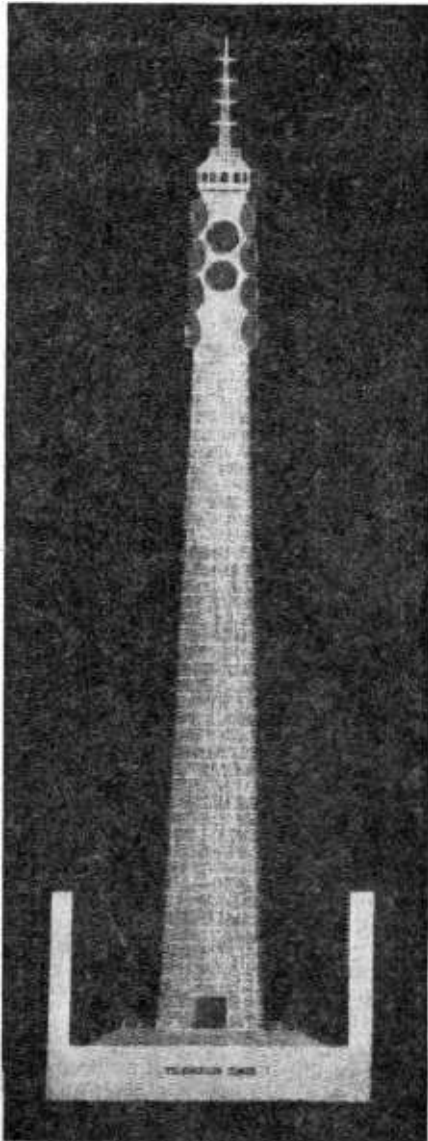


Fig. 17—Recommended design of television tower.

It provides:

1. Rigid mounting of antennas at any height and pointed in any direction.
2. Housing for repeaters at antenna heights to save losses in transmission lines or wave guides.
3. Means of access protected from wind, rain, ice, and snow.
4. Observation platform for visitors.
5. Cost comparable with less-desirable steel towers.
6. Mounting for broadcast antennas when required.

radio service will increase to such a degree that it will be unreasonable to provide radio frequencies and facilities so that all of the airplanes flying over land may communicate by radio over long distances. Furthermore, as the speed and efficiency of airplanes has increased, it has become more unreasonable to provide either large protruding antennas, or powerful equipment, needed to operate on the frequencies required to reach large distances.

Looking ahead it seems inevitable that much of the communication with aircraft must be limited to short distances and carried out on higher frequencies with smaller equipment and without protruding antennas. This will require a large number of ground stations, spread out along the air routes. Substantially these same routes will be followed by the radio-relay systems, and the radio-relay stations are natural sites for airline radio ground stations.

The railroads, long-distance bus and truck lines, and portions of the traveling public have communications needs similar in character to those of the airlines, and radio-relay systems might very well contribute to the fulfillment of these needs.

Radio relays may, of course, be used for long-distance multiplex telephone communication, particularly for the distribution of sound broadcast programs. Sound accompanying television obviously should pass over the radio relays so that its handling may be properly coordinated and so that vision and sound will be subject to equal time delays.

Finally, there is a growing need for means to interconnect a variety of newly developed business machines so that manufacturing, transportation, and merchandising organizations, and the public they serve, may benefit from the advantages of decentralized and widespread operations, with centralized management and control.

With all the pent-up new needs, and the apparent ability of radio-relay systems to fill these needs, what is now needed most to make radio relaying a great new American industry is a more general understanding of its value; a well-defined and stable licensing policy; a relaxation of restraints which dampen the hope of expansion and profit and which discourage joint action by those in need of relay service; and a few good promoters who have caught the vision.

# A MICROWAVE RELAY SYSTEM\*†

BY

LELAND E. THOMPSON

Engineering Products Department, RCA Victor Division,  
Camden, N. J.

*Summary*—A method of double-frequency modulation suitable for long-distance transmission of multichannel signals by means of radio-relay stations is described. Propagation, radio-frequency bandwidth, and radio-frequency power are discussed briefly. The signal-to-noise ratio and distortion of the system are shown by theory and experiment. An experimental circuit between Philadelphia and New York is described and the results are given.

## INTRODUCTION

THE development of microwave power generation and radiation during the war advanced so far that it now seems economically possible to transmit multichannel telephone and telegraph signals over long distances by means of relay stations spaced from 25 to 50 miles apart. Such services require a high degree of reliability. Interruptions due to interference and propagation failures should be entirely absent.

The microwave region from 2000 to 10,000 megacycles is particularly well suited for such transmissions. In this frequency range the received signal over a propagation path only slightly above grazing is near the free-space value.<sup>1</sup> Interference from a station on the same frequency channel at a much greater distance away than the desired station, even under conditions of unusual propagation and without the help of the directivity of the antennas, is considerably reduced just because the distance to the interfering station is greater than that to the desired station. This is a more favorable condition than on lower frequencies where, for example, on 40 to 100 megacycles the received signal at a distance of 25 miles over a propagation path slightly above grazing would be considerably below the free-space value and an interfering signal from a greater distance may be so much nearer the free-space value that, with the same transmitted power, it is actually stronger than the desired signal under unusual propagation conditions.

This more favorable propagation characteristic of microwave fre-

---

\* Decimal classification: R480 X R310.

† Reprinted from *Proc. I.R.E.*, December, 1946.

<sup>1</sup> C. W. Hansell, "Radio-relay-systems development by the Radio Corporation of America," *Proc. I.R.E.*, vol. 33, pp. 156-168; March, 1945.



quencies together with sharply directional antennas provides a much greater opportunity to use the same frequency channel over and over again than was ever possible on lower frequencies.

It is well known that frequency modulation with a large deviation ratio provides a gain in signal-to-noise ratio at the expense of increased bandwidth.<sup>2,3</sup> In other words, for a given signal-to-noise ratio, less radio-frequency power is required than in an amplitude-modulation system, or in a frequency-modulation system with a low deviation ratio. In addition to the economy of a low-power system, there is the advantage of the greater possibility of using the same frequency channel over and over even in the same local geographical area, because of the interference-suppression effect of frequency modulation.

For example, assume that in a terminal station in a metropolitan area, which is the terminating point of several microwave relay circuits, each relay circuit is a two-way circuit and that each radiates from the terminal station in a different direction. All the receivers at the terminal station may use one common frequency channel and all the transmitters may use a second one. Interference between the different circuits would be eliminated by the directivity of the antennas and by the interference suppression of frequency modulation. With an amplitude-modulation system, or any system which would depend on the antenna directivity alone for interference elimination, such common use of one frequency channel would not be practical, at least not with the antenna designs in use at the present time. In this case, although the frequency band required for each of the circuits would be smaller, each circuit would require a separate frequency channel. Probably a total frequency spectrum greater than that used when all the circuits can operate on a common frequency channel would be required.

It is evident that bandwidth alone is not a measure of the "space" required by a particular system. The type of modulation and the amount of radio-frequency power used are of great importance in efficient use of the spectrum.

#### THE DOUBLE-FREQUENCY-MODULATION SYSTEM

The ability to modulate, relay, and demodulate a number of simultaneous signal channels without objectionable noise or cross talk is as important as the ability to generate and to radiate radio-frequency power. This system of modulation makes use of frequency separation

---

<sup>2</sup> Edwin H. Armstrong, "A method of reducing disturbances in radio signaling by a system of frequency modulation," *Proc. I.R.E.*, vol. 24, pp. 689-740; May, 1936.

<sup>3</sup> Murray G. Crosby, "Frequency modulation noise characteristics," *Proc. I.R.E.*, vol. 25, pp. 472-514; April, 1937.

of the various signal channels. The modulation range is from 30 cycles to 150 kilocycles. Any of the systems of channeling used on long wire-line telephone<sup>4</sup> and telegraph<sup>5</sup> systems may be used.

The intelligence or signaling band of frequencies is used to frequency-modulate or phase-modulate a subcarrier to 1.0 megacycle. The modulated subcarrier then frequency-modulates the radio-frequency carrier. A pre-emphasis network is used to increase the deviation of the subcarrier to approximate linearity with increasing modulating frequency between 10 and 150 kilocycles, so that the signal-to-noise ratio on all of the channels will be the same. Below 10 kilocycles, pre-emphasis does not take place. Above 10 kilocycles the modulation is more correctly called phase modulation, since the deviation increases with modulating frequency.

The method of generating and modulating the subcarrier is shown in Figure 1. Two oscillators are frequency-modulated by two reactance-modulator tubes. Each oscillator output is coupled to a tripler stage,

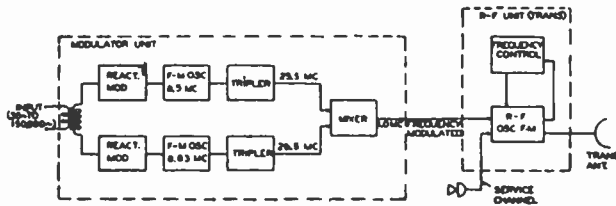


Fig. 1—Block diagram of the terminal transmitter.

and the outputs of the two tripler stages couple to a mixer stage. The plate circuit of the mixer stage is tuned to the frequency difference between the frequencies of the two input voltages. The input modulating voltage is fed in push-pull fashion to the grids of the reactance modulators. The output frequency swing of the 1.0-megacycle subcarrier is, because of the action of the tripler stages, three times the sum of the swings produced by the two modulators. The maximum frequency swing of the subcarrier is plus and minus 400 kilocycles.

The microwave unit of the transmitter uses a reflex oscillator.<sup>6</sup> A relatively low-power oscillator tube has been used in the experimental system. The modulated subcarrier is coupled to the repeller electrode circuit of the oscillator tube to produce the frequency modulation of

<sup>4</sup> B. W. Kendal and H. A. Affel, "A twelve-channel carrier telephone system for open-wire lines," *Bell Sys. Tech. Jour.*, vol. 18, pp. 119-142; January, 1939.

<sup>5</sup> F. B. Bramhall and J. E. Boughtwood, "Frequency-modulated carrier telegraph system," *Trans. A.I.E.E.*, vol. 61, pp. 36-39; January, 1942.

<sup>6</sup> J. R. Pierce, "Reflex oscillators," *Proc. I.R.E.*, vol. 33, pp. 112-118; February, 1945.

the microwave carrier. The frequency swing is plus and minus 2.0 megacycles.

The frequency control consists of a high-Q cavity circuit which stabilizes the frequency of the oscillator by means of an automatic-frequency-control circuit.

At a relay station the signal is received by a superheterodyne receiver with an intermediate frequency of 32 megacycles and a bandwidth of 4 megacycles. Figure 2 is a block diagram of a relay receiver and transmitter. The last limiter in the intermediate-frequency amplifier connects to a 32-megacycle discriminator which has a frequency range from audio frequencies up to about 1.5 megacycles. The frequency-modulated subcarrier output of the discriminator is amplified by a two-stage amplifier and limiter with interstage-coupling circuits

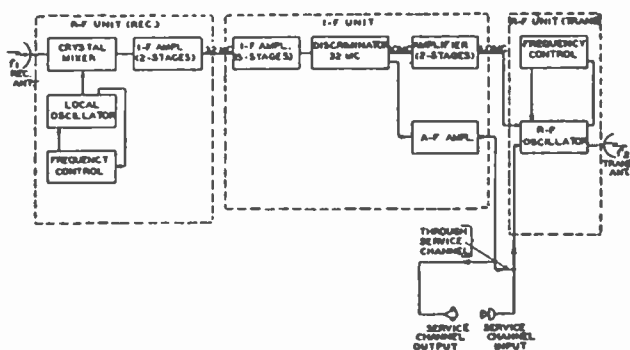


Fig. 2—Block diagram of a relay receiver and transmitter.

broadly tuned to 1.0 megacycle. The output of this amplifier is coupled to the repeller-electrode circuit of the relay-transmitter oscillator and thus frequency-modulates the relay transmitter.

At a terminal receiving station, the output circuit of the subcarrier amplifier connects to a second demodulator. The circuits of the demodulator are shown in block-diagram form in Figure 3. By the use of an oscillator and a balanced mixer circuit, the 1.0 megacycle subcarrier is changed to a frequency of 13.0 megacycles. A three-stage limiter is used before the final discriminator, which operates at the center frequency of 13.0 megacycles.

The modulation characteristic of the transmitter oscillator as well as of the 32-megacycle discriminator need not be linear because the modulation applied to the oscillator and the output voltage of the discriminator are the subcarrier wave, and this is a frequency-modulated wave and not subject to any harmful effects by passing through nonlinear circuits.

A comparatively simple system of relaying is thus provided, since the relay-transmitter radio-frequency circuits contain a single tube, the reflex oscillator.

For successful operation and maintenance of a relay system consisting of a number of relay stations that are normally unattended, a means of communication from a terminal station to any relay station, and also between any two relay stations, is very desirable. A means of locating failures in the system from a terminal station is almost a necessity for prompt repair and servicing. This service channel is provided by frequency-modulating the transmitter oscillator directly with audio frequencies in addition to the subcarrier modulation.

At each relay station, this audio frequency is separated from the subcarrier at the 32-megacycle discriminator and then applied again to the outgoing transmitter oscillator. A microphone and headphone are connected in this circuit at each relay station. This service channel also provides the necessary circuit for the signals which locate failure.

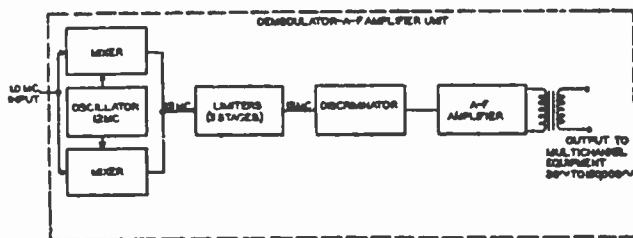


Fig. 3—Block diagram of the demodulator used at a terminal station.

Nonlinearity in the modulation characteristics of the oscillator and the 32-megacycle discriminator cause distortion in this channel, but a relatively high value of distortion here is not objectionable. Because of the large frequency separation, cross modulation with the subcarrier channels does not result.

The radio-frequency circuit components of the experimental equipment are illustrated in Figure 4. The antenna is shown at the top. The transmitter oscillator appears at the lower left. These components were designed for a frequency range of 3000 to 3300 megacycles. The concentric-line output of the oscillator tube is capacitance-coupled to a section of concentric line containing two sliding insulator sections, each a quarter-wavelength long. By adjusting the position of the two insulators, the oscillator tube is matched to the transmission line and antenna. At the lower right in Figure 4 is shown the receiver oscillator and mixer unit. The output of the oscillator tube couples to a quarter-wave concentric-line resonant circuit by means of a capacitance probe. A small loop couples the antenna to the resonant circuit across which

the crystal rectifier is connected. The output terminal shown at the top of the unit connects to the intermediate-frequency amplifier.

#### SIGNAL-TO-NOISE RATIO

The received-carrier-to-noise ratio depends on a number of factors. First, the propagation path should be clear of any obstructions such as hills, trees, etc. The other factors determining the received-carrier-to-noise ratio are transmitter power, diameter of the antenna reflector, wavelength, distance, receiver bandwidth, and receiver noise factor. The value of the carrier-to-noise ratio may be calculated for these latter factors from the formulas given by Hansell.<sup>1</sup>

With either frequency modulation or amplitude modulation the signal-to-noise ratio at the output of the receiver is not the same value as the carrier-to-noise ratio before the last detector; this is the case

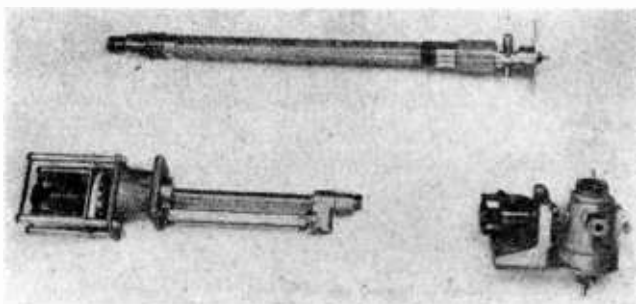


Fig. 4—Experimental radio-frequency circuit components.

if the bandwidth of the intermediate-frequency-amplifier circuits is greater than twice the frequency-response range of the audio circuits. The signal-to-noise ratio is improved by a factor that is determined by the bandwidth reduction. In the case of amplitude modulation the equation for signal-to-noise ratio ( $S/N$ ) is

$$\left( \frac{S}{N} \right)_{AM} = M \sqrt{\frac{(BW)}{2f_a}} \frac{C}{N} \quad (1)$$

where  $(BW)$  is the intermediate-frequency bandwidth,  $f_a$  is the audio-frequency bandwidth,  $M$  is the modulation factor,  $C$  is the carrier voltage, and  $N$  the noise voltage ahead of the last detector. When the frequency-modulation improvement factor<sup>3</sup> is applied to (1), the equation for the signal-to-noise ratio with frequency modulation is

$$\left( \frac{S}{N} \right)_{FM} = \sqrt{3} D \sqrt{\frac{(BW)}{2f_a} \frac{C}{N}} \quad (2)$$

where  $D$  is the ratio between the frequency deviation and the highest modulating frequency.

The signal-to-noise ratio equations for the double-frequency-modulation system are derived in the appendix. The equation for the first or audio-frequency channel is

$$\left( \frac{S}{N} \right)_{DFM} = \frac{\sqrt{3}}{\sqrt{2}} D_1 D_2 \sqrt{\frac{(BW)}{2f_a} \frac{C}{N}} \quad (3)$$

where  $D_1$  is the ratio between the frequency swing of the carrier and the subcarrier frequency, and  $D_2$  is the ratio between the frequency deviation of the subcarrier by the audio frequencies and the highest audio frequency of this channel.

The signal-to-noise ratio equation for the carrier channels above the audio channel, where the subcarrier is phase modulated, is

$$\left( \frac{S}{N} \right)_{PFM} = \frac{1}{\sqrt{2}} D_1 D_3 \sqrt{\frac{(BW)}{2f_a} \frac{C}{N}} \quad (4)$$

where  $D_3$  is the ratio between the frequency deviation of the subcarrier by any one channel and the mid-frequency of this channel and  $f_a$  is the band-width of this signal channel. It is assumed in all of the above cases that the carrier-to-noise ratio is above the threshold value and that the total frequency swing of the subcarrier by all of the signal channels does not exceed the linear range of the subcarrier modulator and demodulator.

#### DISTORTION

Cross talk in a multichannel modulation system depends on the distortion in the system. The sources of distortion in frequency modulation are the amplitude nonlinearity of the modulator and the demodulator as well as the nonlinear phase characteristics of the circuits between the modulator and the demodulator.

Measurements of the distortion in this system with the modulator connected directly to the demodulator are shown by the curve in Figure 5.

The second source of distortion, nonlinear phase characteristics of tuned circuits, is an important factor in a relay system composed of a large number of relay stations. Both Roder<sup>7</sup> and Jaffe<sup>8</sup> show that this distortion is high, even in one circuit, when the frequency swing is near or greater than the bandwidth of the tuned circuit and when the modulating frequency is a high audio frequency. The distortion reduces rapidly with a reduction of frequency swing. However, distortion is still a serious factor when a large number of tuned circuits are used, as in a long relay system.

The nonlinear phase characteristic of the receiver intermediate-frequency-amplifier circuits will first be considered. The action of these circuits on the signal frequencies is of the greatest importance because of the relatively large number of such circuits in the system. It was determined in the experimental system that tuning all these circuits to one side or the other of resonance did not produce a measurable

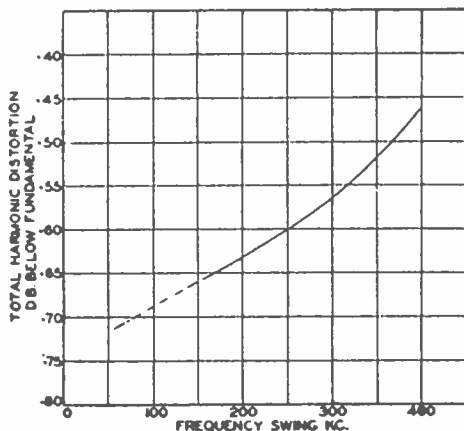


Fig. 5—Over-all distortion of the modulator and demodulator units.

change in the over-all distortion. Also it was found that the over-all distortion did not change with the percentage modulation (or frequency swing) of the carrier. It was concluded that the intermediate-frequency-amplifier circuits are not an important source of distortion in this double-frequency-modulation system.

The subcarrier amplifier and limiter tuned circuits are a source of distortion. By making these circuits sufficiently broad in frequency response, a satisfactory phase characteristic can be obtained such that

<sup>7</sup> H. Roder, "Effects of tuned circuits upon a frequency-modulated signal," *Proc. I.R.E.*, vol. 25, pp. 1617-1647; December, 1937.

<sup>8</sup> David Lawrence Jaffe, "A theoretical and experimental investigation of tuned-circuit distortion in frequency-modulation systems," *Proc. I.R.E.*, vol. 33, pp. 318-333; May, 1945.

a large number of relay stations may be used. An advantage of such low- $Q$  circuits is that they are relatively stable under normal changes of temperature and humidity, and thus make practical the use of phase-corrective networks should they be necessary in an extremely long relay system.

#### COMPARISON WITH SINGLE FREQUENCY MODULATION

It is reasonable to compare the signal-to-noise ratios of this system with a single-frequency-modulation system on the basis of equal transmission bandwidths and equal transmitted powers. Both systems can be designed for any given bandwidth and power, within practical limits.

Comparing (2) for frequency modulation with (3) for double frequency modulation, assuming equal bandwidths, power, and modulating frequencies,

$$\frac{\left(\frac{S}{N}\right)_{FM}}{\left(\frac{S}{N}\right)_{DFM}} = \frac{\sqrt{2}D}{D_1D_2} \quad (5)$$

gives the ratio of the signal-to-noise ratios of the two systems. Assuming values for  $D_1$  and  $D_2$  according to the system described,  $D_1$  is equal to 2 and the ratio of  $D$  to  $D_2$  is 5, since the maximum frequency swing of the subcarrier is 400 kilocycles and the maximum frequency swing for a frequency-modulation system with a bandwidth of 4.0 megacycles would be 2.0 megacycles. The single-frequency-modulation system has a greater signal-to-noise ratio by a factor of 3.5, or about 11 decibels.

In the case of the single-frequency-modulation system, the modulation on the carrier passing through the intermediate-frequency circuits of the receivers is the signaling frequency. To maintain a sufficiently low value of cross talk due to nonlinear phase distortion, it is probable that the full peak-to-peak deviation equal to the bandwidth could not be used, and the signal-to-noise ratio would therefore be reduced. Another factor to be considered in the single-frequency-modulation system (assuming relaying is accomplished without demodulation at the relay stations) is the frequency instability of the transmitters. The instability adds up along the system. That is, the frequency of the received carrier at the final receiver in the chain depends not only on the last transmitter, but on all of the transmitters and all of the receiver oscillators in the chain. A suitable allowance for frequency drift would reduce the permissible peak frequency swing.

While these results have indicated reasons for choice of the double-



frequency-modulation system, it is difficult to make an exact comparison at the present time. The normal progress of development will make a more conclusive comparison possible in the future. However, the experimental results described below tend to confirm the correctness of these conclusions.

#### EXPERIMENTAL RESULTS

An experimental two-way circuit constructed between Philadelphia and New York City was placed in operation in April, 1945. The location of this circuit is shown on the map of Figure 6. Two relay stations are used, one near Bordentown, New Jersey, and the other near New Brunswick, New Jersey, at a site named Ten Mile Run.

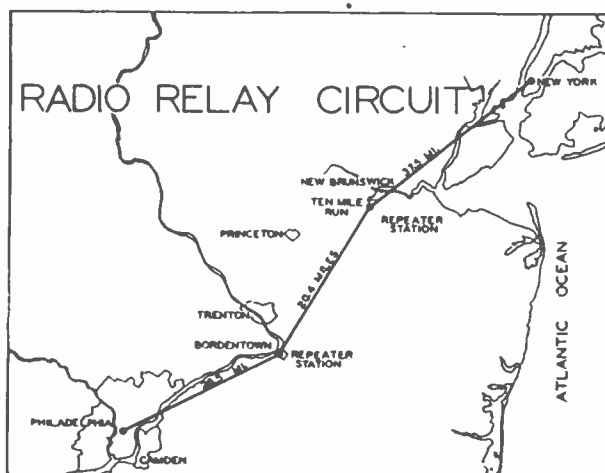


Fig. 6—Location of stations in the experimental circuit.

The photograph of Figure 7 shows the tower with antenna reflectors at the Bordentown relay station. The Ten Mile Run station is similar. The towers are 100 feet in height. The experimental equipment was placed in the enclosure at the top of each tower. The design of later models permits the installation of most of the equipment at ground level, with the transmitter oscillator, receiver oscillator, mixer, and first amplifier located near the antennas.

The facilities for the installation of the terminal stations at both Philadelphia and New York were made available by the Western Union Telegraph Company, the Engineering Department of which organization co-operated in the field tests of the circuit.

The frequencies used in the experimental tests are near 3300 megacycles. Two frequency channels are used for the complete two-way

circuit. At each relay station the transmitters in both directions are on the same channel frequency, and the receivers in both directions operate on the other channel frequency.

The transmitter power is approximately 0.1 watt. The antenna parabolic reflectors are 4 feet in diameter. This dimension gives an antenna gain of about 30 decibels and an angular beam width of about

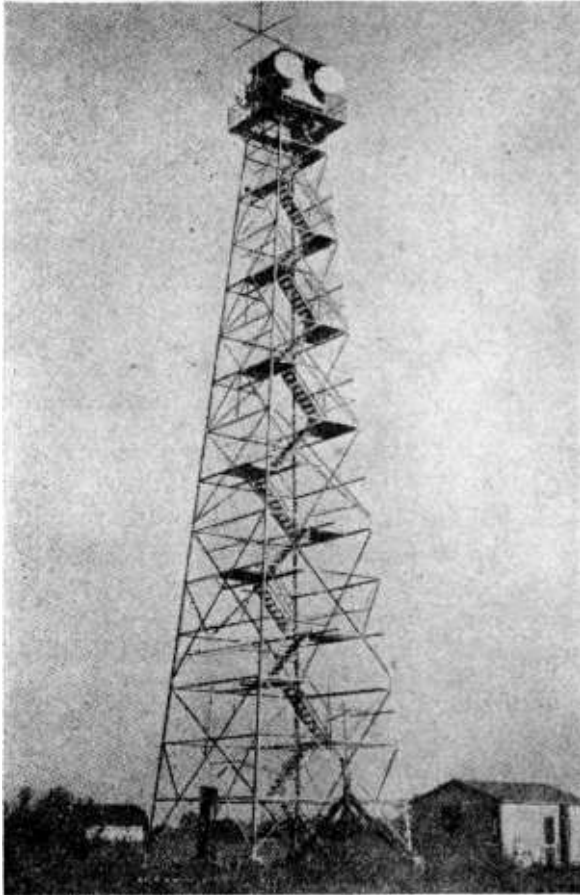


Fig. 7—Relay station near Bordentown, New Jersey.

5.5 degrees at the half-power points. The antennas are dipoles fed by concentric transmission lines.

The propagation path between Philadelphia and Bordentown is sufficiently clear above hilltops to allow a geometrically unobstructed path above trees of normal height. The distance is 26.5 miles. The path of the link between Bordentown and Ten Mile Run is well above

trees and other obstructions. The distance of this link is 20 miles. The propagation path between Ten Mile Run and New York is not sufficiently clear of the terrain to allow for trees and buildings near the center of the path. The distance is 37.5 miles.

The received-carrier-to-noise ratio was measured over each link of the circuit under normal weather conditions when the received signals were constant. The value of this ratio measured on the Ten Mile Run to New York link was 20. Between Ten Mile Run and Bordentown the ratio was 90, and between Bordentown and Philadelphia the ratio was 68.

To obtain an experimental confirmation of the signal-to-noise ratio of (3), a measurement was made under the following conditions. The subcarrier circuit on the New York receiver was connected directly to the transmitter to form a relay station, so that a one-way loop circuit of 168 miles in length was obtained with the transmitting and receiving ends of the circuit in Philadelphia. Measurements were made at audio frequencies with a filter on the receiver output with a noise band of 15 kilocycles. A modulating frequency of 1000 cycles was used with a swing of 60 kilocycles on the subcarrier.

The signal-to-noise root-mean-square voltage ratio measured about 1000, or 60 decibels. From (3) the calculated value is 67 decibels, with the carrier-to-noise ratio of 20 obtained on the lowest signal link in the circuit. There were two such links of about equal strength and therefore 3 decibels should be subtracted from this calculated figure, giving a value of 64 decibels. The noise contributions of the links having the stronger received signals would be small by comparison and were neglected. Other tests made over a single link checked the theoretical value to about the same degree.

The distortion over the circuit, measured at a modulation frequency of 200 cycles and a frequency swing of 240 kilocycles on the subcarrier, was about 0.1 per cent, or 60 decibels below the audio signal. This is about the same value as was measured with the modulator unit connected directly to the demodulator and not going through the radio circuit, as is shown in the data of Figure 5.

The distortion increased with modulating frequency, and at 5000 cycles and a frequency swing of 240 kilocycles, the distortion was 0.7 per cent. This measurement showed the effect of the nonlinear phase characteristic of the subcarrier circuits. Although the frequency swing of 240 kilocycles is very much more than would be used normally with a modulation component at 5000 cycles, the measurement indicated that such distortion can be serious at higher modulation frequencies.

In co-operation with the Engineering Department of the Western

Union Telegraph Company, practical tests were made with the use of two carrier telephone channels, about 50 teleprinter channels, a slow-speed tape-facsimile channel, and an audio channel with a fidelity of 30 cycles to 10,000 cycles. This combined modulation extended to a frequency of about 50 kilocycles. Listening tests showed cross talk and noise to be at an acceptably low level. The operation of the teleprinter channels was satisfactory, with no errors noted during the period of the tests on the single printer that was used at the radio terminal.

Propagation records were made over this circuit for about nine months. Generally the results show quite satisfactory performance with the power of 0.1 watt. It is proposed to conduct further tests at greater distances. These tests may indicate that, with sufficient propagation path clearance, distances of 50 to 60 miles may be practical with this low value of power.

The noise level of the circuit was apparently determined entirely by receiver noise. Both terminal receivers are in locations where the noise level caused by electrical machinery is very high at the receiver intermediate frequency of 32 megacycles. Proper grounding and shielding of the intermediate-frequency circuits was necessary to prevent noise from being introduced directly into the intermediate-frequency amplifier.

#### CONCLUSION

From both a theoretical and a practical viewpoint, the system of radio relaying described is sufficiently promising for multichannel voice and telegraph communication to warrant further development and an extension of the test circuit. Such work is now in progress.

#### ACKNOWLEDGMENT

The author wishes to acknowledge the help of a large number of co-workers in the course of this work. The support and guidance of John B. Coleman and Donald S. Bond is particularly appreciated. The help of F. C. Collings and his group in the early development stage and of G. Gerlach and his group in the later field-test stage contributed materially to the development. The early experience in the microwave field of N. I. Korman and C. G. Sontheimer was of particular value in the course of this work.

The support and interest in the development shown by F. E. d'Humy and H. P. Corwith of the Western Union Telegraph Company is very much appreciated. In particular, the assistance of F. B. Bramhall, J. Z. Miller, and W. B. Sullinger, J. E. Boughtwood, and M. Cantor of the Engineering Department of that company contributed materially to the success of the tests.

APPENDIX

Consider the signal and noise at the first frequency-modulation detector in the receiver. If the frequency-modulation peak-to-peak swing of the carrier by the subcarrier wave before detection is equal to the intermediate-frequency bandwidth, the amplitude of the subcarrier after detection is the same as the amplitude of the carrier ahead of the detector, if the efficiency of the frequency-modulation detector is 100 per cent. Crosby<sup>3</sup> has shown that, if sufficient limiting is used, the efficiency of the detector does not change the output signal-to-noise ratio, both the signal and the noise being reduced with a detector of low efficiency. It is then permissible to assume an efficiency of 100 per cent.

In Figure 8, the rectangle *OABC* represents the average noise-power output of an amplitude-modulation detector, and the area *OBC* represents the average noise-power output of a frequency-modulation de-

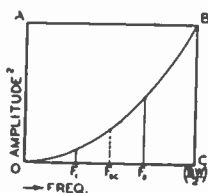


Fig. 8—Amplitude-modulation and frequency-modulation receiver noise-power spectra.

tor. Crosby<sup>3</sup> has shown that the ratio of these two values of power is 3 to 1. This result is found by a comparison of the squared ordinate areas of the two noise-voltage spectra. Similarly, the area *OBC* compared to the area under the curve between  $F_1$  and  $F_2$ , is as the squared ordinate areas, and the power ratio is

$$\frac{\int_0^{(BW/2)} F^2 dF}{\int_{F_1}^{F_2} F^2 dF} = \frac{\left(\frac{BW}{2}\right)^3}{F_2^3 - F_1^3} \tag{6}$$

The subcarrier-to-noise root-mean-square voltage ratio following the first frequency-modulation detector, considering only noise between  $F_1$  and  $F_2$ , is then

$$\frac{C_{sr}}{N} = \sqrt{3} M \sqrt{\frac{\left(\frac{BW}{2}\right)^3}{F_2^3 - F_1^3}} \frac{C}{N} \tag{7}$$

where  $C/N$  is the carrier-to-noise ratio in the intermediate-frequency amplifier ahead of the detector and  $M$  is the amount of frequency swing compared to the bandwidth and is equal to 1 at a frequency swing equal to half the bandwidth.

Following the second frequency-modulation detector, the signal-to-noise ratio improves over that ahead of the detector by the well-known factor  $\sqrt{2}$  times the deviation ratio, and also because of a bandwidth reduction produced by the channel audio-frequency filter following the detector. The signal-to-noise ratio following this filter is

$$\frac{S}{N} = \sqrt{3} D_2 \sqrt{\frac{F_2 - F_1}{2f_a} \frac{C_{sc}}{N}} \tag{8}$$

where  $f_a$  is the audio band of the filter.

Substituting (7) and (8)

$$\frac{S}{N} = 3MD_2 \sqrt{\frac{F_2 - F_1}{2f_a}} \sqrt{\frac{\left(\frac{BW}{2}\right)^3}{F_2^3 - F_1^3} \frac{C}{N}} \tag{9}$$

$$= \frac{3}{\sqrt{2}} D_2 \frac{M\left(\frac{BW}{2}\right)}{\sqrt{F_2^2 + F_1F_2 + F_1^2}} \sqrt{\frac{(BW) C}{2f_a N}} \tag{10}$$

Equation (10) gives the signal-to-noise ratio of the first audio-frequency channel with a filter passing frequencies up to  $f_a$ . If  $F_1$  and  $F_2$  approach  $F_{sc}$ , the frequency of the subcarrier,

$$\frac{M\left(\frac{BW}{2}\right)}{\sqrt{F_2^2 + F_1F_2 + F_1^2}} = \frac{M\left(\frac{BW}{2}\right)}{\sqrt{3} F_{sc}} = \frac{1}{\sqrt{3}} D_1 \tag{11}$$

where  $D_1$  is the ratio of the deviation of the carrier by the subcarrier. Equation (10) then becomes

$$\left(\frac{S}{N}\right)_{DFM} = \frac{\sqrt{3}}{\sqrt{2}} D_1 D_2 \sqrt{\frac{(BW) C}{2f_a N}} \tag{3}$$

In the system described,  $F_1$  is equal to 600 kilocycles and  $F_2$  is equal to 1400 kilocycles, and the error in using (3) instead of (10) is

$$\frac{\sqrt{1.4^2 + 0.6 \times 1.4 + 0.6^2}}{\sqrt{3} \times 1} = \frac{\sqrt{3.16}}{\sqrt{3}} = 1.03. \tag{12}$$

It is not necessary to use a band-pass filter in the subcarrier circuits to eliminate noise components below  $F_1$  and above  $F_2$ , as these components produce noise in the receiver output circuits beyond the modulation range and are eliminated by the channel filters.

Similarly, the signal-to-noise ratio in any band of modulation frequencies between  $F_3$  and  $F_4$  at the output of the second frequency-modulation detector is

$$\frac{S}{N} = \sqrt{3} M_1 \sqrt{\frac{\left(\frac{F_2 - F_1}{2}\right)^3}{F_4^3 - F_3^3}} \frac{C_{sc}}{N} \tag{13}$$

$$= \sqrt{3} M_1 \frac{\left(\frac{F_2 - F_1}{2}\right)}{\sqrt{F_4^2 + F_3 F_4 + F_3^2}} \sqrt{\frac{F_2 - F_1}{2(F_4 - F_3)}} \frac{C_{sc}}{N} \tag{14}$$

where  $M_1$  is the amount of frequency swing of the subcarrier compared to the bandwidth of the subcarrier circuits and is equal to 1 at a frequency swing equal to  $(F_2 - F_1)/2$ .

If  $F_3$  and  $F_4$  approach the mid-channel frequency,  $F_m$ ,

$$M_1 \frac{\left(\frac{F_2 - F_1}{2}\right)}{\sqrt{F_4^2 + F_3 F_4 + F_3^2}} = \frac{M_1 \left(\frac{F_2 - F_1}{2}\right)}{\sqrt{3} F_m} = \frac{1}{\sqrt{3}} D_3 \tag{15}$$

where  $D_3$  is the ratio between the deviation of the subcarrier by the frequencies between  $F_3$  and  $F_4$  and the mid-channel frequency,  $F_m$ . Equation (14) then becomes

$$\frac{S}{N} = D_3 \sqrt{\frac{F_2 - F_1}{2(F_4 - F_3)}} \frac{C_{sc}}{N} \tag{16}$$

$$= D_3 \sqrt{\frac{F_2 - F_1}{2f_a} \frac{C_{ac}}{N}} \quad (17)$$

where  $f_a$  is the bandwidth of any channel above the audio channel. The error introduced by the use of (15) is very small. For example, the error in calculating a channel of 4 kilocycles between 18 and 22 kilocycles would be 0.16 per cent.

Substituting equation (7) in (17) in the same manner as it was substituted in (8), it is found that

$$\left( \frac{S}{N} \right)_{FPM} = \frac{1}{\sqrt{2}} D_1 D_3 \sqrt{\frac{(BW) C}{2f_a N}} \quad (4)$$



## MICRO-WAVE TELEVISION RELAY\*†

BY

W. J. POCH AND J. P. TAYLOR

Engineering Products Department, RCA Victor Division,  
Camden, N. J.*Summary*

*The need for radio links, particularly for use in relaying of television programs for networking purposes, is briefly reviewed and the advantages of microwaves for this purpose are discussed. The paper then describes in detail equipment which is available for use as television relays. This equipment uses the war-developed klystron circuits, operates in the super-high frequency band and is actual production equipment and not of a special or experimental nature. After a brief discussion of system tests, the arrangement of equipment units is described. The paper concludes with a detailed discussion of the transmitter, transmitter control unit, receiver, and receiver control units of this system.*

*(8 pages; 20 figures)*

\* Decimal Classification: R389.1 × R310.

† *EM and Tele.*, August, 1946.

## DEVELOPMENT OF RADIO RELAY SYSTEMS\*†

BY

C. W. HANSELL

Research Department, RCA Laboratories Division,  
Rocky Point, L. I., N. Y.*Summary*

*Radio relay systems for long distance electrical communications over land have been accepted as replacements for wire lines and cables over some of the most heavily loaded telegraph circuits in the world. They are beginning to revolutionize and expand communications over land just as the development of short wave transoceanic communication 20 years ago revolutionized international communications. During the war this company developed the AN/TRC-8 and AN/TRC-5 radio relaying equipments for the U. S. Army Signal Corps; at the end of the war, it developed Types CW-1a and CW-2a radio relay equipment which it demonstrated for the Western Union Telegraph Co., with the result that Western Union has announced plans for establishing a national radio relay network. Long distance radio relaying is expected to be done in a band of frequencies ranging from about 1000 to 8000 megacycles, the upper limit of frequency being set by effect of rain storms upon reliability. Suggested minimum carrier-to-effective or apparent noise power ratios are as follows: for printer telegraph, 18 decibels; for ordinary broadcast material, facsimile, and television, 50 decibels; and for high grade music, 60 decibels. The frequency bandwidth occupied by a phase modulated multichannel radio relay*

\* Decimal Classification: R480.

† *RCA REVIEW*, September, 1946.

system is  $2B + 2Bd/\sqrt{3}$  where  $B$  is the modulation frequency band and  $d$  is the peak phase deviation. Radio relay equipment development is still in a state of flux but, since costs are mostly for sites, towers, and auxiliary facilities, which are permanent, there is no need to delay investment in radio relay systems. Automatic facsimile message communication at television speeds may well be the best answer to competition for the record communications industry.

(18 pages; 3 figures)

## A MICROWAVE RELAY COMMUNICATION SYSTEM\*†

BY

G. G. GERLACH

Engineering Products Department, RCA Victor Division,  
Camden, N. J.

### Summary

*This paper reviews the experimental results obtained with a 4000-megacycle multichannel relay system connecting New York and Philadelphia. The system employs a frequency-modulated subcarrier which in turn is used to frequency-modulate the final carrier. Demodulation to the sub-carrier frequency is effected at relay stations. The microwave relay equipment, which resulted from this experimental work and which will be installed by the Western Union Telegraph Company in a circuit connecting New York, Washington and Pittsburgh, is described.*

(25 pages, 21 figures, 2 tables)

\* Decimal Classification: R480.

† RCA REVIEW, December, 1946.

## PULSE TIME DIVISION RADIO RELAY\*†

BY

B. TREVOR, O. E. DOW, AND W. D. HOUGHTON

Research Department, RCA Laboratories Division,  
Riverhead and Rocky Point, L. I., N. Y.

### Summary

*This paper describes a radio relay set which provides eight telephone circuits and operates in the 1350 to 1500-megacycle band. The set uses a time division multiplex system and pulse position modulation. An explanation of the system is given. The signal-to-noise ratio at threshold signal condition is derived and compared with the measured signal-to-noise ratio. This radio set was developed for the U. S. Army during the war and is designated the AN/TRC-5.*

(14 pages; 10 figures)

\* Decimal Classification: R148.6 × R480.

† RCA REVIEW, December, 1946.

# ATTENUATION OF ELECTROMAGNETIC FIELDS IN PIPES SMALLER THAN THE CRITICAL SIZE\*†

BY

E. G. LINDER

Research Department, RCA Laboratories Division,  
Princeton, N. J.

*Summary*—A theoretical and experimental discussion is given of electromagnetic fields in pipes smaller than the critical size, especially with regard to attenuation, and based upon wave-guide theory. It is shown that the rate of attenuation, as the wavelength increases and passes through the critical value, approaches a high asymptotic value. Confirmatory experimental data are given. Simple formulas for attenuation are included.

RECENTLY several papers<sup>1-3</sup> have appeared in which the propagation of electromagnetic waves in pipes has been discussed. These have indicated that for a given frequency there is a critical pipe size below which wave propagation is not possible, or in other words, for a pipe of a given size there is a cutoff frequency  $f_0$  below which wave propagation does not occur. Aside from this, so far as the writer is aware, no discussion has previously been made of phenomena below cutoff or very near to it. In fact most of the present published theory is not valid for frequencies very near to  $f_0$ . It is the purpose of the present paper to discuss this case somewhat more completely.

The general expressions for the fields in cylindrical tubes may be written in the form<sup>1,2</sup>

$$\left. \begin{aligned} E &= E_1(r, \theta) \exp(j\omega t \pm \gamma z) \\ H &= H_1(r, \theta) \exp(j\omega t \pm \gamma z) \end{aligned} \right\}, \quad (1)$$

whence it is seen that the field along the axis of the tube is controlled by the factor  $\exp(j\omega t \pm \gamma z)$ , where  $\gamma$ , the propagation constant, may be written  $\gamma = \alpha + j\beta$ . The real part of  $\gamma$  is the attenuation constant and the imaginary part is the phase constant.

\* Decimal Classification: R110.

† Reprinted from *Proc. I.R.E.*, December, 1942.

<sup>1</sup> W. L. Barrow, "Transmission of electromagnetic waves in hollow tubes of metal," *Proc. I.R.E.*, vol. 24, pp. 1298-1329; October, 1936.

<sup>2</sup> J. R. Carson, S. P. Mead, and S. A. Schelkunoff, "Hyper-frequency wave guides," *Bell Sys. Tech. Jour.*, vol. 15, pp. 310-333; April, 1936.

<sup>3</sup> G. C. Southworth, "Hyper-frequency wave guides," *Bell Sys. Tech. Jour.*, vol. 15, pp. 284-309; April, 1936.

The forms of propagation constant discussed in the above references<sup>1-3</sup> are not valid for  $f \cong f_0$ , except in Barrow's paper. He gives a form of  $\gamma$  which is valid for the *E*-type wave, over the whole frequency range, but does not discuss it, putting it immediately into a simpler form which does not hold over the whole range. Barrow's general expression is limited only by the assumption that the conductivity of the tube is very large but finite. After making several changes of notation it may be written

$$\gamma = \frac{2\pi}{\lambda_0} \left\{ \left[ 1 - \left( \frac{\lambda_0}{\lambda} \right)^2 - \frac{\lambda_0^2 w}{4\pi^2} \right] + j \frac{\lambda_0^2 w}{4\pi^2} \right\}^{\frac{1}{2}}, \tag{2}$$

where  $\lambda_0$  is the free-space wavelength corresponding to  $f_0$ , i.e., the cutoff wavelength, and

$$w = \frac{\sqrt{2} \omega \epsilon_1}{a} \sqrt{\frac{\omega \mu_2}{\sigma_2}}, \tag{3}$$

- where  $\epsilon_1$  = dielectric constant of the medium (10<sup>-11</sup>/36 $\pi$  farad per centimeter for air)
- $\mu_2$  = permeability of the tube (henries per centimeter)
- $\sigma_2$  = conductivity of the tube (mhos per centimeter)
- $a$  = radius of the tube.

For copper pipes of practical sizes, the  $w$  term is negligibly small except very near cutoff.

The real part of (2) determines the attenuation. It is of interest to consider its variation as  $\lambda$  varies from below to above  $\lambda_0$ . This has been plotted in Figure 1, for the case of  $E_{0,1}$  type of field in a copper tube of radius  $a = 1.58$  centimeters. For  $\lambda < \lambda_0$  the curve is identical with those published previously<sup>1-3</sup>, except as  $\lambda \rightarrow \lambda_0$  the attenuation does not become infinite as previously indicated, but rises very steeply to a comparatively high value, and for  $\lambda > \lambda_0$  it approaches an asymptotic value of 13.2 decibels per centimeter.

The imaginary part of  $\gamma$  determines the form of the field along the  $z$  axis. For  $\lambda < \lambda_0$ , it is seen from (2), the imaginary part is very large compared to the real part; i.e.,  $\beta \gg \alpha$ . Hence we see from (1)

$$E = E_1(r, \theta) \exp(-\alpha z) \exp(-j\beta z),$$

that the field is simple harmonic with small attenuation. However, for  $\lambda > \lambda_0$ , we have  $\beta \ll \alpha$ . The factor  $\exp(-j\beta z)$  is very near unity.

The harmonic variation disappears and the field decreases at a high exponential rate as determined by  $\exp(-\alpha z)$ .

At the cutoff point  $\lambda = \lambda_0$  and  $\gamma = \sqrt{w(-1+j)} = \sqrt{w}(\cos 67.50 + j \sin 67.50)$ . Thus  $\alpha$  and  $\beta$  are of similar magnitude.

It is evident that there is a continuous transition through the cutoff point, from a slightly attenuated simple harmonic wave to a highly

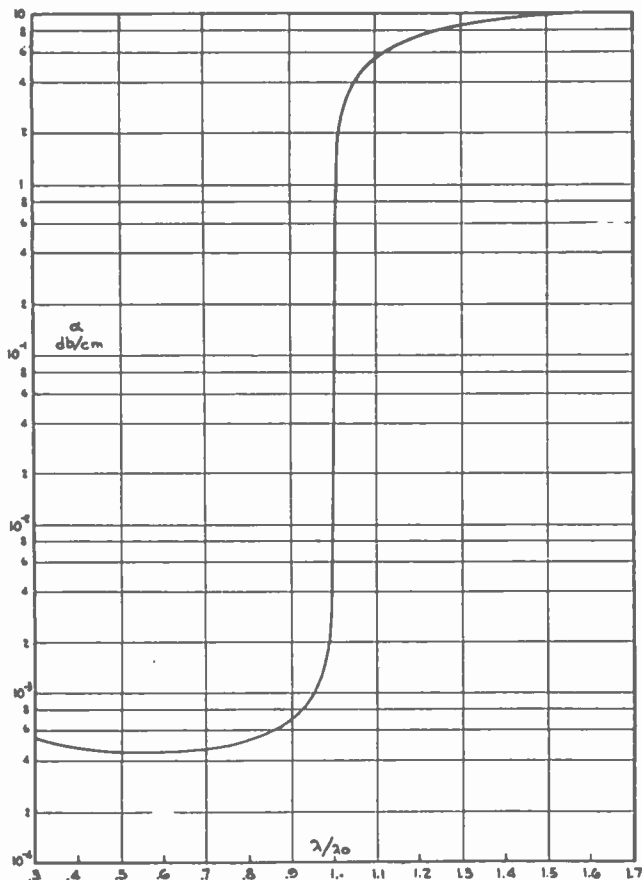


Fig. 1—Attenuation for the case of an  $E_{0,1}$  type of field in a copper pipe of 1.58 centimeters radius, showing the variation through the cutoff point.

attenuated exponential field.

It is possible to derive very simple expressions for the attenuation which are accurate except close to  $\lambda_0$ . To do this write  $\gamma^2$  in the form

$$\gamma^2 = \rho \epsilon^2 \phi,$$

whence

$$\gamma = \sqrt{\rho} e^{\theta}, \quad \alpha = \sqrt{\rho} \cos \phi, \quad \text{and} \quad \beta = \sqrt{\rho} \sin \phi,$$

where, from (2)

$$\rho = \frac{4\pi^2}{\lambda_0^2} \sqrt{\left(1 - \frac{\lambda_0^2}{\lambda^2} - \frac{\lambda_0^2 w}{4\pi^2}\right)^2 + \left(\frac{\lambda_0^2 w}{4\pi^2}\right)^2}.$$

Except very near to  $\lambda_0$  the  $w$  term is negligibly small and this is closely approximated by

$$\rho = \frac{4\pi^2}{\lambda_0^2} \left( \frac{\lambda_0^2}{\lambda^2} - 1 \right), \quad \text{for } \lambda < \lambda_0,$$

and

$$\rho = \frac{4\pi^2}{\lambda_0^2} \left( 1 - \frac{\lambda_0^2}{\lambda^2} \right), \quad \text{for } \lambda > \lambda_0.$$

Consider the two cases:

1.  $\lambda < \lambda_0$ .

Here  $\gamma^2$  has a large negative real part, and a small positive imaginary part, hence  $2\phi$  is almost 180 degrees and  $\phi$  is almost 90 degrees. Hence we may write  $\cos \phi = w/2\rho$ , and  $\sin \phi = 1$ . Therefore

$$\alpha = \sqrt{\rho} \cos \phi = \frac{\lambda_0 w / 4\pi}{\sqrt{\frac{\lambda_0^2}{\lambda^2} - 1}},$$

or, multiplying numerator and denominator by  $\lambda/\lambda_0$ ,

$$\alpha = \frac{\lambda w / 4\pi}{\sqrt{1 - \frac{\lambda^2}{\lambda_0^2}}}, \quad (4)$$

and

$$\beta = \frac{2\pi}{\lambda} \sqrt{1 - \frac{\lambda^2}{\lambda_0^2}}. \quad (5)$$

These are identical with the expressions derived by Barrow;<sup>1</sup> and Carson, Mead, and Schelkunoff<sup>2</sup>, for this case.

2.  $\lambda > \lambda_0$ .

Here  $\gamma^2$  has a large positive real part, and a small positive imaginary part. Hence,  $2\phi$  is nearly zero,  $\cos \phi = 1$ , and  $\sin \phi = w/2\rho$ . Therefore,

$$\alpha = \frac{2\pi}{\lambda_0} \sqrt{1 - \frac{\lambda_0^2}{\lambda^2}}, \quad (6)$$

and

$$\beta = \frac{\lambda_0 w / 4\pi}{\sqrt{1 - \frac{\lambda_0^2}{\lambda^2}}}. \quad (7)$$

It is of interest that the attenuation in this case depends only on  $\lambda$  and  $\lambda_0$  and is independent of the tube material, except for the assumption that it is of high conductivity.

The above discussion applies only to  $E$  waves, since the basic expression (2) was derived for that case only. The case of  $H$  waves for  $\lambda < \lambda_0$  has been discussed in detail by Barrow; Carson, Mead, and Schelkunoff, etc. The case  $\lambda > \lambda_0$  may be handled by noting that the propagation constant for  $H$  waves may be written<sup>4</sup>

$$\gamma = \frac{2\pi}{\lambda_0} \sqrt{1 - \frac{\lambda_0^2}{\lambda^2}},$$

except for  $\lambda$  very near to  $\lambda_0$ . For  $\lambda > \lambda_0$  this is real and thus represents the attenuation, which is seen to be identical with (6). The assumptions are the same in both cases. Hence (6) is valid for both  $E$  waves and  $H$  waves.

Equations (4) and (5) have been discussed in previous publications,<sup>1-3</sup> and will not be dealt with further here. Equations (6) and (7) however appear not to have been mentioned previously.<sup>5</sup> Equation (6) has been checked over the wavelength range from 7 to 10 centimeters for a tube of 1.58 centimeters radius, and for a field configuration of

<sup>4</sup> J. A. Stratton, "Electromagnetic Theory," McGraw-Hill Book Company, New York, N. Y., 1941, p. 539.

<sup>5</sup> R. A. Braden of this laboratory first noticed that our experimental measurements of attenuation rate followed an empirical law similar to equation (6). The similarity of this to expressions occurring in wave-guide theory led to the present investigation.

the  $H_{1,1}$  type. These data, which were obtained by G. Fernsler, are plotted in Figure 2. There is agreement within the accuracy of the measurements.

The extension or fringing of fields into tubes has been discussed in a number of instances<sup>6,7</sup> for static or low-frequency fields. These represent limiting cases given by  $\lambda \rightarrow \infty$ , and for which, from (6),

$$\alpha = 2\pi/\lambda_0. \tag{8}$$

Harnett and Case<sup>7</sup> have described three examples, to which this result is applicable, in which tubes are used as attenuators for signal generators, and in which three different field configurations are employed. The first type has an input electrode consisting of a small circular disk

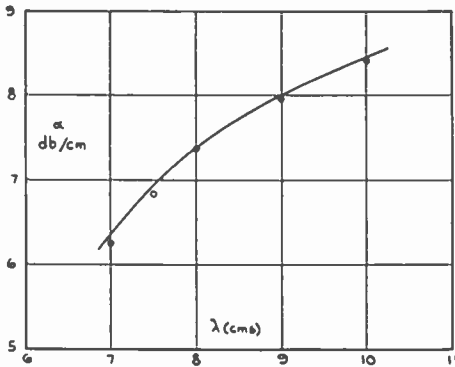


Fig. 2—Attenuation for the case of an  $H_{1,1}$  type of field in a pipe of 1.58 centimeters radius. The circles are experimental points. The line is computed from equation (6).

centrally located in the tube. This produces a radial electric field similar to that of the  $E_{0,1}$  wave. Hence from wave-guide theory,  $\lambda_0 = 2.62a$ . Therefore, from (8),

$$\begin{aligned} \alpha &= \frac{2\pi}{2.62a} \text{ napiers per centimeter} \\ &= \frac{20.9}{a} \text{ decibels per centimeter} \\ &= 20.9 \text{ decibels per radius,} \end{aligned}$$

<sup>6</sup> I. Langmuir and K. T. Compton, "Electrical discharges in gases, Part II," *Rev. Mod. Phys.*, vol. 3, pp. 212-213; April, 1931.

<sup>7</sup> D. E. Harnett and N. P. Case, "The design and testing of multirange receivers," *Proc. I.R.E.*, vol. 23, pp. 578-594; June, 1935. The attenuation formulas given in this paper were derived by H. A. Wheeler, but his derivations have not been published.



which is in agreement with previous results.<sup>6,7</sup> The second type has an input electrode consisting of a coil whose axis is normal to the axis of the tube. This produces a field configuration similar to that of the  $H_{1,1}$  wave. The limiting value of  $\alpha$  is found to be 16.0 decibels per radius. The third type consists of an input electrode in the form of a coil whose axis coincides with that of the tube. The field is analogous to that of the  $H_{0,1}$  wave, and the limiting attenuation is found to be 33.3 decibels per radius. These three cases are in agreement with the limiting values found by H. A. Wheeler, and given in the Harnett and Case paper.

The formulas for  $\lambda > \lambda_0$  for these three cases may be written as follows:

$$E_{0,1} \text{ type, } \alpha = 20.9 \sqrt{1 - \frac{\lambda_0^2}{\lambda^2}} \text{ decibels per radius,} \tag{9}$$

$$H_{1,1} \text{ type, } \alpha = 16.0 \sqrt{1 - \frac{\lambda_0^2}{\lambda^2}} \text{ decibels per radius,} \tag{10}$$

$$H_{0,1} \text{ type, } \alpha = 33.3 \sqrt{1 - \frac{\lambda_0^2}{\lambda^2}} \text{ decibels per radius,} \tag{11}$$

Formulas for other types of waves may be derived by inserting the proper value of  $\lambda_0$  in (6).

The accuracy of (6) and (7), also the derived formulas (9), (10), and (11) may be estimated as follows: From the accurate expression (2) we see that the terms involving  $w$  (which were neglected in obtaining (6) and (7)) affect the order of magnitude of the result only when

$$1 - \frac{\lambda_0^2}{\lambda^2} \approx \frac{\lambda_0^2 w}{4\pi^2} \approx 10^{-4}$$

for copper pipes. This may be written

$$\lambda^2 - \lambda_0^2 = 10^{-4}\lambda^2, \quad \text{or} \quad (\lambda - \lambda_0)(\lambda + \lambda_0) \approx 10^{-4}\lambda^2,$$

$$\text{or} \quad (\lambda - \lambda_0) = \Delta\lambda \approx \frac{10^{-4}\lambda^2}{2\lambda_0}, \quad \text{or} \quad \Delta\lambda \approx 10^{-4}\lambda_0.$$

Thus,  $\lambda$  must be within 0.01 per cent of  $\lambda_0$  before the  $w$  term is equal in magnitude to the sum of the other terms.

# RESONANT-CAVITY MEASUREMENTS\*†

BY

R. L. SPROULL AND E. G. LINDER

Research Department, RCA Laboratories Division,  
Princeton, N. J.

*Summary*—Satisfactory methods are described for measuring the resonant frequency,  $Q$ , and shunt resistance of resonant cavities. Some of the wavemeters and other equipment developed for these measurements are described.

The methods of determining resonant frequencies permit moderate accuracy in absolute measurements and very high precision in the comparison of the resonant frequencies of two cavities.

Three methods of measuring  $Q$  are described which are similar in principle but different in detail.

Shunt resistance has been determined by two methods which are convenient and reliable. By inverting these methods, the dielectric constants and dielectric conductivities of liquids and gases can be measured.

## I. INTRODUCTION

CAVITY resonators are indispensable in the micro-wave art, and in order to exploit them effectively it is necessary to be able to measure their characteristic properties. The parameters generally used to describe cavities are resonant frequency,  $Q$ , and shunt resistance. The methods in use at longer wavelengths for measuring these properties of resonant circuits are not generally applicable in the centimeter-wave region of frequencies. For several years, measuring procedures suitable for resonant cavities in this frequency region have been developed concurrently with applications of cavities. The most satisfactory methods are described here. These methods have been used successfully in the wavelength range from 2 to 12 centimeters and should also be useful at longer and shorter wavelengths.

## II. APPARATUS

The frequency stability of microwave oscillators is usually poor, and it is desirable to avoid reliance on the constancy of frequency of the signal generator in any measurements in this frequency region. A "sweep frequency" technique<sup>1</sup> was therefore used, as sketched in

\* Decimal Classification: R209.

† Reprinted from *Proc. I.R.E.*, May, 1946.

<sup>1</sup> F. E. Terman, "Radio Engineers' Handbook," McGraw-Hill Book Company, New York, N. Y., 1943.

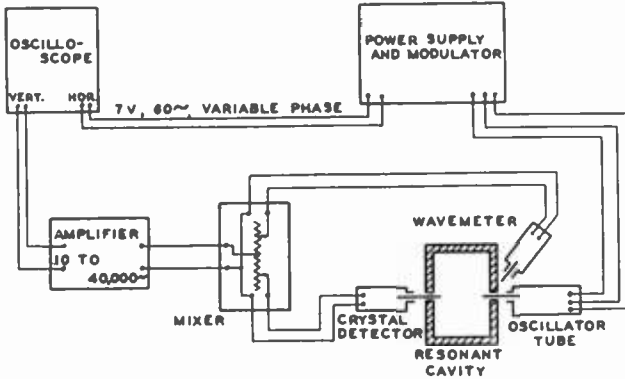


Fig. 1—Diagram of measuring equipment.

Figure 1. The apparatus used is illustrated in Figure 2 and Figure 3.

The frequency of the oscillator is modulated at a 60-cycle rate. A short, tunable transmission line from the oscillator ends in a probe, which may be inserted into the cavity being tested. A similar probe abstracts from the cavity a very small fraction of the oscillator's power, and another short, tunable transmission line connects this probe to a crystal detector. The rectified current from the detector is applied to an audio amplifier, the output of which is connected to the vertical-deflection system of a cathode-ray oscilloscope. The horizontal deflection is at a 60-cycle rate.

The pattern traced out on the oscilloscope screen is, therefore, crystal current as a function of the modulating voltage applied to the oscillator. With some restrictions, this pattern is also a measure of the "response" of the cavity (the square of the absolute magnitude of its impedance) as a function of frequency. These restrictions are: (1)

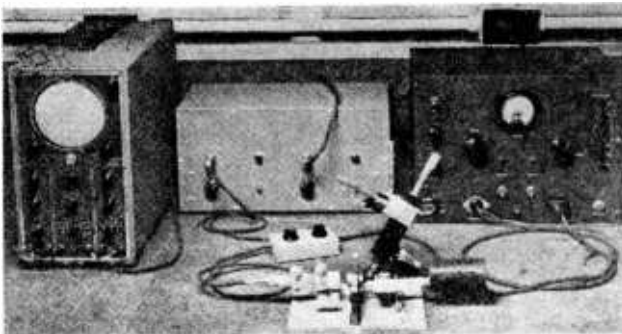


Fig. 2—Photograph of measuring equipment. The oscilloscope, audio amplifier, and power-supply modulator are in the background. The mixer box is in the center. In the foreground are the detector, cavity mounting, wavemeter, and oscillator.

the coupling into and out from the test cavity must be very loose; (2) the crystal must be "square law"; (3) the bandwidth of the coupling systems must be much greater than that of the cavity; (4) the amplifier and oscilloscope amplifiers must not distort the signals applied to them; (5) the oscillator must have negligible amplitude modulation over a frequency region of several times the bandwidth of the cavity; (6) the frequency modulation must be linear; that is; frequency must be a linear function of the modulating voltage.

The first four requirements can be satisfied quite generally, and the last two do not constitute serious difficulties except for very low- $Q$  cavities. The probe coupling has been used in most of the measurements because the only modification of the cavity required for the measurements is the provision of two small holes in the cavity walls. For precise work, waveguide systems have been used, but they suffer from lack of versatility.

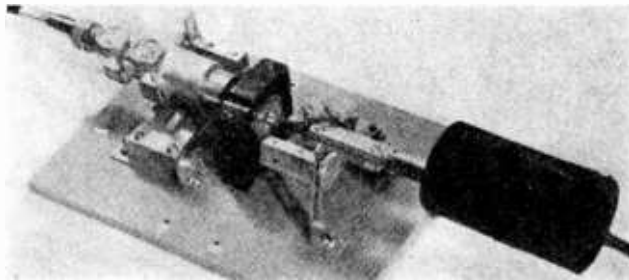


Fig. 3—Detector, cavity mounting, and oscillator. The low- $Q$  crystal detector circuit is a coaxial line, tunable by a rack-and-pinion control. Another rack and pinion controls the insertion of the detector probe into the resonator. The tunable transmission line from the oscillator is terminated by the small wire probe which projects into the cylindrical cavity being tested.

The mixer shown in Figure 1 permits the simultaneous appearance on the screen of resonance curves of two cavities, one of which is usually a wavemeter or secondary frequency standard. When these two cavities are tuned to nearly the same frequency, the oscilloscope vertical deflection is the algebraic sum of the signals from the two detectors. The relative amplitudes of the two signals may be varied by adjusting the coupling of the oscillator to the two cavities, or by adjusting the potentiometers in the mixer.

Three kinds of wavemeters have been used, all based on resonant cavities. A carefully constructed concentric transmission line with **movable terminating piston** has been used as a frequency standard. The  $Q$  of this type of wavemeter is low, of the order of 1000, but it will appear that this does not constitute a serious limitation for

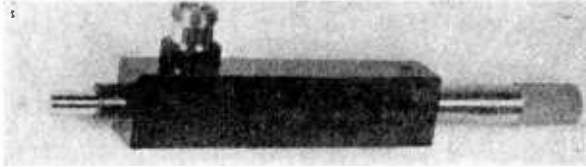


Fig. 4—Resonant-cavity wavemeter. The dielectric-covered antenna is at the left, and the threaded bushing above it and to the right is the connector for rectified crystal current. The micrometer which fixes the piston position is at the right.

most frequency measurements. This meter is not satisfactory for measuring small frequency differences because of its low  $Q$  and small dispersion (small travel of piston and change in scale reading per unit of wavelength change).

A resonant-cavity wavemeter, illustrated in Figure 4, has been developed<sup>2</sup> for more accurate measurements. It consists of a rectangular cavity, the length of which is variable by a piston driven by a micrometer screw; a crystal detector and a small probe antenna are loosely coupled to the cavity. This type of wavemeter has the advantage of a high  $Q$ ; a further advantage is that a given motion of the piston corresponds to a smaller wavelength change than the same motion of the concentric-line plunger. Its chief disadvantage is its limited wavelength range. At the short-wavelength end of the scale the entrance of higher modes of oscillation of the cavity limits the range, while the long-wavelength limit is caused by the proximity of the "cut-off" point. The resonant wavelength can never be longer than twice the width of the cavity, regardless of the piston's position.

For higher dispersion in a much narrower range (about one half per cent of the mean wavelength) a wavemeter has been built using the  $TE_{1,2,0}$  mode, also called the (1, 2, 0) mode<sup>3</sup> of a rectangular cav-

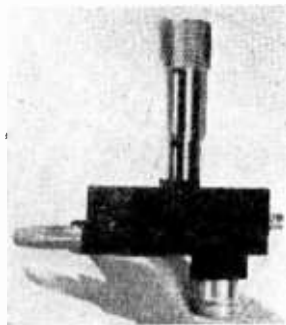


Fig. 5 — Narrow-range resonant-cavity wavemeter. The small pin which varies the resonant frequency is driven by the micrometer screw.

<sup>2</sup> D. Blitz and E. G. Linder.

<sup>3</sup> E. U. Condon, "Principles of microwave radio," *Rev. Mod. Phys.*, vol. 14, p. 347; October, 1942.

ity, as shown in Figure 5. The end of a micrometer screw was ground to form a small pin which was inserted through, but without touching the rim of, a small hole in the center of the broad side of the cavity. This arrangement permits very slight current flow on the part of the pin which lies outside the cavity, and secures maximum linearity of resonant wavelength as a function of the depth of insertion of the pin. Since the whole scale of the micrometer corresponds to only a fraction of a per cent change in a resonant wavelength, high dispersion is obtained. This wavemeter is made of Invar to minimize the temperature coefficient of frequency.

### III. RESONANT-FREQUENCY COMPARISONS

No effort has been made in this work to attain great accuracy in the measurement of the absolute resonant frequencies of resonant cavities. The accuracy of such measurements has been limited by the accuracy of the frequency standards employed. The absolute accuracy of the coaxial-line wavemeter is probably no better than  $\pm 0.1$  per cent in the centimeter region.

It is frequently desirable to be able to compare the resonant frequencies of cavities with a precision much higher than this accuracy of the absolute measurement of frequency. Measurement of small frequency differences or the construction of an internally consistent set of secondary frequency standards require such high precision. The frequency-comparison method described here is capable of as great precision as can be profitably employed at the present stage of the microwave art.

As an introduction to the method actually used, it is worthwhile to describe a more rudimentary method. If, in the system shown in Figure 1, the range of frequencies generated by the oscillator includes the resonant frequencies of both the wavemeter and the cavity under test, the pattern on the oscilloscope screen will resemble Figure 6(a).<sup>1</sup> In this and subsequent figures, the wavemeter resonant frequency and  $Q$  are called  $f_w$  and  $Q_w$ ;  $f_c$  and  $Q_c$  are the properties of the cavity being tested. As  $f_w$  becomes nearly equal to  $f_c$ , the pattern of Figure 6(b) results, and Figure 6(c) portrays exact equality of frequencies. It is impossible to determine equality of frequencies with much less error than that represented by Figure 6(b), and even the difference between Figure 6(b) and Figure 6(c) is difficult to detect if the amplifier gain

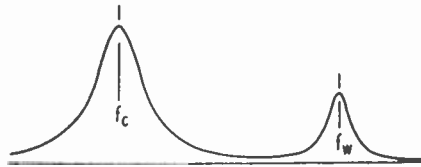
<sup>1</sup> E. U. Condon, "Forced oscillations in cavity resonators," *Jour. Appl. Phys.*, vol. 12, pp. 129-132; February, 1941. Figures 6, 7, and 9 are computed from the known form of a high- $Q$  cavity's transfer impedance as a function of frequency, when the coupling is very loose and the coupling systems are of low  $Q$ . The resonance curves are of the form  $[1 + 4Q^2(f - f_c)^2]^{-1}$ .

or oscillator power fluctuates. This constitutes a frequency-comparison precision of about  $\pm (10/Q_r)$  per cent. While this is sufficient for many purposes, it is not adequate for measuring small differences in resonant frequency, such as will be encountered in shunt-resistance measurements.

The frequency-comparison method actually used is a distinct improvement over this simple arrangement. In the improved method

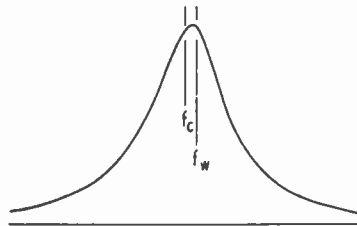
Fig. 6 — Oscilloscope patterns for first method of frequency comparison.

- (a) Horizontal scale compressed. Wavemeter resonant frequency ( $f_w$ ) and cavity resonant frequency ( $f_c$ ) considerably different.



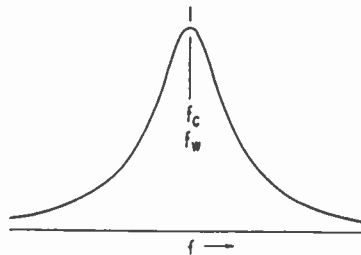
(a)

- (b)  $f_w$  nearly equal to  $f_c$ ,  
 $f_w = f_c + (f_c/10Q_r)$ .



(b)

- (c)  $f_w$  exactly equal to  $f_c$ .



(c)

the detector outputs are combined in such a way that the signal from the wavemeter crystal decreases the deflection produced by the crystal coupled to the cavity under test. This may be accomplished by using crystals which differ in the sign of the rectified current or merely by reversing the leads from one crystal to the mixer. The oscilloscope patterns thus obtained are shown in Figure 7(a) for  $f_w \neq f_c$ , in Figure 7(b) for  $f_w \cong f_c$ , and in Figure 7(c) for  $f_w = f_c$ . The inequality in

resonant frequencies is obvious from the unequal heights of the two limbs in Figure 7(b), even though the frequency difference is only  $1/Q_c$  per cent. One therefore has only to tune the wavemeter until the

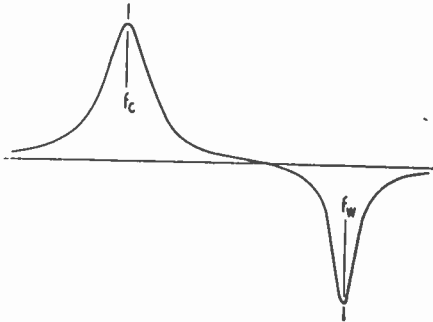
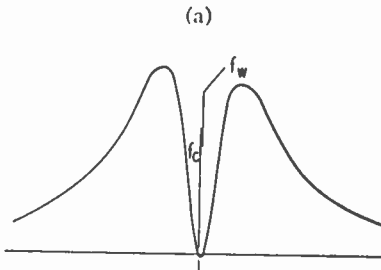
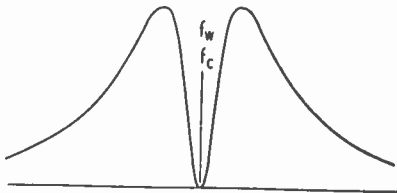


Fig. 7 — Oscilloscope patterns for second precision method of frequency comparison.

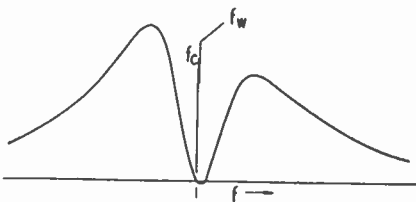
(a) Horizontal and vertical scales compressed.  $f_w$  considerably different from  $f_c$ .  $Q_w = 2Q_c$ .



(b)  $f_w$  nearly equal to  $f_c$ .  
 $f_w = f_c + 0.01 (f_c/Q_c)$ ;  
 $Q_w = 2Q_c$ .



(c)  $f_w$  exactly equal to  $f_c$ .  
 $Q_w = 2Q_c$ .



(d)  $f_w$  nearly equal to  $f_c$ , but a value of  $Q_w/Q_c$  different from parts (a), (b), and (c).  $f_w = f_c + 0.008 (f_c/Q_c)$ ;  $Q_w = 1.10Q_c$ . Vertical scale expanded.

heights of these two limbs are approximately equal to obtain precise equality of  $f_w$  and  $f_c$ .

This comparison is particularly sensitive when the wavemeter  $Q$



is nearly equal to that of the cavity. The mixer is then adjusted to give equal amplitudes to the two resonance curves. If  $Q_w = Q_r$  and  $f_w = f_r$ , a straight line appears on the oscilloscope, and the slightest departure from equality of  $f_w$  and  $f_r$  is immediately apparent. A number of cavities and a wavemeter with  $Q$ 's within 10 per cent of 8000 have been used in this measurement work. Figure 7(d) is typical of the patterns encountered with these cavities; the existence of a frequency difference is obvious, yet the difference is only one millionth of the resonant frequency  $f_r$ .

It is essential to this method that the amplitudes of the two resonance curves be of the same order of magnitude, but only when  $Q_w \cong Q_r$  is it necessary to make them approximately equal. Some advantage is obtained when  $Q_w \neq Q_r$  if the higher  $Q$  resonance is given a somewhat larger amplitude. Fluctuations in the power or frequency of the oscillator or in the gain of the amplifiers cannot cause errors. Amplitude modulation of the oscillator can cause a slight error, but this error is much smaller than its analogue in the former method. The resonance curves of both wavemeter and cavity must be undistorted, any resonances in the transmission lines must be of very low  $Q$ , and the coupling to the cavities must be loose. It is not necessary that the frequency modulation be linear, though linearity is a convenience in detecting distortion. The crystal capacitance and distributed capacitance of wiring must be kept low enough that it does not cause a significant phase delay of the signal from one crystal relative to that from the other. This is easily possible because of the low repetition frequency (60 cycles).

This method has proved reliable and convenient in operation. Photographs of the oscilloscope screen are shown in Figure 8.

In the precision measurement of frequency using cavity wavemeters, corrections must be applied for atmospheric properties and cavity temperature. If the parts of the wavemeter which determine the dimensions of the resonant cavity are of a single metal, the temperature coefficient of wavelength is the coefficient of linear expansion of the metal. The temperature and humidity of the atmosphere within the wavemeter must be known in order to convert wavelength in this atmosphere to wavelength *in vacuo*, and hence to frequency. When comparing the frequencies of a wavemeter and a resonant cavity, both open to the same atmosphere, these corrections for the dielectric constant of the air need not be applied; but a correction for thermal expansion of the cavity dimensions must be applied whenever the cavities being compared are of different metals.

IV. *Q* MEASUREMENTS

The oscilloscope presentation of a cavity-resonance curve permits measurement of *Q* value by measuring the difference  $\Delta f$  in frequency

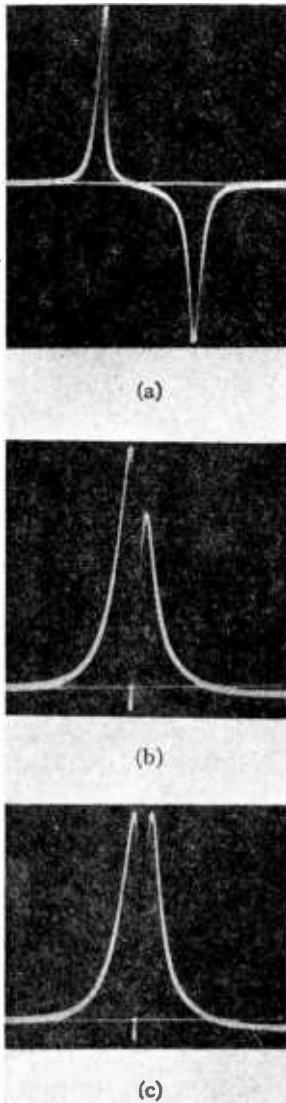


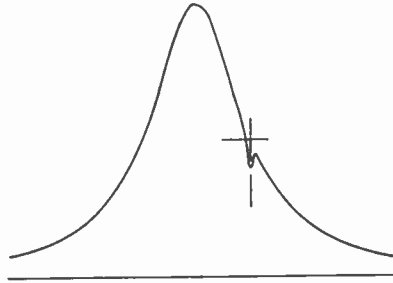
Fig. 8—Photographs of oscilloscope screen. The conditions correspond roughly to those of Fig. 7(a), (b), and (c).

at the two half-power points and using the value of  $f_c$  already obtained to compute  $Q_c \equiv f_c/\Delta f$ . Under the conditions of coupling, linearity, etc., noted in the second section, the half-power points are the points

where the vertical deflection is one half the maximum deflection. If a wavemeter of sufficiently high  $Q$  is available, the wavemeter detector signal may be combined with the resonance curve and the two frequencies at the half-power points determined directly; Figure 9(a) shows a wavemeter tuned to one of these two frequencies, where the wavemeter  $Q_w$  is 15 times the  $Q_c$  of the cavity.

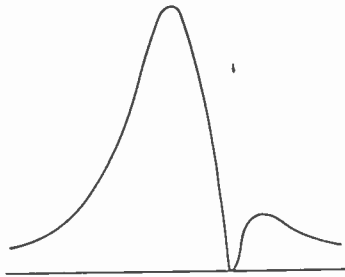
Fig. 9 — Oscilloscope patterns for measurement of  $Q$ .

- (a) Method suitable when  $Q_w/Q_c \gg v$ .  
 $Q_w = 15Q_c$ ;  
 $f_w = f_c + (f_c/2Q_c)$ .



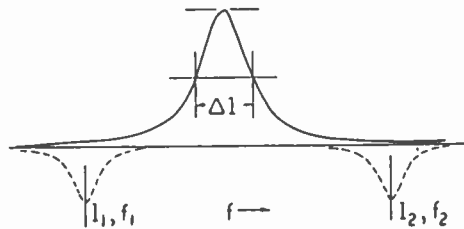
(a)

- (b) Method suitable for any  $Q_w/Q_c$  but not accurate if  $Q_c$  is extremely large.  $Q_w = 4Q_c$ ;  $f_w = f_c + (f_c/2Q_c)$ .



(b)

- (c) Method suitable for any  $Q_w/Q_c$ .



(c)

This method becomes less accurate as the ratio  $Q_w/Q_c$  becomes smaller than 10 or 15, since it becomes increasingly difficult to determine the half-power points in the presence of the wavemeter signal. To overcome this difficulty, the amplitude of the wavemeter signal may be made exactly one half of that of the cavity. The wavemeter may

then be set to a half-power point by tuning it until it produces a dip in the resonance curve which just reaches the reference base line for the resonance curve, as in Figure 9(b). This method may be used for any  $Q_r/Q_e$  ratio, but becomes unsatisfactory if  $Q_e$  is so large that the number of scale divisions of the wavemeter corresponding to the frequency difference becomes small.

When measuring high- $Q$  cavities it is often found that the wavemeter dispersion is insufficient for accurate measurements; the frequency difference between half-power points may correspond to only a fraction of a scale division of the wavemeter. It is then desirable to "calibrate the screen" of the oscilloscope as in Figure 9(c). The frequencies  $f_1$  and  $f_2$  corresponding to two well-separated points  $l_1$  and  $l_2$  on the screen are determined by tuning the wavemeter until the peak of its resonance curve coincides with each of these points in turn. If the linear separation on the screen of the half-power points of the cavity being tested is  $\Delta l$ , then

$$\Delta f = \Delta l \left( \frac{f_2 - f_1}{l_2 - l_1} \right). \quad (1)$$

This is valid, of course, only if the frequency modulation and oscilloscope horizontal deflection are linear functions of the modulating voltage, and nonlinearity of modulation constitutes the most troublesome source of error in this method. This method also requires that the generated frequency at any one modulator voltage remain constant for the few seconds required to tune the wavemeter. None of the other methods described here has this limitation.

If the  $Q$  is very low, it may be necessary to correct the measurements for amplitude modulation of the signal generator. The amplifier must pass an undistorted resonance curve for accurate measurements with any value of  $Q$ , which requires that its gain and time delay be constant from 60 to about 6000 cycles. The input and output couplings of the cavity must be very small if the measured  $Q$  is to be the "unloaded"  $Q$  of the cavity. This last requirement means that the power transmission into the detector must be very small. For example, if the measured  $Q$  is to be within 5 per cent of the unloaded  $Q$ , the power into the detector can be at most only 0.5 per cent of the power which could have been obtained from the same oscillator when coupled for maximum power transfer into the detector.

## V. SHUNT-RESISTANCE MEASUREMENTS

In many applications of cavity resonators it is necessary to know

the shunt resistance of the cavity, which is its shunt impedance at resonance. This is particularly true if the resonator is to be excited by an electron beam, as in a microwave oscillator.

The shunt resistance  $R_0$  of a cavity, like that of a conventional "lumped" circuit, can be defined from the relation

$$R_0 = \frac{V_2}{2W_1} \tag{2}$$

where  $W_1$  is the power dissipated per second in the cavity (watts) and  $V$  is the amplitude of the "voltage" between two points on the cavity walls. By "voltage" is meant the line integral of the alternating elec-

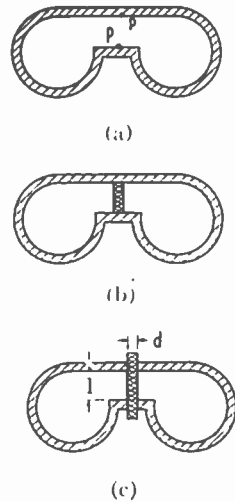


Fig. 10—Measurement of shunt resistance in a doughnut-shaped resonant cavity. Cylindrical symmetry about  $pP$ . The shunt resistance between the points  $p, P$  is required. In (b) a dielectric cylinder is inserted, and in (c) the dielectric has been inserted in an easier manner, which gives approximately correct results when  $l/d \gg 1$ .

tric field.<sup>5</sup> For a given  $W_1$ , the value of  $V$ , and hence of  $R_0$ , depends on the two points chosen; this corresponds to the different values of resistance obtained by "tapping" at different turns of the coil in a coil-and-capacitor resonant circuit.  $R_0$  also depends, in the case of a resonant cavity, upon the choice of the path between these two points over which  $V$  is evaluated. In most applications of resonant cavities, the particular value of  $R_0$  of most interest is that obtained by choosing end points and path such that the maximum  $R_0$  is obtained. The  $R_0$  thus evaluated is consistent with the usual definition<sup>5</sup> and will be used in the remainder of this section.

In applications involving electron beams, one is generally interested in cavities such that the amplitude of the electric field is nearly constant over the required path; such a case is illustrated in Figure 10(a),

<sup>5</sup> See p. 365 of footnote reference 3.

where  $R_0$  is to be evaluated over the straight-line path between  $p$  and  $P$ . Only such constant-field cases are susceptible to the following measuring methods.

Two methods of measuring shunt resistance have been developed, and they will be called the "resistance-insertion" and "capacitance-insertion" methods. In the former, a small resistor is inserted between the two points where  $R_0$  is required and the effect upon the  $Q$  of the cavity is observed; in practice, this "resistor" is usually a rod of lossy dielectric. In the latter method, a small dielectric cylinder is inserted as before, but the effect upon the resonant frequency of the cavity is observed.

A small dielectric cylinder of cross-sectional area  $A$  and length  $l$  is inserted between the points  $p$  and  $P$  in Figure 10(a), such that the ends are in intimate contact with the cavity walls and the axis of the cylinder is perpendicular to the cavity walls. Since the electric field in the neighborhood of the dielectric is nearly constant and parallel to the elements of the cylinder, the electric field at the surface of the dielectric is entirely tangential to this surface, and hence is the same intensity inside the dielectric as it is just outside. If the cross-sectional area, dielectric constant, and conductivity of the rod are sufficiently small, the  $Q$  will remain of the order of 100 or more and the change in resonant frequency can be kept of the order of one per cent or less. Under these circumstances the electric and magnetic fields at resonance will not be substantially changed by the presence of the dielectric, and  $R_0$  can be calculated from either the change in  $Q$  or the change in  $f_0$ .

The algebraic expressions relating  $R_0$  to the observables in the two methods can be derived in several ways. Using the energy-decrement definition of  $Q$  and (2), and obtaining the power dissipated in the lossy dielectric from Maxwell's equations, the expression for the resistor-insertion method may be obtained. The relation for the capacitance-insertion method may be derived from the change in the average stored electric energy when the dielectric is inserted and the requirement that the average electric and magnetic energies must be equal at resonance.<sup>6</sup> Also, both expressions may easily be verified directly from Maxwell's equations for the special cases of cavities the geometrical shapes of which permit analytical solutions for the fields before the dielectric was inserted. Derivations based on the "lumped"-circuit

---

<sup>6</sup> See p. 351 of footnote reference 3. This property of resonance holds for systems of electromagnetic standing waves, provided one sums the energies over an integral number of half wavelengths of the standing-wave pattern, which is what is done in computing the electric and magnetic energies of a cavity at its resonant frequency.

analogy are given below. The relations derived by any of these methods are identical and subject to the same restrictions.

In lumped circuits

$$Q_c = 2\pi f_c C R_0. \tag{3}$$

The essence of the methods for measuring  $R_0$  of cavities is to express the unmeasurable quantity  $C$  in terms of observable quantities. In the resistance-insertion method a resistance  $R$  inserted between the points  $p$  and  $P$ , as in Figures 10(a) and (b), is essentially a resistance in parallel with the shunt resistance  $R_0$  between these points. If  $f_c$  and  $Q_c$  were the resonant frequency and  $Q$  before the resistor was inserted, and  $f_c'$  and  $Q_c'$  the new values with the resistor,  $Q_c'$  will be related to the parallel combination of  $R$  and  $R_0$  in the same way that (3) related  $Q_c$  to  $R_0$ :

$$\frac{1}{Q'} = \frac{1}{2\pi f_c' C'} \left( \frac{1}{R_0} + \frac{1}{R} \right) = \left( \frac{f_c C}{f_c' C'} \right) \frac{R_0}{Q_c} \left( \frac{1}{R_0} + \frac{1}{R} \right). \tag{4}$$

If the resistor's size and dielectric constant are sufficiently small,  $f_c C$  nearly equals  $f_c' C'$ ; setting  $f_c C = f_c' C'$  and rearranging terms gives

$$R_0 = R(Q_c/Q_c' - 1). \tag{5}$$

Because of the limitation to situations of constant field, where the electric field is known to be substantially the same inside the resistor as it is outside, the effective resistance  $R$  of the cylinder is just the resistance calculated in the usual way:  $R = l/\sigma A$ . Skin effect need not be considered since the skin depth is much larger than the diameter of the cylinder for all useful values of  $A$  and  $\sigma$ . Therefore

$$R_0 = \frac{l}{\sigma A} (Q_c/Q_c' - 1) \text{ ohms.} \tag{6}$$

Of course one must use the value of  $\sigma$ , the dielectric conductivity<sup>7</sup> which pertains to the frequency at which the measurements are made. Note that in using (6) the change in frequency upon insertion of the resistor must be small compared to the frequency itself, the resistor must be of constant cross section and parallel to the electric field, its

---

<sup>7</sup>  $\sigma$  is related to the tangent of the angle  $\delta$  of loss by  $\tan \delta = \sigma/2\pi f \kappa \epsilon_0$ . The "Q" of the dielectric is  $Q = 1/\tan \delta$  and  $\sin \delta$  is its "power factor."  $\sigma$  here is measured in m-k-s units (mhos per meter), but (6) may be used with  $l$  and  $A^{1/2}$  in centimeters and  $\sigma$  in mhos per centimeter.

ends must make good contact with the cavity walls, and the amplitude of the electric field must be constant in the neighborhood of the resistor. The "good-contact" restriction frequently may be removed, as explained below.

This method has been successfully used on a variety of cavities. The limitations associated with (6) make metallic resistors impractical, but lossy liquids and glasses exhibit the correct orders of magnitude of conductivities for use as resistors. The conductivities of common glasses and some common liquids range from about 0.015 (Corning 705BA glass) to 15 (water) mhos per meter in the centimeter-wavelength region. For most cavities a thin Pyrex capillary tube containing water, water-ethyl-alcohol mixtures, or carbon tetrachloride has produced a satisfactory resistor. With bores of the order of  $10^{-3}$  or  $10^{-4}$  square centimeter and lengths of 0.1 to 1 centimeter, resistances of the order of 1000 ohms to 10 megohms may be obtained. The size and conductivity of the dielectric are so chosen that  $Q_c/Q_c'$  is substantially different from unity, in order to avoid the situation where a small error in measuring  $Q_c/Q_c'$  introduces a large relative error in the determination of  $R_0$ . On the other hand,  $Q_c'$  must not be too low or difficulty will be encountered in measuring it because of the limited frequency-modulation range of the oscillator.

In the capacitance-insertion method, the insertion of the small dielectric cylinder increases the capacity by the amount  $\Delta C = (\kappa - 1)\epsilon_0 A/l$ . This comes about because the contribution to the total cavity capacitance of the volume occupied by the dielectric was  $\epsilon_0 A/l$  before the dielectric was inserted and  $\kappa\epsilon_0 A/l$  afterwards.  $\kappa$  is the dielectric constant of the material,  $\epsilon_0 = 8.85 \times 10^{-12}$  farads per meter, and  $l$  and  $A^{1/2}$  are expressed in meters.

The rate of change of resonant frequency with change in capacitance is obtained by differentiating  $2\pi f_c = (LC)^{-1/2}$  and it is

$$\frac{\partial f_c}{\partial C} = -\frac{f_c}{2C}.$$

For small finite changes it is approximately true that

$$\Delta f_c = -\left(\frac{f_c}{2C}\right)\Delta C = \frac{-f_c(\kappa - 1)\epsilon_0 A}{2Cl}. \quad (7)$$

Using (7) in (3) to eliminate the unknown and unmeasurable quantity  $C$ , one obtains



$$R_0 = \frac{-Q_c l (\Delta f_c)}{\pi f_c^2 (\kappa - 1) \epsilon_0 A} . \tag{8}$$

A simpler and more convenient relation is obtained by expressing the frequency change  $\Delta f_c$  in terms of a resonant-wavelength change  $\Delta \lambda_c$ ; when this is done and the approximation  $(\pi c \epsilon_0)^{-1} = 120$  ohms is used, (8) becomes

$$R_0 = 120 \frac{Q_c l (\Delta \lambda_c)}{(\kappa - 1) A} \text{ ohms.} \tag{9}$$

M-k-s units have been used to derive (9) but of course it is valid if  $l$ ,  $\Delta \lambda_c$ , and  $A^{1/2}$  are in the same units, whether or not these units are meters. The restrictions mentioned in connection with (6) apply as well to (9).

This capacitance-insertion method is more convenient and accurate than the resistor method, since only one  $Q$  measurement is required in the former and the change in resonant wavelength, even though it may be very small, can be measured quite accurately by the method portrayed in Figure 7. But the capacitance method is less flexible because the range of  $\kappa$ 's of available materials is small compared to the range of  $\sigma$ 's. This means that for cavities of very low shunt resistance,  $A$  must be larger than in the resistor-insertion method in order to preserve a  $\Delta \lambda_c$  of sufficient magnitude.

In using either of these methods, it is much more convenient to drill small holes in the cavity walls and insert the dielectric cylinder through these holes than to install it completely inside the cavity. This "short-cut" is illustrated in Figure 10(c). It is satisfactory provided  $d \ll l$ ; under these circumstances the fringing field in the dielectric near the cavity walls is not a serious source of error, and the contact of the dielectric rod with the walls is not important in either method. Tests have shown that even if  $d \cong l/4$  the methods are still reliable.

Both methods of measuring shunt resistance have been tested by measuring  $R_0$  of rectangular and cylindrical cavities, where the ratio of  $R_0$  to  $Q_c$  could be calculated. The measured ratio agreed with the theoretical  $R_0/Q_c$  within a few per cent for all the cavities investigated. Since this ratio depends only on the cavity geometry and not upon the material or surface condition of the cavity walls, comparing experimental and theoretical values of this ratio is a better test of the measuring method than comparison of  $R_0$  values.

The methods for measuring shunt resistance may be reversed to provide methods for measuring the conductivity  $\sigma$  and dielectric constant  $\kappa$  of solids and liquids at very high frequencies. A cavity of

simple geometrical shape is employed and  $R_0/Q_c$  is computed from the known electric and magnetic fields in the cavity. Then from measurements of  $Q_c$ , and of  $Q_c'$  and  $\Delta\lambda_c$  when a dielectric cylinder is inserted,  $\sigma$  and  $\kappa$  may be obtained from (6) and (9). This method has been used for many different materials, and wherever comparison with values of  $\sigma$  and  $\kappa$  obtained by other methods was possible, good agreement was secured.

# ABSORPTION OF MICROWAVES BY GASES. II\*†

By

JOHN E. WALTER AND W. D. HERSHBERGER

Research Department, RCA Laboratories Division,  
Princeton, N. J.

*Summary*—The absorption coefficients and dielectric constants of sixteen gases have been measured at the two wavelengths  $\lambda = 1.24$  cm and  $\lambda = 3.18$  cm. The gases are  $\text{H}_2\text{S}$ ,  $\text{COS}$ ,  $(\text{CH}_3)_2\text{O}$ ,  $\text{C}_2\text{H}_6\text{O}$ ,  $\text{C}_2\text{H}_5\text{Cl}$ ,  $\text{SO}_2$ ,  $\text{NH}_3$ , six halogenated methanes and three amines. Certain improvements in technique are described; these improvements permit detection of absorption coefficients as small as  $0.2 \times 10^{-4} \text{ cm}^{-1}$  and measurement of larger coefficients with an accuracy of  $\pm 5$  percent. The measured dielectric constants at these wave-lengths are essentially equal to the static values. A quantitative interpretation of the absorption coefficients in terms of the known structure and spectra of the individual molecules is given. The theory indicates that all non-planar molecules which possess a permanent dipole moment should show appreciable absorption in the microwave region.

## INTRODUCTION

RESULTS of an investigation on the absorption of microwaves by gases were given in an earlier paper.<sup>1</sup> Measurements on absorption are taken by noting the power loss suffered by a microwave transmitted through a rectangular wave guide operating in the  $\text{TE}_{10}$  mode. Dielectric constants are measured by comparing the wave-length in the guide when evacuated with the wave-length after the gas under study is admitted to the guide. Measurements are reported at two wave-lengths: 3.18 cm and 1.24 cm. The experimental values of the absorption coefficients  $\alpha$  (in  $\text{cm}^{-1}$ ) are given in Table 1; the experimental values of the dielectric constants are listed in Table 2. The purpose of the present paper is to report improvements in technique, to give the theory underlying the observed absorption, and to present new data and analyses of these data.

## TECHNIQUES AND ACCURACY OF MEASUREMENT

One factor which has limited the accuracy with which small absorption coefficients may be measured is the standing wave in the test section of guide. This effect was troublesome in the work reported earlier but has now been eliminated by placing a wedge of lossy solid material

\* Decimal Classification: R110.

† Reprinted from *Jour. Appl. Phys.*, October, 1946.

<sup>1</sup> W. D. Hershberger, *J. App. Phys.* 17, 495 (1946).

Table 1—Observed absorption coefficients.

	$\alpha \times 10^4$ ( $\lambda = 3.18$ )	$\alpha \times 10^4$ ( $\lambda = 1.24$ )
NH <sub>3</sub>	15.5	78.0
CH <sub>3</sub> F	7.6	10.0
CH <sub>3</sub> Cl	5.5	8.0
CH <sub>3</sub> Br	4.2	6.2
C <sub>2</sub> H <sub>5</sub> Cl	8.7	15.0
CHFCl <sub>2</sub>	5.2	10.6
CHF <sub>2</sub> Cl	7.2	12.0
CF <sub>2</sub> Cl <sub>2</sub>	0.3	3.1
H <sub>2</sub> S	~0.0	~0.3
SO <sub>2</sub>	1.1	5.0
COS	—	0.8
(CH <sub>3</sub> ) <sub>2</sub> O	0.7	3.9
C <sub>2</sub> H <sub>5</sub> O	1.0	6.8
CH <sub>3</sub> NH <sub>2</sub>	2.1	10.5
(CH <sub>3</sub> ) <sub>2</sub> NH	—	7.0
C <sub>2</sub> H <sub>5</sub> NH <sub>2</sub>	3.1	10.2

in this section near the input window. The loss introduced by the wedge is 10 db and, since it is not inserted until the standing wave has been minimized by the usual tuning adjustments, no measurable standing wave now exists when measurements are taken. The procedure for tuning is first to fill the 30-foot test section with ammonia which effectively isolates the receiver from the generator and then adjust the tuner which is adjacent to the input window for a minimum standing wave. Next, the ammonia is removed and the tuner adjacent to the output window is adjusted for a minimum standing wave. As a result

Table 2—Dielectric constants.

	$\delta_0 \times 10^3$ (calculated)	$\delta \times 10^3$ ( $\lambda = 3.18$ )	$\delta \times 10^3$ ( $\lambda = 1.24$ )
NH <sub>3</sub>	6.3	5.3	5.5
CH <sub>3</sub> F	9.2	8.1	8.4
CH <sub>3</sub> Cl	10.3	9.4	9.9
CH <sub>3</sub> Br	9.7	9.5	10.0
C <sub>2</sub> H <sub>5</sub> Cl	12.7	11.1	11.6
CHFCl <sub>2</sub>	6.2	4.9	5.2
CHF <sub>2</sub> Cl	6.7	5.2	5.7
CF <sub>2</sub> Cl <sub>2</sub>	3.1	2.9	3.1
H <sub>2</sub> S	3.6	3.0	3.5
SO <sub>2</sub>	7.9	7.5	8.6
COS	2.6	—	2.6
(CH <sub>3</sub> ) <sub>2</sub> O	6.2	5.5	6.1
C <sub>2</sub> H <sub>5</sub> O	10.4	10.2	10.7
CH <sub>3</sub> NH <sub>2</sub>	5.3	4.8	5.3
(CH <sub>3</sub> ) <sub>2</sub> NH	4.4	—	4.0
C <sub>2</sub> H <sub>5</sub> NH <sub>2</sub>	6.0	5.3	4.5

of this adjustment receiver power very nearly attains its maximum value. Finally, the 10-db wedge is placed inside of the test section of guide and the operation of the system is relatively insensitive to changes in the frequency of the generator. The result is that an absorption coefficient as small as  $0.2 \times 10^{-4}$  neper per cm may be measured, but of course the accuracy in this range is low. Thus if the received power falls to 98 per cent of its initial value on introducing a gas into a 30-foot section of guide the absorption coefficient is  $0.18 \times 10^{-4}$  neper per cm, while if the power drops to 97 per cent of its initial value, the coefficient is  $0.27 \times 10^{-4}$  neper per cm. When a gas with large absorption is used, the fact that absorption vanishes as the pressure is reduced is of great aid in following the course of a pressure vs. absorption curve.

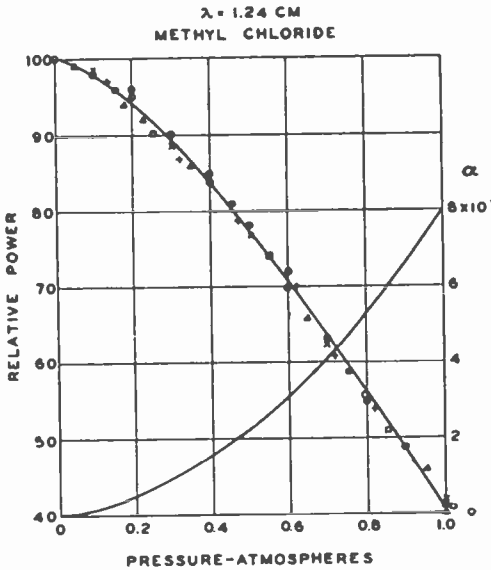


Fig. 1—Absorption of methyl chloride at  $\lambda = 1.24$  cm.

When the absorption coefficient is of the order of  $10^{-3}$  neper per cm or 40 times the minimum measurable absorption, the consistency of the results obtained is such that the accuracy of the absorption coefficients reported is estimated to be somewhat better than 5 per cent. Approximately the same accuracy is realized in the measurement of  $\delta$ , which is the amount by which the dielectric constant exceeds unity.

Figure 1 represents the experimental points obtained in six absorption runs with methyl chloride. These readings lie in the range of pressure and absorption for which accuracy is high, using the 30-foot section of guide.

## GENERAL THEORY

The essential parameters which characterize an absorption line are  $\nu_0$ , the frequency of the center of the line, and the half-width  $\Delta\nu$ , which is the difference between  $\nu_0$  and the frequency at which the absorption has fallen to one-half of the absorption at the center of the line. In the microwave region the observed broadening of an absorption line is to be attributed to collision broadening; Doppler broadening and natural line breadth are negligible at these frequencies. Since at one atmosphere  $\Delta\nu$  is found to be of the same order of magnitude as  $\nu_0$ , if  $\nu_0$  is in the microwave region, the exact shape of the absorption line becomes a matter of considerable interest. This problem of the shape of collision-broadened lines has been re-examined by Van Vleck and Weisskopf,<sup>2</sup> who have shown that the classical formula of Lorentz requires revision. The fundamental difference between the assumptions made in the two theories, in applying them to absorption by molecules possessing a permanent dipole moment, is the following: Lorentz assumed that after each collision all orientations of the dipole with respect to the direction of the electric field are equally probable; Van Vleck and Weisskopf assumed that the probability of a given orientation is given by the corresponding Boltzmann factor. The absorption coefficient  $\alpha_\nu$ , for electromagnetic radiation of frequency  $\nu$  is calculated by the latter authors to be

$$\alpha_\nu = \frac{8\pi^3\nu N}{3hc} \cdot \frac{\sum_j \sum_i |\mu_{ij}|^2 f(v_{ij}\nu)}{\sum_j e^{-W_j/kT}} e^{-W_j/kT}, \quad (1)$$

$$f(v_{ij}\nu) = \frac{1}{\pi} \frac{\nu}{\nu_{ij}} \left\{ \frac{\Delta\nu}{(\nu_{ij} - \nu)^2 + \Delta\nu^2} + \frac{\Delta\nu}{(\nu_{ij} + \nu)^2 + \Delta\nu^2} \right\}, \quad (2)$$

where  $N$  = number of molecules per cc,

$\mu_{ij}$  = electric dipole moment matrix element for the two states  $i$  and  $j$  which have a frequency separation  $\nu_{ij}$ ,

$W_j$  = energy of  $j$ th state, and

$\Delta\nu$  = half-width of a line =  $1/2\pi\tau$ , where  $\tau$  is the mean time between molecular collisions.

The other symbols have their usual significance. The summations are to be extended over all the states of the molecule. Equations (1) and (2) differ from the Lorentz result by the inclusion of the factor

<sup>2</sup> J. H. Van Vleck and V. F. Weisskopf, *Rev. Mod. Phys.* 17, 227 (1945).

$\nu/\nu_{ij}$  in (2) and by the change in the sign of the second term in (2). For a molecule with large moments of inertia and a permanent dipole moment  $\mu_0$ , these equations reduce to the familiar Debye formula

$$\epsilon_\nu'' = \frac{\alpha_\nu c}{2\pi\nu} = \frac{4\pi N \mu_0^2}{3kT} \frac{\nu \Delta\nu}{\nu^2 + \Delta\nu^2} \tag{3}$$

for the complex part of the dielectric constant.

For our purposes it is convenient to specialize Equations (1) and (2) so that they apply directly to the ammonia problem.  $\text{NH}_3$  is a symmetrical top molecule with rotational energy levels specified by the quantum numbers  $J$  and  $K$ .<sup>3</sup> Each rotational level is split into a close doublet as a result of the tunneling effect; the two components of the doublet are specified by the designation + and -. The selection rules for rotational transitions are  $\Delta J = 0, \pm 1$ ;  $\Delta K = 0$ ;  $+\leftrightarrow-$ . The "inversion spectrum" frequency corresponding to  $\Delta J = 0, \Delta K = 0$ ;  $+\leftrightarrow-$  is about  $0.8 \text{ cm}^{-1}$  while the lowest frequency in the rotation spectrum corresponding to  $\Delta J = \pm 1$  is about  $20 \text{ cm}^{-1}$ . For  $\nu < 1.0 \text{ cm}^{-1}$  only the absorption associated with the inversion spectrum need be considered, and Equation (1) can be reduced to<sup>2</sup>

$$\alpha_\nu = \frac{8\pi^3 \nu N}{6ckT} \frac{\sum_j \sum_i |\mu_{ij}|^2 f(\nu_{ij}, \nu) \nu_{ij} e^{-W_j/kT}}{\sum_j e^{-W_j/kT}}, \tag{4}$$

where  $j$  and  $i$  now refer to the two components of a given doublet. The reduction follows from the relation  $h\nu_{ij} \ll kT$ . Aside from the negligible difference in the Boltzmann factor, we obtain the same contribution to the sum in the numerator from the transition  $j \rightarrow i$  as from the transition  $i \rightarrow j$ . If  $W(J, K)$  is the mean energy of a given doublet, and  $g(J, K)$  is the total weight of the rotational level with quantum numbers  $J$  and  $K$ , Equation (4) becomes

$$\alpha_\nu = \frac{4\pi^2 N \nu^2}{3ckT} \frac{\sum_{J, K} g(J, K) |\mu(J, K)|^2 f'[\nu(J, K), \nu] e^{-W(J, K)/kT}}{\sum_{J, K} g(J, K) e^{-W(J, K)/kT}}, \tag{5}$$

where

$$f'[\nu(J, K), \nu] = \frac{\Delta\nu}{[\nu(J, K) - \nu]^2 + \Delta\nu^2} + \frac{\Delta\nu}{[\nu(J, K) + \nu]^2 + \Delta\nu^2}, \tag{6}$$

<sup>3</sup> G. Herzberg, *Infra-Red and Raman Spectra* (D. Van Nostrand Company, New York, 1945), pp. 26-34.

and where the sums over the rotational levels in the excited vibrational states have been omitted.  $\mu(J, K)$  is the electric moment matrix element for the transition  $\Delta J = 0, \Delta K = 0, + \longleftrightarrow -$  and is equal to<sup>4</sup>

$$|\mu(J, K)|^2 = \frac{K^2}{J(J+1)} \mu_0^2, \quad (7)$$

where  $\mu_0$  is the permanent dipole moment of the molecule. For an accidentally symmetrical top the weights  $g(J, K)$  are  $(2J+1)$  for  $K=0$ , and  $2(2J+1)$  for  $K \neq 0$ . For  $\text{NH}_3$  or  $\text{CH}_3\text{Cl}$  the presence of the threefold symmetry axis and the nuclear spin of the hydrogen atoms introduce the additional factor 4 for  $K$  divisible by 3 and the factor 2 for  $K$  not divisible by 3.<sup>5</sup> Since both numerator and denominator of (5) involve the same set of weights, only the relative values are important. Factors such as the spin of N or Cl, which would change the absolute weights, will not affect the relative weights. In the sums we can therefore use the weights

$$g(J, K) = (2J+1) \text{ times } 4, 4, 4, 8, 4, 4, 8, 4 \dots$$

for  $K = 0, 1, 2, 3, 4, 5, 6, 7 \dots$  (8)

If these weights are used, the sum in the denominator, which we denote by  $Q$ , becomes (in the high temperature approximation)

$$Q = 8/3(Q_{\text{class}}) = 8/3(1.027) [T^3/B^2A]^{\frac{1}{2}}, \quad (9)$$

where  $Q_{\text{class}}$  is the classical rotational partition function for a symmetrical top with rotational constants  $B$  and  $A$ , and  $T$  is the absolute temperature. The energy levels, in wave numbers, are

$$W(J, K) = BJ(J+1) + (A-B)K^2. \quad (10)$$

If  $\nu(J, K) = \nu_0$  independently of  $J$  and  $K$ , the absorption coefficient is given by

$$\alpha_\nu = \beta N \nu^2 \left[ \frac{\Delta\nu}{(\nu_0 - \nu)^2 + \Delta\nu^2} + \frac{\Delta\nu}{(\nu_0 + \nu)^2 + \Delta\nu^2} \right], \quad (11)$$

where  $\beta$  is a constant which can be calculated from the sums in (5). We also note that

<sup>4</sup> Reference 3, p. 422.

<sup>5</sup> Reference 3, p. 28.



$$\int_0^{\infty} f'[\nu(J, K), \nu] d\nu = \pi, \tag{12}$$

independently of  $\nu(J, K)$  and  $\Delta\nu$ . Therefore, from (12) and (5), we have, as a measure of the total absorption arising from this inversion spectrum

$$\int_0^{\infty} \frac{\alpha_{\nu} d\nu}{\nu^2} = \frac{4\pi^3 N}{3ckT} \frac{\mu_0^2}{Q} \sum_{J, K} g(J, K) \frac{K^2}{J(J+1)} e^{-W(J, K)/kT} \tag{13}$$

independently of any assumptions as to the detailed positions or breadths of the individual lines.

Since our measurements are limited to two frequencies, they do not give any direct information on the half-widths  $\Delta\nu$  of the absorption lines. From the kinetic theory of gases and the relation  $\Delta\nu = 1/2\pi\tau$  one would expect to find  $\Delta\nu \sim 0.05 \text{ cm}^{-1}$  or less at room temperature and atmospheric pressure. Adel and Barker<sup>6</sup> find  $\Delta\nu = 0.067 \text{ cm}^{-1}$  for zero slit width for the lines in  $\text{N}_2\text{O}$ , which is a linear molecule with a very small dipole moment. For molecules with a large dipole moment much larger values of  $\Delta\nu$  have been reported; for example, Cornell<sup>7</sup> reports  $\Delta\nu \sim 0.3$  for  $\text{H}_2\text{O}$  and larger values for  $\text{NH}_3$  and  $\text{HCN}$  (not corrected for slit width). These larger values are to be expected in dipole molecules, since a "collision," as the word is applied to line broadening, means that the molecules have come sufficiently close to cause a perturbation of the energy levels, not that they have collided in a billiard-sense. The "optical" collision diameters are as computed from observed values of  $\Delta\nu$  are usually several times larger than the kinetic theory diameters.

#### AMMONIA

Although the absorption of microwaves by  $\text{NH}_3$  has been known for a long time and the general features understood,<sup>8</sup> the details of the structure of the line are not clear. Let us assume for the moment that the  $\nu(J, K)$ 's are all essentially equal, so that the absorption is given by (11). Since  $\Delta\nu$  is inversely proportional to the mean time  $\tau$  between collisions, and since  $\tau$  is inversely proportional to the pressure  $P$ ,  $\Delta\nu \sim P$ . Also,  $N \sim P$ . For the non-resonant case, with  $\nu_0$  very different from  $\nu$ , Equation (11) shows that  $\alpha_{\nu} \sim P^2$  as long as  $(\nu_0 - \nu) \gg \Delta\nu$ .

<sup>6</sup> A. Adel and E. F. Barker, *Rev. Mod. Phys.* 16, 236 (1944).

<sup>7</sup> S. D. Cornell, *Phys. Rev.* 51, 739 (1937).

<sup>8</sup> C. E. Cleeton and N. H. Williams, *Phys. Rev.* 45, 234 (1934). A complete discussion of the ammonia spectrum and references to the original literature may be found in reference 3, pp. 33, 221, 257, 416.

For the resonant case, with  $\nu_0 \cong \nu$ ,  $\alpha_\nu$  should rise very rapidly with increasing pressure and become relatively independent of  $P$  when  $\Delta\nu \gg (\nu_0 - \nu)$ . These conclusions are in qualitative agreement with the observed behavior of the pressure dependence of the  $\text{NH}_3$  absorption (Figure 2); the curve for  $\nu = 0.81 \text{ cm}^{-1}$  ( $\lambda = 1.24 \text{ cm}$ ) is of the type corresponding to  $\nu \cong \nu_0$ , that for  $\nu = 0.32 \text{ cm}^{-1}$  ( $\lambda = 3.18 \text{ cm}$ ) is of the type corresponding to  $\nu \ll \nu_0$ . The situation is less favorable if looked at from a quantitative viewpoint. The  $\text{NH}_3$  curve for  $\nu = 0.81$  rises linearly with pressure above 0.1 atmos., and this rise continues to at least 2.5 atmos. The details of the curve cannot be accounted for by Equation (11) if  $\Delta\nu$  is assumed to be proportional to  $P$ . Any other variation of  $\Delta\nu$  with  $P$  would have no theoretical justification at present. If we assume  $\nu_0 \cong 0.80 \text{ cm}^{-1}$ ,  $\alpha_\nu$  should decrease with frequency more

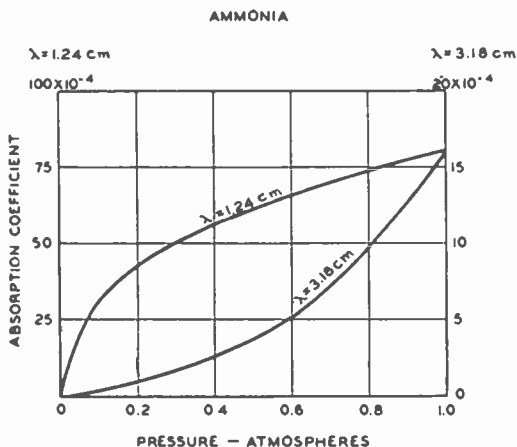


Fig. 2—Absorption of ammonia employing 5-foot guide.

rapidly than  $\nu^2$  in the region  $\nu < 0.80 \text{ cm}^{-1}$ . This is in serious disagreement with the observed decrease. Actually, the  $\nu(J, K)$ 's are not identical. The centrifugal distortion of the molecule caused by rotation produces a change in the effective barrier height and thus a change in the doublet separation. This dependence of the doublet separation on  $J$  and  $K$  has been calculated by Sheng, Barker, and Dennison,<sup>9</sup> who obtain the result

$$\nu(J, K) - \nu_0 = -0.0011 (J^2 + J) + 0.0016K^2, \quad (14)$$

where  $\nu_0$  is the doublet separation in the non-rotating molecule. If the Boltzmann distribution is taken into account, one finds that there are

<sup>9</sup> H. Y. Sheng, E. F. Barker, and D. M. Dennison, *Phys. Rev.* 69, 786 (1941).

lines of appreciable intensity spread over a region about  $0.06 \text{ cm}^{-1}$  wide (at zero pressure). If the ammonia inversion spectrum consists of a series of lines starting at  $\nu \sim 0.80 \text{ cm}^{-1}$  and extending to considerably lower frequencies, the observed features of the absorption curve are more readily understood. This distribution of frequencies would increase the absorption at  $\nu = 0.32 \text{ cm}^{-1}$  relative to that at  $\nu = 0.81 \text{ cm}^{-1}$  above that expected for a single line near  $\nu = 0.80 \text{ cm}^{-1}$ , and would also produce a pressure variation similar to that observed at  $\nu = 0.81 \text{ cm}^{-1}$ . Such a distribution would also explain the apparent discrepancy between the doublet separation as obtained from the pressure curves ( $\nu_0 \cong 0.80 \text{ cm}^{-1}$ ) and from the far infra-red spectra ( $\nu_0 \cong 0.66 \text{ cm}^{-1}$ ) as observed by Wright and Randall.<sup>10</sup> It would seem, however, that a spread greater than that by Equation (14) would be required. Van Vleck and Weisskopf<sup>2</sup> have pointed out that a variation of  $\Delta\nu$  with  $J$  and  $K$  would also tend to increase the absorption at the edge of the line relative to the absorption at the center. It appears that a quantitative description of the  $\text{NH}_3$  absorption must be postponed until an investigation at low pressures reveals further information about the  $\nu(J, K)$ 's.

Application of Equation (13) to  $\text{NH}_3$  yields

$$\int_0^\infty \frac{\alpha_\nu d\nu}{\nu^2} = 74 \times 10^{-14} \text{ (theoretical)}. \tag{15}$$

(The  $\text{NH}_3$  constants are  $A = 6.31$ ,  $B = 9.94$ ,  $\mu_0 = 1.49 \times 10^{-18}$ . The ratio  $\Sigma/Q$ , where  $\Sigma$  represents the sum in (13), is equal to 0.39 for  $\text{NH}_3$  at  $T = 300^\circ \text{K}$ .) From the data of Cleeton and Williams<sup>8</sup>

$$\int_0^\infty \frac{\alpha_\nu d\nu}{\nu^2} \cong 35 \times 10^{-11} \text{ (experimental)}. \tag{16}$$

The origin of this discrepancy is not clear. Comparisons of this type often lead to even more serious disagreements,<sup>11</sup> but these are usually attributed to errors arising from finite slit width. Foley and Randall<sup>12</sup> have made a similar comparison on the line  $J = 14 \rightarrow J = 15$  of  $\text{NH}_3$  at a pressure of 20 cm and have found the experimental value to be only about 20 per cent lower than the theoretical value. It would be of

<sup>10</sup> N. Wright and H. M. Randall, *Phys. Rev.* 44, 391 (1933).

<sup>11</sup> C. Shaefer and F. Matossi, *Das Ultrarote Spectrum* (Verlagsbuchhandlung, Julius Springer, Berlin, 1930).

<sup>12</sup> H. M. Foley and H. M. Randall, *Phys. Rev.* 59, 171 (1941).

interest to see whether or not the above discrepancy persists at low pressures.

Figure 3 shows the effect of the admixture of oxygen on the ammonia absorption. Almost identical curves are obtained from  $\text{NH}_3 - \text{CH}_4$  and  $\text{NH}_3 - \text{H}_2$  mixtures. The dotted curves connect points of equal  $\text{NH}_3$  partial pressure; if these lines were horizontal it would mean that the  $\text{NH}_3$  absorption is a function of the  $\text{NH}_3$  partial pressure only, since the absorption of  $\text{O}_2$  is negligible. The addition of  $\text{O}_2$  to  $\text{NH}_3$  changes the line breadth  $\Delta\nu$  in the latter molecule and so effects the absorption. We can make a rough estimate of the relative collision cross sections for  $\text{NH}_3 - \text{O}_2$  and  $\text{NH}_3 - \text{NH}_3$  collisions as follows. If the pressure of  $\text{NH}_3$  is greater than 0.1 atmos., the absorption is,

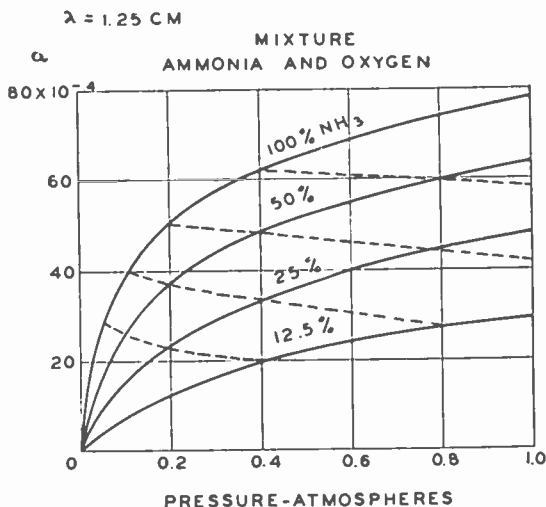


Fig. 3—Absorption of mixtures of ammonia and oxygen.

according to Equation (11), essentially proportional to  $1/\Delta\nu$  if the concentration of  $\text{NH}_3$  is constant. If we follow the dotted line which starts at  $\alpha \times 10^4 = 40$ , we find that  $\Delta\nu$  increases by a factor  $(1.00 + 0.48)$  as the total pressure is increased from 0.1 atmos. to 0.8 atmos. by the addition of oxygen. A corresponding increase in pressure caused by the addition of  $\text{NH}_3$  should increase  $\Delta\nu$  by a factor  $(1.00 + 7.00)$ . The relative cross sections for the two-collision process are thus in the ratio 14.5:1, and the relative collision diameters about in the ratio 4:1. Since optical collision diameters are considerably larger than kinetic theory diameters, we see that, roughly at least, the  $\text{NH}_3 - \text{O}_2$  collision diameter is close to the kinetic theory value.

## METHYL HALIDES

The methyl halides  $\text{CH}_3\text{F}$ ,  $\text{CH}_3\text{Cl}$ ,  $\text{CH}_3\text{Br}$  all show the type of variation  $\alpha_\nu \sim P^2$  which is characteristic of absorption at a frequency far removed from the resonant frequency (Figure 4). In this figure the curves for  $\text{CH}_3\text{Cl}$  are not shown. For this gas, at a given wavelength, the curve absorption coefficient vs. pressure lies between the corresponding curves for  $\text{CH}_3\text{F}$  and  $\text{CH}_3\text{Br}$ . The absolute magnitude of the absorption, the variation of  $\alpha_\nu$  with  $\nu$ , and the similarity of the absorption in the three gases are all inconsistent with the assumption that the observed absorption arises from rotational transitions. Com-

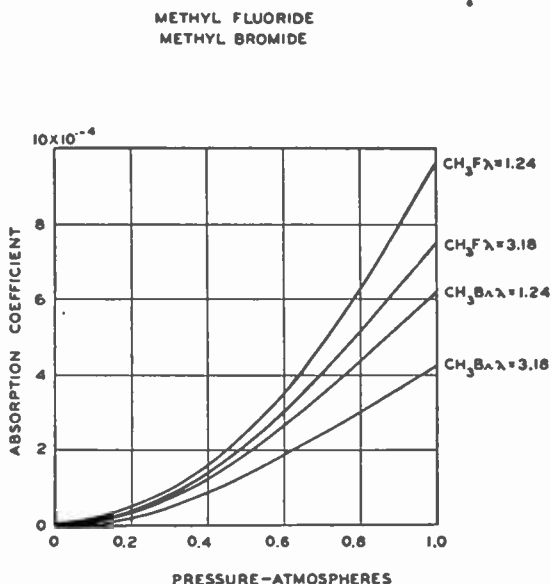


Fig. 4—Absorption of methyl fluoride and methyl bromide.

paring the observed absorption at  $\nu = 0.81 \text{ cm}^{-1}$  and  $\nu = 0.32 \text{ cm}^{-1}$  with Equation (11), we conclude immediately that  $\nu_0$  is very small.

From a formal viewpoint, the energy levels of  $\text{CH}_3\text{X}$  are exactly the same as those of  $\text{NH}_3$ , and the selection rules are identical. Each rotational level characterized by the quantum numbers  $J$  and  $K$  is double, the two components being designated by the symbols  $+$  and  $-$ . The separation of this doublet depends on the height of the potential barrier which must be overcome if the molecule is to be turned into its mirror image. In  $\text{NH}_3$  this barrier (for the passage of N through the plane of the H's) is low and the corresponding doublet separation is large. The potential barrier preventing inversion in  $\text{CH}_3\text{X}$  (perhaps

most easily visualized as an internal rotation of a  $\text{CH}_2$  group relative to the rest of the molecule) would be expected, on the basis of ordinary chemical concepts, to be much higher than the barrier for inversion in  $\text{NH}_3$ , and the doublet separation would be expected to be much smaller. From (11), we see that the absorption becomes

$$\alpha_\nu = \beta' \nu^2 \Delta\nu / (\nu^2 + \Delta\nu^2), \quad (17)$$

for  $\nu \gg \nu_0$ , which is independent of the exact value of  $\nu_0$ . The experimental results can be fitted to an equation of this form if we assume  $\Delta\nu$  proportional to the pressure. The selection rules, statistical weights, and matrix elements are the same as in the ammonia problem.  $\beta'$  is then given by

$$\beta' = \frac{8\pi^2 N}{3kT} \frac{\mu_0^2}{Q} \sum_{J,K} g(J,K) \times \frac{K^2}{J(J+1)} \cdot e^{-W(J,K)/kT}, \quad (18)$$

if, in (17), the  $\nu$ 's and  $\Delta\nu$ 's are in  $\text{cm}^{-1}$ .

The experimental values of  $\alpha_\nu$  were corrected for the contribution arising from rotational absorption; this contribution was estimated from the theory to be 0.00004 for  $\text{CH}_3\text{Cl}$  and 0.00005 for  $\text{CH}_3\text{Br}$  at  $\nu = 0.81 \text{ cm}^{-1}$  and negligible in other cases. The experimental values of  $\beta'$  and  $\Delta\nu$  were computed from the corrected values of  $\alpha_\nu$  for  $\nu = 0.81 \text{ cm}^{-1}$  and  $0.32 \text{ cm}^{-1}$  and  $P = 1.0$  atmos. The variation of  $\alpha_\nu$  with  $P$  is reproduced satisfactorily by Equation (17) with these values of the constants. The experimental values of  $\Delta\nu$  are of the correct order of magnitude. The theoretical values of  $\beta'$  are 30-40 per cent higher than the experimental values; this agreement may be regarded as sufficiently exact to verify the correctness of the assumed theory. The results are compared in Table 3; it is to be noted that the variation of  $\beta'$  is not identical with the variation in  $\mu_0$  since the sums in (18) are appreciably different for the different molecules.

Since we have assumed the doublet separation to be negligibly small, and the frequency associated with the absorption to be essentially zero, we should arrive at the same result if we simply consider the molecules to be rigid rotators, characterized by the quantum numbers  $J$  and  $K$ . Now a non-rotating dipole molecule can absorb energy from an electromagnetic field because of the effect of collisions; the absorption is given by the Debye formula (3), which can be derived from classical theory. The mechanism can be visualized as the following: After each collision the dipole has a tendency to be oriented parallel to the field; between collisions the dipole is stationary. If the field is varying with time, the

net effect of this mechanism is the production of a polarization which lags behind the field. The polarization current then has a component parallel to the field, resulting in an absorption of energy. The dipole moment vector of a symmetrical top molecule such as  $\text{CH}_3\text{Cl}$ , in the state characterized by  $J$  and  $K$ , can be resolved into a component parallel to the direction of the total angular momentum vector and a component perpendicular to this direction. The former component is stationary in space, and hence gives a full contribution to the Debye absorption; the latter component has a time average equal to zero and hence gives no Debye absorption. The square of the component of the permanent dipole moment  $\mu_0$  parallel to the total angular momentum vector is, since the dipole moment vector is along the symmetry axis, equal to  $M_K^2\mu_0^2/M^2$  where  $M_K$  is the angular momentum about the symmetry axis of the molecule and  $M^2$  is the total angular momentum. From quantum mechanics  $M_K^2 = K^2\hbar^2/2\pi$ ,  $M^2 = J(J+1)\hbar^2/2\pi$ ; the square of this component is thus equal to  $K^2\mu_0^2/J(J+1)$ . If, in Equation (3), we replace  $\mu_0^2$  by this last expression, and sum over all values of  $J$  and  $K$  weighted by the proper statistical factors, we arrive exactly at Equations (17) and (18). In other words, the quantum-mechanical theory and the essentially classical theory of Debye lead to identical results. This is no accident, since the Debye theory is the limiting form of the general theory as the resonant frequency approaches zero.<sup>2</sup> It should be emphasized that the Debye theory cannot be applied in the form (3), the essential modification being that  $\mu_0^2$  in (3) must be replaced by the square of that component of  $\mu_0$  which is stationary in space. Although the two viewpoints concerning the  $\text{CH}_3\text{X}$  absorption are formally equivalent, the Debye picture is perhaps more in agreement with our conventional ideas.

Table 3

	$\Delta\nu$ (exp)	$\beta'$ (exp)	$\beta'$ (theor.)	$\mu_0 \times 10^{18}$
$\text{CH}_3\text{F}$	0.20	0.0053	0.0067	1.81
$\text{CH}_3\text{Cl}$	0.22	0.0037	0.0054	1.87
$\text{CH}_3\text{Br}$	0.21	0.0029	0.0038	1.78

## COS

From the known moment of inertia of the linear molecule COS, namely,  $1.37 \times 10^{-38}$  g-cm<sup>2</sup>, the wave-length for the transition  $J=1 \longleftrightarrow J=2$  is very nearly 1.24 cm, the operating wave-length. The wave-length is given by

$$\lambda_0 = \frac{4\pi^2 c I}{h(J+1)}. \quad (19)$$

The computed absorption is given by

$$\alpha_0 = \frac{2\mu_0^2 \nu_0^2 h^2}{3cI(kT)^2} \times \frac{N}{\Delta\nu}, \quad (20)$$

where  $\mu_0$  for COS is 0.65 Debye units,  $\nu_0$  is  $2.4 \times 10^{10}$  cycles per second, and  $N$  is the number of molecules per cc. At one atmosphere, we obtain the observed value for  $\alpha_0$  namely  $0.8 \times 10^{-4}$  neper 1 cm, when  $\Delta\nu$  is taken to be about  $3 \times 10^9$  or  $0.10 \text{ cm}^{-1}$ . The form of Eq. (20) shows that if both  $N$  and  $\Delta\nu$  vary linearly with pressure,  $\alpha_0$  is independent of pressure. The curve in Figure 5, showing the absorption of COS, is of the resonant type as expected. In view of the above

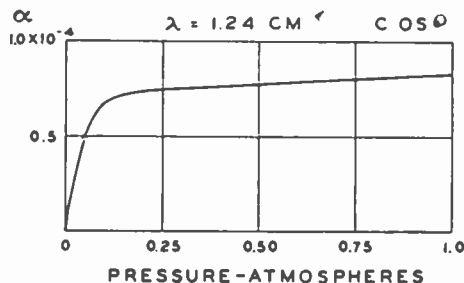


Fig. 5—Absorption of carbonyl sulphide.

mentioned result  $\Delta\nu = 0.067 \text{ cm}^{-1}$  on the rather similar molecule  $\text{N}_2\text{O}$ , this seems to be a very reasonable value, and indicates a verification of the theory.

### $\text{H}_2\text{S}$

A survey of the known rotational levels of  $\text{H}_2\text{S}$  reveals no energy separations in the region  $0 < \nu < 3.0 \text{ cm}^{-1}$  which corresponds to an allowed transition.<sup>13</sup> The microwave absorption in  $\text{H}_2\text{S}$  should, therefore, be very small, as is observed. The small absorption at  $\nu = 0.81 \text{ cm}^{-1}$  ( $\alpha_\nu \times 10^4 \cong 0.3$ ) is probably the cumulative effect of the numerous lines at higher frequencies.

### $\text{SO}_2$

The rotational levels of  $\text{SO}_2$  are not known experimentally, so a detailed calculation is not possible. The levels can be computed if the

<sup>13</sup> P. C. Cross, *Phys. Rev.* 47, 7 (1935).



molecule is considered to be a rigid unsymmetrical top. It is found that there are, up to  $J = 12$ , about 10 lines in the frequency range  $0 < \nu < 1.50 \text{ cm}^{-1}$  which correspond to allowed transitions. At  $J = 12$  the Boltzmann factor is about 0.80, so there will undoubtedly be many strong lines in this frequency range arising from transitions involving levels higher than  $J = 12$ . It is, therefore, reasonable to assume that the observed absorption  $\text{SO}_2$  could be accounted for on the basis of ordinary rotational transitions, indeed, no other mechanism seems possible.

#### OTHER MOLECULES

The other molecules listed in Table 1 are non-planar unsymmetrical tops. As we proceed from a symmetrical top to an unsymmetrical top, we find that each  $K$  level splits into two levels, and a transition between these two levels is generally allowed. Transitions of this type, corresponding to  $\Delta J = 0$ ,  $\Delta K = 0$  in the symmetrical top, will produce a series of lines from  $\nu \cong 0$  upward. Also, certain transitions corresponding to  $\Delta K \neq 0$  are allowed in unsymmetrical tops. The moments of inertia of these molecules are large; therefore, transitions corresponding to  $\Delta J = \pm 1$  will involve low frequencies. The net result is that we have a very complicated rotational spectrum, containing many lines with frequencies from  $\nu \sim 0$  upward, and thickly scattered throughout the microwave region. Any exact calculations are almost impossible; however, we should expect the magnitude of the absorption to be about the same as for the methyl halides. The pressure curves often show a behavior intermediate between the resonant and non-resonant types, which is accounted for by the distribution of lines described above. Figure 6 shows such curves for ethylamine.

In general, one would expect all heavy non-planar unsymmetrical top molecules which have a large dipole moment to show an appreciable absorption in the microwave region. Since the selection rules are more stringent for planar and linear molecules, each molecule must be considered individually. Non-planar symmetrical top molecules should be analogous to the methyl halides.

#### DIELECTRIC CONSTANTS

Van Vleck and Weisskopf<sup>2</sup> have given the appropriate formula for the computation of that part of  $\delta$  which arises from the permanent dipole moment  $\mu_0$ . To this must be added the contribution arising from the electronic polarization  $P_A$ . For zero frequency,  $\delta$  is given by

$$\delta_0 = \frac{3(P_B + P_A)}{V} + \frac{4\pi N\mu_0^2}{3kT}, \quad (21)$$

where  $V$  is the molar volume.<sup>14</sup>  $\delta$  should not differ very much from  $\delta_0$  in the microwave region, since this is on the low frequency side of the region of large absorption. This is illustrated by the comparison of calculated static values and observed values in Table 2. The necessary data were taken from Smyth's text,<sup>14</sup> except for the substituted methanes, for which the data were taken from later papers by Smyth and his co-workers.<sup>15</sup>

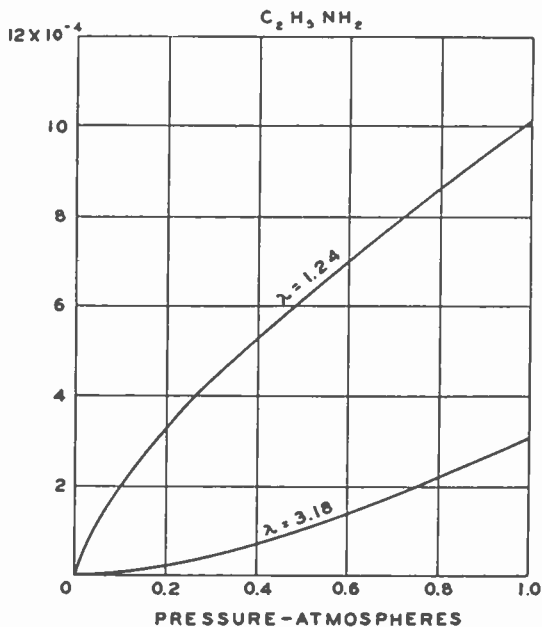


Fig. 6—Absorption of ethylamine.

For the methyl halides, the contribution to  $\delta$  arising from the frequencies near zero (the ones to which we attributed the absorption) is given by

$$\delta_v' = \frac{4\pi N\mu_0^2}{3kT} \sum_Q \frac{\Delta v^2}{v^2 + \Delta v^2}, \quad (22)$$

<sup>14</sup> C. P. Smyth, *Dielectric Constant and Molecular Structure* (Chemical Catalog Company, New York, 1931).

<sup>15</sup> C. P. Smyth and R. H. Wiswall, Jr., *J. Chem. Phys.* 9, 356 (1941); C. P. Smyth and K. B. McAlpine, *J. Chem. Phys.* 1, 190 (1933); and *J. Chem. Phys.* 2, 499 (1934).

where  $\Sigma$  is the sum of the numerator of (18). For the complex part of the dielectric constant we have

$$\epsilon_v'' = \frac{\alpha_v c}{2\pi\nu} = \frac{4\pi N\mu_0^2}{3kT} \frac{\Sigma}{Q} \frac{\nu\Delta\nu}{\nu^2 + \Delta\nu^2}. \quad (23)$$

If we assume that the contribution to  $\delta$  arising from the rotational frequencies is equal to the static value of this contribution, the above equations lead to

$$\delta_\nu = \delta_0 - \epsilon_v'' (\nu/\Delta\nu) = \delta_0 - (\alpha_v/2\pi\Delta\nu). \quad (24)$$

Insertion of the observed values of  $\alpha_\nu$  for  $\text{CH}_3\text{Cl}$  gives  $\delta \times 10^3 = 9.9$  at  $\lambda = 3.18$  and  $\delta \times 10^3 = 9.7$  at  $\lambda = 1.24$ , as compared with the observed values 9.4 and 9.9. This agreement is not too good, but perhaps is within the limits of error of the measurements. The observed increase in  $\delta$  as  $\lambda$  is decreased from 3.18 cm to 1.24 cm if real, must be attributed to the effect of the absorption lines at higher frequencies. As the frequency is increased from zero upward, the  $\delta$  value of  $\text{NH}_3$  should first increase above the static value and then decrease as the microwave absorption band is approached. The observed values are both lower than the static value; the meaning of this result is uncertain.

#### ACKNOWLEDGMENTS

We wish to express our indebtedness to George W. Leck, Jr., for invaluable help in building microwave generating and power measuring equipment and to Elizabeth T. Bush for constructing wave guide components, preparing gases in the laboratory not readily available commercially, and taking many measurements. Also we express our appreciation to Irving Wolff of these Laboratories for support and encouragement, and to John Turkevich of Princeton University, for critical and helpful discussions during the course of the investigation.

*Note added in proof, July 9, 1946.*—Figure 4 in the paper referred to in reference 1 shows the absorption of ammonia at reduced pressure at three different wave-lengths. The information in this figure is quite consistent with the map of the fine structure of ammonia published by Bleaney and Penrose in the March 16, 1946, issue of *Nature*. The curve in Figure 4 at 1.243 centimeters rises steeply at low pressure, but, after a few millimeters of pressure are reached, bends over and rises less steeply. A curve of this character indicates that the observations were taken near the maximum of one of the spectral lines. True enough, Bleaney and Penrose map an unresolved pair of lines at this wave-length to which they assign the quantum numbers (4,4) and (10,9). The curve at 1.320 centimeters also exhibits a point of inflection and these observations were taken on the complex and unresolved absorption line designated (5,4), (4,3), and (6,5). By contrast, the experimental curve at  $\lambda = 1.227$  is linear which is consistent with the fact that this wave-length falls *between* the (4,4) and (5,5) lines.

WAVE GUIDES AND THE SPECIAL  
THEORY OF RELATIVITY\*†

BY

W. D. HERSHBERGER

Research Department, RCA Laboratories Division,  
Princeton, N. J.*Summary*

*The Lorentz transformation is applied to the  $H_{11}$  solution of Maxwell's equations used to describe wave propagation in conducting pipes of rectangular cross section. When group velocity for the wave is employed in the transformation, the solution obtained is that one characterizing wave-guide operation at cut-off frequency, thus demonstrating that the speed associated with power or signal transmission is group velocity. When phase velocity for the wave is employed in the transformation, and we treat all quantities appearing in the new solution as real, we find that the problem has been reduced to one in magnetostatics and the significance of this solution is pointed out. The use of the inverse Lorentz transformation to find wave guide solutions from known solutions of problems in statics is indicated.*

*(4 pages; 5 figures)*

---

\* Decimal Classification: R118.

† *Jour. Appl. Phys.*, August, 1945.

## THE ABSORPTION OF MICROWAVES BY GASES\*†

BY

W. D. HERSHBERGER

Research Department, RCA Laboratories Division,  
Princeton, N. J.*Summary*

*The absorption by ammonia of electromagnetic waves having a length in the one-centimeter range has been known for some years. An investigation has been made to determine whether other gases show similar absorption for microwaves and as a result fourteen additional gases have been found whose absorption is comparable to that of ammonia. Among these gases are dimethyl ether, a variety of amines and alkyl halides, and several others. Measurements on the absorption coefficient and dielectric constant of these gases taken at 1.25 cm at room temperature and a pressure of one atmosphere are given. The frequency at which the absorption coefficient attains its maximum value may be inferred from the curve; absorption coefficient vs. pressure. Data on the absorption of several gas mixtures are given. Possible molecular mechanisms adequate to account for the large absorptions observed are discussed together with the conclusions reached.*

*(6 pages; 5 figures; 1 table)*

---

\* Decimal Classification: R110.

† *Jour. Appl. Phys.*, June, 1946.

## THERMAL AND ACOUSTIC EFFECTS ATTENDING ABSORPTION OF MICROWAVES BY GASES\*†

BY

W. D. HERSHBERGER, E. T. BUSH, AND G. W. LECK

Research Department, RCA Laboratories Division,  
Princeton, N. J.

### Summary

*As a result of an investigation of the absorption spectra of gases at microwave frequencies, it has been found that of the 50-odd materials that are gaseous at room temperature and a pressure of one atmosphere, 15 strongly absorb microwaves. The experimental techniques used in taking measurements are described and the theoretical interpretation of the observed absorption for some of the simpler molecules is given. The energy absorbed by the gas from the microwaves reappears as heat and sound. Thermal conversion is demonstrated by confining an absorbing gas in a cavity resonator which communicates with a U-tube. The gas not only absorbs the microwaves but serves as the thermometric substance of a gas thermometer. A 12-inch deflection of the U-tube column is obtained when the average input power is ten watts. Acoustic conversion is shown by exposing a gas-filled balloon to a modulated microwave field; the sound frequencies generated depend on the modulation. The absorbing gas may be confined in an organ pipe closed at one end by a disk in contact with a piezo-electric crystal. This organ pipe is resonant electromagnetically to the impressed microwave frequency and acoustically to the modulation frequency. A detector of this type has a square law response and is sufficiently sensitive to detect 10 milliwatts of power.*

*(10 pages; 4 figures; 1 table)*

---

\* Decimal Classification: R110.

† RCA REVIEW, September, 1946.

## MICA WINDOWS AS ELEMENTS IN MICROWAVE SYSTEMS\*†

BY

L. MALTER, R. L. JEPSEN AND L. R. BLOOM

Tube Department, RCA Victor Division,  
Lancaster, Pa.

### Summary

*The design of a virtually reflectionless, vacuum-tight window made of mica for use in a waveguide system is described. The technique of manufacture and the experimental results with a number of models are given. Such mica windows have many applications but are particularly useful for the transmission of microwave power or electro-magnetic radiation in particular portions of the spectrum.*

*(12 pages; 11 figures)*

---

\* Decimal Classification: R310.

† RCA REVIEW, December, 1946.

## RECEIVER INPUT CONNECTIONS FOR U-H-F MEASUREMENTS\*†

BY

JOHN A. RANKIN

RCA License Laboratory, New York

*Summary*—Three methods of obtaining push-pull output voltage from a signal generator with single-sided output are discussed in relation to u-h-f receiver measurements. The three circuits are compared from the standpoint of output voltage accuracy, impedance presented to the receiver input circuit, and operating convenience. It is pointed out that for accurate voltage measurements the proper dummy antenna resistance must be used, and that the receiver input circuit must be connected to the receiver chassis.

The most convenient input connection for making u-h-f receiver measurements is a direct connection between the signal-generator output and the receiver input. This connection requires no special equipment, and is adequately accurate for most receiver measurements. Certain precautions in making the ground return path correct in length are necessary and are discussed fully in the text.

THE technique of making overall receiver measurements on television and frequency-modulation receivers is complicated by the fact that these receivers are frequently designed with balanced or push-pull antenna input systems, while standard signal generators are equipped with single-sided output. Furthermore, receivers designed with balanced input systems are intended to be used with a balanced transmission-line input from the antenna. The antenna and transmission-line system will generally look to the antenna circuit like a pure resistance load equal to the characteristic impedance of the transmission line, so that any measurements made with a signal generator should present the same loading to the input circuit. In the case of television receivers, if the loading presented to the antenna circuit is different than that out of which the antenna circuit is designed to work, reflection may exist.

The problem of obtaining a balanced output from a standard signal generator with single-sided output, and of having this output present the correct loading to the input circuit, will be discussed in this paper. Three methods of interconnection will be presented, any one of which will give satisfactory results, but with various degrees of operating convenience.

---

\* Decimal Classification: R243 X R361.114

† Reprinted from *RCA REVIEW*, April, 1942.

## TRANSFORMER COUPLING

A transformer, the circuit of which is illustrated in Figure 1, will transform single-sided r-f voltage from a signal generator to a balanced r-f voltage.

The transformer coils are wound on  $\frac{5}{8}$ -inch tubing with the two-turn primary winding located between the two secondary windings which are three turns each. All of the coils are wound with No. 36 enameled wire close spaced so as to provide the maximum coupling. The coupling is 69 per cent, a value which requires that the leakage reactance be tuned out, otherwise the device will not present a pure resistance input load to the receiver under test. The leakage reactance is tuned out by means of the ganged tuning condensers  $C_1$  and  $C_2$  which have a range of 8 to 140  $\mu\mu\text{f}$  per section. The capacitor range provides a frequency coverage of 20 to 63 Mc. Because this range is not suffi-

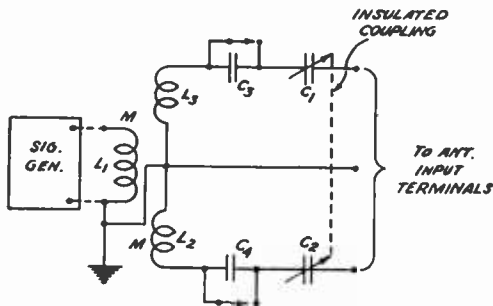


Fig. 1

cient to cover all of the television bands, it was extended by adding the series condensers  $C_3$  and  $C_4$  which in combination with  $C_1$  and  $C_2$  provide an additional tuning range of from 64 to 90 Mc. It would be possible to lower the self-inductance of the secondary coils and raise the frequency range to some extent with  $C_3$  and  $C_4$  shorted. However, this procedure results in a lower coefficient of coupling and, hence, a higher percentage of leakage reactance, and, therefore, is not as beneficial as it might first appear. The reduction of the coefficient of coupling is due in part to the fact that an appreciable amount of the leakage reactance is in the leads, hence, can not be changed by coil changes.

The tuning out of the leakage reactance is best accomplished by terminating the primary with a resistance equal to the output resistance of the signal generator that is to be used, and adjusting the tuning condenser to the setting that makes the output impedance look like a pure resistance. An impedance bridge or impedance-measuring device may be used to indicate the nature of the output impedance and

the establishment of the tuning points for the calibration of the tuning condensers. It would be possible to determine the correct tuning point of  $C_1$  and  $C_2$  if a receiver with balanced input that presents a pure resistance to the antenna were available. However, most receiver input circuits do not look like a pure resistance, but have a reactance component as well. If a reactance component is present in the input circuit of the receiver, an erroneous calibration of  $C_1$  and  $C_3$  will result, as in this case  $C_1$  and  $C_3$  will tune out the total reactance in the circuit rather than that residing only in the balanced input device.

The voltage gain from a single-sided input to a balanced output measured in a high-impedance secondary load is tabulated below for the two operating ranges.

<i>Range</i>	<i>Frequency</i>	<i>Gain</i>
Low	30 Mc	2.1
"	35	2.1
"	40	2.1
"	45	2.1
"	50	2.0
"	55	1.8
"	60	2.0
High	65	1.7
"	70	1.3
"	75	1.5
"	80	1.5
"	85	1.7

The impedance transformation or step-up is four to one when the input is terminated in a resistor of the order of 15 ohms.

In the use of this device some precautions are necessary if reliable results are to obtain: The lead lengths to and from the device must be short. A separate calibration of tuning, voltage gain, and impedance transformation ratio for each different unit should be made, as small mechanical changes in such a coil arrangement lead to seriously large electrical changes. In making measurements it is necessary to set the condensers  $C_1$  and  $C_2$  for each new frequency and to use the corresponding gain factor.

Another method of constructing such a transformer is to use a trifilar winding. In this case the three wires comprising the separate circuits are twisted together. While somewhat higher coupling may be secured by this winding method, the same precautions should be observed as with the transformer described above.



TRANSMISSION-LINE COUPLING

A balanced transmission line may be so connected with respect to ground that the short-circuiting effect of the ground return is not present due to the standing-wave phenomenon existing on the ground return. Such an arrangement is shown in Figure 2. In effect two transmission lines are used, one is indicated by  $L_1$ , the twisted pair, (not necessarily a twisted pair in practice), and the second is made up of the ground return "G" and the two wires of " $L_1$ " acting together as a single conductor. This second transmission line is indicated in Figure 2 as " $L_2$ " and is seen to be an open wire line.

The physical length and electrical length of an open wire transmission line are equal for all practical purposes and the characteristic impedance of the line may be made relatively high by merely increasing the spacing between the two wires. Impedance in excess of 1000 ohms are easily obtained in practice.

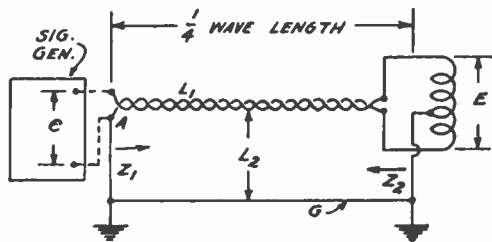


Fig. 2

The input impedance of a  $\frac{1}{4}$  wave length transmission line is

$$Z_{in} = \frac{Z_o^2}{Z_T}$$

Where  $Z_o$  = the characteristic impedance of the line and,  
 $Z_T$  = far end terminating impedance.

The physical length (and electrical length) of the open wire line  $L_2$  of Figure 2 is made  $\frac{1}{4}$  wave length at the mean operating frequency and the characteristic impedance is made high (say 1000 ohms) by spacing the two conductors.

With the above factors in mind, the magnitudes of the impedance looking into either end of the line  $L_2$  may be determined with sufficient accuracy to evaluate the shunting effect of the ground-return circuit.

First consider the impedance  $Z_2$  between the ground return lead "G", and the side of the transmission line  $L_1$  that connects to the ground side of the signal generator at A. The terminating resistance  $Z_T$  in this case is a short-circuit; therefore,  $Z_2$  looks like an infinite impedance (or open-circuit) and no short-circuiting action takes place at the receiving end.

In determining the magnitude of  $Z_2$  for the side of the transmission line  $L_1$  connected to the high side of the signal generator, it is necessary to know the apparent output impedance of the signal generator. The apparent output impedance of the signal generator will usually be such as to correctly terminate the transmission line  $L_1$ . Most transmission lines currently used for connection between the antenna and receiver have approximately 100 ohms characteristic impedance, so that it is reasonable to assume the apparent signal-generator output impedance to be 100 ohms. From this assumption the value of  $Z_2$  may be determined for the side of the line  $L_1$  connected to the high side of the signal generator, bearing in mind that the characteristic impedance of line  $L_2$  may be of the order of 1000 ohms or higher.

$$Z_2 = \frac{Z_o^2}{Z_T} = \frac{1000^2}{100} = 10,000 \text{ ohms}$$

This value is high compared to the impedance across half of the antenna input circuit, so may be disregarded so far as its shorting effect is concerned.

The value of  $Z_1$  may be determined in a similar fashion to that above. However, the impedance between either side of this antenna input circuit and its center tap can never be greater than one-half the characteristic impedance of the transmission line  $L_1$ , provided  $L_1$  is properly terminated at the signal-generator end. Assume again the same values of characteristic impedances for lines  $L_1$  and  $L_2$ , namely 100 and 1000 ohms; then,  $Z_1$  for either side of the line  $L_1$  will never be less than

$$Z_1 = \frac{Z_o^2}{Z_T} = \frac{1000^2}{\frac{100}{2}} = 20,000 \text{ ohms.}$$

This value is also high compared to the output impedance of the signal generator and, hence, has no short-circuiting action on it.

The frequency range over which this system will operate satisfactorily is approximately 1.5 to one.

From the above discussion it is evident that the ground return connection " $G$ " acts electrically as if it were not present and that a single-sided voltage is effectively transformed into a push-pull voltage by the circuit of Figure 2.

The transmission through the line  $L_1$  from signal generator to receiver may be considered to be loss free, due to the short length of line used, when the line is properly terminated. If the line is not correctly terminated, the transfer loss is still negligible if the mismatch is of the order of two or three to one. For a transfer loss of 10 per

cent the mismatch may be 2.5 to one. Such an error in receiver sensitivity measurements is not excessive at ultra-high frequencies.

The impedance that the line  $L_1$  presents to the receiver antenna circuit will be the characteristic impedance of the transmission line when the line is correctly terminated at the signal generator end. For a line not so terminated but with negligible loss the impedance at the receiving end is

$$Z_R = \frac{Z_G \cos \theta + j Z_o \sin \theta}{\cos \theta + j \frac{Z_G}{Z_o} \sin \theta}$$

where  $Z_G$  = Signal generator output impedance,  
 $Z_o$  = Characteristic impedance of line  $L_1$  and  
 $\theta$  = The electrical length of the line in radians.

This method of obtaining push-pull voltage from a signal generator with single-sided output is convenient provided the transmission  $L_1$

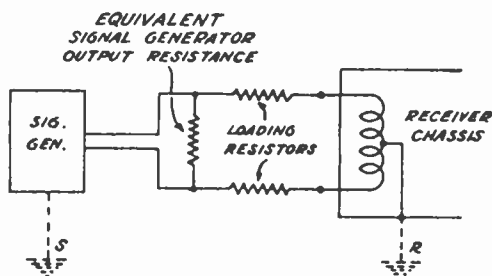


Fig. 3A.

has a characteristic impedance equal to the impedance out of which the antenna circuit is designed to work, and that the apparent signal-generator output impedance is made equal to the characteristic impedance of the line.

#### DIRECT CONNECTION BETWEEN SIGNAL GENERATOR AND RECEIVER

The circuit for direct connection between signal generator and receiver is shown in Figure 3A with an equivalent circuit in Figure 3B. In the circuit of Figure 3A two ground points are shown; one, the output of the signal generator at "S" which is connected to the chassis of the signal generator; and the other, the center tap of the antenna input circuit connected to the receiver chassis at "R". The ground path through the chassis of the two units back through the power line is shown as an impedance  $Z$  in the equivalent circuit of Figure 3B. At frequencies in the u-h-f range,  $Z$  has generally been found to be so high in any practical set up as to be entirely negligible in its effect

on shunting one-half of the input circuit. At frequencies at which the return circuit is close to series resonance (an even number of quarter-wave lengths), this impedance may drop to an undesirably low value. Changing the physical length of the return circuit will correct this and may be used as a test for low impedance in this circuit.

This type of operation is illustrated by a series of sensitivity measurements on a typical receiver at 43 Mc. In this series of measurements the only changes that were made were changes in the connections between the signal generator and the receiver. The signal generator used had an output resistance of 15 ohms, while the antenna input circuit was designed to operate out of a 100-ohm balanced transmission line. It was, therefore, necessary to add an 85-ohm dummy antenna between the signal generator and receiver input terminals.

Twelve different methods of connecting the signal generator to the receiver are illustrated in Figure 4. The ground points shown on the circuits of Figure 4 represent connection from the signal source to

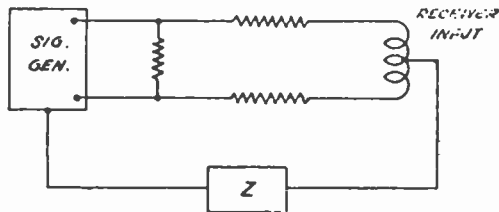


Fig. 3B.

the chassis of the signal generator, and from the primary winding to the receiver chassis, respectively. The two ground points on each of the Figures 4A to 4J inclusive are connected together as shown by the impedance  $Z$  of Figure 3B. It must be kept in mind that these two ground points are not a common or low-impedance ground connection, but rather the ground points of the two units.

The output for each measurement, illustrated by Figure 4, was maintained at the same level. The antenna input necessary to produce this standard output is tabulated on Figure 4 along with the different connections. It is to be noted that the input circuit is unbalanced in some of the measurements. This was done to show that the point of grounding the antenna primary winding is not critical, so far as this introduced voltage is concerned.

The circuits of Figures 4K and 4L have the primary ground removed and are not reliable. The input necessary with the circuit of 4L shows the largest departure from the average of any of the circuits considered.

The average input required to produce standard output for the connections shown by Figures 4A to 4J inclusive is 9.53 microvolts.

NOTE:  
ALL GND. SHOWN ON THIS PAGE  
AS  $\nabla$  INDICATES CHASSIS.

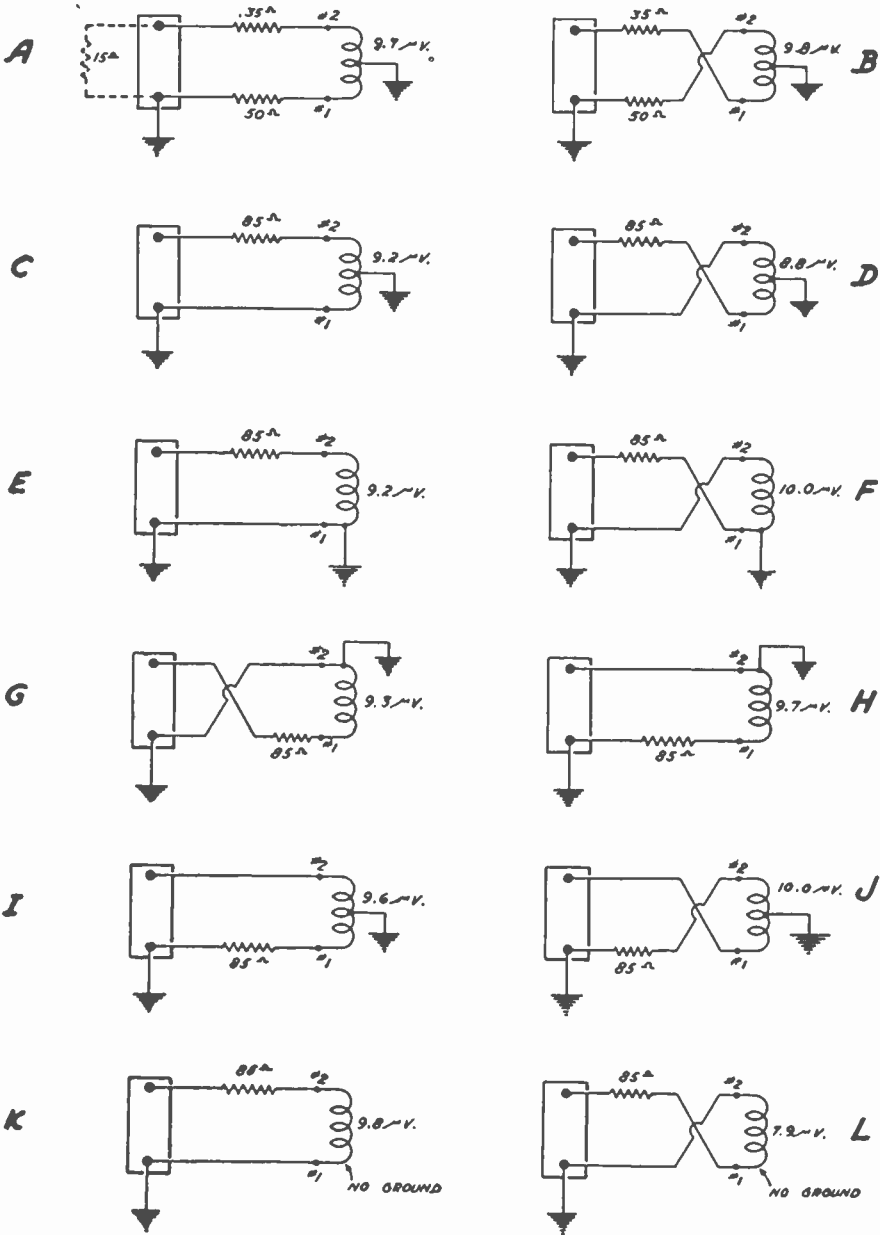


Fig. 4.

The departure from the average of Figure 4D is the largest of any of the cases with a ground connection on the primary winding. However, the departure is only eight per cent, an error which is believed to be very small for receiver sensitivity measurements at these frequencies.

For these sensitivity measurements, the dummy antenna resistance was varied, both above and below the correct value of 100 ohms. The sensitivity followed the variations of the dummy antenna very closely when the impedance of the input circuit was taken into consideration.

The series of sensitivity measurements discussed above leads to two conclusions regarding the use of a direct connection between the output of a single-sided signal generator and the input of a balanced antenna circuit; first, the primary of the antenna input circuit must be connected to the ground point of the input circuit, and second, the correct value of dummy antenna resistance must be used. In using this direct connection between the signal generator and receiver, it is well to make two simple tests to be sure that measurements are valid. First, the polarity of the signal-generator output should be reversed, and second, the power-line connection for either the signal generator or the receiver should be moved to a different outlet. Normally no change in receiver sensitivity should be observed on making either of these two changes.

Other methods of obtaining balanced output from a single-sided generator have suggested themselves. However, in view of the simplicity offered by the last, of the three methods discussed, they do not appear to be attractive.

# A COAXIAL-LINE DIODE NOISE SOURCE FOR U-H-F\*†

BY

HARWICK JOHNSON

Research Department, RCA Laboratories Division  
Princeton, N. J.

*Summary*—The 50-ohm coaxial line construction of the present diode extends the usefulness of temperature-limited diode noise sources in untuned circuits through the ultra-high frequency region. A direct measurement of receiver sensitivity is obtained by doubling the noise power output of the receiver. The noise factor is given by the diode current in milliamperes except for a transit time correction and a minor correction for spurious responses of the receiver. A maximum temperature-limited emission of 100 milliamperes enables the measurement of receiver noise factors up to about 20 decibels. The transit time reduction of noise is 3 decibels at 3000 megacycles which is probably the upper limit of usefulness of the diode. The effect of standing waves introduced by the diode and its termination on the accuracy of measurement is discussed.

## INTRODUCTION

THE temperature-limited diode has proved to be a convenient known noise source in receiver measurement work. However, its use at ultra-high frequencies has been limited by the lack of tubes of suitable construction and, even at very-high-frequencies where present tubes must be used in conjunction with tuned circuits, the temperature-limited diode has lost much of its convenience. The purpose of this work has been the development of a diode that may be used as a noise source at ultra-high frequencies and, moreover, that will be adaptable for use with untuned circuits.

This is accomplished in the present tubes following the suggestion of E. W. Herold‡ in 1942 to construct the diode as a section of coaxial line with the electron stream flowing between the inner and outer conductors. By the use of suitable electrode spacing a structure is obtained in which the electron transit time is small and which is readily adapted to wide-range coaxial-line circuits. Developmental tubes known as the R-6212 were designed and constructed by H. A. Finke# during 1944.

---

\* Decimal Classification: R261.2 × R361.114.

† Reprinted from *RCA REVIEW*, March, 1947.

‡ RCA Laboratories Division, Princeton, N. J.

# Formerly RCA Laboratories Division, Princeton, N. J.

The internal structure of this early type was subsequently revised to produce the type R-6212A described in this paper. This tube is a laboratory development only.

The noise diode as a means of determining the noise factor of a receiver is first considered with some generality. The construction of the R-6212A is then described and the operating characteristics of the tube given. This is followed by consideration of various factors which affect the accuracy of measurement when using the noise diode as a noise source. These factors include the transit time reduction of noise, for which an approximate calculation is given, and sources of reflection due to the diode such as the diode filament capacitance. The diode termination is briefly discussed and the results of experimental measurements are given.

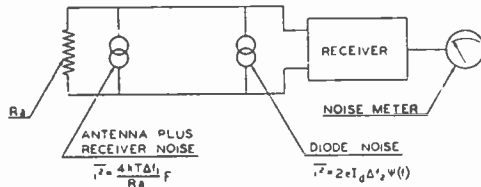


Fig. 1—Equivalent circuit for receiver sensitivity measurements.

### THE NOISE DIODE IN RECEIVER NOISE FACTOR MEASUREMENTS

As a noise source, one of the most important applications for the noise diode is the measurement of the noise factor of a receiver. The use of a noise source in such a measurement will be shown to be much simpler than the conventional method using a signal generator.

Since, at present, no standard definition for the noise factor of a receiver has been established, it is well to point out that the noise factor referred to herein is that based on the use of the noise bandwidth of the *useful signal channel alone* as the noise bandwidth of the receiver.<sup>1</sup> This definition, as far as is known, is that most often used in laboratory measurements using signal generators. Thus agreement should be secured in the quotation of noise factors measured by the conventional signal generator procedure and those measured by a diode noise generator as described below.

<sup>1</sup> D. O. North, "Noise Figures of Radio Receivers" (Contributed discussion), *Proc. I.R.E.*, Vol. 33, No. 2, p. 125-126, February, 1945.

For the original definition of noise factor see D. O. North, "The Absolute Sensitivity of Radio Receivers," *RCA REVIEW*, Vol. VI, No. 3, pp. 332-343, January, 1942.



If  $F$  is the noise factor of a receiver, the total noise output of a receiver may be considered to result from a noise current generator of value (Figure 1)

$$\overline{i_n^2} = \frac{4kT \Delta f_1}{R_a} F \quad (1)$$

at the receiver input, where  $k$  is Boltzmann's constant ( $1.38 \times 10^{-23}$  joules per degree Kelvin),  $T$  is the temperature in degrees Kelvin,  $\Delta f_1$  is the noise bandwidth of the useful signal channel alone and  $R_a$  is the antenna resistance.

If a temperature-limited diode carrying an average current,  $I$ , is placed across the receiver terminals, this diode may also be represented by a current generator of value<sup>2</sup>

$$\overline{i^2} = 2eI \Delta f_2$$

where  $e$  is the electronic charge ( $1.60 \times 10^{-19}$  coulombs) and  $\Delta f_2$  is the overall receiver noise bandwidth including possible responses at image frequency or in the vicinity of frequencies harmonically related to that of the local oscillator.

For use at ultra-high frequencies, with tubes in which the electron transit time is an appreciable part of a period, the diode noise must be modified to account for the transit time reduction of noise.<sup>3</sup> In this case

$$\overline{i^2} = 2eI \Delta f_2 \Psi(f) \quad (2)$$

where  $\Psi(f)$  is the frequency-dependent correction for the transit time reduction of noise. This correction will be discussed later.

With the system shown in Figure 1, the noise factor of the receiver may be most readily obtained in the following manner. With the diode turned off, the noise output of the receiver is observed on the receiver output meter. This meter may be of any type capable of being calibrated in terms of noise power. The diode is turned on and its filament emission increased until the noise output power of the receiver is double its original reading. The diode current  $I_d$  is recorded. This procedure of doubling noise output of the receiver means that the current generator representing the diode is equivalent to that representing the

<sup>2</sup> W. Schottky, "Spontaneous Current Fluctuations in Various Conductors," *Ann. Physik*, Vol. 57, p. 541, 1918.

<sup>3</sup> S. Ballantine, "Schrot-Effect in High Frequency Circuits," *Jour. Frank. Inst.*, Vol. 206, p. 159, August, 1928.

receiver noise, and (1) and (2) may be equated using  $I_d$  for the diode current

$$\frac{4kT \Delta f_1}{R_a} F = 2eI_d \Delta f_2 \Psi(f)$$

whence

$$F = \frac{e}{2kT} R_a I_d \frac{\Delta f_2}{\Delta f_1} \Psi(f) \tag{3}$$

Many ultra-high frequency receivers are designed to work from an antenna impedance of 50 ohms as seen through a standard connect-

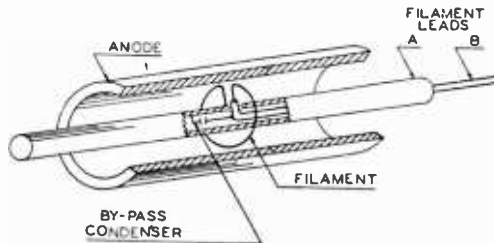


Fig. 2—Outline drawing of coaxial-line noise diode.

ing cable of 50-ohm characteristic impedance; thus, if  $R_a$  is 50 ohms and  $T$  is taken as 290° Kelvin,

$$F = I_d' \frac{\Delta f_2}{\Delta f_1} \Psi(f) \tag{4}$$

where  $I_d'$  is the diode current in milliamperes.

Further, in the many cases where the spurious responses of the receiver are negligible, the bandwidth correction,  $\Delta f_2/\Delta f_1$ , becomes unity so that

$$F = I_d' \Psi(f) \tag{5}$$

Expressing the noise factor in decibels the expression is simply

$$F_{(db)} = 10 \log_{10} \{ I_d' \Psi(f) \}$$

It is thus seen that the noise factor is readily measured using a temperature-limited diode by the simple procedure described above, requiring only a single observation made without tuning adjustments

or knowledge of the receiver bandwidth. If the bandwidth correction,  $\Delta f_2/\Delta f_1$ , must be evaluated to obtain an accurate measurement of noise factor, the noise diode loses some of its convenience.

### DESCRIPTION OF THE NOISE DIODE

The R-6212A coaxial-line noise diode is shown in outline in Figure 2 and consists of an outer cylinder (anode) and a central conductor whose diametric ratio is that of a coaxial line of 50-ohm characteristic impedance. The tungsten wire filament is supported from the central conductor into which is constructed a mica condenser to by-pass the filament lead brought in coaxially through one end of the center con-

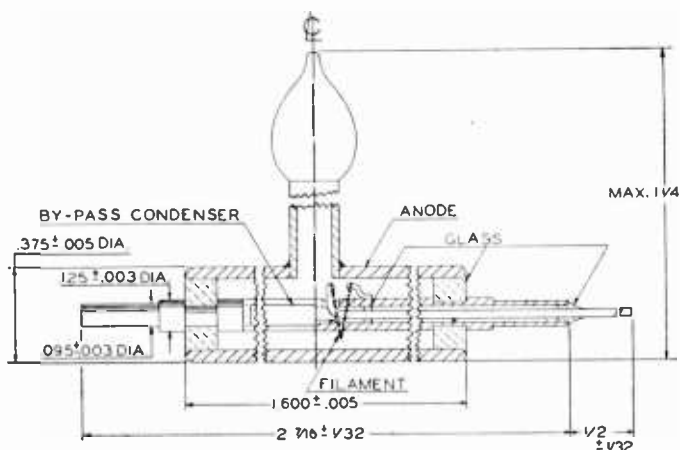


Fig. 3—Details and dimensions of coaxial-line noise diode.

ductor. This construction makes both filament terminals available at one end of the tube. The constructional details of the tube are shown in Figure 3, while the photograph of Figure 4 shows the central conductor subassembly, the anode outer conductor, and the completed tube. The central conductor is undercut at the position of the glass seals to compensate partially for the change in characteristic impedance at this point due to the presence of the glass.

The operating data for the tube are given in Table I. With an anode voltage of 300 volts the filament emission is temperature-limited up to about 100 milliamperes. From Equation (4) it is seen that this emission enables noise factors up to about 20 decibels to be measured at low frequencies by the method described above. Transit time effects reduce this to about 17 decibels near the upper end of the ultra-high frequency band.

*Table I*

Anode Voltage	300 Volts
Anode Current	100 milliamperes (maximum)
Filament Voltage	3.0-3.5 volts (approximately)
Filament Current	2.5 amperes (approximately)

Static characteristics of three sample tubes are shown in Figure 5. Differences result from a variation of the geometry of the .005-inch

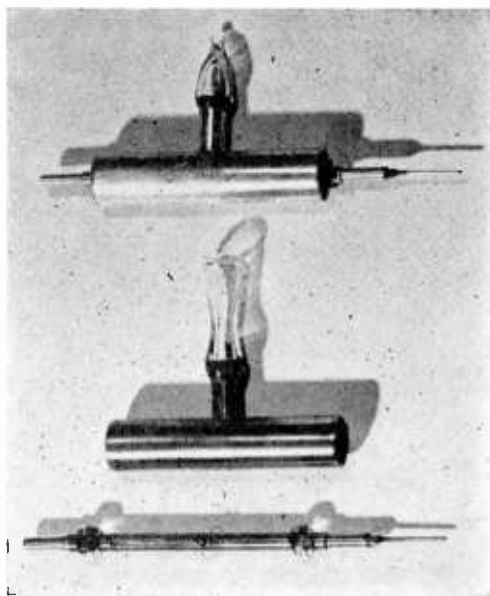


Fig. 4—Central conductor subassembly, anode outer conductor and the completed tube.

tungsten filament with respect to the anode; however, all tubes are temperature-limited at the operating voltage of 300 volts. It is necessary to provide means of cooling the anode when the anode dissipation exceeds 18 watts. This is most readily accomplished by thermal conduction to the adjoining radio-frequency plumbing.

Figure 6 shows the calculated<sup>4</sup> minimum life expectancy of the tungsten filament, by computation of the time for 10 per cent evaporation (by weight) of the filament.

<sup>4</sup> Calculations by H. A. Finke based on data published by Howard A. Jones and Irving Langmuir "The Characteristics of Tungsten Filaments as Functions of Temperature—Part II" *G.E. Review*, Vol. 30, No. 7, pp. 354-361, July, 1927.

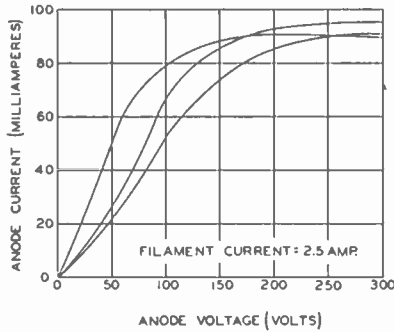


Fig. 5—Typical static characteristics of coaxial-line noise diode.

TRANSIT TIME CORRECTION

The Schottky equation for the shot noise in a temperature-limited diode

$$\overline{di^2} = 2eI df$$

is based on the assumption that the current induced by the passage of one electron through the diode is (in the limit of negligible transit time) an impulse function whose Fourier transform shows the energy distribution to be uniform throughout the frequency spectrum. However, as the transit time of an electron approaches an appreciable part of the period of the frequency components of interest, the current pulse due to the passage of one electron can no longer be idealized as an impulse function and the induced current pulse must be analyzed in

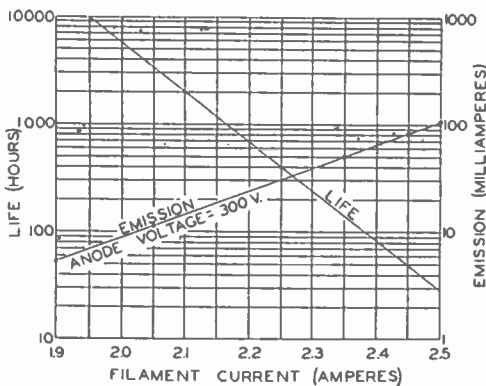


Fig. 6—Minimum life expectancy and measured emission of noise diode.

order to determine the distribution. It is evident that under such conditions the high frequency components will be of reduced amplitude. An analysis for the parallel-plane diode has been given in the literature.<sup>3</sup>

While the R-6212A coaxial-line noise diode resembles a cylindrical diode there are important differences bearing on the transit time reduction of noise. The tube geometry essential for this discussion is shown in Figure 7. In this construction it is obvious that those electrons leaving the innermost part of the filament experience a different field and hence have a different transit time than those leaving the outermost portion of the filament wire. The transit time correction must, therefore, be an integrated effect accounting for the difference

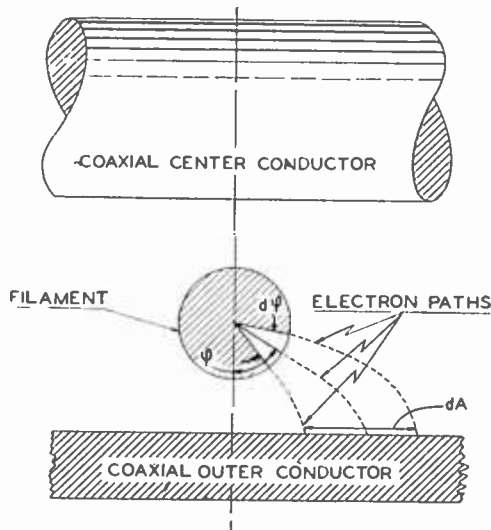


Fig. 7—Geometry of noise diode on an axial plane through one half of diode.

in the electron paths (the shape of the induced current pulse) and the electron transit times (duration of the induced current pulse).

A rigorous computation of the transit time correction would involve the calculation of the shape of the current pulse for each electron path, an adjustment to the proper time scale as determined by the transit time for each path and a summation to find the integrated effect. This is a difficult procedure for the geometry involved; the correction term to be calculated here will be the result of simplifying assumptions in order to obtain at least the approximate correction.

Consider the elementary diode indicated in Figure 7 composed of an emitting surface covering an angle  $d\phi$  of the filament wire and the

corresponding active anode surface  $dA$  as determined by the connecting electron paths. Let the current pulse induced by the passage of an electron through this elementary diode be

$$i(\phi, t) = e h(\phi, t)$$

where  $e$  is the electronic charge and  $\phi$  may be considered a parameter identifying the elementary diode. The shot noise due to this elementary diode is then

$$\overline{di^2} = 2eI_\phi |H^2(\phi, \omega)| df$$

where  $H^2(\phi, \omega)$  is the Fourier transform of  $h(\phi, t)$  and  $I_\phi$  is the average current through the elementary diode.

The filament wire is assumed to emit uniformly so that

$$I_\phi = \frac{I}{2\pi} d\phi$$

and the total shot noise in a frequency band  $df$  being upon integration over the entire emitting surface

$$\overline{di^2} = 2eI df \frac{1}{\pi} \int_0^\pi |H^2(\phi, \omega)| d\phi$$

Now  $H^2(\phi, \omega)$  is a slowly varying function over the bandwidth of a receiver so that an integration over  $df$  gives

$$\overline{i^2} = 2eI \Delta f \frac{1}{\pi} \int_0^\pi |H^2(\phi, \omega)| d\phi$$

For the purpose of this approximate calculation  $H^2(\phi, \omega)$  will be approximated by the form for the parallel plane diode given by Ballantine<sup>3</sup> in the form  $H^2(\omega\tau)$  where  $\tau$  is the transit time and in this case is a function of  $\phi$ . Writing  $\theta$  (the transit angle) for  $\omega\tau$ , Ballantine gives

$$|H^2(\theta)| = \frac{4}{\theta^4} \{2(1 - \cos \theta) + \theta(\theta - 2 \sin \theta)\} \quad \text{whence}$$

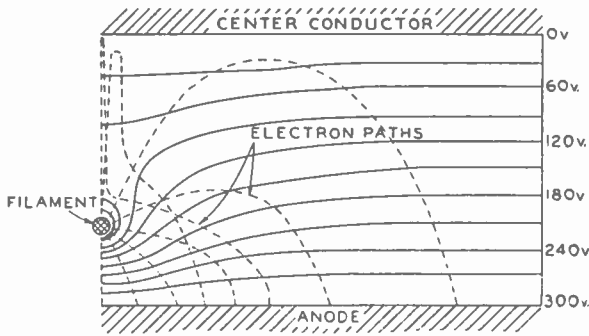


Fig. 8—Approximate field plot and electron paths.

$$\bar{i}^2 = 2eI \Delta f \frac{1}{\pi} \int_0^\pi \frac{4}{\theta^4} \{2(1 - \cos \theta) + \theta(\theta - 2 \sin \theta)\} d\phi$$

where  $\theta$  is a function of  $\phi$  and the frequency.

The integral term is evidently the transit time correction  $\Psi(f)$  of equation (2), that is

$$\Psi(f) = \frac{1}{\pi} \int_0^\pi \frac{4}{\theta^4} \{2(1 - \cos \theta) + \theta(\theta - 2 \sin \theta)\} d\phi \quad (6)$$

where  $\theta = 2\pi f \tau$  and  $\tau$  is a function of  $\phi$ .

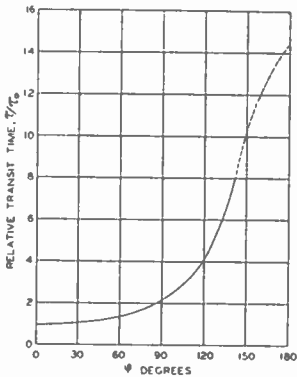


Fig. 9—Variation of transit time with  $\phi$ .

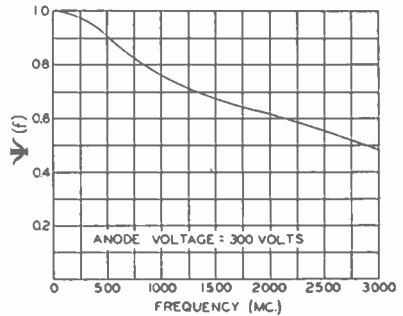


Fig. 10—Calculated approximate transit time reduction of noise in noise diode.



The approximate calculation of  $\Psi(f)$  was then made in the following manner. An approximate field plot of the geometry of Figure 7 was obtained in an electrolytic tank with parallel electrodes. From this field plot, together with data from rubber membrane studies, the electron paths were laid out as shown in Figure 8. The transit times for the various paths could then be computed numerically, thus supplying an explicit relation between the transit time (or transit angle for a given frequency) and  $\phi$  as shown in Figure 9. The numerical integration of (6) to determine  $\Psi$  could then be performed for a particular frequency.

The resulting transit time correction factor  $\Psi(f)$  as a function of frequency is shown in Figure 10. It is seen that the diode noise output drops off to about  $\frac{1}{2}$  (3 decibels) at 3000 megacycles.

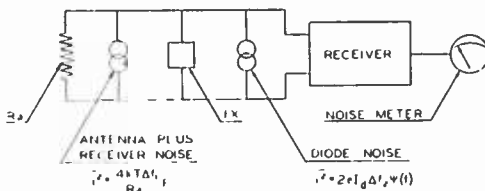


Fig. 11—Equivalent circuit including diode filament capacitance for receiver sensitivity measurements.

#### EFFECT OF DIODE CAPACITANCE

In the equivalent circuit of Figure 1 it is implied that the diode may be introduced into the antenna circuit without affecting the circuit constants. This is not entirely valid for the R-6212A at ultra-high frequencies because of the impedance discontinuities introduced by the diode. It is of interest to consider the circuit of Figure 11 in which a reactance  $jX$  has been added, where this may be considered to be the capacitance added across the line by the diode filament.

In Figure 11,  $F'$  is the noise factor of the receiver with an antenna impedance of  $R_a$  and  $jX$  in parallel. It is evident that a measurement procedure such as that described above will result in the measurement of  $F'$  which, however, may differ from  $F$  of Figure 1 which is the desired noise factor.

If the receiver is considered to have been adjusted previously for minimum noise factor with respect to changes in the operating parameters, then  $F'$  is not sensibly different from  $F$  for small changes in the antenna impedance caused by the addition of  $jX$ . The extent to which the circuit of Figure 11 may be used to determine the noise

factor of the circuit of Figure 1 depends, under these conditions, on the broadness of the minimum noise factor adjustment with respect to changes in  $X$ . This is a characteristic of the receiver and no general statement may be made concerning the limits of its validity.

Lacking specific knowledge of the receiver characteristics it is of interest, in order to gain an insight into the magnitude of the effect of the diode filament capacitance, to consider the variation of the noise power input (i.e. antenna circuit noise or diode noise) into a receiver as the reactance  $X$  is varied. It will be assumed that the input impedance of the receiver is matched to a transmission line whose characteristic impedance  $Z_o$  equals  $R_a$ . This is very close to the condition of minimum noise factor for ultra-high frequency receivers.

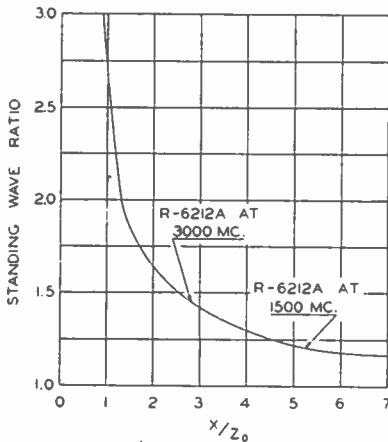


Fig. 12 — Variation of standing wave ratio with filament capacitance.

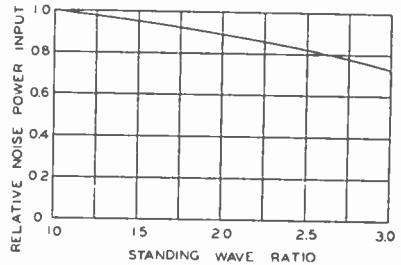


Fig. 13 — Variation of receiver noise power input with standing wave ratio due to filament capacitance.

Since ultra-high-frequency impedance measurements are generally made by means of standing wave measurements on a transmission line, it is desirable to discuss the effect of the diode filament capacitance in terms of the standing wave ratio it introduces in a transmission line which is otherwise terminated in its characteristic impedance. This standing wave ratio,  $\eta$ , is given in Figure 12 as a function of  $X/Z_o$ . The two points indicated for  $\eta = 1.2$  and  $\eta = 1.4$  indicate the calculated effect of the R-6212A filament capacitance at 1500 and 3000 megacycles respectively.

The variation of the noise power input as a function of the standing wave ratio is shown in Figure 13. It is seen that the change in the noise power input is not large for standing wave ratios less than

1.5. In view of the small changes in noise power input (less than 5 per cent) caused by these values of the standing wave ratio, it appears reasonable to expect the presence of the filament capacitance alone would not seriously limit the operation of the tube up to nearly 3000 megacycles. Thus, in an experimental system, if the filament capacitance is so small that the noise input due to the diode is not greatly in error (Figure 13) and, if the noise output of a receiver when connected to the antenna impedance of  $R_a$  and  $jX$  in parallel differs only a few per cent from that when connected to an antenna impedance  $R_a$ , the error in the measured noise factor should be negligible.

The above discussion has been concerned with the effect of the diode filament capacitance alone. In an actual circuit, other sources of reflection are present, for example—the glass beads of the tube, the cable connectors or an improper termination for the diode. A general

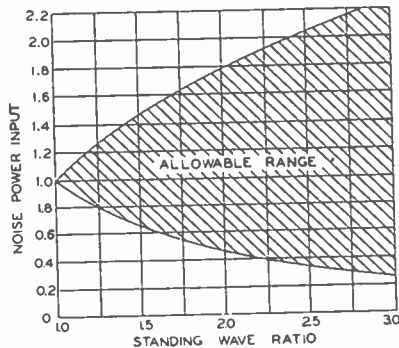


Fig. 14—Ratio of receiver noise power input to that for unity standing wave ratio.

calculation of their effect is not practicable since these sources are disposed along the transmission line and, as mentioned above, one has no knowledge (except in a limited region near the minimum noise factor) of the variation of receiver noise due to these reflections. An insight into the uncertainties of attempting to predict the behavior of a system possessing these distributed sources of reflection may be gained by consideration of the following simple calculation. Let all the sources of reflection lie on the terminated side of the diode filament and assume that the receiver input impedance is that of the characteristic impedance of the connecting transmission line. Then the variation of the noise power input to the receiver from the diode will be in the shaded region of Figure 14 depending on the magnitude and phase of the reflection coefficient associated with the standing wave ratio. It is therefore evident that any usable system must be made as reflectionless as possible.

## WIDE BAND TERMINATIONS

One of the principal objectives for the construction of the R-6212A diode in the form of a coaxial line is to make possible its use in wide range (untuned) ultra-high frequency circuits. The circuit techniques to achieve a wide-range circuit equivalent to that of Figure 1, or Figure 11, are more difficult than appears at first sight. This complication arises from the necessity of providing heating power for the diode filament. Although a minimum of work has been done on this aspect of the problem, the development of a suitable termination is essential to the exploitation of the full possibilities of the tube.

Methods of introducing the filament leads through the simpler forms of radio-frequency chokes are generally subject to the criticism of narrow band operation. Possibilities of introducing the filament current through the receiver end of the diode are rejected as undesirable in a generally useful device.

Probably the simplest general method of providing a wide band termination is that of a long "lossy" line. This suggests that the long "lossy" line be constructed of two concentric coaxial pairs as shown in Figure 15 which shows a typical circuit with the R-6212A diode for the noise factor measurement of an ultra-high frequency receiver. In Figure 15, coaxial pair "B" is used for the filament connections and pair "A" having a characteristic impedance of 50 ohms is used for the diode termination. The termination loss may be introduced in the dielectric of pair "A", the outer conductor of pair "A", the inner conductor of pair "A" or a combination of these. If the loss is introduced in the inner conductor of pair "A", this conductor should be a high conductivity tube clad with a high resistivity material. This would provide a low resistance path for the filament current but still introduce loss in pair "A".

Long "lossy" lines are relatively bulky items to handle. To avoid this inconvenience it should be possible to attain relatively wide band operation with a termination in which a high resistivity material is introduced into the interconductor space of pair "A" if the material is introduced in the proper manner. This would make possible a less bulky termination.

Alternatively, the "lossy" line may be made in the form of a two-wire shielded pair; the two inner conductors would be operated in parallel for radio frequencies and serve as the filament connections. The losses are introduced by one of the methods described above. This type of termination, with the loss introduced in the dielectric of the two-wire shielded pair, was used for the experimental checks on the tube performance to be described later. The reasons dictating the use

of this termination were simply those of available materials and facilities. Since the available two-wire line had a 34-ohm characteristic impedance, a tapered section was necessary to transform this impedance to the 50 ohms required for the diode termination. A variant of this type of termination is that of a parallel connection of two coaxial pairs.

EXPERIMENTAL MEASUREMENTS

The noise factor of a receiver was measured both by the conventional signal generator method and by the noise diode using the termination described above. A comparison of the results of several measurements for different receiver adjustments is given in Table II.

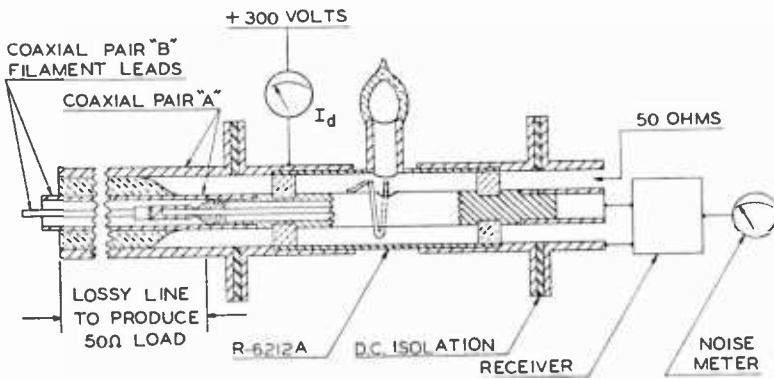


Fig. 15—A typical circuit for measurement of receiver sensitivity with the noise diode.

Table II

Noise Factor Measurement Comparison

(A) Frequency 750 Megacycles  $\Psi(f) = 0.83$

$$\Delta f_2 / \Delta f_1 = 1.1$$

$$F = 1.1 \times 0.83 I_d'$$

Signal Generator		Diode		Difference $\Delta F (db)$
$F$	$F (db)$	$F$	$F (db)$	
12.2	10.9	13.6	11.3	+ 0.4
12.9	11.1	13.6	11.3	+ 0.2
10.2	10.1	10.4	10.2	+ 0.1
38.5	15.9	42.7	16.3	+ 0.4

(B) Frequency 1500 megacycles

$$\Psi(f) = 0.67$$

Due to an oversight  $\Delta f_2/\Delta f_1$  was not evaluated. It is assumed to be the same as in A.

$$F = 1.1 \times 0.67 I_d'$$

Signal Generator		Diode		Difference
$F$	$F(db)$	$F$	$F(db)$	$\Delta F(db)$
40	16.0	42.9	16.3	+ 0.3
45	16.5	44.0	16.4	- 0.1

The termination previously described and used for the above measurements had a standing wave ratio of 1.1 and 1.25 at 750 and 1500 megacycles, respectively, including the cable connectors. With the R-6212A diode inserted, the standing wave ratio was 1.4 and 1.15 at 750 and 1500 megacycles, respectively. At 750 megacycles it was determined that the presence of the filament was the greatest single contributing factor in affecting the standing wave ratio. Since this was the case, the system was expected to satisfy the conditions previously set forth for a usable system, permitting experimental checks to better than 1 decibel. As indicated in Table II such was the case.

\* \* \* \*

It is well to point out that general precautionary measures are necessary when making receiver noise measurements by any method. Noise due to hum and interference signals may be attributed to thermal and tube noise in overall receiver output noise measurements unless required steps are observed. It is often necessary to shut down or isolate certain circuits to gain a true evaluation of the effect of thermal and tube noise effects in receiver output noise.

### CONCLUSIONS

The convenience of a temperature-limited diode as a noise source in receiver measurement work has been demonstrated, in particular for the determination of the noise factor of a receiver. The development of the R-6212A coaxial-line noise diode has made possible the application of these procedures at ultra-high frequencies. This is due principally to the coaxial form of construction permitting it to be incorporated readily into coaxial-line circuits.

While the R-6212A diode, when used as a standard noise source, must be corrected for transit time effects, experimental measurements of receiver noise factors have shown that the use of the approximate correction calculated above results in agreement on the order of the

experimental accuracy (better than 0.5 decibels) with measurements up to 1500 megacycles using a conventional signal generator. Increased accuracy may be obtained with an experimental calibration.

The usable high-frequency limit of the tube is determined by the reflections arising from imperfections in the tube. Insufficient circuit work was undertaken to establish definitely this upper limit. While the measurement of noise factor has been particularly stressed in this report, the tube may also be used in other applications requiring an ultra-high frequency noise source.

It must be emphasized that the R-6212A coaxial-line noise diode was developed purely as a laboratory and not as a commercial product.

#### ACKNOWLEDGMENT

Acknowledgment is made of the valuable advice and suggestions so generously contributed by Mr. E. W. Herold during the course of this work.

# AN ULTRA-HIGH-FREQUENCY LOW-PASS FILTER OF COAXIAL CONSTRUCTION\*†

By

C. I. CUCCIA AND H. R. HEGBAR

Research Department, RCA Laboratories Division,  
Princeton, N. J.

*Summary*—The design of an ultra-high-frequency low-pass filter of coaxial construction is described. The design equations and design criteria are derived and are applied to two coaxial filters whose cut-off frequencies are 800 megacycles and 1800 megacycles, respectively, and whose mechanical details and transmission characteristics are discussed.

**D**URING the course of an investigation of modes of oscillation in cavity magnetron blocks by means of cold-resonance measurements, it was found that the harmonics in the output of the test oscillator excited modes belonging to multiplets other than the fundamental one. These cold-resonance tests were conducted for modes existing in the range from 600 to 1500 megacycles and troublesome oscillator harmonics were identified up to 10,000 megacycles. It was evident that a filter with low-pass characteristics could be used to eliminate this difficulty without modification of the oscillator or the other elements of the testing apparatus and a simple coaxial filter that was successfully utilized will be described.

It was required that the low-pass filter, which was to be designed for this application, have a minimum number of pass bands above the cut-off frequency. Since the phase shift and input impedance variation over the low-pass band were not of primary importance, these aspects are not considered here. To be most useful, a filter for experimental work at these frequencies should be fitted with coaxial connectors permitting rapid connection to coaxial cables, and should be completely closed to prevent radiation and coupling with other apparatus. It is always desirable that such units be of simple and rugged mechanical construction.

After consideration of various filter designs which might be satisfactory, it was decided that the most direct approach to the problem was to construct a constant-K, T-type, low-pass filter in which the lumped series inductances and shunt capacitances used in low-pass filters were to be replaced by lengths of coaxial transmission line whose distributed parameters would closely simulate the lumped parameters.

---

\* Decimal Classification: R310 × R386.2.

† Reprinted from *RCA REVIEW*, December, 1947.



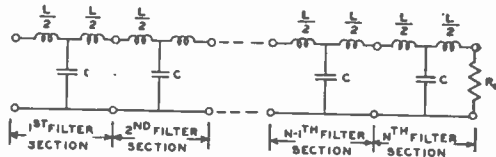


Fig. 1—Lumped parameter constant-K T-type low-pass filter with N sections.

The design of the filter was carried out in the following way: It is known<sup>1</sup> that for the low-pass, constant-K, T-type filter shown in Figure 1,

$$C = \frac{1}{\pi f_c R_o} \text{ farads} \quad (1)$$

$$L = \frac{R_o}{\pi f_o} \text{ henries} \quad (2)$$

where  $f_c$  is the cut-off frequency in cycles per second and  $R_o$  is the terminating resistance in ohms.

In the ultra-high-frequency coaxial filter being described, a section of coaxial line having a large characteristic impedance with respect to  $R_o$  is used as the inductance element and a section of coaxial line having a small characteristic impedance with respect to  $R_o$  is used as the capacitance element. The conditions for which a short length of coaxial line will appear to be a series inductance or a shunt capacitance are derived in the Appendix and are listed there in Equations (5-a), (6-a), and (10-a).

The geometry used for the coaxial filters is shown in Figure 2. Expressions for the characteristic impedance of the inductance and capacitance sections are

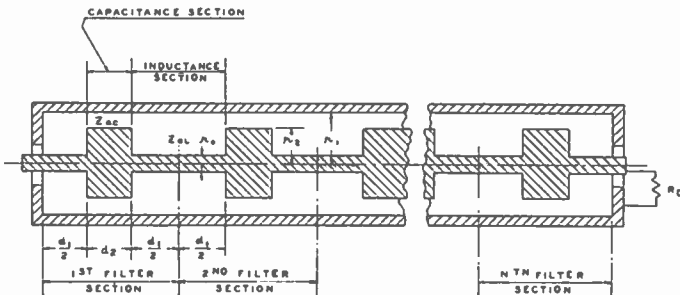


Fig. 2—Detail of UHF low-pass coaxial filter with N sections.

<sup>1</sup> Ware and Reed, COMMUNICATION CIRCUITS, John Wiley and Sons, New York, N. Y., 1944 (Equations 9-14, 9-15, pp. 126-127.)

$$Z_{oL} = 138 \text{ Log}_{10} \frac{r_1}{r_o} \text{ (ohms)} \quad (3), \quad Z_{oc} = 138 \text{ Log}_{10} \frac{r_1}{r_2} \text{ (ohms)}. \quad (4)$$

The total inductance of the inductance section of length,  $d_1$ , is approximately

$$L \cong \frac{Z_{oL} d_1}{v} \quad (5)$$

and, neglecting fringing, the total capacitance of the capacitance section of length,  $d_2$ , is approximately

$$C \cong \frac{d_2}{Z_{oc} v} \quad (6)$$

where  $v$  is the velocity of light. Equations (5) and (6) are suitable representations for lumped inductance and capacitance if

$$\tan \frac{2\pi f L_o d_1}{Z_{oL}} \approx \frac{2\pi f L_o d_1}{Z_{oL}} \quad (7)$$

and  $\tan 2\pi f Z_{oc} C_o d_2 \approx 2\pi f Z_{oc} C_o d_2$  (8)

as specified in Equation (6-a).  $L_o$  and  $C_o$  are the inductance and capacitance per unit length of line, respectively.

Substituting Equations (5) and (6) into Equations (1) and (2), the following design relationships are obtained:

$$d_1 = \frac{R_o \lambda_o}{138 \pi \text{ Log}_{10} \frac{r_1}{r_o}} \quad (9) \quad d_2 = \frac{138 \lambda_o}{\pi R_o} \text{ Log}_{10} \frac{r_1}{r_2} \quad (10)$$

where  $d_1$  and  $d_2$  are in centimeters and  $\lambda_o$  is the cut-off wavelength in centimeters. It is evident that Equations (9) and (10) may be combined to yield the general relationship

$$\lambda_c = \pi \sqrt{d_1 d_2 \frac{\text{Log}_{10} \frac{r_1}{r_o}}{\text{Log}_{10} \frac{r_1}{r_2}}} \quad (11)$$

in terms of the lengths,  $d_1$  and  $d_2$ , and the radii,  $r_o$ ,  $r_1$ , and  $r_2$  which are interrelated by Equations (9) and (10).

The design relations—Equations (9), (10), and (11)—for a practical ultra-high-frequency coaxial filter will be valid if the following criteria are observed:

$$d_2 < d_1 \ll \lambda_c/8 \quad (12)$$

$$2\pi r_1 < \lambda_c \quad (13)$$

$$r_1 - r_2 < d_2/4 \quad (14)$$

$$r_1 - r_o < d_1/4 \quad (15)$$

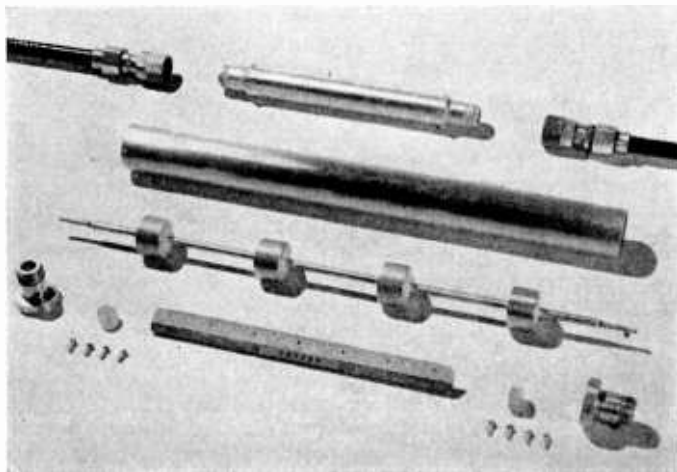


Fig. 3—Photograph of the 800-megacycle and 1800-megacycle coaxial low-pass filters. The 800-megacycle filter is shown dismantled.

Equation (12) is deduced from Equations (7) and (8). Equation (13) is specified so that the design of the filter will be made for the fundamental mode of any of the component sections of coaxial line. Equations (14) and (15) are intended to minimize end effects and represent an average of information which has been yielded by numerous field plots.

Two of the filters which were constructed were designed using Equations (9) and (10) for cut-off frequencies of 800 and 1800 megacycles and are pictured in Figure 3 with the 800-megacycle filter shown dismantled. The center structure was made by soldering discs at proper intervals on a center rod. Army-Navy coaxial cable connectors were used at both ends of the structure and served to hold and position the center conductor in the enclosing cylinder. All of the metal components were made of brass and were silver plated.

The details of these filters are tabulated as follows, with the dimensions in inches:

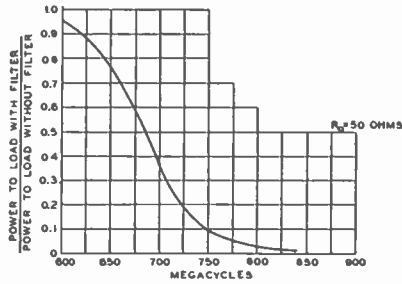


Fig. 4—Transmission curve of 800-megacycle coaxial filter in the vicinity of cutoff.

$f_c$	Number of Sections	$R_o$	$r_o$	$r_1$	$r_2$	$d_1$	$d_2$
800	4	50	0.0937	0.500	0.450	2.34	0.583
1800	4	50	0.0468	0.3125	0.275	0.95	0.312

Measurements were made with and without the filters between an oscillator and a 50-ohm load using 50-ohm coaxial cable for frequencies in the range of 500 to 3750 megacycles. The ratio of the power to the load with and without the filter for both filters is shown in Figures 4 and 5 in the vicinity of cut-off. Although the actual power transfer through the filter is a function of the impedance reflected back to the oscillator and so will vary with different oscillators and filters, the cut-off frequency of the filter will not be appreciably affected by the over-all circuit and it is this cut-off region which is of interest. The 800-megacycle filter design adheres closely to Equations (12-15) and Figure 4 shows its experimentally observed cut-off to be closely in accord with the predicted value. The 1800-megacycle filter's experi-

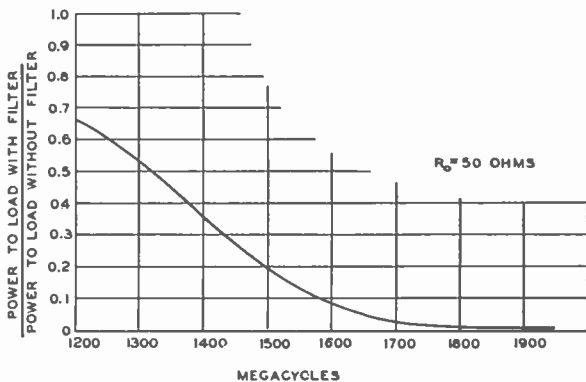


Fig. 5—Transmission curve of 1800-megacycle filter in the vicinity of cutoff.

mentally observed cut-off in Figure 5 does not agree exactly with the predicted cut-off since it is evident from the dimensions listed in the table that Equation (12) is exceeded to such an extent that the angle in Equation (7) is not an accurate approximation of the tangent of the angle. The effective cut-off of the 1800-megacycle filter is seen in Figure 5 to be in the neighborhood of 1650 megacycles and represents an over-all error of about eight per cent.

There are frequencies above cut-off where pass bands will result due to resonances on the part of either the capacitance or the inductance sections. At 2690 megacycles, for example, the 800-megacycle filter was found to have an extremely sharp pass band in which considerable transmission was observed. This is precisely that frequency at which the inductance section length,  $d_1$ , is equal to a half wavelength and the filter becomes a line composed of a series of resonant sections connected by short lengths of low characteristic impedance line. Resonance on the part of the capacitance section will also produce a pass band. These pass bands may be predicted and if, in general,  $d_1$  and  $d_2$  are made very small compared to the cut-off wavelength, the resonant pass bands will be far removed from the main pass band of the filter. It is possible to decrease the transmission in these pass bands by including sections in the structure with different  $d_1$  and  $d_2$  which are designed to cut-off at the correct frequency.

Since the coaxial low-pass filter will decrease in size as the cut-off frequency is increased, the upper limit of design and usage will be determined by mechanical considerations which will become important above 5000 megacycles. It is particularly important at these higher frequencies that the connectors do not introduce reflections of large magnitude and that the termination be made as close to  $R_0$  in value as possible. In the specific application of the filters being described, a termination made up of a small 50-ohm resistor which was bent into the shape of a loop was found to function satisfactorily, but at higher frequencies the termination must be carefully engineered to preserve the cut-off characteristic of the filter.

When installed into the cold-resonance equipment for which they were designed, the low-pass coaxial filters were found to be completely satisfactory with respect to performance and during the course of numerous experiments, indications due to higher modes getting through the high-pass bands of the filters were not observed.

#### ACKNOWLEDGMENT

The authors are indebted to L. S. Nergaard for numerous suggestions and to L. E. Norton for aiding in transmission measurements.

APPENDIX

A. Consider the use of a short length of coaxial transmission line, having zero dissipation, as a series-lumped inductance in series with a terminating impedance,  $Z_L$ . Let the characteristic impedance of this line be  $Z_o$  and let it be terminated by  $Z_L$  such that the input impedance,  $Z_1$ , may be written

$$Z_1 = Z_o \frac{Z_L \cos \beta l + j Z_o \sin \beta l}{Z_o \cos \beta l + j Z_L \sin \beta l} \tag{1-a}$$

where the length of the line is  $l$  and

$$Z_o = \sqrt{\frac{L_o}{C_o}} \tag{2-a} \quad \beta l = \omega \sqrt{L_o C_o} l \tag{3-a}$$

$L_o$  and  $C_o$  are the inductance and capacitance per unit length of line, respectively. Equation (1-a) may be rewritten

$$Z_1 = \frac{Z_L + j Z_o \tan \beta l}{1 + j \frac{Z_L}{Z_o} \tan \beta l} \tag{4-a}$$

If the length,  $l$ , and the ratio,  $\frac{Z_L}{Z_o}$ , are such that

$$\left| \frac{Z_L}{Z_o} \tan \beta l \right| \ll 1 \tag{5-a}$$

and  $\tan \beta l \approx \beta l$  (6-a) then  $Z_1 = Z_L + j \omega L_o l$  (7-a)

which shows that the short length of line will appear to be a series inductance if (5-a) and (6-a) are adhered to.

B. Consider the use of a short length of coaxial transmission line, having zero dissipation, as a lumped capacitance in shunt with a terminating impedance  $Z_L$ . Let the characteristic impedance of this line be  $Z_o$  and let it be terminated by  $Z_L$  such that the input admittance,  $Y_1$ , may be written

$$Y_1 = \frac{1}{Z_o} \frac{Z_o \cos \beta l + j Z_L \sin \beta l}{Z_L \cos \beta l + j Z_o \sin \beta l} \quad (8-a)$$

$$= \frac{\frac{1}{Z_L} + j \frac{1}{Z_o} \tan \beta l}{1 + j \frac{Z_o}{Z_L} \tan \beta l} \quad (9-a)$$

If the length,  $l$ , and the ratio,  $\frac{Z_o}{Z_L}$ , are such that

$$\left| \frac{Z_o}{Z_L} \tan \beta l \right| \ll 1 \quad (10-a)$$

and  $\tan \beta l \approx \beta l$  (6-a) then  $Y_1 = \frac{1}{Z_L} + j \omega C_o l$  (11-a)

which shows that the short length of line will appear to be a shunt capacitance if (10-a) and (6-a) are adhered to.

If the radius of the outer conductor,  $r_o$ , is much larger than the radius of the inner conductor,  $r_b$ , fringing may not be neglected and it is convenient to include an approximate fringing factor such that

$$Y_1 \cong \frac{1}{Z_L} + j \omega \left[ 1 + \frac{r_o - r_b}{l} \right] C_o l \quad (12-a)$$

#### BIBLIOGRAPHY

"An Easily Constructed 'High-Pass' Coaxial Filter", Harvard Radio Research Laboratory Report 411-115A, U. S. Dept. of Commerce Publication PB 14175.

L. R. Quarles, "Transmission Lines as Resonant Circuits", *Communications*, Vol. 26, pp. 22-52, May, 1946.

L. R. Quarles, "Transmission Lines as Filters", *Communications*, Vol. 26, pp. 34-48, June, 1946.

Laurance M. Leeds, "Concentric Narrow-Band-Elimination Filter", *Proc. I.R.E.*, Vol. 26, No. 5, pp. 576-589, May, 1938.

## MEASUREMENT OF IRON CORES AT RADIO FREQUENCIES\*†

BY

DUDLEY E. FOSTER AND ARTHUR E. NEWLON

RCA License Laboratory,  
New York, N. Y.

### Summary

*Iron cores are used in radio-frequency coils primarily to obtain increased inductance. The amount of inductance increase due to the iron core depends upon the physical dimensions of the coil and the core, and on the effective permeability of the core. In addition to the inductance increase, the iron core increases the effective radio-frequency resistance of the coil due to hysteresis and eddy-current losses in the iron. This paper describes a method of measuring the effective permeability and loss factor of iron at radio frequencies, and develops expressions by means of which the characteristics of a given coil can be predicted when the iron constants are known. The measurement method described is employed to measure several cores. Sample calculations and curves are given to illustrate the use of the formulas developed herein.*

(11 pages, 17 figures, 4 appendices)

---

\* Decimal Classification: R231 × R232.3

† *Proc. I.R.E.*, May, 1941

## DIRECT-READING WATTMETERS FOR USE AT RADIO FREQUENCIES\*†

BY

GEORGE H. BROWN, J. EPSTEIN AND D. W. PETERSON

Research Department, RCA Laboratories Division,  
Princeton, N. J.

### Summary

*The principle upon which the operation of direct-reading wattmeters is based has been known for many years. The contribution of this paper lies in the application of this principle to a practical operating instrument for the measurement of high power at radio frequencies. Two instruments are described. The first is useful in the range of frequencies from 500 to 2000 kilocycles. This instrument contains circuits which permit operation at any frequency in this band with no tuning or other change in the instrument. The second instrument operates in the region near 50 megacycles. It is inherently a single-frequency device constructed from sections of transmission lines. The theory of operation is discussed, as well as calibration methods. Test data taken with the instruments with loads having a wide*

---

\* Decimal Classification: 621.374.6 × R251

† *Proc. I.R.E.*, August, 1943



*range of power factors are compared with power measurements made on water-cooled loads.*

*(8 pages, 12 figures, 2 tables)*

## SPECIAL APPLICATIONS OF ULTRA-HIGH-FREQUENCY WIDE-BAND SWEEP GENERATORS\*†

BY

JOHN A. BAUER

Engineering Products Department, RCA Victor Division,  
Camden, N. J.

### *Summary*

*Three unusual uses of wide-band frequency-modulated signal generators are described. Instruments suitable for two uses immediately applicable to television receiver development are also shown. These applications are as follows:*

- 1. Radio-frequency impedance measurements;*
- 2. Overall frequency response measurements of television receivers;*
- 3. Microwave frequency measurements.*

*Practicality has already been demonstrated with resulting large laboratory and factory test time savings.*

*(12 pages, 7 figures)*

---

\* Decimal Classification: R355.913.2 × R200

† *RCA REVIEW*, September, 1947

## AN OMNIDIRECTIONAL RADIO-RANGE SYSTEM\*†

## Part I—Principles of Operation

BY

DAVID G. C. LUCK‡

Research Laboratories, RCA Manufacturing Co., Inc.,  
Camden, N. J.*Summary*

*Radio navigation may be done with direction-finding receivers on mobile craft, with fixed direction finders on the ground or with directional beacon transmitters on the ground. Each method has its unique merits and faults, but the last seems especially suited for aircraft guidance in the United States and has, in the form of four-course radio "range" beacons, rendered outstanding service. The disadvantages of limited choice of courses and of difficulty in definitely determining on which course a craft may be, inherent in the present four-course ranges, may be avoided by rotating a transmitted radio beam and timing its passage over the receiving craft, to determine uniquely the bearing of that craft from the known location of the beacon transmitter. A rotating beam, of figure-eight shape, may be produced without mechanical motion by setting up two fixed antenna systems, having figure-eight directivity, at right angles and feeding them with radio-frequency signals modulated at the desired rotation frequency, the modulation of the separate supplies to the two crossed antennas being in phase quadrature. Unmodulated carrier to resolve the ambiguity of the figure-eight beam, by changing its shape to a limaçon, is radiated from a non-directive antenna, and a timing reference is provided by interrupting all transmission momentarily just as the beam points north. The audio output from a receiver tuned to this beacon comprises a sine wave produced by the sweep of the beam and a train of impulses produced by the reference keying. The sine component is filtered, split in phase and used to drive a cathode-ray beam in a circle, in step with the rotation of the transmitted beam. The impulses are used to slow up the beam electrons momentarily, marking the swept circle, with an outward jog and so indicating receiver bearing directly. The impulses also actuate a zero-center meter, while the sine wave renders this meter insensitive at a certain moment of the cycle and oppositely sensitive just before and just after that moment. By adjusting the sine wave phase, the meter may be centered when the receiver is on any desired bearing, and thereafter will indicate any departure from that bearing. A special broadcast transmission may be used to check adjustments of receiving indicators. Certain conditions as to modulation phases and amplitudes, antenna-current phases and amplitudes, antenna geometry and cathode-ray inductor voltage phases, amplitudes and tube geometry must be fulfilled if accurate bearings are to be obtained. Study of these conditions shows all adjustment tolerances to be of reasonable magnitude, though considerable care in antenna construction is necessary to insure adequate symmetry of antenna-current phase.*

*(27 pages, 7 figures)*

\* Decimal Classification: R526.1

† RCA REVIEW, July, 1941

‡ Now with the Research Department, RCA Laboratories Division, Princeton, N. J.

## AN OMNIDIRECTIONAL RADIO-RANGE SYSTEM\*†

## Part II — Experimental Apparatus

BY

DAVID G. C. LUCK‡

Research Laboratories, RCA Manufacturing Co., Inc.,  
Camden, N. J.*Summary*

*Experimental omnidirectional ranges have been developed and tested in flight at frequencies of 6425 kilocycles per second and 125 megacycles per second. In each case, a radiating system consisting of five vertical antennas and a metallic ground mat was used. Each transmitter was of a normal radiotelephone type, supplemented by a pair of balanced modulators, an impulse keyer, and a set of modulation controls. Full monitoring of the effect of all transmitter adjustments was provided. Essentially normal aircraft receivers and antennas were employed. Both cathode-ray azimuth indicators and pointer-type deviation from course indicators were provided.*  
(26 pages, 17 figures)

---

\* Decimal Classification: R526.1

† RCA REVIEW, January, 1942

‡ Now with Research Department, RCA Laboratories Division, Princeton, N. J.

## AN OMNIDIRECTIONAL RADIO-RANGE SYSTEM\*†

## Part III — Experimental Results and Methods of Use

BY

DAVID G. C. LUCK‡

Research Laboratories, RCA Manufacturing Co., Inc.,  
Camden, N. J.*Summary*

*Tests of experimental omnidirectional ranges have been made at 6425-kilocycles and 125-megacycle operating frequencies. Ground measurements at the higher frequency showed directive pattern shapes to be imperfect but acceptable and showed overall instrumental errors of indicated azimuth averaging less than one degree. Flight tests at both frequencies showed considerably larger errors, apparently related to terrain or transmitter-site characteristics. Sky-wave operation at the lower frequency was found satisfactory in the absence of violent fading. Standing wave effects were sought but not found in the ultra-high-frequency field. Trouble*

---

\* Decimal Classification: R526.1

† RCA REVIEW, March, 1946

‡ Now with the Research Department, RCA Laboratories Division, Princeton, N. J.

was experienced in the higher-frequency tests with spurious modulation of receiver signals produced by spinning propellers and imperfect structural bonding of aircraft, as well as with ignition interference. Behavior of the experimental equipment itself was on the whole satisfactory. Omnidirectional ranges may be used to fly straight radial courses to or from range stations, in which service the technique of their use is rather similar to that employed with other visual course-type ranges, or they may be used for general cross-country navigation following a uniquely simple technique. Omnidirectional ranges lend themselves well to safe air-traffic control.

(24 pages, 8 figures)

## RADIATING SYSTEM FOR 75-MEGACYCLE CONE-OF-SILENCE MARKER\*†

By

EDMUND A. LAPORT‡ AND JAMES B. KNOX

RCA Victor Company, Ltd.,  
Montreal, Quebec, Canada

### Summary

*A brief description is given of a new 75-megacycle cone-of-silence marker radiating system developed for use on the Canadian airways. This system provides a sharper marker beam and reduces orientation error over previous marker radiating systems.*

(3 pages, 4 figures)

---

\* Decimal Classification: R526.1

† *Proc. I.R.E.*, January, 1942

‡ Now Chief Engineer, RCA International Division, New York, N. Y.

## SHORAN PRECISION RADAR\*†

By

STUART WILLIAM SEELEY

Manager, Industry Service Laboratory, RCA Laboratories Division,  
New York, N. Y.

### Summary

*Shoran navigational radar is generally credited with being the most precise system of its type devised by man. The history of the conception and development of the principles employed, as well as a description of the physical make-up of the equipment are discussed in this paper. The history traces the development from the fall of 1938 through to the actual application of Shoran equipment both in the European and Far Eastern*

---

\* Decimal Classification: R526 × R537

† *Elec. Eng.*, April, 1946

*theaters of war in 1944 and 1945. Following the historical section, the Shoran system is described in general. The specific plane and ground equipment is then covered in some detail and a statement concerning operational results is included.*

*(9 pages, 12 figures)*

## TELERAN\*†

### Part I— Air Navigation and Traffic Control by Means of Television and Radar

BY

D. H. EWING AND R. W. K. SMITH

Engineering Products Department, RCA Victor Division,  
Camden, N. J.

#### *Summary*

*Wartime développement of radar techniques offer a new approach to the problem of improving air navigation and traffic control, two fields in which existing equipment is obsolescent. Since no one military equipment appears to be ideally suited for solving the many problems, a re-investigation of the requirements necessary to handle very heavy traffic is first made. After analyzing the requirements, a system is described which appears to fulfill these requirements and offers unique advantages. In this system (Teloran), aircraft position information is presented to ground observers and controllers on a series of plan position indicators. One indicator is used for each altitude layer. Information on the position of aircraft in a given altitude layer is superimposed on a map of the region covered by the ground radar; this, together with weather, traffic control, and other desired information, is transmitted by television to each aircraft in the region. Each cooperating aircraft is equipped with a transponder beacon which serves not only to reinforce the radar echo but also to provide an altitude-dependent reply which allows the ground station to differentiate among aircraft by altitude. The application of this system to concrete problems of navigation and traffic control is also discussed. Included are the problems of enroute navigation, approach and landing procedures, automatic flight and landing, collision prevention, personal identification and communication, and air traffic control.*

*(21 pages, 12 figures)*

---

\* Decimal Classification: 629.132.5 × R583 × 537

† RCA REVIEW, December, 1946

## TELERAN\*†

## Part II — First Experimental Installation

BY

D. H. EWING, H. J. SCHRADER AND R. W. K. SMITH

Engineering Products Department, RCA Victor Division,  
Camden, N. J.*Summary*

*A set of equipment designed to demonstrate the principles of Teleran as outlined in a previous paper is described. Liberal use of conventional circuits and practices has been made and only those new circuits designed specifically for Teleran are described here. Pictures of the airborne equipment are included. The paper covers in detail the choice of television parameters, synchronizing equipment, the television transmitter, altitude coding, cameras and mixing, the landing display, the airborne beacon, and the airborne television receiver.*

*(21 pages, 6 figures)*

---

\* Decimal Classification: 629.132.5 × R583 × R537

† RCA REVIEW, December, 1947

---

NOTE—It is planned to publish Part III of this series, concerning experimental tests and operational results, in RCA REVIEW soon after these tests have been completed, possibly late during 1948 or early in 1949.

## APPENDIX I

---

# RADIO AT ULTRA-HIGH FREQUENCIES

### A Bibliography of Technical Papers by RCA Authors 1925 — 1947

---

This listing includes some 330 technical papers on ultra-high frequencies and closely related subjects, selected from those written by RCA Authors and published during the period 1925-1947.

Papers are listed chronologically except in cases of multiple publication. Papers which have appeared in more than one journal are listed once, with additional publication data appended.

Abbreviations used in listing the various journals are given on the following pages.

Any requests for copies of papers listed herein should be addressed to the publication to which credited. However, *RCA Licensee Bulletins* are not published and are issued only as a service to licensees of the Radio Corporation of America.

---

## ABBREVIATIONS

(Note—Titles of periodicals not listed below, as well as book titles, are not abbreviated.)

<i>Amer. Jour. Phys.</i> .....	AMERICAN JOURNAL OF PHYSICS
<i>Amer. Rev.</i> .....	AMERICAN REVIEW
<i>An. Amer. Acad. Polit. Soc. Sci.</i> .....	ANNALS OF THE AMERICAN ACADEMY OF POLITICAL AND SOCIAL SCIENCES
<i>ASTM Bulletin</i> .....	BULLETIN OF THE AMERICAN SOCIETY FOR TESTING MATERIALS
<i>Bell Sys. Tech. Jour.</i> .....	BELL SYSTEM TECHNICAL JOURNAL
<i>Broad. Eng. Jour.</i> .....	BROADCAST ENGINEERS JOURNAL (A.T.E. JOURNAL)
<i>Comm. and Broad. Eng.</i> .....	COMMUNICATION AND BROADCASTING ENGINEERING
<i>Elec. Eng.</i> .....	ELECTRICAL ENGINEERING (TRANSACTIONS A.I.E.E.)
<i>Electronic Ind.</i> .....	ELECTRONIC INDUSTRIES
<i>FM and Tele.</i> .....	FM AND TELEVISION
<i>G.E. Review</i> .....	GENERAL ELECTRIC REVIEW
<i>ICS</i> .....	INTERNATIONAL CORRESPONDENCE SCHOOLS
<i>Ind. Eng. Chem.</i> .....	INDUSTRIAL AND ENGINEERING CHEMISTRY
<i>Ind. Standard.</i> .....	INDUSTRIAL STANDARDIZATION (AMERICAN STANDARDS ASSOCIATION JOURNAL)
<i>Inter. Project</i> .....	INTERNATIONAL PROJECTIONIST
<i>Jour. Acous. Soc. Amer.</i> .....	JOURNAL OF THE ACOUSTICAL SOCIETY OF AMERICA
<i>Jour. A.I.E.E.</i> .....	JOURNAL OF THE AMERICAN INSTITUTE OF ELECTRICAL ENGINEERS
<i>Jour. Appl. Phys.</i> .....	JOURNAL OF APPLIED PHYSICS
<i>Jour. Amer. Ceramic Soc.</i> .....	JOURNAL OF THE AMERICAN CERAMIC SOCIETY
<i>Jour. Amer. Concrete Inst.</i> .....	JOURNAL OF THE AMERICAN CONCRETE INSTITUTE
<i>Jour. Amer. Pharmaceutical Assc.</i> .....	JOURNAL OF THE AMERICAN PHARMACEUTICAL ASSOCIATION
<i>Jour. Bacteriology</i> .....	JOURNAL OF BACTERIOLOGY
<i>Jour. British Inst. Cine.</i> .....	JOURNAL OF THE BRITISH INSTITUTE OF CINEMATICS
<i>Jour. Chem. Phys.</i> .....	JOURNAL OF CHEMICAL PHYSICS
<i>Jour. Eng. Educ.</i> .....	JOURNAL OF ENGINEERING EDUCATION
<i>Jour. Frank. Inst.</i> .....	JOURNAL OF THE FRANKLIN INSTITUTE
<i>Jour. Opt. Soc. Amer.</i> .....	JOURNAL OF THE OPTICAL SOCIETY OF AMERICA
<i>Jour. Sci. Inst. (Brit.)</i> .....	JOURNAL OF SCIENTIFIC INSTRUMENTS (BRITISH)
<i>Jour. Soc. Mot. Pic. Eng.</i> .....	JOURNAL OF THE SOCIETY OF MOTION PICTURE ENGINEERS
<i>Jour. Tele. Soc. (Brit.)</i> .....	JOURNAL OF THE TELEVISION SOCIETY (BRITISH)
<i>Phys. Rev.</i> .....	PHYSICAL REVIEW
<i>Proc. Amer. Phil. Soc.</i> .....	PROCEEDINGS OF THE AMERICAN PHILOSOPHICAL SOCIETY
<i>Proc. I.R.E.</i> .....	PROCEEDINGS OF THE INSTITUTE OF RADIO ENGINEERS



## ABBREVIATIONS (Continued)

<i>Proc. Nat. Elec. Conf.</i> .....	PROCEEDINGS OF THE NATIONAL ELECTRONICS CONFERENCE
<i>Proc. Rad. Club Amer.</i> .....	PROCEEDINGS OF THE RADIO CLUB OF AMERICA
<i>Project. Jour. (Brit.)</i> .....	PROJECTIONISTS JOURNAL (BRITISH)
<i>Product Eng.</i> .....	PRODUCT ENGINEERING
<i>Project. Eng.</i> .....	PROJECTION ENGINEERING
<i>QST</i> .....	QST (A.R.R.L.)
<i>Radio and Tele.</i> .....	RADIO AND TELEVISION
<i>Radio Eng.</i> .....	RADIO ENGINEERING
<i>Radio Tech. Digest</i> .....	RADIO TECHNICAL DIGEST
<i>RCA Rad. Serv. News</i> .....	RCA RADIO SERVICE NEWS
<i>Rev. Mod. Phys.</i> .....	REVIEWS OF MODERN PHYSICS
<i>Rev. Sci. Instr.</i> .....	REVIEW OF SCIENTIFIC INSTRUMENTS
<i>RMA Eng.</i> .....	RMA ENGINEER
<i>Sci. Monthly</i> .....	SCIENTIFIC MONTHLY
<i>Sci. News Ltr.</i> .....	SCIENCE NEWS LETTER
<i>Short Wave and Tele.</i> .....	SHORT WAVE AND TELEVISION
<i>TBA Annual</i> .....	ANNUAL OF THE TELEVISION BROADCASTERS ASSOCIATION
<i>Teleg. &amp; Teleph. Age</i> .....	TELEGRAPH AND TELEPHONE AGE
<i>Tele. News</i> .....	TELEVISION NEWS
<i>The T &amp; R Bulletin (Brit.)</i> .....	BULLETIN OF THE RADIO SOCIETY OF GREAT BRITAIN
<i>Trans. Amer. Soc. Mech. Eng.</i> .....	TRANSACTIONS OF THE AMERICAN SOCIETY OF MECHANICAL ENGINEERS
<i>Trans. Electrochem. Soc.</i> .....	TRANSACTIONS OF THE ELECTRO-CHEMICAL SOCIETY

## U-H-F BIBLIOGRAPHY

	Year
"Frequency Multiplication Principles and Practical Application of Ferro Magnetic Methods", N. E. Lindenblad and W. W. Brown, <i>Jour. A.I.E.E.</i> .....	1925
"Transmission and Reception of Photoradiograms", R. H. Ranger, <i>Proc. I.R.E.</i> (April) .....	1926
"Polarization of Radio Waves", E. F. W. Alexanderson, <i>Jour. A.I.E.E.</i> .....	1926
"Some Practical Aspects of Short-Wave Operations at High Power", H. E. Hallborg, <i>Proc. I.R.E.</i> (June) .....	1927
"Photoradio Developments", R. H. Ranger, <i>Proc. I.R.E.</i> (June) .....	1929
"Image Transmission by Radio Waves", A. N. Goldsmith, <i>Proc. I.R.E.</i> (September) .....	1929
"The Selection of Standards for Commercial Radio Television", J. Weinberger, T. A. Smith and G. Rodwin, <i>Proc. I.R.E.</i> (September) .....	1929
"Antennas", H. H. Beverage, Section of RADIO LIBRARY, International Textbook Co. ....	1928
"Mechanical Developments of Facsimile Equipment", R. H. Ranger, <i>Proc. I.R.E.</i> (September) .....	1929
"20-40 KW High-Frequency Transmitter", I. F. Byrnes and J. B. Coleman, <i>Proc. I.R.E.</i> (March) .....	1930
"Improving the Short Wave Receiver", Berthold Sheffield, <i>Radio News</i> (November) .....	1930
"Quartz Crystals In Radio Receiving Circuits", D. Grimes and W. S. Barden, <i>RCA Licensee Bulletin LB-113</i> (December 2) .....	1930
"Looking Ahead with Short Waves", A. N. Goldsmith, <i>Short-Wave Craft</i> (January) .....	1931
"Diversity Receiving System of RCA Communications, Inc. for Radiotelegraphy", H. H. Beverage and H. O. Peterson, <i>Proc. I.R.E.</i> (April) .....	1931
"Diversity Telephone Receiving System of R.C.A. Communications, Inc.", H. O. Peterson, H. H. Beverage and J. B. Moore, <i>Proc. I.R.E.</i> (April) .....	1931
"Application of Frequencies Above 30,000 kc to Communication Problems", H. H. Beverage, H. O. Peterson and C. W. Hansel, <i>Proc. I.R.E.</i> (August) .....	1931
"Development of Directive Transmitting Antennas by R.C.A. Communications, Inc.", P. S. Carter, C. W. Hansell and N. E. Lindenblad, <i>Proc. I.R.E.</i> (October) .....	1931
"Efficient System for Complete Modulation of Amateur Radio Transmitters", L. E. Barton, <i>QST</i> (November) .....	1931
"Mica Condensers in High-Frequency Circuits", I. G. Maloff, <i>Proc. I.R.E.</i> (April) .....	1932
"Circuit Relations in Radiating Systems and Applications to Antenna Problems", P. S. Carter, <i>Proc. I.R.E.</i> (June) .....	1932
"The Precision Frequency Measuring System of RCA Communications, Inc.", H. O. Peterson and A. M. Braaten, <i>Proc. I.R.E.</i> (June) .....	1932
"New Forms of Short Wave Tubes", I. E. Mourontseff, G. R. Kilgore, H. V. Noble, <i>Electronics</i> (September) .....	1932
"Magnetostatic Oscillators for Generation of Ultra Short Waves", G. R. Kilgore, <i>Proc. I.R.E.</i> (November) .....	1932
"Transoceanic Reception of High-Frequency Telephone Signals", R. M. Morris and W. A. R. Brown, <i>Proc. I.R.E.</i> (January) .....	1933
"Notes on Propagation of Waves Below Ten Meters in Length", B. Trevor and P. S. Carter, <i>Proc. I.R.E.</i> (March) .....	1933
"A Study of Propagation of Wavelengths Between 3 and 8 Meters", L. F. Jones, <i>Proc. I.R.E.</i> (March) .....	1933
"Tubes to Fit the Wavelength", B. J. Thompson, <i>Electronics</i> (August) .....	1933
"Super-Regeneration and Its Application to High-Frequency Reception", D. Grimes and W. S. Barden, <i>RCA Licensee Bulletin LB-267</i> (November 8) .....	1933

	Year
"Vacuum Tubes of Small Dimensions for Use at Extremely High Frequencies", B. J. Thompson and G. M. Rose, Jr., <i>Proc. I.R.E.</i> (December) .....	1933
"An Efficient C-W and Phone Transmitter Using the New Tubes and Circuits", L. C. Waller, <i>QST</i> (December) .....	1933
"Transoceanic Radio and Solar Activity", W. A. R. Brown, <i>Transactions of the American Geophysical Union</i> .....	1933
"The 150-Watt Mobile Transmitters", C. Dietsch, <i>Broad. Eng. Jour.</i> (January) .....	1933
"Transmission and Reception of Centimeter Waves", I. Wolff, E. G. Linder and R. A. Braden, <i>Proc. I.R.E.</i> (January) .....	1934
"Note on Paper Condensers in Short Wave Receivers", W. S. Barden, <i>RCA Licensee Bulletin LB-286</i> (April 27) .....	1934
"A Short Wave Coil Study", W. S. Barden, <i>RCA Licensee Bulletin LB-287</i> (April 27) .....	1934
"The Input Impedance of Vacuum Tubes", J. Yolles, <i>RCA Licensee Bulletin LB-290</i> (April 28) .....	1934
"Improved Magnetron Oscillator for the Generation of Microwaves", E. G. Linder, <i>Phys. Rev.</i> (May 1) .....	1934
"Notes on an Ionized Gas Modulator for Short Radio Waves", E. G. Linder and I. Wolff, <i>Proc. I.R.E.</i> (June) .....	1934
"Multi-Range Receiver Problems", M. Clay, <i>RCA Licensee Bulletin LB-292</i> (June 1) .....	1934
"The Double Doublet Antenna", W. Hollander Bohlke, <i>Radio News</i> (September) .....	1934
"Design and Use of 'Acorn' Tubes for Ultra-High Frequencies", B. Salzberg, <i>Electronics</i> (September) .....	1934
"The Radio-Relay Link for Television Signals", C. J. Young, <i>Proc. I.R.E.</i> (November) .....	1934
"An Electron Oscillator with Plane Electrodes", B. J. Thompson and P. D. Zottu, <i>Proc. I.R.E.</i> (December) .....	1934
"Transmission and Reception of Centimeter Waves", I. Wolff, E. G. Linder and R. A. Braden, <i>Proc. I.R.E.</i> (January) .....	1935
"A Method of Measuring Noise Levels on Short-Wave Radio-Telegraph Circuits", H. O. Peterson, <i>Proc. I.R.E.</i> (February) .....	1935
"New Antenna System for Operating Control of Radiation", J. L. Reinartz, <i>QST</i> (February) .....	1935
"A Review of Radio Communications in the Mobile Services", I. F. Byrnes, <i>Proc. I.R.E.</i> (May) .....	1935
"Notes on Propagation at a Wavelength of Seventy-three Centimeters", B. Trevor and R. W. George, <i>Proc. I.R.E.</i> (May) .....	1935
"Development of Transmitters for Frequencies Above 300 Megacycles", N. E. Lindenblad, <i>Proc. I.R.E.</i> (September) .....	1935
"Recent Developments in Miniature Tubes", B. Salzberg and D. G. Burnside, <i>Proc. I.R.E.</i> (October) .....	1935
"Crystal Control for Ultra Short Waves", Berthold Sheffield, <i>Electronics</i> (November) .....	1935
"Transmission of 9 CM Electro-Magnetic Waves", I. Wolff, <i>Broadcast News</i> (December) .....	1935
"Antennas", E. A. Laport, Section of RADIO ENGINEERS' HANDBOOK, Henney, McGraw-Hill Book Co., New York, N. Y. ....	1935
"Input Resistance of Vacuum Tubes as Ultra-High-Frequency Amplifiers", W. R. Ferris, <i>Proc. I.R.E.</i> (January) .....	1936
"Analysis of the Effects of Space Charge on Grid Impedance", D. O. North, <i>Proc. I.R.E.</i> (January) .....	1936
"A Detector Circuit for Reducing Noise Interference in Phone Reception", L. E. Thompson, <i>QST</i> (February) .....	1936
"Sun Spots and Short Waves", O. B. Hanson, <i>Today</i> (February 1) ..	1936
"A Turnstile Antenna for Use at Ultra-High Frequencies", G. H. Brown, <i>Electronics</i> (March) .....	1936
"Terrestrial Magnetism and Its Relation to World-Wide Short-Wave Communications", H. E. Hallborg, <i>Proc. I.R.E.</i> (March) .....	1936

	Year
"Ultra-High-Frequency Receiver Considerations", S. W. Seeley, <i>RCA Licensee Bulletin LB-350</i> (March 9) .....	1936
"Frequency Control by Low Power Factor Line Circuits", C. W. Hansell and P. S. Carter, <i>Proc. I.R.E.</i> (April) .....	1936
"Description and Characteristics of the End-Plate Magnetron", E. G. Linder, <i>Proc. I.R.E.</i> (April) .....	1936
"A Quarter Kilowatt on Four Bands, Rapid QSY", L. R. Moffett, <i>Radio</i> (May) .....	1936
"An Urban Field Strength Survey at 30 and 100 Mc", R. S. Holmes and A. H. Turner, <i>Proc. I.R.E.</i> (May) .....	1936
"Ultra-High-Frequency Bands for All-Wave Receivers", H. B. Deal, <i>RCA Licensee Bulletin LB-360</i> (May 19) .....	1936
"Frequency Modulation Propagation Characteristics", M. G. Crosby, <i>Proc. I.R.E.</i> (June) .....	1936
TELEVISION, Vol. I, RCA Institutes Technical Press, New York, N. Y. (July) .....	1936
"The New York-Philadelphia Ultra-High-Frequency Facsimile-Relay System", H. H. Beverage, <i>RCA REVIEW</i> (July) .....	1936
"Micro-Waves in NBC Remote Pickups", R. M. Morris, <i>RCA REVIEW</i> (July) .....	1936
"Magnetron Oscillators for the Generation of Frequencies Between 300 and 600 Megacycles", G. R. Kilgore, <i>Proc. I.R.E.</i> (August) .....	1936
"Ultra-High-Frequency Transmission Between RCA Building and Empire State Building in New York City", P. S. Carter and G. S. Wickizer, <i>Proc. I.R.E.</i> (August) .....	1936
"Electrical Measurements at Wavelengths Less than Two Meters", L. S. Nergaard, <i>Proc. I.R.E.</i> (September) .....	1936
"Fade-Out Observations at Riverhead, N. Y.", A. M. Braaten, <i>The T. &amp; R. Bulletin (Brit.)</i> (September) .....	1936
"Harbor Telephone Service", I. F. Byrnes, <i>RCA REVIEW</i> (October) .....	1936
"Television Radio Relay", B. Trevor and O. E. Dow, <i>RCA REVIEW</i> (October) .....	1936
"5-Meter Crystal Controlled Push-Pull 800 Output", J. L. Reinartz, <i>QST</i> (October) .....	1936
"Multitube Oscillators for the Ultra-High-Frequencies", P. D. Zottu, <i>QST</i> (October) .....	1936
"A Study of the Characteristics of Noise", V. D. Landon, <i>Proc. I.R.E.</i> (November) .....	1936
THE ULTRA-HIGH FREQUENCY DOMAIN, A. N. Goldsmith, University of Chicago Press, Chicago, Ill. ....	1936
"Fixed Services Above 30,000 Kc", C. B. Jolliffe, Statements Made by RCA before FCC .....	1936
"Some Notes on Ultra-High-Frequency Propagation", H. H. Beverage, <i>RCA REVIEW</i> (January) .....	1937
"Directional Antennas", G. H. Brown, <i>Proc. I.R.E.</i> (January) .....	1937
<i>Broadcast News</i> (June) .....	1937
"Frequency Assignments for Television", E. W. Engstrom and C. M. Burrill, <i>RCA REVIEW</i> (January) .....	1937
"Reply to C. R. Burrow's Discussion on 'An Urban Field Strength Survey at 30 and 100 Mc'", R. S. Holmes and A. H. Turner, <i>Proc. I.R.E.</i> (January) .....	1937
"A Coupling System for Rod Antennas", D. E. Foster and G. Mountjoy, <i>RCA Licensee Bulletin LB-387</i> (February 16) .....	1937
"UHF Diode with Movable Anode", Berthold Sheffield, <i>Electronics</i> (March) .....	1937
"Frequency Modulation Noise Characteristics", M. G. Crosby, <i>Proc. I.R.E.</i> (April) .....	1937
"Some Problems of Aviation Radio", F. X. Rettenmeyer, <i>RCA REVIEW</i> (April) .....	1937
"A New Method of Measurement of Ultra-High-Frequency Impedance", S. W. Seeley and W. S. Barden, <i>RCA Licensee Bulletin LB-392</i> (April 27) .....	1937

	Year
"Determination of the Radiating System which will Produce a Specified Directional Characteristic", I. Wolff, <i>Proc. I.R.E.</i> (May).....	1937
"The Ultra-High-Frequency Domain", A. N. Goldsmith, <i>Elec. Eng.</i> (June) .....	1937
"Recent Developments in Diversity Receiving Equipment", J. B. Moore, <i>RCA REVIEW</i> (July) .....	1937
"Television Transmitters Operating at High Power and Ultra-High Frequencies", J. W. Conklin and H. E. Gihring, <i>RCA REVIEW</i> (July) .....	1937
TELEVISION, Vol. II, RCA Institutes Technical Press, New York, N. Y. (October) .....	1937
"The Magnetron as a High-Frequency Generator", G. R. Kilgore, <i>Jour. Appl. Phys.</i> (October) .....	1937
"A Novel Relay Broadcast Mobile Unit", M. W. Rife, <i>RCA REVIEW</i> (October) .....	1937
"Televsual Use of Ultra-High Frequencies", A. N. Goldsmith, TELEVISION, Vol. II (October) .....	1937
"Some Notes on Ultra-High-Frequency Propagation", H. H. Beverage, TELEVISION, Vol. II (October) .....	1937
"The Requirements and Performance of a New Ultra-High-Frequency Power Tube", W. G. Wagener, <i>RCA REVIEW</i> (October) .....	1937
"Field Strength Observations of Transatlantic Signals, 40 to 45 Megacycles", H. O. Peterson and D. R. Goddard, <i>RCA REVIEW</i> (October) .....	1937
<i>Proc. I.R.E.</i> (October) .....	1937
"On the Optimum Length for Transmission Lines Used as Circuit Elements", B. Salzberg, <i>Proc. I.R.E.</i> (December) .....	1937
"A Compact 56 Mc Portable-Mobile Transmitter Receiver", H. C. Lawrence, Jr., <i>QST</i> (December) .....	1937
"Effects of Space Charge in the Grid-Anode Region of Vacuum Tubes", A. V. Haefl and B. Salzberg, <i>RCA REVIEW</i> (January) .....	1938
"Time-Division Multiplex in Radiotelegraphic Practice", R. E. Mathes, J. L. Callahan and A. Kahn, <i>Proc. I.R.E.</i> (January) .....	1938
"Oscillator Frequency Stability in Relation to Receivers with Spread Short Wave Bands", D. E. Foster, <i>RCA Licensee Bulletin LB-418</i> (January 8) .....	1938
"High Fidelity Broadcasting at Ultra-High-Frequencies", E. W. Herold, <i>Proc. I.R.E.</i> (March) .....	1938
"Excess Energy Electrons and Electron Motion in High Vacuum Tubes", E. G. Linder, <i>Proc. I.R.E.</i> (March) .....	1938
"Putting the Harmonic Generator to Work", J. L. Reinartz, <i>QST</i> (April) .....	1938
"A Rotatable Mast for Beam Antennas", W. van B. Roberts, <i>Radio</i> (April) .....	1938
"The Developmental Problems and Operating Characteristics of Two New Ultra-High-Frequency Triodes", W. G. Wagener, <i>Proc. I.R.E.</i> (April) .....	1938
"Equipment and Methods Developed for Broadcast Facsimile Service", C. J. Young, <i>RCA REVIEW</i> (April) .....	1938
"Facsimile Broadcasting", D. E. Foster, <i>RCA Licensee Bulletin LB-426</i> (April 25) .....	1938
"Effect of High-Energy Electron Random Motion Upon the Shape of the Magnetron Cut-off Curve", E. G. Linder, <i>Jour. Appl. Phys.</i> (May) .....	1938
"The NBC Type ND-32 UHF Cue Receiver", <i>NBC Eng. Notice (Apparatus) No. 10</i> (June 10) .....	1938
"The NBC Type ND-31 UHF Pack Transmitter", <i>NBC Eng. Notice (Apparatus) No. 11</i> (June 10) .....	1938
"The NBC Type ND-20 UHF Portable Transmitter", <i>NBC Eng. Notice (Apparatus) No. 12</i> (June 10) .....	1938
"Photoradio Transmission of Pictures", H. Shore, <i>RCA REVIEW</i> (July) .....	1938

	Year
"The Relation Between Radio-Transmission Path and Magnetic-Storm Effects", G. W. Kenrick, A. M. Braaten and J. General, <i>Proc. I.R.E.</i> (July) .....	1938
"Carrier and Side-Frequency Relations With Multitone Frequency or Phase Modulation", M. G. Crosby, <i>RCA REVIEW</i> (July) .....	1938
"Phase Shift Measurement", A. A. Barco, <i>RCA Licensee Bulletin LB-442</i> (August 16) .....	1938
RADIO FACSIMILE, Vol. I, RCA Institutes Technical Press, New York, N. Y. (October) .....	1938
"Review of Ultra-High-Frequency Vacuum-Tube Problems", B. J. Thompson, <i>RCA REVIEW</i> (October) .....	1938
"Selective Side-Band Versus Double-Side-Band Transmission of Telegraph and Facsimile Signals", B. Trevor, J. E. Smith and P. S. Carter, <i>RCA REVIEW</i> (October) .....	1938
"A Survey of Ultra-High-Frequency Measurements", L. S. Nergaard, <i>RCA REVIEW</i> (October) .....	1938
"Propagation Requirements for Facsimile", R. E. Mathes and J. E. Smith, RADIO FACSIMILE, Vol. I (October) .....	1938
"A Narrative Bibliography of Radio Facsimile", J. L. Callahan, RADIO FACSIMILE, Vol. I (October) .....	1938
"Tape Facsimile: Historical and Descriptive Note", C. J. Young, RADIO FACSIMILE, Vol. I (October) .....	1938
"U-H-F Equipment for Relay Broadcasting", W. A. R. Brown, <i>RCA REVIEW</i> (October) .....	1938
"Photoradio Apparatus and Operating Technique Improvements", J. L. Callahan, J. N. Whitaker and Henry Shore, RADIO FACSIMILE, Vol. I (October) .....	1938
"Practical Application of an Ultra-High-Frequency Radio-Relay Circuit", J. E. Smith, F. H. Kroger and R. W. George, <i>Proc. I.R.E.</i> (November) .....	1938
"A Study of Ultra-High-Frequency Wide-Band Propagation Characteristics", R. W. George, <i>Proc. I.R.E.</i> (January) .....	1939
"Analysis and Design of Video Amplifiers—Part II", S. W. Seeley and C. N. Kimball, <i>RCA REVIEW</i> (January) .....	1939
"Charts for Transmission-Line Measurements and Computations", P. S. Carter, <i>RCA REVIEW</i> (January) .....	1939
"Construction and Alignment of Television Receiver", C. C. Shumard, <i>QST</i> (January) .....	1939
"New Television Amplifier Receiving Tubes", A. P. Kauzmann, <i>RCA REVIEW</i> (January) .....	1939
"Observations on Sky-Wave Transmission on Frequencies Above 40 Megacycles", D. R. Goddard, <i>Proc. I.R.E.</i> (January) .....	1939
<i>RCA REVIEW</i> (January) .....	1939
"Recent Developments in Radio Transmitters", J. B. Coleman and V. E. Trouant, <i>RCA REVIEW</i> (January) .....	1939
"Input Loading of Receiving Tubes at Radio Frequencies", <i>RCA Tube Dept. Applic. Note No. 101</i> (January 25) .....	1939
"An Ultra-High-Frequency Power Amplifier of Novel Design", A. V. Haeff, <i>Electronics</i> (February) .....	1939
"Communication by Phase Modulation", M. G. Crosby, <i>Proc. I.R.E.</i> (February) .....	1939
"Transmitter Circuit Design for Frequencies Above 100 Mc", O. E. Dow, <i>Proc. Rad. Club Amer.</i> (March) .....	1939
"Wide-Band Variable-Frequency Testing Transmitters", G. L. Usselman, <i>RCA REVIEW</i> (April) .....	1939
"Antennas", H. H. Beverage, <i>Radio and Tele.</i> (April) .....	1939
<i>RCA REVIEW</i> (July) .....	1939
"Field Strength Measuring Equipment for Wide-Band U-H-F Transmission", R. W. George, <i>RCA REVIEW</i> (April) .....	1939
"Measurements of Admittances at Ultra-High Frequencies", J. M. Miller and B. Salzberg, <i>RCA REVIEW</i> (April) .....	1939

	Year
"Television Transmitting Antenna for Empire State Building", N. E. Lindenblad, <i>RCA REVIEW</i> (April) .....	1939
"Directional Antennas", G. H. Brown, <i>Broadcast News</i> (May) .....	1939
"Radio Frequency Generator for Television Receiver Testing", A. H. Turner, <i>RMA Eng.</i> (May) .....	1939
"A Push-Pull Ultra-High-Frequency Beam Tetrode", A. K. Wing, <i>RCA REVIEW</i> (July) .....	1939
<i>Radio Tech. Digest</i> (November, December) .....	1939
"Effect of Electron Transit Time on Efficiency of a Power Amplifier", A. V. Haeff, <i>RCA REVIEW</i> (July) .....	1939
"The Use of Gas-Filled Lamps as High-Dissipation, High-Frequency Resistors, Especially for Power Measurements", Ernest G. Linder, <i>RCA REVIEW</i> (July) .....	1939
"Notes on the Random Fading of 50-Megacycle Signals Over Non-optical Paths", K. G. MacLean and G. S. Wickizer, <i>Proc. I.R.E.</i> (August) .....	1939
"Resonant Impedance of Transmission Lines", B. Salzberg and L. S. Nergaard, <i>Proc. I.R.E.</i> (September) .....	1939
"Ultra-High-Frequency Propagation", M. Katzin, <i>Proc. Rad. Club Amer.</i> (September) .....	1939
"A Theoretical Analysis of Single Side-Band Operation of Television Transmitters", L. S. Nergaard, <i>Proc. I.R.E.</i> (October) .....	1939
"Simple Television Antennas", P. S. Carter, <i>RCA REVIEW</i> (October) .....	1939
"Radio in Navigation", C. D. Tuska, <i>Jour. Frank. Inst.</i> (October, November) .....	1939
"Ultra-High-Frequency Propagation Formulas", H. O. Peterson, <i>RCA REVIEW</i> (October) .....	1939
"Radio Facsimile by Subcarrier Frequency Modulation", J. N. Whitaker and R. E. Mathes, <i>RCA REVIEW</i> (October) .....	1939
"The Anode-Tank-Circuit Magnetron", Ernest G. Linder, <i>Proc. I.R.E.</i> (November) .....	1939
"Transatlantic Reception of London Television Signals", D. R. Goddard, <i>Proc. I.R.E.</i> (November) .....	1939
"Note on Early Fade-Out Investigations", Arthur M. Braaten, <i>Terrestrial Magnetism and Atmospheric Electricity</i> (December) .....	1939
"Application of the Abelian Finite Group Theory to Electromagnetic Refraction", K. A. Whiteman, <i>RCA REVIEW</i> (January) .....	1940
"The Service Range of Frequency Modulation", M. G. Crosby, <i>RCA REVIEW</i> (January) .....	1940
"Television Reception in an Airplane", R. S. Holmes, <i>RCA REVIEW</i> (January) .....	1940
"Frequency Modulation", S. W. Seeley, <i>RCA Licensee Bulletin LB-505</i> (January 19) .....	1940
"A Cathode Ray Frequency Modulation Generator", Robert E. Shelby, <i>Electronics</i> (February) .....	1940
"Directional Antenna Gain Chart", W. S. Duttera, <i>Electronics</i> (February) .....	1940
"Propagation of Ultra-High Frequency Waves", D. E. Foster, <i>RCA Licensee Bulletin LB-509</i> (February 15) .....	1940
"Sound Broadcasting on Ultra-High Frequencies with Special Reference to Frequency Modulation", A. F. Van Dyck, <i>RCA Licensee Bulletin LB-518</i> (March 14) .....	1940
"The Limits of Inherent Frequency Stability", W. Van B. Roberts, <i>RCA REVIEW</i> (April) .....	1940
"Mobile Field Strength Recordings of 49.5, 83.5, and 142 Mc from Empire State Building, New York—Horizontal and Vertical Polarization", G. S. Wickizer, <i>RCA REVIEW</i> (April) .....	1940
"Motorboat Ship-Shore Radiocommunication System", H. B. Martin, <i>Proc. Rad. Club Amer.</i> (April) .....	1940
"A Method of Measuring Frequency Deviation", M. G. Crosby, <i>RCA REVIEW</i> (April) .....	1940

	Year
"Selective Sideband Transmission in Television", R. D. Kell and G. L. Fredendall, <i>RCA REVIEW</i> (April) .....	1940
RADIO AT ULTRA-HIGH FREQUENCIES, Vol. I, RCA Institutes Technical Press, New York, N. Y. (April) .....	1940
"A New Method for Measurement of Ultra-High-Frequency Impedance", Stuart W. Seeley and William S. Barden, RADIO AT ULTRA-HIGH FREQUENCIES, Vol. I (April) .....	1940
"Simple Antennas and Receiver Input Circuits for Ultra-High Frequencies", R. S. Holmes and A. H. Turner, RADIO AT ULTRA-HIGH FREQUENCIES, Vol. I (April) .....	1940
"A Compact 112-Mc. Station", H. C. Lawrence, Jr., <i>QST</i> (May) .....	1940
"Antennas and Transmission Lines at the Empire State Building", Nils E. Lindenblad, <i>Communications</i> (May) .....	1940
(April, May) .....	1941
"Direction Finding on 1.67-meter Waves", Luke C. L. Yuan, <i>Science</i> (May) .....	1940
"U.H.F. Oscillator Frequency Stability Considerations", S. W. Seeley and E. I. Anderson, <i>RCA Licensee Bulletin LB-524</i> (May 6) .....	1940
"A 500-Megacycle Radio-Relay Distribution System for Television", F. H. Kroger, B. Trevor, and J. E. Smith, <i>RCA REVIEW</i> (July) .....	1940
"An Efficient U.H.F. Unit for the Amateur Television Transmitter", L. C. Waller, <i>QST</i> (July) .....	1940
"An Ultra-High-Frequency Antenna of Simple Construction", G. H. Brown and J. Epstein, <i>Communications</i> (July) .....	1940
"Field Strength Measuring Equipment at 500 Megacycles", R. W. George, <i>RCA REVIEW</i> (July) .....	1940
"Field-Strength Survey, 52.75 Megacycles from Empire State Building", G. S. Wickizer, <i>Proc. I.R.E.</i> (July) .....	1940
"Measurements of Frequency Modulated Field Intensity", B. W. Robins, <i>Broadcast News</i> (July) .....	1940
"Ultra-High-Frequency Propagation Through Woods and Underbrush", Bertram Trevor, <i>RCA REVIEW</i> (July) .....	1940
"U-II-F Oscillator Stability Considerations", E. I. Anderson, S. W. Seeley, and W. Stuart, <i>RCA REVIEW</i> (July) .....	1940
"Compact U.H.F. Antennas", D. E. Foster and A. E. Newlon, <i>RCA Licensee Bulletin LB-530</i> (July 10) .....	1940
"An Ultra-High-Frequency Superheterodyne Receiver for Direction Finding", Luke C. L. Yuan and C. E. Miller, <i>Rev. Sci. Instr.</i> (September) .....	1940
"Field Strength of Motor Car Ignition Between 40 and 450 Megacycles", R. W. George, <i>Proc. I.R.E.</i> (September) .....	1940
"NBC Frequency-Modulation Field Test", R. M. Morris and R. F. Guy, <i>RCA REVIEW</i> (October) .....	1940
<i>Radio</i> (January) .....	1941
"Vertical vs. Horizontal Polarization", G. H. Brown, <i>Electronics</i> (October) .....	1940
"Input Connections for U.H.F. Measurements", J. A. Rankin, <i>RCA Licensee Bulletin LB-537</i> (October 9) .....	1940
"More About Horizon Distances", A. M. Braaten, <i>T and R Bulletin (Brit.)</i> (December) .....	1940
"The RCA Miniature Tubes", <i>RCA Tube Dept. Applic. Note No. 106</i> .....	1940
"A New Ultra-High Frequency Tetrode and Its Use in a One Kilowatt Television Sound Transmitter", A. K. Wing and F. E. Young, <i>Proc. I.R.E.</i> (January) .....	1941
"A Transmitter for Frequency Modulated Broadcast Service Using a New Ultra-High-Frequency Tetrode", A. K. Wing and J. E. Young, <i>RCA REVIEW</i> (January) .....	1941
"A Vestigial Side-Band Filter for Use With a Television Transmitter", G. H. Brown, <i>RCA REVIEW</i> (January) .....	1941
"Impulse Noise in FM Reception", V. D. Landon, <i>Electronics</i> (February) .....	1941



Year

"The Distribution of Amplitude with Time in Fluctuation Noise", V. D. Landon, *Proc. I.R.E.* (February) ..... 1941

"A New Series of Insulators for Ultra-High-Frequency Tubes", L. R. Shardlow, *RCA REVIEW* (April) ..... 1941

"Short Wave Radio Transmission and Geomagnetism", H. E. Hallborg, *RCA REVIEW* (April) ..... 1941

"Water-cooled Resistors for Ultra-High Frequencies", G. H. Brown and J. W. Conklin, *Electronics* (April) ..... 1941

"Correlations of Short Wave Radio Transmission Across Atlantic with Magnetic Conditions", H. E. Hallborg, *Proc. Amer. Phil. Soc.* (May) ..... 1941

"Measurement of Iron Cores at Radio Frequencies", D. E. Foster and A. E. Newlon, *Proc. I.R.E.* (May) ..... 1941

"An Omnidirectional Radio Range System", David G. C. Luck, *RCA REVIEW* (July) ..... 1941

"Duplex Transmission of Frequency-Modulated Sound and Facsimile", D. E. Foster and Maurice Artzt, *RCA REVIEW* (July) ..... 1941

"NBC Short-Wave Listening Post", G. O. Milne, *RCA REVIEW* (July) ..... 1941

"Applications of the Inductive Output Tube", O. E. Dow, *Proc. Rad. Club Amer.* (August) ..... 1941

"A Simplified Television System for the Radio Amateur and Experimenter", L. C. Waller and P. A. Richards, *RCA REVIEW* (October) ..... 1941

"Narrow Band FM Police Receiver", H. E. Thomas, *RCA REVIEW* (October) ..... 1941

"Behavior of Electron Multipliers as a Function of Frequency", L. Malter, *Proc. I.R.E.* (November) ..... 1941

"The Orbital-Beam Secondary-Electron Multiplier for Ultra-High Frequency Amplification", H. M. Wagner and W. R. Ferris, *Proc. I.R.E.* (November) ..... 1941

"Voltage-Controlled Electron Multipliers", B. J. Thompson, *Proc. I.R.E.* (November) ..... 1941

"An Analysis of the Signal-to-Noise Ratio of U-H-F Receivers", E. W. Herold, *RCA REVIEW* (January) ..... 1942

"An Omnidirectional Radio Range System—Part II", David G. C. Luck, *RCA REVIEW* (January) ..... 1942

"Radiating System for 75-Mc. Cone-of-Silence Marker", E. A. Laport and James B. Knox, *Proc. I.R.E.* (January) ..... 1942

"The Absolute Sensitivity of Radio Receivers", D. O. North, *RCA REVIEW* (January) ..... 1942

"The Design and Development of Three New Ultra-High-Frequency Transmitting Tubes", C. E. Haller, *Proc. I.R.E.* (January) ..... 1942

"Impedance Determinations of Eccentric Lines", G. H. Brown, *Electronics* (February) ..... 1942

"Receiver Input Connections for U-H-F Measurements", J. Rankin, *RCA REVIEW* (April) ..... 1942

"Ultra-High Frequency and Frequency Modulation", A. F. Van Dyck, *RCA License Bulletin LB-595* (August) ..... 1942

"Discussion on 'The Distribution of Amplitude with Time in Fluctuation Noises'", V. D. Landon, *Proc. I.R.E.* (September) ..... 1942

"Attenuation of Electromagnetic Fields in Pipes Smaller Than The Critical Size", E. G. Linder, *Proc. I.R.E.* (December) ..... 1942

"Direct-Reading Wattmeters for Use at Radio Frequencies", G. H. Brown, J. Epstein and D. W. Peterson, *Proc. I.R.E.* (August) .... 1943

"FM and UHF", R. F. Guy, *Communications* (August) ..... 1943

"Practical Analysis of Ultra-High Frequency", J. R. Meagher and H. J. Markley, Booklet, RCA Service Co., Inc., Camden, N. J. (August) ..... 1943

"Some Aspects of Radio Reception at U-H-F, Part I—Antenna and Receiver Input Circuits", E. W. Herold and L. Malter, *Proc. I.R.E.* (August) ..... 1943

	Year
"Use of Subcarrier Frequency Modulation in Communication Systems", W. H. Bliss, <i>Proc. I.R.E.</i> (August) .....	1943
"Some Aspects of Radio Reception at U-H-F, Part II—Admittances and Fluctuation Noise of Tubes and Circuits", E. W. Herold and L. Malter, <i>Proc. I.R.E.</i> (September) .....	1943
"Some Aspects of Radio Reception at U-H-F, Part III—Signal-to-Noise Ratio of Radio Receivers", E. W. Herold and L. Malter, <i>Proc. I.R.E.</i> (September) .....	1943
"Ultrashort Electromagnetic Waves, Part VI—Reception", B. Trevor, <i>Elec. Eng.</i> (September) .....	1943
"Characteristics of Resonant Transmission Lines", J. B. Epperson, <i>Electronics</i> (October) .....	1943
"Some Aspects of Radio Reception at U-H-F, Part IV—General Superheterodyne Considerations at U-H-F", E. W. Herold and L. Malter, <i>Proc. I.R.E.</i> (October) .....	1943
"Some Aspects of Radio Reception at U-H-F, Part V—Frequency Mixing in Diodes", E. W. Herold and L. Malter, <i>Proc. I.R.E.</i> (October) .....	1943
"The ND-28 (The 'Beer Mug' Miniature UHF Transmitter)", <i>NBC Eng. Notice (Apparatus) No. 5</i> (November 15) .....	1943
"The ND-25 UHF Program Receiver", <i>NBC Eng. Notice (Apparatus) No. 7</i> (November 15) .....	1943
"Antenna Arrays Around Cylinders", P. S. Carter, <i>Proc. I.R.E.</i> (December) .....	1943
"Television? FM? Facsimile?", O. B. Hanson, Pamphlet, National Broadcasting Co., Inc., New York, N. Y. (December) .....	1943
"Sunspots and Radio", H. E. Hallborg, <i>Radio Craft</i> (January) .....	1944
"Grounded-Grid Radio-Frequency Voltage Amplifiers", M. C. Jones, <i>Proc. I.R.E.</i> (July) .....	1944
"Coverage Curves for FM Antennas", R. D. Duncan, Jr., <i>Broadcast News</i> (August) .....	1944
"Sun, Earth and Short Wave Propagation", H. E. Hallborg, <i>Proc. Rad. Club Amer.</i> (December) .....	1944
"Television Coverage Curves For Turnstile Antennas", R. D. Duncan, Jr., <i>Broadcast News</i> (January) .....	1945
"The Use of Radio Frequencies to Obtain High Power Concentrations for Industrial Heating Applications", W. M. Roberds, <i>Proc. I.R.E.</i> (January) .....	1945
"Radio Relay Systems Development by the Radio Corporation of America", C. W. Hansell, <i>Proc. I.R.E.</i> (March) .....	1945
"Experimentally Determined Impedance Characteristics of Cylindrical Antennas", G. H. Brown and O. M. Woodward, Jr., <i>Proc. I.R.E.</i> (April) .....	1945
"Radio Relay Systems Development", C. W. Hansell, <i>Proc. Nat. Elec. Conf.</i> (May 15) .....	1945
"Wave Guides and the Special Theory of Relativity", W. D. Hersberger, <i>Jour. Appl. Phys.</i> (August) .....	1945
"Artificial Antenna", S. Wald, <i>Electronics</i> (November) .....	1945
"Range Prediction Chart for FM Stations", F. C. Everett, <i>Communications</i> (November) .....	1945
"Frequency-Modulation Distortion Caused By Multipath Transmission", M. S. Corrington, <i>Proc. I.R.E.</i> (December) .....	1945
"High Output Transmitter-Receiver", B. W. Southwell, <i>CQ</i> (January) .....	1946
"RCA Micro-Wave Relay System", H. F. Mickel, <i>Broadcast News</i> (January) .....	1946
"The Grounded-Grid Amplifier", C. J. Starnier, <i>Broadcast News</i> (January) .....	1946
"The Super Turnstile Antenna", R. W. Masters, <i>Broadcast News</i> (January) .....	1946
"Radio-Frequency Resistors as Uniform Transmission Lines", D. R. Crosby and C. H. Pennypacker, <i>Proc. I.R.E.</i> (February) .....	1946
"RCA Time-Division Multiplex", R. Hutchens, <i>Relay</i> (February) .....	1946

	Year
"The Teleran Proposal", P. J. Herbst, I. Wolff, D. Ewing, and L. F. Jones, <i>Electronics</i> (February) .....	1946
"Transmission of Television Sound on the Picture Carrier", G. L. Fredendall, K. Schlesinger, and A. C. Schroeder, <i>Proc. I.R.E.</i> (February) .....	1946
"An Omnidirectional Radio Range System—Part III", D. G. C. Luck, <i>RCA REVIEW</i> (March) .....	1946
"Induction Heating in Radio Electron-Tube Manufacture", E. E. Spitzer, <i>Proc. I.R.E.</i> (March) .....	1946
"Local Oscillator Radiation and Its Effect on Television Picture Contrast", E. W. Herold, <i>RCA REVIEW</i> (March) .....	1946
"Merchant Marine Radar", I. F. Byrnes, <i>RCA REVIEW</i> (March) ..	1946
"Frequency Converter Considerations at 100 Mc.", H. A. Finke, and A. A. Barco, <i>RCA Licensee Bulletin LB-665</i> (March 25) .....	1946
"Grounded-Grid Power Amplifiers", E. E. Spitzer, <i>Electronics</i> (April) .....	1946
"Shoran Precision Radar", S. W. Seeley, <i>Electronics</i> (April) .....	1946
"Shoran Precision Radar", S. W. Seeley, <i>Elec. Eng.</i> (April) .....	1946
"Super Turnstile Antenna", R. F. Holtz, <i>Communications</i> (April) ..	1946
"Radar Aids to Navigation—Loran, Teleran, Television", I. Wolff, <i>Princeton Eng.</i> (May) .....	1946
"Resonant-Cavity Measurements", R. L. Sproull and E. G. Linder, <i>Proc. I.R.E.</i> (May) .....	1946
"A Multi-Channel VHF (Radio Communications Systems)", J. B. Knox and C. H. Brereton, <i>RCA REVIEW</i> (June) .....	1946
"An Experimental Color Television System", R. D. Kell, G. L. Fredendall, A. C. Schroeder, and R. C. Webb, <i>RCA REVIEW</i> (June) ..	1946
"Development of an Ultra Low Loss Transmission Line for Television", E. O. Johnson, <i>RCA REVIEW</i> (June) .....	1946
"Development of Pulse Triodes and Circuit to Give One Megawatt at 600 Megacycles", R. R. Law, D. G. Burnside, R. P. Stone, and W. B. Whalley, <i>RCA REVIEW</i> (June) .....	1946
"FM Field Survey Techniques", P. B. Laeser, <i>Broadcast News</i> (June) ..	1946
"Frequency Modulation Mobile Radiotelephone Services", H. B. Martin, <i>RCA REVIEW</i> (June) .....	1946
"Pulse Communication", C. W. Hansell, <i>Electronics</i> (June) .....	1946
"Radar Aids to Air Navigation", I. Wolff, <i>RCA Lab. News</i> (June) ..	1946
"The Absorption of Microwaves by Gases", W. D. Hershberger, <i>Jour. Appl. Phys.</i> (June) .....	1946
"Problems in the Design of High-Frequency Heating Equipment", W. M. Roberds, <i>Proc. I.R.E.</i> (July) .....	1946
"Canada's New Short Wave Transmitters", H. B. Seabrook and F. R. Quance, <i>Electronic Ind.</i> (July) .....	1946
"New RCA 160 MC Mobile and Fixed Station EQT", R. W. Obenour, <i>Calling All Chiefs</i> (July) .....	1946
"Micro-Wave Television Relays, Operating on 6,800 to 7,050 Mc.", W. J. Poch and J. P. Taylor, <i>FM and Tele.</i> (August) .....	1946
"Rotating Joints for U.H.F. Transmission Lines", Tom Gooteé, <i>Radio News</i> (September) .....	1946
"Thermal and Acoustic Effects Attending the Absorption of Microwaves by Gases", W. D. Hershberger, E. T. Bush and G. W. Leck, <i>RCA REVIEW</i> (September) .....	1946
"Characteristics of the Pylon FM Antenna", R. F. Holtz, <i>FM and Tele.</i> (September) .....	1946
"Miniature Airborne Television Equipment", R. D. Kell and G. C. Sziklai, <i>RCA REVIEW</i> (September) .....	1946
"Development of Radio Relay Systems", C. W. Hansell, <i>RCA REVIEW</i> (September) .....	1946
"A 100-KW Portable Radar Transmitter", H. C. Lawrence, <i>Communications</i> (September) .....	1946
"Wave-Guide Output Magnetrons with Quartz Transformers", L. Malter and J. L. Moll, <i>RCA REVIEW</i> (September) .....	1946

	Year
"Naval Airborne Television Reconnaissance System", R. E. Shelby, F. J. Somers and L. R. Moffett, <i>RCA REVIEW</i> (September) . . . .	1946
"Absorption of Microwaves by Gases, II", J. E. Walter and W. D. Hershberger, <i>Jour. Appl. Phys.</i> (October) . . . . .	1946
"And Now the 'Pylon' Antenna", R. F. Holtz, <i>Broadcast News</i> (October) . . . . .	1946
"Microwave Equipment for Television Relay Service", W. J. Poch and J. P. Taylor, <i>Broadcast News</i> (October) . . . . .	1946
"Grounded-Grid Power Amplifiers", E. E. Spitzer, <i>Broadcast News</i> (October) . . . . .	1946
"Electromagnetic Horns and Parabolic Reflectors", T. Goot�e, <i>Radio News</i> (November) . . . . .	1946
"The RCA Antennalyzer—An Instrument Useful in the Design of Directional Antenna Systems", G. H. Brown and W. C. Morrison, <i>Proc. I.R.E.</i> (December) . . . . .	1946
"Frequency Modulation Distortion Caused by Common- and Adjacent-Channel Interference", M. S. Corrington, <i>RCA REVIEW</i> (December) . . . . .	1946
"Teloran", D. H. Ewing and R. W. K. Smith, <i>RCA REVIEW</i> (December) <i>Proc. Nat'l Elec. Conf.</i> . . . . .	1946
"A Microwave Relay Communication System", G. G. Gerlach, <i>RCA REVIEW</i> (December) <i>Proc. Nat'l Elec. Conf.</i> . . . . .	1946
"Mica Windows as Elements in Microwave Systems", L. Malter, R. L. Jepsen, and L. R. Bloom, <i>RCA REVIEW</i> (December) . . . . .	1946
"Simultaneous All Electronic Color Television", <i>RCA REVIEW</i> (December) . . . . .	1946
"A Microwave Relay System", L. E. Thompson, <i>Proc. I.R.E.</i> , (December) . . . . .	1946
"Television Equipment for Aircraft", M. A. Trainer and W. J. Poch, <i>RCA REVIEW</i> (December) . . . . .	1946
"Pulse Time Division Radio Relay", B. Trevor, O. E. Dow, and W. D. Houghton, <i>RCA REVIEW</i> (December) . . . . .	1946
RADAR—WHAT RADAR IS AND HOW IT WORKS, O. E. Dunlap, Jr., Harper and Bros.—New York . . . . .	1946
"Military Television", George M. K. Baker, <i>TELEVISION</i> , Volume IV (January) . . . . .	1947
"Multi-Channel Radiotelephone for Inland Waterways", G. G. Bradley, <i>Tele-Tech</i> (January) . . . . .	1947
<i>TELEVISION</i> , Volume III (1938-1941), <i>RCA REVIEW</i> , RCA Laboratories Division, Princeton, N. J. (January) . . . . .	1947
<i>TELEVISION</i> , Volume IV (1942-1946), <i>RCA REVIEW</i> , RCA Laboratories Division, Princeton, N. J. (January) . . . . .	1947
"A Coaxial-Line Diode Noise Source for U-II-F", H. Johnson, <i>RCA REVIEW</i> (March) . . . . .	1947
"Excess Noise in Cavity Magnetrons", R. L. Sproull, <i>Jour. Appl. Phys.</i> (March) . . . . .	1947
"The Maximum Efficiency of Reflex-Klystron Oscillators", E. G. Linder and R. L. Sproull, <i>Proc. I.R.E.</i> (March) . . . . .	1947
"The Pocket Ear", J. L. Hathaway and W. Hotine, <i>RCA REVIEW</i> (March) . . . . .	1947
<b>THEORY AND APPLICATION OF RADIO-FREQUENCY HEATING</b> , G. H. Brown, C. N. Hoyer and R. A. Bierwirth, D. Van Nostrand Company, Inc., New York, N. Y. (March) . . . . .	1947
"Comparator for Coaxial Line Adjustments", O. M. Woodward, Jr., <i>Electronics</i> (April) . . . . .	1947
"Teloran", D. H. Ewing and R. W. K. Smith, <i>Airways Radio Journal</i> (April and June) . . . . .	1947
Reprinted from <i>RCA REVIEW</i> (December) . . . . .	1946
"Input Admittance of Receiving Tubes", <i>RCA Application Note AN-118</i> , RCA Tube Department, Harrison, N. J. (April 15) . . . . .	1947
"Use of the 2E24 and 2E26 at 162 Megacycles", <i>RCA Application Note AN-119</i> , RCA Tube Department, Harrison, N. J. (May 15) . . . . .	1947

	Year
"The AN/ART-13 Radio Transmitter—Characteristics and Tests", <i>NBC Eng. Notice (Apparatus) No. 33</i> , National Broadcasting Co., Inc., New York, N. Y. (June) .....	1947
"Circularly-Polarized Omnidirectional Antenna", G. H. Brown and O. M. Woodward, Jr., <i>RCA REVIEW</i> (June) .....	1947
"Coaxial Tantalum Cylinder Cathode for Continuous-Wave Mag- netrons", R. L. Jepsen, <i>RCA REVIEW</i> (June) .....	1947
"Input Impedance of a Folded Dipole", W van B. Roberts, <i>RCA RE- VIEW</i> (June) .....	1947
"Miniature Tubes in War and Peace", N. H. Green, <i>RCA REVIEW</i> (June) .....	1947
"Phase-Front Plotter for Centimeter Waves", H. Iams, <i>RCA RE- VIEW</i> (June) .....	1947
"Precision Device for Measurement of Pulse Width and Pulse Slope", H. L. Morrison, <i>RCA REVIEW</i> (June) .....	1947
"Radar for Merchant Marine Service", F. E. Spaulding, Jr., <i>RCA REVIEW</i> (June) .....	1947
"The Radio Mike", J. L. Hathaway and R. Kennedy, <i>RCA REVIEW</i> (June) .....	1947
"Stabilized Magnetron for Beacon Service", J. S. Donal, Jr., C. L. Cuccia, B. B. Brown, C. P. Vogel and W. J. Dodds, <i>RCA REVIEW</i> (June) .....	1947
"Compensation of Frequency Drift", W. A. Harris and D. P. Hea- cock, <i>RCA Licensee Bulletin LB-715</i> (June 12) .....	1947
"Operation of the RCA-6SB7-Y Converter", <i>RCA Application Note AN-120</i> , RCA Tube Department, Harrison, N. J. (June 16)....	1947
"A Frequency-Modulated Magnetron for Super-High Frequencies", G. R. Kilgore, C. I. Shulman, and J. Kurshan, <i>Proc. I.R.E.</i> (July) .....	1947
"Propagation Studies on 45.1, 474, and 2800 Megacycles Within and Beyond the Horizon", G. S. Wickizer, and Arthur M. Braaten, <i>Proc. I.R.E.</i> (July) .....	1947
"A 1-Kilowatt Frequency-Modulated Magnetron for 900 Megacycles", J. S. Donal, Jr., R. R. Bush, C. L. Cuccia, and H. R. Hegbar, <i>Proc. I.R.E.</i> (July) .....	1947
"The NBC ND-310 Receiver", <i>NBC Eng. Notice (Apparatus) No. 29</i> , National Broadcasting Co., Inc., New York, N. Y. (August)..	1947
"Beam-Deflection Control for Amplifier Tubes", G. R. Kilgore, <i>RCA REVIEW</i> (September) .....	1947
"An Experimental Simultaneous Color-Television System, Part III— Radio-Frequency and Reproducing Equipment", K. R. Wendt, G. L. Fredenall and A. C. Schroeder, <i>Proc. I.R.E.</i> (September)..	1947
"Special Applications of U-H-F Wide Band Sweep Generators", J. A. Bauer <i>RCA REVIEW</i> (September) .....	1947
"An Experimental Simultaneous Color Television System", <i>RCA Licensee Bulletin LB-729</i> (September 3) .....	1947
"The Behavior of 'Magnetic' Electron Multipliers as a Function of Frequency", L. Malter, <i>Proc. I.R.E.</i> (October) .....	1947
"Variation of Bandwidth with Modulation Index in Frequency Modu- lation", M. S. Corrington, <i>Proc. I.R.E.</i> (October) .....	1947
"Laboratory Antenna Distribution System", F. Mural, <i>RCA Licensee Bulletin LB-730</i> (October 6) .....	1947
"Compensation of Frequency Drift", <i>RCA Application Note AN-122</i> , RCA Tube Department, Harrison, N. J. (October 15).....	1947
"Frequency Allocations", P. F. Siling, <i>RCA REVIEW</i> (December)..	1947
"Slot Antennas", N. E. Lindenblad, <i>Proc. I.R.E.</i> (December) .....	1947
"Small-Signal Analysis of Traveling-Wave Tube", C. I. Shulman and M. S. Heagy, <i>RCA REVIEW</i> (December) .....	1947
"Storage Orthicon and Its Application to Teleran", S. V. Forgue, <i>RCA REVIEW</i> (December) .....	1947
"TELERAN—Part II, First Experimental Installation", D. H. Ewing, H. J. Schrader and R. W. K. Smith, <i>RCA REVIEW</i> (December)..	1947
"Ultra-High-Frequency Low-Pass Filter of Coaxial Construction", C. L. Cuccia and H. R. Hegbar, <i>RCA REVIEW</i> (December).....	1947

## APPENDIX II

---

Summaries of papers published in RADIO AT ULTRA-HIGH FREQUENCIES, Volume I (which is now out of print), are included below as basic reference material on earlier developments. Original publication data are shown in each case.

---

### RADIO AT ULTRA-HIGH FREQUENCIES

#### Volume I

#### Summaries

---

PAPERS PUBLISHED IN FULL IN VOLUME I

---

### SIMPLE TELEVISION ANTENNAS\*†

BY

P. S. CARTER

Engineering Department, RCA Communications, Inc.,  
Rocky Point, N. Y.

*Summary*—The frequency band widths demanded by high-definition television have considerable range when considered in relation to resonant circuits. The transmitting antenna and transmission-line systems must, therefore, meet stringent requirements if multiple images or ghosts in the received picture are to be avoided.

Before discussing the characteristics of particular antenna systems, the transmitting and receiving antenna problems are considered. The input impedance of a transmission line, even when loaded with a resonant circuit having a  $Q$  as low as 2, undergoes considerable variation with frequency within the transmission band. If the television receiver is designed to present a pure resistance to its transmission line, equal to the characteristic impedance of the latter throughout the transmission frequency band, the receiving antenna requirements are not difficult to meet.

The measured impedance-frequency characteristic of a half-wave dipole of large diameter conductors, when compared with that obtained for a similar antenna of small diameter conductors, shows the advantages of the former.

A method of impedance matching has been devised whereby the usual narrowing of the useful frequency band caused by impedance transformation is overcome.

The "folded dipole" antenna and combinations of these units are superior to ordinary dipoles for television purposes. Measurements indicate that ground and other reflecting surfaces considerably affect the impedance-frequency characteristics of antennas.

---

\* Decimal Classification: R326.6.

† RCA REVIEW, October, 1939.

*The use of a type of antenna called the "double cone" or "hour glass" antenna results in a very flat impedance-frequency characteristic at the input terminals of a transmission line over a wide range of frequency. By properly proportioning the dimensions of this antenna its impedance can be made to match the characteristic impedance of all practical open-wire transmission lines. The current and electric field distributions along the surfaces of the conical conductor have been measured. The theory of this antenna is briefly considered.*

*Curves of the characteristics of the systems discussed are included. For comparison purposes the measurements of line reflection vs. frequency for the several antenna systems considered are shown by a family of curves in a single figure.*

*(18 Pages; 27 Figures)*

## TELEVISION TRANSMITTING ANTENNA FOR EMPIRE STATE BUILDING\*†

BY

NILS E. LINDENBLAD

Transmitter Laboratory, RCA Communications, Inc.,  
Rocky Point, N. Y.

*Summary—The theory for a new approach to the design of wide-band radiators for vision antennas is set forth and demonstrated in its application both to models and to the television antenna recently installed on top of the Empire State Building in New York City. A band width was obtained which is several times that required to meet television standards in the United States.*

*The design principles of a sound antenna capable of being located close to the vision antenna without causing mutual interference, are described and demonstrated.*

*The paper also deals with important transmission line phenomena and circuit problems, particularly as they occur in connection with this antenna. A short description of mechanical and auxiliary details is included.*

*(22 Pages; 22 Figures)*

---

\* Decimal Classification: R326.61.

† RCA REVIEW, April, 1939.

## A TURNSTILE ANTENNA FOR USE AT ULTRA-HIGH FREQUENCIES\*†

BY

GEORGE H. BROWN

RCA Manufacturing Co., Inc., Camden, N. J.

*Summary—The Turnstile antenna provides a circular horizontal radia-*

---

\* Decimal Classification: R321.32.

† Electronics, April, 1936.

tion pattern, with a concentration of energy in the vertical plane. This paper describes the antenna, its theoretical aspects, the experimental tests made on the antenna, as well as the procedure and the circuits necessary in its operation.

(12 Pages; 13 Figures)

## FREQUENCY CONTROL BY LOW POWER FACTOR LINE CIRCUITS\*†

BY

CLARENCE W. HANSELL AND PHILIP S. CARTER

RCA Communications, Inc., Rocky Point, L. I., New York

*Summary*—This paper points out the advantages of concentric conductor lines as low power factor or high Q resonant circuits for controlling the frequency of very high frequency oscillators. The electrical characteristics of lines of various dimensions at various frequencies is given. Several forms of temperature compensated lines are described. Oscillator circuits, circuit combinations, and precautions for obtaining stable transmitter frequencies are suggested. Photographs of typical line controlled transmitters are included. The results obtained with line control indicate that the method has great potential usefulness comparable with the usefulness of piezoelectric crystal control.

(23 Pages; 17 Figures)

---

\* Decimal Classification: R355.6.

† *Proc. I.R.E.*, April, 1936.

## CARRIER AND SIDE-FREQUENCY RELATIONS WITH MULTI-TONE FREQUENCY OR PHASE MODULATION\*†

BY

MURRAY G. CROSBY

RCA Communications, Inc., Riverhead, N. Y.

*Summary*—The equation for the carrier and side frequencies of a frequency or phase-modulated wave is resolved for the case of two applied modulating tones. It is shown that when more than one modulating tone is applied, the amplitude of the carrier is proportional to the product of the zero-order Bessel Functions of all of the modulation indexes involved. The amplitudes of the side frequencies are proportional of the products of Bessel Functions equal in number to the number of tones applied and having orders respectively equal to the orders of the frequencies involved in the side frequency. Beat side frequencies are produced which have higher-order amplitude and do not appreciably widen the band width occupied by frequency modulation.

(4 Pages)

---

\* Decimal Classification: R630.1.

† *RCA REVIEW*, July, 1938.



## A CATHODE-RAY FREQUENCY-MODULATION GENERATOR\*†

BY

R. E. SHELBY

Engineering Staff, National Broadcasting Company, Inc.,  
New York, N. Y.

*Summary*—A new device is described for phase or frequency modulating a carrier wave obtained from a source of constant frequency and phase. It consists essentially of an electron gun, a target anode of special design and a means for deflecting the cathode-ray beam. Deflection of the beam is by means of two carrier voltages derived from a common source, but differing in phase by  $90^\circ$  and applied in such a way that the electron stream traces a circular path on the target anode. When amplitude modulation is applied to the deflection voltages, a phase-modulated signal is obtained in the circuit associated with the target anode. Frequency modulation may be obtained by proper pre-distortion of the audio-frequency signal prior to modulation.

A U-H-F radio transmitter set-up used in testing such a device is described.

(10 Pages; 8 Figures)

---

\* Decimal Classification: R630.3.

† *Electronics*, February, 1940.

## A STUDY OF ULTRA-HIGH-FREQUENCY WIDE-BAND PROPAGATION CHARACTERISTICS\*†

BY

R. W. GEORGE

RCA Communications, Inc., Riverhead, N. Y.

*Summary*—Signals reflected from buildings and other large objects introduce distortion in the received signal because of their relative time delay and phase relations. This distortion is especially evident in the form of blurred and multiple images in television reception. Data on the relative merits in this respect, of vertically and horizontally polarized waves transmitted from the Empire State Building in New York City, were obtained at the two frequency ranges of 81 to 86 megacycles and 140 to 145 megacycles. Some data using circular polarization at the lower frequency range were also obtained.

The effects of indirect-path signals were indicated on recorded curves showing field strength versus frequency. The methods and equipment used to record these data at a number of representative receiving locations are briefly described.

A minimum of indirect-path signal interference was found to be generally had with horizontal polarization at both signal-frequency ranges. In this respect, circular polarization was found to be slightly preferable to

---

\* Decimal Classification: R113.7.

† *Proc. I.R.E.*, January, 1939.

vertical polarization. Horizontal polarization also gave somewhat greater average field strength.

Miscellaneous data and observations are described, including sample propagation-characteristic curves. In conclusion, some relations between direct- and indirect-path signals and propagation path are discussed.

(17 Pages; 11 Figures; 2 Tables)

## ULTRA-HIGH-FREQUENCY PROPAGATION\*†

BY

M. KATZIN

RCA Communications, Inc., Riverhead, N. Y.

*Summary*—This paper presents a short summary of the subject of ultra-high-frequency propagation, with theoretical and experimental results presented side by side, to show the general agreement between them. The quasi-optical behavior of u-h-f waves is exhibited in the phenomena of reflection, diffraction, and refraction. The reflecting properties of the ground, and their application in explaining propagation over plane earth, are shown. The presence of multipath reflections in urban areas and their effect on wide-band transmission is discussed. Diffraction and refraction are discussed, the variable nature of refraction giving rise to fading experienced beyond the horizon. Coverage data of the Empire State television transmitter are used to illustrate the practical application of many of the points discussed in the paper.

(36 Pages; 34 Figures)

---

\* Decimal Classification: R112 × R113.

† Proc. Radio Club of America, September, 1939.

## FREQUENCY MODULATION PROPAGATION CHARACTERISTICS\*†

BY

MURRAY G. CROSBY

RCA Communications, Inc., Riverhead, N. Y.

*Summary*—Early work on frequency modulation is described wherein the propagation characteristics of frequency modulation were determined for frequencies between 9000 and 18,000 kilocycles. Oscilloscopic wave form and aural program observations, taken on a circuit between California and New York, showed that frequency modulation is much more distorted by the effects of multipath transmission than is amplitude modulation. The distortion is greatest at the lower modulation frequencies and higher depths of modulation where the side frequencies are most numerous.

Oscilloscopic observations of the Lissajou figures formed by placing the outputs of receivers connected to spaced antennas on opposite oscillo-

---

\* Decimal Classification: R148.

† Proc. I.R.E., June, 1936.

scope plates showed that the diversity characteristics of frequency modulation are similar to those of amplitude modulation. That is, the detected outputs of the receivers tend to remain in phase for the lower modulation frequencies and become more phase random as the modulation frequency is increased. However, this tendency is almost obliterated on the lower modulation frequencies of frequencies modulation by the presence of unequal harmonic distortion in the two receiver outputs.

Theory is given analyzing the distortion encountered in a two-path transmission medium under various path amplitude and phase relation conditions. The theory explains phenomena observed in the tests and points out the extreme distortion that can be encountered.

(17 Pages; 8 Figures)

## FREQUENCY MODULATION NOISE CHARACTERISTICS\*†

BY

MURRAY G. CROSBY

RCA Communications, Inc., Riverhead, L. I., New York

*Summary*—Theory and experimental data are given which show the improvements in signal-noise ratio effected by frequency modulation over amplitude modulation. It is shown that above a certain carrier-noise ratio in the frequency modulation receiver which is called the "improvement threshold," the frequency modulation signal-noise ratio is greater than the amplitude modulation signal-noise ratio by a factor equal to the product of a constant and the deviation ratio (the deviation ratio is equal to the ratio between the maximum frequency deviation and the audio modulation band width). The constant depends upon the type of noise, being slightly greater for impulse than for fluctuation noise. In frequency modulation system with high deviation ratios, a higher carrier level is required to reach the improvement threshold than is required in system with low deviation ratios; this carrier level is higher for impulse than for fluctuation noise. At carrier-noise ratios below the improvement threshold, the peak signal-noise ratio characteristics of the frequency modulation receiver are approximately the same as those of the amplitude modulation receiver, but the energy content of the frequency modulation noise is reduced.

An effect which is called "frequency limiting" is pointed out in which the peak value of the noise is limited to a value not greater than the peak value of the signal. With impulse noise this phenomenon effects a noise suppression in a manner similar to that in the recent circuits for reducing impulse noise which is stronger than the carrier in amplitude modulation reception.

When the power gain obtainable in certain types of transmitters by the use of frequency modulation is taken into account, the frequency modulation improvement factors are increased and the improvement threshold is lowered with respect to the carrier-noise ratio existing in a reference amplitude modulation system.

(43 Pages; 16 Figures)

\* Decimal Classification: R148 X R270.

† Proc. I.R.E., April, 1937.

## THE SERVICE RANGE OF FREQUENCY MODULATION\*†

BY

MURRAY G. CROSBY

Engineering Department, RCA Communications, Inc.,  
Riverhead, N. Y.

*Summary*—An empirical ultra-high-frequency propagation formula is correlated with experimentally confirmed frequency modulation improvement factors to develop a formula for the determination of the relation between signal-noise ratio and distance in a frequency-modulation system. Formulas for the distance between the transmitter and the point of occurrence of the threshold of frequency-modulation improvements, as well as formulas for the signal-noise ratio occurring at this distance, are also developed.

Results of calculations and listening tests are described which evaluate the signal-noise ratio gain obtained by applying pre-emphasis to the higher modulation frequencies of both amplitude and frequency modulation systems.

Examples using a typical set of conditions are given and discussed.

(23 Pages; 10 Figures)

---

\* Decimal Classification: R113.7 × R630.1.

† RCA REVIEW, January, 1940.

## PRACTICAL APPLICATION OF AN ULTRA-HIGH-FREQUENCY RADIO-RELAY CIRCUIT\*†

BY

J. ERNEST SMITH, FRED H. KROGER, AND R. W. GEORGE

RCA Communications, Inc., New York, N. Y.

*Summary*—The utilization of an ultra-high-frequency radio circuit for the transmission of telegraph, teletype printer, and facsimile signals is described. The operating procedure is stressed throughout, particularly with regard to equipment maintenance tests and the methods employed to determine the conditions of the circuit such as degree of modulation, signal-to-noise ratio, etc. Considerations are presented with respect to the most efficient division of the total modulation band into the communication channels, as well as the signal-to-noise ratios required for the different types of service. It is found that fading, static, and weather conditions at these frequencies are of little importance as to their effect on the economic use of the circuit. However, diathermy machines and similar sources of disturbance are troublesome and their effect must be minimized. Experience during the past year and a half indicates that the dependability of the ultra-high-frequency radio circuit is of a high order.

(16 Pages; 10 Figures; 2 Tables)

---

\* Decimal Classification: R480.

† Proc. I.R.E., November, 1938.

## WIDE-BAND VARIABLE-FREQUENCY TESTING TRANSMITTERS\*†

By

G. L. USSELMAN

Engineering Department, RCA Communications, Inc.,  
Rocky Point, N. Y.

*Summary*—A wide-band variable-frequency transmitter, designed primarily for testing purposes is described. The transmitter consists of a single-tube oscillator stage with a high degree of frequency control. Two models have been built which operate in the frequency range of 40 to 100 megacycles, with 500 to 1000 watts output. Means are also provided for telegraphically keying the transmitters. This type of transmitter supplies a need for a source of high-frequency power which is continuously variable over a wide range of frequency, but which will accurately maintain any frequency to which it is adjusted.

(7 Pages; 3 Figures)

---

\* Decimal Classification: R355.15.

† RCA REVIEW, April, 1939.

## FIELD STRENGTH MEASURING EQUIPMENT FOR WIDE BAND U-H-F TRANSMISSION\*†

By

R. W. GEORGE

RCA Communications, Inc., Riverhead, N. Y.

*Summary*—Mainly in the interest of television service, some quantitative data were required on the characteristics of ultra-high-frequency propagation paths. Portable measuring equipment and methods devised to obtain these data are described.

Transmitter systems giving constant output over the ranges of 81 to 86 Mc and 140 to 145 Mc were used, the frequency of each transmitter varied at the rate of 166 kc per second from one extreme of its range to the other. Field strength was measured at each 70-kc increment of the frequency range, a measurement being recorded automatically as the signal frequency passed through the receiver pass-band. The circuits were arranged to hold the recorder indication until changed by the following measurement. About 70 measurements were recorded in one-half minute by means of a novel automatic tuning arrangement.

The signal generator and calibration methods used are also described.

(10 Pages; 6 Figures)

---

\* Decimal Classification: R270.

† RCA REVIEW, April, 1939.

## U-H-F EQUIPMENT FOR RELAY BROADCASTING\*†

BY

W. A. R. BROWN

Assistant Development Engineer, National Broadcasting Company, Inc.,  
New York, N. Y.

*Summary*—Several types of portable transmitting and receiving equipment, which have recently been developed to meet the increasing demands imposed upon operating facilities by the constantly expanding scope of ultra-high-frequency relay broadcasting are described, and their functions in relay-broadcast operations outlined in this paper.

(13 Pages; 10 Figures)

---

\* Decimal Classification: R310.

† RCA REVIEW, October, 1938.

## A NEW METHOD FOR MEASUREMENT OF ULTRA-HIGH FREQUENCY IMPEDANCE\*†

BY

STUART W. SEELEY AND WILLIAM S. BARDEN

License Laboratory, Radio Corporation of America,  
New York, N. Y.

*Summary*—A technique for measuring impedances at ultra-high frequencies with a high degree of accuracy is described. A vacuum-tube voltmeter, and a small air condenser, the value of which need only be known on an incremental basis, are the critical elements required in the measurements. A detailed description as well as an analytical explanation of the method is given.

(22 Pages; 7 Figures)

---

\* Decimal Classification: R244.

† Original material—not reprinted.

## A SURVEY OF ULTRA-HIGH-FREQUENCY MEASUREMENTS\*†

BY

L. S. NERGAARD

Research and Engineering Department, RCA Manufacturing Company, Inc.,  
Harrison, N. J.

*Summary*—A simple magnetron signal generator is described. The more useful transmission-line and skin-effect formulas are listed. In connection

---

\* Decimal Classification: R200.

† RCA REVIEW, October, 1938.

with transmission lines, it is pointed out that even at very high frequencies the quadrature component of the characteristic impedance cannot be neglected. Methods which have been used for the measurement of the following quantities are described:

(1) *Wavelength*—Wavelength has been measured by reflection of waves in free-space and transmission-line wavemeters. A method of determining the end correction of a transmission-line wavemeter is described.

(2) *Power*—Thermocouples for the measurement of small powers are described. The use of incandescent lamps for the measurement of large powers is discussed.

(3) *Voltage*—Diode voltmeters and thermocouples have been used for the measurement of voltage. The errors of these voltmeters are discussed.

(4) *Reactance*—Reactance has been measured by tuning the unknown reactance to resonance with a transmission line of known characteristics. The method is illustrated by two examples: the determination of the resonant wavelength, the inductance and capacitance of a diode, and the calibration of a variable condenser.

(5) *Resistance*—Resistance has been measured by the substitution method, the resistance-variation method, and the reactance-variation method. The reactance-variation method has been used in all of its forms, namely, capacitance variation, line-length variation and frequency variation. The pertinent formulas and examples of the methods are given. A transmission line and condenser for the measurement of resistance by the capacitance-variation method are described.

(6) *Current*—The measurement of current with thermocouples is discussed.

(40 Pages; 15 Figures)

## VACUUM TUBES OF SMALL DIMENSIONS FOR USE AT EXTREMELY HIGH FREQUENCIES\*†

BY

B. J. THOMPSON AND G. M. ROSE, JR.

Research and Engineering Department, RCA Manufacturing Company, Inc.,  
Harrison, N. J.

*Summary*—This paper describes the construction and operation of very small triodes and screen-grid tubes intended for reception at wavelengths down to 60 centimeters with conventional circuits.

The tubes represent nearly a tenfold reduction in dimensions as compared with conventional receiving tubes, but compare favorably with them in transconductance and amplification factor. The interelectrode capacitances are only a fraction of those obtained in the larger tubes.

The triodes have been operated in a conventional feed-back oscillator circuit at a wavelength of 30 centimeters with a plate voltage of 115 volts and a plate current of 3 milliamperes.

Receivers have been constructed using the screen-grid tubes which afford tuned radio-frequency amplification at 100 centimeters and 75 centimeters, a gain of approximately four per stage being obtained at the longer wavelength.

(15 Pages; 15 Figures)

\* Decimal Classification: R331.

† *Proc. I.R.E.*, December, 1933.

## SIMPLE ANTENNAS AND RECEIVER INPUT CIRCUITS FOR ULTRA-HIGH-FREQUENCIES\*†

BY

R. S. HOLMES AND A. H. TURNER

RCA Manufacturing Company, Inc., Camden, N. J.

*Summary*—This paper describes some of the factors affecting the performance of antennas, transmission lines and receiver input circuits. The effect of antenna selectivity, directivity and gain is discussed, and selectivity curves for some simple antenna arrangements are given. Some of the factors governing selectivity, gain and signal-to-receiver hiss ratio are discussed. The discussion covers both narrow and wide band circuits.

(11 Pages; 7 Figures)

---

\* Decimal Classification: R326.7.

† Original material—not reprinted.

## MAGNETRON OSCILLATORS FOR THE GENERATION OF FREQUENCIES BETWEEN 300 AND 600 MEGACYCLES\*†

BY

G. R. KILGORE

Research and Engineering Department, RCA Manufacturing Company, Inc.,  
Harrison, N. J.

*Summary*—The need for vacuum tube generators capable of delivering appreciable power at frequencies from 300 to 600 megacycles is pointed out and the negative resistance magnetron is suggested as one of the more promising generators for this purpose.

An explanation of the negative resistance characteristic in a split-anode magnetron is given by means of a special tube which makes possible the visual study of electron paths. In this manner it is demonstrated how most of the electrons starting toward the higher potential plate reach the lower potential plate.

From the static characteristics it is shown how the output, efficiency, and load resistance can be calculated, and from this analysis it is concluded that the negative resistance magnetron is essentially a high efficiency device at low frequencies.

Measurements of efficiency at ultra-high frequencies are given for several magnetrons under various operating conditions. It is concluded from these measurements that the decrease of efficiency at very high frequencies is mainly due to electron-transit-time effects. A general curve is given showing efficiency as a function of the "transit-time ratio." This curve indicates that for a transit time of one-fifteenth of a period, approximately fifty per cent efficiency is possible; for one-tenth of a period, thirty per cent; and for one-fifth of a period, the efficiency is essentially zero.

---

\* Decimal Classification: R355.9.

† Proc. I.R.E., August, 1936.



Two methods are described for increasing the plate-dissipation limit. One method is that of increasing the effective heat-dissipating area by the use of an internal circuit of heavy conductors. The other method is that of a special water-cooling arrangement which also makes use of the internal circuit construction.

Examples of laboratory tubes are illustrated, including a radiation-cooled tube which will deliver fifty watts at 550 megacycles and a water-cooled tube which will deliver 100 watts at 600 megacycles.

(18 Pages; 16 Figures)

## AN ULTRA-HIGH-FREQUENCY POWER AMPLIFIER OF NOVEL DESIGN\*†

By

ANDREW V. HAEFF

Research and Engineering Department, RCA Manufacturing Company, Inc.,  
Harrison, N. J.

*Summary*—For many high-frequency applications a non-regenerative power amplifier is of primary importance. It is the purpose of this paper to describe an amplifier of a novel type, consisting of a new tube combined with a tank circuit. Successful operation is obtained at frequencies much higher than those which can be handled by conventional devices of comparable power capabilities.

(8 Pages; 7 Figures)

---

\* Decimal Classification: R363.1.

† *Electronics*, February, 1939.

## DEVELOPMENT OF TRANSMITTERS FOR FREQUENCIES ABOVE 300 MEGACYCLES\*†

By

N. E. LINDENBLAD

RCA Communications, Inc., Rocky Point, L. I., N. Y.

*Summary*—The fundamental functions of the electrons and their work cycle, in the interelectrode space of high vacuum tubes, are discussed. It is shown how the triode feed-back circuit becomes inoperable at very high frequencies due to space-time and reactance characteristics. It is further shown how the space-time conditions can be organized to benefit the maintenance of oscillation instead of becoming a detriment. Some of the more familiar arrangements, such as the Barkhausen and the magnetron circuits, which are based on this principle, are discussed in some detail. With these illustrations as a background the author describes a new method of frequency multiplication at very high frequencies. This method yields much

---

\* Decimal Classification: R355.5.

† *Proc. I.R.E.*, September, 1935.

greater power outputs than hitherto possible and promises to become very useful.

Various means for frequency stabilization are referred to and the merits of frequency controlling devices, such as crystals and low power factor circuits, are compared.

Special problems encountered in the application of modulation at very high frequencies are described and reference is made to methods developed to meet these problems.

Practical considerations of circuit arrangements are described in some detail. Several examples of transmitter design are given. These sections are illustrated with photographs.

Important points in connection with antennas and transmission lines are discussed and the results of some measurement are given.

The paper ends with a brief reference to some propagation results obtained by RCA Communications engineers and others.

(35 Pages; 23 Figures; 1 Table)

## TRANSMISSION OF 9-CM. ELECTRO-MAGNETIC WAVES\*†

BY

IRVING WOLFF AND E. G. LINDER

Research Division, RCA Manufacturing Company, Inc.,  
Camden, N. J.

*Summary*—A 9-cm beam transmitter and a receiver are described for making tests of the transmission of electromagnetic waves of this wavelength.

Using this transmitter with the receiver placed at a series of locations from  $\frac{1}{2}$  up to a line of sight distance of 16 miles, measurements of field strength failed to show any noticeable attenuation due to the atmosphere. A series of more accurate tests comparing the transmission over a 2-mile distance during alternate clear and rainy periods indicated that the attenuation due to rainfall was less than .1 db per mile.

(9 Pages; 9 Figures; 1 Table)

---

\* Decimal Classification: R113.5.

† *Broadcast News*, December, 1935.

## PAPERS PUBLISHED IN SUMMARY FORM IN VOLUME I

## FREQUENCY ASSIGNMENTS FOR TELEVISION\*†

BY

E. W. ENGSTROM AND C. M. BURRILL

RCA Manufacturing Company, Camden, N. J.

*Summary*—This article is not a report of original work, but is a correlation or synthesis of information pertinent to the subject, available to the authors within the RCA Services or through published papers. Since the results of all have been taken into account it has not seemed feasible or desirable to give credit to individual sources except to mention the article by H. H. Beverage entitled "Some Notes on Ultra Short Wave Propagation" appearing in this number of RCA REVIEW, and the bibliography forming a part of that article. Much credit is due collectively to the many workers in this field, who have made possible the drawing with reasonable certainty of the conclusions here stated. The basic plan of any new service must always be determined by the work of such pioneers before commercial experience has made everything plain. Because fundamental plans for broadcast television are now in the making, it is hoped that this brief article will be found both timely and interesting.

(6 Pages)

\* Decimal Classification: R007.1 × R583.

† RCA REVIEW, January, 1937.

THE REQUIREMENTS AND PERFORMANCE OF A  
NEW ULTRA-HIGH-FREQUENCY POWER TUBE\*†

BY

W. G. WAGENER

Formerly with Research and Engineering Department, RCA Manufacturing Company, Inc.,  
Harrison, N. J.

*Summary*—Large values of power are difficult to obtain in the ultra-high-frequency region. At the limiting frequencies it is increasingly more difficult to find vacuum tubes that will deliver such power and perform efficiently. The principal factors that affect the design and performance of the tubes are those involving the electrical circuit, the size requirements for the power desired, and the transit time of the electrons within the evacuated space of the tube.

The design principles that result from a consideration of these factors have been used in the development of a new ultra-high-frequency triode. A triode capable of delivering approximately 700 watts at 100 megacycles is described. This tube, which is cooled by water and air, is capable of operation as a neutralized power amplifier up to 200 megacycles with an output of approximately 500 watts.

(7 Pages; 5 Figures)

\* Decimal Classification: R334 × R339.2.

† RCA REVIEW, October, 1937.

## TELEVISION TRANSMITTERS OPERATING AT HIGH POWERS AND ULTRA-HIGH FREQUENCIES\*†

By

J. W. CONKLIN AND H. E. GIHRING

RCA Manufacturing Company, Inc., Camden, N. J.

*Summary*—A general review of some of the unusual problems encountered in the development of high-power ultra-high-frequency transmitters and particularly television power amplifiers. Tube and circuit problems are discussed and also some of the difficulties encountered with associated components.

(15 Pages; 12 Figures)

---

\* Decimal Classification: R583.4.

† RCA REVIEW, July, 1937.

## EFFECT OF ELECTRON TRANSIT TIME ON EFFICIENCY OF A POWER AMPLIFIER\*†

By

ANDREW V. HAEFF

Research and Engineering Department, RCA Manufacturing Company, Inc.,  
Harrison, N. J.

*Summary*—Measurements of the plate efficiency of a neutralized triode amplifier operated at high frequencies are reported. The results are compared with those obtained for an oscillator operated at the same frequency. At a frequency at which the oscillator efficiency approaches zero the amplifier efficiency is found to be reduced to only 50 per cent of the low-frequency value. It is shown that the difference in efficiency is primarily due to a large phase angle between the plate current and the grid voltage produced by the electron transit time.

(9 Pages; 5 Figures)

---

\* Decimal Classification: R334 × R339.2.

† RCA REVIEW, July, 1939.

## ON THE OPTIMUM LENGTH FOR TRANSMISSION LINES USED AS CIRCUIT ELEMENTS\*†

By

BERNARD SALZBERG

Research and Engineering Department, RCA Manufacturing Company, Inc.,  
Harrison, N. J.

*Summary*—The existence of an optimum length for transmission lines

---

\* Decimal Classification: R117.1.

† Proc. I.R.E., December, 1937.

which are tuned by low-loss capacitor to give maximum sending-end impedance is discussed. This optimum length is found to be  $0.185\lambda$  for a shorted line and  $0.472\lambda$  for an open-circuited line, resulting in impedances 14 and 3 per cent higher, respectively, than can be obtained from lines without tuning condensers.

(4 Pages; 2 Figures)

## OBSERVATIONS ON SKY-WAVE TRANSMISSION ON FREQUENCIES ABOVE 40 MEGACYCLES\*†

BY

D. R. GODDARD

RCA Communications, Inc., Riverhead, L. I., N. Y.

*Summary*—The results of daily observations at Riverhead, L. I., N. Y., since September, 1937, of European 40-to-45 megacycle transmitters are reported. Measurements of field strength were made on English, French, and German television signals. Multipath propagation of the English video-frequency channel was observed optically and the difference in path length determined.

(4 Pages; 5 Figures)

---

\* Decimal Classification: R112.4.

† *Proc. I.R.E.*, January, 1939.

## NOTES ON THE RANDOM FADING OF 50-MEGACYCLE SIGNALS OVER NON-OPTICAL PATHS\*†

BY

K. G. MACLEAN AND G. S. WICKIZER

RCA Communications, Inc., Riverhead, L. I., N. Y.

*Summary*—To obtain data on the variation of field strength beyond the horizon, simultaneous recordings were made at three locations, one within the optical path of the transmitter, one 700 feet below the line of sight, and one 11,400 feet below the line of sight. All three locations were on the same line from the transmitter. Recordings extended over a two-week period, chosen at a time when atmospheric refraction was likely to be favorable. Analysis of the recorded data indicates several things of interest. The variation of field strength at each location was random and showed no correlation with any other location; the range of field-strength variation exceeded 49 decibels at the most remote location; maximum fields generally occurred at night; and previous data on the rate of attenuation beyond the horizon were confirmed.

(5 Pages; 12 Figures; 2 Tables)

---

\* Decimal Classification: R113.1.

† *Proc. I.R.E.*, August, 1939.

## A STUDY OF THE PROPAGATION OF WAVE-LENGTHS BETWEEN THREE AND EIGHT METERS\*†

BY

L. F. JONES

RCA Manufacturing Company, Inc., Camden, N. J.

*Summary*—A description is given of the equipments used in an air-plane, dirigible, automobile and indoors to measure the propagation characteristics of wavelengths between about three and eight meters. The majority of observations were of television transmissions from the Empire State building.

The absorption of ultra-short-waves traveling through or around large buildings is shown to be in terms of amplitude about 50 per cent every 500 feet for seven meters and 50 per cent every 200 feet for three meters. A number of reflection phenomena are discussed and the influence of interference patterns on receiving conditions is emphasized. It is shown that any modulation frequency is partly or completely suppressed if propagation to the receiver takes place over two paths differing in length by half of the hypothetical radio wavelength of the modulation frequency. For a good television picture this corresponds to a difference of about 500 feet.

Various types of interference are mentioned. There are maps of the interference patterns measured in a typical residential room. The manner in which traffic movements cause severe fluctuations in ultra-short wave field strengths at certain indoor points is shown by recorded field strengths.

It is shown that the service range of the Empire State transmitters includes most of the urban and suburban areas of New York, and that the interference range is approximately 100 miles. Variations of field strength with altitude, beyond line of sight, are shown. Observations made at a distance of 280 miles are described.

An empirical ultra-short-wave propagation formula is proposed. Curves are then calculated showing the relations between wavelength, power, range, attenuation, and antenna height.

(38 Pages; 28 Figures; 2 Tables)

\* Decimal Classification: R112.

† Proc. I.R.E., March, 1933, and Television, Vol. 1, 1936.

## AN URBAN FIELD-STRENGTH SURVEY AT THIRTY AND ONE HUNDRED MEGACYCLES\*†

BY

R. S. HOLMES AND A. H. TURNER

RCA Manufacturing Company, Inc., Camden, N. J.

*Summary*—A description is given of the transmitter and receiver equipment used in making field strength surveys in the Camden-Philadelphia area for a low power transmitter whose antenna is 200 feet above the ground, at frequencies of thirty and one hundred megacycles.

\* Decimal Classification: R270.

† Proc. I.R.E., May, 1936, and TELEVISION, Vol. 1, 1936.

Field strength contour maps for the area within approximately ten miles of the transmitter are given. From these maps the average field strength obtained at various distances from the transmitter was determined, and the attenuation of the signal was found to be proportional to the 1.84 power of the distance for thirty megacycles and the 2.5 power of the distance for one hundred megacycles for the region between one and ten miles from the transmitter.

Curves showing the variation from the average field strength of the signal along three routes radiating fifteen miles from the transmitter are given, and these variations are compared with the elevation profiles of the respective routes. It is shown that the signal is usually strongest on the brows of hills facing the transmitter.

Measurements were made in three representative residences, and from these data, curves showing the power required at the transmitter to furnish one hundred microvolts input to receivers with short indoor antennas located in houses at various distances up to ten miles from the transmitter were computed for the two frequencies.

(16 Pages; 14 Figures; 1 Table)

## ELECTRICAL MEASUREMENTS AT WAVE-LENGTHS LESS THAN TWO METERS\*†

BY

LEON S. NERGAARD

Research and Engineering Department, RCA Manufacturing Company, Inc.,  
Harrison, N. J.

*Summary*—In this paper the measurement of power and voltage at ultra-short waves is considered. A signal generator delivering adequate power output with satisfactory stability over the wave-length range from twenty to 200 centimeters is described. The requirements of thermocouples satisfactory for the measurement of power are considered and a set of thermocouples covering the power range from 0.1 milliwatt to fifty watts is described. A study of vacuum tube voltmeters has shown that diode voltmeters have very small loading (of the order of  $10^5$  ohms) on the circuits to which they are connected, whereas conventional triode voltmeters using RCA-955's have an input impedance of about  $10^4$  ohms at a wave length of one meter. The errors of diode voltmeters at ultra-short wave lengths have been studied and found to be of two kinds:

1. An error due to partial series resonance between the lead inductances and the interelectrode capacity.
2. An error due to a transit time effect. This has been called "premature cutoff." These errors have been studied experimentally and theoretically, the results being in qualitative agreement. In the course of the experimental work very small diodes have been built, the smallest diode having an anode diameter of only 0.0065 inch. Calibrations for these diode voltmeters have been obtained. The calibration of the diode having an anode diameter of nine mils at a wavelength of 100 centimeters differs from the sixty-cycle calibration by less than one per cent due to premature cutoff and by about six per cent due to resonance error. Voltmeters of this

\* Decimal Classification: R243.1 X R245.

† *Proc. I.R.E.*, September, 1936.

type have been supplied to other workers and have been found to give very useful and consistent results.

The RCA-955 acorn tube with grid and plate tied together has been studied as a diode voltmeter. From this study it is concluded that the RCA-955 is useful as a voltmeter down to the sixty-centimeter wave length, but that small diodes are necessary for precise measurements below 150 centimeters and for general measurements below sixty centimeters.

(23 Pages; 15 Figures)

## APPLICATION OF ABELIAN FINITE GROUP THEORY TO ELECTROMAGNETIC REFRACTION\*†

BY

R. A. WHITEMAN

Instructor of Physics, RCA Institutes, Inc., New York

*Summary*—This paper presents the direct relationship between the group theory and indices of refraction encountered in the solution of optical problems. The properties and advantages of the group theory are made available by using the double-subscript notation when designating the indices of refraction. The notation is developed from fundamental concepts of refraction at a plane surface and applied to two specific refraction problems in the following order:

- a. refraction the Kennelly-Heaviside layer (radio waves)
- b. electronic refraction (electron optics)

The criterion to be used in determining the applicability of the method developed in this paper to any refraction problem is reduced to a simple equation.

(9 Pages; 3 Figures)

---

\* Decimal Classification R113.605 × R138.3 × 510.  
† RCA REVIEW, January, 1940.

## THE USE OF GAS-FILLED LAMPS AS HIGH-DISSIPATION, HIGH-FREQUENCY RESISTORS, ESPECIALLY FOR POWER MEASUREMENTS\*†

BY

ERNEST G. LINDER

RCA Manufacturing Company, Inc., Camden, N. J.

*Summary*—A type of hydrogen-filled lamp suitable for use as a high-frequency resistance is described, which possesses unusually great heat-dissipation ability. This dissipation may be several hundred times that obtainable with vacuum lamps, and the gain is greatest for filaments of

---

\* Decimal Classification: R245 × R383.  
† RCA REVIEW, July, 1939.



the smallest diameter. Other advantages are pointed out. The theory of heat loss in a gaseous atmosphere is summarized. Details of experimental lamps are given. Design data are presented in the form of a chart which includes, watts dissipated, resistance, temperature, and filament diameter.

(6 Pages; 1 Figure; 2 Tables)

## MEASUREMENTS OF ADMITTANCES AT ULTRA-HIGH FREQUENCIES\*†

BY

JOHN M. MILLER‡ AND BERNARD SALZBERG

Research and Engineering Department, RCA Manufacturing Company, Inc.,  
Harrison, N. J.

*Summary*—A substitution method is described for determining admittances at ultra-high frequencies. Typical measurements of resistors and insulators are given.

The method employs a short transmission line excited by an ultra-high-frequency oscillator. The receiving end of the line is short-circuited and the sending end is shunted by a variable capacitor and the unknown admittance. A vacuum-tube voltmeter indicates the resonant voltage at a point on the line. The unknown admittance is removed, resonance restored by the variable capacitor and the same voltage obtained by sliding a known resistor along the line. The unknown admittance is then determined by the frequency, capacitance change, and the position of the known resistor. With proper line constants, the equivalent sending-end resistance of the resistor is equal to the product of its resistance and the square of the ratio of the total line length to the distance of the resistor from the receiving end.

(19 Pages; 4 Figures; 5 Tables)

---

\* Decimal Classification: R244.1.

† RCA REVIEW, April, 1939.

‡ Formerly with RCA Manufacturing Company.

## RADIO-FREQUENCY GENERATOR FOR TELEVISION RECEIVER TESTING\*†

BY

A. H. TURNER

RCA Manufacturing Company, Inc., Camden, N. J.

*Summary*—An automatic recording signal generator is described which has proven extremely useful in the development of television receivers. The more important specifications and characteristics of this signal generator are as follows:

---

\* Decimal Classification: R355.913.2.

† RMA Engineer, May, 1939.

1. Consists of push-pull r-f oscillator and push-pull modulated r-f amplifier.
2. Frequency range (motor-driven linear control) 40 to 100 megacycles.
3. R-F output (motor-driven continuously variable control and uniform logarithmic scale) 1 to 100,000 microvolts.
4. Modulation (from external source or 400 cycles internal) 30 to 3,000,000 cycles for both side-bands or may be altered for 30 to 5,000,000 cycles for single side-band.
5. R-F output impedance-50 ohms approximately.
6. Slow, normal, and fast curve-paper frequency scales selected by gear shift.
7. Receiver output may be set and held constant at any level between 0.5 volt and 25 volts by the automatic mechanism.

(2 Pages; 2 Figures)

## INPUT RESISTANCE OF VACUUM TUBES AS ULTRA-HIGH-FREQUENCY AMPLIFIERS\*†

BY

W. R. FERRIS

Research and Engineering Department, RCA Manufacturing Company, Inc.,  
Harrison, N. J.

*Summary*—Vacuum tubes which when operated as voltage amplifiers at low frequency require no measurable grid input power have been found to take very serious amounts of power at ultra-high frequencies. The grid input conductance is shown to be very accurately represented for electrodes of any shape by the expression

$$g_o = K s_m f^2 \tau^2$$

where  $g_o$  is the input conductance,  $s_m$  the grid-plate transconductance,  $f$  the frequency, and  $\tau$  the electron transit time.  $K$  is a parameter which is a function of the geometry of the tube and the voltage distribution. A physical picture of the effect, a simple theoretical derivation, and experimental proof with conventional tubes are given.

The magnitude of  $g_o$  is such that it is the principal limitation for amplifiers at frequencies of the order of 100 megacycles, and it seriously affects the amplification at frequencies as low as fifteen megacycles. The input resistance of a typical commercial tube, the RCA-57, is approximately 20,000 ohms at thirty megacycles. Other commercial tubes, being of the same general construction and size, have input resistances of the same order. The use of very small tubes, such as the RCA-954, with correspondingly short transit times is shown to be a practical means of increasing the amplification obtainable with conventional circuits.

Input capacity variation with frequency is found to be negligible with the RCA-57 even up to eighty megacycles and higher. However, the grid-cathode capacity is a function of the applied voltage; the ratio of this capacity under operating conditions to that with the tube cold having a value of four thirds for its minimum. The change in input capacity from cold to hot is of the order of one micromicrofarad for the RCA-57. No change in grid-screen capacity is indicated.

\* Decimal Classification: R240 X R339.2.

† Proc. I.R.E., January, 1936.

The plate resistance of screen-grid tubes is found to vary with frequency but with the RCA-57 at eighty megacycles it is over twenty times the grid resistance and thus constitutes a negligible amount of the total loss in the circuit.

(24 Pages; 13 Figures)

## MULTI-TUBE OSCILLATORS FOR THE ULTRA-HIGH FREQUENCIES\*†

BY

PAUL D. ZOTTU

Formerly with Research and Engineering Department, RCA Manufacturing Company, Inc.,  
Harrison, N. J.

*Summary*—An important limitation on the effective use of the ultra-high frequencies is the fact that with present methods the output power that can be developed is small. With the feedback type of oscillator, output decreases approximately inversely as the square of the frequency. Although the use of two tubes in push-pull permits doubling the output of a single-tube oscillator, in the region of 300 Mc this increase amounts to only a few watts with commercially-available tubes. Paralleling of tubes is out of the question because this method causes tube capacities to add and therefore requires reduction of inductance to maintain the same frequency. At the frequencies considered, inductance is already at a premium and further reduction necessitates making the oscillatory circuit inside the tube. Another disadvantage of the direct-parallel system is that the generated frequency changes with the addition or subtraction of a unit. It is evident, therefore, that a means of combining the output of two or more independent oscillators in such a way that these disadvantages are overcome would be highly desirable.

By proper utilization of two well-known effects in the operation of oscillators, a method for combining several oscillators in the desired manner becomes possible. Consider first a simple oscillator coupled to a tuned circuit which will be termed the secondary circuit. If the coupling is very loose, the secondary tuning will have negligible effect on the oscillator frequency, except in a small region near the point where the two circuits are in resonance, where a slight change in oscillator frequency will occur. With closer coupling, a considerably greater change in frequency results; as the coupling is still further increased, a "jump" in frequency as the secondary is tuned through resonance will occur. The behavior is modified somewhat by the presence of a load on the secondary, although the general effect is the same. The interesting point is that, depending upon the coupling and load, the oscillator frequency is seriously affected by the tuning of the secondary circuit.

The power output to the secondary circuit depends upon the coupling and tuning; with small values of coupling the output rises as the secondary is tuned into resonance, decreases on tuning away. With coupling values greater than the critical, two points of maximum power output will appear, with a minimum point occurring at resonance. The important thing is that maximum output of the oscillator can be obtained with coupling values equal to or greater than critical.

(4 Pages; 7 Figures)

\* Decimal Classification: R355.912.

† QST, October, 1936.

## ANALYSIS OF THE EFFECTS OF SPACE CHARGE ON GRID IMPEDANCE\*†

BY

D. O. NORTH

Research and Engineering Department, RCA Manufacturing Company, Inc.,  
Harrison, N. J.

*Summary*—Previous theory of transit-time phenomena in high vacuum diodes is extended and augmented to provide an explanation of the high-frequency behavior of high- $\mu$  amplifiers with parallel plane electrodes. For mathematical reasons the analysis is restricted to triodes with plate at alternating-current ground and to tetrodes with screen grid at alternating-current ground. Expressions for internal input loading and capacity are derived, showing the dependence upon frequency, voltages, and tube dimensions, and it is shown how the theory in its present form can be made quantitatively applicable to many commercial tubes of cylindrical design.

In agreement with both elementary theory and observation, the theory shows that at the threshold of the effect the input loading varies as the square of the frequency. For the RCA-57 there is calculated an internal input resistance of 21 megohms at one megacycle, dropping to 2100 ohms at 100 megacycles. These figures are in excellent agreement with actual measurement, and illustrate the tremendous importance of transit times in the design of tubes for ultra-high frequencies. It is likely that internal input power losses of this character, together with closely allied losses in transconductance, are primarily responsible for high-frequency failure of both amplifiers and oscillators.

"Hot" input capacity exceeds the "cold" value. The magnitude and dependence upon tube parameters is given, the increase is primarily due to space charge but also depends upon  $\tau_2/\tau_1$ , the ratio of the electron transit time between control grid and plate to the transit time between cathode and control grid. In agreement with observation, the theory indicates very slight frequency dependence.

There is included a brief account of temperature-limited diodes, illustrating their possibilities as a source of high-frequency negative resistance.

(29 Pages; 3 Figures)

---

\* Decimal Classification: R138.1  $\times$  R339.2.

† *Proc. I.R.E.*, January, 1936.

## RECENT DEVELOPMENTS IN MINIATURE TUBES\*†

BY

BERNARD SALZBERG AND D. G. BURNSIDE

Research and Engineering Department, RCA Manufacturing Company, Inc.,  
Harrison, N. J.

*Summary*—The development of two indirectly heated miniature tubes, a triode and a sharp cut-off amplifier pentode especially suited for use at

---

\* Decimal Classification: R330  $\times$  R339.2.

† *Proc. I.R.E.*, October, 1935.

high frequencies, is described. The electrical and mechanical factors involved in the design and application of these tubes are discussed and their novel structural appearances is described.

Because of their decreased lead impedances, interelectrode capacitances, and transit times, these miniature tubes allow considerable improvement to be made in high-frequency receiving equipment. It is possible to operate the triode as an oscillator in a conventional circuit down to a wavelength of approximately 40 centimeters. The pentode can be operated as a radio-frequency amplifier down to a wavelength of approximately 70 centimeters. It is practicable to obtain stable gains with it of from ten to fifteen at three meters, a wavelength at which standard tubes are almost entirely ineffectual. Both tubes can be used, down to much lower wavelengths, in exactly the same manner and for the same applications that the corresponding conventional tubes are used; i.e., as oscillators, amplifiers, detectors, converters, and as negative-resistance devices.

The small size of the tubes and their novel structural design allow compact and convenient receiving equipment to be built. Even at the longer wavelengths, they are applicable to a large number of uses for which their excellent characteristics, small size, and low weight make them particularly useful.

(16 Pages; 13 Figures; 2 Tables)

## EFFECTS OF SPACE CHARGE IN THE GRID-ANODE REGION OF VACUUM TUBES\*†

BY

BERNARD SALZBERG AND A. V. HAEFF

Research and Engineering Department, RCA Manufacturing Company, Inc.,  
Harrison, N. J.

*Summary*—The effects of space charge in the region between grid and anode of a vacuum tube, for the case where the planes of the grid and plate are parallel are determined from the results of a simple analysis. The main effects of the space charge are (a) to introduce departures from the linear potential distribution of the electrostatic case; (b) to set an upper limit, under certain conditions, for the anode current; (c) to introduce instabilities and hysteresis phenomena in the behavior of the tube; and (d) to increase the electron transit time in this region.

Four modes of potential distribution which may exist in this region are treated: (1) Neither potential minimum nor virtual cathode exist; (2) potential minimum exists; (3) space-charge-limited virtual cathode exists; and (4) temperature-limited virtual cathode exists (negative anode potentials). For each of the various states of operation, expressions are derived for the distribution of potential and electric intensity throughout the region; the time of flight of electrons from grid to anode, and from grid to the plane of zero potential; and the location and magnitude of the minimum potential. An expression is also derived for the dependence of the anode current on the space current, grid-anode distance, grid voltage, and anode voltage. Curves are plotted from these expressions, and it is shown how the behavior of a large variety of practical tubes can be predicted and explained

\* Decimal Classification: R138.1 × R339.2.

† RCA REVIEW, January, 1938.

with their aid. The assumptions which underlie the theory are stated, and the effects of the neglected phenomena are discussed qualitatively.

Anode-current vs. anode-voltage and anode-current vs. space-current curves representing observations made on a specially constructed tetrode are presented by way of experimental verification of the theoretical results.

For purposes of illustration, application is made of these results to elucidate the theory of the type of power-amplifier tube which employs a minimum potential, formed in front of the anode as a result of the space charge of the electrons, to minimize the passage of secondary electrons from anode to grid. In addition, it is shown how the decrease of anode current with increasing space current which occurs when a space-charge-limited virtual cathode is formed in the grid-anode region, may be utilized to provide negative transconductance amplifiers and oscillators.

(39 Pages; 21 Figures)

## NEW TELEVISION-AMPLIFIER RECEIVING TUBES\*†

BY

A. P. KAUZMANN

Research and Engineering Department, RCA Manufacturing Company, Inc.,  
Harrison, N. J.

*Summary*—Television circuits require amplifying tubes of high grid-plate transconductance and low input and output capacitances to realize a voltage gain per stage sufficient to keep the amplifying stages at a reasonable number. To this end the 1851 and 1852, sharp cut-off, 9000-micromho grid-plate transconductance tubes—and the 1953, semi-remote cut-off, 5000-micromho grid-plate transconductance tube were developed. The improvements are the result of decreasing the control-grid-to-cathode spacing, and at the same time decreasing the pitch and diameter of the control-grid wires.

The maximum allowable resistance in the control-grid circuit is determined from the grid-plate transconductance of the tube, the cathode-bias resistor, and the screen voltage-dropping series resistor. Also, the use of a small un-bypassed resistor in the cathode circuit to neutralize the changes in input capacitance and input loading with varying plate current is presented.

The 1851 and 1852 have the highest ratios of grid-plate transconductance to plate current of any commercially available tubes with the result that they have high signal-to-noise ratios. The high grid-plate transconductances also result in high-conversion transconductance when these tubes are used as mixer tubes; the 1851 and 1852 give a maximum of 3500 micromhos, and the 1853 a maximum of 1500 micromhos. With practical circuits the 1851 and 1852 have produced gains per stage of 3.5 to 7.0 at 50 megacycles, and of 20 to 45 at 11 megacycles. Similarly, the 1853 has produced gains per stage of 2 to 4 at 50 megacycles, and of 6.5 to 13 at 11 megacycles. All of these values are for a band-pass of 2.5 megacycles.

(19 Pages; 14 Figures; 2 Tables)

\* Decimal Classification: R339.2.

† RCA REVIEW, January, 1939.

## AN ELECTRON OSCILLATOR WITH PLANE ELECTRODES\*†

BY

B. J. THOMPSON AND P. D. ZOTTU‡

Research and Engineering Department, RCA Manufacturing Company, Inc.,  
Harrison, N. J.

*Summary*—This paper describes a new type of thermionic tube capable of producing ultra-high frequencies by means of electron oscillations. Tubes of this type are characterized by having parallel plane electrodes, instead of cylindrical electrodes as in the conventional Barkhausen-Kurz tubes, and a fourth element called a backing plate.

The relations between wavelength and amplitude of oscillation and the various electrode potentials are shown by measurements on a typical tube. It is found that in these tubes the filament voltage is not critical, space-charge-limited operation being satisfactory, and that only one mode of oscillation is obtained. Both of these factors appear to give these tubes an advantage in stability over cylindrical Barkhausen-Kurz tubes.

A tube of the flat type is described which has produced oscillations at a wavelength of less than 10 cm in the fundamental mode with a positive grid potential of 150 volts.

(12 Pages; 14 Figures)

\* Decimal Classification: R138.4.

† Proc. I.R.E., December, 1934.

‡ Formerly with RCA Manufacturing Company.

## THE DEVELOPMENTAL PROBLEMS AND OPERATING CHARACTERISTICS OF TWO NEW ULTRA-HIGH-FREQUENCY TRIODES\*†

BY

WINFIELD G. WAGENER

Formerly with Research and Engineering Department, RCA Manufacturing Company, Inc.,  
Harrison, N. J.

*Summary*—Large values of power are difficult to obtain in the ultra-high-frequency region. At the limiting frequencies it is increasingly more difficult to find vacuum tubes that will deliver such power and perform efficiently. The principal factors that affect the design and performance of the tubes are those involving the electrical circuit, the size requirements for the power desired, and the transit time of the electrons within the evacuated space of the tube.

The design principles that result from a consideration of these factors have been used in the development of two new ultra-high-frequency triodes. A triode capable of delivering approximately 700 watts at 100 megacycles is described. This tube, which is cooled by water and air, is capable of

\* Decimal Classification: R339.2.

† Proc. I.R.E., April, 1938.

operation as a neutralized power amplifier up to 200 megacycles with an output of approximately 500 watts. A second triode is described which is a radiation-cooled glass tube with a 300-watt plate-dissipation rating. Normal efficiency is obtained up to 40 megacycles and operation as a neutralized power amplifier is possible up to 100 megacycles. The efficiency at 100 megacycles is approximately 60 per cent.

(14 Pages; 10 Figures)

## A PUSH-PULL ULTRA-HIGH-FREQUENCY BEAM TETRODE\*†

BY

A. K. WING

Research and Engineering Department, RCA Manufacturing Company, Inc.,  
Harrison, N. J.

*Summary*—The design of a vacuum tube capable of delivering 10 watts useful power output at frequencies of the order of 250 megacycles and with a d-c plate voltage of 400 volts and good economy of space and cathode power, is discussed. In order to keep the physical dimensions of the tube small and to make it adaptable to straightforward circuit arrangements, the tube was designed as a push-pull beam tetrode. Unusual constructional features include the use of short, heavy leads sealed directly into the moulded glass bulb.

Characteristics of the tube are given. Tests show that the tube will operate as a stable Class C amplifier at frequencies up to 250 megacycles. At that frequency a power output of the order of 13 watts with an efficiency of 45 per cent has been obtained. Satisfactory operation as a frequency multiplier is possible in the same frequency range. Oscillator operation has been obtained at considerably higher frequencies. The variation of output and efficiency with frequency is shown.

(11 Pages; 6 Figures)

---

\* Decimal Classification: R339.2.

† RCA REVIEW, July, 1939.

## DESIGN AND USE OF "ACORN" TUBES FOR ULTRA-HIGH FREQUENCIES\*†

BY

BERNARD SALZBERG

Research and Engineering Department, RCA Manufacturing Company, Inc.,  
Harrison, N. J.

*Summary*—Early work on the extension of the high-frequency limit of receiving equipment indicated that in conventional circuits employing

---

\* Decimal Classification: R339.2.

† Electronics, September, 1934.



standard tubes, the tubes became less and less effective as the frequency was increased and that ultimately, at frequencies of the order of 200 megacycles, tubes were practically useless. B. J. Thompson and G. M. Rose, Jr., conclusively demonstrated that the limitations to the successful operation of vacuum tubes at the higher frequencies may be overcome by reducing the dimensions of the tubes. The small tubes, which they built, being intended for a research study, were not suited for manufacture. However, the possibilities of these tubes aroused an interest sufficiently widespread to warrant their further development for use by experimenters. This article deals with the factors which were involved in the design and application of the first of such tubes, a Lilliputian triode.

(3 Pages; 4 Figures)

## REVIEW OF ULTRA-HIGH-FREQUENCY VACUUM-TUBE PROBLEMS\*†

BY

B. J. THOMPSON

Research and Engineering Department, RCA Manufacturing Company, Inc.,  
Harrison, N. J.

*Summary*—The effects of electron transit time and of lead inductance and interelectrode capacitance which become of importance at ultra-high frequencies are reviewed. It is shown that, in radio-frequency amplifier tubes for use in receivers, the most serious effect is the high ratio of input conductance to transconductance, which is independent of the transconductance and is proportional to the square of the frequency. This ratio may be reduced by reducing the electron transit time, the lead inductances, and the interelectrode capacitances. In power amplifiers and oscillators for transmitters, the important effects are much the same as in receiving tubes. The solution is complicated, however, by the problem of obtaining sufficient power output in a small structure.

(10 Pages; 2 Figures)

---

\* Decimal Classification: R339.2.

† RCA REVIEW, October, 1938.

## CONSTRUCTION AND ALIGNMENT OF THE TELEVISION RECEIVER\*†

BY

C. C. SHUMARD

Research and Engineering Department, RCA Manufacturing Company, Inc.,  
Harrison, N. J.

*Summary*—The design of coupling circuits which will pass the extraor-

---

\* Decimal Classification: R583.5.

† QST, January, 1939.

*dinarily wide frequency band necessary for good picture reception is one of the most critical features of a television receiver. In this article the construction of these circuits is discussed in detail. The exact dimensions given, as well as the carefully worked out alignment procedure, should enable the constructor to get the receiver into operation with a minimum of trouble. In conjunction with the deflection circuits for small cathode-ray tubes described in October QST, it constitutes a complete television receiving system.*

(9 Pages; 15 Figures)

## NOTES ON PROPAGATION AT A WAVELENGTH OF SEVENTY-THREE CENTIMETERS\*†

BY

B. TREVOR AND R. W. GEORGE

RCA Communications, Inc., Riverhead, L. I., N. Y.

*Summary—Quantitative field strength observations have been made on a wavelength of 73 centimeters with improved apparatus. The methods are described. Propagation data have been obtained with the receiver installed in an automobile and an airplane. Further observations were made on the ground at a distance of 113 miles, 8,000 feet below the line of sight from the transmitter. The results show the nature of the propagation of 73-centimeter waves over distances up to 175 miles. Below the transmitter's horizon, rapid attenuation occurs with increase in distance from the transmitter, the plane of polarization of the transmitted signal remains unchanged, and various types of fading are observed.*

(9 Pages; 5 Figures)

---

\* Decimal Classification: R113.

† *Proc. I.R.E.*, May, 1935.

## DESCRIPTION AND CHARACTERISTICS OF THE END-PLATE MAGNETRON\*†

BY

ERNEST G. LINDER

RCA Manufacturing Company, Inc., Camden, N. J.

*Summary—A new type of magnetron is described which is especially adapted to the generation of centimeter waves. It possesses several advantages over the simple magnetron, namely: (1) greater stability with respect to fluctuations of supply voltages, (2) less tendency to oscillate at undesired long wavelengths, (3) greater efficiency, (4) greater output, and (5) greater ease of adjustment. Static and dynamic characteristics are discussed. The*

---

Decimal Classification: R355.912.1.

† *Proc. I.R.E.*, April, 1936.

*effect of space charge on electron motion and tube performance is treated mathematically, and supporting experimental data are presented. Evidence is given that for best operation an optimum space-charge condition is required, which can conveniently be established and maintained by the use of end plates. Power output is limited by a type of instability involving electron bombardment of the filament, and apparently initiated by excessive space charge.*

*(21 Pages; 18 Figures)*

## THE MAGNETRON AS A HIGH-FREQUENCY GENERATOR\*†

BY

G. ROSS KILGORE

Research and Engineering Department, RCA Manufacturing Company, Inc.,  
Harrison, N. J.

*Summary*—The search for methods of generating ultra-high frequencies has followed two main paths. One has been the improvement of the negative grid tube as an oscillator and amplifier so as to extend its upper frequency limit. The other has been the investigation of less conventional vacuum tubes that appear to be applicable at high frequencies. Of the latter group the magnetron now stands out as one of the most promising tubes.

The device first called a "magnetron" by Hull in 1921 is well known as a vacuum tube having cylindrical plate structure and coaxial filament, with a uniform magnetic field directed along the electrode axis. Its use as a generator of high frequency currents has developed mainly in the past decade and its investigation has claimed the attention of a large number of research workers in many countries.

Magnetrons in a variety of structural forms and in a number of operating modes have been used for oscillation generation. Broadly speaking, magnetron oscillators can be divided into two classes; one using an alternating magnetic field, and other using a constant magnetic field. The alternating-field type described by Elder, in which the field coil is part of the oscillating circuit, is obviously limited to low frequencies and need not be considered in the present discussion. The constant field types which are useful in generating ultra-high frequencies can be subdivided as negative resistance oscillators and transit time oscillators.

The negative resistance magnetron oscillator may be defined as one which operates by reason of a static negative resistance between its electrodes and in which the frequency is equal to the natural period of the circuit. In Europe this type is sometimes called "dynatron magnetron" or Habann oscillator.

The transit time magnetron oscillator may be defined as one which operates by reason of electron transit time phenomena and in which the frequency is determined by the electron transit time. This type is often referred to as an "electronic oscillator" and sometimes as a "magnetostatic oscillator."

\* Decimal Classification: R355.912.1.

† *Jour. of Applied Physics*, October, 1937.

*It is the purpose of the present paper to survey the various types of magnetron generators with particular reference to their performance and limitations at ultra-high frequencies.*

*(11 Pages; 15 Figures)*

## MICRO-WAVES IN NBC REMOTE PICK-UPS\*†

BY

ROBERT M. MORRIS

Development Engineer, National Broadcasting Company, N. Y.

*Summary—The National Broadcasting Company in its efforts to best serve the public interest has constantly endeavored to take its microphones to more and more remote points. To do this has required the use of radio to an increasing extent. In many cases wire lines have not been available in time to do the job. In other instances the very nature of the pick-up point (ship, airplane, balloon, etc.) has necessitated the use of radio circuits. Radio apparatus for these special events or spot news broadcasts has in general fallen into two classifications; first, portable units of from 10 to 100 watts and second, self-contained pack-sets of less than 1 watt, and light enough to be carried by one person. The extreme mobility of this latter type of equipment has made it of special interest for unusual or difficult broadcasts.*

*(8 Pages; 8 Figures)*

---

\* Decimal Classification: R310.

† RCA REVIEW, July, 1936.

## APPLICATION OF FREQUENCIES ABOVE 30,000 KILOCYCLES TO COMMUNICATION PROBLEMS\*†

BY

H. H. BEVERAGE, H. O. PETERSON, AND C. W. HANSELL

RCA Communications, Inc.,  
New York, Riverhead and Rocky Point, N. Y.

*Summary—The authors briefly describe the results of a number of experiments with frequencies above 30,000 kc covering a period of several years. Since the major interests of radio communications companies has been in long-distance communications, this paper includes some qualitative data covering propagation beyond the optical, or direct vision, range. The authors have found that the altitude of the terminal equipment location has a marked effect on the signal intensity, even beyond the optical range.*

*Frequencies below about 43,000 kc appear to be reflected back to earth*

---

\* Decimal Classification: R531.84.

† Proc. I.R.E., August, 1931.

at relatively great distances in the daytime in north-south directions, but east-west transmission over long distances is extremely erratic.

Frequencies above about 43,000 kc do not appear to return to earth beyond the ground wave range, except at rare intervals, and then for only a few seconds or a few minutes. These frequencies, which do not return to earth, also appear to be free of echoes and multiple path transmission effects. Therefore, they are free from distortion due to selective fading and echoes. The range is also limited to the ground wave range, so these frequencies may be duplicated at many points without interference. As the frequency is raised, the range tends to approach the optical distance as a limit. Experiments with frequencies above 300,000 kc have, so far, indicated that the maximum range is limited to the optical distance. A number of possible applications are suggested, based on the unique properties of these frequencies. A specific application to telephony between the Islands of the Hawaiian group is briefly described.

(21 Pages; 11 Figures)